

IRSN

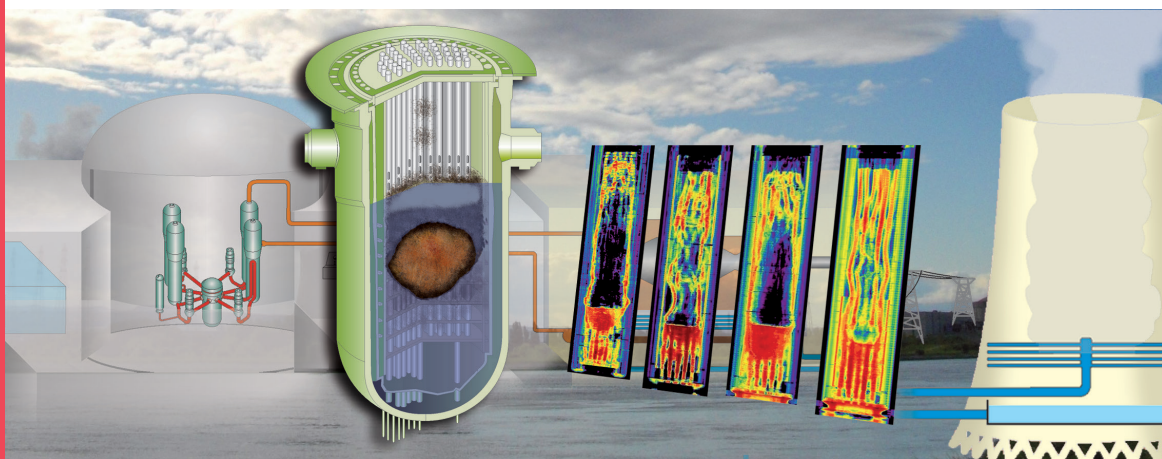
INSTITUT
DE RADIOPROTECTION
ET DE SÛRETÉ NUCLÉAIRE

Enhancing nuclear safety

Didier Jacquemain, Coordinator

Nuclear Power Reactor Core Melt Accidents

Current State of Knowledge



edp sciences



Science and Technology Series

Nuclear Power Reactor Core Melt Accidents

Current State of Knowledge

Ahmed Bentaïb, Hervé Bonneville, Gérard Cénérino,
Bernard Clément, François Corenwinder, Michel Cranga,
Gérard Ducros, Florian Fichot, Didier Jacquemain,
Christophe Journeau, Vincent Koundy, Denis Leteinturier,
Daniel Magallon, Renaud Meignen, Frédérique Monroig,
Georges Nahas, Frédérique Pichereau, Emmanuel Raimond,
Jean-Marie Seiler, Bruno Tourniaire, Jean-Pierre Van-Dorselaere

Didier Jacquemain, Coordinator

Cover illustration: Radiographic image of Phebus FP test devices and an artist's impression of the TMI-2 reactor core after fuel melt.

Printed in France
ISBN: 978-2-7598-1835-8

All rights reserved for all countries. This document may not be translated, adapted or reproduced by any means without permission. Pursuant to paragraphs 2 and 3 of Article 41 of the Act of 11 March 1957 only "copies or reproductions strictly reserved for the copyist's private use and not intended for collective use" are authorised. Regarding analyses and brief quotations intended as examples and illustrations, paragraph 1 of Article 40 of the same Act stipulates that "any representation, in whole or in part, made without the consent of the author or his/her successors or assignees is illicit." Such representation or reproduction, made by whatever means, therefore constitutes an infringement punishable under Articles 425 et seq. of the French Penal Code.

Preface

This new publication on what are referred to as “severe” core melt accidents, which may occur in pressurised light-water reactors, is the result of one of the most comprehensive surveys ever conducted on this subject. The knowledge it contains is presented with a strong educational focus. I would like to take this opportunity to thank all those mentioned in the foreword who contributed to this vast project, with a special mention for its coordinator [D. Jacquemain](#).

Although the project was not yet completed, considerable headway had already been made when the [Fukushima Daiichi](#) disaster struck. This was the world’s third severe accident and resulted in the destruction of three nuclear power reactors and the release of large quantities of radioactive material to the sea and atmosphere. It raised the question as to whether the project should be postponed to take into account feedback from these major events. It was however decided to complete the book as soon as possible as it would be several years before any detailed scientific information from the Fukushima Daiichi accident became available. Furthermore, the knowledge and models already available within [IRSN](#) on the phenomenology of this type of accident had enabled the Institute to carry out valuable real-time assessments of changes in the state of the reactors.

For more than thirty years, [IRSN](#) has been carrying out experimental studies on the phenomena that lead to reactor core melt and those induced by this type of event. Back in the 1960s when the first nuclear power reactors were designed, a core melt was considered impossible because of the design measures taken to prevent it, such as design margins and redundant safety systems to halt the chain reaction and remove the heat generated in the reactor core. Consequently, no measures were included in reactor design to mitigate the impact of this type of event. This approach had to be rethought following the accident at the Three Mile Island nuclear power plant in the United States in 1979. It was then necessary to determine how fuel could be damaged in a reactor core and, more especially to understand the melting process induced by a loss of cooling that

could ultimately lead to failure of the reactor coolant system – and the reactor vessel in particular. The next step was to grasp how chemical or radiolytic reactions could induce a significant release of hydrogen and many fission products exhibiting varying degrees of volatility and toxicity.

An experimental programme unlike any other in the world was then launched using [Phebus](#), a reactor built by the CEA at Cadarache in the south of France. As part of the programme, fuel melt tests were performed on a reduced scale, representative of the actual operating conditions in a pressurised water reactor. New knowledge was to emerge from this impressive programme, including some surprises that called into question certain theoretical predictions. Models aimed at simulating these extreme phenomena in a full-scale reactor were then developed and incorporated in computer tools and validated during these tests.

As knowledge of severe accidents grew over the years, some countries took concrete steps to improve the safety of power reactors – whether existing or planned.

[SARNET](#), an international network of experts and researchers led by [IRSN](#) from 2004 to 2013, coordinated continuous improvement of knowledge and the standards of models used to simulate severe accident phenomena in various types of reactor. This collaboration is being continued as part of the European NUGENIA association. Further experiments are needed, however, to reduce uncertainty on various phenomena with a significant impact on the consequences (especially for health) of a severe accident, although, based on data from the [Phebus](#) programme, such experiments are now designed as analytical tests, known as separate-effect tests. These are designed to target individual phenomena for which greater knowledge is required: what happens if an attempt is made to “reflood” a severely damaged, partially melted reactor core? What happens to the corium – the chemically and thermally aggressive mixture of fuel and molten metal – once it is released from the reactor core? Another question, of prime importance for radiation protection, concerns the behaviour of the different chemical species of radioactive iodine and ruthenium which are produced in large quantities inside the reactor containment, with varying degrees of volatility.

[IRSN](#) and its national and international research partners will continue to devote considerable resources in these areas over the coming years. For the past fifteen years, the Institute has never lost sight of the fact that severe accident research is vital. Unfortunately, the accident at [Fukushima](#) proved it right. The knowledge already acquired, as well as that yet to come, should be used not only to go on improving existing reactors wherever possible, but also to ensure that in the future, the nuclear industry at last develops reactors that no longer expose countries opting for nuclear energy to the risk of accidents, and the ensuing radioactive contamination of potentially large areas, that most human societies consider unacceptable. I hope that this publication helps to disseminate existing knowledge on this crucial topic as the new generation of nuclear engineers takes over from the old. I also hope it serves to illustrate how important it is to continue research and industrial innovation, without which no essential progress can be made in the field of [nuclear safety](#).

Jacques Repussard
[IRSN](#) Director-General

List of abbreviations

Institutions

AEAT: Atomic Energy Authority Technology, UK (AEC Technology plc)

AECL: Atomic Energy of Canada Limited, a nuclear science and technology research institute

AEKI: Atomic Energy Research Institute, Budapest, Hungary

ANCCLI: *Association nationale des comités et commissions locales d'information* (French National Association of Local Information Commissions and Committees)

ANL: Argonne National Laboratory, USA

ANR: *Agence nationale de la recherche* (National Research Agency, France)

ASN: *Autorité de sûreté nucléaire* (Nuclear Safety Authority, France)

AVN: *Association Vinçotte nucléaire* (Vinçotte Nuclear Association, Belgium)

BARC: Bhabha Atomic Research Centre, India

BNL: Brookhaven National Laboratory, USA

CEA: *Commissariat à l'énergie atomique et aux énergies alternatives* (Alternative Energies and Atomic Energy Commission, France)

CLI: *Commission locale d'information* (French Local Information Commission)

CNL (formerly AECL): Canadian Nuclear Laboratories

CNRS: *Centre national de la recherche scientifique* (French National Centre for Scientific Research)

CSNI: Committee on the Safety of Nuclear Installations, OECD

EDF: *Électricité de France* (French power utility)

EPRI: Electric Power Research Institute, USA

FAI: Fauske & Associates, Inc., USA

FzD: *Forschungszentrum Dresden-Rossendorf* (research laboratory in Dresden, Germany)

FzK: *Forschungszentrum Karlsruhe* (Karlsruhe Institute of Technology, Germany)

GRS: *Gesellschaft für Anlagen – und Reaktorsicherheit*, (reactor safety organisation in Germany)

IAEA: International Atomic Energy Agency, Vienna, Austria

IAE-NNC-RK: Institute of Atomic Energy – National Nuclear Centre – Republic of Kazakhstan

IBRAE: Nuclear Safety Institute of Russian Academy of Sciences

ICRP: International Commission on Radiological Protection

IKE: *Institut für Kernenergetik und Energiesysteme, Universität Stuttgart* (Institute for Nuclear Technology and Energy Systems, University of Stuttgart, Germany)

INEL: Idaho National Engineering Laboratories, Idaho, USA

INL: Idaho National Laboratory, USA

INSA: *Institut national des sciences appliquées* (National Institute of Applied Science, France)

IPSN: *Institut de protection et de sûreté nucléaire* (Institute for Nuclear Safety and Protection, France)

IREX: *Institut pour la recherche appliquée et l'expérimentation en génie civil* (Institute for Applied Research and Experimentation in Civil Engineering, France)

IRSN: *Institut de radioprotection et de sûreté nucléaire* (Institute for Radiological Protection and Nuclear Safety, France)

ISS: Innovative Systems Software, USA

ISTC: International Science and Technology Centre, EC

JAEA: Japan Atomic Energy Agency

JAERI: Japan Atomic Energy Research Institute

JNES: Japan Nuclear Energy Safety

JRC: Joint Research Centre, EC

JSI: Jozef Stefan Institute, Slovenia

KAERI: Korea Atomic Energy Research Institute, South Korea

KAIST: Korea Advanced Institute of Science and Technology, South Korea

KINS: Korea Institute of Nuclear Safety, South Korea

KIT (ex-FzK): *Karlsruher Institut für Technologie* (Karlsruhe Institute of Technology, Germany)

KTH, see RIT

LUCH: Scientific Manufacturer Centre, Russia

MIT: Massachusetts Institute of Technology, USA

NEA: Nuclear Energy Agency, OECD

NIIAR: Scientific Research Institute of Atomic Reactors, Russia

NITI: Aleksandrov Scientific Research Technological Institute, Saint Petersburg, Russia

NRC-KI (formerly RRC-KI): National Research Centre Kurchatov Institute, Moscow, Russia

NUPEC: Nuclear Power Engineering Corporation, Japan
OECD: Organisation for Economic Co-operation and Development
ORNL: Oak Ridge National Laboratory, USA
PSI: Paul Scherrer Institute, Switzerland
RIT (formerly KTH): Royal Institute of Technology, Stockholm, Sweden
SKI: Swedish Nuclear Power Inspectorate
SNL: Sandia National Laboratory, USA
UCLA: University of California, Los Angeles, USA
UCSB: University of California, Santa Barbara, USA
UJV: Nuclear Research Institute Rez, Czech Republic
US NRC: United States Nuclear Regulatory Commission, USA
VTT: Technical Research Centre, Finland

Technical abbreviations

Ag-In-Cd: Silver-Indium-Cadmium
AICC: Adiabatic Isochoric Complete Combustion
ARTIST: Aerosol Trapping in a Steam Generator (experimental programme carried out by the Paul Scherrer Institute [PSI])
ATWS: Anticipated Transient Without Scram (automatic reactor shutdown without insertion of control rods or transients with failure of the automatic reactor shutdown system – also known as ATWR for anticipated transient without (reactor) trip)
AVS: Annulus Ventilation System (1300 MWe, 1450 MWe reactors and EPR)
BIP: Behaviour of Iodine Project (international programme on iodine behaviour under the auspices of the OECD)
BL: Electrical Building
BWR: Boiling Water Reactor
CANDU: CANada Deuterium Uranium reactor (a heavy-water reactor)
CCWS: Component Cooling Water System
CFD: Computational Fluid Dynamics
CHF: Critical Heat Flux
CHRS: Containment Heat Removal System (a reactor spraying system in the EPR designed for use in severe accidents)
CODIR-PA: French Post-accident Management Steering Committee
CRP: Coordinated Research Programme on Severe Accident Analysis, IAEA
CSA: Complementary Safety Assessment
CSARP: Cooperative Severe Accident Research Programme (coordinated by the US NRC)
CSD: Severely Degraded Fuel
CSS: Containment Spraying System
CVCS: Chemical and Volume Control System
DAC: Facility construction licence

DCH: Direct Containment Heating (of gases)
DDT: Deflagration-Detonation Transition
E3B: Extension of the third containment barrier
EEE: Containment annulus (1300 MWe, 1450 MWe reactors and EPR)
EFWS: Emergency Feedwater System
ENACEEF: Flame acceleration facility, an experimental installation of the CNRS/ICARE in Orleans, France
EPR: European Pressurised Water Reactor
EPS: Emergency Power Supply
ESWS: Essential Service Water System
ETY: Hydrogen Reduction and Measurement System
FB: Fuel Building
FNR: Fast Neutron Reactor
FP: Fission Products
FP + number: European Commission Framework Programme for research and technological development (e.g., FP6, FP7 for the sixth and seventh framework programmes)
FPCPS: Fuel Pool Cooling and Purification System
FWLB: Feedwater Line Break
GAEC: Assistance Guide for Emergency Response Teams
GCR: Gas-Cooled, Graphite-Moderated Reactor
GIAG: Severe Accident Operating Guidelines
HHSI: High Head Safety Injection
HRA: Human Reliability Analysis
HTR: High Temperature Reactor
IRWST: In-containment Refuelling Water Storage Tank (borated water tank located inside the EPR containment building)
ISP: International Standard Problem
ISTP: International Source Term Programme
LHF: Lower Head Failure (failure in the lower part of the reactor vessel)
LHSI: Low Head Safety Injection (or Low Head Safety Injection System according to context)
LOCA: Loss-of-Coolant Accident
LUHS (H1): Loss of Ultimate Heat Sink (H1 in France)
MCCI: Molten Core-Concrete Interaction
MFWS: Main Feedwater System
MHPE: Maximum Historically Probable Earthquake
MHSI: Medium Head Safety Injection
MOX: Mixed Oxide Fuel (fuel composed of a mixture of UO₂ + PuO₂)
MPL: Maximum Permissible Level (of radioactivity)

NAB: Nuclear Auxiliary Buildings
OLHF: OECD Lower Head Failure (OECD research programme on failure in the lower part of the reactor vessel)
ORSEC: French emergency response plan
PBMR: Pebble Bed Modular Reactor (a type of high-temperature reactor or HTR)
PDS: Plant Damage State
PHWR: Pressurised Heavy Water Reactor
PPI: Off-site Emergency Plan
PRT: Pressuriser Relief Tank
PSA: Probabilistic Safety Assessment
PUI: On-site Emergency Plan
PWR: Pressurised Water Reactor
RB: Reactor Building
RBMK: *Reactor Bolshoy Moshchnosty Kanalny* (high-power Russian reactor with pressure tubes)
RCS (transients): Transients on the Reactor Coolant System
RCS: Reactor Coolant System
RFS: Basic Safety Rule
RHRS: Residual Heat Removal System
SAB: Safeguard Auxiliary Buildings
SARNET: Severe Accident Research NETwork of excellence, a European research project to study core melt accidents in water reactors
SBO (H3): Station Blackout
SERENA: Steam Explosion REsolution for Nuclear Applications (an OECD research programme)
SG: Steam Generator
SGTR: Steam Generator Tube Rupture
SI: Safety Injection
SIS: Safety Injection System
SLB: Steam Line Break
SME: Seismic Margin Earthquake
SOAR: State-of-the-Art Report
TAM: Equipment hatch
TGT: Thermal Gradient Tube
TGTA-H2: Accident with total loss of steam generator feedwater supply and failure of “feed and bleed” operating mode (or transients on the secondary system)
TMI: Three Mile Island, USA
TMI-2: Reactor 2 at the Three Mile Island NPP, USA
VCI: Pre-service Inspection

VD: Ten-Yearly Outage Programme

V-LOCA: Loss of Coolant Accident (containment bypass accidents or loss-of-coolant accidents outside the containment building)

VVER: *Vodo-Vodyanoi Energetichesky Reaktor* (Russian water-cooled, water-moderated nuclear power reactor)

ZPP: Population Protection Zone

ZST: Reinforced Environmental Monitoring Zone

Foreword

This summary of knowledge on core melt accidents is a collective work written for the most part by authors from the *Institut de Radioprotection et de Sûreté Nucléaire* (French Institute for Radiological Protection and Nuclear Safety or [IRSN](#)). Some sections include contributions from authors from the *Commissariat à l'énergie atomique et aux énergies alternatives* (French Alternative Energies and Atomic Energy Commission or CEA). Experts from both these organisations and from EDF, a French power utility, also took part in carefully proofreading various chapters. We would like to express our thanks to all those who contributed in one way or another to this publication.

Didier Jacquemain from [IRSN](#), who was the project coordinator.

Contributions were made by the following authors:

- Chapters 1, 2, 3 and 9: Didier Jacquemain;
- Chapter 4: Gérard Cénérimo, François Corenwinder, Didier Jacquemain and Emmanuel Raimond from IRSN;
- Chapter 5: Ahmed Bentaïb from IRSN (Section 5.2.2), Hervé Bonneville from IRSN (Section 5.1.4), Bernard Clément from IRSN (Section 5.5), Michel Cranga from IRSN (Sections 5.3, 5.4.2 and 5.4.3), Gérard Ducros from CEA (Section 5.5), Florian Fichot from IRSN (Sections 5.1.1, 5.1.2 and 5.4.1), Christophe Journeau from CEA (Section 5.4.3), Vincent Koundy from IRSN (Section 5.1.3), Daniel Magallon from CEA (Section 5.2.3), Renaud Meignen from IRSN (Sections 5.2.1 and 5.2.3), Jean-Marie Seiler from CEA (Section 5.4.1) and Bruno Tourniaire from CEA (Sections 5.3 and 5.4.2);
- Chapter 6: François Corenwinder, Denis Leteinturier, Frédérique Monroig, Georges Nahas and Frédérique Pichereau from IRSN;

- Chapter 7: Bernard Clément (Section 7.3) and Didier Jacquemain (Sections 7.1 and 7.2);
- Chapter 8: Jean-Pierre Van-Dorsselaere from IRSN.

The following experts were involved in proofreading in their specialist fields:

- for IRSN: Jean Couturier, Cécile Debaudringhien, Anna Duprat, Patricia Dupuy, Jean-Michel Evrard and Grégory Nicaise;
- for CEA: Georges Berthoud and Étienne Studer;
- for EDF: François Andréo, Kresna Atkhen, Thierry Dagusé, Alain Dubreuil-Chambardel, François Kappler, Gérard Labadie and Andreas Schumm.

Randall O. Gauntt from the US Nuclear Regulatory Commission (USA) and Jonathan Birchley from the Paul Scherrer Institute (Switzerland) approved the section on the MELCOR computer code in Chapter 8.

Denis Boulaud, Bernard Chaumont, Bernard Clément, Richard Gonzalez, Didier Jacquemain, Daniel Quéniart, Jean Peltier, Frédérique Pichereau from IRSN and Michel Durin from CEA proofread the whole work several times to ensure consistency.

Georges Goué, Odile Lefèvre and Sandrine Marano from IRSN prepared the work for publication.

Lastly, this work would not have been possible without the active participation of IRSN's Scientific Directors Jean-Dominique Gobin and Michel Schwarz, and its Director-General Jacques Repussard.

Tim Haste from IRSN largely contributed to improve the quality of the present English version by proof-reading minutely many chapters.

Summary

Preface	III
List of abbreviations	V
Foreword	XI

Chapter 1

Introduction

1.1. General objectives of the book	1
1.2. Structure of the book.....	3
1.3. Objectives and approach of R&D on core melt accidents	4
1.3.1. Objectives.....	4
1.3.2. International R&D.....	5
1.3.3. Approach.....	7

Chapter 2

Design and Operation of a Pressurised Water Reactor

2.1. General information about reactor operation.....	11
2.2. The pressurised water reactors in France's nuclear power plant fleet	13
2.3. Description of a pressurised water reactor and its main loops	18
2.3.1. Facility overview	18
2.3.2. Description of the main components of a PWR	21
2.4. Reactor operation under normal and accident conditions	33
2.4.1. Systems used under normal reactor operating conditions.....	33

2.4.2. Systems used under reactor incident or accident conditions.....	35
2.5. Reactor control under normal and accident conditions	38
2.5.1. Control room.....	38
2.5.2. Reactor control.....	39
2.6. Conclusion.....	42

Chapter 3

Safety Principles for Pressurised Water Reactors in the French Nuclear Power Plant Fleet

3.1. Introduction.....	43
3.2. Concept of defence-in-depth.....	44
3.3. Role of the probabilistic approach.....	47
3.4. Conclusion.....	48

Chapter 4

Safety Principles for France's Pressurised Water Reactors

4.1. Concept of severe accident.....	51
4.2. Accident scenarios that may lead to core melt	52
4.2.1. Description of PSA level 1 accident scenarios	52
4.2.2. Melt frequencies by scenario type determined by the level 1 PSA for the 900 MWe reactors	59
4.2.3. Accident progression beyond core melt	60
4.3. General progression of core melt accidents and their management at reactors in operation in France and for EPR.....	60
4.3.1. Physics of core melt and associated phenomena.....	60
4.3.2. Containment failure modes.....	67
4.3.3. Management of core melt accidents at PWRs in operation in France	69
4.3.4. Approach adopted for EPRs.....	81
4.4. Level 2 PSAs: method and lessons from core melt accidents.....	86
4.4.1. Methods of conducting level 2 PSAs.....	88
4.4.2. Applications of level 2 PSAs in France.....	92
4.4.3. Conclusion on level 2 PSAs.....	98

Chapter 5

Development of the core melt accident

5.1. Development of the accident in the reactor vessel.....	101
5.1.1. Progression of the core melt in the reactor vessel	101
5.1.2. Corium behaviour in the lower head.....	111

5.1.3. Reactor vessel failure	120
5.1.4. High-pressure core melt	127
5.2. Phenomena liable to result in early containment failure.....	146
5.2.1. Direct containment heating	146
5.2.2. Hydrogen risks and means of mitigating their consequences.....	161
5.2.3. Steam explosions.....	177
5.3. Phenomena that could lead to delayed containment failure: Molten Core-Concrete Interaction (MCCI).....	200
5.3.1. Introduction.....	200
5.3.2. Physical phenomena involved	200
5.3.3. Experimental programmes.....	203
5.3.4. Computer modelling and simulation software	209
5.3.5. Application to a power reactor.....	213
5.3.6. Summary and outlook	217
5.4. Retention and cooling of corium inside and outside the reactor vessel.....	222
5.4.1. In-vessel corium retention	222
5.4.2. Cooling of corium under water during MCCI.....	233
5.4.3. Corium spreading for the EPR.....	241
5.5. Release of fission products during a core melt accident	255
5.5.1. Inventory and relative importances of FPs	256
5.5.2. Release of FPs into the reactor vessel	259
5.5.3. Fission product transport in the reactor coolant system and secondary loops (fission gases excluded).....	269
5.5.4. Ex-vessel fission product releases	274
5.5.5. Behaviour of aerosols in the containment	275
5.5.6. Fission product chemistry	278
5.5.7. Conclusion.....	293

Chapter 6

Behaviour of Containment Buildings

6.1. Introduction.....	301
6.2. Behaviour of containment buildings under design-basis conditions	303
6.2.1. Single wall containment buildings (900 MWe reactors).....	304
6.2.2. Double-wall containment buildings (1300 and 1450 MWe reactors).	306
6.2.3. Double-wall containment on the EPR	307
6.2.4. Monitoring the integrity and leak tightness of containment buildings.....	308

6.3. Mechanical behaviour of containments in the event of a core melt accident ...	311
6.3.1. Introduction.....	311
6.3.2. Mechanical behaviour of the containments of 900 MWe PWR power plants.....	311
6.3.3. Mechanical behaviour of the containments of 1300 MWe PWR power plants.....	322
6.3.4. Summary and outlook concerning studies performed by IRSN regarding the mechanical behaviour of containment buildings under core melt accident conditions	326
6.4. Containment bypass.....	327
6.4.1. Introduction.....	327
6.4.2. Possibilities for containment bypass.....	329
6.4.3. Types of containment bypass that could occur during reactor operation	330
6.4.4. Types of containment bypass that could occur during a design-basis accident.....	331
6.4.5. Types of containment bypass that could occur during a core melt accident.....	332
6.5. Conclusion.....	334

Chapter 7

Lessons Learned from the Three Mile Island and Chernobyl Accidents and from the Phebus FP Research Programme

7.1. Lessons learned from the Three Mile Island accident.....	337
7.1.1. Introduction.....	337
7.1.2. Accident and core-degradation sequence.....	339
7.1.3. Environmental and public health consequences of the accident.....	348
7.1.4. Lessons learned from the accident with regard to the physics of core melt accidents	349
7.1.5. Lessons learned from the accident for the safety of French nuclear power plants.....	350
7.1.6. Conclusion.....	355
7.2. Lessons learned from the Chernobyl disaster.....	356
7.2.1. Introduction.....	356
7.2.2. Accident sequence, releases and consequences.....	357
7.2.3. Lessons learned in France regarding safety	365
7.2.4. Lessons learned in France regarding “nuclear crisis” management.....	366
7.2.5. Conclusion.....	367

7.3. The Phebus FP programme	367
7.3.1. Background	367
7.3.2. Description of the Phebus FP test setup and test matrix.....	368
7.3.3. Main lessons regarding fuel rod degradation.....	370
7.3.4. Releases from the core	374
7.3.5. Transport of fission products and aerosols in the RCS.....	377
7.3.6. Thermal-hydraulics and aerosol behaviour on the containment vessel.....	379
7.3.7. Iodine chemistry in the containment vessel	380
7.3.8. Use of Phebus FP test results in safety analyses	383

Chapter 8

Numerical Simulation of Core Melt Accidents

8.1. Integral and mechanistic computer codes	389
8.1.1. Integral codes.....	390
8.1.2. Mechanistic codes	393
8.2. General approach to code development and validation	394
8.2.1. Code development.....	394
8.2.2. Code validation	394
8.3. ASTEC.....	396
8.3.1. Capabilities.....	397
8.3.2. Validation status mid-2015.....	399
8.3.3. ASTEC upgrade prospects	401
8.4. MAAP	401
8.4.1. Capabilities.....	402
8.4.2. Validation status mid-2015.....	404
8.4.3. MAAP upgrade prospects	405
8.5. MELCOR	405

Chapter 9

Conclusion

Chapter 1

Introduction

1.1. General objectives of the book

The operation of nuclear power reactors utilising nuclear fission involves risks of possible radioactive substance dispersion and human and environmental exposure to radiation. In order to mitigate these risks, the nuclear industry attaches the greatest importance to the safety of its facilities. The nuclear facilities are therefore designed, constructed and used in such a way as to prevent potential abnormal and emergency situations and limit their consequences. Furthermore, measures are taken to continuously improve the facilities' level of safety by acting upon feedback on their design and operation, periodically reassessing their safety and integrating advances in scientific knowledge and the applicable techniques.

Despite all the measures taken, however, the possibility of an accident resulting in partial or complete melting of the nuclear fuel contained in the reactor core and, over the relatively long term, large quantities of radioactive substances being released into the environment cannot be excluded, as the [Fukushima Daiichi](#) accident in Japan in March 2011 has shown. Studying this type of accident, which is commonly classified as a "severe accident", is an important element of the safety approach adopted for nuclear fission power reactors. It is done with the aim of setting up suitable measures to reduce the probability of such an accident and, should one nevertheless occur, to mitigate its impact upon populations and the environment. All stakeholders in the nuclear industry have conducted considerable research in France and worldwide with the aim of achieving this objective and so improving the equipment and procedures of the reactors currently in operation.

The objective of this book is to present the scientific aspects of core melt accidents, and notably the knowledge acquired through the research carried out over the course of the last thirty years in order to understand and model the physical phenomena that can occur in such an accident. It is intended for any reader wishing to obtain an overview of the knowledge acquired, any remaining gaps and uncertainties, and past and present research in the field of core melt accidents.

It therefore reviews the current state of knowledge and prospects regarding research in the field, little more than thirty years after the Three Mile Island (TMI) accident in the United States which resulted in the partial melting of the core but fortunately caused very minor radioactive releases, nearly four years after the Fukushima Daiichi accident which resulted in a core melt in three reactors and major radioactive releases, and during the construction of the first third-generation pressurised water reactors (PWRs) in France; in the case of these reactors, core melt accidents are being addressed at the design stage.

The preliminary lessons learned from the Fukushima Daiichi accident do not seem to fundamentally challenge the existing state of knowledge regarding the phenomenology of core melt accidents or highlight new, hitherto unknown phenomena. Four years after the accident, however, the full sequence of events is still not exactly known. Feedback from the TMI accident, in which the damage to the reactor core could only be seen when the damaged reactor pressure vessel was opened around seven years after the accident, leads us to suppose that it will take several years to reconstruct the detailed scenario of the accident that caused the radioactive releases. As long as the cores of the three damaged reactors remain inaccessible, the available data will be too limited to allow the progression of the damage to be reconstructed. It therefore seems too early to present any lessons learned from the Fukushima accident regarding the phenomenology of nuclear core melt accidents at this stage¹.

It should be noted that although the physical phenomena described in this book can occur in different models of French or foreign pressurised water reactors currently in operation or under study as well as widely in the boiling water reactors such as those at the Fukushima Daiichi site, this book focuses more specifically on the reactors currently in operation and under construction or planned in France: the second-generation 900, 1300 and 1450 MWe pressurised water reactors and third-generation 1600 MWe European Pressurised Water Reactors (EPRs).

-
1. Following the Fukushima Daiichi accident, the consequences of external hazards such as flooding and earthquakes have been assessed in greater detail with a view to preventing and mitigating the effects of a core melt accident. In France, the Prime Minister asked the President of the French Nuclear Safety Authority (ASN) to conduct a safety audit of the French nuclear facilities in 2011, giving priority to the power reactors, regarding the following five points: the flooding risks, the seismic risks, the loss of electrical power, the loss of the heat sink, and the operational management of accident situations. ASN therefore asked the nuclear facility operators to conduct additional safety assessments on their facilities with the aim of learning the first lessons from the events that occurred at the Fukushima Daiichi nuclear power plant, firstly in order to assess the robustness of the French nuclear facilities in confronting severe external events, and secondly in order to reinforce the existing safety measures to increase their robustness.

1.2. Structure of the book

Following this introduction, which describes the structure of this book and highlights the objectives of R&D on core melt accidents, this book briefly presents the design and operating principles (Chapter 2) and safety principles (Chapter 3) of the reactors currently in operation in France, as well as the main accident scenarios envisaged and studied (Chapter 4). The objective of these chapters is not to provide exhaustive information on these subjects (the reader should refer to the general reference documents listed in the corresponding chapters), but instead to provide the information needed in order to understand, firstly, the general approach adopted in France for preventing and mitigating the consequences of core melt accidents and, secondly, the physical phenomena, studies and analyses described in Chapters 5 to 8.

Chapter 5 is devoted to describing the physical phenomena liable to occur during a core melt accident, in the reactor vessel and the reactor containment. It also presents the sequence of events and the methods for mitigating their impact. For each of the subjects covered, a summary of the physical phenomena involved is followed by a description of the past, present and planned experiments designed to study these phenomena, along with their modelling, the validation of which is based on the test results. The chapter then describes the computer codes that couple all of the models and provide the best current state of knowledge of the phenomena. Lastly, this knowledge is reviewed while taking into account the gaps and uncertainties, and the outlook for the future is presented, notably regarding experimental programmes and the development of modelling and numerical simulation tools.

Section 5.1 provides a detailed description of the sequence of events of a core melt accident in the reactor vessel; it discusses the core damage in the reactor vessel (Section 5.1.1), the behaviour of the corium² at the bottom of the reactor vessel (Section 5.1.2), the reactor vessel failure (Section 5.1.3) and high-pressure core melt (Section 5.1.4). Section 5.2 concerns the phenomena that can result in an early³ failure in the containment, consisting of direct heating of the gases within the containment building (Section 5.2.1), the "hydrogen risk" (Section 5.2.2) and the "steam explosion" risk (Section 5.2.3). Corium erosion of the concrete basemat of the containment building, which is one of the phenomena that can result in the containment failing later⁴, is discussed in Section 5.3. Section 5.4 focuses on the phenomenology of corium retention and cooling, both within the reactor vessel by reflooding the reactor coolant system and outside it by reflooding the reactor pit (Section 5.4.1), as well as of the under-water cooling of the corium during the corium-concrete interaction (Section 5.4.2) and of corium spread (Section 5.4.3). Section 5.5 discusses the release and transport of the fission products (FPs). It covers the release of FPs both within the vessel (Section 5.5.2) and outside the vessel (Section 5.5.4), the transport of FPs within the primary and secondary coolant

2. The mixture of melt materials resulting from the degradation of the structures comprising the reactor core (the fuel rods, control rods, spacer grids and plates within the core).
3. The word "early" means within such a very short time that it is not possible to set up measures to limit the spread of the radioactivity in the environment and its potential consequences upon the populations.
4. "Later" is used as the opposite of "early".

systems (Section 5.5.3), the behaviour of the aerosols (Section 5.5.5) and the chemistry of the FPs (Section 5.5.6) within the containment building.

Chapter 6 focuses on the behaviour of the containment enclosures during a core melt accident. After summarising the potential leakage paths of radioactive substances through the different containments in the case of the accidents chosen in the design phase, it presents the studies of the mechanical behaviour of the different containments under the loadings that can result from the hazards linked with the phenomena described in Chapter 5. Chapter 6 also discusses the risks of containment building bypass⁵ in a core melt accident situation.

Chapter 7 presents the lessons learned regarding the phenomenology of core melt accidents and the improvement of nuclear reactor safety from:

- the Three Mile Island accident that occurred on 28 March 1979 in the United States;
- the **Chernobyl** accident that occurred on 26 April 1986 in the Soviet Union's Ukrainian territory;
- the integral simulation testing of core melt accidents in the **Phebus FP** international research programme, which took place between 1993 and 2004.

For the reasons stated above (Section 1.1), it is too early to draw detailed lessons from the core melt accidents during the **Fukushima Daiichi** accident; as a result, this book does not contain a specific section on this accident. Further information on this accident is contained in the public report listed as reference document [1], which describes the initial analyses of the accident and its consequences one year after the accident.

Lastly, Chapter 8 presents a review of development and validation efforts regarding the main computer codes dealing with "severe accidents", which draw on and build upon the knowledge mainly acquired through the research programmes: ASTEC, which is jointly developed by IRSN and its German counterpart, GRS (*Gesellschaft für Anlagen- und Reaktorsicherheit*), MAAP-4, which is developed by FAI (Fauske & Associates, Inc.) in the United States and used by EDF and by utilities in many other countries, and MELCOR, which is developed by SNL (Sandia National Laboratories) in the United States for the US Nuclear Regulatory Commission (US NRC).

1.3. Objectives and approach of R&D on core melt accidents

1.3.1. Objectives

Analysis of the feedback, which includes an analysis of the incidents and, therefore, of the accidents, must be supplemented by research on safety notably relating to core melt accidents, as this is essential in maintaining and improving the safety of the nuclear reactors currently in operation.

5. An accident in which the containment building is bypassed can result in the direct release of radioactive products into the environment.

Research and studies of core melt accidents will undoubtedly not only provide a better understanding of the conditions under which the accidents occur as well as their sequence of events, but also improve our knowledge of their phenomenology with the aim of developing measures to stop them progressing and limit their effects. The results of this research can therefore be used to develop, on the basis of existing experience and knowledge, simulation tools and models that can predict the accidents' sequence of events and consequences, as these tools are used in the nuclear facilities' safety studies.

The knowledge acquired as a result of this research can also help to develop new concepts for improving safety and thereby reduce the risks and consequences of core melt accidents. This research includes that relating to the "core catcher" developed for the EPR with the aim of limiting the consequences of a core melt accident, which are described in Section 5.4.3.

1.3.2. *International R&D*

Even before the Three Mile Island accident, which occurred in 1979 in the United States (Section 7.1), probabilistic safety assessments were performed on core melt accidents that occurred in the United States, with the aim of assessing the risks of radioactive releases into the environment and the consequences of these releases upon the populations [2]. At the time, these studies were widely considered to be theoretical.

More advanced research programmes on core melt accidents began at the beginning of the 1980s, following the awareness caused by the Three Mile Island accident, which clearly demonstrated that a nuclear reactor core melt accident was possible. Most of the countries using nuclear reactors (United States, Finland, France, Japan, Germany, Belgium, Canada, South Korea, United Kingdom, Netherlands, Switzerland, Sweden, Russia as well as some central Europe and eastern European countries [Hungary, Czech Republic, Slovakia, Slovenia, Lithuania and Ukraine]) have conducted research programmes in the field of core melt accidents. The [Chernobyl](#) accident, which occurred in 1986 in the Ukraine (Section 7.2), has merely underlined the need to continue and extend the research in this field. In general, each of these countries has focused on one or more particular aspects of the issue, as the field is too vast to allow the investigation of all phenomena in any one national programme.

The United States was the first country to conduct major research in the field. The research programmes were directed by the US NRC and based on national laboratories including the Electric Power Research Institute (EPRI), SNL and the Oak Ridge National Laboratory (ORNL) [3].

In France, the first major research programmes on core melt accidents began at the beginning of the 1980s and include the [Phebus](#) CSD (severely degraded fuel) programme. Bearing in mind the number of its nuclear power plants, France, like the United States, has developed national or international programmes on almost all subjects relating to core melt accidents. This research is primarily conducted by [IRSN](#), CEA, EDF and AREVA. All these entities either develop or help to develop simulation software and have facilities in which they conduct testing.

Extensive research has been carried out in the field of core melt accidents, involving very considerable human and financial resources as a result of their great complexity, as well as collaboration between nuclear stakeholders, industry groups, research centres and safety authorities, at both the national and the international levels. In France, IRSN, CEA, EDF and AREVA have conducted joint programmes on many subjects and participate in international programmes, including those supported by the European Commission through its Framework Programmes for Research and Development and those conducted under the auspices of the OECD. In particular, IRSN has jointly conducted the Phebus FP integral test programme with CEA from the end of the 1980s onwards, thereby structuring international research efforts regarding core melt accidents (Section 7.3).

As part of the Sixth Framework Programme, a Network of Excellence called SARNET (Severe Accident Research NETwork of excellence) was set up to optimise the use of the available resources and increase the knowledge acquired in Europe regarding core melt accidents, coordinated by IRSN. Between 2004 and 2008, SARNET consisted of around fifty organisations belonging to 19 European Union countries as well as Switzerland. As well as increasing the scientific knowledge acquired regarding core melt accidents, it has also defined new research programmes and set up the resources needed to ensure the sustainability of the knowledge gained and to transfer the knowledge on a wider level. In 2008, operation of the SARNET network ensured the consistency of the current state of knowledge and of the main remaining uncertainties regarding core melt accidents. As a result, the highest-priority areas for improvement have been identified and new research programmes proposed in order to fill in the remaining gaps [4]. The activities of the network, which include the new proposed subjects of research, have continued as part of the Seventh Framework Programme, as the network has now been joined by the US NRC, Canadian Nuclear Laboratories (CNL, formerly AECL) and two South Korean organisations (KINS and KAERI). This book benefits from the scientific consensus reached in this field [4].

Many international collaborative projects have also been set up with the help of the OECD. The work of the OECD Nuclear Energy Agency Committee for the Safety of Nuclear Installations (CSNI) encourages the kick-off and implementation of research programmes intended to reach a consensus regarding scientific and technical issues of joint interest, notably in the field of core melt accidents [5]. Their subjects are chosen as part of its working groups, which identify questions that have not been fully resolved as well as programmes or facilities that could be the subject of international collaborative projects (for example, see reference [6]). Since the OECD does not have its own budget for this type of action, it relies on contributions from participants.

In the field of simulation tools, CSNI has formed expert working groups with the aim of setting up validation matrices; it also organises International Standard Problems (ISPs), which compare the experimental results obtained by teams using different computer software for a given problem, improving the software concerned as a result [7]. Lastly, State-of-the-Art Reports (SOARs) are produced on subjects of joint interest, such as hydrogen distribution, hydrogen combustion and aerosol behaviour. These SOARs provide the widest possible view of a given problem by reviewing current knowledge and the remaining uncertainties, and may recommend areas for further research [5].

1.3.3. Approach

The objective of core melt accident research is to produce and collect scientific information that enables us to improve our understanding and description of the physical phenomena that take place when such an accident occurs. The characteristics of these physical phenomena are generally rarely experienced and studied outside the nuclear field. They involve specific materials whose chemistry and interactions are complex and must be studied under extreme temperature — and sometimes, radioactivity — conditions. In addition, the physics of core melt accidents combine the disciplines of energy with those of material physics, as well as those of aerosol physics and of fission product physics and chemistry. Couplings between elementary phenomena involving different technical or scientific disciplines must also be taken into account. These special characteristics complicate both the experimental approach and the theoretical approach.

The experimental approach is further complicated by a particular difficulty: accurately reproducing all or part of an accident transient can rarely be envisaged, both for questions of scale as well as for various technological reasons including the radioactivity of the materials involved, which can only be used experimentally in small quantities. As it is impossible to perform full-scale testing in this field and reproduce all accident situations, elementary tests (so-called “analytical” experiments) aimed at providing a detailed understanding of the elementary phenomena contributing to the situation under study must be conducted instead, and more general tests must be performed to confirm that nothing has been forgotten, considering the many interactions between the different physical phenomena. All this must be done at scales that are compatible with the facilities’ technical and economic capacities while also maintaining the highest possible level of representativeness, allowing the acquired knowledge to be extrapolated to the full-scale power reactor — often using qualified models.

These characteristics lead us to choose a research approach that combines the following:

- analytical experiments that study the elementary phenomena while limiting the effects of other phenomena as much as possible within a range of parameters that is representative of what can be expected in a core melt accident; the obtained results can be used to develop and qualify the models and determine the associated uncertainties;
- the assembly and coupling of all elementary models within computer codes with predictive capabilities;
- more global experiments intended to simulate as accurately as possible the situations that can be met in a power reactor in an actual accident scenario. These global experiments are used to validate the calculation tools in order to ensure that no important phenomena have been forgotten and the coupling of the phenomena has been modelled correctly. If any unexpected behaviour is noticed, the modelling is reviewed or a new campaign of analytical experiments may even be run. Due to their complexity and their generally high cost, few global tests are performed. As each of the tests involves a set of coupled

phenomena, the results are often difficult to interpret. The **Phebus FP** programme is a notable example of this type of testing, and its lessons are presented in Section 7.3 of this book.

The computer codes contain the knowledge produced by analysing the experimental data. The transposition of the experimental results to the power reactors is therefore based on these codes. Considering the importance of these computer codes, it is essential to assess their ability to correctly describe the accident. This explains the importance attached to physically qualifying the computer codes.

All of the experimental data used (analytical experiments and global experiments) form the experimental basis of the physical qualification of the computer code. Despite the degree of sophistication presently achieved by the computer codes developed in the field of core melt accidents (Chapter 8), these computer tools all still suffer from many uncertainties that must be carefully considered when used in safety studies. These uncertainties are of two main types:

- those resulting from the simplification of the physical models introduced in the calculation software, the representativeness limits of the software experimental qualification base and the lack of precision in the numerical resolution schemes;
- those resulting from the simplification introduced in the simulation tools used to describe an actual facility.

This somewhat theoretical description should enable the reader to form an idea of how core melt accident research operates. The approach described here will be illustrated in Chapter 5 of this book for each of the phenomena involved.

Reference documents

- [1] “**Fukushima, one year later** – Initial analyses of the accident and its consequences” IRSN/DG report 2012-001, www.irsn.fr, 2012.
- [2] N. Rasmussen *et al.*, Reactor Safety Study. An Assessment of Accident Risks in US Commercial Nuclear Power Plants, WASH-1400 (NUREG-75/014), Washington DC, US Nuclear Regulatory Commission, 1975.
- [3] See the US NRC website containing the NUREG reports on core melt accidents: <http://www.nrc.gov/reading-rm/doc-collections/nuregs/>.
- [4] (a) T. Albiol *et al.*, SARNET: Severe accident research network of excellence, *Progress in Nuclear Energy* 52, 2-10, 2010.
(b) B. Schwinges *et al.*, Ranking of severe accident research priorities, *Progress in Nuclear Energy* 52, 11-18, 2010.
(c) W. Klein-Hessling *et al.*, Conclusions on severe accident research priorities, *Annals of Nuclear Energy*, available on-line, <http://dx.doi.org/10.1016/j.anucene.2014.07.015>.

-
- [5] See the OECD/NEA/CSNI website containing the NEA/CSNI reports on core melt accidents: <http://www.oecd-nea.org/nsd/docs/>.
- [6] Nuclear Safety Research in OECD Countries: Support Facilities for Existing and Advanced Reactors (SFEAR), Nuclear Safety, [NEA/CSNI/R\(2007\)6](#), ISBN 978-92-64-99005-0, 2007.
- [7] CSNI International Standard Problems: Brief Description (1975-1999), [NEA/CSNI/R\(2000\)5](#), 2000.

Chapter 2

Design and Operation of a Pressurised Water Reactor

2.1. General information about reactor operation

The nuclei of some isotopes contained in nuclear fuel, such as ^{235}U and ^{239}Pu , can split up (fission) into two¹ smaller fragments called “fission products”. These fragments have large amounts of kinetic energy that is mainly released as kinetic thermal energy in the surrounding fuel material. This release of energy is used to generate electricity in power reactors. Fission into two fragments can either be induced by neutrons (induced fission) or occur spontaneously in the case of heavy isotopes (spontaneous fission). Fission is accompanied by the release of two to three neutrons. Some of these neutrons may in turn initiate other fissions (the principle behind a nuclear chain reaction), be absorbed into the fuel without initiating any nuclear fission, or escape from the fuel.

Neutrons produced by fission from the neutrons of one generation form the neutrons of the next generation. The effective neutron multiplication factor, k , is the average number of neutrons from one fission that cause another fission. The value of k determines how a nuclear chain reaction proceeds:

- where $k < 1$, the system is said to be “subcritical”. The system cannot sustain a chain reaction and ends up dying out;

1. In about 0.4%-0.6% of cases the fission can be into three fission products, this is termed “ternary fission”.

- where $k=1$, the system is “critical”, i.e., as many neutrons are generated as are lost. The reaction is just maintained. This situation leads to a constant power level;
- where $k > 1$, the system is “supercritical”. For every fission there will be an average of k fissions in the next generation. The result is that the number of fissions increases exponentially.

There are in fact two types of supercritical situation: prompt supercriticality and delayed supercriticality. Nearly all fission neutrons are immediately emitted (for example, 99.3% of neutrons are released as 10^{-7} s for ^{235}U); these neutrons are called “prompt neutrons”. However, a small fraction of fission products are de-excited by beta decay (β decay) and subsequently emit what are termed “delayed neutrons”. β decay occurs any time from a few tenths of a second to several tens of seconds after the fission event. The fraction of delayed neutrons is typically less than 1% of all the neutrons generated at any time in a chain reaction. During the interval between $k=1$ and $k = 1/(1 - \beta) \approx 1 + \beta$, supercriticality is referred to as “delayed”; when $k > 1/(1 - \beta) \approx 1 + \beta$, supercriticality is referred to as “prompt”. The value of the fraction of delayed neutrons representing the interval between delayed and prompt supercriticality is defined as a “dollar” and depends on the isotope.

To produce energy, nuclear reactors operate in the region of delayed supercriticality for it is in this region that, thanks to the presence of delayed neutrons, changes in reaction rates occur much more slowly than with prompt neutrons alone. Without delayed neutrons, these changes would occur at speeds much too fast for neutron-absorbing systems to control.

The order of magnitude commonly used to express system departure from criticality is known as “reactivity” ρ , $\rho = 1 - 1/k$. Positive ρ values correspond to supercritical states and negative values correspond to subcritical states.

Chain reactions in nuclear reactors must be controlled, i.e., zero or negative reactivity must be maintained with the aid of neutron-absorbing elements. In pressurised water reactors, these elements are either placed inside mobile devices called control rods (containing chemical elements such as cadmium and boron) or dissolved in the cooling water (boron).

In some low-probability accidents, the reactivity of the reactor may reach high positive values that cause the chain reaction to become supercritical. If the measures taken are insufficient to bring the reactor back to a safe condition, such accidents could lead to an uncontrollable power increase that could result in severe reactor damage like that which occurred during the [Chernobyl](#) accident (Section 7.2).

The reactivity of a reactor is affected primarily by the temperature of both the fuel and the coolant and by the coolant void fraction. The influence of each of these parameters is characterised by a reactivity coefficient, which is the derivative of the reactivity with respect to the parameter considered. In the case of fuel, an increase in power results in an increase in fuel temperature and an increase in neutron capture by ^{238}U . The reactivity coefficient, called the temperature coefficient or the Doppler coefficient, is therefore negative. In the case of coolant, the reactivity coefficient is related

to changes in the coolant density (temperature coefficient) or void fraction (void coefficient). These coefficients are negative in pressurised water reactors² to ensure reactor stability and limit the maximum power that could be reached during an accident.

Some fission products formed are radioactive. This radioactivity results in, even after the chain reaction stops, energy being released in the form of heat (called “decay heat”). This heat decreases over time and, one hour after reactor shutdown, amounts to approx. 1.5% of its level during operation³.

The energy released by fissions and fission products must be continuously removed to avoid an excessive rise in reactor temperature. In pressurised water reactors, this energy is removed during normal conditions by three successive loops whose main purpose is to prevent the radioactive water exiting the core from leaving the plant (Figure 2.3):

- the first loop is the reactor coolant system (RCS). It cools the core by circulating water at an average temperature of around 300 °C and a pressure of 155 bar;
- the secondary loop extracts the heat from the RCS by means of steam generators, which supply steam to the turbine generator to produce electricity;
- the tertiary system consists of a condenser and rejects the remaining heat to a river or the sea or to the atmosphere by means of cooling towers.

This brief description of the operation of a nuclear reactor identifies the basic safety functions that must be ensured at all times:

- reactivity control;
- heat removal;
- containment of fission products and, more generally, radioactivity (some activation products in the RCS⁴ are also radioactive).

2.2. The pressurised water reactors in France’s nuclear power plant fleet

Various types of nuclear reactor are used to generate electricity in France. They use different fissile materials (natural uranium, uranium enriched in uranium-235, plutonium, etc.) and different neutron moderators (graphite, water, heavy water, etc.)⁵. They

2. Water is used as the moderator in pressurised-water reactors. It decelerates neutrons produced by fission (these neutrons lose their kinetic energy by colliding with the nuclei of the water’s hydrogen atoms) and increases fission product yields. As the temperature inside the reactor core increases, the water expands. This reduces the water’s ability to slow down neutrons and results in fewer fission reactions. The temperature coefficient of the water is thus negative.
3. One hour after reactor shutdown, a 900 MWe reactor generates 40 MW of heat and a 1300 MWe reactor generates 58 MW of heat. One day after shutdown, this heat output drops to 16 MW for a 900 MWe reactor and 24 MW for a 1300 MWe reactor.
4. Radioactive substances may be formed under irradiation by activation of the metal components in the RCS and be entrained into the reactor coolant by corrosion mechanisms.
5. The moderator reduces the velocity of the neutrons, thereby increasing their likelihood of producing a fission reaction.

are also characterised by the type of coolant (ordinary water in liquid or vapour form, heavy water, gas, sodium, etc.) used to remove heat from the core (where fission reactions occur) and transfer it either to the loops supplying the turbine generators or to the turbine generators directly.

The nuclear power plants currently in operation in France use enriched uranium in oxide form that may be mixed with plutonium oxide recovered from the reprocessing of spent fuel. They use ordinary water as the heat-transfer fluid. This water is maintained under high pressure (155 bar) so that it remains in liquid form at its operating temperature (300 °C). They are known as pressurised water reactors (PWRs) and belong to what is commonly known as the second generation of nuclear power reactors⁶.

A distinctive feature of France's reactor fleet is its standardisation. The technical similarity of many of the country's reactors justifies the generic overview given in this chapter. The 19 nuclear power plants in operation in France have two to six PWRs, giving a total of 58 reactors. This reactor fleet consists of three series: the 900 MWe series, the 1300 MWe series, and the 1450 MWe (or N4) series (Figure 2.1).

The thirty-four 900 MWe reactors are split into two main types:

- CP0, which consists of the two reactors at Fessenheim and the four reactors at Bugey;
- CPY (consisting of types CP1 and CP2), which encompasses the 28 other reactors (four reactors at Blayais, four at Dampierre, six at Gravelines, four at Tricastin, four at Chinon, four at Cruas-Meysses and two at Saint-Laurent-des-Eaux).

The twenty 1300 MWe reactors are split into two main types:

- the P4, which consists of eight reactors: two at Flamanville, four at Paluel and two at Saint-Alban;
- the P'4, which consists of 12 reactors: two at Belleville-sur-Loire, four at Cattenom, two at Golfech, two at Nogent-sur-Seine and two at Penly.

Lastly, the N4 series consists of four 1450 MWe reactors: two at the Chooz nuclear power plant and two at the Civaux nuclear power plant.

Despite the deliberate standardisation of France's fleet of nuclear power reactors, technological innovations have been introduced during the design and construction of each plant. The creation of France's fleet occurred in four main stages:

- the CP0 900 MWe "preproduction" series was brought into operation between 1977 and 1979;
- the CPY 900 MWe series was brought into operation between 1980 and 1987;

6. Reactors built before the 1970s make up the first generation. The Generation-I reactors in France were graphite moderated, cooled by carbon dioxide, and fuelled with natural uranium metal. They were a type of gas-cooled reactor (GCR).

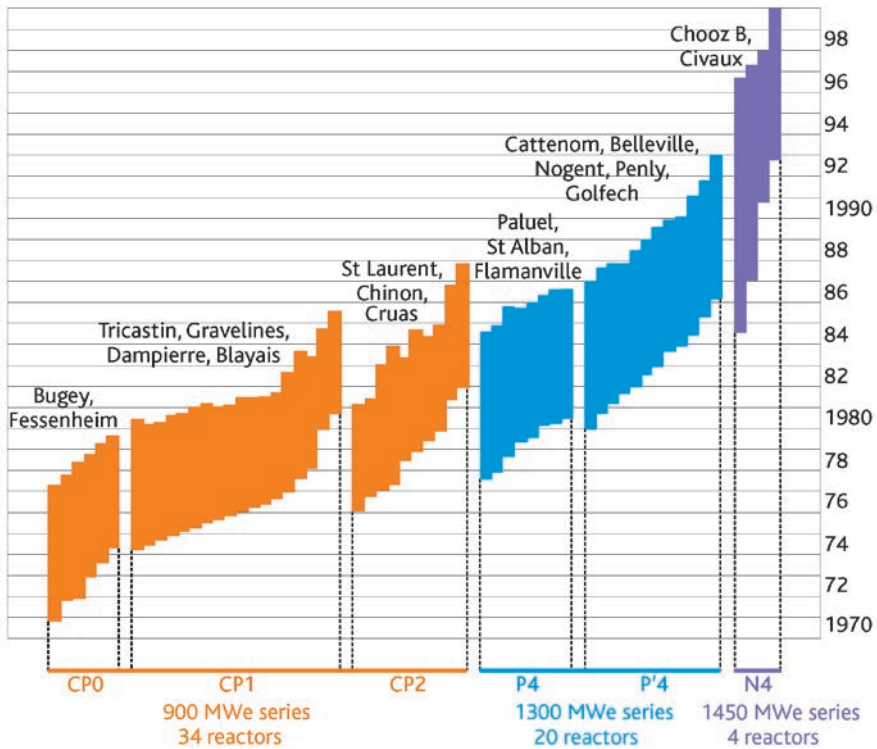


Figure 2.1. Construction periods and distribution of the three series of 900, 1300 and 1450 MWe power reactors in operation in France in 2015.

- the P4 and P'4 1300 MWe series were brought into operation between 1984 and 1993;
- the 1450 MWe (or N4) series was brought into operation between 2000 and 2002.

The CPY reactors benefited from the feedback obtained from the design studies, construction and operation of the CP0 reactors. Unlike the design studies for the CP0 series, which were conducted separately for each site, the design studies for the CPY series were conducted for all the sites. As a result, the CPY series differs from the CP0 series in terms of building design (in particular, the containment building was modified to facilitate operations), siting of the engineered safety systems (which were modified to increase the independence of the systems' trains and increase their reliability) and more flexible reactor control (particularly via the use of control rods and the addition of control rods with less neutron-absorbing capacities⁷). In the case of the CP2 reactors, the orientation of the

7. The control-rod clusters are made up of 24 rods. There are two types of control-rod cluster, "black" and "grey". Black clusters have 24 neutron-absorbing rods (consisting of a silver, indium and cadmium alloy (Ag-In-Cd) or boron carbide [B₄C]). Grey clusters consist of rods made of materials with varying degrees of absorbcency (e.g., only eight Ag-In-Cd or B₄C absorbing rods and 18 rods made of steel, which is more transparent to neutrons). Moving these clusters at different rates in the core makes it possible to optimise the spatial power distribution, control changes in reactor power and adjust the mean temperature of the reactor coolant.

control room was shifted by 90 degrees to prevent projectiles generated by rupture of the turbine generator from damaging the reactor containment vessel (Figure 2.2).

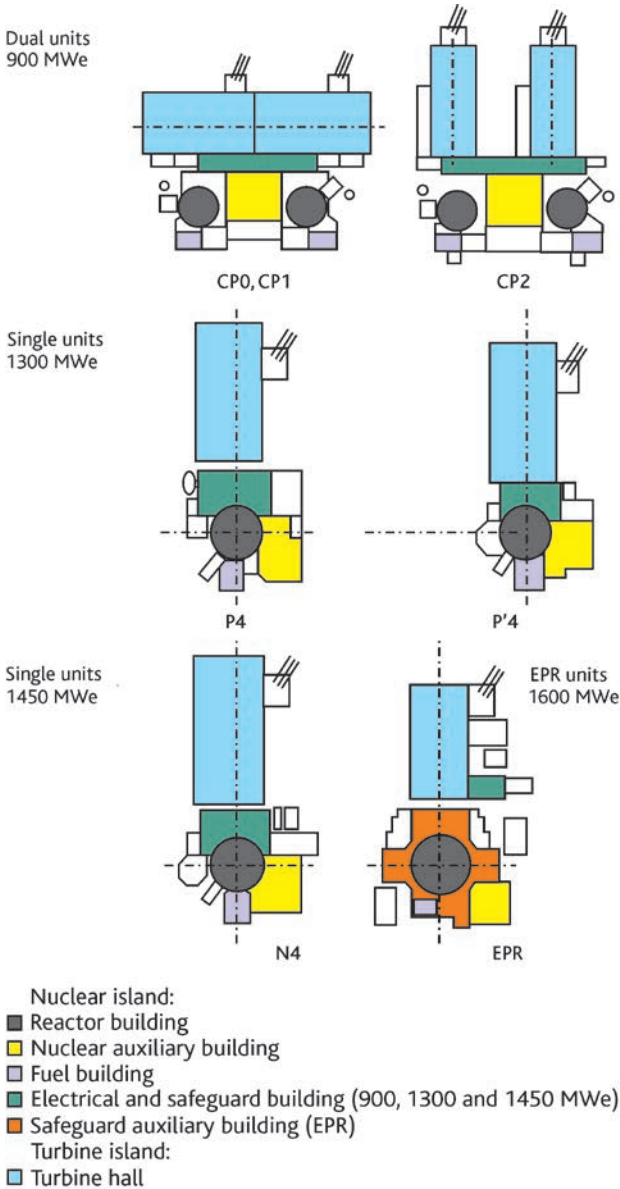


Figure 2.2. Schematic plant layout showing the buildings of the different reactor series in operation in France.

The 1300 MWe reactors differ from the 900 MWe reactors in terms of the design of their core, loops and reactor protection system as well as their buildings. The increase

in power was achieved by increasing the size of the reactor. In order to remove the increased heat (from 900 to 1300 MWe), the cooling capacity of the RCS was increased by the installation of an additional cooling loop (thus changing the number of loops from three for the 900 MWe reactors to four for the 1300 MWe reactors) (Figure 2.3). The components of each RCS are also larger than those of the preceding series. In terms of the locations of the buildings, the new series are single-unit plants, whereas the preceding series were dual-unit plants (Figure 2.2). The engineered safety systems and auxiliary systems are located in buildings specific to each unit so as to improve the safety of their operation. In addition, each containment vessel has a double concrete wall (an inner wall of prestressed concrete and an outer wall of reinforced concrete) instead of the single wall of steel-lined prestressed concrete on the 900 MWe reactors. New microprocessor-based instrumentation and control technologies using programmable memory are used. The P'4 series differs from the P4 series in that the installation of the buildings and structures was optimised with the primary goal of reducing costs. The result is a denser plant layout and smaller buildings and structures.

Lastly, the main differences between the 1450 MWe reactors and those of the preceding series are the larger reactor core, smaller steam generators (SG) that delivery steam at higher pressure, the design of the reactor coolant pump (higher flow rate) and the computerised control system.

The next generation of reactor that EDF is planning to put into service in France will consist of a design known as the European Pressurised Water Reactor, or EPR). A reactor with a power output of around 1600 MWe is currently under construction at EDF's Flamanville site, on France's Cotentin Peninsula on the English Channel. These new PWRs incorporate evolutionary improvements over earlier designs. They therefore benefit from extensive operating experience feedback from the current fleet and meet more stringent safety objectives. They also benefit research findings, particularly regarding core melt accidents, which were factored in right from the design phase. Their main differences with the Generation-II PWRs are the design of the loops, the reactor protection system and the site buildings (particularly the containment), which offer a higher degree of protection in the event of an accident.

The design of the RCS and the main components and the configuration of the loops are quite similar to those of the N4 series. The main evolutionary improvements are as follows:

- increase in the volumes of primary and secondary water (particularly in the steam generators) to increase the thermal inertia of the reactor;
- organisation of the engineered safety systems and the support systems (safety injection system [SIS], steam generator emergency feedwater system [EFWS], component cooling-water system [CCWS], essential service-water system [ESWS], emergency power supplies [EPS]) into four independent trains located in physically separate rooms. This physical separation ensures that the engineered safety systems remain available in the event of an internal or external hazard (e.g., fire, earthquake or flood).

Regarding the containment, in addition to the reinforcement of its structure (more specifically the outer concrete wall, see Section 2.3.2.3), the following changes have been made in relation to those of the N4 series:

- placement of the borated-water storage tank inside the containment, hence the name “in-containment refuelling water storage tank” (IRWST). The IRWST feeds the safety injection system and the containment heat-removal system (CHRS);
- installation of a system for containing and cooling molten corium inside a special compartment in the event of a vessel melt-through during a core melt accident. The purpose of this system is to provide long-term protection of the basemat from erosion should such an accident occur;
- installation of a steel liner on the inner wall of the double-wall containment.

Another notable difference with the N4 series is that more rooms are protected by the reinforced-concrete outer wall (airplane crash [APC] shell). In addition to the reactor building, the fuel building and two of the rooms housing the engineered safety systems are covered by the outer concrete wall.

The layout of the buildings (Figure 2.2) was changed so that the four independent trains of the engineered safety systems and support systems could be housed in separate rooms and thus prevent leaks being released directly into the environment from the containment. All the containment penetrations lead into buildings located around the reactor building and equipped with ventilation and filtration systems.

To provide the reader with the information needed to understand the concepts presented in this document, the rest of this chapter provides a relatively generic, summary overview of the main components of the reactors in operation in France and of how these reactors function under normal and accident conditions. The specific features of the EPR are described whenever they relate to core melt accidents.

2.3. Description of a pressurised water reactor and its main loops

2.3.1. Facility overview

Each reactor comprises a nuclear island, a turbine island, water intake and discharge structures and, in some cases, a cooling tower (Figures 2.2 and 2.3).

The main parts of the nuclear island are:

- the reactor building (RB), which contains the reactor and all the pressurised coolant loops as well as part of the loops and systems required for reactor operation and safety (Figures 2.3, 2.6 and 2.7);
- the fuel building (FB), which houses the facilities for storing and handling new fuel (pending its loading into the reactor) and spent fuel (pending its transfer to reprocessing plants). The fuel building also contains the equipment in the

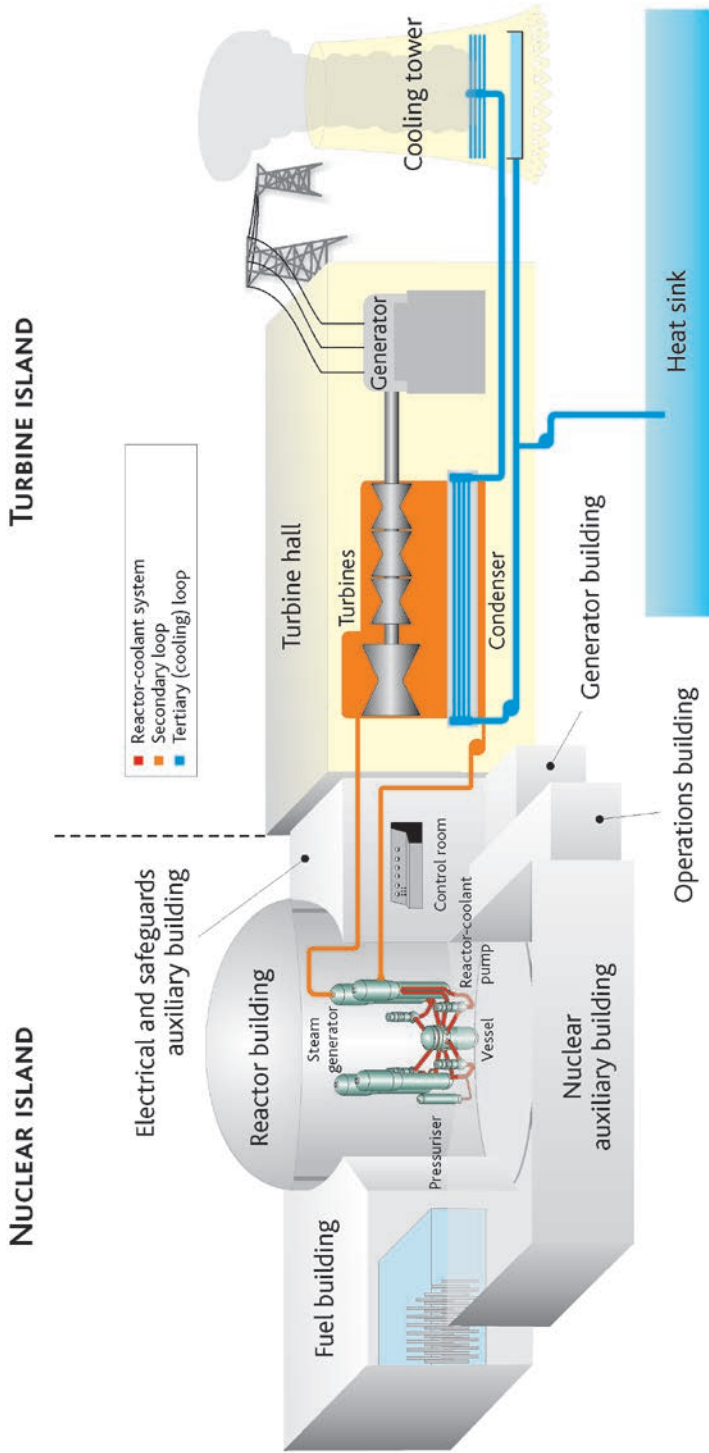


Figure 2.3. Schematic diagram of a PWR (1300 MWe or N4) and its main loops.

fuel pool cooling and purification system (FPCPS) and, for units in operation, the equipment in the steam generator emergency feedwater system (EFWS). The EPR itself has four independent steam generator emergency feedwater trains. Each train is located in one of the four divisions of the safeguard auxiliary building;

- a safeguard auxiliary building (SAB) with electrical equipment rooms. The main engineered safety systems are located in the SAB's bottom half and the electrical equipment rooms are located in its top half. These two halves do not communicate with each other. The rooms in the SAB contain equipment, particularly that of the safety injection system (SIS), the containment spray system (CSS), the component cooling water system (CCWS) and ventilation equipment. The electrical equipment rooms contain all the means for controlling the unit (the control room and operations facilities, electric power supplies, and the instrumentation and control [I&C] system). Note that, in the case of the 900 MWe series, there is only one SAB with electrical equipment rooms for two adjoining units. In the case of the 1300 MWe and N4 series, there is only one building per unit. The EPR has four independent engineered safety systems. Each is located, with its support systems, in a room that is physically separate from the others. These rooms are known as the "divisions" of the SAB. Divisions 2 and 3 of the SAB are protected by the reinforced-concrete outer wall. The control room is located in division 3 of the SAB;
- a nuclear auxiliary building (NAB) housing the auxiliary systems required for normal reactor operation. This building houses the equipment of the chemical and volume control system (CVCS), the gaseous waste processing system, the reactor coolant effluent processing system and the boron recycle system;
- two geographically separate buildings, each housing a diesel generator (emergency power supply). In the case of the EPR, the offsite emergency power supplies consist of two sets of four diesel generators (each set being housed in its own building) and two station blackout (SBO) generators;
- an operations building.

The turbine-island equipment converts the steam generated by the nuclear island into electricity and supplies this electricity to the transmission system. The main parts of the turbine island are:

- the turbine hall, which houses the turbine generator (it receives the steam generated by the nuclear island and converts it into electricity) and its auxiliary systems;
- a pump house to cool the facility under normal operating conditions and provide emergency cooling with the related hydraulic structures;
- a cooling tower in the case of closed-loop cooling.

Some of these items of equipment contribute to reactor safety. The secondary loops are the interface between the nuclear island and the turbine island.

2.3.2. Description of the main components of a PWR

2.3.2.1. Reactor core

The reactor core is made up of fuel assemblies (Figure 2.4). Each assembly consists of 264 fuel rods (Figure 2.4, left), 24 tubes to contain the rods of a control rod cluster and a guide tube. All are arranged in a 17×17 square lattice (Figure 2.4, right). The fuel rods are made up of zirconium alloy tubes also known as “cladding” (zirconium has low neutron-absorbing properties and good corrosion resistance). Zircaloy, which contains 98% zirconium, is the alloy most frequently used in France’s PWRs. The cladding, which is 0.6 mm thick and 9.5 mm in diameter, is held in place by Zircaloy grids. Pellets made of uranium dioxide (UO_2) or a mixture of uranium and plutonium oxides ($(\text{U,Pu})\text{O}_2$, commonly referred to as MOX fuel) and measuring 8.2 mm in diameter are stacked inside the rods. These pellets make up the nuclear fuel. The level of ^{235}U enrichment varies

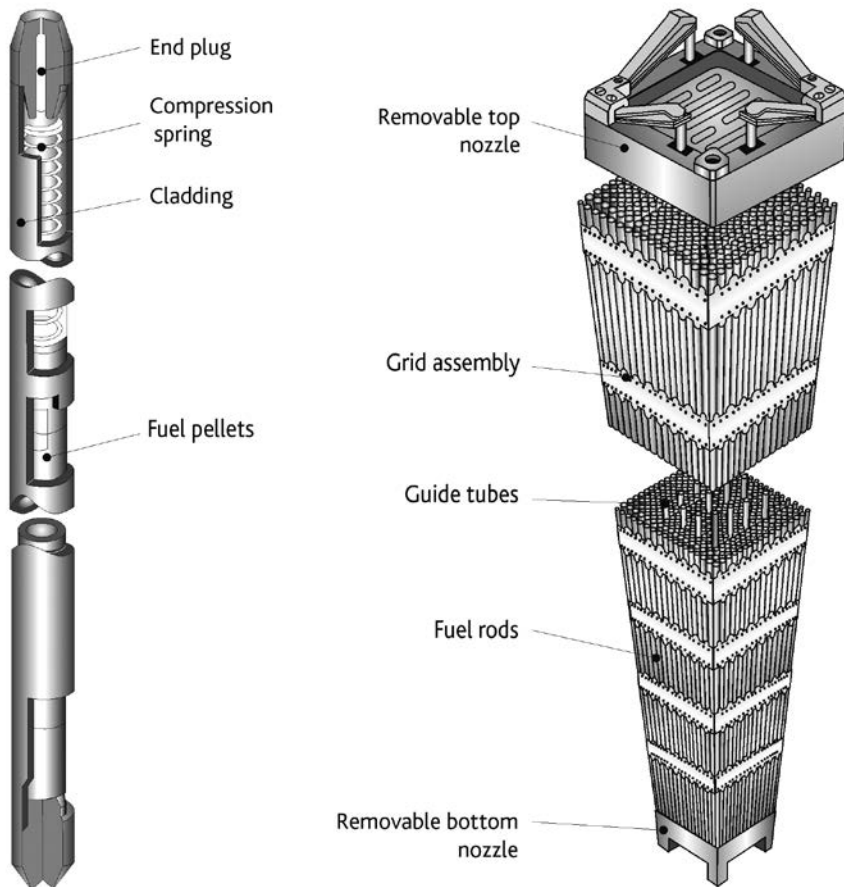


Figure 2.4. Diagram of a fuel rod (left) and of the main components of a fuel assembly (right).

between 3% and 4.5% depending on the method of fuel management⁸. The fuel assemblies are similar for all the series. Only their lengths change. One-third to one-fourth of the fuel is replenished once every 12 to 18 months during reactor outages.

The main characteristics of the fuel and the core are given for each series in Table 2.1.

Table 2.1. Characteristics of the cores of each series.

Series	900 MWe	1300 MWe	1450 MWe	EPR
Number of fuel assemblies	157	193	205	241
Total height of the fuel pellets in each assembly rod (m)	3.66	4.27	4.27	4.20
Number of control rod clusters Absorbing material	57 Ag-In-Cd	65 Ag-In-Cd + B ₄ C	73 Ag-In-Cd + B ₄ C	89 Ag-In-Cd + B ₄ C
Mass of enriched uranium (t)	72.5	104	110.5	144.2

The core is located inside a vessel made of 16MND5 low-carbon steel fitted with an upper head that is removed for refuelling purposes (Figure 2.5). Inside the vessel are

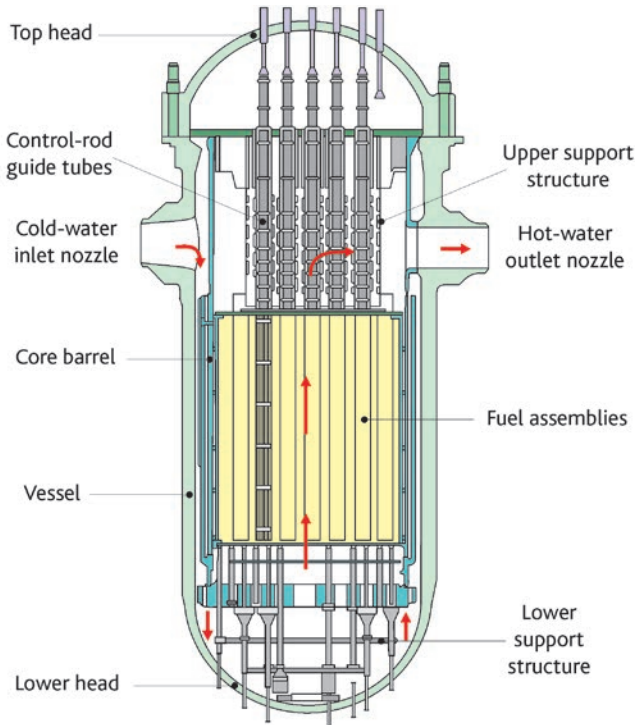


Figure 2.5. Cutaway of the PWR vessel at Fessenheim.

8. During reactor operation, the amount of fissile material in the fuel diminishes, requiring the spent fuel rods to be replaced by new assemblies. The method of managing this replacement depends on the initial enrichment of fissile material within the fuel.

metal structures (known as internals) that can be completely removed to facilitate periodic inspections:

- the lower structures support the core;
- the side structures (core barrel) separate the cold fluid entering the vessel from the hot fluid exiting the core;
- the upper structures are made up of the control rod guide tubes.

The dimensions of the vessels of each series are given in Table 2.2.

Table 2.2. Dimensions of the vessels of each series.

Series	900 MWe	1300 MWe	1450 MWe	EPR
Inside diameter (m)	4.00	4.39	4.486	4.885
Height (m)	12.3	13.6	13.645	13.105
Cladding thickness at core level (m)	0.20	0.22	0.225	0.25

2.3.2.2. Reactor coolant system and secondary loops

The reactor coolant system (RCS) carries heat away from the reactor core by circulating pressurised water (known as reactor coolant) through the heat transport loops (there are three for a 900 MWe reactor, four for a 1300 MWe reactor, a 1450 MWe reactor or an EPR). Each loop is connected to the reactor vessel, which contains the core, and is equipped with a reactor coolant pump (RCP). This pump circulates the coolant heated through contact with the fuel elements to heat exchangers, called steam generators, where the coolant transfers its heat to the secondary loops and flows back to the reactor (Figures 2.3 and 2.6). The RCPs are fitted with seals that are continuously cooled by pressurised water to prevent reactor coolant from leaking outside the RCS.

The steam generators are evaporators composed of a bundle of U-tubes and a secondary side with integral moisture-separation equipment. The reactor coolant enters the inverted U-tubes and heats the secondary-side water, which flows in through a nozzle located above the tube bundle. The steam generated rises through the moisture separators and exits through the top of the steam generator.

A tank, called a pressuriser, allows the coolant to expand and maintains the RCS pressure at 155 bar so that the coolant (heated to over 300 °C) remains in liquid form. The reactors in operation have three letdown lines, each of which has an isolation valve and a safety valve. In particular, these valves enable emergency blowdown of the RCS to prevent high-pressure core melt.

The upper section of the EPR pressuriser has three letdown lines, each of which has a pilot valve fitted with a position sensor. The EPR also has an emergency RCS blowdown system consisting of a set of motor-operated valves that are actuated to avert high-pressure core melt. This system consists of two parallel letdown lines connected to the same nozzle at the top of the pressuriser. Each line is fitted with two motor-operated

valves and is connected to a shared letdown line that leads to the pressuriser relief tank. This system is described in Section 4.3.4.

The normal operating conditions of the RCS for each series are given in Table 2.3.

For each unit, the RCS is completely located inside the containment.

Table 2.3. Normal operating conditions of the RCS for each series.

Series	900 MWe	1300 MWe	1450 MWe	EPR
Number of loops	3	4	4	4
Nominal absolute RC pressure (bar)	155	155	155	155
Nominal flow rate (m ³ /h)	21,250	23,325	24,500	27,195
RCS volume, pressuriser included (m ³)	271	399	406	460
Nominal temperature of the water at the vessel inlet (°C)	286	293	292	296
Nominal temperature of the water at the vessel outlet (°C)	323	329	330	330

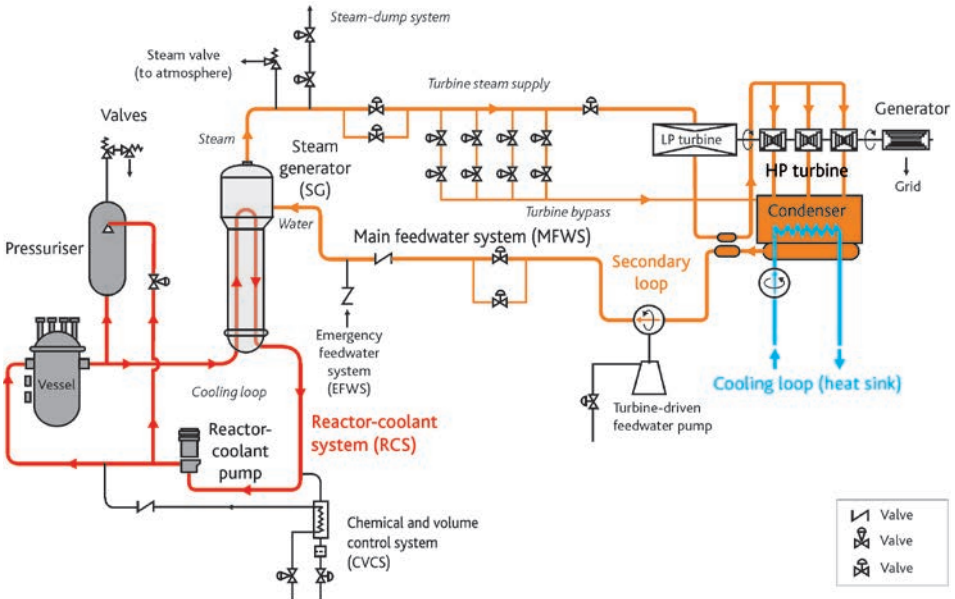


Figure 2.6. Schematic diagram of the main components of the RCS and the secondary loops.

During normal operation, the secondary loops convert the thermal energy produced by the core into electrical energy. To prevent radioactive coolant from leaving the containment, the secondary loops are separated from the RCS by the pipes of the steam generators. The reactor coolant flows through these pipes, where its heat is transferred

to the water in the secondary loops. This water is vaporised then expands in the steam turbine connected to the generator (Figure 2.6). The steam is generated in these loops at a pressure of 58 bar absolute (900 MWe reactors), 65 bar absolute (1300 MWe reactors), 73 bar absolute (1450 MWe reactors) or 77 bar absolute (EPR). It exits the turbine and flows into a condenser that is cooled by water from a river or sea. In some instances, the water is cooled by contact with air inside a cooling tower.

The upper sections of the steam generators are connected to the turbine's steam chest *via* three or four lines⁹ (one per steam generator) (Figure 2.6). Each line has:

- a flow restrictor inside the outlet pipe of the steam generator;
- a steam dump system equipped with an isolation valve and a control valve;
- seven (two for the N4 series and the EPR) safety valves with steam dump pipes;
- an isolation valve that closes in a matter of seconds.

The flow restrictor slows down the rate of cooling and depressurisation of the secondary loop and reduces the forces exerted on the tube bundle in the event of a steam line break. The valves protect the loop against overpressure if the steam can no longer be dumped. The bypass is used to temporarily send steam directly to the condenser without passing through the turbine or activating the valves. It is used especially to remove heat from the core during startup, hot shutdown or cold shutdown of the reactor and until the residual heat removal system (RHRS) is turned on (Figure 2.7). The steam dump system discharges the residual heat, thus cooling the reactor core if it can no longer be cooled by the normal systems, and avoids having to open the safety valves in the event of rupture of one or more steam generator lines. This system consists of one line per steam generator for the 900 and 1300 MWe series, two lines per steam generator for the N4 series, and only one line for the EPR. Each line has a dump valve and an isolation valve.

The characteristics of the secondary loops are given for each series in Table 2.4.

Table 2.4. Characteristics of the secondary loops for each series.

Series	900 MWe	1300 MWe	1450 MWe	EPR
Number of steam generators (SG)	3	4	4	4
Secondary-side steam pressure at the SG outlet (bar absolute)	58	65	73	77
Heat-transfer area in an SG (m ²)	4746	6940	7308	7960
Steam flow rate (t/h) per SG	1820	1909	2164	2197
Steam temperature at the SG outlet (°C)	273	281	288	293

9. In the EPRs, each of the four lines is located in a separate room.

2.3.2.3. Containment

The containment is made up of the reactor building, which houses the RCS, a portion of the secondary loops (including the steam generators), and a number of auxiliary operating and safety systems. The reactor building is a concrete cylinder topped by a concrete dome. It forms a strong barrier that offers the specified level of integrity (see Chapter 6 for more details), prevents radioactive substances from escaping into the outside environment, and protects the reactor from external hazards. The reactor buildings of PWRs currently in operation are designed to withstand the pressure (4 to 5 bar absolute) expected during a loss-of-coolant accident (LOCA with a double-ended guillotine break of a main coolant pipe) or rupture of a steam line inside the containment. They ensure a satisfactory level of integrity should either situation occur. The containment of the EPR is designed to withstand a higher pressure of approx. 6.5 bar absolute.

Whatever the reactor type, the concrete walls of the containment rest on a foundation, or basemat, which is also made of concrete. The walls are topped by a concrete dome that forms the roof of the building. The reactor building is designed to withstand the effects of a seismic margin earthquake (SME) (the magnitude of the SME is determined based on the magnitudes of the maximum historically probable earthquakes [MHPE] and by taking into account a safety margin that covers uncertainties, amongst other aspects) and environmental hazards (extreme weather conditions, aircraft crashes, explosions, etc.).

The reactor building penetrations are distinctive points of the containment. Pipes, electrical wiring and ventilation ducts are routed through orifices in the containment walls. There are also access hatches, or locks, for personnel and large items of equipment. Lastly, there is a canal, or pipe, for transferring fuel assemblies between the reactor building and the fuel building. Some water and steam pipes, particularly the portions of the secondary loops inside the reactor building and the outer portions leading to the isolation valves, are an extension of the containment. The secondary shell of the steam generators and the tube bundles on the primary side are also an extension of the containment.

All these penetrations have a specified level of integrity (see Chapter 6 for more details). With the exception of the water and steam penetrations on the secondary loops, these penetrations are fitted with isolation devices located inside the containment. These isolation devices, which are closed before or during an accident, are located on the fluid inlets and outlets. The isolation valves for the water and steam penetrations on the secondary loops are located inside the containment and after the safety valves (see the description of the secondary loops in the preceding section).

Before the reactor is first brought online, the containment is inspected and tested to determine its overall integrity and its resistance to forces under normal and accident conditions. All these aspects are explained in Chapter 6 of this document.

Internal components (known as internals) support equipment, provide biological shielding of personnel, and physically separate the loops (particularly the coolant loops) and some items of equipment.

Table 2.5. Characteristics of the containments of each series.

Series	900 MWe	1300 MWe P4	1300 MWe P'4	N4	EPR
Total volume (m ³)	60,000	98,000	83,700	86,000	102,700
Free volume (m ³)	50,400	82,000	70,500	73,000	75,500
Overall height above ground level (m)	51.3 (FES)* 52.9 (BUG)* 56.6 (CPY)	71.9	61.8	63.2	62.2
Inside diameter of the cylindrical portion (m)	37	45.00 (inner wall) 50.80 (outer wall)	43.80 (inner wall) 49.80 (outer wall)	43.80 (inner wall) 49.80 (outer wall)	48.00 (inner wall) 53.00 (outer wall)
Standard thickness of the cylindrical portion (m)	0.85 (CP0) 0.90 (CPY)	0.90 (inner wall) 0.55 (outer wall)	1.20 (inner wall) 0.55 (outer wall)	1.20 (inner wall) 0.55 (outer wall)	1.30 (inner wall) 1.30 (outer wall)
Height above ground level of the cylindrical portion (m)	41	54.15 (inner wall) 55.04 (outer wall)	46.60 (inner wall) 51.15 (outer wall)	51.00 (inner wall) 55.55 (outer wall)	43.90 (inner wall) 46.60 (outer wall)
Standard thickness of the dome (m)	0.75 (CP0) 0.80 (CPY)	0.87 (inner wall) 0.40 (outer wall)	0.82 (inner wall) 0.40 (outer wall)	0.82 (inner wall) 0.40 (outer wall)	1.00 (inner wall) 1.80 (outer wall)
Steel liner thickness (mm)	6	no liner	no liner	no liner	6

* FES = Fessenheim; BUG = Bugey.

With the exception of EPRs¹⁰, the containments of France's reactors are fitted with a decompression and filtration system (also known as a filtered venting system) to prevent sudden containment failure in the event of a slow rise in the internal pressure during a core melt accident. To reduce the release of radioactive substances, the steam inside the containment is sent through this system to a system fitted a metal prefilter with a sand bed to trap most of the radioactive aerosols. This system is opened according to a specific procedure, known as U5 (see Section 2.5.2.1).

► Description of the containment walls

The 900 MWe reactor containments consist of a single wall of prestressed reinforced concrete that is lined on the inside with steel plate (known as the liner). The purpose of the steel liner is to act as a leaktight barrier, including during an accident. The purpose of the concrete containment is to withstand pressures and temperatures during an accident, seismic loads and external hazards.

10. In its opinion 2012-AV-0139 of 3 January 2012 concerning the complementary safety assessments of the priority nuclear facilities in the light of the accident at the Fukushima-Daiichi nuclear power plant, ASN recommends that "EDF will have to identify the existing or additional systems to be included in the EPR's "hardened safety core", in particular to control the pressure inside the containment in the event of a severe accident." This recommendation may result in a reconsideration of the installation of a filtered venting system on reactors of this type.

The containments of the 1300 MWe and 1450 MWe reactors have two walls:

- an inner wall made of unlined prestressed concrete and designed to withstand pressures and temperatures resulting from an accident and participate in ensuring a degree of leak tightness;
- an outer wall of reinforced concrete. Leakage from the inner wall is collected in the space between the inner and outer walls, or annulus. The annulus is maintained at negative pressure by the annulus ventilation system (AVS) so that any leaks from the inner wall and the penetrations can be collected and filtered before their release. The outer wall also protects the reactor from external hazards (extreme weather conditions, aircraft crashes, explosions, etc.).

Like the containments of the 1300 MWe and 1450 MWe reactors, the containment of the EPR (Flamanville 3) has two walls with a dynamic containment system. Furthermore, the inner wall of the containment is lined with steel plate, which ensures most of the integrity. The reinforced-concrete outer wall on the EPR has been made stronger than that of the preceding generation so that, in the event of a severe accident, it will withstand hydrogen explosions, meet requirements for no direct radioactive leaks to the environment, and consolidate its protection against external hazards.

► Description of the containment basemat

The reactor building sits on a prestressed-concrete slab, or basemat. This basemat forms the foundation of the containment's concrete walls and internal structures and confines the bottom half of the building. The configuration of the basemat varies with each site and is designed according to the seismic and geotechnical characteristics of each site. The thickness of the basemat also varies with each site. It is 1.5 m thick at Fessenheim, 2.25 m at Bugey, approx. 4 m for the CPY units, 3 m for the P4 units, 2.8 m for the P'4 units, approx. 3 m for the N4 units, and approx. 4 m for EPRs.

The basemat has access galleries for stretching the prestressing tendons, a drainage system and, where necessary, measuring systems.

The basemat under the EPR is also fitted with a core catcher, a system for containing and cooling molten corium in the event of vessel melt-through during a core melt accident. This system is described in detail in Section 4.3.4 of this document (see also Figure 4.7).

► Description of the reactor pit

The reactor pit is bordered by a cylindrical concrete hoop around the reactor vessel. The bottom has an opening to allow access inside the reactor pit (this opening is closed when the reactor is operating). The void between the vessel and the concrete of the reactor pit is occupied mainly by the vessel insulation. The reactor pit supports the reactor building's internal structures and rests on the containment basemat (Table 2.6).

Table 2.6. Characteristics of the reactor pits of each series.

Series	900 MWe	1300 MWe P4	1300 MWe P'4	1450 MWe N4	EPR
Inside diameter (m)	5.20	5.85	5.26	5.56	6.15
Thickness (m)	1.80 to 2.10	2.00	2.00	2.00	2.70

Chases at the top accommodate the neutron flux measurement systems and shafts accommodate the reactor coolant piping (hot legs and cold legs).

The role of the reactor pit is to support the reactor vessel as well as shield workers from ionising radiation during work on the RCS and adjacent equipment during operation of the reactor.

The reactor pit of the 900, 1300 and 1450 MWe reactors may contain water, particularly after an accident with RCS break. The water in the pit may also come from the CSS (Section 2.3.2.4).

The reactor pit of the EPR is designed to prevent molten corium from spreading into the containment after a vessel melt-through during a core melt accident. The aim of this system is to eliminate the risk of direct heating of the containment (Section 5.2.1). It is also designed to remain dry to prevent potential steam explosions from a corium-water interaction in the event of vessel melt-through (Section 5.2.3) and allow molten corium to flow to the core catcher (Section 5.4.3). The consideration of core melt accidents in the design of the EPRs is explained in detail in Section 4.3.4.

2.3.2.4. The main auxiliary systems and engineered safety systems

During normal operation, shutdown or restart of the reactor, the auxiliary systems contribute to fulfilling the basic safety functions (reactivity control, removal of heat from the RCS and of residual heat, containment of radioactive materials; see Section 2.1). The two main auxiliary systems are the chemical and volume control system (CVCS) and the residual heat removal system (RHRS). They are schematically illustrated in Figure 2.7, which relates to reactors in operation (EPRs excluded).

During reactor operation, the CVCS is used to adjust the boron concentration in the reactor coolant by drawing in demineralised or borated water during reactor power changes. It is also used to adjust the water inventory in the RCS during temperature variations. The CVCS is also used to maintain the chemistry of the reactor coolant by adding chemicals (e.g., corrosion inhibitors) to reduce its concentration of corrosion products. This system has one or more water letdown lines leading from the RCS, a boric-acid tank, a purification unit, and one or more charging lines for reinjecting water into the RCS. Lastly, it continuously supplies water to the seals of the RCPs to ensure their integrity.

During normal reactor shutdown, the functions of the RHRS are to remove the residual heat generated by the fuel in the vessel and maintain the reactor coolant at a moderate temperature while fuel remains in the core. When the chain reaction stops,

the reactor core continues to produce heat. This heat must be removed, otherwise the fuel may become severely damaged. The RHRS, which has two motor-driven circulation pumps, collects water from a primary loop at the reactor outlet, transfers it to heat exchangers, and sends it back into another primary loop at the reactor inlet. The heat exchangers are cooled by the component cooling water system (CCWS), which is cooled by the essential service-water system (ESWS).

In the case of the EPR, residual-heat removal (RHR) is carried out by the low-head safety injection system (LHSI). The EPR therefore has four separate, independent RHR trains.

The function of the engineered safety systems is to control accident situations and mitigate their consequences. They consist primarily of the safety injection system (SIS), the containment spray system (CSS) for the reactors in operation (EPRs excluded), and the steam generator emergency feedwater system (EFWS). These systems are schematically illustrated in Figure 2.7, which relates to non-EPR reactors.

In the event of a loss-of-coolant accident (LOCA), the SIS is used to inject borated water into the reactor core in order to halt the nuclear reaction and maintain the water inventory in the RCS. In the case of the reactors in operation (EPRs excluded) it is also used, in some cases of system operation¹¹, to remove residual heat.

In the case of the reactors in operation (EPRs excluded), the SIS has pressurised accumulator tanks of borated water, a boric-acid tank (refuelling water storage tank, RWST), and pumps with discharge rates and pressures that can handle the various LOCA cases (breaks of different sizes). The reactors in operation have a high-head safety-injection system and a low-head safety-injection system. The 1300 MWe reactors also have a medium-head safety-injection system.

The EPR has four separate, independent low-head and medium-head safety-injection trains. The four trains are supplied with borated water from the in-containment refuelling water storage tank (IRWST), so named because it is located inside the containment¹² (whereas the RWSTs of the reactors in operation are located outside the containments).

The operation of these systems is described in Section 2.4.2.

In the event of an accident leading to a significant increase in pressure in the reactor building, a water-spray system (CSS) is turned on to lower the pressure and thus preserve the integrity of the containment. This system is also used to wash radioactive

11. As with the CSS described below, the SIS can inject water either directly from the fuel pool cooling and purification system (FPCPS) or indirectly using the water collected at the bottom of the containment (recirculation). Residual heat removal by the SIS is achieved with direct injection only. In recirculation mode, the residual heat is removed by the CSS (Section 2.4.2.2).

12. The heat exchangers in the low-head safety injection system remove residual heat from the containment of the EPR without having to use the CSS, like on the reactors in operation. The EPR has a residual heat removal system, but it is used only for severe accident situations. The IRWST also provides the water needed to cool the molten corium in the core catcher in the event of a core melt accident with vessel melt-through.

normal operation while the reactor is at hot shutdown to keep water in the steam generators. The EFWS has two motor-driven pumps and either one pump (900 MWe) or two pumps (other series) that are driven by a steam turbine supplied by the steam generators. These pumps draw in feedwater from a tank with a capacity of 700 m³ (900 MWe), 1440 m³ (P4), 1723 m³ (P'4) or 1488 m³ (N4) and inject this water on the secondary side of the steam generators.

In the case of the EPR, the EFWS has four separate, independent trains, each of which has its own water tank that is supplied by a shared 2600 m³ tank. These trains are used only if the MFWS fails. The EPR is also equipped with a system that feeds water to the steam generators during reactor startup and shutdown.

2.3.2.5. Other systems

Other systems or circuits important to reactor safety include:

- the CCWS, which cools a number of items of equipment important to reactor safety (the RCPs and the CVCS pumps; the ventilation systems; the SIS and CSS for units at operation; the residual-heat-removal system (RHRS or SIS/RHRS for EPRs). The CCWS operates in a closed loop between the auxiliary systems and the engineered safety systems on the one hand, and the ESWS on the other (see next bullet, below) It should be noted that the CCWS at the Fessenheim reactors does not contribute to cooling of the CVCS, the RCPs, the CSS or the ventilation systems. These systems and items of equipment are cooled directly by the ESWS. The engineered safety systems in all the other reactors are cooled by two CCWS trains. In the EPRs, they are cooled by four CCWS trains;
- the ESWS, which cools the CCWS through the heat sink (river or sea). The series in operation have two ESWS trains; the EPRs have four trains;
- the fuel pool cooling and purification system (FPCPS), which, amongst other things, is used to remove decay heat generated by the fuel elements stored in the spent-fuel pool;
- the ventilation systems, which play an essential role in the containment of radioactive materials by placing rooms at negative pressure and filtering releases;
- the fire-protection circuits and systems;
- the instrumentation and control (I&C) system and the electrical systems. The systems important to reactor safety are powered by redundant power supplies consisting of two independent electrical trains for the reactors in operation and four independent electrical trains for the EPRs. Each electrical train is supplied by a switchboard that itself is supplied by either the transmission grid (two independent high-voltage lines) or a diesel generator. In addition, a third diesel generator (900 MWe series) or a backup turbine (1300 MWe and 1450 MWe series) or two SBO diesel generators (EPRs) may be used if necessary.

2.4. Reactor operation under normal and accident conditions

2.4.1. Systems used under normal reactor operating conditions

Normal reactor operating conditions refer to the following states:

- at-power and hot-shutdown states, during which cooling is provided by the steam generators, which are supplied on their secondary sides by the MFWS);
- shutdown states, with the RCS closed, during which cooling is provided by either the RHRS or the steam generators supplied on their secondary sides by the EFWS);
- shutdown states, with the RCS open, during which cooling is provided by the RHRS.

The basic safety functions – reactivity control, heat removal and containment of radioactive substances – must be ensured at all times for each reactor state. The systems used to ensure each of these functions are described on the following pages.

2.4.1.1. Reactivity-control systems

Two methods are used to control reactivity. The first method consists of adding boron (an effective neutron absorber) to the RCS to offset slow reactivity changes in the long term. The second method entails using the control-rod clusters (Section 2.3.2.1), which consist of 24 stainless-steel rods containing a silver-indium-cadmium alloy (all reactors) or boron carbide (1300 MWe and 1450 MWe reactors, EPRs) and which slide up and down inside Zircaloy guide tubes. The clusters are inserted into or removed from the core either by the facility's control systems or manual controls operated by facility operators.

In the interval between a hot and cold reactor shutdown, the temperature coefficient is negative. This drop in temperature causes the reactivity in the core to increase (Section 2.1). In this situation, the boron concentration in the RCS is increased to make up for the inability of the control rods to control the reactivity.

Boric acid is injected into the RCS during plant operation or shutdown by the CVCS (see Section 2.3.2.4 for a description of the CVCS).

2.4.1.2. Heat-removal systems

At power, the heat generated in the reactor core is removed by the RCS and transferred to the steam generators by the RCPs. The steam produced on the secondary side of the steam generators is expanded in the steam turbine and exhausted to the condenser. The condenser is cooled by a tertiary loop, which is a heat sink consisting of the sea or a river (open-loop system) or the atmosphere (via cooling towers [closed-loop system]). The condensed water is pumped back to the steam generators by the MFWS (Figures 2.3 and 2.6).

When the reactor is shut down, the decay heat from the fission products is much lower (less than 1% of nominal power) and decreases over time. This heat is removed by various systems depending on whether the RCS is open or closed. When the RCS is closed, the decay heat may be transferred to the steam generators by means of natural convection and without using the RCPs. Water may be supplied to the steam generators by either the MFWS or the EFWS. When it is supplied by the EFWS, the steam generated is dumped to the atmosphere by control valves (Figure 2.6).

An alternative method of heat removal for reactors in operation (EPRs excluded) is the RHRS. The RHRS may be used when the vessel is either closed or open (see Section 2.3.2.4, Figure 2.7 for a description of these systems).

In the case of the EPR, residual heat is removed by the low-head safety-injection system (LHSI, Section 2.3.2.4).

2.4.1.3. Containment systems for radioactive substances

During normal operation, the reactor coolant contains small amounts of radioactive substances. These substances consist of corrosion products in the RCS, which are irradiated during their time in the reactor core, and fission products in the form of gases or particles from leaks in the fuel-rod cladding.

The reactor coolant is continuously purified by the CVCS. The particles contained in it are captured by filters and the gaseous products are stored in tanks for subsequent treatment.

Containment systems are used to prevent these radioactive substances from leaking out into the environment:

- rooms or buildings containing radioactive substances in the form of gases or particles are placed at a pressure below the outdoor air pressure. So-called "iodine-risk" rooms are placed at a pressure below that of the rooms surrounding them;
- gas leaks are collected by either special systems (in particular the gaseous waste processing system) for storage and inspection before being released, or by the nuclear auxiliary building's ventilation systems, which are fitted with iodine traps;
- liquid leaks are collected by sumps, retention pits, containment basins and collection lines for treatment and inspection before being stored in special tanks.

In the case of the EPR, design provisions have been made to prevent radioactive substances from leaking directly into the environment. All the containment penetrations lead into buildings equipped with ventilation and filtration systems.

Radiation is measured in the rooms housing the auxiliary systems (activity of the ambient air, activity of the sump water) to monitor the integrity of these systems, and in the CCWS and the steam system to monitor the integrity of these heat exchangers.

2.4.2. *Systems used under reactor incident or accident conditions*

During normal facility operation (including normal operation transients), the essential physical parameters remain within their set value ranges. In the event of an accident, some of these parameters may go beyond their ranges, tripping the systems (protection and engineered safety systems, see Sections 2.3.2.4 and 2.3.2.5) designed to bring the reactor back to a state ensuring the three basic safety functions: reactivity control, heat removal and containment of radioactive substances.

2.4.2.1. Reactivity-control systems

Reactivity is controlled by inserting the control rods¹³ into the core. These rods fall by gravity into the core within 2-3 seconds of a power failure (reactor trip). The values of some parameters are continuously compared against thresholds (e.g., reactor power, RCS pressure, RCP velocity, temperatures). When any of these thresholds is exceeded, the protection system initiates a reactor trip and may also trip other systems. For example, under some accident conditions, the SIS are also tripped to pump borated water into the RCS to control the reactivity. The CVCS may also be activated to make up the borated water lost from the RCS through small leaks.

2.4.2.2. Residual-heat-removal systems

In accident situations without a break in the RCS, residual heat may be removed first by the EFWS, which is automatically initiated if the MFWS is not available (Figure 2.7).

In some accident situations, a break in the RCS may be caused by a loop failure or the opening of the safety valves. If this occurs, residual heat can be removed only if the water inventory in the RCS remains sufficient and the heat transferred into the containment by the coolant flowing out of the break is removed. For example, if a small break occurs on the RCS, the heat from the reactor core is not completely carried away by the coolant flowing out of the break and into the containment. A portion of this heat must be removed by the EFWS.

► Maintaining the RCS water inventory

A sufficient water inventory is maintained in the RCS by the SIS, which pumps sufficient amounts of water into the RCS to compensate for breaks up to and including double-ended breach (complete rupture) of the RCS.

In the case of the 900 MWe reactors, this function is carried out for breaks of all sizes by two pumps that inject borated water at high pressure (trip threshold of 170 bar) and two pumps that inject borated water at low pressure (trip threshold: 10 bar). In addition, accumulator tanks containing borated water and pressurised with nitrogen empty their

13. Failure of a drive mechanism may lead to ejection of a control rod and uncontrolled increase in the reactivity of the affected assembly. This type of reactivity accident is the subject of many studies and much research, particularly within the scope of IRSN's international Cabri programme. This programme is beyond the scope of this document.

contents into the RCS if its pressure drops below 40 bar. The 1300 MWe and 1450 MWe reactors have a medium-head safety-injection system (consisting of two pumps that inject borated water into the cold legs at a trip threshold of 120 bar), a low-head safety-injection system (two pumps that inject borated water into the cold and hot legs at a trip threshold of 20 bar) and four accumulator tanks that empty their contents into the RCS if its pressure drops below 40 bar.

In the case of the reactors in operation (EPRs excluded), the SIS is automatically initiated by the protection system if the pressure measured in the pressuriser becomes low (trip thresholds given earlier for each series). When the SIS is initiated, borated water is pumped into the RCS from a storage tank located in the reactor building and known as the in-containment refuelling water storage tank (IRWST). When there is no more water in the IRWST, the SIS actuates the CSS. The CSS operates in a closed loop using water condensed from the steam inside the containment and which flows into sumps located at the bottom of the containment.

The SIS can also maintain a sufficient water inventory in the RCS during accident situations without RCS breaks and where the steam generators are unavailable. In these situations, the RCS safety valves and the SIS are actuated to maintain a sufficient water inventory in the RCS, protect the RCS against overpressure, and remove the residual heat ("feed and bleed"). The low-temperature water (approx. a few dozen °C) injected by the SIS flows through the core and exits the valves in the form of steam.

The EPRs have a medium-head safety-injection system (consisting of four pumps that inject borated water into the cold legs at a trip threshold of approx. 90 bar), a low-head safety-injection system (four pumps that inject borated water into the cold and hot legs at a trip threshold of 20 bar) and four accumulator tanks that empty their contents into the RCS if its pressure drops below 40 bar. The water injected into the RCS comes from the in-containment refuelling water storage tank (IRWST).

► Removal of heat released into the containment

If an RCS break occurs in the reactors in operation (EPRs excluded), the CSS is actuated to lower the heat and pressure inside the containment. It does so by drawing in water from the RWST by means of two motor-driven pumps. When the RWST is empty, the CSS draws water from the sumps at the bottom of the containment (all series). The water used by the CSS is cooled by the CCWS, which itself is cooled by the ESWS (at Fessenheim, this cooling is provided directly by the ESWS) (Figure 2.7).

In some accidents with core melt that jeopardise the integrity of the containment, the heat inside the containment may be removed by the containment's filtered venting system. This system limits the peak pressure inside the containment (U5 procedure; Section 2.5.2.1).

If an RCS break occurs on the EPR, the temperature and pressure inside the containment are decreased by the low-head safety-injection system via the heat exchangers on the SIS/RHRS, which has four motor-driven pumps that draw in water from the IRWST.

A specific system, the CHRS, has been installed to lower the temperature and pressure inside the containment during a core melt accident. The CHRS consists of a two-train spray system, heat exchangers and a specific heat sink.

In the event of a core melt accident with vessel melt-through, the water in the IRWST is used to flood and cool the molten corium in the core catcher. The CHRS, which is used for severe accidents, supplies water to the core catcher, limits vaporisation of the water covering the molten corium, and limits the rise in pressure inside the confinement.

2.4.2.3. Containment systems for radioactive substances

Under accident conditions, the integrity of the fuel-rod cladding may become compromised when the heat inside the fuel rods is not adequately removed. The rise in temperature causes creepdown and collapse of the cladding as well as oxidation of the zirconium by water vapour.

In the case of incident conditions estimated to occur relatively frequently over the life of the reactor, containment of fission products is ensured primarily by the fuel-rod cladding, which is designed to remain leaktight during such conditions. The reactor coolant pressure boundary (RCPB) and the containment are two additional barriers ensuring containment of fission products in the event of fuel-rod-cladding failure and in the presence of the activation products in the reactor coolant in the primary circuit.

In the case of situations estimated to occur less often and for which the cladding and the RCPB are no longer leaktight, containment is ensured by the reactor building, which is designed to remain adequately leaktight. Leaks from the systems penetrating the containment are prevented by isolation valves placed on all the containment penetrations and which automatically close when the pressure inside the containment exceeds a set threshold (containment isolation). The purpose of these provisions is to ensure a very low rate of leakage from the containment to the atmosphere.

The radioactive products (primarily fission products) carried under accident conditions by the water flowing through the RCS, the SIS and the containment spray system (CSS for the reactors in operation; CHRS in the event of a severe accident in the case of the EPR) are another source of radioactive releases. In order to reduce atmospheric releases from leaks on these systems, parts of which are located outside the reactor building, the buildings in which they are housed are maintained at negative pressure by ventilation systems equipped with filters.

Containment of radioactive substances must therefore be ensured under any situation that, due to certain kinds of equipment damage, would allow the reactor coolant to leak directly outside the containment, i.e., either inside the peripheral buildings or directly into the outdoor environment. Known as containment bypass events, these situations are described in detail in Section 6.4. A case in point is rupture of the steam generator tubes, which allows reactor coolant to enter the secondary loops and can result in radioactivity being released to the atmosphere by the steam dump valves and safety

valves on the steam generators. The risks of such an event occurring are prevented by periodically inspecting the condition of the tubes; placing plugs on weak or corroded tubes; replacing the steam generators when necessary; controlling the chemistry and activity of the reactor coolant; and implementing operating procedures that avoid actuating the dump valves of the steam generators.

2.5. Reactor control under normal and accident conditions

2.5.1. Control room

A reactor is run by operators located in the control room. The control room contains all the control, display and monitoring equipment and systems required to operate a reactor under normal, incident and accident conditions.

After the TMI-2 accident of 1979 (Section 7.1), ergonomic improvements were made to the control rooms of the units in operation (900 MWe and 1300 MWe reactors). The layouts of the controls and display systems were improved and the information on the display systems was made clearer and more reliable. The goal was to display clearer information about the state of the systems used to operate the reactor. An aid, called the safety parameter display system (SPDS) was installed in each control room to aid in implementation of incident and accident procedures. Connected to the data-acquisition system, the SPDS provides a summary of the parameters required for implementing the facility's operational procedures. It also allows operators to quickly ascertain the availability of systems important to safety (containment isolation systems, engineered safety systems, electric power supplies, etc.). In an accident situation, it provides operators with the most relevant information (state of the systems, water level and margin to in-core boiling, containment integrity, etc.).

Reactor operation is centralised in the control room provided it is accessible by staff. If the control room is not accessible (for example, after being evacuated during a fire or other emergency), a safe-shutdown panel located in another room is used, under some conditions, to shut down the unit and maintain the reactor in safe state. This supplementary control room must remain accessible in the event the main control room has to be evacuated. In this case, the controls on the safe-shutdown panel override the controls in the main control room. There are also distributed control panels for specific functions (waste processing, water demineralisation, local control of diesel generators, etc.).

Each unit also has an emergency-response centre that is made available to the emergency-response team formed on the site during an accident. The equipment in this room helps the local emergency-response team to ascertain the main parameters of the unit and share them with other emergency-response teams located around the country and which are familiar with the unit. This way, the local and national emergency-response teams have the same information about the parameters of the situation and can manage it accordingly.

The control rooms of the N4 series differ from those of the preceding series in that heavy use is made of computerised systems. In the control rooms of the N4 series, operating procedures are displayed on screens and logic processing and monitoring are automated. An additional means of emergency response, the auxiliary panel, is installed in the control room. Its role is to safely shut down the unit and control accident situations if the computer system is down. The control rooms of the EPRs are technologically identical to those of the N4 series.

2.5.2. Reactor control

2.5.2.1. Operating procedures

During normal operation and incident and accident transients, the facility is controlled according to a set of procedures whose purpose is to keep the reactor in a safe state or drive it into this state.

Each initiating event liable to lead to an incident or accident is associated with a standard method of operation that is denoted by an "I" (for incidents) or an "A" (for accidents). These operating procedures are established based on the foreseeable development of an incident or accident so as to keep the reactor in a safe state or drive it into this state. They apply if an event occurs alone (not in a combination) and has been correctly identified. This method is known as the "event-based approach".

Supplementary procedures have been established for operating conditions involving simultaneous failure of the redundant trains of systems important to safety and for failure of equipment used over the long term (several months) after a loss-of-coolant accident (LOCA). Known as "H procedures" ("H" for *hors dimensionnement*, or, beyond design basis), these supplementary procedures may require the installation of new, supplementary equipment (e.g., addition of a turbine generator that produces electricity from the steam in the secondary loop to supply a power source for some essential systems, or the installation of a special generator [for the 900 MWe reactors] or a combustion turbine [for the 1300 MWe and 1450 MWe reactors]). These procedures are as follows:

- procedure H1 for total loss of the heat sink or associated systems;
- procedure H2 for total loss of the steam generator feedwater supply (MFWS and EFWS);
- procedure H3 for total loss of the offsite and onsite power sources (loss of both offsite power sources, unsuccessful house-load operation, and loss of both generators);
- procedure H4 for total loss of the SIS or CSS over the long-term phase following a LOCA (future total loss of pumping or heat-exchange systems);
- procedure H5 for protection of some riverside sites against flooding above the thousand-year flood level.

In addition to the aforementioned accidents, there remains the possibility that a series of events could lead to radioactivity being released outside the facility. This is the case of core melt accidents. The following emergency procedures have been created to mitigate or delay core damage and radiological consequences:

- procedure U1 for averting core meltdown in situations where no A or H procedures would be suitable or effective. This procedure recommends, based on changes in the core outlet temperature and the availability of the systems and equipment, the best actions to be taken in terms of using the steam generators, SIS, and the relief valves on the pressuriser and the RCPs to prevent core meltdown;
- procedure U2 for locating and isolating containment leaks;
- procedure U3 for implementing mobile emergency equipment for the SIS and CSS and which supplements procedure H4;
- procedure U4 for implementing means of prevention of early radioactive releases in the event of vessel breach and corium erosion of the basemat;
- the U5 procedure for relieving the pressure inside the containment *via* the sand-bed filter.

In such a situation, the emergency-response teams use the Assistance Guide for Emergency-Response Teams (GAEC) and the Severe Accident Operating Guidelines (GIAG), which define the actions to be taken to ensure containment of radioactive substances for as long as possible.

2.5.2.2. Choice of procedure and the state-oriented approach

To determine the appropriate operating procedure, the state of the reactor must first be diagnosed. This diagnosis is made based on an analysis of the relevant alarms and physical variables.

Making this diagnostic and selecting the right procedure are not always easy in the case of situations with multiple failures. Indeed, the combinations of events caused by multiple failures can be endless. On the other hand, the possible physical states of the reactor are limited in number. They can be identified from a limited number of data characterising the physical state of the main reactor components: subcriticality of the reactor core; RCS water inventory; efficiency of (residual) heat removal; integrity of, and water level in, the steam generators; and integrity of the containment. In addition, the actions to be taken may generally be inferred from knowledge of the reactor's physical state without necessarily having to identify the sequence of events that led up to this state. The entire approach that consists of the identifying the physical state of the facility, defining the operation to be achieved based on this state, and setting priority actions to be taken to control the situation is known as the "state-oriented approach".

In the state-oriented approach, the operational objective and strategy may be redefined at any time based on developments in the situation (physical state of the

reactor, equipment failures, human errors). Unlike with the event-based approach, operation is no longer defined solely by an initial diagnosis of the cause of the incident or accident. This type of operation makes it possible to cover all thermal-hydraulic incidents or accidents (RCS breaks, secondary-loop breaks, core heating, etc.), be they single or multiple, occurring alone or compounded by system failures, power failures or even human errors.

2.5.2.3. Control under incident and accident conditions

The operating procedures describe the operations to be carried out to return the reactor to a safe state. They primarily address:

- controlling reactivity through operation of the systems used to add boron to the RCS after rod drop;
- maintaining the RCS water inventory through operation of the CVCS and the SIS;
- removing residual heat through operation of the core cooling systems:
 - the steam generators (if available): the heat generated in the reactor is removed by spraying water from the secondary loops. This water is then either cooled by the condenser or discharged to the atmosphere. The necessary makeup water is provided by either the MFWS or the EFWS);
 - the engineered safety systems (CSS and SIS) in the event of a LOCA or total loss of the steam generators;
 - the RHRS after reactor shutdown (RHRS for the units in operation – EPRs excluded – or LHSI for the EPRs);
- containment of radioactive substances through closure, where necessary, of the devices used to ensure the integrity of the containment.

By monitoring the systems used, the operators can detect if any of them fail and, if possible, implement stopgap measures while the failed systems are being repaired.

In order ensure human redundancy, the shift manager then the facility safety engineer are called into the control room as soon as an accident procedure is implemented. Their role is to monitor the situation as it progresses and meet the following objectives:

- ensure that the necessary safety-related actions are carried out;
- ensure that operators correctly follow the procedure relating to the reactor's state;
- monitor the state and availability of the safety systems used.

In the event of an accident involving a risk of radioactive release, the local and national emergency-response teams are set up in a matter of hours and use the Assistance Guide for Emergency-Response Teams (GAEC) and the Severe Accident Operating Guidelines (GIAG) to manage the situation (Section 2.5.2.1).

2.6. Conclusion

The preceding sections present the main components, systems and loops found in PWRs as well as their main principles of operation under normal and accident conditions. PWRs are complex facilities with specific risks related to the presence of large amounts of radioactive products. Safety must be a constant concern at each stage of their life (design, construction, operation, dismantling) to reduce risks, particularly the dissemination of radioactive substances.

Provisions are made at each stage in the life of a reactor to protect people and the environment against the effects of radiation. These provisions aim to:

- ensure the normal operation of facilities;
- prevent incidents and accidents;
- mitigate the consequences of a potential incident or accident.

The approach used to implement these safety measures is described in the next chapter.

References

- [1] P. Coppolani, N. Hassenboehler, J. Joseph, J.-F. Petretot, J.-P. Py, J.-S. Zampa, *La chaudière des réacteurs à eau sous pression*, EDP Sciences, collection INSTN, 2004.
- [2] J. Bourgeois, P. Tanguy, F. Cogne, J. Petit, *La sûreté nucléaire en France et dans le Monde*, Polytechnica, 1996.
- [3] J. Libmann, *Éléments de sûreté nucléaire*, EDP Sciences, collection IPSN, 2000.

Chapter 3

Safety Principles for Pressurised Water Reactors in the French Nuclear Power Plant Fleet

3.1. Introduction

The goal of this chapter is not to provide an exhaustive explanation of [nuclear safety](#) principles and practices at facilities in France (for a discussion on this topic, see the work of J. Libmann [1]), but to illustrate the two complementary safety approaches, deterministic and probabilistic, by introducing a key concept of the first, defence-in-depth, and a general description of probabilistic safety assessments (PSAs), which are part of the second.

Nuclear facilities, in particular those for producing electricity, present specific risks related to the presence of often significant quantities of radioactive substances that can cause individuals, population groups and the environment to be exposed to ionising radiation.

[Nuclear safety](#) is composed of a set of technical and organisational measures taken during all phases in the life of a facility (design, construction and commissioning, operation, decommissioning and dismantling) to protect workers, the general public and the environment from the effects of radioactive substances. It involves:

- ensuring normal operation of facilities without excessive exposure for workers and excessive releases of radioactivity in radioactive effluents;

- preventing incidents and accidents;
- limiting the consequences of incidents and accidents that occur despite prevention measures that have been implemented.

Containment of radioactive substances is achieved by placing “barriers” between the substances and people. In diagrammatic terms, for pressurised water reactors (PWRs) of the type operated in France, there are three successive barriers between radioactive substances and the environment: the fuel rod cladding, the reactor coolant system and the containment building. Optimal leak tightness of these barriers in the various situations of normal and emergency operation shall be sought in the design phase. However, in normal operation, the barriers are not generally perfectly leaktight: cladding ruptures and leaks in the reactor coolant system and the containment building of limited significance may occur¹.

It is important to mention in this context the particular case of PWR steam generator tubes, which are part of the second and third barriers, since the rupture of a tube may cause the safety valves of the steam generator to open, thus creating a containment bypass.

The goal of defence-in-depth, introduced in the following section, is to ensure basic safety functions, i.e., controlling reactivity, cooling irradiated fuel and containing radioactive substances; these safety functions are necessary to ensure all barriers remain effective.

3.2. Concept of defence-in-depth

The defence-in-depth concept was introduced in the [nuclear safety](#) field in the early 1970s. In nuclear facilities, it is achieved by implementing levels of defence based on the intrinsic characteristics of the facility, equipment measures and procedures put in place to prevent accidents, and if prevention fails, limit accident consequences. Defence-in-depth is a concept that applies to all stages in the life of a facility, from design to dismantling.

How the concept of defence-in-depth is implemented has evolved over time to take into account operational experience from facilities, including incidents and accidents that have occurred, in order to build an ever more effective defence.

For reactors currently in operation, defence-in-depth is based on five levels (see INSAG-10 [2] and Table 3.1) intended to prevent the occurrence and limit the consequences of technical, human and organisational failures. The various levels of defence-in-depth apply in the various states of the facility, from normal operation to core melt accidents. At each level of defence-in-depth, except for level 5, there are measures designed to prevent the occurrence of more severe situations.

The design of current reactors included only three levels of defence-in-depth.

1. Leaks during normal operation will nevertheless meet operating technical specifications.

Level 1: prevention of operating anomalies and system failures

Prevention of operating anomalies and failures in components, equipment and systems assumes prudent design (with adequate safety margins) and components, equipment and systems that have been manufactured and operated to the highest quality standards. This level corresponds to the normal domain of operation for the facility with general rules and operating procedures designed to maintain the plant unit within its normal operating domain.

Level 2: failure detection and comprehensive management of operating malfunctions

This level includes resources and systems designed to control operating malfunctions, which assumes monitoring that will ensure failures are detected. This includes automatic functions and control systems that can return the facility to its normal operating mode. These systems are designed to correct an abnormal change in facility parameters.

Level 3: comprehensive accident management (including design-basis accidents)

The first two levels of defence-in-depth reduce the risks of failure at the facility. It is nevertheless assumed that accidents can occur during reactor operation. Accidents considered at this level result from a single initiating event (e.g., the failure of a component essential for a basic safety function – comprehensive management of reactivity, cooling of nuclear fuel or containment of radioactive substances). Resources that limit the consequences of such accidents and ensure basic safety functions are implemented: at this level defence-in-depth consists of implementing safeguards that ensure the integrity of the core structure and limit releases into the environment in the event of an accident (considered for the design-basis of the facility). This level also includes defining emergency operating procedures.

After the accident at Three Mile Island Unit 2 (TMI-2) in the United States in 1979, the concept of defence-in-depth was enlarged to include accidents that had not been explicitly considered during facility design. In particular, lessons from the initial probabilistic safety assessments (Section 3.3) and the TMI-2 accident (Section 7.1) demonstrated the need to take into account accidents resulting from multiple failures and those leading to core melt. These developments led to defining an additional level of defence-in-depth.

Level 4: comprehensive management of severe accidents

This level of defence-in-depth includes procedures and equipment used to handle situations that are not covered by the first three levels of defence-in-depth; these are accidents that could result in reactor core melt. At level 4, the objective is to prevent accidents from resulting in core melt and to limit releases outside the site by ensuring containment of radioactive substances in the event core melt nevertheless does occur.

This level of defence-in-depth includes emergency procedures and associated equipment resources (Section 2.5.2), specific equipment (e.g., hydrogen recombiners), the severe accident operating guidelines and the facility's on-site emergency plan. The licensee prepares and implements the on-site emergency plan. When the plan is implemented, the facility's emergency response teams are mobilised in order to contain the accident and avoid the release of radioactive substances. The purpose of the on-site emergency plan is to protect staff working at the site in the event of an incident or accident and to limit off-site consequences of an accident.

Level 5: limiting consequences of radiation in the event of radioactive releases

Despite all the measures described above, radioactive releases may occur. Additional measures, taken by public authorities, are then implemented to protect the public, on-site staff and property from the consequences of these releases.

Measures for protecting the public from radioactive releases include evacuation, shelter in hardwall accommodation, taking of potassium iodide tablets and restrictions on the consumption of foodstuffs. This level includes off-site emergency plans prepared for each site. Public authorities implement the off-site emergency plan, which organises emergency operations to limit public exposure to radiation in the event of releases.

Table 3.1. The various levels of defence-in-depth.

Level	Objective	Main measures	Corresponding facility condition
1	Preventing operating malfunctions and system failures	Prudent design (including safety margin) and well-designed and well-run facility	Normal operation
2	Detecting failures and comprehensive management of operating malfunctions	Systems for control, protection and review (for maintaining the facility within its normal operating domain) and monitoring (preventing failures)	Operating malfunctions or failures
3	Comprehensive accident management (including design-basis accidents)	Safeguard systems and accident procedures	Accidents including "design-basis accidents" (single initiating event)
4	Comprehensive management of severe accidents, prevention of accident progression and mitigation of consequences	Additional measures and accident management (emergency procedures and associated equipment resources, severe accident operating guidelines, on-site emergency plan)	Multiple failures Core melt accidents
5	Limiting radiological consequences in the event of a release of radioactive substances	Off-site emergency plan	Accidents with radioactive releases

For third-generation reactors, multiple failure and core melt accidents are considered in the initial design of the reactors, which signifies a major step in the range of accident situations for which measures are taken to prevent accidents and limit the consequences must be planned from the design stage. Even if the measures taken for these reactors cannot all be applied in practice to second-generation reactors, they can help identify safety improvements for reactors that are currently in operation and improve defence-in-depth for the reactors.

3.3. Role of the probabilistic approach

Probabilistic safety assessments (PSAs) were first developed in the 1960s for nuclear power plants. The Rasmussen report [3], published in the United States in 1975, which sought to compare risks for the public from nuclear reactors with other industrial and natural risks, demonstrated the value of a probabilistic analysis for assessing nuclear reactor risks. Since then, all nuclear power plants in commercial operation worldwide have been subject to PSAs.

PSAs supplement traditional deterministic analyses and enable a systematic investigation of the numerous possibilities of event combinations and sequences that constitute accident scenarios. They consist of a set of technical analyses for assessing the risks at a facility in terms of accident frequency, e.g., core melt, and their consequences. They provide an overall view of reactor safety, including both equipment resistance and operator behaviour. They can show topics for which changes both in design and operation can be studied and even judged necessary.

There are three major types of PSAs based on consequences under examination:

- level 1 PSA: used to identify sequences leading to core melt and quantifying their frequency;
- level 2 PSA: used to assess the nature, significance and frequency of releases of radioactive substances outside the containment building;
- level 3 PSA: used to assess the probabilities of consequences on the public in terms of dosimetry and contamination (even in terms of frequency of cancers or other effects on health).

The Rasmussen report [3] is the first example of a level 3 PSA. As will be seen in Section 4.3.2 later, this report remains a reference for an approach to managing core melt accidents. PSAs carried out until now in France for 900, 1300 and 1450 MW plant units and the EPR have been level 1 and 2 [4–9] (see also Sections 4.2 and 4.4). They are prepared by EDF and IRSN with the studies by EDF considered as the reference cases. They are updated by EDF and IRSN, particularly during safety reviews, to take into account changes in knowledge and operating experience and are used for safety assessments of PWRs according to the conditions stated in basic safety rule 2002-01 [10]. The results of level 1 PSAs and the method and applications of level 2 PSAs prepared by IRSN are described in Section 4.4.

Compared with assessments of the same type performed abroad, level 1 and 2 PSAs in France benefit from the standardisation of plant units in France, which helps assess the

reliability of equipment and the probability of certain initiating events on broader statistical bases. In addition, French assessments consider all reactor states: operation at full and intermediate power and maintenance outage. Taking into account the specific operating configurations in these states, including the lesser degree of automatic safeguard actions, French PSAs have demonstrated that these reactor states play a significant role in the probability of core melt. The results brought about improvements in operation (technical specifications and procedures) and design (implementation of alarms and controllers).

The same PSAs also provided a more quantitative assessment of the value of measures taken to improve accident management. Level 2 PSAs are also used to evaluate measures given in severe accident operating guidelines that operators on-site should implement in such situations, particularly to ensure maximum containment of radioactive substances [11–13].

The PSAs however have certain limitations due to uncertainties associated with them that require using caution when interpreting results and using them for making decisions. The existing French PSAs are thus not exhaustive in terms of coverage, since they only partially take into account internal and external hazards. In addition, uncertainties stem from quantitative input data and simplifications and assumptions adopted for the design study [14]. A non-exhaustive list would include uncertainties associated with the choices in combining initiating events, supporting scenarios for thermal-hydraulic and neutronic calculations, modelling of physical phenomena and human actions, estimating the reliability of software and equipment, the choice of event trees (events and chronological order) and probabilistic quantification software (see Section 4.4 for further details).

Global safety PSAs are thus used to support or supplement traditional deterministic safety analyses both for a more quantitative assessment of the level of safety at plant units in France and to constitute analytical tools for these plant units. Insofar as comparison of the results of PSAs to standard criteria must be done with caution given the uncertainties mentioned above, the probabilistic approach is useful for determining weaknesses related to plant units under consideration and to assess, for example, the relative benefit of changes in design or operation.

3.4. Conclusion

The deterministic and probabilistic approaches to safety constitute an ensemble that contributes to preventing and limiting the consequences of accidents, especially severe core melt accidents and thus ensure a heightened level of safety at nuclear facilities. The approaches continue to evolve and it is important not to overlook the permanent interaction between the level of safety at facilities and the current state of knowledge available from research on core melt accidents, which is presented here in Chapter 5; more detailed studies (such as PSAs), given in Section 4.4; operating experience; and incident and accident analysis.

Following the Fukushima Daiichi accident, French nuclear facilities underwent complementary safety assessments (CSAs) which focused on five key points regarding power reactors: risks of flooding, earthquakes, loss of power, loss of heat sink, and operational

management of accident situations. These assessments are aimed at determining the robustness of French reactors in response to extreme external events and adding to existing safety provisions to enhance this robustness.

In particular, efforts are under way at IRSN to expand the scope of PSAs by including recent knowledge from research, handling hazards such as flooding and earthquakes and taking into account operational feedback from facility operation: the goal of these efforts is improved assessment of power reactor risks and measures taken for emergency operation.

References

- [1] J. Libmann, *Éléments de sûreté nucléaire*, Collection IPSN, EDP Sciences, 1996.
- [2] International Nuclear Safety Advisory Group Report, INSAG-10, IAEA Report, Vienna, 1996.
- [3] N. Rasmussen *et al.*, Reactor safety study, WASH-1400, Washington D.C., US NRC, 1975.
- [4] A. Ellia-Hervy, F. Corenwinder, J.-M. Lanore, V. Sorel, Les Études Probabilistes de Sûreté de niveau 1: les méthodes, les connaissances utilisées, les résultats», *Revue Générale Nucléaire* 1, 12-16, 2003.
- [5] E. Kalalo, D. Brenot, "Rôle et limites des EPS", *Revue Contrôle* 155, 39-42, 2003.
- [6] A. Dubreuil-Chambardel, G. Body, V. Sorel, Qu'est-ce qu'une étude probabiliste de sûreté de niveau 2? Exemple de la troisième visite décennale des REP 900 MWe, *Revue Générale Nucléaire* 1, 88-92, 2010.
- [7] E. Raimond, Apport des études probabilistes de sûreté de niveau 2 dans l'analyse de sûreté – Point de vue de l'IRSN, *Revue Générale Nucléaire* 1, 99-105, 2010.
- [8] E. Raimond, N. Rahni, K. Chevalier-Jabet, T. Durin, L'EPS de niveau 2 pour les REP 900: du développement aux enseignements de l'étude, IRSN, Rapport scientifique et technique, 2008.
- [9] E. Raimond, C. Caroli, B. Chaumont, Status of IRSN level 2 PSA, CSNI/WG Risk Workshop, Cologne, Germany, 2004.
- [10] Règle fondamentale de sûreté n° 2002-01 – Développement et utilisation des études probabilistes de sûreté pour les réacteurs nucléaires à eau sous pression, document ASN (2002); <http://www.asn.fr/index.php/Les-actions-de-l-ASN/La-reglementation/Regles-fondamentales-de-surete-et-guides-de-l-ASN/Guides-de-l-ASN-et-RFS-relatives-aux-REP/RFS-2002-1-du-26-12-2002>.
- [11] E. Raimond, B. Laurent, N. Rahni, K. Chevalier-Jabet, T. Durin, Application des EPS de niveau 2 et des techniques de fiabilité dynamique à la validation des guides d'intervention en cas d'accident grave, IRSN, Rapport scientifique et technique, 2007.

- [12] E. Raimond, T. Durin, B. Laurent, K. Chevalier-Jabet, Level 2 PSA: a dynamic event tree approach to validate PWR severe accident management guidelines, *Conference PSA2008*, Knoxville, USA, 2008.
- [13] E. Raimond, K. Chevalier-Jabet, F. Pichereau, Link between level 2 PSA and off-site emergency preparedness, *Conference PSAM8*, New Orleans, USA, 2006.
- [14] E. Raimond, N. Rahni, M. Villermain, Method implemented by the IRSN for the evaluation of uncertainties in level 2 PSA, *Workshop on the evaluation of uncertainties in relation to severe accidents and level 2 PSA*, Cadarache, France, 2005.

Chapter 4

Safety Principles for France's Pressurised Water Reactors

4.1. Concept of severe accident

A severe accident or core melt accident at a PWR is an accident during which the reactor fuel is significantly damaged with more or less extensive melting of the reactor core. This melting is caused by extended loss of core cooling by the coolant and, in turn, a significant increase in the temperature of the exposed fuel rods. Owing to the preventive measures in place (see Section 3), such an accident occurs only following a series of failures (multiple human or equipment failures). The failure, in 1979, of the second reactor at the Three Mile Island nuclear power plant nevertheless confirmed that a series of failures could lead to a core melt accident. Fortunately, the accident did not have significant environmental consequences (Section 7.1). The [Fukushima-Daiichi](#) accident in 2011 showed that external hazards (tsunami triggered by an earthquake) with a magnitude greater than a facility's design basis could also lead to core meltdowns. Unfortunately, this accident resulted in significant amounts of radioactivity being released into the environment.

If core degradation cannot be stopped inside a reactor vessel through cooling of the degraded core (in-vessel reflooding with coolant), the core melt accident may ultimately lead to loss of containment integrity and large releases of radioactivity into the environment. Because of the significant consequences of such releases into the environment, and in accordance with the defence-in-depth approach (see Section 3), many efforts are being made to study this type of accident and mitigate its consequences. The first step

in studying core melt accidents involves identifying the main scenarios that may lead to them. These scenarios are described in the following section.

4.2. Accident scenarios that may lead to core melt

This section describes the main accident scenarios as they appear in the light of level 1 probabilistic safety assessments (level 1 PSAs). Each scenario involves a series of equipment or human failures that may lead to core uncover and, if core cooling cannot be restored, to core melt. The severity of core melt is not specified in the following presentation. Some scenarios may result in nearly total fuel melt while others may simply lead to very limited fuel degradation. The magnitude and kinetics of the corresponding releases are assessed during level 2 PSAs. These assessments are presented in Section 4.4.

Accident sequences likely to result from external hazards are not described here; such PSAs are now in the course of development.

4.2.1. Description of PSA level 1 accident scenarios

4.2.1.1. Introduction

As mentioned in Section 3.3, the aim of level 1 PSAs is to determine which accident scenarios – ranging from simple cladding failure to fuel melt – result in partial or total fuel degradation. EDF develops such PSAs for four reactor types (900 MWe, 1300 MWe, N4 and EPR). These PSAs constitute reference studies used to support safety analyses. IRSN develops its own level 1 PSAs for the 900 and 1300 MWe series and the EPR in order to analyse EDF's findings more deeply and identify specific points that need to be examined more in detail.

The scenarios presented on the following pages are based on the findings of the level 1 PSAs developed by EDF and IRSN for the 900 MWe reactors.

The description and operation of the systems of these reactors that come into play during normal and accident situations are presented in Chapter 2 (particularly in Section 2.3.2.4 and Figures 2.6 and 2.7). The acronyms for some systems (especially FPCCS, RHRS, CSS, CVCS, CCWS, EFWS, U5, SIS) are defined in Chapter 2 as well.

The following description of the accident scenarios is for illustrative purposes only. It does not aim to provide all the details given in the PSAs.

4.2.1.2. Loss-of-coolant accidents (LOCA): large breaks, intermediate breaks and small breaks

LOCA are initiated by breaks in the reactor-coolant system (RCS) or any of the connecting circuits. These breaks do not include vessel failure or failure of one or more steam generator tubes (the latter case is discussed in Section 4.2.1.5). Such breaks cause reactor coolant to leak out and the RCS to become depressurised. The level 1 PSA

distinguishes several scenarios depending on the reactor's initial state and the size and location of the break.

In the event of a LOCA, the depressurisation of the RCS induces an automatic reactor trip and automatically initiates the safety injection system (SIS). In the case of large breaks, the rapid increase in pressure inside the containment automatically initiates the containment spray system (CSS).

The protection and engineered safety systems must perform the following functions to mitigate the consequences of the accident:

- reactivity control;
- maintaining the water inventory in the reactor vessel;
- removal of the residual heat generated by the fuel.

Reactivity control is provided by the automatic reactor trip and the injection of boric acid into the core.

Water is maintained inside the reactor vessel by the SIS, which operates in two phases: an injection phase and a recirculation phase. In the first phase, the SIS injects water from the RWST. In the second, it recirculates water drawn from the sumps at the bottom of the containment building.

The heat generated by the fuel is removed through cooling by the water flowing inside the vessel (by the break, which allows the water heated by the fuel to be removed, by the steam generators and, in the longer term, by the RHRS). However, this system can be used only if the RCS break is not too big. When the SIS recirculates the water contained in the sumps in the containment building, heat is removed from the containment building by the CSS.

The RHRS and CSS are cooled by the CCWS¹.

The accident scenarios that lead to core melt assume the failure of one or more engineered safety systems. Scenarios involving one of the following failures are considered for a reactor initially at power:

- failure of the SIS;
- failure of the CSS while in the injection and/or recirculation phase.

The level 1 PSA accident scenarios for reactor-trip states differ depending on the initial state of the RCS (closed, partially open or completely open). Whatever the case, however, they are always associated with failure to maintain a sufficient level of water in the RCS to cool the core following a human error or an equipment failure.

1. Except at Fessenheim, where the CSS is cooled directly by the ESWS (see Section 2.4.2.2).

4.2.1.3. Loss-of-coolant accidents with containment bypass (V-LOCA)

These accidents, which are caused by loss of coolant *via* a break occurring outside the containment building but in a loop connected to the RCS loop and not isolated from it, have two specific characteristics:

- since coolant is lost outside the containment, the recirculation phase of safety injection is not possible;
- there is a risk of fission products being released directly outside the containment as long as the break is not isolated from the RCS.

An example of an accident of this type is a break in the thermal barrier of any of the RCPs.

4.2.1.4. Steam-line break accidents (FWLB, SLB)

These accidents are caused by:

- small or large breaks occurring in a steam generator feedwater line (FWLB) upstream of the isolation valve of the MFWS and EFWS systems (see Figures 2.6 and 2.7). These lines are located inside the containment (the lines located outside the containment have check valves to isolate breaks and prevent the steam generators from being completely emptied);
- small or large breaks occurring in a steam line connected to the secondary side of a steam generator (SLB). Breaks may occur inside or outside the containment. Those that occur outside it can be localised either between the containment and the steam isolation valves or downstream of the steam isolation valves. Breaks that occur downstream of the valves can be isolated by closing the valves;
- a dump valve on the secondary loops becoming stuck open.

When a break in the feedwater line of a steam generator occurs, the steam generator is rapidly voided of water and the flow rate of the steam in the generator's secondary side rises suddenly. This results in increased removal of heat from the RCS by the affected steam generator, initiation of an automatic reactor trip and startup of the SIS.

Operators must isolate the affected steam generator by closing the steam isolation valves to prevent the other steam generators from voiding and thus preserve the possibility of cooling by the secondary loops.

A break on a steam line connected to the secondary side of a steam generator will cause the flow of steam in the secondary loops to suddenly rise. This causes more heat to be removed from the RCS, which in turn causes the RCS pressure and temperature to drop. The effect of this cooling is that it reduces the available reactivity shutdown margin. If a large break occurs, the SIS is rapidly initiated (automatic injection of highly borated water) and the isolation valves on the steam lines automatically close to isolate the steam generators.

The following functions must be performed in the event of SLB or FWLB:

- reactivity control, which is initiated by the automatic reactor trip and, where necessary, the injection of borated water by the SIS;
- residual-heat removal, which is provided by the unaffected steam generators, which are supplied with water by the EFWS until the EFWS tank is empty;
- for scenarios involving a large break inside the containment, heat is removed from the containment by the CSS.

The most likely accident scenarios where FWLB leads to core melt involve either (i) several control rods becoming stuck outside the core and preventing reactivity control or (ii) failed closure of the isolation valves on the lines of the steam generator affected by the break (thus preventing the secondary loops from cooling the reactor) followed by failure of maintaining a feed-and-bleed stream (see Section 2.4.2.2).

With regard to SLBs, three scenarios leading to core melt can be mentioned as examples:

- *a large break* inside the containment followed by complete failure of the CSS. The pressure and temperature inside the containment could exceed the qualification range of the instrumentation used to operate the facility under accident conditions. Furthermore, loss of reactivity control might occur if at least two control rods are mechanically stuck outside the core;
- *a small break* followed by a control rod becoming stuck combined with failure, due to human error, to isolate the steam lines of the affected steam generator. In this case, reactivity control might not be provided;
- reactor trip followed by failure of the EFWS followed by a human error involving the injection of water into the RCS (no feed and bleed).

4.2.1.5. Steam generator tube rupture accidents (SGTR)

These accidents range from major leaks to complete ruptures of one or more steam generator tubes (SGTR category) and secondary-line breaks (water or steam) resulting in virtually immediate rupture of one or more steam generator tubes (combination of SLB and SGTR).

Leakages or ruptures on a steam generator tube will induce a drop in the RCS pressure, an automatic reactor trip and actuation of the SIS and steam generator auxiliary feedwater systems.

When this occurs, operating personnel must identify and isolate the affected steam generator, shut down the SIS and cool the RCS *via* the unaffected steam generators to establish the operating conditions required to actuate the RHRS. If too much time elapses before the affected steam generator is isolated or the SIS is turned off, the steam generator fills up with water. This water may block open the discharge devices on the corresponding secondary loop (steam-dump valves and safety valves), thus allowing

coolant to leak outside the containment. If this occurs, the RCS must be depressurised to stop the leak.

SGTR (one tube or two tubes) accident scenarios that may lead to core melt include total loss of coolant from the secondary loop and failure of the SIS or implementation of feed and bleed by operators.

4.2.1.6. Accidents with total loss of heat sink or associated systems (H1)

These accidents involve either loss of the heat sink (unavailability of cooling water pumped in from a river or sea) at all the site's units and directly leading to loss of the cooling systems (particularly that of the ESWS) or failure of the cooling systems used to remove heat *via* the heat sink (particularly loss of the ESWS, the CCWS or the RHRS).

Loss of heat sink initiates a reactor trip; the RCS is cooled by the secondary loops, which are fed by the EFWS. However, the EFWS tanks are not limitless. If the heat sink is not restored after a certain time, cooling by the secondary loops will no longer be possible.

Loss of the CCWS leads to:

- shutdown of the RCS pumps;
- shutdown of cooling of the thermal barriers of the RCPs. This may lead to an RCS break in the event of failure of the flow of injection water to the RCPs;
- failure of cooling of the water released from the CVCS;
- failure of cooling of some ventilation systems, which may lead to equipment failures (e.g., some pumps);
- eventually, failure of containment cooling during operation of the SIS and the spray system during recirculation of the water in the containment sumps. The rise in the temperature of the water in the sumps may cause the recirculation pumps to fail.

In such an accident, intervention is required to bring the reactor back to a state where the flow of water to the RCP seals can be stopped without risk of damage to the seals (RCS pressure of no more than 45 bar and reactor-coolant temperature of no more than 190 °C). The RCPs are shut off and the RCS is cooled by the secondary loops with natural circulation through the RCS.

Core melt in a reactor at power may be caused by failure of the EFWS to supply the steam generators followed by failure to initiate feed and bleed or failure to maintain a sufficient amount of water in the RCS in the event of a break on the RCP seals.

In the case of the various reactor shutdown states and depending on the initial reactor state, core melt may be caused by failure of the EFWS, failure to maintain a sufficient amount of water in the RCS during the closed and partially open states of the reactor, or even failure of the makeup water when the RCS is initially open.

4.2.1.7. Accidents with total loss of the steam generator feedwater supply (TGTA-H2)

These accidents are caused by equipment failures that lead to simultaneous unavailability of the MFWS and the EFWS.

In these accidents, the secondary sides of the steam generators are quickly voided and lose their efficiency. The RCS heats up and its pressure rises to the set pressure of the pressuriser safety valves. The RCS empties and remains at high pressure until core uncover and melt occur. Core melt can thus occur while the RCS is pressurised. This poses a short-term threat for containment of the radioactivity released during core melt (ejection of corium into the containment during pressure-induced rupture of the vessel, resulting in "direct heating" of the containment (see Section 5.2.1), steam generator tube breaks).

To avert high-pressure core melt, reactor operators must:

- open the pressuriser safety valves (SEBIM valves) and actuate the SIS (feed-and-bleed operation) to cool the core;
- ultimately, restore the feedwater supply to the steam generators so as to establish the operating conditions allowing operation of the RHRS.

The accident scenarios most likely to lead to core melt assume here failure of feed and bleed in either the short term (failure of the SIS to actuate or operator error) or in the longer term (failure of the SIS to operate, failure of the CSS to cool the containment).

4.2.1.8. Accidents with station blackout (SBO – H3)

These accidents are initiated by the quasi-simultaneous failure of the two 6.6 kV emergency switchboards (LHA and LHB) or loss of offsite then onsite power due to a series of events damaging to the power sources and which in turn trips the reactor and cuts off power to the reactor's engineered safety systems.

If the RCS is closed when such an accident occurs, operators must attempt to bring the reactor back to a state where injection of water to the RCP seals is no longer necessary. They must do this using the turbine generator (LLS), the test pump (injection to the RCP seals), the TDAFWP (turbine-driven auxiliary feedwater pump) and the steam-dump valves. This state is characterised by an RCS temperature of no more than 190 °C and an RCS pressure of no more than 45 bar.

If the RCS is partially open when such an accident occurs, operators must attempt to bring the reactor back to an intermediate state where the RCS temperature is no more than 190 °C and the RCS pressure is no more than 45 bar. The test pump compensates for the water lost through the RCS vents.

If the RCS is open when such an accident occurs, a gravity-fed water-makeup system must be implemented as a short-term measure. This system is to be supplemented in the medium term by water injection by the adjacent unit's charging pump (900 MWe series) or the petrol water pump (1300 MWe and N4 series).

In all cases of SBO, the SBO generator (900 MWe series) or the combustion turbine (1300 MWe and N4 series) must be connected very quickly so that the systems enabling the reactor to return to a safe state may be restored to service.

The accident scenarios that may result in core melt include:

- failure of the TDAFWP (900 MWe series), the TDAFWPs (1300 MWe and N4 series) or injection of water to the RCP seals (which could lead to a break due to the loss of cooling) when the RCS is initially closed;
- failure of the RCS makeup when the RCS is open.

4.2.1.9. Loss of onsite power

The accidents discussed here are caused by loss of voltage on one or more low-voltage switchboards.

In some cases, this loss of voltage may lead to partial unavailability of the feedwater supply to the steam generators and of the injection of water to the RCP seals.

The accident scenarios that may lead to core melt therefore are primarily "TGTA-H2" scenarios (total loss of the steam generator feedwater supply and failure of feed and bleed) and scenarios that lead to breaks on the RCP seals and failure to maintain a sufficient amount of water in the RCS.

4.2.1.10. Transients involving automatic shutdown failure (ATWS)

The corresponding scenarios are caused by failure of the reactor to automatically trip upon insertion of the control rods following an internal initiating event that should result in an automatic trip.

These transients lead to loss of the MFWS and the EFWS is unable to remove the heat generated by the reactor core.

There may be three consequences:

- loss of integrity of the RCS when its design-basis pressure is exceeded;
- core damage (especially in the event of failure of cooling by the secondary side of the steam generators followed by failure of core cooling by feed and bleed);
- rupture of the steam generator tubes caused by the large difference in pressure between the primary and secondary loops.

4.2.1.11. RCS transients

The corresponding scenarios encompass RCS transients caused in particular by inadvertent operation of the SIS, uniform dilution (gradual drop in the boron concentration in the reactor coolant), non-uniform dilution (formation in the RCS of a water slug with low boron concentration that is subsequently injected into the reactor core), CVCS failure or uncontrolled rod withdrawal. These scenarios may lead to fuel degradation at each of the reactor's operational states.

In the levels 1 PSAs (both those of EDF and IRSN), the frequency of core melt due to uniform dilution is low compared to that of non-uniform dilutions. Based on studies to date of the potential consequences of non-uniform dilution, it is not possible to assess the risks of failure of containment integrity. For this reason, both EDF's and IRSN's level 2 PSAs use a simplifying assumption, i.e., short-term failure of containment integrity. As a result, in these level 2 PSAs, non-uniform dilution contributes significantly to the risk of large early releases. Licensees must therefore aim to "practically eliminate" the corresponding scenarios.

4.2.2. Melt frequencies by scenario type determined by the level 1 PSA for the 900 MWe reactors

As mentioned earlier, the level 1 PSA developed by EDF is the reference assessment. It results in a core melt frequency of around 4.6×10^{-6} per year and per reactor for all the scenarios described in Section 4.2.1.

After completing its level 1 PSA, following an update to take into account changes planned during the third ten-yearly outages (VD3) for the 900 MWe reactors, IRSN estimated core melt frequency² to be around 7.5×10^{-6} per year and per reactor for all reactor operational states. The contributions of the various types of scenario described in Section 4.2.1 are shown in Table 4.1.

Table 4.1. Distribution, by scenario type, of core melt frequency according to the findings of IRSN's post-VD3 level 1 PSA for the CPY 900 MWe series.

Scenario type	IRSN (post-VD3 update)	
	Core melt frequency (per year/reactor)	% of total core melt frequency
Loss-of-coolant accidents (LOCA)	1.2×10^{-6}	16%
Loss-of-coolant accidents occurring with containment bypass (V-LOCA)	2.2×10^{-7}	2.9%
Steam line break accidents (FWLB, SLB)	5×10^{-8}	0.7%
Steam generator tube rupture accidents (SGTR)	1.1×10^{-8}	0.1%
Total loss of heat sink or associated systems (H1)	1.3×10^{-6}	17%
Total loss of the steam generator feedwater supply (TGTA-H2)	1×10^{-6}	14%
Station blackout (H3)	2.9×10^{-6}	38%
Loss of onsite power (PDS)	5.1×10^{-7}	6.8%
Transients involving automatic shutdown failure (ATWS)	3.3×10^{-8}	0.4%
RCS transients ³	3×10^{-7}	4%
Total core melt frequency	7.5×10^{-6}	100%

- As indicated above, the term "core melt" encompasses situations leading to simple cladding failure as well as situations leading to total meltdown of the fuel in the reactor vessel.
- At the time of publication of this document, non-uniform dilution (which numbers among the accidents that can occur on the RCS) was undergoing a thorough review by IRSN in order to assess the new provisions proposed by EDF to prevent this type of accident.

The findings of EDF and IRSN's assessments show that the predominant scenarios are those caused by SBO.

4.2.3. Accident progression beyond core melt

The previous sections present the wide variety of scenarios liable to lead to core damage. However, it should be noted that although these scenarios can be triggered by different initiating events, they may lead to similar developments after core melt.

Indeed, understanding some of the characteristics of the state of the reactor at the time of core uncovering is sufficient to determine the subsequent evolution of the accident. These characteristics are used particularly in the interface between the level 1 PSAs and the level 2 PSAs, which will be discussed in Section 4.4. Examples of these characteristics include:

- **the point at which the core melt accident occurs**, as this determines the amount of residual heat in the core and thus the rate of progression of the accident;
- **the pressure in the RCS during the core melt accident**: particularly accidents where failure of the RHRS leads to high-pressure core melt situations, which lead to specific risks of damage to the containment;
- **the state of the engineered safety systems**, especially the availability of the CSS, which removes heat from the containment and removes airborne radioactive substances from the containment atmosphere;
- **core subcriticality**;
- **the state of the containment**, particularly its isolation or the presence of a bypass (loss of coolant through a break outside the containment) or even failed closure of the equipment hatch.

The similarities in the expected progression of the various core melt accidents make it possible to generically assess the various phenomena that may come into play during these accidents. These phenomena are presented in Section 4.3.

4.3. General progression of core melt accidents and their management at reactors in operation in France and for EPR

4.3.1. Physics of core melt and associated phenomena

4.3.1.1. Core uncovering

► Start of core uncovering

Core uncovering begins when the fuel rods are no longer completely covered by coolant due to a loss of coolant in the reactor core. Depending on the initial state of the reactor,

the initiating event of the accident, system failures and any operating errors, core uncover can be reached within a matter of minutes, hours or days of the initiating event. Core uncover leads to core melt only if a sufficient level of cooling cannot be restored.

For example, a 10 cm break in the RCS would, if water is not injected into the RCS by the SIS, lead to complete uncover of the fuel rods in 30 minutes.

► Core uncover with a pressurised RCS

The progression and consequences of the accident will vary depending on the pressure in the vessel at the time of uncover and vessel breach (as will be seen in subsections 5.1.4 and 5.2.1). In practice, a high-pressure core melt accident occurs when the vessel pressure is greater than approx. 15-20 bar (order of magnitude) at the time of breach.

A high-pressure core melt accident can occur in the following cases in particular:

- failure of the secondary side of the steam generators to cool the RCS;
- delayed core reflooding that causes the RCS pressure to rise to above 15-20 bar just before the vessel lower head is breached.

4.3.1.2. In-vessel fuel degradation (failure of the first containment barrier)

The physical phenomena involved in the progression of in-vessel accidents are discussed in Section 5.1. Section 5.1.1 explains core degradation in detail. Section 5.1.2 deals entirely with the behaviour of molten materials in the vessel lower head before it is breached. This section describes the steps involved in in-vessel fuel degradation.

► Oxidation and failure of fuel-rod cladding

As the water level drops in the reactor core, the uncovered part heats up under the action of the residual heat.

At normal operation, the Zircaloy cladding surrounding the core fuel is at a maximum temperature of 350 °C. At temperatures of 700-900 °C, the cladding becomes deformed due to the degradation of its mechanical properties.

During the accident, the pressure in the vessel may or may not be greater than the pressure of the gases⁴ in the fuel rods:

- if the pressure in the vessel is lower than the pressure of the gases in the fuel rods, the heat causes the cladding to swell until it bursts (Figure 4.1);

4. These are inert fill gases introduced into the rods during manufacture, and noble gases (particularly xenon and krypton) produced by the nuclear fission reactions that occur in the fuel pellets inside the rods. The pressure of these gases depends on the fuel irradiation time. For example, it can vary between 80 and 140 bar for a 1300 MWe PWR.

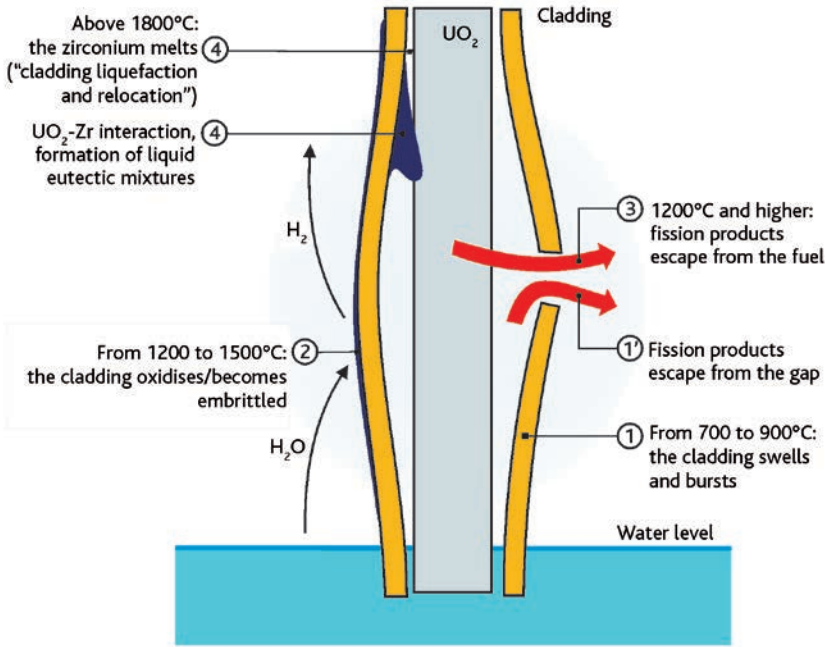


Figure 4.1. Degradation mechanisms of fuel cladding during severe accidents, at low pressure (gap: the space between the fuel pellet and the cladding which is filled with gas).

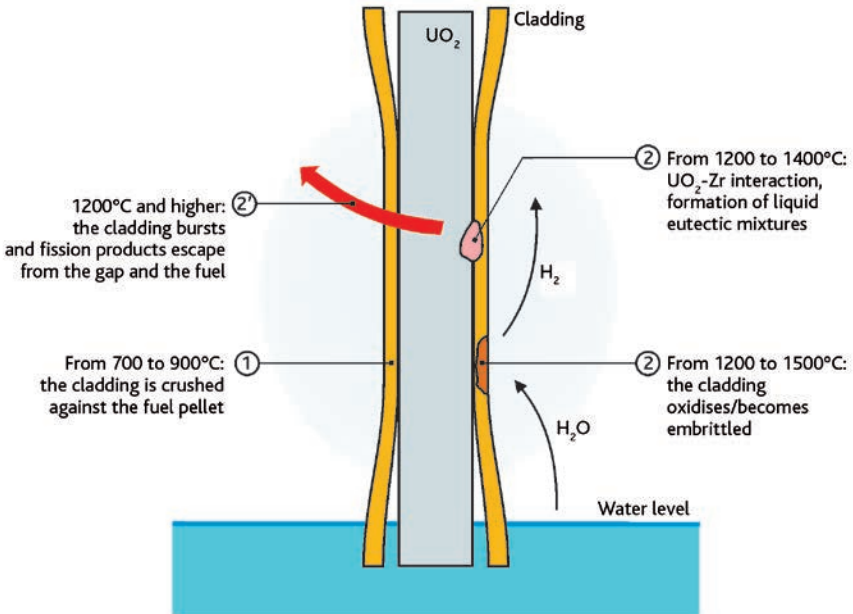


Figure 4.2. Degradation mechanisms of fuel cladding during severe accidents, at high pressure (gap: the space between the fuel pellets and the cladding which is filled with gas).

- if the pressure in the vessel is higher than the pressure of the gases in the fuel rods, the heat causes the cladding to push against the fuel pellets, promoting formation of uranium dioxide–zirconium ($\text{UO}_2\text{-Zr}$) eutectic with a melting point of 1200–1400 °C (Figure 4.2).

► Hydrogen release and melting of the core materials

During fuel uncover and degradation, the zirconium in the fuel-rod cladding oxidises on contact with the superheated steam⁵.

The oxidation reaction starts at around 1200 °C and accelerates considerably⁶ at around 1500 °C. However:

- oxidation is a highly exothermic chemical reaction. It locally releases heat that is more than the residual heat. If cooling is unable to remove this heat, both the temperature of the materials and the oxidation rate rise. This phenomenon is known as “reaction runaway”;
- the reaction releases hydrogen⁷ into the RCS. This hydrogen is carried all the way to the containment. If this hydrogen ignites inside the containment, it can cause a deflagration that, under certain conditions, leads to a detonation (the hydrogen risk in the containment is discussed in detail in Section 5.2.2);
- the cladding is embrittled and more vulnerable to thermal shock.

Furthermore, the rate at which fission products are released increases with the increase in the temperature of the fuel pellets.

Schematically:

- between 900 and 1800 °C, the metal components of the core either melt or vaporise (control-rod components, structural steel, non-oxidised Zircaloy in the cladding);
- above 1800 °C, the other core components (oxides, etc.) begin to melt.

Figure 4.3 shows schematically the main phenomena involved in degradation of core materials.

Temperatures of the order of 2800 °C are required before the uranium oxide will begin melting. However, the presence of eutectic mixtures with the zirconium and steel of the control rods may cause molten materials to melt and relocate at lower

5. According to the reaction $\text{Zr} + 2 \text{H}_2\text{O} \rightarrow \text{ZrO}_2 + 2 \text{H}_2$, with a ΔH of – 600 to – 700 kJ/mole of Zr and 0.0442 kg of H_2 produced per kg of oxidised Zr.
6. At 1500 °C, a cubic ZrO_2 phase appears in the oxidised cladding, in equilibrium with a tetragonal ZrO_2 phase, which is stable at temperatures below 1500 °C. As the oxygen diffusion coefficient is higher in the cubic ZrO_2 phase than in the tetragonal phase, the oxidation rate of the Zr speeds up very quickly.
7. Complete oxidation of 1 kg of Zircaloy produces around 0.5 m³ of hydrogen at normal temperature and pressure. Given the quantities of zirconium in the cores of the PWR units, this amounts to the production of around 1 kg of hydrogen per MWe.

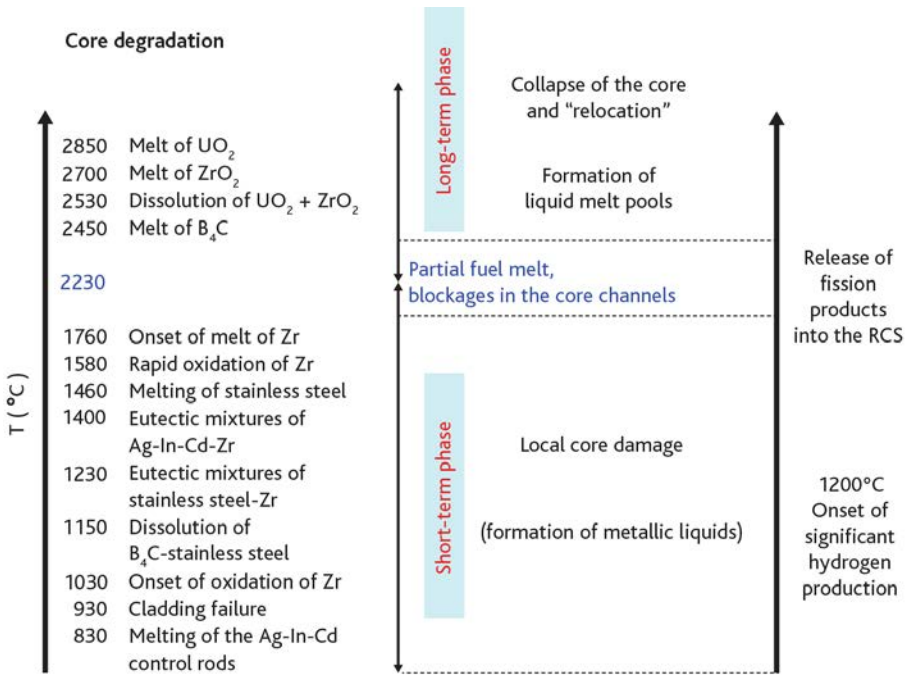


Figure 4.3. Main phenomena involved in reactor-core degradation.

temperatures. This melting causes a local then general collapse of the reactor core and the formation of corium, a molten mixture of fuel and the materials of the structures that support the fuel in the vessel during normal reactor operation. This mixture is kept molten by the residual heat from radioactive decay of the fission products trapped in the corium.

At these temperatures, the most volatile fission products almost entirely escaped from the fuel (Section 4.3.1.6).

4.3.1.3. RCS failure during a core melt accident (failure of the second containment barrier)

► Vessel-lower head failure

The lower head of the vessel may be breached within a matter of tens of minutes or hours following collapse of the component elements of the core. This interval depends on the corium mass in the vessel lower head, the heat released by this mass and the presence or absence of water to remove part of this heat through evaporation. Vessel failure is discussed in Section 5.1.3.

► Induced steam generator tube rupture

During fuel degradation, the hot steam exiting the reactor core and circulating by natural convection through the RCS causes the RCS structures to heat up excessively. If the RCS is pressurised during in-vessel core melt, these structure may yield and break. Induced rupture of the steam generator tubes would cause fission products to be released directly to the outside atmosphere *via* the safety valves on the secondary loops (for example, the safety valves on the 900 MWe units are set at 76 bar). The phenomenology associated with high-pressure core melt accidents is discussed in Section 5.1.4.

4.3.1.4. Phenomena that can cause early failure of the containment during a core melt accident (failure of the third containment barrier)

► Direct heating of gases in the containment

If the RCS is pressurised when the vessel is breached, corium may disperse into the containment as it flows out of the vessel and cause a sharp rise in pressure as the heat contained in the molten corium is rapidly transferred to the gases in the containment atmosphere. This phenomenon is known as "direct containment heating" and is discussed in detail in Section 5.2.1.

► "Hydrogen risk"

Hydrogen risk is the possibility of loss of containment leak tightness and integrity during hydrogen ignition. Hydrogen is mainly produced by oxidation of the zirconium in the cladding and of structures of the fuel elements during core degradation and by oxidation of the metals in the corium during the MCCI phase (Section 4.3.1.5). This hydrogen builds up inside the containment and can locally reach high concentrations that exceed the flammability threshold in the $H_2 + O_2 + H_2O$ gas mixture. The hydrogen risk is discussed in detail in Section 5.2.2.

► Steam explosion

The corium produced during a core melt accident may come into contact with water if it is present in the vessel lower head (if the molten corium relocates here) or in the reactor pit (if the vessel lower head is breached). As the corium is at a much higher temperature than the water, this contact can trigger a very energetic interaction. On contact with the water, the corium may be highly fragmented and cause massive, instantaneous vaporisation of the water. Known as a steam explosion, this phenomenon is discussed in detail in Section 5.2.3.

4.3.1.5. Phenomena that can ultimately lead to failure of containment integrity after a core melt accident

On contact with the corium, the concrete of the containment's basemat in the reactor pit begins to decompose under the effect of the heat emitted by the corium. Known as the molten core-concrete interaction or MCCI, this phenomenon leads to the production of a large amount of gases that causes the pressure inside the containment to progressively rise. It is discussed in detail in Section 5.3.

4.3.1.6. Release of fission products

When cladding failure occurs, the fission gases (krypton [Kr], xenon [Xe]) and other volatile fission products (mostly iodine [I], caesium [Cs], bromine [Br], rubidium [Rb], tellurium [Te] and antimony [Sb]) that have accumulated in the free volumes inside the fuel rods during operation of the reactor are released into the RCS. The same also occurs for a small portion of fission products in the fuel pellets.

The volatile fission products initially present in the fuel pellets are then progressively released as degradation of the in-core fuel propagates. Nearly all the volatile fission products will have escaped from the fuel by the time it starts melting. The various phases of release of fission products are described more in detail in Section 5.5.2.

Releases to the environment depend on physical and chemical conditions that affect the transfer of fission products in the facility from the reactor vessel to the containment. These transfers are determined primarily by the type of fission products (gas or aerosol) and their chemical form.

The mass of aerosols (fission products, heavy nuclei, materials of the structures and control rods) released into the containment during fuel degradation may be high (e.g., around 1500 kg for a 900 MWe PWR). These aerosols agglomerate and sediment. This results in reduction factors for the aerosol mass suspended in the containment atmosphere of between 300 (around 24 hours after the last releases) and 2500 (48 hours after the last releases). However, these values do not take into account aerosols that may be resuspended by, for example, dynamic phenomena inside the containment.

Special attention is focused on the behaviour of iodine given its complexity and the potential short-term radiological consequences of releases of radioactive iodine to the environment.

The main physical and chemical forms of iodine that can be found in the containment after a core melt accident are gaseous molecular iodine (I_2), particulate iodine (i.e., in aerosol form, such as caesium iodide [CsI]) and gaseous organic iodine (e.g., methyl iodide [CH_3I]). Among these three physical and chemical forms, organic iodine is the hardest for existing filtration systems to trap.

Very broadly speaking, during fuel-rod degradation iodine is released in the form of particles and gas into the RCS and then the containment.

In the containment, the gaseous molecular iodine:

- is rapidly adsorbed by the paint on the walls of the containment and reacts with this paint or the organic compounds emitted by it to create gaseous organic iodine. This organic iodine may be converted by radiation into iodine oxides, which are comparable to very fine aerosols;
- mixes with the water in the containment sumps if the CSS is actuated;
- is released outside the containment by direct or filtered leaks.

The iodine aerosols are deposited on the relatively cool walls and floors of the containment and, for example, are entrained to the containment sumps by the condensed water vapour. Depending on the physical and chemical conditions in the sumps and under the effect of the radioactivity, the iodine aerosols may enter into complex chemical reactions, the net effect of which is the production of gaseous molecular iodine that escapes into the containment atmosphere.

The noble gases (Xe, Kr) and the gaseous organic iodine are not deposited but instead released outside the containment by direct or indirect leak paths.

Releases, transfers and the chemistry of fission products are discussed in more detail in Section 5.5.

4.3.2. Containment failure modes

4.3.2.1. The Rasmussen report

4.3.2.1.1. Background

At the request of the US Nuclear Regulatory Commission, Professor Norman C. Rasmussen of the Massachusetts Institute of Technology (MIT), conducted from 1972 to 1975 a scientific investigation into hazards created by the use of nuclear-power reactors (pressurised water reactors and boiling water reactors).

This overall survey gave a systematic analysis of possible accident scenarios. The report's general conclusions were given as graphs showing the relationship between accident probabilities and "expected" numbers of cancer fatalities.

Published in 1975 under reference numbers WASH-1400 and NUREG 75-014, the Rasmussen report [1] is the first example of a comprehensive probabilistic safety assessment (PSA) giving figures for the probable impact on the population (level 3 PSA).

Despite the considerable uncertainties of the probabilities and consequences, French and international safety authorities tried to draw practical conclusions from this study to improve the safety of power reactors and intervention by public authorities in the event of an accident.

The Three Mile Island accident of 1979 (Section 7.1) fuelled discussions on these subjects.

4.3.2.1.2. Classification of the possible containment failure modes

Rasmussen's classification of the possible containment failure modes is still in use today. The five main modes are shown in Figure 4.4:

- mode α : steam explosion in the vessel or reactor pit caused by an interaction between the corium and the coolant, inducing loss of containment integrity in the short term;
- mode β : initial or fast-induced loss of containment integrity;
- mode γ : hydrogen explosion in the containment, inducing loss of its integrity;
- mode δ : slow overpressurisation of the containment, inducing loss of its integrity;
- mode ϵ : basemat melt-through by the corium, inducing basemat breach.

Mode V, which corresponds to bypasses of the containment by outgoing pipes, is dealt with separately, since it does not directly concern the behaviour of the containment building.

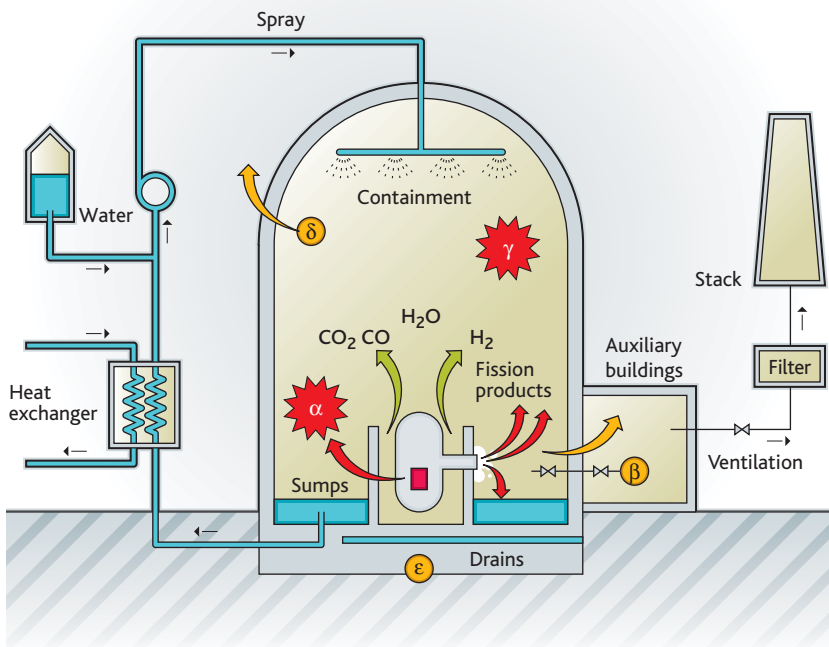


Figure 4.4. Schematic diagram of the possible containment failure modes according to the Rasmussen report [1].

4.3.2.2. Other failure modes

The possibility of loss of containment integrity by "direct containment heating" was identified in the early 1980s in the USA after the publication of the Rasmussen report.

Discussions held between 1987 and 1990 after the [Chernobyl](#) accident (Section 7.2) led to the identification of high-frequency accidents that can lead to significant reactivity insertion into reactor cores. Reactivity insertion is followed by a sudden and significant increase in the nuclear-power output of the reactor core and can trigger an explosion that would damage both the vessel and the containment.

Given its crucial importance for the consequences of a core melt accident, containment behaviour and its failure modes are the subject of many studies (Section 4.3.3.3). Chapter 6 of this document is devoted entirely to them.

4.3.3. *Management of core melt accidents at PWRs in operation in France*

4.3.3.1. Introduction

The resumption of core cooling and the preservation of the integrity of both the vessel and the containment resulted in very little radioactive material being released to the environment during the core melt accident at TMI-2 (Section 7.1).

Yet, for several days the plant's management as well as local and federal US authorities wondered how the accident would progress and if it could lead the reactor to explode or the containment to fail and release significant amounts of radioactivity to the environment. The contradictory information given by the authorities, which were unable to assess the severity of the accident, spread panic throughout the populations within the vicinity of the nuclear-power plant. Nearly 200,000 people fled the area. Although its radiological consequences remained very limited, the accident prompted a major national crisis. It became apparent that it was vital to devise provisions and means for managing core melt accidents in a less improvised manner.

A twofold approach was adopted: (i) implement short-term provisions and means to better prevent core melt accidents and mitigate their consequences and (ii) expand research to improve knowledge of the physics of this type of accident. The provisions and means put in place included implementing specific procedures and a new operating organisation (see Section 2.5.2), improving the integration of operating experience feedback and the development of simulation tools and resources for managing emergencies.

It therefore quickly became apparent that if the authorities were to be able to take the most appropriate and timely decisions to ensure the protection of people and the environment, it was vital to have a deeper understanding of the behaviour of containments, even under conditions far removed from those considered for their design, and the implementation of tools for simulating the potential developments of an accident, the corresponding releases and their transfer to the environment.

Studies were therefore conducted to:

- investigate the possible containment failure modes (presented in the previous section) and assess the resources required to address them under the best possible conditions. This type of study subsequently went hand in hand, both at EDF and IRSN, with the development of level 1 and level 2 probabilistic safety assessments (Section 4.2 and Section 4.4);
- determine the environmental releases corresponding to different core melt baseline accidents (Section 4.3.3.2).

EDF used the lessons learnt from this work to draft severe-accident operating guidelines (GIAG) (Section 4.3.3.4). These guides define the specific actions to be taken during severe accidents in order to ensure, for as long as possible, the best possible containment of radioactive substances.

The French public authorities plan to implement measures to protect populations near nuclear sites (Section 4.3.3.5) in addition to the general measures enacted as part of the ORSEC-RAD plan.

The main provisions taken in France to manage core melt accidents in operating reactors are described in the following sections and are summarised in Figure 4.5.

4.3.3.2. Classification of releases associated with core melt accidents

► Definition

IRSN has determined specific types of releases, known as “source terms”. A source term is a specific type of release characteristic of a family of reactors and representative of a type of accident, i.e., in general a containment failure mode following complete core melt. The source term is taken into consideration when defining corrective actions to be taken to protect people under these conditions.

Three source terms, listed in decreasing order of severity, were defined in 1979:

- source term S1 corresponds to short-term containment failure occurring no more than a few hours after the onset of the accident;
- source term S2 corresponds to direct releases to the atmosphere following loss of containment integrity occurring one or more days after the onset of the accident;
- source term S3 corresponds to indirect, delayed releases to the atmosphere through pathways allowing a significant amount of fission products to be retained.

Table 4.2 lists the orders of magnitude for these source terms for a 900 MWe reactor.

Broadly speaking, the primary aim of the research conducted on severe accidents to improve the safety of facilities was to eliminate, *via* adequate provisions and means, accidents liable to lead to S1 and S2 releases.

IRSN and EDF are currently conducting research to mitigate the consequences of accidents regardless of their severity in addition to eliminating the most severe accidents.

Table 4.2. Source terms S1, S2 and S3 for a 900 MWe PWR expressed as percentages of the initial activity of the radioactive substances present in the reactor core.

Source term	S1	S2	S3
Noble gases	80	75	75
Inorganic iodine	60	2.7	0.3
Organic iodine	0.7	0.55	0.55
Caesium	40	5.5	0.35
Tellurium	8	5.5	0.35
Strontium	5	0.6	0.04
Ruthenium	2	0.5	0.03
Lanthanides and actinides	0.3	0.08	< 0.005

► Radiological consequences

The initial S3 source term comes from the now-dated investigation of an accident scenario in the Rasmussen report [1] that was adapted to French reactors. It was partially updated in the late 1980s after emergency procedures were put in place in French reactors. One procedure of note is the U5 procedure, which is associated with a system for decreasing the pressure inside the containment in the event of an accident (venting line with a sand filter that was subsequently retrofitted with a metal prefilter placed in the containment).

Since then, the baseline S3 source term is represented for studies by a delayed release filtered through the sand-bed filter. The release is assumed to spread somewhere between 24 hours and 48 hours after the onset of the accident. This source term is now periodically reassessed to take account of improved understanding of the behaviour of fission products.

The S3 source term was used in the 1970s to establish the technical foundations of offsite emergency plans (PPI), which are implemented to ensure short-term protection of people from environmental releases. The S3 source term is assessed for accident scenarios chosen for being "reasonably conservative" in terms of releases to the environment and offsite radiological consequences.

The doses received by people for an S3 release are estimated using the dose coefficient values established by key international organisations (defined in the publications of the International Commission on Radiological Protection [ICRP] [2]). These estimated doses are used to determine whether measures implemented as part of offsite emergency plans (evacuation, sheltering) to ensure short-term protection of people are "satisfactory" for S3 releases.

The radiological consequences for the environment depend primarily on short-term releases of iodine and longer-term releases of caesium (Section 5.5.1). In practical terms,

iodine releases “govern” short-term “management” of the accident while caesium releases govern medium- and long-term “management” of the accident.

► Improvement of understanding

Since the Three Mile Island accident, many experimental results have been obtained around the world regarding the phenomena associated with core melt accidents (see all of Chapter 5). France (in particular IRSN) played a major role in obtaining these results, particularly through the *Phebus-FP* programme, which was conducted at the Cadarache nuclear research centre (Section 7.3). Knowledge and understanding of the complex phenomena involved in such accidents have grown considerably. Likewise, abilities to predict changes in reactor-core state with the help of simulation tools have been significantly improved (see Section 7.1.4).

Nevertheless, new experimental data on issues such as the behaviour of iodine and ruthenium inside the RCS and containment, the interaction between corium and concrete of containment basemats and in-vessel reflooding of damaged cores during core melt accidents are expected to be obtained in the coming five years. International research programmes conducted to improve knowledge of the progression of core melt accidents and the associated releases are presented in Chapter 5.

4.3.3.3. Investigation of the possible containment failure modes

► Introduction

While the source terms were being defined, studies being conducted in France following the publication of the Rasmussen report looked at the various possible modes of containment failure at France's nuclear-power plants as well as the ways to strengthen this last barrier to release.

These studies were conducted with realism in mind. The aim was not to perform a safety demonstration using conservative assumptions but rather to pragmatically find ways to improve facilities having a set basic design and define procedures for protecting the population under the best possible conditions. A number of these improvements and procedures called for implementing additional equipment.

It was thus in the wake of the TMI-2 accident that ultimate procedures (U procedures) and associated provisions designed to avoid or mitigate the radiological consequences of core melt accidents were progressively introduced at all units in France's nuclear-power-plant fleet (Section 2.5.2). The Severe-Accident Operating Guideline (GIAG) defines the specific measures to be taken and, where imposed by the progression of an accident, implementation of ultimate procedures designed to ensure the best containment of radioactive substances for the longest possible time. Figure 4.5 summarises the main provisions taken in France to manage core melt accidents in operating reactors.

► Initial containment failure

During normal operation, containment integrity is continuously monitored by a system that is based on pressure measurements and is able to detect a large leak (open penetration or hatch). The isolation devices of the containment penetrations are periodically and individually inspected to ensure their integrity. Lastly, pressurising the containment (before the reactor is loaded for the first time then once every 10 years) makes it possible to compare the overall leakage rate of the containment with the technical requirements. All these inspections, which are presented in detail in Chapter 6, are carried out to assess containment leakage and prevent large leaks from forming when an accident occurs. It should be noted that direct leaks (uncollected leaks, discharged directly to the environment) are particularly important on account of their radiological consequences.

During an accident, direct leaks can occur if automatic isolation of containment penetrations fails or if the integrity of the containment hatches is lost. This mode of containment failure (referred to as mode β) is very important as it can allow radioactivity to be released directly to the environment from virtually the very start of an accident. Ensuring "satisfactory" protection of nearby populations would be impossible under such circumstances.

To cope with this, EDF developed the U2 procedure entitled "*What to do in the event of loss of containment integrity*". It defines the methods for monitoring containment integrity during accident situations (even non-severe accidents) once radioactivity rises to a specific threshold and for detecting and localising integrity breaches in order to correct them wherever possible. It supplements continuous monitoring of the containment leakage rate during normal operation, which only makes it possible to detect very large leaks.

The U2 procedure encompasses:

- conditions for containment monitoring by measuring the activity released by the stack and the activity in the containment sumps, the peripheral rooms and their ventilation systems; and by checking the states of the isolation devices;
- the actions to be taken, such as confirming isolation orders; localising leaks and implementing means to eliminate them; containment of rooms or, where the situation is under control and allows some containment penetrations to be reopened, reinjection into the reactor building of liquid waste collected in the peripheral buildings.

► Direct containment heating

The main risk associated with this phenomenon, which would be caused by corium breaching the vessel under pressure, is loss of containment integrity due to a rapid rise in the containment pressure. This rise in pressure is associated with corium fragmentation and diffusion of corium particles in the containment atmosphere, which cause the gases in the containment to heat up and may lead to combustion of the hydrogen there.

Direct containment heating is prevented by reducing the possibility of high-pressure core melt. This ultimately involves *intentionally* reducing the pressure in the RCS so that the pressure in the vessel is below 15 or 20 bar (order of magnitude) when it is breached.

Direct containment heating is presented in detail in Section 5.2.1.

► Hydrogen explosion in the containment

Combustion of all the hydrogen produced by oxidation of the Zircaloy cladding in the active part of the core (amounting to 80% of the total mass of Zr in the core) would produce a pressure pulse that could affect the containment integrity of French PWRs.

Faced with this risk of loss of containment integrity from hydrogen combustion, in 2001 ASN asked EDF to install passive autocatalytic hydrogen recombiners in all the reactors of France's fleet. EDF complied with ASN's request. This decision took into account neighbouring countries' decisions (e.g., Belgium, Switzerland and Germany) to install hydrogen recombiners.

The production and combustion of hydrogen as well as the associated risks (a hydrogen explosion in a containment can lead to loss of containment integrity [mode γ]) and the operation of a passive autocatalytic hydrogen recombiner are described in Section 5.2.2.

► Steam explosion in the vessel or reactor pit

A steam explosion may occur when hot, fragmented corium comes into contact with water present in either the vessel lower head or, after vessel melt-through, the reactor pit (water from the CSS).

The mechanical energy of a steam explosion in the vessel could cause the vessel to burst and generate missiles that could endanger the integrity of the containment and particularly the vessel head. Mode α , as defined in the Rasmussen report, corresponds to an in-vessel steam explosion that induces loss of vessel integrity and rips off the vessel head.

Mechanical studies of in-vessel steam explosions conducted by several international experts have led to the conclusion that a direct loss of containment integrity induced by mode α is highly unlikely. However, vessel breach caused by an in-vessel steam explosion cannot be completely ruled out.

The energy released by a steam explosion induced by a flow of corium into a flooded reactor pit could compromise the strength of the structures adjacent to the reactor pit (particularly the adjoining walls and floors) and the strength of the various components of the RCS and especially the containment. R&D investigations are still being conducted on reactor-pit steam explosions. These investigations aim to demonstrate that such explosions do not lead to loss of containment integrity.

French operating units do not at present implement special procedures or provisions regarding the risk of containment failure in the event of steam explosions in a reactor vessel or flooded reactor pit.

One possibility could be to limit the amount of water in reactor pits to reduce or even eliminate (if the pits can be kept dry) the risk of steam explosions occurring in them. However, it should be emphasised that a large amount of water in reactor pits would make it possible to cool part of the corium before it comes into contact with the concrete basemat of the containment and could delay erosion of the basemat by the corium and even, in some cases, prevent basemat melt-through. Managing the water in reactor pits in the event of a severe accident is the subject of supplementary studies incorporating the R&D results for steam explosions.

Steam explosions are presented in detail in Section 5.2.3.

► Slow rise in the containment pressure

Mode δ corresponds to loss of containment integrity from overpressure due to heating of the containment atmosphere caused by insufficient removal of the heat generated by the fission products and to the progressive formation of a very large amount of gases during erosion of the basemat concrete by corium. Added to these gases may be steam from the water used to cool the corium in an attempt to slow its progress.

If the containment atmosphere is not cooled, its internal pressure will rise inexorably and could lead to a loss of containment integrity after a period of 24 hours.

In the face of the possibility of irreversible loss of containment integrity, it was found appropriate to have a means of controlling the pressure inside the containment by allowing filtered releases.

The adopted solution consisted in using a containment penetration intended to vent pressure from the containment during its initial and subsequent periodic pressure tests. Known as "filtered venting", this system consists of a set of valves, a relief valve and a sand-bed filter with a surface area of 42 m² and a thickness of 80 cm. The system is located outside the containment and sandwiched between the penetration and the stack.

Filtered venting is used to:

- limit then reduce the pressure inside the containment;
- reduce the activity of the aerosols in the released gases by a factor of at least 10;
- direct the filtered gases to the stack, where their activity is measured.

Tests of the filtration efficiency of such a sand bed and the optimisation of its geometry and the flow conditions through it were conducted in the early 1990s by IPSN in its research facilities in collaboration with EDF. These tests showed that it was possible to achieve, and even exceed, the minimum efficiency sought (i.e., a reduction factor of 10 for aerosols). The FUCHIA tests (at a filter scale of 1) showed that the filtration efficiency

of the filter sand was higher by one order of magnitude than the minimum efficiency sought for aerosols.

Nonetheless, in the event of an accident, the build-up of radionuclides in the filter sand could have led to problems of onsite radiation protection and filter cooling. Furthermore, the rapid condensation of the water vapour in the pipes could have caused a hydrogen deflagration (the hydrogen/steam mixture from the containment was made explosive by the rapid decrease in the steam concentration). Various additional provisions were thus implemented. One measure consisted in the addition of a prefilter on the filtered venting system inside the containment to filter aerosols while another entailed the addition of a heater on the line outside the containment upstream of the sand-bed filter. The prefilter lowers the radioactivity levels in the sand-bed filter. The line heater prevents the condensation of steam.

In the event of a core melt accident, the containment filtered venting procedure (known as U5) would be used only in close collaboration with the public authorities. The filtered venting system cannot be opened until at least 24 hours following the onset of an accident. This interval ensures that the system is used only when the concentrations of airborne radioactive substances inside the containment have sufficiently abated and allows time to implement appropriate measures to protect people (preventive evacuation, sheltering) from the releases that will be discharged to the environment by the filtered venting system.

► Melt-through of the containment concrete basemat by corium

Mode ϵ corresponds to loss of containment integrity due to corium melt-through of the containment basemat.

Basemat melt-through

In the current state of nuclear facilities and according to current knowledge, corium can completely melt through the basemat within a period of time that depends on the characteristics of the basemat (concrete type⁸, basemat thickness⁹) but is always greater than 24 hours¹⁰.

The MCCI and the associated risks are presented in Section 5.3.

8. Siliceous concrete or silico-calcareous concrete.
9. The basemat thickness varies between 2.25 and 4.0 m depending on the series. It was initially only 1.5 m thick at the units at Fessenheim (see Section 2.3.2.3 for more details), but was recently thickened by 50 cm.
10. In response to the conclusions of the safety review conducted during the Fessenheim plant's third ten-yearly outage, ASN asked EDF to implement provisions to increase the melt-through time in the event of a severe accident with vessel breach in Fessenheim units. EDF therefore increased the basemat thickness by 50 cm in the reactor pit and in an additional corium spreading area that was provisioned for corium spreading and cooling.

► U4 provisions

The initial design of the basemats of EDF's nuclear-power plants includes a network of drain pipes and penetrations (particularly for the basemat monitoring systems). Construction measures were therefore taken to prevent direct contact of corium with the environment in the event of basemat erosion (filling with injected mortar or sealing with adequate metal plugs welded on the ends of pipes that had not initially been closed off).

The units at the Cruas site posed a specific challenge. Each unit rests on a top basemat that is connected to a bottom basemat by anti-seismic bearings. The empty space between these basemats is connected to the outside air and, in the event of a core melt accident, could allow unfiltered releases to escape outdoors. This prompted EDF to establish specific provisions (known as U5 – Cruas and U4 – Cruas, respectively) to prevent such releases. These provisions entail:

- venting the pressure inside the containment until it equals that of the space between the basemats at the time of melt-through of the top basemat so that the contents of the containment atmosphere are not ejected into this space;
- completely flooding this space with water to reduce releases to the environment under the resulting effects of dilution, filtration and cooling, and adding sodium hydroxide to this water to obtain a basic solution that will dissolve the iodine in it.

► Bypass of the containment by outgoing pipes (mode V)

Loss-of-coolant accidents with containment bypass (known as V-LOCA) occur when coolant is lost through a break outside the containment in a loop connected to, but not isolated from, the RCS. V-LOCAs have two specific characteristics:

- as coolant is lost outside the containment, the recirculation of water in the SIS is impossible;
- in the event of core melt, fission products would be released directly outside the containment if the break is not isolated in time.

To prevent loss of containment integrity due to a V-LOCA, EDF implemented design and operation retrofits at all the reactors in France's fleet. In particular, these retrofits addressed the risk of containment bypass in the event of a break on the thermal barrier of a reactor-coolant pump and the portion of the affected CCWS. These retrofits are designed to practically eliminate V-LOCAs that might lead to significant short-term releases.

Containment bypasses are discussed in Section [6.4](#).

► Rapid reactivity insertion accidents

Cases of rapid reactivity insertion due to accidental injection of a water slug with a low boron concentration into the reactor core (these non-uniform dilution accidents may be caused by operator error, failure of the auxiliary systems or leaks on

steam generator tubes) are the subject of detailed studies that consist of the following three steps:

- definition of a maximum volume of a de-borated water slug for which core sub-criticality is demonstrated, on the basis of neutronic and thermal-hydraulic codes related to core subcriticality independent of the dilution accident considered;
- definition of provisions designed to ensure that this maximum volume is not exceeded during each of the dilution accidents considered;
- performance of a probabilistic assessment to determine the adequacy of the provisions implemented.

4.3.3.4. Severe-Accident Operating Guideline (GIAG)

The purpose of EDF's Severe-Accident Operating Guidelines (GIAG) is to provide emergency-response teams with the guidance needed to ensure that radioactive substances are contained as best as possible. The GIAG describes the possible actions and recommendations for mitigating the consequences of severe accidents. These actions and recommendations are the subject of discussions between EDF and IRSN's experts to take into account advances in the understanding of severe accidents.

When the GIAG is implemented¹¹, the priority is placed on safeguarding the containment rather than the reactor core.

When implemented, the GIAG overrides all other emergency operating procedures and responsibility for plant operation is transferred from the control-room operators to the emergency-response teams. The GIAG provides the emergency-response teams with the necessary guidance for defining the best system-usage strategies for safeguarding the containment. The control-room operators implement the operating actions requested by the local emergency-response team.

During their third ten-yearly outages, specific instrumentation is installed in the 900 MWe reactors to allow emergency-response teams to better assess the progress of core melt accidents and better inform the authorities about these accidents (containment hydrogen monitoring; detection of corium on the basemat of the reactor pit).

4.3.3.5. Radiological consequences of the S 3 source term and response plans of the public authorities

In the early 1980s the French public authorities explored the realistic possibilities of implementing measures to protect people (sheltering, evacuation) near France's nuclear sites. Based on the characteristics of these sites, the French authorities estimated that evacuating people located within a 5-km radius of a site and sheltering people located within a 10-km radius of a site would be possible within 12-24 hours

11. Main implementation criterion: the temperature of the gases exiting the core is greater than 1100 °C.

of the onset of an accident¹². They observed that implementing these measures would ensure a satisfactory level of short-term public protection against releases corresponding to the S3 source term, which at the time had been assessed in the light of the response levels recommended then by international organisations.

When assessing radiological consequences, the S3 source term can be described as a release resulting from use of the containment filtered venting system to vent the containment 24 hours after the onset of an accident leading to core melt¹³.

The radiological consequences are calculated based on the weather conditions. The results are expressed in terms of effective doses from the radioactive plume (external and internal exposure), ground fallout, ingestion and equivalent doses to the thyroid (primarily due to iodine). The results are assessed in the light of the applicable public-safety measures.

The public-safety measures that can be implemented during the emergency phase are indicated in the offsite emergency plans (PPI). The prefect may consider a number of public-safety measures:

- sheltering;
- ingestion of potassium-iodide tablets: people who may be affected by releases of radioactive iodine ingest the prescribed dose of potassium iodide when the order is issued by the prefect;
- evacuation.

The ICRP, first in publication 103 (2007) then in publication 109 (2009) [2] issued its recommendations for the protection of people in emergency exposure situations. The primary purpose of these recommendations is to contribute to ensuring an appropriate level of protection of the population and of the environment against the harmful effects of radiation exposure, including in emergency situations.

By virtue of ASN decision 2009-DC-0153 of August 2009, sanctioned by the Order of 20 November 2009, the French public authorities set the response levels for radiological emergencies at:

- an effective dose of 10 mSv for sheltering;
- an effective dose of 50 mSv for evacuation;
- an equivalent dose to the thyroid of 50 mSv for potassium-iodide administration.

These levels are intended to guide the public authorities in taking public-safety measures in the event of an accident. For example, in the event of an accident with releases forecasted to result in effective doses of 10 mSv throughout a 1-km radius, the French public authorities would shelter people located in a more than 1-km radius.

12. These distances have been adopted as the radii of action in the French authorities' offsite emergency plans (PPI) for all EDF sites in France.

13. Such a release is assessed for early-release accidents with large RCS break and failure of the SIS and CSS.

For the S3 source term, IRSN estimated that the doses for the most radiosensitive individuals would remain below the response levels within a radius of up to 6 km for evacuation and up to 18 km for potassium-iodide administration for average¹⁴ weather conditions and along the axis of the wind, assumed here to be constant. However, due to uncertainties in the understanding of the phenomena involved in core melt accidents and the dispersion phenomena of radioactive materials in the environment, it has not yet been deemed advisable to change the radii of the offsite emergency plans (PPI) for France's nuclear-power plants.

Independent of its immediate radiological consequences, the Chernobyl accident (Section 7.2) highlighted the extent of long-term social and economic disruptions due in particular to contamination of food supply chains.

Restrictions on the distribution of foodstuffs, set beforehand by the European Commission (maximum permitted levels [MPL] of radioactive contamination of foodstuffs), and which would be automatically enforced in the event of a new accident, are very low. In the case of releases corresponding to the S3 source term, distribution could be prohibited across distances far from the release site (more than 100 km) for periods of varying length depending on the radionuclides released.

These observations prompted a search for ways to significantly reduce the maximum conceivable releases for Generation III reactors (see Section 4.3.4 on EPRs) and to attempt to reduce, to the greatest possible extent, possible releases from operating reactors as part of a process of continual safety improvement.

Following the interministerial directive of 7 April 2005 on the measures to be taken by the public authorities in case of an event leading to a radiological emergency, ASN set up a steering committee for management of the post-accident phase of nuclear accidents or radiological emergencies (CODIRPA). The committee's mandate is to develop the policy on organisation of the actions of the public authorities following an accident. The first policy elements arising from CODIRPA's work (to read a general summary of CODIRPA's work, see the 29 January 2008 report on ASN's website www.asn.fr) led to the proposal of taking immediate actions (where warranted) right from the end of the emergency phase for the short-term post-accident phase and the long-term post-accident phase to:

- limit the exposure of the population;
- reduce land contamination;
- prohibit the consumption and distribution of contaminated foodstuffs;
- manage contaminated food waste;
- monitor radiation levels in exposed populations.

14. Normal diffusion and wind velocity of 7 m/s.



Accident progression	Provisions for preventing accidents and mitigating their consequences		Control
Loss of core cooling	H4-U3 procedures: mobile water-injection equipment (core engineered safety system)	Containment monitoring provisions: U2 procedure (containment isolation)	Emergency operating procedures
Cladding oxidation Melt	Catalytic recombiners for limiting the risks of an H2 explosion	U4 measure (with specific actions for the Cruas plant)	Severe-Accident Operating Guideline (GIAG) Priority placed on safeguarding the containment
Vessel melt-through	Provisions designed to avert high-pressure core melt and direct heating of the gases in the containment Improvement in reliable opening of the pressuriser valves Depressurisation of the RCS		Specific instrumentation for severe accidents (containment pressure, hydrogen content, detection of vessel melt-through)
Corium-water interaction Molten core concrete interactions (MCCI)	Water makeup operation strategy (SIS, accumulators, etc.) to cool the corium outside the vessel		Severe-Accident Operating Guideline (GIAG)
Radioactive releases	U5 procedure: filtered venting Containment venting Filtration of releases		ORSEC-PPI plan and ORSEC-RAD plan

Figure 4.5. Main provisions taken in France to manage core melt accidents in operating PWRs.

4.3.4. Approach adopted for EPRs

Ambitious safety targets have been set for France’s EPR since 1993. These targets aim in particular at significantly reducing radioactive releases that may result from all conceivable accident situations, including accidents with core melt. These targets have led to implementation of the design provisions described on the following pages.

The corium catcher, a new system engineered for EPRs, is an example of these provisions (Section 4.3.4.3). Its operation will have to be specifically demonstrated taking account of the related uncertainties.

4.3.4.1. General safety targets

The general EPR safety targets pertaining to severe accidents are specified in reference [4].

Accidents with core melt that may lead to large early releases (Section 4.3.2) must be practically eliminated. If they cannot be considered as physically impossible, design provisions must be taken to prevent them. This applies in particular to accidents with high-pressure core melt.

Accidents with low-pressure core melt must be managed such that the associated maximum conceivable releases only require public-safety measures that are very limited in terms of scope and duration. This may involve:

- no permanent relocation;
- no need for emergency evacuation beyond the immediate vicinity of the nuclear site;
- limited sheltering;
- no long-term restrictions on the consumption of foodstuffs.

As regards accidents with low-pressure core melt, given the wide range of possible accident conditions, compliance with this target must be demonstrated by calculating the radiological consequences of various representative accidents that have been defined by taking account of the detailed design of the facility.

4.3.4.2. “Practical elimination” of accidents that could lead to large early releases

“Practical elimination” of accidents that could lead to large early releases is a matter of judgement. Each type of situation must be considered separately. Practical elimination can be demonstrated by deterministic or probabilistic considerations, taking into account uncertainties due to limited understanding of certain physical phenomena. However, practical elimination cannot be demonstrated simply by compliance with a generic probabilistic cut-off value.

Accidents with core melt that must be practically eliminated through design are as follows:

- high-pressure core melt accidents that could lead to direct containment heating or steam generator tube rupture;
- rapid reactivity insertion accidents, in particular those caused by rapid injection of insufficiently borated water in the reactor core;
- in-vessel and ex-vessel steam explosions and global hydrogen detonations that could endanger containment integrity;
- core melt accidents with containment bypass (*via* the steam generators or the loops connected to the RCS).

► “Practical elimination” of high-pressure core melt situations

In order to avoid high-pressure vessel melt-through (pressure greater than an order of magnitude of 15-20 bar) or a steam generator tube rupture, the top of the pressuriser of the EPR has three pressure relief valves and two other valves, that provide either feed-and-bleed or emergency blowdown of the RCS for severe accidents. The three pressure relief valves protect the RCS from overpressurisation. For the other valves, the

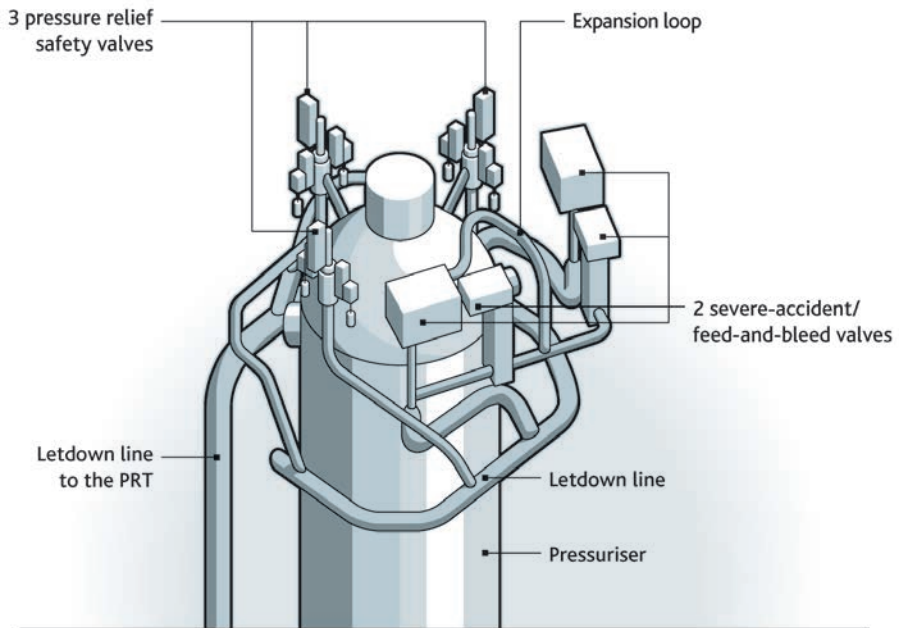


Figure 4.6. EPR – Emergency RCS blowdown system.

feed-and-bleed mode is used in the event of total loss of the steam generator feedwater supply; the emergency RCS blowdown mode is used to prevent high-pressure core melt. Either valve may be used for feed-and-bleed operation and emergency blowdown of the RCS. The three pressure relief valves and the two feed-and-bleed/high-pressure melt valves discharge to the same letdown line, which carries the water, steam or water/steam mixture to the pressuriser relief tank (PRT) (Figure 4.6).

In addition, design provisions have been adopted to limit the diffusion of fragmented corium particles in the containment atmosphere in the event of vessel lower head melt-through so as to avoid direct containment heating. These design provisions relate to the reactor pit and its ventilation system and are intended to prevent large amounts of corium exiting the reactor vessel from being carried from the reactor pit to the free volume of the containment.

► “Practical elimination” of rapid reactivity insertion accidents

Practical elimination of rapid reactivity insertion accidents by injection of a water slug with low boron concentration into the reactor core requires a detailed investigation of the various possible dilution scenarios that takes into account all the lines of defence for each scenario.

The investigation consists of the three steps discussed in Section 4.3.3.3.

► “Practical elimination” of the risk of steam explosion

In order to prevent steam explosions in the event of high-temperature corium flows into the reactor pit, EPRs are designed with provisions for preventing water from entering the reactor pit before vessel breach occurs, even in the event of rupture of an RCS pipe.

EPRs also feature design provisions that avert steam explosions by preventing water from entering the spreading compartment of the corium catcher before the corium reaches it.

► “Practical elimination” of the risk of hydrogen detonation

The design-basis pressure and temperature of the inner containment wall must ensure the integrity and leak tightness of the containment even after a global deflagration of the maximum amount of hydrogen that may be in the containment during low-pressure core melt accidents.

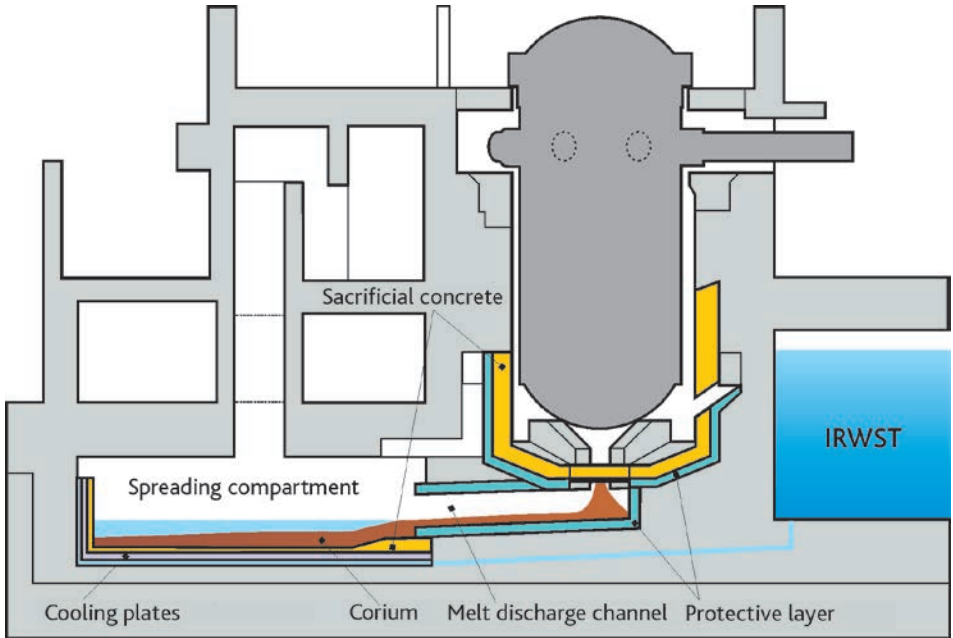
In addition, the volume of the containment and the mitigation means, such as the passive autocatalytic recombiners, must make it possible to reduce the hydrogen concentrations in the containment atmosphere to prevent the possibility of a global hydrogen detonation.

Lastly, the design of the containment internals must prevent, as far as reasonably possible, the possibilities of high local hydrogen concentrations. If it is not possible to demonstrate that the local hydrogen concentration remains below 10%, the absence of deflagration-to-detonation transition (DDT) and fast deflagration must be demonstrated. Failing this, adequate provisions must be implemented, such as reinforcement of the walls of the corresponding compartments and of the containment.

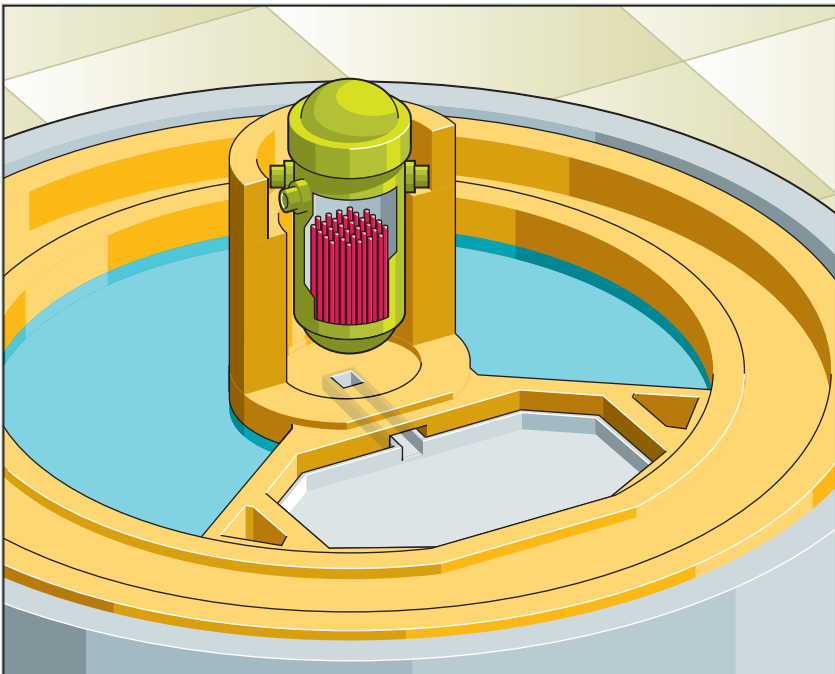
4.3.4.3. Provisions for low-pressure core melt

Design provisions have been adopted for low-pressure core melt accidents in order to comply with the aforementioned general safety targets. The main provisions are as follows:

- a corium catcher located at the bottom of the containment is used to retain and cool corium following vessel lower head melt-through (Figure 4.7). The corium catcher is designed to protect the containment basemat from MCCI. Corium is cooled in a spreading compartment. This compartment is separated from the reactor by a grid covered with a layer of sacrificial concrete and a discharge channel to protect it from thermomechanical loading caused by failure of the reactor vessel. Design provisions prevent water from any part of the containment from entering this compartment before the corium spreads along its surface. The reactor pit and spreading compartment are lined with layers of sacrificial concrete to obtain the adequate characteristics of the molten mixture. Once spread along the layer of sacrificial concrete in the spreading compartment, the surface



(a)



(b)

Figure 4.7. EPR. Diagram of the corium catcher: (a) cutaway view; (b) top view with the spreading compartment in the foreground.

of the corium is cooled by flooding it with water from the IRWST. In addition, the thermal loads imposed on the basemat are limited by a thick steel plate that is located under the layer of sacrificial concrete and cooled by cooling channels connected to the CHRS (see below);

- the design-basis pressure and temperature of the inner containment wall make it possible to ensure containment integrity and leak tightness in the event of a severe accident:
 - for at least 12 hours without removal of residual heat from the containment;
 - after a global deflagration of the maximum amount of hydrogen that could be present in the containment.
- a containment cooling system is used to remove residual heat, control the pressure inside the containment and preserve the long-term integrity and leak tightness of the containment in the event of a severe accident. This dual-train system is composed primarily of the IRWST, a specific heat exchanger and heat sink and a CSS. As mentioned above, this system may also be used to cool corium in the catcher. The dispositions for practical elimination of the risk of hydrogen detonation are given above;
- all the containment penetrations (including the equipment hatch) lead to buildings where the inside air is ventilated and filtered. There must not be any direct leakage pathway between the containment and the outside environment. Loops that may be used to carry radioactive substances outside the containment are contained inside peripheral buildings with suitable confinement capacities. Pressure-resistant penetrations in the containment must be designed to withstand loads resulting from core melt accidents.

Specific R&D programmes were required to develop the corium catcher and spreading compartment. These programmes are presented in Section 5.4.3.

4.4. *Level 2 PSAs: method and lessons from core melt accidents*

Over the past three decades, and particularly since the Three Mile Island accident in the USA, level 2 PSAs have occupied an increasingly greater place in nuclear-reactor safety assessments in France and abroad. Level 2 PSAs are now either required or recommended by national safety regulators around the world. In the case of Generation III reactors, these requirements or recommendations apply right from the design phase. For example, EDF provided ASN with a level 2 PSA for the commissioning of its Flamanville-3 EPR.

For each accident leading to core melt identified in the level 1 PSA, the level 2 PSA aims to determine, based on knowledge of the physics of core melt accidents and studies conducted with computer codes simulating such accidents, the evolution of the

accident, possible failures of the containment and the range and kinetics of radioactive releases into the environment with the corresponding probabilities.

Level 2 PSAs therefore make it possible to assess the type and extent of radioactive releases outside the containment that could be caused by core melt with the corresponding frequencies and contribute to assessing the overall safety of the facility. They make it possible to verify that the estimated frequencies of accidents that could lead to large releases to the environment are very low.

Level 2 PSAs are also used to assess the benefits of improvements to equipment (and particularly to existing systems) and procedures designed to reduce the probabilities of containment failure modes or mitigate the consequences of such failures in terms of releases. They may also contribute to the definition and introduction of systems for preventing severe accidents and mitigating their consequences as well as for improving the GIAG.

Lastly, they may also contribute to identifying and setting priorities for research programmes designed to improve understanding and modelling of the physics of core melt accidents.

In France, EDF and IRSN each developed level 2 PSAs for the 900 MWe reactors and, more recently, the 1300 MWe reactors. The PSAs developed by EDF are reference studies. In the period 2004-2009, the level 2 PSAs were used in particular to review safety during the third ten-yearly outages of the 900 MWe reactors. The rest of this section presents, for illustrative purposes, the method used by IRSN and gives examples of application of the level 2 PSA for the 900 MWe reactors as part of the safety reviews

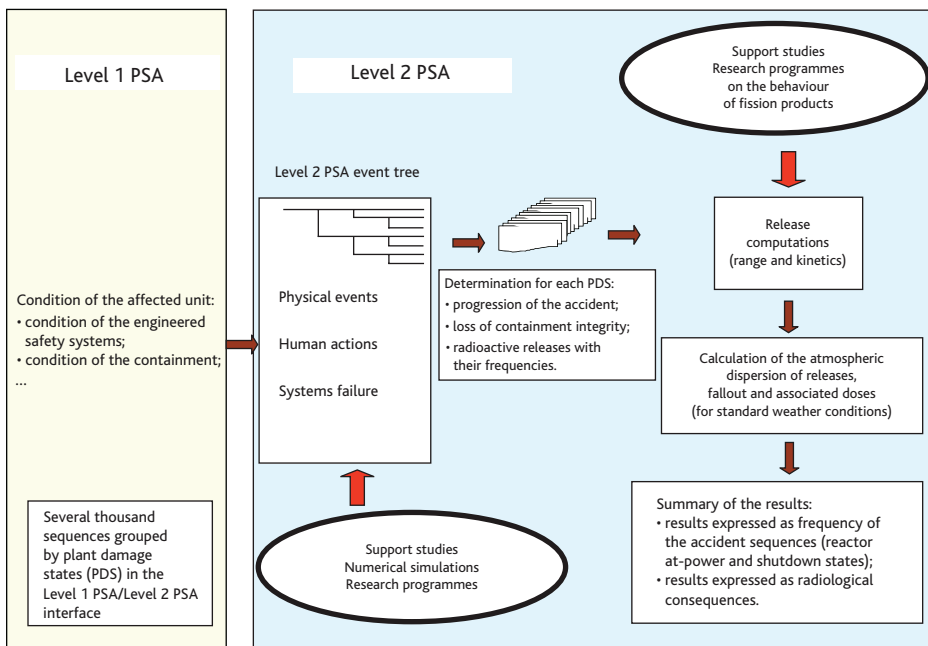


Figure 4.8. Method used for the level 2 PSA conducted by IRSN for the 900 MWe reactors.

conducted during the third ten-yearly outages of these reactors. This method is presented in Figure 4.8 and described in the following sections.

4.4.1. Methods of conducting level 2 PSAs

4.4.1.1. Interface with the level 1 PSA

Creating an interface with the level 1 PSA is the first step in carrying out a level 2 PSA. This interface must:

- ensure transmission of information on the state of the affected unit at the end of the level 1 PSA (particularly the state of the engineered safety systems, the containment, the RCS pressure, etc.) that might significantly affect the subsequent evolution of the accident and the possible containment failure modes and the extent of the releases in particular;
- group together sequences in the level 1 PSA (which generally has several thousand sequences) when they lead to an equivalent subsequent progression. Sequences having the same set of interface variables are grouped together in the same plant damage state (PDS).

The PDSs adopted make up the initiators of the event trees in the level 2 PSAs. Depending on the study methods used and the desired level of detail, as many as several dozen or several hundred PDSs may be considered when carrying out a level 2 PSA.

For example, in the case of the level 2 PSA conducted by IRSN for the 900 MWe reactors (known as EPS2 REP900), a little more than 300 PDSs were defined to group together the level 1 PSA sequences leading to core melt.

4.4.1.2. Severe accident event tree

The central element of the level 2 PSA is the event tree. This tree is used to describe all the events that may affect the progression of the severe accident up to the release of radioactive substances to the environment. The events in this tree may correspond to:

- physical events (core degradation and formation of a corium pool; cladding oxidation and hydrogen production; formation of breaks in the RCS for high-pressure accidents; steam explosions that may lead to failure of the reactor vessel and possibly the containment; direct heating of the gases in the containment due to a pressure failure in the vessel and leading to containment failure; corium erosion of the concrete basemat; mechanical failure of the containment; release of radioactive substances outside the core and their transfer into the facility);
- human actions such as recovery of a means of water injection for in-vessel cooling of the core or corium; depressurisation of the RCS; recovery of cooling by the steam generators; actuation of the CSS; actuation of the containment filtered venting system as well as errors in implementing the GIAG;
- system failures.

Once constructed, the event tree is used to determine, for each PDS, the various possible ways in which the accident may progress and the potential losses of containment integrity as well as assess the corresponding radioactive releases with their frequencies.

The models associated with the events are used to:

- assign conditional probabilities, particularly to human actions (success or failure of the action based on the quality of the available information, lead times, complexity of the decision process and the actions to be taken) or equipment failures;
- update the state of the facility following the event (e.g., state of containment integrity after an energetic phenomenon).

Models of physical events are developed primarily from numerical simulations conducted with tools such as the ASTEC code presented in Chapter 8 of this document.

Quantification of the events thus requires a large number of support studies (Section 4.4.1.4) designed to best determine the plant's behaviour.

IRSN's level 2 PSA for the 900 MWe reactors looks at more than 100 events, resulting in the quantification of the frequencies of several thousands of different sequences.

In addition, a Monte Carlo algorithm is used to explain and assess uncertainties during quantification of the level 2 PSA event tree.

4.4.1.3. Release categories

As the radioactive releases for each sequence in the level 2 PSA cannot be assessed, the sequences are grouped to obtain a limited number of release categories associated with a containment failure mode as well as a range and a kinetic of the radioactive releases. The range of the releases can then be estimated using severe accident computer codes, such as ASTEC or MAAP (see Chapter 8) or simplified models developed specifically for level 2 PSAs.

The various release categories and the associated frequencies make up the outcome of a level 2 PSA.

4.4.1.4. Level 2 PSA support studies

Developing a level 2 PSA requires conducting a large number of support studies to be able to determine the progression of the different level 2 PSA sequences and quantify their frequencies. Table 4.3 presents an indicative list of the aspects to be looked at in the case of a pressurised water reactor.

Drawn up as part of the ASAMPSA2 project¹⁵ of the 7th European Framework Programme for Research and Technological Development (FP7), this list illustrates two

15. The objective of the ASAMPSA2 (Advanced Safety Assessment Methodologies: Level 2 PSA) project was to develop best-practice guidelines for the development and implementation of level 2 PSAs based on feedback from 21 European partners involved in reactor safety. The project ended in 2012.

facts: (i) defining and conducting support studies make up most of the work involved in conducting level 2 PSAs and (ii) these support studies are largely based on research findings in the field of severe accidents. More information on this is provided in the subsequent chapters of this document.

While creating an event tree, determining the frequencies of the various categories of radioactive release and presenting the study findings constitute a smaller workload, they require methods that are specifically developed to the applications envisaged for level 2 PSAs.

Table 4.3. Studies required in order to conduct a level 2 PSA for a PWR.

Level 1 PSA/level 2 PSA interface
Level 1 PSA sequences are grouped together into PDSs that lead to the same type of severe accident progression, particularly in terms of containment failure mode and extent of the releases. Transients leading to core melt are investigated.
Human reliability analysis (HRA)
Identification of the human actions that may occur during the sequence (actions set out in the operating guidelines, emergency-response support, system recovery, etc.).
Quantification of the probabilities of failure of the various actions set out in the operating procedures.
Quantification of the physical phenomena and resulting loads for the containment In-vessel accident progression phase
Definition and calculation of representative thermal-hydraulic sequences for each PDS.
Fuel degradation.
Rupture of the RCS including rupture of the steam generator tubes induced by a high-pressure core melt accident.
Hydrogen production.
Restoration of core cooling (reinjection of water in the core).
Vessel cooling from outside through flooding of the reactor pit.
Investigation of the consequences of in-vessel water injection (corium cooling, increase in the kinetics of the production of hydrogen by oxidation of the zirconium in the fuel cladding, rise in vessel pressure, etc.).
Investigation of the composition of the containment atmosphere (role of the hydrogen recombiners and the CSS) and possible rise in the containment pressure.
Effect of opening of the containment filtered venting system.
Studies of the distribution and combustion of the hydrogen released into the containment.
Investigation of the risk of criticality from corium.
Investigation of the possibilities of in-vessel steam explosion and the associated consequences (leak in the RCS, mechanical failure of the vessel, loss of containment integrity).
Investigation of a vessel rupture (mechanical failure) (time before rupture, type of rupture, etc.).
Quantification of the physical phenomena and resulting loads for the containment Vessel rupture phase
Investigation of the phenomenon of direct containment heating if the vessel ruptures while it is pressurised.
Investigation of the consequences of a steam explosion in the reactor pit.
Investigation of the risk of criticality from corium.

Quantification of the physical phenomena and resulting loads for the containment Ex-vessel phase (MCCI)
Corium coolability.
Radial and axial erosion of the reactor pit walls and basemat (MCCI).
Impact of water injection (corium cooling, rise in containment pressure).
Assessment of the production of noncondensable gases (H_2 , CO, CO_2 , etc.) and steam during the MCCI.
Investigation of the change in the composition and pressure of the containment atmosphere.
Investigation of the distribution and combustion of hydrogen and carbon monoxide released into the containment.
Effects of opening of the containment filtered venting system.
Investigation of containment performance (integrity)
Investigation of the initial leakage rate (normal leakage rate, possible losses of integrity of some devices between periodic tests).
Investigation of the reliability of the containment isolation system.
Assessment of containment performance (integrity) under severe accident conditions.
<i>1 – Mechanical response of the containment when subjected to quasi-static or slow pressure or temperature loads – Assessment of the maximum mechanical strength and fragility curves of the containment. Break size assessment.</i>
<i>2 – Assessment of the response of the containment assumed to be subjected to specific loads (effects of a steam explosion in the reactor pit on the adjacent structures, effects of a local hydrogen deflagration, etc.).</i>
Assessment of containment penetration performance (integrity) under severe accident conditions.
Identification of possible containment bypasses (e.g., pipes in the basemats of some containments).
Investigation of containment in the auxiliary buildings (ventilation, filtration, dynamic containment, etc.).
Investigation of systems behaviour under severe accident conditions
Sump water recirculation and cooling system (removal of heat from the containment).
RCS safety valves (reliability of RCS depressurisation under severe accident conditions).
Steam generators (integrity of the steam generator tubes, steam generator cooling efficiency).
Instrumentation (availability of the reactor instrumentation under severe accident conditions).
Passive systems (hydrogen recombiners, etc.)
Core catcher (EPRs).
Quantification of radioactive releases outside the containment
Identification of key parameters for source-term assessment and definition of release categories.
Categorisation of fission product (FP) isotopes according to three volatility class (volatile FPs, noble gases, and semi-volatile or low-volatile FPs; see Section 5.5 for more information) and their physical form (aerosol or gas) in the containment.
Calculation of releases for representative sequences (use of integral codes such as ASTEC, MAAP or MELCOR (see Chapter 8), or use of simplified models developed specifically for level 2 PSAs.
Calculation of the radiological consequences for the level 2 PSA release categories (optional depending on the presentation of the level 2 PSA findings).

4.4.2. Applications of level 2 PSAs in France

Conducting a level 2 PSA entails conducting highly comprehensive studies on the expected behaviour of a facility in the event of reactor core melt.

These studies may be used to support identification of ways to improve reactor safety through better design or operation. Nevertheless, the numerical results of level 2 PSAs should be interpreted with great caution and associated, wherever possible, with an assessment of the uncertainties and considerations on the accuracy of the underlying assumptions (simplifications may be necessary for a level 2 PSA conducted during the design stage of a reactor whereas more detailed studies may be conducted at a later time once the design and operating procedures have been completed).

4.4.2.1. Use of level 2 PSAs during safety analyses

The 2002 basic safety rule (BSF) on the development and use of PSAs [5] established that PSAs, known as reference PSAs, must be carried out by the licensees of nuclear power plants and be submitted to ASN. As a result, IRSN reviewed these PSAs using independent studies of the same type.

Level 2 PSAs were used for the first time in a safety analysis, for reactors in operation, in the safety review associated with the third ten-yearly outages of EDF's 900 MWe reactors (VD3 900) between 2004 and 2009. The analysis of the level 2 PSA showed the main sequences that contribute to the risk of radioactive releases and the points for which design or operating changes had to be studied or implemented. A few examples are described in Section 4.4.2.2 below.

Since this first application, a level 2 PSA has been conducted for the safety review associated with the third ten-yearly outages of EDF's 1300 MWe reactors (VD3 1300) between 2010 and 2015. Level 2 PSAs are planned for all the following reviews.

4.4.2.2. Examples of application within the context of the safety review for 900 MWe reactors

4.4.2.2.1. Reinforcement of the equipment hatch

The containment of the 900 MWe reactors are designed to ensure their mechanical integrity and leak tightness against an absolute internal pressure of approx. 5 bar. Each containment is equipped with an internal steel liner to ensure its leak tightness. The mechanical integrity and leak tightness of the containments are checked periodically, particularly during the ten-yearly tests (tests at 5 bar absolute in air, see Section 6.2). Considering the vital role the containment can play in controlling severe accidents and their consequences, it was found appropriate to assess the ultimate mechanical strength of the containments beyond their design-basis pressure. As a result, mechanical strength tests were performed on containment models and detailed models for assessing the mechanical behaviour of these containments were developed (Figure 4.9). The findings of this research and studies are discussed more in detail in Section 6.3 of this document.

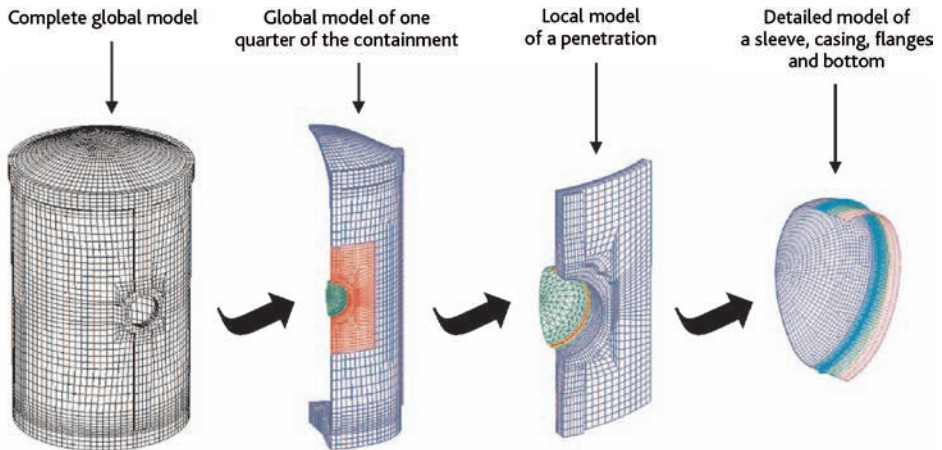


Figure 4.9. Example of models of the containments of the CPY 900 MWe units used to conduct detailed mechanical studies of these containments and illustrating in particular the detailed modelling performed for the equipment hatch.

Based on the results of the mechanical strength tests performed on the models and the results of the numerical simulations, IRSN and EDF deduced that the walls of the containments retained a satisfactory level of mechanical strength and leak tightness up to pressures well above their design-basis pressure (approx. 10 bar absolute) but that the equipment hatch closure system was a relative weak spot.

While developing its level 2 PSA for the 900 MWe PWRs, IRSN conducted detailed mechanical studies of the containment by constructing a fine-mesh model of the singular zones of the containment, particularly the equipment hatch. The results of these studies showed that, for some phenomena that may occur during a severe accident (direct containment heating [DCH] following mechanical failure of the pressurised vessel, hydrogen combustion after reflooding of the in-vessel core), the calculated loadings could jeopardise the integrity of the equipment hatch closure system.

Drawing on the results of these mechanical studies, the level 2 PSAs showed that these energetic phenomena (DCH, hydrogen combustion) that lead to a sharp rise in containment pressure contributed significantly to the risk of radioactive releases.

This conclusion led the licensee to reinforce the equipment hatch during the third ten-yearly outages. The planned reinforcement will make it possible to ensure the integrity of the equipment hatch up to a pressure of 8 bar absolute, which is significantly higher than the design-basis pressure of the containments.

Figure 4.10 shows the frequencies calculated during the level 2 PSA for the 900 MWe reactors conducted by IRSN for accidents leading to loss of containment integrity due to DCH or hydrogen combustion. Reinforcement of the equipment hatch closure system significantly reduces the risk of radioactive releases related to these energetic phenomena (frequency reduced by a few 10^{-7} /reactor-year). It should be noted that failure of the equipment hatch would result in direct releases to the environment.

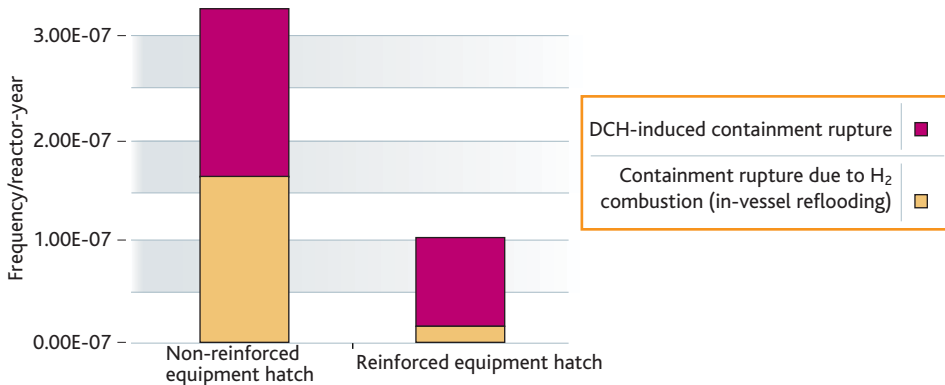


Figure 4.10. Effect of mechanical reinforcement of the equipment hatch closure system on the estimated frequency of accidents leading to loss of containment integrity.

4.4.2.2.2. Risk related to a steam explosion in the reactor pit

Due to the geometric characteristics of the reactor pit of the 900 MWe reactor series, the reactor pit and the top of the containment communicate. As a result, water may build up in the reactor pit if the CSS is operated. In the event of core melt and mechanical failure of the vessel, molten corium (at a temperature of around 1700 °C) may then flow into this water and trigger an explosive phenomenon known as a steam explosion.

While conducting its level 2 PSA for the 900 MWe reactors, IRSN studied this phenomenon using two codes: MC3D (to quantify the corium-water interaction phenomena) and EUROPLEXUS (to assess the strength of the structures). The study's conclusions showed that, under certain conditions, a steam explosion could generate vibrations violent enough to adversely affect the containment integrity.

The results obtained during the level 2 PSA for the 900 MWe reactors also showed that there are large uncertainties concerning the preceding conclusion. Figure 4.11 shows the calculated frequencies of accidents that may lead to large early releases and illustrates the results obtained in terms of the uncertainties about the frequencies of accidents leading to containment failure.

The positive aspects of the presence of water in the reactor pit (vessel cooling from the outside, cooling of corium prior to its interaction with the basemat) must be assessed further in order to determine whether the reactor pit should be intentionally flooded in the event of core melt.

Given the positive and negative effects of the presence of water in the reactor pit, IRSN therefore deemed it better to wait for the results of the R&D work on steam explosions to be consolidated before considering changing the design of the reactors or their operation under severe accident conditions. The assessment of the advantages and disadvantages of the various possible reactor pit flooding strategies is thus one of the matters that will be looked at during the third ten-yearly outages of the 1300 MWe reactors (2010-2015).

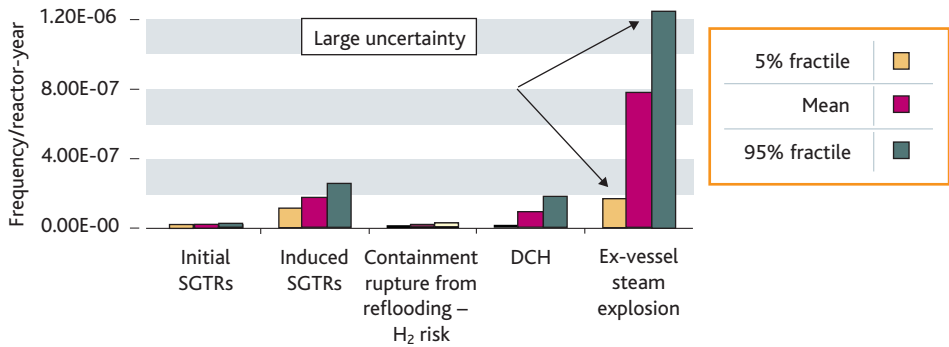


Figure 4.11. Quantification of the probability of containment failure – level 2 PSA for the 900 MWe reactors (EPS2 REP900)¹⁶.

4.4.2.2.3. Detection of mechanical vessel failure

During a core melt accident, very high temperature corium flows to the vessel lower head and may damage the vessel and lead to its mechanical failure (vessel melt-through). Calculating the progression of corium-induced vessel damage and the time to vessel failure is a decisive factor in predicting the progression of the accident.

If the RCS remains pressurised without any influx of water, vessel failure will inevitably occur shortly after corium reaches the vessel lower head. In all other cases, however, strong uncertainties exist as to the time to vessel failure (and even the possibility of such failure occurring).

These findings prompted IRSN, during the safety review associated with the third ten-yearly outages of EDF’s 900 MWe reactors, to recommend the installation of a means of detecting vessel failure to allow the emergency response teams to assess the progression of the accident.

As a result, ASN asked EDF to install a thermocouple in the reactor pit during the third ten-yearly outages of its 900 MWe reactors in order to be able to detect corium in the reactor pit. It also asked EDF to ensure the availability of this thermocouple over time.

4.4.2.3. Feedback on R&D

Conducting a level 2 PSA reveals areas where additional results should be obtained through R&D (i.e., cases where assessing the significance of one or more phenomena for the progression of an accident does not seem robust enough to allow clear operational conclusions to be drawn).

Three examples are discussed below.

16. SGTR: steam-generator tube rupture. Initial SGTRs (rupture of one or more steam-generator tubes weakened by corrosion, fatigue or wear) are accident initiators. Induced SGTRs are triggered by high-pressure core melt.

4.4.2.3.1. Strategy for managing severe accidents prior to vessel failure

During a severe accident, core cooling failure may lead to degradation and melting of the fuel rods. If the operators are able to restore the SIS and CSS during the accident, two actions may be taken to limit the progression of the accident:

- use the SIS to send water back into the vessel in order to cool the fuel;
- decrease the pressure in the containment if necessary and use the SIS to remove airborne fission products.

Precautions must be taken considering that:

- injecting water into a vessel with a damaged core may accelerate the production of hydrogen and repressurise the RCS;
- using the CSS to decrease the pressure in the containment will make the containment atmosphere less inert and increase the risk of hydrogen combustion (the CSS causes the steam – an inerting agent – in the containment atmosphere to condense).

While conducting their level 2 PSA for the 900 MWe reactors, IRSN and EDF closely studied these control actions and their possible consequences in order to propose recommendations in the GIAG. These studies showed:

- the existence of a strong coupling of the phenomena (e.g., starting up the CSS whilst reducing the containment pressure also helps to limit the amplitude of pressure spikes that may result from a hydrogen combustion event);
- the difficulty in using the available simulation tools to predict hydrogen production, the rise in pressure in the containment and the possibility of corium cooling during in-vessel reflooding of a partially melted core.

Implementing the current recommendations in the GIAG for operating the in-vessel water makeup and the CSS to prevent hazardous situations is complex. The findings of IRSN's level 2 PSA reinforce the recommendations in the GIAG for limiting the risk of containment failure during in-vessel core melt. However, they also show that special attention must be placed on the possibilities of human error occurring during implementation of these recommendations. The only way to reduce the possibilities of human errors would be to simplify the GIAG.

In the light of this, IRSN launched two R&D programmes with EDF's support. The programmes are designed to obtain a better understanding of reflooding of a partially degraded or melted core and the hydrogen risk related to use of the CSS as well as develop the associated models:

- a programme on reflooding of a degraded core with formation of a bed of solid debris in the vessel (configuration that was observed in the vessel of the damaged reactor at Three Mile Island, see Section 7.1). This programme will include experiments in the PEARL facility designed by IRSN as well as the development of models for the ASTEC code to verify whether it is possible to cool debris beds

with varying properties (debris size, homogeneity and porosity of the debris bed, etc.) This programme is discussed more in detail in Section 5.4.1;

- the ENACEFF programme (with CNRS), which consists of tests designed to better characterise situations of hydrogen combustion in the presence of droplets produced by the CSS. The objective is to determine the effect of the droplets on flame acceleration in the event of hydrogen combustion and verify whether this acceleration can lead to a transition to detonation. This programme is discussed more in detail in Section 5.2.2.

4.4.2.3.2. Strategy for managing severe accidents after vessel failure

As explained above, the studies conducted by IRSN in support of the level 2 PSA for the 900 MWe PWRs revealed a probability of containment failure in the event of a steam explosion in the reactor pit as well as strong uncertainties about the occurrence of this phenomenon.

Margins on the preservation of containment integrity may be due to the mechanical strength of the civil engineering structures. However, their assessment requires the use of more accurate (3D) and validated models.

Furthermore, the possible positive effects of the presence of water in the reactor pit have yet to be adequately determined. Indeed, it is currently hard to assess just how much the water in the reactor pit would cool corium and prevent it from melting through the basemat.

Only advances in knowledge will make it possible to answer these questions more precisely. That is why IRSN is involved:

- in programmes designed to better characterise the phenomena involved in steam explosions through tests in the KROTOS (CEA) and TROI (KAERI) facilities (see Section 5.2.3). Although the OECD's SERENA2 programme on the subject ended in 2012, the lessons it provided show that R&D remains necessary in order to better assess the effects of steam explosions on containment integrity and leak tightness;
- in the development and qualification of the MC3D code (*ditto*);
- in the performance of 3D simulations of the mechanical resistance of the structures adjoining the reactor pit;
- in experimental programmes designed to better assess the interaction between corium and the concrete of containment basemats and the possibilities of stopping basemat erosion by corium (VULCANO [CEA] tests, MCCI [ANL] tests, etc.) and the development of simulation tools (Section 5.3).

4.4.2.3.3. Behaviour of hydrogen recombiners during severe accidents

Before being installed in the reactors in operation, the passive autocatalytic hydrogen recombiners were qualified, including by their manufacturers, to verify their efficiency under core melt accident conditions. Some tests conducted by IRSN showed that even though the gas mixture near the recombiners is inflammable, the high temperatures of the catalyst plates (heated by the recombination reaction between hydrogen and oxygen) could trigger hydrogen combustion. IRSN considered that it was necessary to determine the conditions that allow such combustion to occur and to better assess the risk of ignition of the containment atmosphere by the recombiners as well as the consequences on containment integrity. The possibility of the recombiners initiating hydrogen combustion is the subject of additional studies and research programmes of the OECD and SARNET. More information about these research programmes is provided in Section 5.2.2.

4.4.3. Conclusion on level 2 PSAs

Between 1990 and 2015, significant strides were made in understanding severe accidents and the tools used to study and simulate them as well as in the development of level 2 PSAs. IRSN's approach was to emphasise conducting realistic studies to determine priority areas for improvement of the design or operation of facilities. The realism of these studies increases with the advances made by the research programmes. In this way, the level 2 PSAs and codes for severe accidents presented in Chapter 8 contribute to integrating the most advanced knowledge for assessing the safety of facilities.

As regards the level 2 PSAs, and more generally severe accidents, international discussions and collaborations are very important today because they make it possible to confirm methods, studies and their conclusions [6], reach an international consensus on R&D priorities [7], and share the funding and findings of complex R&D programmes.

Level 2 PSAs were first applied for safety analyses with the safety reviews associated with the third ten-yearly outages of EDF's 900 MWe reactors. They were subsequently extended to the safety reviews associated with the third ten-yearly outages for EDF's 1300 MWe reactors and the review of the licence application for the Flamanville 3 EPR.

Efforts are also being made at IRSN to expand the scope of application of the PSAs to external hazards such as floods and earthquakes. The events that led up to the Fukushima-Daiichi accident show that such developments are necessary in order to better assess the risks at nuclear facilities.

References

- [1] N. Rasmussen *et al.*, *Reactor Safety Study*, WASH-1400, Washington D.C., US NRC, 1975.
- [2] (a) The 2007 Recommendations of the International Commission of Radiological Protection, ICRP Publication 103, *Annals of ICRP* 37 (2-4), 2007.

- (b) Application of the Commission's Recommendations for the Protection of People in Emergency Exposure Situations, [ICRP Publication 109](#), *Annals of ICRP* **39** (1), 2009.
- [3] Arrêté du 20 Novembre 2009 portant homologation de la décision n°2009-DC-0153 de l'Autorité de sûreté nucléaire du 18 août 2009 relative aux niveaux d'intervention en situation d'urgence radiologique, NOR: SASP0927660A.
- Accessible on <http://www.legifrance.gouv.fr>
- [4] Décret n° 2007-534 du 10 avril 2007 autorisant la création de l'installation nucléaire de base dénommée Flamanville 3, comportant un réacteur nucléaire de type EPR, sur le site de Flamanville (Manche), NOR: INDI0700460D, version consolidée au 11 avril 2007.
- Accessible sur <http://www.legifrance.gouv.fr>
- [5] ASN – Règle fondamentale de sûreté n°2002-01 – Développement et utilisation des études probabilistes de sûreté pour les réacteurs nucléaires à eau sous pression. <http://www.asn.fr/Informer/Actualites/Regle-fondamentale-de-surete-RFS-n-2002-01>
- [6] E. Raimond, S. Güntay, C. Bassi, D. Helton, A. Lyubarskiy, Some international efforts to progress in the harmonization of Level 2 PSA development and their applications (European (ASAMPSA2), US NRC, OECD-NEA and IAEA activities), OECD/NEA Workshop on Implementation of Severe Accident Management Measures (ISAMM 2009), Switzerland, OECD/NEA/CSNI/R(2010)10, Dec. 2010, <https://www.oecd-nea.org/nsd/docs/2010/csni-r2010-10-vol1.pdf>
- [7] (a) T. Albiol *et al.*, SARNET: Severe accident research network of excellence, *Progress in Nuclear Energy* **52**, 2-10, 2010.
- (b) B. Schwinges *et al.*, Ranking of severe accident research priorities, *Progress in Nuclear Energy* **52**, 11-18, 2010.

Chapter 5

Development of the core melt accident

5.1. Development of the accident in the reactor vessel

5.1.1. Progression of the core melt in the reactor vessel

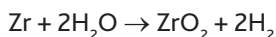
5.1.1.1. Introduction

If the reactor core remains dry for a considerable length of time, the temperature of the fuel rods rises and may locally reach levels that cause significant and irreversible core degradation. The mechanisms of this degradation are both chemical and mechanical. Depending on the local temperature levels, degradation may result in more or less severe hydrogen production, fission product (FP) release, and molten corium formation and propagation towards the lower head. These phenomena have been studied in many national and international research programmes [1, 2, 11, 12, 15, 22]. The main degradation mechanisms that appear as the core temperature rises, as well as their consequences, are described in Section 5.1.1.2. This description is followed by a presentation of the main experimental programmes that have increased the state of knowledge of the degradation mechanisms, as well as a description of the modelling and computer codes that capitalise on that knowledge. The main mechanisms involved in the evolution of the fuel rod and core degradation are schematically shown in Figures 4.1, 4.2 and 4.3 of the previous chapter.

5.1.1.2. Physical phenomena

5.1.1.2.1. Cladding oxidation and hydrogen formation

At temperatures above approximately 1300 K, the zircaloy in the cladding is exothermically oxidised by the steam. This reaction plays a major role in aggravating the core degradation, as the thermal power that it releases can become significantly higher than the residual power. The equation of this oxidation reaction is as follows:



with an enthalpy reaction ΔH between -600 and -700 kJ/mole of zirconium and 0.0442 kg of hydrogen produced per kg of oxidised zirconium.

This oxidation produces a zirconia (ZrO_2) layer on the external surface of the cladding. The mass of oxygen absorbed by the cladding and the thickness of the oxide formed are governed by a parabolic time law. The square of the increase in the mass of oxygen fixed by the zirconium ΔM_o is proportional to the time interval Δt , that is to say:

$$(\Delta M_o)^2 = K_o(T)\Delta t$$

The reaction rate $K_o(T)$ varies as an exponential function of the inverse of temperature (Arrhenius law) and, at temperatures above 1600–1700 K, the energy supplied to the cladding by the reaction cannot be evacuated by convection with the steam; the reaction rate then increases rapidly, resulting in the cladding temperature exceeding the zirconium melting temperature (2100 K). Numerous experimental and theoretical studies have focused on this phenomenon, which is now well understood. The hydrogen produced can escape from the RCS (through a break, if there is one) into the containment building atmosphere; this results in an explosion risk regarding which the strength of the containment must be assessed. Knowing how to predict hydrogen production is therefore an important aspect of the safety studies, as we have already discussed in Section 4.3.

In the case of the 1300 MWe PWRs, the control rods are partly composed of boron carbide B_4C (Section 2.3.2.1). This can also oxidise at temperatures above 1600 K, producing hydrogen. Little hydrogen is produced through this reaction, however, in comparison with the volume of hydrogen produced by the zirconium oxidation reaction. In the case of 900 MWe PWRs, the Ag-In-Cd alloy in the control rods does not oxidise.

5.1.1.2.2. Meltdown of materials and interactions with the intact rods

The control rods melt at lower temperatures than the fuel rods, either through meltdown (the Ag-In-Cd alloy melts at temperatures above 1100 K) or, in the case of the 1300 MWe reactors, through a chemical reaction resulting in their liquefaction (with steel, the B_4C forms a liquid eutectic mixture at temperatures above 1500 K). The B_4C may also oxidise once the steel cladding and the zircaloy guide tube have disappeared. B_4C oxidation is an exothermic process, effectively accelerating control rod degradation. It also produces hydrogen (always through steam decomposition, as for Zr oxidation), and part of the boron is in gaseous form (HBO_2).

After they melt, the control rod materials (including some steel) flow into the core and come into contact with the fuel rods, thereby weakening the cladding of those that are still intact through chemical interactions (forming eutectic liquids). It should be noted that the spacer grids made in Inconel may also react with the zirconium cladding. The major dissolution reactions include the Ag-Zr and Fe-Zr interactions, both of which form a eutectic liquid whose melting point is considerably lower than that of zircaloy. Experimental studies have been conducted on these interactions; the existing knowledge of these interactions and their modelling is satisfactory. Some uncertainties still remain regarding the influence of B_4C , however, as it seems to cause the cladding of the fuel rods to degrade at a lower temperature than that indicated by the models developed using the current state of knowledge.

5.1.1.2.3. Cladding failure

The increased fuel temperature and the formation of fission gas within the pellets increase fuel rod internal pressure. The zircaloy cladding begins to distort when the temperatures exceed 1000 K, due to the degradation of their mechanical properties. In some cases, the pressure inside the fuel rods can exceed the pressure inside the reactor vessel. This overpressure within the fuel rod causes the cladding to swell as a result of creep. This phenomenon, which is called “ballooning”, can cause a mechanical failure in the cladding before they are oxidised. Some major distortion, referred to as “flowering”, has also been observed. This is the result of the fuel pellets growing in volume, causing additional stresses in the cladding. There are sufficient experimental data on these phenomena, and their modelling is satisfactory.

During a core melt accident, not all of the fuel rod cladding suffers from mechanical failures before they oxidise. The oxidised cladding that has not failed mechanically may lose its integrity as a result of other mechanisms occurring at higher temperatures. These other mechanisms are much less well-known, however. The current hypotheses used to take them into account are based on experimental findings; consequently, it is accepted that the zirconia layer breaks above a certain temperature (typically around 2300 to 2500 K). Another mode of failure may occur when the thickness of the zirconia layer is less than a certain value (approximately 300 μm). The rupture mechanism involved is still poorly known, and it is modelled using a correlation deduced from the results of integral experimental programmes such as [Phebus](#) and CORA (Section 5.1.1.3.1), which use a rupture temperature that varies according to the thickness of the zirconia layer. In order to improve our understanding of the mechanism involved, it would be necessary to perform experiments that are both difficult and costly. Such experiments are not planned, as most users of the computer codes consider that the modelling described above is adequate for representing this mechanism in the computer codes used to simulate core melt accidents. It should nevertheless be remembered that the zirconia layer rupture criterion is a key parameter in these codes, as it defines the threshold for liquid zircaloy relocation towards the lower parts of the core.

5.1.1.2.4. Zircaloy melting and fuel dissolution

When the zircaloy melting point is reached, the UO_2 fuel is partially dissolved by the liquid metal (which does not flow out of the cladding as long as the zirconia layer remains intact). This may result in the mechanical integrity of the fuel rods being lost and the fragments produced in certain areas of the core accumulating long before the UO_2 melting point is reached (approximately 3100 K). The resulting fusion-dissolution, mechanical degradation and relocation of core materials within the reactor vessel (melts of molten materials and local accumulations of fragments) determine how the distribution of the degraded materials in the reactor core evolves during the course of the accident, and these must be taken into account in the modelling in order to realistically predict the degraded condition of the core. This can then be used to predict which areas are likely to be cooled if water is injected (reflooding) and which areas cannot be cooled because molten materials have accumulated, thereby preventing water from reaching them. Many experimental studies have been conducted in order to study changes in the distribution of the degraded materials in the core during the course of a core melt accident and considerable knowledge has been gained as a result, but the modelling is not yet satisfactory, undoubtedly due to the complexity of the phenomena involved. Despite the progress made (the development of mechanistic models based on detailed analyses of tests conducted on fuel rod clusters), some experimental results are still difficult to explain or interpret using the existing models, particularly the finding that fuel pellet dissolution exceeds the possible values based on the phase diagrams. It also remains difficult to model the simultaneous phenomena of fuel pellet dissolution and cladding oxidation. An ISTC (International Science and Technology Centre, a European Commission body) project named THOMAS, led by IBRAE (the Nuclear Safety Institute of the Russian Academy of Sciences in Moscow) resulted in the development of a model capable of computing the oxidation of a large corium pool (with natural convection processed in 2D or 3D) and the formation and dissolution of solid crusts at the edge of the pool.

5.1.1.2.5. Corium flow

The flow of the molten materials through the degraded core and their solidification in its colder areas may result in considerable localised reductions in coolant flow cross-sections (Figure 5.1 clearly shows this phenomenon), which directly affects coolant flow and the cooling of the degraded core. This flow depends on various factors including the viscosity of the molten mixture, which is a function of its oxidation degree. In the 2100–2900 K temperature range, the viscosity of a U-Zr-O mixture is an increasing function of the oxygen content. Knowing how to calculate the oxidation of such mixtures is thus particularly critical in determining the corium flow. The current understanding of this phenomenon is incomplete, notably because, in most of the experiments conducted (Phebus, CORA and PBF, described in Section 5.1.1.3.1), the corium globally flows in a single direction (a one-dimensional flow). It is likely, however, that corium radial flow would be just as important if not predominant¹ in the case of an accident affecting a reactor core. Various corium flow models provide partially satisfactory results, i.e. they

1. This is illustrated by the example of the Three Mile Island core melt accident, although this accident scenario is a special case (Section 7.1).

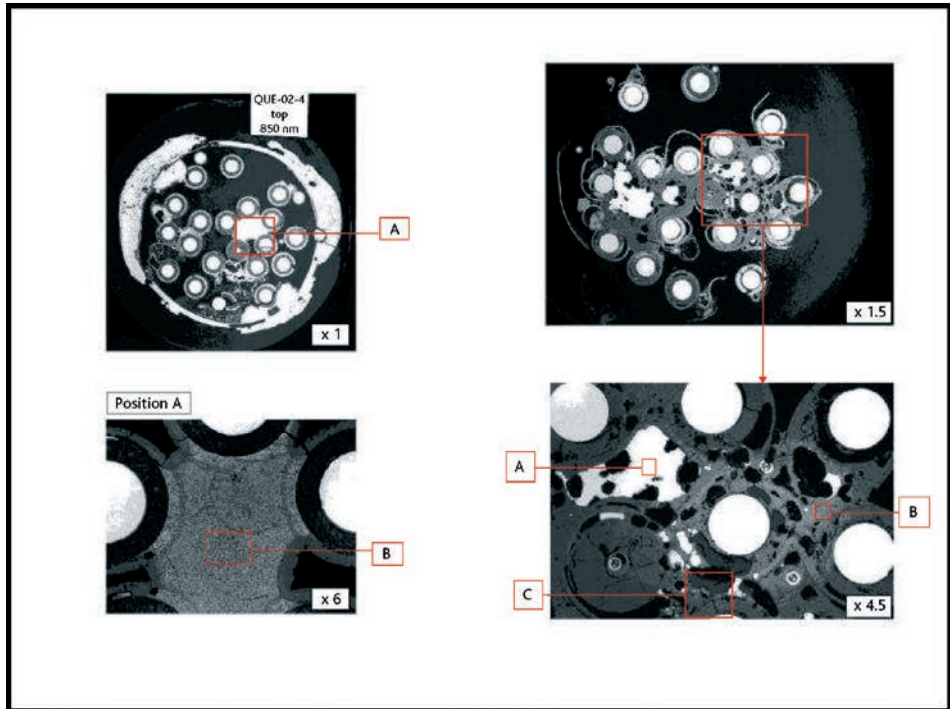


Figure 5.1. Photographs of two cross-sections of the fuel assembly after the QUENCH-02 test. These show the distribution of the solidified molten materials (melts) between the rods and the impact of these melts upon their degradation. The solidified melts are visible between the rods. They either totally block the spaces between the rods (position A, lower left) or partially block the spaces, leaving porosities (photograph, lower right).

generally predict the place in which the molten materials accumulate, but they are not capable of accurately predicting the resulting porosity (experimentally, it is found that the molten materials still do not occupy all of the available space). For the moment, however, it is not possible to improve them on the basis of existing experimental data. In the experiments conducted with corium melts, the corium flow is closely linked both with the localised temperatures reached in the tested fuel assemblies and with the degree of oxidation in the corium. These data cannot be determined sufficiently accurately from the experimental results or computed from the models, due to the complexity of the phenomena involved. Furthermore, in most of these experiments, corium progression is one-dimensional. The flow models have not been validated using sufficiently large-scale two- or three-dimensional test data. Uncertainties also remain regarding the physical properties of corium, notably its solidus and liquidus temperatures, as well as regarding the apparent viscosity (the viscosity of the liquid-solid mixture) where the solid and liquid phases are present simultaneously. These properties directly influence the corium flow.

5.1.1.2.6. Oxidation of the molten mixtures

When the corium flows through the core, it contains zircaloy that has not been completely oxidised. On contact with the steam, the zircaloy continues to oxidise. No experimental measurements of a U-Zr-O liquid mixture oxidation rate are available. However, during integral tests such as QUENCH (reflooding of an assembly of already-oxidised rods), substantial hydrogen production has been observed over a very brief period in the case of scenarios involving reflooding or a local increase in steam flow rate. This observation is particularly important when assessing the hydrogen explosion risk, as reflooding may lead to the instant hydrogen release rate within the containment temporarily exceeding the capacity of the hydrogen recombiners in the containment building concerned.

The QUENCH tests were the first that could be used to understand this effect, but they had two disadvantages. Firstly, the use of ZrO_2 pellets instead of UO_2 pellets forms a corium that is a Zr-O mixture instead of the U-Zr-O mixture that would be formed in a reactor core melt accident. Secondly, it is difficult to distinguish between the oxidation itself and the other phenomena (flow, cooling, etc.) in these integral tests; as a result, it is not possible to determine whether the materials oxidise while they are flowing or afterwards. The most likely explanation regarding the prolonged and intense oxidation of zircaloy is that of a relatively slow melt consisting of the very hot U-Zr-O liquid mixture (progressing at a speed of up to a few mm/s) along the fuel rods. The oxidation kinetics of such a mixture depend on the ability of steam to access the zircaloy and, therefore, on the porosity of the medium. The more the liquid mixture fills the open spaces, the lower the oxidation kinetics are. From this point of view, the zircaloy oxidation phenomenon is globally understood and most computer codes include models for calculating core melt progression in the reactor vessel. The validation of these models is still often very succinct, however. In particular, more analytical test results are needed; these could be used to determine the oxidation rates for U-Zr-O melt mixtures. The hypothesis of zirconia layer spalling in the event of reflooding (detaching zirconia layers from the rods, bringing the metal zircaloy into contact with the water or steam) does not provide a valid explanation for the intensified oxidation process while the rods are being reflooded. To date, no experimental results support the existence of such spalling in the case of the zircaloy 4 or the M5 alloy (there is very little experimental data for the latter), which are used as cladding materials in the PWRs. It has only been found in the case of alloys that are not used in the French PWRs, such as the E110 (Zr-Nb) used in the Russian PWRs (VVER).

5.1.1.2.7. Formation of a corium pool and corium flow into the lower head

If the temperature reaches the melting point of UO_2 , a "molten pool" forms in the reactor core. Due to the formation of the eutectic liquids, the melting temperature may be several hundred degrees below that of the UO_2 melting point (3100 K).

As the eutectic molten mass increases, the pool expands axially and radially in the core until it reaches either the baffle or the core support plate (internal structure; see Section 2.3.2). At this moment, the corium flows into the lower head. Considering its

low surface/volume ratio, the corium pool formed in this way is very difficult to cool; as a result, it may grow by incorporating the rods located around it, even if it is reflooded. This is what occurred in the Three Mile Island accident (Section 7.1).

It is essential to predict the weight, composition and temperature of the materials reaching the lower head during the course of the accident, as well as the instants when these materials do so, in order to study the subsequent sequence of events of the accident. These phenomena are modelled in most computer codes. Their level of validation and detail are satisfactory, considering the experimental data available. Only partial data is available, however, as they exist either for small-scale, virtually one-directional fuel rod assemblies (around twenty rods, in the case of the *Phebus* assemblies), or for preformed debris beds, which are also small (RASPLAV, ACRR and *Phebus-FPT4*; these programmes are described in Section 5.1.1.3.1 and Section 5.1.2.3.1). At present, there are no experimental data allowing detailed characterisation of corium pool formation and flow in the core. More representative data are still to be obtained in order to characterise the evolution of a corium pool through two-dimensional rod assemblies.

The degradation may ultimately result in very different configurations in the core simultaneously, ranging from intact or barely degraded rods to the formation of a corium pool or a bed of debris. These different degraded core conditions are described in greater detail in Section 5.4.1.

5.1.1.3. Experimental programmes, modelling and computer codes

5.1.1.3.1. Experimental programmes

This section provides a brief description of the main experimental programmes, ranging from the oldest to those still under way or scheduled in 2015, to study the degradation of the core materials. The programmes performed have provided data for validating the computer codes. An OECD summary report presents all the tests whose results have been used to validate the core melt accident simulation computer codes [13].

Separate effect tests on the oxidation kinetics of fuel rod materials and the associated chemical interactions: many tests conducted by different teams including Forschungszentrum Karlsruhe (PzK) of Germany, and Atomic Energy of Canada Limited (AECL) of Canada have determined the oxidation kinetics of zircaloy, UO_2 dissolution by the molten zircaloy, B_4C oxidation (FzK and IRSN), zircaloy dissolution by the molten steel, etc.

Separate effect tests on cladding failure mechanisms: these tests (for example, the EDGAR tests conducted by CEA) have helped to determine the cladding creep law based on the cladding temperatures and the oxidation conditions.

LOFT-FP [19]: this test programme, which was completed in 1985, was conducted by the Idaho National Laboratory (INL) of the United States on an assembly consisting of 121 UO_2 fuel rods with in-pile nuclear heating. It consisted of tests on fuel assembly degradation and FP release, and involved temperatures up to 2400 K (locally). Steam cooling was used, followed by water reflooding.

PBF-SFD [20]: this test programme, which was completed in 1985, was conducted by INL on an assembly consisting of 32 UO_2 fuel rods with in-pile nuclear heating. It also included tests on fuel assembly degradation and FP release, but at temperatures up to 2600–3100 K (locally). Steam cooling was used, followed by water reflooding (for certain tests).

NRU-FLHT [14]: this test programme, which was completed in 1987, was conducted by AECL on an assembly consisting of 16 non-irradiated UO_2 fuel rods with in-pile nuclear heating. These degradation tests were unusual because they used fuel rods 3.7 m high (full-scale).

ACRR-MP [8]: this test programme, which was completed in 1992, was conducted by the Sandia National Laboratory (SNL). It consisted of in-pile tests of small debris bed melting ($\text{UO}_2 + \text{ZrO}_2$) in an inert atmosphere, at temperatures up to 3000–3200 K. The formation and then flowing of a corium pool were observed.

CORA [17, 18]: this test programme, which was completed in 1993, was conducted by KIT (formerly FzK) on an assembly consisting of 25 non-irradiated UO_2 fuel rods with electric heating. It consisted of tests in which fuel rod temperature reached 2200 K (locally). Each test included a steam pre-oxidation phase, followed by reflooding with water or steam at a high flow rate.

QUENCH [21]: this test programme, which was still under way in 2013, was conducted by FzK on an assembly consisting of 25 non-irradiated ZrO_2 fuel rods with electric heating. It consisted of degradation tests and involved temperatures up to more than 2000 K (locally). Steam cooling was used, followed by water reflooding. Recent tests have studied the behaviour of cladding materials other than zircaloy-4, such as E110 or M5 (Zr-Nb alloys).

Phebus FP [5]: this test programme, which was completed in 2004, was conducted by IRSN on an assembly consisting of 21 irradiated UO_2 fuel rods with in-pile nuclear heating. It involved degradation and FP release tests with temperatures up to 2600–3100 K (locally). Steam cooling was used.

ISTC 1648 (QUENCH): this test programme, funded by the International Science and Technology Centre (ISTC), was conducted by NIIAR (Scientific Research Institute of Atomic Reactors) in Russia. It aimed at studying the reflooding of a core that has reached temperatures exceeding 2000 K (locally), and performed three tasks: conducting degradation and reflooding tests using irradiated VVER fuel components, performing reflooding tests using a new VVER assembly of 31 rods, and developing a reflooding model for the SVECHA code by IBRAE (Nuclear Safety Institute of the Russian Academy of Sciences). The results of this programme have not been publicly published, but some reports are available by contacting ISTC.

PARAMETER: this test programme, funded by ISTC and launched by LUCH (Scientific Manufacturer Centre, Russia), studied the degradation of fuel assemblies consisting of 19 non-irradiated prototype fuel rods for VVER reactors (the tests were similar to those of the QUENCH project, but used UO_2 pellets instead). The experimental apparatus was

used to refill the system from above or below, at temperatures up to 2300 K at the moment it was refilled. Three tests had been conducted by the end of 2009. After the apparatus had been considerably degraded in the first test, care was taken to ensure that the temperature did not exceed 1870 K at the hottest point during the preliminary oxidation phase in the subsequent tests, in order to preserve the integrity of the fuel assembly holder. A fourth test was conducted in 2010, with a preliminary oxidation phase in air intended to simulate the entry of air into the reactor vessel. This programme's experimental data have not been publicly published either, but some publications discuss the validation of computer codes using some results of these tests.

Few in-pile experimental programmes study the phenomena involved when core melts go so far as to form a debris bed or corium pool in the core and corium flows into the lower head, with the exception of *Phebus FP* and ACRR. The LOFT and PBF tests attained late-phase fuel degradation but did not involve detailed analysis of rod melt and corium progression.

The Three Mile Island accident remains the only available source of knowledge on the condition of a reactor core following massive melting (Section 7.1). This accident and the condition of the reactor core have been analysed in detail; the results have been published and are publicly available [4, 15, 26, 27]. Figure 7.7 shows the condition of the core following the accident. Of particular interest are the large molten pool within the core, the collapse of a large portion of the rods above the pool (forming a debris bed) and partial corium relocation towards the lower head. Two aspects of the accident scenario are worth noting: the high-pressure sequence, and the corium melt in the lower head after the core was, at least partially, refilled.

5.1.1.3.2. Core melt modelling and computer codes

This Section provides a brief description of the main dedicated models and computer codes used to simulate the phenomena of reactor core material degradation occurring in a core melt accident (it does not describe the integral computer codes used to process all of the phenomena involved in a reactor when a core melt accident occurs, as these are presented in Chapter 8).

SCDAP/RELAP (US NRC, United States Nuclear Regulatory Commission) is a mechanistic² computer code developed by INEL. It is the result of coupling the RELAP 5 thermal-hydraulic code with the SCDAP core degradation modelling code. Its core modelling is based on parallel, one-dimensional channels and includes several models for simulating various aspects of fuel rod changes during the course of their degradation: heat transfers, residual power, cladding oxidation, fuel dissolution, cladding failures and FP release. This computer code is no longer developed by NRC but a private version known as SCDAPSIM is still developed [3, 6].

2. A "mechanistic" computer code consists of models that, whenever possible, are based on a physical or chemical description of the phenomena involved rather than adopting an empirical approach (based on correlations obtained using experimental results). In reality, mechanistic computer codes always include several empirical models.

ATHLET-CD (GRS, Gesellschaft für Anlagen - und Reaktorsicherheit, Germany) is a mechanistic computer code that is the result of coupling the ATHLET thermal-hydraulic code with a core degradation computer module. Much like SCDAP/RELAP, its core modelling is based on parallel, one-dimensional channels and includes several models for simulating various aspects of fuel rod changes during the course of their degradation: heat transfers, residual power, cladding oxidation, fuel dissolution, cladding failures and FP release. GRS is continuing to develop this computer code, notably with the addition of the MEWA module relating to the formation of a corium pool in the core [23, 25].

ICARE/CATHARE (IRSN) is a mechanistic computer code that simulates PWR core melt accidents. It is the result of coupling the CATHARE thermal-hydraulic code with the ICARE code that simulates core degradation and is similar to SCDAP/RELAP, except that considerable development has been carried out to simulate the phenomena involved when large-scale melting leads to significant degradation of the core (the formation of a debris bed or corium pool, and corium flows). It also allows axisymmetrical 2D modelling of the core and the reactor vessel. Several models simulate changes in the core fuel rods over time, as well as those occurring in the corium in the core and the lower head; they process heat transfers, residual power, cladding oxidation, fuel dissolution, cladding failures, FP release, 2D corium flow modelling, flow oxidation, fuel rod collapse and corium pool development. Development of this computer code is being continued by IRSN and includes a model of degraded core reflooding and complete modelling of corium behaviour in the lower head [7, 9].

RATEG/SVECHA (IBRAE, Russia) is a mechanistic computer code that is the result of coupling the RATEG thermal-hydraulic code with the SVECHA core degradation simulation computer module. This computer code includes highly detailed modelling of certain phenomena, notably cladding oxidation, fuel dissolution, cladding failure and FP release. The computer code is designed to describe in detail fuel assembly degradation (or that of a representative fuel rod). Its major limitation lies in its inability to process the radial propagation of degradation; notably, it does not process corium pool formation in the core, but it is able to simulate a molten pool in the lower plenum. IBRAE is continuing to develop this computer code, including the development of a module relating to corium flow oxidation [24].

5.1.1.4. Summary and outlook

The physics relating to the evolution of a PWR core melt accident is now well understood and modelled for the main processes. This notably concerns fuel rod cladding oxidation and failure. The complex phenomena involved in the later phases of the accident can only be modelled with significant uncertainties, however. This is particularly true of fuel rod collapse and corium oxidation. Additional experimental data would be needed in order to refine the modelling, but no related programmes are ongoing or planned in 2015. Given the high cost of the potential tests, which would have to be conducted with real irradiated materials, it seems unlikely that new experimental programmes (national or international) will be initiated in the near future. To reduce the remaining uncertainties, the only alternative is to perform additional analysis on past tests (which were often insufficiently investigated) and develop more detailed models.

5.1.2. *Corium behaviour in the lower head*

5.1.2.1. Introduction

In most of the expected cases, the lower head is filled with water when the corium coming from the hottest area of the core flows into it. The results of the fuel assembly melt tests in the [Phebus](#), QUENCH and CORA programmes show that the zircaloy in the assemblies at the end of the tests is only partially oxidised. In the assemblies' hottest areas, 20 to 100% of the zircaloy is oxidised; total oxidation is only seen locally in the areas in which the temperatures and steam concentrations have been high enough to provide intense oxidation over a long period. The corium that flows in the lower head therefore contains a percentage of unoxidised zircaloy that is estimated to be 25 to 80% of the zircaloy (depending on the scenario, following the general trend that a large break sequence leads to a low percentage of oxidised Zr whereas a small break sequence leads to a high percentage of oxidised Zr). This corium is said to be substoichiometric while its composition is not $(U-Zr)O_2$, which corresponds to its composition after complete oxidation.

The interaction of corium (above 2500 K) with water leads to more or less fine-grained fragmentation of the corium into particles, on the one hand, and intense steam production capable of substantially increasing the pressure in the RCS, on the other hand. When the partially fragmented corium has accumulated in the lower head, it forms what is called a debris bed. This bed is either very compact if there is little cooling (part of the corium is not solidified), or composed of porous solid debris. It is unlikely that a large debris bed can be cooled effectively. In all cases, the corium gradually evaporates the water present in the lower head. If there is no additional water supply and the debris configuration is such that it cannot be cooled effectively, the materials' temperature gradually rises until it reaches the melting point of the steel structures (plates, tubes, etc.) located in the lower head. A substantial quantity of molten steel then gradually enters the corium. As the temperature rises, first the zircaloy and then the oxide debris melt and either form a pool or become part of an existing pool. The formation of this corium pool in the lower head is a critical step in a PWR core melt accident: in this situation, there is a considerable heat flux at the interface between the pool and the reactor vessel that can lead to reactor vessel failure. Reactor vessel failure is described in detail in [Section 5.1.3](#).

5.1.2.2. Physical phenomena

When the hot corium pours into the lower head filled with water, steam is produced, leading to a pressure peak or even a steam explosion in the reactor vessel ([Section 5.2.3](#)), which creates mechanical stresses likely to damage the RCS. In addition, the reactor vessel is subjected to a heat flux that can locally be very high, resulting in melt erosion of the vessel walls and potentially leading to its failure. Regarding the last point, studies seek to determine the likelihood of in-reactor vessel corium retention or the conditions under which the reactor vessel would fail (timing, location, and characteristics of the corium flowing from the reactor vessel into the containment). It is thus important to be able to predict the changes the corium will undergo, from its relocation towards the lower head to its cooling or flow out of the reactor vessel. The main phenomena governing these changes are briefly described below.

5.1.2.2.1. Corium fragmentation and debris formation

When a corium melt comes into contact with the water present in the lower head, the corium becomes fragmented (Figure 5.2). Corium fragmentation is described in detail in Section 5.2.3 on steam explosions. The fragmentation is very complex to model and includes considerable uncertainties [34, 40].

5.1.2.2.2. Direct impact of a corium melt upon the reactor vessel

If there is little water in the lower head or there is a substantial mass of relocated corium, the corium melt only partially interacts with the water and part of this very hot melt comes into direct contact with the reactor vessel.

This situation can rapidly lead to reactor vessel failure during its period of contact with the corium melt. Although few experimental studies have been conducted on this phenomenon (a few CORVIS tests with molten materials simulating a corium, notably a molten thermite mixture [a mixture of iron and alumina], arriving on a mock-up of a BWR vessel), this phenomenon is relatively well-known. In such a situation, it would probably form an insulating — and therefore protective — crust between the corium and the reactor vessel, given the very large difference between the temperature of the reactor vessel and the corium solidification temperature. In the TMI-2 accident (Section 7.1), such a crust was probably formed; this would explain why, although a massive corium melt flowed into the lower head, the vessel was not damaged³. One of the key parameters is the degree of corium overheating above its melting point; this degree directly influences the thickness and, therefore, the efficiency of the protective crust.

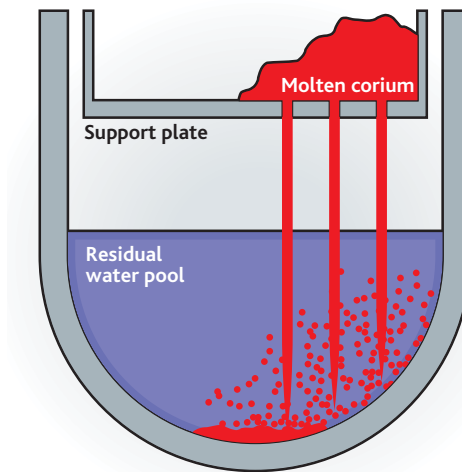


Figure 5.2. Schematic diagram of molten corium arriving in the lower head and fragmenting upon contact with water.

3. In the case of TMI-2, the presence of water in the lower head undoubtedly also contributed to the efficient cooling of the reactor vessel during the corium melt.

5.1.2.2.3. Steam explosion

The interaction between a corium melt and the water can result in a steam explosion (Section 5.2.3). Although the physics of this phenomenon are generally understood, it is not yet possible to predict with certainty under which conditions this phenomenon can occur. Despite the relatively low probability of an explosion occurring that had been observed in the tests conducted in order to study the interaction between very hot corium and water, such an explosion cannot be entirely ruled out and so the phenomenon is studied because of its possible consequences for the containment. It should be noted that in the TMI-2 accident, corium melt arrival did not lead to a steam explosion despite the presence of water in the lower head. This could indicate that there was no fine-grained fragmentation of the corium on contact with the water. It could also be due to the high pressure in the reactor vessel (approximately 100 bar).

5.1.2.2.4. Debris bed dry-out and possible reflooding

Corium melt fragmentation produces corium drops that cool and solidify on contact with the water, forming particles that settle in the lower head and create a "debris bed". This debris bed may be very compact if the cooling of the corium drops resulting from the fragmentation is insufficient to solidify them totally. In this case, the formed debris bed cannot be cooled effectively because the water cannot access some regions of the debris bed due to its low permeability. The debris bed then continues to heat up, gradually drying up the lower head and then melting to form a corium pool that is much more difficult to cool. The final risk is that the corium pool builds up and comes into contact with the reactor vessel and causes it to rupture. The possibility of avoiding the lower head drying and cooling down such a debris bed with the water present in the lower head or with an additional injection of water from the RCS is therefore under study (Section 5.4.1).

One of the parameters currently used to estimate the possibilities of cooling a debris bed is the "critical dry-out heat flux" (CHF), which corresponds to the maximum residual power density of the debris bed multiplied by the height of the bed within which it does not lead to a local dry-out. Below the CHF, the water is present everywhere in the debris bed and the temperature of the debris bed remains low. The CHF depends on the characteristic parameters (debris size, bed geometry and porosity, etc.) of the debris bed. Typical values are approximately 0.2 MW/m₂ for particles with a diameter of 1 mm and 1.2 MW/m₂ for particles with a diameter of 7 mm.

In a core melt accident, water may re-enter the reactor vessel whereas the debris bed is partly or totally dry. In such a situation, reflooding the debris bed may produce a large quantity of steam in a very short time, which can rapidly build up the pressure in the RCS and cause major oxidation of the unoxidised zircaloy in the hot upper parts of the core to resume. Few studies have been conducted on the phenomenology of debris bed reflooding and research programmes are still studying the subject in 2015 (notably the PEARL test programme conducted by IRSN).

5.1.2.2.5. Corium pool formation

As mentioned above, the dry-out of a large volume of a debris bed is a key step in the evolution of a core melt accident because it determines when corium pool formation begins or, if only a portion of the corium is fragmented into solid particles, when the propagation of the existing pool begins. Thanks to the results of the ACRR-MP, *Phebus* FPT4 and RASPLAV AW-200 tests [39, 32, 28], the molten pool formation is now quite well modelled when it occurs under conditions that do not result in significant corium oxidation and the main components of the corium are UO_2 , Zr and ZrO_2 . The pool may also contain a large quantity of molten steel. Although the interactions between the liquid steel and a (U-Zr)-O corium have been studied for some time, the effect of these interactions upon the evolution of the corium in the lower head (see later in this document) when the corium is in inert atmosphere was only revealed at the beginning of the 2000s, notably in the OECD's MASCA project [37]. The evolution of a debris bed containing steel under oxidising conditions requires further study. This is because the residual power causes the steam to circulate within the debris, which is likely to oxidise as a result (Figure 5.3). The melting of the debris and the development of a corium pool under oxidising conditions have never been studied experimentally, notably because of the high cost of the tests, which would require the use of real materials. The uncertainties regarding the degree of oxidation of the materials in the formed corium pool are processed in the core melt accident simulation computer codes by means of sensitivity studies.

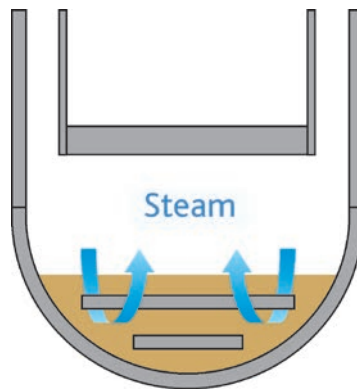


Figure 5.3. Schematic diagram of corium configuration after the lower head has dried out: a debris bed (which is more or less porous, depending on the degree of fragmentation of the corium) around steel structures, with steam circulating through natural convection.

5.1.2.2.6. Convection movements in the corium pool

The power released by the corium pool can be evacuated both through its lateral edges (thus *via* the vessel wall) and through its upper surface (through convective exchange with any water present, or through radiative transfer). These heat transfers cause natural convection movements of the molten materials in the corium pool (Figure 5.4). One of the key parameters when taking into account this phenomenon is the relationship between the upward heat flux and the lateral flux evacuated through

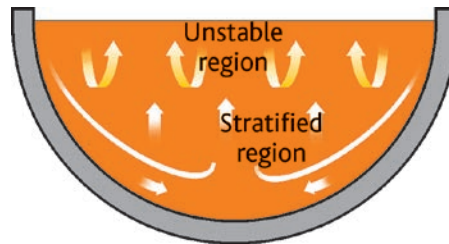


Figure 5.4. Schematic diagram of convection movements in a turbulent corium pool with top-down and lateral cooling. These movements cause the corium to flow downwards along the reactor vessel then rise (slowly) in the centre. The top of the pool is the site of considerable agitation in the form of thermoconvective cells (Rayleigh-Besnard instability).

the vessel wall. The movements in the corium pool are mainly turbulent, except in some highly stratified regions at temperatures in which there is almost no convection (the bottom part, for example). This phenomenon is relatively well understood for simple corium pool configurations, and correlations have been established for heat exchanges at the edges of the pool (see Section 5.4.1.1 and the reference documents [33, 41]).

5.1.2.2.7. Corium oxidation (in the form of particles or a pool), and hydrogen production

When the corium is being fragmented, it may be oxidised. This oxidation, if it occurs, produces hydrogen, on the one hand, and determines the later evolution of the corium, on the other hand. The ZREX/ZRSS tests (by Sandia National Laboratory, with a Zr + ZrO₂ or Zr-stainless steel mixture) and CCM tests (by Argonne National Laboratory, with a UO₂ + ZrO₂ corium mixture containing 24% steel) have provided partial information on corium oxidation. These tests suggest that, in the absence of a steam explosion, the fragmentation is not fine enough to result in significant debris oxidation. Nevertheless, tests with water at saturation have led to the oxidation of up to 30% of the metallic masses present in the corium. In the event of a steam explosion, oxidation may be complete. Not enough tests have been conducted to allow sufficient quantification of this phenomenon (because of the risks involved).

As to corium pool oxidation, this phenomenon has not been extensively studied and models are inadequate as a result in 2015. The MASCA-2 programme tests (on the evolution of a stratified pool under oxidising conditions, see reference document [37]) have provided some information on this subject, but not enough to allow the oxidation kinetics to be measured; in addition, it is very difficult to extrapolate their small-scale data to the scale of a power reactor lower head.

5.1.2.2.8. Metal/oxide stratification in the corium pool

The MASCA MA and STFM tests [37], which were conducted at high temperatures with a corium containing uranium, zirconium and iron in the form of metals and oxides, have revealed the existence of two immiscible liquid phases at equilibrium, one metallic and the other consisting of oxides. Depending on the initial composition of the mixture,

the metallic phase, consisting mainly of steel, may contain uranium and zirconium and become denser than the oxide phase. This results in pool stratification with the metallic phase at the bottom of the reactor vessel (Figure 5.5). Phase composition at equilibrium can be predicted using thermochemical databases such as NUCLEA (developed by Thermodata for IRSN and CEA). Pool stratification depending on the evolution of density over time is rarely modelled in the computer codes used to simulate core melt accidents, however. Although stratification of two immiscible liquids is a known phenomenon, the coupled interaction between mass exchange (thermochemistry) and flow dynamics (natural convection and stratification) remains a difficult process to model. In 2015, some computer codes incorporate simplified modelling of the oxide and metallic layers' evolution based on changes in their density.

The challenge lies in being able to predict under what conditions the molten metal layer is lighter than the oxide layer, resulting in the heat flux in the reactor vessel being "concentrated" in the metallic layer (when it is thinner than approximately 50 cm); this phenomenon is named the "*focusing effect*". In the initial studies on corium retention in the reactor vessel, which adopted a "conventional" approach (for the Westinghouse AP600 reactors, for example), the metal was supposed to merely contain steel and so be lighter than the oxide. The heat flux transferred to vessel wall is then higher in the metallic layer, particularly when it is thin: as a first-order approximation, the heat flux transferred to the vessel wall is inversely proportional to the thickness of the molten metal layer thickness. A thin molten metal layer above a corium pool therefore has the effect of "concentrating" the heat delivered to the wall. This phenomenon, which is rather well understood and modelled [44], is one of the main threats to reactor vessel integrity. It is explained in detail in Section 5.4.1.1.

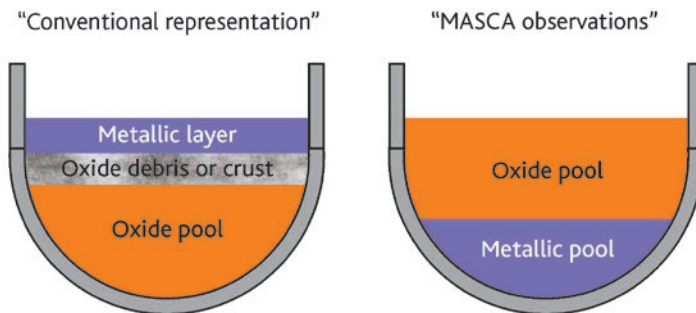


Figure 5.5. Layout of the potential metallic, oxide and debris layers resulting from corium fragmentation, as supposed in the "conventional" approach (left) and as observed in the MASCA tests (right).

5.1.2.2.9. Dissolution of reactor vessel steel at temperatures below its melting point

As a result of the formation of eutectic mixtures (Fe-U-Zr), reactor vessel steel may dissolve at temperatures above 1360 K. This can lead to erosion of vessel steel if it is in contact with a corium containing uranium oxide, zirconia and zirconium. The

METCOR tests (studying the interaction between a high-temperature corium containing uranium, zirconium and oxygen, and a steel sample representing a reactor vessel) have made it possible to estimate the erosion kinetics of reactor vessel steel, but the need remains for a more detailed understanding of the process. However, the rate of creep above 1300 K is such that the steel no longer has any mechanical strength at such temperatures (Section 5.1.3). This phenomenon can therefore be considered of secondary importance.

5.1.2.3. Experimental programmes, modelling and computer codes

5.1.2.3.1. Experimental programmes

This section provides a brief description of the main experimental programmes dedicated to the behaviour of corium in the lower head, ranging from the oldest to those still under way or planned in 2015.

DEBRIS [43]: the purpose of this test programme, conducted by the University of Stuttgart Institute of Research (IKE) in Germany, is to measure pressure losses and cooling (caused by water flow) for two-phase flows in a heated debris bed. The experimental system is one-dimensional and consists of steel balls heated by induction. Initially, a set of measurements taken for an isothermal water-air flow through the bed of balls was used to determine the two-phase pressure losses, as a knowledge of these values is essential in predicting the "critical dry-out heat flux" (CHF). Since 2008, the experimental system has been modified in order to perform debris bed reflooding tests. As the preliminary tests were satisfactory, more quantitative tests have been performed since 2011 to measure debris bed cooling through reflooding.

SILFIDE [29]: the purpose of this test programme conducted by EDF and completed in 2000 was to measure the CHF of a debris bed heated within its volume. The experimental system was two-dimensional and therefore differed from the DEBRIS test programme. The debris bed consisted of steel balls heated by induction. Useful results were obtained despite the challenge of establishing a homogeneous power distribution within the balls. In particular, local fluxes were sometimes observed to be higher than the theoretical critical flux (for 3 mm particles, the maximum flux measured in the SILFIDE tests was 1.7 MW/m² instead of the approximately 1 MW/m² predicted by the Lipinski correlation). Researchers also observed temporary, localised dry-out prior to reflooding.

RASPLAV [28]: this experimental programme, which was completed in 2000, was conducted under the auspices of the OECD by the Kurchatov Institute of Moscow in Russia. IRSN, CEA and EDF also participated in this project. Its purpose was to study the two-dimensional thermal hydraulics of a corium pool composed of "real" materials (the corium was composed of UO₂, ZrO₂ and Zr). The tests, involving up to 200 kg of corium, produced heat fluxes in accordance with predictions using the correlations developed from tests with simulants. However, it was revealed that the interactions between the materials could result in a non-homogeneous corium composition, notably due to stratification, but this phenomenon is minor compared with the stratification observed in the presence of iron during the MASCA tests (see below).

MASCA: this experimental programme, which was completed in 2006, was conducted under the auspices of the OECD by the Kurchatov Institute of Moscow in Russia. [IRSN](#), CEA and EDF also participated in this project. The experimental facilities used for the MASCA programme were found to provide useful results on material interactions and their impact upon heat flux distribution in a corium pool. The MASCA experiments studied how material interactions affected stratification of the corium pool and, consequently, flows and heat exchanges at the edges of the pool. The main tests were used to study the addition of steel, fission products or B_4C to a corium pool composed of UO_2 , ZrO_2 and Zr. At the same time, certain thermophysical properties of metallic alloys composed of uranium, zirconium and iron or oxides were measured, such as their density, viscosity, and solidus and liquidus temperatures. The programme's second phase was aimed at studying the evolution of a stratified corium pool in an oxidising atmosphere.

SIMECO [45]: this experimental programme, which was completed in 2009, was conducted by the Royal Institute of Technology (RIT) in Stockholm, Sweden. Its purpose was to study the heat fluxes in a stratified pool in which a thermal power was generated. In tests using simulants (salts or paraffins), three-layer pool configurations were produced, consisting of a heavy "metallic" layer, an "oxide" layer where most of the power was dissipated and a light "metallic" layer. This allowed the heat flux distribution across the corium pool to be measured. In 2015, the results have yet to be interpreted in greater detail, but it already seems that they will help to modify the distribution estimated on the basis of conventional correlations.

METCOR: this experimental programme by the International Science and Technology Centre (ISTC), which was completed in 2009, was conducted by the Alexandrov Scientific Research Technological Institute (NITI) in Saint Petersburg, Russia. Its purpose was to study the erosion of a steel sample representing the reactor vessel by a corium ($UO_2 + ZrO_2 + Zr$). The sample was externally cooled and subjected to a heat flux representative of conditions in a large corium pool, with a temperature gradient of over 1000 K across the sample [30]. The results of this programme seem to show that the erosion does not weaken the reactor vessel, as its mechanical strength mainly depends on the profile of temperatures in the wall under core melt accident conditions.

LIVE: this experimental programme, which began in 2004 and still under way in 2015, is conducted by Forschungszentrum Karlsruhe GmbH Technik und Umwelt (FzK) in Germany, with support from the European Commission. Its purpose is to study the behaviour of a corium using simulants in a hemispherical lower head (approximately 1 m in diameter). The chosen simulant is a mixture of $NaNO_3$ and KNO_3 . The first test studied the steady-state thermal hydraulics of the pool (distribution of thermal fluxes at the wall). The second studied the corium melt and its spread in the lower head, with the formation of a crust through solidification. Other tests performed between 2011 and 2013 have studied the effect of stratification, the melting of debris and the effect of top cooling. Those tests were partially funded by the European network of excellence [SARNET-2](#), with support from the European Commission. These new tests have completed our knowledge of the temperature at the solid-liquid interface and crust stability.

INVECOR: this experimental programme supported by the European Commission in the context of the ISTC was conducted between 2006 and 2010 by IAE-NNC-RK (Kazakhstan). Its purpose was to study the interactions between a liquid corium ($\text{UO}_2 + \text{ZrO}_2 + \text{Zr}$) and a steel hemispherical lower head approximately 80 cm in diameter by maintaining a constant power density using electrodes inserted into the corium pool. Four tests were carried out. Each test used 60 kg of corium, which was poured into the reactor vessel mock-up then heated, and then cooled using water. The results are quite difficult to interpret because of the presence of the electrodes, which have a considerable influence upon convection in the pool as well as its cooling. The results are primarily qualitative. They reveal that the upper layer of the corium pool is fragmented, encouraging its cooling. It therefore seems that reflooding the lower head, even after a corium melt, are beneficial in retaining the corium in the reactor vessel (in addition to external cooling of the reactor vessel).

5.1.2.3.2. Models and computer codes

This section provides a brief description of the main models and dedicated computer codes used to simulate the behaviour of a corium pool and its interactions with the lower head (the integral computer codes used to simulate core melt accidents, which are presented in Chapter 8, are not presented here).

CFD computer codes: these computer codes solve Navier-Stokes equations for compressible or incompressible fluids in any geometry (2D or 3D). These include the FLUENT and CFX codes, which were both developed by ANSYS and are used for many industrial applications involving 3D flows. These computer codes generally use numerical resolution methods that are efficient and fast, and their user interfaces are designed for ease of use. Offering many optional models (turbulence, material transfers and chemistry), they are increasingly used to study pools of molten materials. They are intended for rather generic applications, however, and may prove of limited use for modelling a particular phenomenon (such as solid particle formation and stratification, for example).

MC3D (CEA/IRSN): this mechanistic computer code simulates in detail the interactions between a corium and water (fragmentation and steam explosion). It is described in Section 5.2.1 [31].

CONV 2D/3D (IBRAE): this code solves Navier-Stokes equations for incompressible fluids, regardless of geometry (2D or 3D). It can be used to calculate the evolution of a corium pool and its spread outside the reactor vessel, and is similar to a CFD code. It does not have a turbulence model (essential when simulating large pools) or a model for processing the chemical interactions within the corium (no material transfers or chemical kinetics), however [35]. It was used in the preparation of the RASPLAV and INVECOR tests.

TOLBIAC (CEA): this is a dedicated model for simulating corium pools in the lower head. It takes into account the existence of two immiscible liquids that can stratify in either direction; it also accounts for potential crust formation on the upper surface of the pool or along its edges. It can be used to calculate transient changes in axisymmetrical 2D domains [46].

SURCOUF (CEA/IRSN joint development for the ASTEC integral computer code): this module, which was developed for the ASTEC integral computer code (see Chapter 8) is designed to model the evolution of debris in the lower head by integrating the coupled interaction between thermochemistry and thermal hydraulics. The 0D approach accounts for the existence of several layers (light metal, heavy metal, oxide and solid debris) and can be used to calculate their respective positions, based on changes in density. This code has been replaced by the PROCOR code which is significantly improved. PROCOR is also used by EDF, with a coupling to MAAP.

ICARE/CATHARE (IRSN): this mechanistic software calculates core degradation under core melt accident conditions. It offers axisymmetrical 2D modelling of the reactor vessel and includes several models designed to simulate the behaviour of corium in the lower head: corium melt fragmentation, debris bed dry-out, debris melting, metal/oxide stratification, corium oxidation and debris reflooding. The lower plenum mesh is still rather crude, however, and the numerical methods used do not provide as much accuracy as the CFD models [36, 38, 42]. The lack of precision in the mesh is nevertheless acceptable, given the uncertainties regarding the properties of materials or some physical phenomena.

5.1.2.4. Summary and outlook

There are still many uncertainties in the description of corium behaviour in the lower head. Firstly, the effects of the material interactions (stratification, oxidation and dissolution) seem very important and are not all properly modelled yet (notably because the experimental results are very recent); this should be improved by analysing the latest results, obtaining more experimental data and developing more advanced models (that, among other things, address the problem that thermodynamic equilibria are not currently processed at the local (mesh) scale). Secondly, the effects of scale are difficult to estimate, and it is sometimes tricky to transpose reduced-scale test results to a full-sized power reactor. Further analysis and modelling is required to make this transposition possible by reducing these uncertainties, considering the fact that it is hardly feasible to perform full-scale tests.

5.1.3. *Reactor vessel failure*

5.1.3.1. Introduction

When a core melt accident occurs in a PWR, the integrity of the reactor vessel may be threatened by three main phenomena. The corium flowing into the lower head may erode the reactor vessel immediately upon direct contact, or the reactor vessel may be damaged by a potential steam explosion immediately the corium comes into contact with the liquid water present; if the reactor vessel withstands this transient phase, its integrity may then be threatened by the effect of a corium pool forming in the lower head.

The reactor vessel is more intensely eroded if the volume of the corium melt is large, or if the water present in the lower head is shallow. In theory, this can result

in the reactor vessel very rapidly failing on contact with the melt. Some experiments have shown that a crust forms between the melts and the molten metal, substantially slowing the rate of erosion [47]. If the temperature of the corium in the melts is higher than 2500 K, however, this insulating crust may not form (Section 5.1.2). Other factors probably reduce the degree of erosion, such as the point of contact of the melt rapidly changing over time, resulting in a very short contact time for a given point in the reactor vessel and the presence of water in the lower head.

When a corium melt and water come into contact, this can also very rapidly produce a large quantity of steam, resulting in a very high pressure peak and possibly a steam explosion capable of damaging the reactor vessel (see Section 5.2.3 and references [48, 49]).

Should molten corium form a pool in the lower head, heat exchange between the pool and the reactor vessel may provoke localised, partial melting of the reactor vessel, possibly resulting in reactor vessel rupture. This heat exchange is even greater for high-mass corium pools. Nevertheless, reactor vessel failure does not occur in all cases, as the Three Mile Island-2 accident showed in 1979 (see Section 7.1 and references [50, 51]). When this accident occurred, the reactor vessel remained intact even though a corium pool formed in the lower head. Subsequent analysis concluded that 1) the corium debris was porous, allowing some cooling, and 2) a gap existed between the pool and the inner surface of the reactor vessel. The gap is believed to have allowed water or steam to circulate. It should also be noted that high pressure in the primary coolant system may have a favourable impact on corium cooling when the corium melts (increased critical flux and reactor vessel deformation from creep or plasticity, potentially enlarging the gap).

It should lastly be noted that the reactor vessels of operational PWRs are equipped with a number of guide thimble passageways (also called “penetrations”) for insertion of instruments to measure the neutron flux in the reactor core. Reactor vessel rupture may be initiated in the zones around these passageways, due to the presence of singularities and welds. If guide thimble passageways fail in the reactor vessel (by melting, for example), water, steam, fission products and corium may leave the reactor vessel *via* the interior of these guide thimbles.

5.1.3.2. Physical phenomena

This document only describes the physical phenomena involved in the case of a corium pool in the lower head resulting in the reactor vessel failing. Three parameters must be determined that are important in the later sequence of accident events outside the reactor vessel: the moment when the reactor vessel fails, the location of the break in the lower head, and the size of the break.

The moment when the reactor vessel fails mainly depends on the pressure of the reactor coolant system (RCS) and reactor vessel temperature (linked with the mass and configuration of the corium pool). RCS pressure is generally uniform throughout the reactor vessel, but it may rapidly increase if water is injected into the reactor vessel.

Reactor vessel temperature is closely linked with the heat flux evacuated through its thick walls.

The location of the break mainly depends on the temperature distribution within the reactor vessel. The area that has been subjected to the greatest heat is the most likely to fail first, excluding singularities and welds; the other sensitive areas are those in which the thickness of the reactor vessel may have been eroded by corium melts, as well as those with singularities due to the presence of the guide thimble passageways and their welds.

Reactor vessel failure may be triggered either by plastic instability or by creep. Plastic instability occurs when the membrane stress acting on the thickness of the reactor vessel exceeds the ultimate tensile strength of the steel, which decreases considerably at higher temperatures. Creep, however, generally occurs at temperatures above 800 K. When the temperature rises throughout the thickness of the reactor vessel, creep may occur even if pressure levels remain low.

Once the reactor vessel begins to crack, the cracking spreads; the final size of the break greatly depends on the method of propagation, and this is directly related to the metallurgical characteristics of the reactor vessels' steels (see later in this document). Differences in chemical composition (even regarding trace elements) can change reactor vessel behaviour at high temperatures; the failure may be either brittle or ductile. Tests conducted on reactor vessel mock-ups [52, 53] have shown that if two materials behave differently at high temperatures (hot shortness vs. ductility), the final break sizes will also differ considerably.

5.1.3.3. Experimental programmes, modelling and computer code

In the context of experimental research on lower head behaviour, CEA conducted the RUPATHER programme [60] from 1995 to 1999 in collaboration with EDF and FRAMATOME. Its objective was to determine the tensile and creep properties (between 300 K and 1600 K) of 16MND5 grade steel (the steel used for French PWR reactor vessels) and model the mechanical behaviour of a PWR reactor vessel subjected to accident loads. The specimens used for the validation tests consisted of cylindrical tubes that were subjected to internal pressure and heated to very high temperatures (between 1000 K and 1600 K). The programme revealed certain deficiencies (both in the modelling and in the mechanical characterisation of 16MND5 grade steel). There were also other difficulties, mainly related to the metallurgical complexity of the steel (the effect of elements present in the steel, even at low levels, notably sulphur). The results have also shown that the metallurgical properties of the steel greatly affect its rupture behaviour. Additional programmes were subsequently carried out.

These included two experimental programmes entitled "*Lower Head Failure*" (LHF, 1994-1999) and "*OECD Lower Head Failure*" (OLHF, 1999-2002), which were carried out by the US Sandia National Laboratories (SNL) to study the strength of reactor vessels produced in US steel (SA533B1) subjected to complex thermomechanical loads representative of those resulting from the presence of a corium pool in the lower head [52, 53].

The second of these programmes, which was an extension of the first, was led by OECD. The LHF programme involved eight tests, and the OLHF programme involved four. Although the same type of 1/5th scale mock-up was used for both programmes, the wall thickness was doubled for the OLHF programme in order to study the impact of the temperature gradient across the reactor vessel wall. Several methods were used to heat the mock-up in the LHF tests, namely a superheated azimuthal band (representing a corium pool in the lower head with maximum heat flux at the free surface of the pool), superheating a localised zone (representing a lower head hotspot) and finally, uniform heating throughout the lower head area. The experimental protocol called for increasing the temperature at a constant rate until the mock-up failed. The LHF tests were carried out under constant pressure (seven tests at 100 bar and one test at 50 bar). Two of them studied the behaviour of the guide thimble passageways. In the case of the OLHF tests, only uniform heating was applied (Figure 5.6) and two pressures were applied: 50 and 100 bar. One OLHF programme test studied the influence of a rapid pressure increase from 50 to 100 bar upon reactor vessel failure mode. Another test studied the behaviour of the guide thimble passageways (at a pressure of 50 bar). During tests with guide thimble passageways, weld leaks generally occurred, resulting in the experiments being terminated before the lower head actually failed.

The FOREVER tests [58, 59] were carried out between 1999 and 2002 by RIT (Royal Institute of Technology in Stockholm, Sweden). These tests used 1/10th scale mock-ups of a PWR reactor vessel in 16MND5 steel. The experimental protocol consisted in pouring a mixed oxide melt (30% by weight of CaO; 70% by weight of B₂O₃) into the reactor vessel simulating the corium at a temperature of approximately 1500 K. This melt was then maintained at approximately this temperature, and the reactor vessel was then subjected to a pressure of 25 bar until it failed.

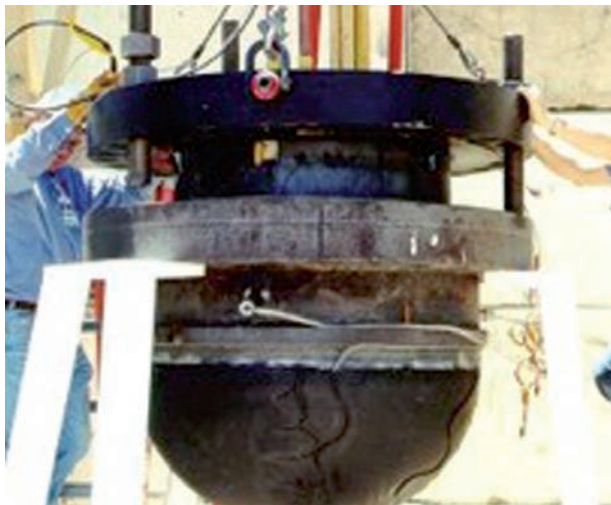


Figure 5.6. Lower head mock-up for carrying out the 1/5th scale OLHF tests, and setting up of its internal induction heating system.

In these three series of tests, particular attention was paid to the instant of reactor vessel failure and its mode, as well as the size of the resulting breaks. These tests were used to develop and validate numerical models for the thermomechanical behaviour of a PWR lower head under pressure prior to its failure. The models developed in this way are briefly described below:

- IRSN developed two simplified models, one one-dimensional (1D) and one two-dimensional (2D): the 2D simplified model has been introduced into the ICARE-CATHARE and ASTEC [54] computer codes;
- models with 2D finite elements have been developed by the Association Vinçotte Nucléaire (AVN: the Samcef code), the French Alternative Energies and Atomic Energy Commission (CEA: the Cast3M code), Electricité de France (EDF: the Aster code), the German laboratories Forschungszentrum Dresden Rossendorf (FZD: the Ansys code) and Gesellschaft für Anlagen- und Reaktorsicherheit (GRS: the Adina code), the US Sandia National Laboratories (SNL: the Abaqus code), the Czech Republic's UJV (the Systus code), and the Finnish VTT technical research centre's Pasula code;
- 3D finite-element models have been developed by AVN, CEA and SNL.

Two successive comparison exercises were carried out in order to compare the results of the 1D and 2D models with the experimental results of the OLHF1 test. The first exercise was carried out as part of the OLHF project, and the second was carried out by the European SARNET (Severe Accident Research NETwork of excellence) [55, 56]. These have established that the instant and location of the failure were generally accurately predicted by the models. Figure 5.7 shows that the elongation in lower head steel estimated by the different numerical models for the OLHF1 test is also consistent with the experimental results.

The 3D models also determined an initial failure time and initiating breaking zone that are compatible with the experimental results [56]. Additional work by CEA on the Cast3m code for the OLHF1 test produced a crack propagation simulation and an

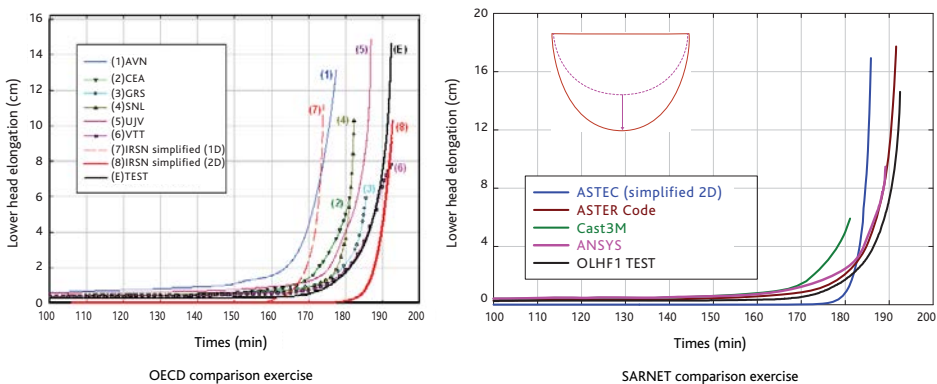


Figure 5.7. Comparison between the final elongation in the lower head steel estimated by different numerical models and the experimental results of the OLHF1 test.

estimate of the final break size that were both totally in keeping with the experimental results. The 3D models, on the other hand, did not give satisfactory results for the LHF tests, and this has been attributed to the variability of the steels used in the tests (ductile steels were used for the OLHF tests, whereas steels that were brittle at around 1300 K were used for the LHF tests).

The following conclusions were drawn from the analysis and interpretation of the test results [57]:

- the LHF and OLHF tests revealed variations in the behaviour of reactor vessel steels (brittle or ductile) at around 1300 K, influencing the final break size and difficulty in integrating the results into existing numerical models. This variability seems to be strongly linked to the presence of certain elements in the steels (sulphur, aluminium nitride, etc.);
- the experimental results could not be used to develop a method of estimating the size of the break in function of the mechanical loads applied to the reactor vessel. In order to develop a method applicable to the power reactors, it seems necessary to use a 3D finite-element calculation with a failure criterion that takes into account the variability of the behaviour of the studied steels, notably in the LHF and OLHF tests.

In order to clarify the variability in reactor vessel steel behaviour, IRSN launched a research programme in collaboration with CEA and INSA Lyon in 2003 [61]. This programme focused on the steels used in French reactor vessels and had a twofold objective: to complete the characterisation database for these steels, and to apply the study results to French reactors.

The programme began with an inventory of the metallurgical properties and compositions of the steels used to manufacture French reactor vessels (carried out by AREVA NP) and then turned to the selection of five study materials with sufficiently different metallurgical and mechanical properties to cover the range of steels used.

Samples of the five materials were then heated to a temperature of around 1300 K in order to identify their behaviour (brittle or ductile); these tests confirmed the brittleness of certain steels (ductility trough). Identification of the metallurgical factors responsible for this brittleness under heating also revealed aluminium nitrate precipitates and manganese sulphide precipitates at the grain boundaries and provided an insight into their role. Concurrently, high-temperature characterisation tests (at between 1200 and 1300 K) were carried out on CT (compact tension) specimens to determine the reactor vessel steels' metallurgical and mechanical properties that define the crack propagation kinetics. The results of these tests were used to develop a crack propagation model [62]. Lastly, INSA Lyon conducted tests on the steel tubes at high temperatures to measure the dependence of crack propagation kinetics on the properties of the tested steel. The reference documents present the state of knowledge in this R&D programme [63, 67].

Several theoretical studies and the CORVIS tests [65], which were conducted by the Institut Paul Scherrer (IPS) in Switzerland, have focused on guide thimble and

guide thimble passageway behaviour under core melt accident conditions with corium in the lower head. These investigations targeted the corium penetration into the guide thimbles and studied various possibilities of guide thimble passageway failure (see the summary [64]). It has been found that even if corium penetrates quite far into the guide thimbles, the resulting heat flux is usually not sufficient to melt the thimble walls and the RCS pressure and temperature conditions should not cause any plastic instability resulting in their rupture. Tube ejection following the failure of the welds between the lower head and the guide thimble sleeve or the melting of the retaining flange is also unlikely.

It should be noted that two finite-element models for studying guide thimble passageway behaviour have been developed by the Finnish VTT institute as part of the OLHF programme [66]. The results from these models are consistent with the experimental findings.

5.1.3.4. Summary and outlook

In order to better appreciate the thermomechanical behaviour of a PWR lower head in the event of a core melt accident and determine the consequences of the potential failure in particular upon the subsequent sequence of events in the accident, the essential parameters consist of the time of failure, the failure mode and the break zone and size.

The numerical models (2D simplified or finite-element models) developed in the context of the RUPATHER, LHF, OLHF and FOREVER programmes have shown their ability to predict the time before lower head failure and the location of the break. The results obtained agree with the experimental data.

Only the 3D finite-element models can be used to provide a more accurate model of the crack and its propagation until a break is created. However, no 3D finite-element model is currently able to correctly assess the size of the break, as this depends on reactor vessel failure mode at high temperature. The failure criterion used in the models must take into account the behavioural variability of the steels used to form the reactor vessels (ductility or hot shortness).

In order to improve the failure criterion and better assess the size of the break in the different cases of core melt accidents, IRSN undertook a collaborative research programme with CEA and INSA Lyon in 2003 on cracking in French reactor vessel steels. Although this programme provided very accurate high-temperature steel cracking kinetic measurements, a crack propagation model is very complex to develop.

The programme has been redirected towards carrying out studies to identify, among the plausible core melt accident scenarios, those for which the propagation of the crack could play an important role in the development of the accident. In the case of accident scenarios with a low pressure in the RCS when the reactor vessel fails (a pressure of less than 20 bar) and with no external cooling of the reactor vessel, these studies show that the reactor vessel failure occurs rather as a result of vessel wall melting. At pressures above 40 bar, on the other hand, cracking of the reactor vessel wall may play an

important role in reactor vessel failure. With the aim of completing the results of these studies, other accident scenarios, notably those with external cooling of the reactor vessel, are currently under study.

5.1.4. High-pressure core melt

5.1.4.1. Introduction – accident definition and possible consequences

A PWR core melt accident can occur at a high pressure mainly as a result of the following:

- an equipment failure or human error resulting in the RCS valves not being opened;
- a rapid pressure increase in the RCS when it is partly or completely depressurised; such a pressure increase can, for example, be caused when a degraded core is reflooded, due to a very fast interaction between the reflooding water and the core's materials at very high temperatures, or even melt.

These accidents are known as “high-pressure melt” accidents.

At high pressures, the different components of the RCS (hot legs, steam generators, etc.) are simultaneously subjected to the following:

- high temperatures;
- high stresses (mainly due to pressure forces).

The combination of both these factors can result in one of these components failing, i.e. creating a break in it. Such a break is qualified as an “induced break” in the terminology used for PWR core melt accidents.

An induced break can be either of the following:

- a break induced by creep in a hot leg, the steam generator's tubes or even in another RCS component; this mechanical failure occurs under the effect of heating coupled with a high pressure;
- a reactor vessel rupture at high pressures (if no other RCS rupture has occurred previously). In this case, the corium present in the lower head can be ejected into the reactor pit and then into the containment and cause it to heat up directly in a process named “Direct Containment Heating” (DCH), which can result in its failure (see Section 5.2.1).

The creation of an “induced break” reduces the pressure in the RCS, thereby reducing the possibility of DCH occurring. If an induced break in the RCS occurs in the steam generator tubes, however, radioactive substances may be directly discharged into the environment.

It is therefore important to study the behaviour of the RCS in the event of a melt under pressure in order to fully appreciate the associated risks. This chapter solely concerns the induced breaks, as DCH is discussed in Section 5.2.1.

5.1.4.2. Physical phenomena

As we have seen in the preceding sections, when a core melt accident occurs in a power reactor, the reduction in the water inventory in the RCS exposes the fuel rods, resulting in the temperature rising and the reactor core's component elements progressively melting. Part of the power released in the core's unflooded zones is then removed from the core through natural convection, i.e. the hot gases (mainly the steam/water vapour that gradually replaces the liquid water as it evaporates) transport a certain quantity of heat from the core into the coldest regions of the RCS. The hot gases are themselves replaced in the core by the cooler gases. As a result, loops form in which the gases flow from the hot areas of the RCS to its cooler ones and the gases that have been cooled in the cooler areas then flow back into the core's hot ones; these are referred to as "convection loops". These movements are "driven" by buoyancy forces according to Archimedes' Principle, i.e. the forces resulting from the difference in density between the hot (and, therefore, lighter) gases and the cold (and, therefore, heavier) gases.

Theoretically, there are two possible modes of gas circulation in the RCS, as shown in Figure 5.8:

- in the first (shown in the left part of Figure 5.8), the gases leaving the core pass through the hot legs of the RCS, the steam generators, the intermediate legs and cold legs before being reinjected into the core's lower part;
- in the second (shown in the right part of Figure 5.8), a water slug remains present in the so-called "intermediate" legs, located, in the case of each RCS loop, between the steam generator outlet and the RCS pump; due to their shape, the intermediate legs (which are called "U" legs) in the loops of the RCS create a siphon (Figure 5.8) in which water can stagnate, forming a slug. The superheated steam leaving the core passes through some of the steam generator tubes (referred to as the "direct tubes") where they cool down, and then return to the reactor vessel through some of the other tubes (referred to as the "indirect tubes") and through the hot leg (which is therefore the seat of a counter-current flow: the hot gases flow from the reactor vessel to the steam generator through the upper part of the hot legs and the cold gases flow from the steam generators to the reactor vessel through the lower part of the same hot legs, as shown in Figure 5.8). This flow pattern has been experimentally demonstrated in a scale mock-up and seems to be the most probable (IRSN's computer models predict high water slug stability; if the slug disappears in a loop, the steam follows the path described in the previous paragraph).

These convective phenomena are not specific to high-pressure melt scenarios, however, a high pressure has the following consequences:

- convective exchanges are much greater at high pressures than at low pressures;
- the pressure present in the RCS generates stresses that are sufficiently great to cause a significant risk of a creep rupture in some of the pipes (the hot leg, SG tube, etc.).

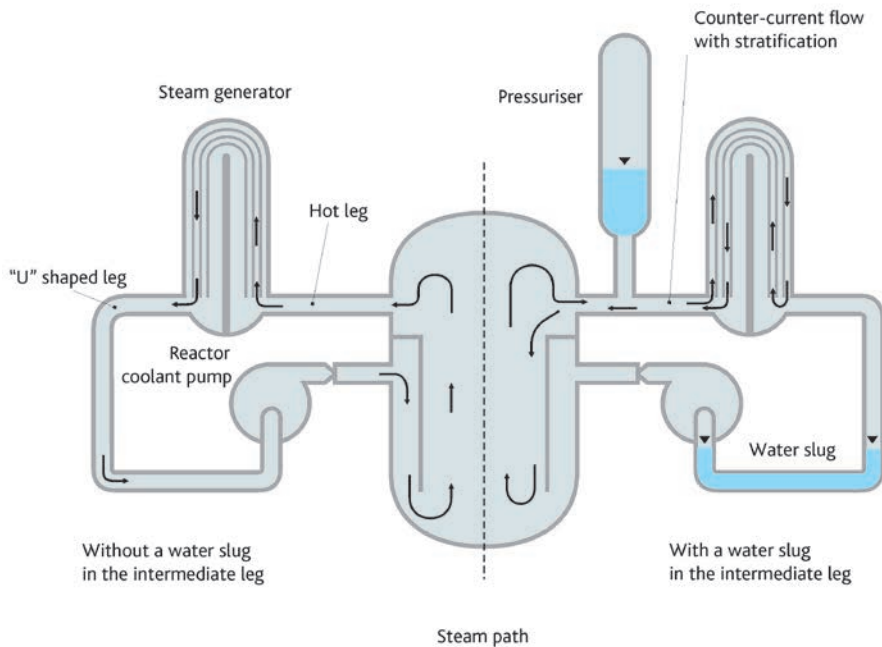


Figure 5.8. Modes of steam circulation in the RCS.

In order to determine the location of the break in the RCS, the time sequence of possible RCS failures must be assessed, thereby identifying the earliest. This means that the mechanical and thermal conditions (thermal and mechanical loads) acting on the components of the RCS (SG tubes, RCS piping, etc.) must be known, as well as the behaviour of the corresponding materials at high temperatures.

The mechanical loads are due to the pressure and the thermal expansion of the structures involved (the structures cannot freely expand under the action of heat; they are constrained to do so in a specific way, notably because they are connected to other equipment).

The thermal loads mainly depend on three factors:

- the power released in the core (residual power and power released by the exothermic oxidation reaction of the Zr);
- the transport of heat from the core and into the RCS by means of superheated steam;
- the residual power released by the fission products when they are transported in the RCS (see Section 5.5 for further details of how the fission products are transported in the RCS).

In order to determine the thermal loads, therefore, it is important to be able to model the different convection loops and the release, transport and deposition phenomena of

the fission products in the RCS. Other elements must also be modelled in order to assess correctly the thermal loads: whether or not water continues to be injected at the RCS pump seals (a seal failure can result in an RCS rupture), the behaviour of the pressuriser steam bleed SEBIM valves (if a valve jams open, the RCS would be depressurised after a certain number of cycles), and the potential formation of hydrogen "slugs" in the upper part of the SG tubes (hydrogen is mainly produced as a result of oxidation of the zirconium in the cladding by the steam) resulting in the gas flow being blocked.

Studies of high-pressure core melt accidents therefore consist of two parts:

- a thermal-hydraulic part to determine the temperatures (and, also the pressures) in the different parts of the RCS;
- a mechanical part, based on the results of the thermal-hydraulic studies and the properties of the materials involved, to assess when and where the RCS fails.

5.1.4.3. Experimental programmes, modelling and computer code

All of the research programmes on core degradation, the release of fission products, corium melt and lower head mechanical strength more or less directly provide data for the high-pressure core meltdown studies. Experimental and modelling programmes specific to this type of situation have also been performed, however.

The first programmes to specifically address high-pressure meltdown were carried out in the United States at the beginning of the 1980s. These notably revealed, in mock-ups, the gas flow patterns. Different existing computer codes were modified in order to model this flow circulation using a simplified geometry; these enabled the thermal loads of the structures to be better assessed. Finite-element mechanical studies were then conducted using these thermal load models. These studies provided more precise models of structural response to the different thermal and mechanical loads. At the beginning of the years 2000, mechanical tests confirmed the validity of this approach and provided data for the modelling of RCS welds.

The improved performance of the computational models can be used to perform Computational Fluid Dynamics (CFD) simulations, which solve 3D fluid mechanics equations, in order to calculate the velocity and temperature fields in the hot legs and the steam generators at a given moment. These methods can partially compensate for the lack of experimental data and help to develop simplified models (for assessing the number of direct tubes and the number of indirect tubes in the steam generators, for example).

5.1.4.3.1. Experimental programmes

Westinghouse tests: a test programme conducted by Westinghouse at the beginning of the 1980s, funded by the Electric Power Research Institute (EPRI) in the United States, concerning gas flows and thermal exchanges in the event of a PWR core melt accident. These tests were conducted in a 1/7th scale mock-up reproducing one side of a four-loop Westinghouse PWR (the mock-up reproduced the reactor vessel, two hot

legs and two steam generators) and were carried out with sulphur hexafluoride (SF_6) in place of superheated steam (this gas behaves like superheated steam under pressure and temperature conditions similar to atmospheric conditions, which greatly simplifies the tests). In particular, these tests revealed circulation flows in the hot legs and SG tubes, the mixing of hot and cooler gases in the SG inlet plenums, and gas stratification in the hot legs. The tests also estimated certain flow data: the mixing ratio in the SG inlet plenums as well as the ratio between the number of "direct" SG tubes (i.e. in which the gases flow from the inlet plenum to the outlet plenum) and the number of "indirect" SG tubes (i.e. in which the gases flow in the opposite direction). These tests are described in several publications, but only partially [68, 69], and were used to qualify computational tools [70, 71]. The ROSA tests, which are mentioned below, aim to provide additional information.

MECI programme: conducted by CEA between 2000 and 2004 and financed by [IRSN](#), this programme:

- included a part to determine the mechanical properties of RCS component materials;
- conducted tube burst tests representing the hot legs (half-scale mock-up);
- conducted tube burst tests representing the hot legs (full-scale mock-up).

The material characterisations of the MECI tests added to the existing data on the various grades of steel of the RCS hot legs. They also made it possible to assess uncertainties under creep conditions, determine the properties of the materials used in the burst tests and compare their properties with those available in the literature (including the inventory of RCS material properties compiled by AREVA).

The high-pressure tube burst tests then validated the methods of assessing the failure times for the various structures. They were conducted on the SG tubes and on the tubular test specimens representative of hot leg geometry (half-scale straight tubes) and materials. At constant pressure, the test specimens were subjected to a "temperature ramp" thermal load (heating to provide a constant rate of temperature increase) until they burst.

The tests conducted on the specimens representing the hot legs were mainly intended to determine the behaviour of various grades of materials present in the RCSs. The programme included mock-up tests carried out upon a single material (in other words, entirely consisting of 16MND5 steel, the grade of steel used to construct the French reactor vessels, or 316L steel, the grade of steel used to manufacture the hot leg components) as well as tests conducted upon welded mock-ups representative of the actual welded joints (between the hot legs and the reactor vessel, and between a hot leg's different components, including the joints with the SGs). As a result, two types of welds were studied: "homogeneous" joints (HJ), represented by a welded assembly consisting of two 316L steel tubes (a half-scale study of the links between a hot leg's components), and bimetallic joints (BMJ), represented by the welded joint between two half-mock-ups in 16MND5 and 316L grade steels (to study the links between the hot legs and the reactor vessel).

The test grid is shown in Table 5.1. The first column indicates the component material, the second states the tube's thickness, the third the membrane stress (σ in MPa; the stress as defined here is a pressure that "measures" the effect of the forces applied to the structure) and the fourth the temperature heat-up rate (in degrees per second).

In the case of the SG tube tests, two pressure loads were studied: that of a high-pressure secondary coolant system, and that of a depressurised secondary coolant system. These tests were reproduced for various temperature ramp rates, with intact tubes or with tubes containing a notch or recess defect (see Table 5.2). It should be noted, however, that such defects are obtained by machining the parts and so are not completely representative of the defects found in the PWRs.

Table 5.1. "Hot leg" mock-up burst test grid.

Material	Thickness (mm)	σ (MPa)	$\Delta T/\Delta t$ ($^{\circ}\text{C}/\text{s}$)
316L	10.5	107	0.2
316L	10.5	107	0.05
316L	15	75	0.2
316L	15	75	0.05
16MND5	10.5	107	0.2
16MND5	10.5	107	0.05
16MND5	15	75	0.2
16MND5	15	75	0.05
BMJ (16MND5L/316L)	15	75	0.2
BMJ (16MND5L/316L)	15	75	0.2
BMJ (16MND5L/316L)	15	75	0.05
BMJ (16MND5L/316L)	15	75	0.05
HJ (316L/316L)	15	75	0.2
HJ (316L/316L)	15	75	0.2
HJ (316L/316L)	15	75	0.05
HJ (316L/316L)	15	75	0.05

Table 5.2. SG tube burst test grid.

Sample reference	Internal pressure (bar)		Rate of temperature increase ($^{\circ}\text{C}/\text{s}$)		Defect geometry		
	80	150	0.05	0.1	None	Notch	Recess
0	•			•	•		
1	•			•	•		
2		•		•	•		
3		•	•		•		

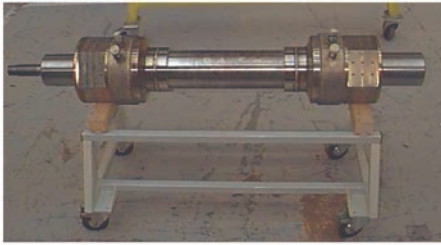
Sample reference	Internal pressure (bar)		Rate of temperature increase (°C/s)		Defect geometry		
	80	150	0.05	0.1	None	Notch	Recess
4	•		•		•		
5		•		•		•	
6		•		•		•	
7	•			•		•	
8	•		•			•	
9		•	•			•	
10		•	•				•
11	•		•				•
12	•		•				•

Figure 5.9 shows the experimental system and the condition of a “hot leg” mock-up after the test.

ROSA-V programme: the ROSA experimental programme began in 1970 in Japan and mainly studied the thermal-hydraulic phenomena occurring in PWRs during accident scenarios. The fifth segment of this programme, ROSA-V, was conducted between 2005 and 2009 in the ROSA/LSTF facility of the Japan Atomic Energy Agency (JAEA) and involved many partners including EDF, AREVA, CEA and IRSN in a four-party agreement. The purpose of these tests was to contribute to the development and validation of the thermal-hydraulic models utilised in the computer codes used to compute accident transients that can occur in PWRs by providing “benchmark tests”, notably for studying high-pressure core melt accidents. These tests were used to perform comparative exercises between the computer codes used to simulate the thermal hydraulics of the RCS and assess their ability to compute thermal-hydraulics during accident transients. The ROSA/LSTF loop consists of a 1/48th scale mock-up (regarding the volumes; the vertical dimensions are respected) and two loops of a four-loop 1100 MWe PWR. The last tests conducted simulated the natural convection phenomena when superheated steam was present in the loops.

ARTIST programme: the ARTIST-1 (*AeRosol Trapping In a Steam-generaTor*) experimental programme, in which IRSN participated, was launched by the Paul Scherrer Institute (PSI, Switzerland) in 2001. It is intended to reproduce the circulation and retention, for the secondary (cold) side of a steam generator, of the fission products (FPs) present in the form of aerosols in the event of a SG tube rupture; its objective is to obtain an experimental database that can be used for safety studies or for the development of models to analyse the retention of FPs, notably in the case of high-pressure melt accidents resulting in an induced break in SG tubes.

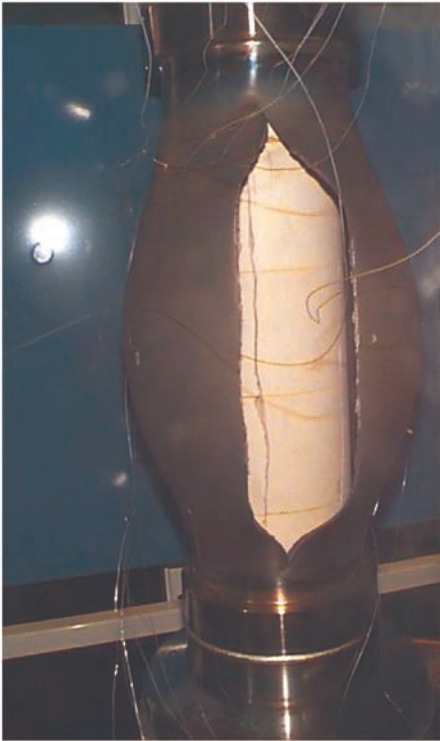
The transport and retention of FPs in the RCSs and Secondary Coolant Systems (SCSs) are described in detail in Section 5.5.3.1 of this document.



▲ Tube 2 before being set up on the test bench



▲ Overview of the damage; view of a damaged shield



Close-up of one end of the crack ►



Figure 5.9. Overview of the burst in tube no. 2 in 316L steel with a temperature ramp of $0.05\text{ }^{\circ}\text{C/s}$ and a membrane stress of 107 MPa.

5.1.4.3.2. Models

In order to assess the strength of the RCS (resistance to failure), so-called “integral” computer codes are used to simulate a complete accident sequence (these integral computer codes are described in Chapter 8) and, therefore, notably to assess the temperature changes of the different components of the RCS over time (thermal loads).

Given the current possibilities of computation, these complex computer codes generally use highly simplified models of one-dimensional coolant systems to compute the temperature fields. The thermal loads computed with these codes are therefore subject to significant uncertainties.

Complementing the integral computer codes, specialist computer codes are used to perform much more detailed local simulations, notably those of the temperature fields and gas circulation flows, and to assess the thermal loads more precisely. The initial detailed models of convective heat transfers in the RCS in the event of accident transients date back to the 1980s [68]. Subsequent progress in computation has resulted in CFD codes that can be used to conduct thermal-hydraulic studies or to perform finite-element calculations in thermomechanical studies to model convection more precisely without the need for large-scale experimental tests that are difficult to implement.

► Modelling of high-pressure core melt in integral computer codes

The integral computer codes presented in Chapter 8 can be used to simulate all of the phenomena that may be involved in a core melt accident, and notably the core degradation and fluid circulation flows in the RCSs and SCSs. They generally use a one-dimensional representation of these systems. To enable the circulation flows and the mixing of hot and cold gases in the SG inlet plenums to be simulated, they are represented in this type of computer code by several volumes, and the gas transfers are performed between the volumes.

The computations performed using the ICARE-CATHARE code can be used to assess the mechanical strength of all of the components of the RCS when a high-pressure core melt accident occurs, depending on the computed thermal loads; some calculations compute the risk of a break occurring in the RCS pump seals. It should be noted, however, that the case of a pressuriser valve jamming in the open position has not been specifically examined (but its modelling would not create any problems). The calculations performed with the code have shown that, if there is a water slug in the intermediate leg of the RCS (see Figure 5.8), it remains in place throughout the period of the accident transient. They have also revealed that the risk of a hydrogen slug forming in the upper part of SG tubes could be avoided.

These computational results must be used with care, however, because of the uncertainties in the thermal load computations. These uncertainties are due to the simplified models used for the coolant systems, on the one hand, and to certain simplified aspects inherent in the ICARE-CATHARE computer code, on the other hand: the code does not model the transport and possible deposition of the FPs released when the core is degraded; furthermore, the core is represented in a highly simplified way, as the code's user must predefine the heat transfers outside the core (two-dimensional [axisymmetrical] modelling of the core can compensate for this simplification, but these models are very costly in terms of computation time).

► Modelling of RCS thermal-hydraulics

The approach described in the previous paragraph results in a model of the hot legs or SG inlet plenums consisting of several volume elements (a few dozen at most). By its nature, therefore, it is highly simplified. On the other hand, it can be used to simulate an accident transient lasting several hours.

The CFD approach can be used to model these zones by means of thousands of unit cells and so can numerically simulate the circulation flows of the gases in a RCS loop more realistically than with an “integral” computer code. It requires a long computation time, however, thereby making the calculation of the complete sequence of events in an accident impossible. We must limit ourselves to studying the gas circulation flows at a given moment. The CFD approach has been adopted by the United States Nuclear Regulatory Commission (NRC) in the FLUENT computer code [71] and by IRSN in its CFX and TRIO computer codes (in the latter case, as part of a collaboration with CEA) [72]. The current means of computation restricts the number of unit cells in a model. A steam generator tube bundle (which consists of several thousand tubes) is modelled by a smaller bundle (consisting of approximately ten times fewer tubes), composed of equivalent tubes whose characteristics are determined so that, for example, the total flow cross-section of the tubes of the equivalent bundle is equal to the total flow cross-section of the actual bundle’s tubes. The modelling is restricted to the RCS: the exchanges with the SCSs are defined in the form of limit conditions (in other words, only the temperature, which is assumed to be uniform, of the steam in the SCS and a thermal exchange coefficient used to calculate the thermal fluxes between the PCSs and the SCSs are defined). The computations of this type provide a detailed view of the flows in the SG tubes at a given moment and can be used to assess some of their characteristics (mixing ratio in an SG plenum, and the number of “direct” SG tubes and “indirect” SG tubes).

This type of computation provides more precise thermal load results that can then be used to improve the thermal modelling in the integral computer codes as well as to improve the assessment of the mechanical strength of RCS components. Computations performed using the TRIO computer code have, for example, revealed that besides the SG direct and indirect tubes, there were also many tubes with no significant gas circulation flows. They also revealed the possibility of triple stratification occurring in the hot legs, with a “warm” layer between the hot and cold layers.

In addition, they provide 3D profiles of the gas temperatures in the RCS loops. Figure 5.10 shows an example of a thermal profile in a hot loop and a steam generator, calculated using the TRIO-U code. The colours represent the gas temperature ranges (in degrees Kelvin). The superheated steam leaving the reactor vessel passes through the upper part of the hot leg and then cools down when it enters the SG plenum and mixes with the “cooler” steam found there. “Relatively” cold steam flows back towards the reactor vessel through the lower part of the hot leg. A prior computation performed using an integral computer code provides this simulation’s “limit conditions” (flow rate and temperature of the hot gases as they enter the hot leg, and SCS temperature).

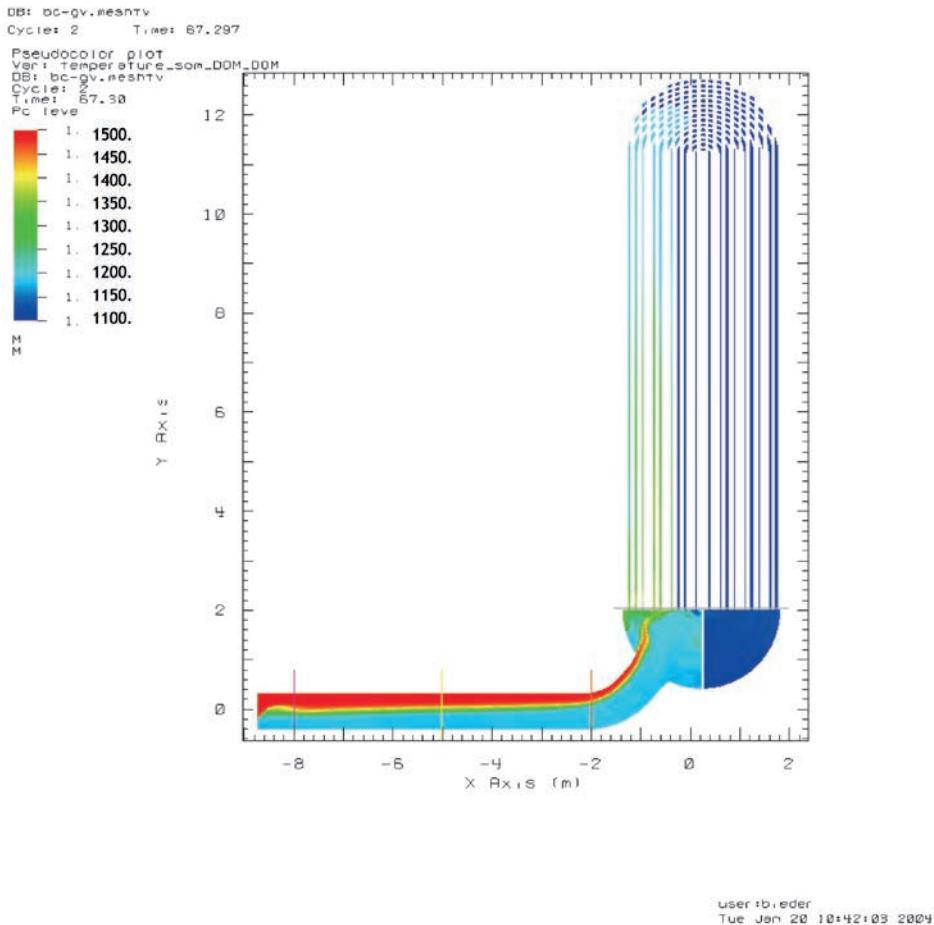


Figure 5.10. Example of a thermal field in a hot leg and the associated steam generator, determined using a TRIO-U calculation. The temperature scale is in degrees Kelvin.

The US NRC has conducted similar studies [72]. In particular, it focused on studying the thermal-hydraulic consequences of SG tube leaks existing prior to the accident and showed that such leaks very considerably increased the risk of SG tube failures.

► Modelling of RCS component mechanics

In order to simulate the mechanical phenomena, CEA performed finite-element calculations for the assembly comprising a hot leg and the lower head of a steam generator with the CAST3M code at IRSN's request. The mechanical phenomena have been used to study the effects of hot leg expansion upon the mechanical stresses and, consequently, upon the times and places at which it failed. The developed model used takes into account a "realistic" spatial distribution, provided by CFD computations, of the hot and cold layers in a hot leg (in other words, it takes into account the fact that a hot leg is not divided into a cold lower half and a hot upper half and uses the geometrical profile

of the separation zone obtained through the CFD computations). To a certain degree, special use of the computational results can be used to take into account the uncertainties regarding material properties as well as those regarding welds.

Figure 5.11 shows a cross-section view of damage to the hot leg at the moment of the failure for a specific thermal load (obtained for a simulation of a total loss of electrical power). One side of the hot leg is welded to the reactor vessel *via* a sleeve (visible at the right side of the figure), and the other side is welded to the lower head of the steam generator *via* an elbow and a conical trunk tube (visible at the left side of the figure). The start of the pressuriser's expansion line that connects the hot leg to the pressuriser can be seen in the figure.

In the computation performed with the CAST3M code, the reactor vessel and the steam generator have been simulated by means of special limit conditions.

The colours represent the level of damage suffered. The damage is a coefficient whose value is between 0 and 1 and is calculated at all points of the unit cell mesh and at every computation step by means of different models specific to the material. A value of 1 represents a failure, whereas a value of 0 represents an intact structure. In this case, the break begins at the beginning of the inner wall of the elbow before the steam generator.

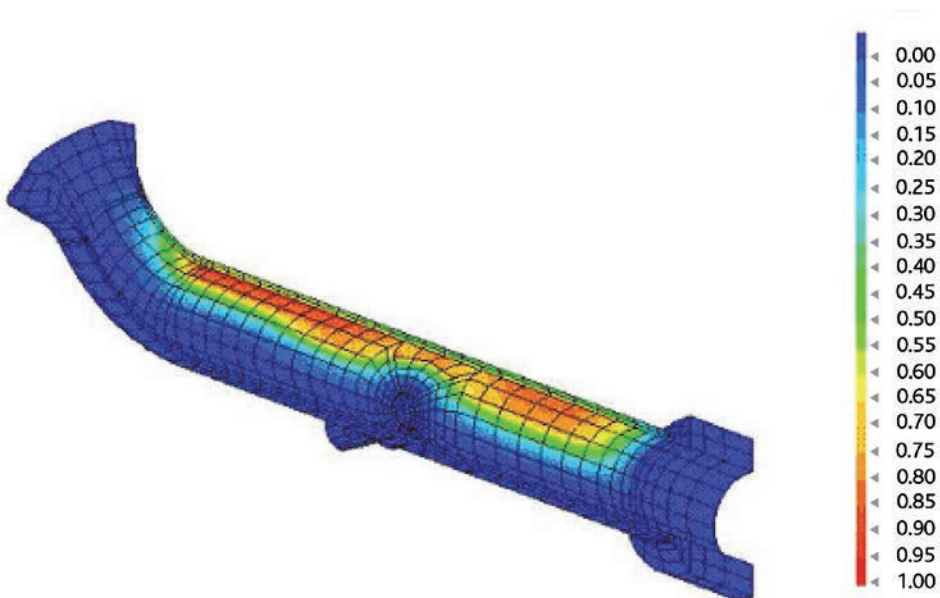


Figure 5.11. CAST3M mechanical computation of the strength of the hot leg – damage level at the moment of the “break” (see text for further details).

5.1.4.4. Summary and outlook

Research has helped to improve our understanding of high-pressure core melt accidents by increasing our knowledge of the thermal and mechanical loads to which the different components of the RCS are subjected as well as our knowledge of the mechanical behaviour of these components in such situations. Given the complexity of the phenomena involved, notably the RCS gas circulation flows that govern the temperatures of the RCS components, however, it is still difficult to predict with certainty where the first failure in the RCS will occur. The studies performed by IRSN are based on the results of this research; they tend to show that, when a high-pressure core melt accident occurs, the first failure would occur in a SG tube when the SGs are depressurised on the secondary side, or in the hot legs if not.

In the case of the modelling tools, progress could be made in validating the existing tools (notably on the basis of the ROSA test results) or improving the 3D modelling of RCS thermal-hydraulics. This is because only a 3D approach can take into account the complex natural convection phenomena that govern RCS temperature. As things are, it is sufficient to model the mechanics of RCS components, given the uncertainties associated with the thermal load computations.

From the point of view of PWR safety, measures have been taken in France to avoid a high-pressure core melt accident occurring (as in other countries), given the potential consequences of this type of accident, notably in the event of direct containment heating. These provisions include deliberate depressurisation of the RCS if possible before the core melts. This can be achieved by opening the pressuriser steam relief valves. The action of depressurising the RCS is included in the emergency operating procedures and must be performed immediately by the operators as soon as the Severe Accident Operating Guidelines (GIAG) is in use (see Section 4.3.3.4 of the Severe Accident Operating Guidelines).

It should be noted that it has been decided to modify the opening control of the pressuriser steam bleed valves in third ten-yearly outage programme of 900 MWe reactors, in order to make their operation more reliable and thereby make it possible to depressurise the RCS during a core melt accident.

In the case of the EPR, design provisions have been made aiming to "practically eliminate" high-pressure core melt accidents. These are described in Section 4.3.4.2.

Reference documents

- [1] B. Adroguer *et al.*, Core Loss During a Severe Accident (COLOSS project), *Proceedings of the FISA-01 meeting*, Luxembourg, Nov. 2001.
- [2] B. Adroguer *et al.*, Corium Interactions and Thermochemistry, *CIT project, FISA-99 Symposium*, Luxembourg, EUR 19532 EN, Nov. 1999.

- [3] C.M. Allison, J.L. Rempe, S.A. Chavez, Final design report on SCDAP/RELAP5 model improvements – debris bed and molten pool behavior, INEL-96/0487, December 1996.
- [4] J. Broughton, P. Kuan, D. Petti, E. Tolman, A Scenario of the Three Mile Island Unit 2 Accident, *Nuclear Technology* **87**, 34-53, 1989.
- [5] B. Clément, N. Hanniet-Girault, G. Repetto, D. Jacquemain, A.V. Jones, M.P. Kissane, M.P. von der Hardt, LWR severe accident simulation: synthesis of the results and interpretation of the first Phebus FP experiment FPT0, *Nuclear Engineering and Design* **226** (1), 5-82, 2003.
- [6] E.W. Coryell, Summary of Important Results and SCDAP/RELAP5 Analysis for OECD LOFT Experiment LP-FP-2, NUREG/CR-6160, [NEA/CSNI/R\(94\)3](#), EGG-2721, April 1994.
- [7] F. Fichot, O. Marchand, P. Drai, P. Chatelard, M. Zabiégo, J. Fleurot, Multi-dimensional approaches in severe accident modelling and analyses, *Nuclear Engineering and Technology* **38** (8), 733-752, 2006.
- [8] R.D. Gasser, R.O. Gauntt, S.C. Boursier *et al.*, Late-phase melt progression experiment: MP-2. Results and analysis, Report NUREG/CR--6167; SAND--93-3931, 1997.
- [9] V. Guillard, F. Fichot, P. Boudier, M. Parent, R. Roser, ICARE/CATHARE coupling: three-dimensional thermal-hydraulics of severe LWR accident, *Proceedings of ICONE-9*, Nice, France, 2001.
- [10] S. Hagen, P. Hofmann, V. Noack, L. Sepold, G. Schanz, G. Schumacher, Comparison of the quench experiments CORA-12, CORA-13, CORA-17, Report FZKA 5679, 1996.
- [11] T. Haste *et al.*, Degraded Core Quench: A Status report, OCDE/GD(97)5, [NEA/CSNI/R\(96\)14](#), August 1996.
- [12] T. Haste, K. Trambauer, Degraded Core Quench: Summary of Progress 1996-1999, [NEA/CSNI/R\(99\)23](#), February 2000.
- [13] T. Haste, B. Adroguer, Z. Hozer, D. Magalon, K. Trambauer, A. Zurita, In-Vessel Core Degradation Code Validation Matrix, Update 1996-1999, OECD/GD(94)14, [NEA/CSNI/R\(95\)21](#), 1996.
- [14] G.M. Hesson, N.J. Lombardo, J.P. Pilger, W.N. Rausch, L.L. King, D.E. Hurley, L.J. Parchen, F.E. Panisko, Full-length high-temperature severe fuel damage test No. 2. Final safety analysis, Report PNL—5547, 1993.
- [15] R. Hobbins, M. Russel, C. Olsen, R. Mc Cardell, Molten Material Behaviour in the Three Mile Island Unit 2 Accident, *Nuclear Technology* **87**, 1005-1012, 1989.
- [16] R. Hobbins, D. Petti, D. Osetek, D. Hagrman, Review of experimental results on light water reactor core melt progression, *Nuclear Technology* **95**, 287-307, 1991.

- [17] P. Hofmann *et al.*, Chemical-Physical Behaviour of Light water reactor core components tested under severe reactor accident conditions in the CORA facility, *Nuclear Technology* **118**, 200-224, 1997.
- [18] P. Hofmann, S. Hagen, G. Schanz, A. Skokan, Reactor Core Materials Interactions at Very High Temperatures, *Nuclear Technology* **87**, August 1989.
- [19] S.M. Jensen, D.W. Akers, Post-irradiation examination results from the LP-FP-2 center fuel module, Report EGG-M-90152; CONF-9005179—2, 1990.
- [20] D.A. Petti, Z.R. Martinson, R.R. Hobbins, C.M. Allison, E.R. Carlson, D.L. Hagrman, T.C. Cheng, J.K. Hartwell, K. Vinjamuri, L.J. Seifken, Power Burst Facility (PBF) severe fuel damage test 1-4 test results report, Report NUREG/CR-5163; EGG-2542, 1989.
- [21] L. Sepold, P. Hofmann, W. Leiling, A. Miasoedov, D. Piel, L. Schmidt, M. Steinbrück, Reflooding experiments with LWR-type fuel rod simulators in the QUENCH facility, *Nuclear Engineering and Design* **204** (1-3), 205-220, 2001.
- [22] I. Shepherd *et al.*, Investigation of Core Degradation, *COBE project, FISA-99 Symposium*, Luxembourg, EUR 19532 EN, Nov. 1999.
- [23] K. Trambauer, Coupling methods of thermal-hydraulic models with core degradation models in ATHLET-CD, ICON-6, © ASME 1998.
- [24] M.S. Veshchunov, K. Mueller, A.V. Berdyshev, Molten corium oxidation model, *Nuclear Engineering and Design* **235** (22), 2431-2450, 2005.
- [25] A.B. Wahba, International activities for the analysis of the TMI-2 accident with special consideration of ATHLET calculations, *Nuclear Engineering and Design* **118**, 43-53, 1990.
- [26] R. Wright, Current understanding of in-vessel core melt progression, *Proceedings of the Dubrovnick meeting*, IAEA-SM-296/95, 1995.
- [27] Progress Made in the Last Fifteen Years through Analyses of TMI-2 Accident Performed in Member Countries, Rapport [NEA/CSNI/R\(2005\)1](#), 2005.
- [28] V. Asmolov *et al.*, RASPLAV Application Report, *OECD RASPLAV Seminar*, Munich (Germany), 2000.
- [29] K. Atkhen, G. Berthoud, Experimental and numerical investigations on debris bed coolability in a multidimensional and homogeneous configuration with volumetric heat source, *Nuclear Technology* **142** (3), 2003.
- [30] S.V. Bechta, B. Khabensky, V.S. Granovsky, E.V. Krushinov, S.A. Vitol, V.V. Gusarov, V.I. Almiashhev, D.B. Lopukh, W. Tromm, D. Bottomley, M. Fisher, P. Piluso, A. Miasoedov, E. Alstadt, H.G. Willschutz, F. Fichot, Experimental Study of Interactions Between Suboxidized Corium and Reactor Vessel Steel, *Proceedings of ICAPP'06*, Reno, NV USA, June 4-8, 2006.

- [31] G. Berthoud, M. Valette, Description des lois constitutives de la version 3.2 du logiciel de prémélange MC3D, NT SMTH/LM2/99-39, 1999.
- [32] P. Chapelot, A.C. Grégoire, G. Grégoire, Final FPT4 Report, IRSN/DPAM-DIR 2004-0135, PH-PF IP-04-553, 2004.
- [33] T.C. Chawla, C.H. Chan, Heat Transfer from Vertical/Inclined Boundaries of Heat Generating Boiling Pools, *Journal of Heat Transfer* **104**, 465-473, 1982.
- [34] D.H. Cho, D.R. Armstrong, W.H. Gunther, S. Basu, Experiments on interactions between Zirconium-containing melt and water (ZREX): Hydrogen generation and chemical augmentation of energetics, *Proceedings of JAERI Conference*, 97-011, Japan, 1997.
- [35] V.V. Chudanov, A.E. Aksenova, V.A. Pervichko, Development of 3D unified computational tools to thermalhydraulic problems, *Proc. 10-th International Topical Meeting on Nuclear Reactor Thermal Hydraulics (NURETH-10)*, Seoul, Korea, October 5-9, 2003.
- [36] F. Fichot, V. Kobzar, Y. Zvonarev, P. Bousquet Mélou, The Use of RASPLAV Results in IPSN Severe Accident Research Program, in OECD-NEA, editor, *Proceedings of RASPLAV Seminar*, Munich, 2000.
- [37] F. Fichot, J.-M. Seiler, V. Strizhov, Applications of the OECD MASCA Project Results to Reactor Safety Analysis, MASCA Application Report, OECD-NEA, 2003.
- [38] F. Fichot, F. Duval, N. Trégourès, M. Quintard, The impact of thermal non-equilibrium and large-scale 2D/3D effects on debris bed reflooding and coolability, *Proceedings of NURETH-11 Conference*, Avignon, France, 2005.
- [39] B.D. Gasser, R.O. Gaunt, S. Bourcier, Late Phase Melt Progression Experiment MP-1. Results and Analyses, NUREG/CR-5874, SAND92-0804, 1992.
- [40] D. Magallon, The FARO programme recent results and synthesis, *Proceedings of CSARP Meeting*, Bethesda, USA, 1997.
- [41] F. Mayinger *et al.*, Examination of thermo-hydraulic processes and heat transfer in core melt, Final Report BMFT RS 48/1. Technical University, Hanover, Germany, 1975.
- [42] M. Salay, F. Fichot, Modelling of metal-oxide corium stratification in the lower plenum of a reactor vessel, *Proceedings of NURETH11 Conference*, Avignon, France, 2005.
- [43] P. Schäfer, M. Groll, W. Schmidt, W. Widmann, M. Bürger, Coolability of Particle Beds: Examination and Influence of Friction Laws, *International Congress on Advances in Nuclear Power Plants (ICAPP'04)*, Pittsburgh, PA, USA, June 13-17, 2004.
- [44] J.M. Seiler, K. Froment, Material effects on multiphase phenomena in late phases of severe accidents of nuclear reactors, *Multiphase Science and Technology* **12**, 117-257, 2000.

- [45] A.V. Stepanyan, A.K. Nayak, B.R. Sehgal, Experimental Investigations of Natural Convection in a Three-layer Stratified Pool with Internal Heat Generation, *Proceedings of NURETH11 Conference*, Avignon, France, 2005.
- [46] S. Vandroux-Koenig *et al.*, TOLBIAC version 2.2 code description, NT SMTH/LM2/99-36, 1999.
- [47] M. Saito *et al.*, Melting attack of solid plates by a high-temperature liquid jet – effect of crust formation, *Nuclear Engineering and Design* **121** (1), 11-23, 1990.
- [48] T. G. Theofanous *et al.*, Lower head integrity under steam explosion loads, *Nuclear Engineering and Design* **189** (1-3), 7-57, 1999.
- [49] B. R. Sehgal *et al.*, Assessment of reactor vessel integrity (ARVI), *Nuclear Engineering and Design* **235** (2-4), 213-232, 2005.
- [50] J. R. Wolf *et al.*, OECD-NEA-TMI-2 Vessel Investigation Project. Report TMI V(93)EG10, 1993.
- [51] L. A. Stickler *et al.*, OECD-NEA-TMI-2 Vessel Investigation Project. Calculations to estimate the margin-to-failure in the TMI-2 vessel, Report TMI V(93)EG01, 1993.
- [52] T. Y. Chu *et al.*, Lower Head Failure Experiments and Analyses, NUREG/CR-5582, SAND98-2047.
- [53] L. L. Humphries *et al.*, OECD Lower Head Failure Project Final Report, OECD/NEA/CSNI/R(2002)27.
- [54] V. Koundy, N. H. Hoang, Modelling of PWR lower head failure under severe accident loading using improved shells of revolution theory, *Nuclear Engineering and Design* **238**, 2400-2410, 2008.
- [55] V. Koundy *et al.*, Progress on PWR lower head failure predictive models, *Nuclear Engineering and Design* **238**, 2420-2429, 2008.
- [56] L. Nicolas *et al.*, Results of benchmark calculations based on OLHF-1 test, *Nuclear Engineering and Design* **223**, 263-277, 2003.
- [57] OLHF Seminar 2002 - *Nuclear Safety* – NEA/CSNI/R(2003)1.
- [58] Sehgal *et al.*, Assessment of reactor vessel integrity (ARVI), *Nuclear Engineering and Design* **221** (1-3), 23-53, 2003.
- [59] Sehgal *et al.*, Assessment of reactor vessel integrity (ARVI), *Nuclear Engineering and Design* **235** (2-4), 213-232, 2005.
- [60] J. Devos *et al.*, CEA programme to model the failure of the lower head in severe accidents, *Nuclear Engineering and Design* **191**, 3-15, 1999.
- [61] V. Koundy *et al.*, Study of tearing behaviour of a PWR reactor pressure vessel lower head under severe accident loadings, *Nuclear Engineering and Design* **238**, 2411-2419, 2008.

- [62] P. Matheron, S. Chapuliot, L. Nicolas, V. Koundy, C. Caroli, Characterization of PWR vessel steel tearing under severe accident condition temperatures, *Nuclear Engineering and Design* **242**, 124-133, 2012.
- [63] V. Koundy, Défaillance du fond d'une cuve REP en situation accidentelle grave et programme de recherche sur la déchirure des matériaux de cuve française, Rapport scientifique et technique (RST), IRSN, 2008.
- [64] B. Autrusson, G. Cénérino, Synthèse des études concernant le comportement mécanique du fond de cuve, Note technique DPEA/SEAC/97-069 – Référence non publique.
- [65] S. Brosi *et al.*, CORVIS. Investigation of light water reactor lower head failure modes, *Nuclear Engineering and Design* **168**, 77-104, 1997.
- [66] K. Ikonen, R. Sairanen, FEM Analysis of OLHF tests with and without penetration, OLHF Seminar 2002, Madrid, June 26-27, 2002 - (Paper from VTT, *Nuclear Energy*, Finland).
- [67] N. Tardif, Étude du comportement à haute température d'une fissuration instable dans l'acier 16MND5 et application au calcul de la rupture d'un fond de cuve en cas d'accident grave, thèse de doctorat, n° d'ordre 2009-ISAL-0105, LaMCoS – UMR CNRS 5259 – INSA de Lyon.
- [68] W. A. Stewart *et al.*, Experiments on natural circulation flows in steam generators during severe accidents, *Proceedings of the international ANS/ENS topical meeting on thermal reactor safety*, San Diego, California, USA, 1986.
- [69] W. A. Stewart *et al.*, Experiments on natural circulation flow in a scale model PWR reactor system during postulated degraded core accidents, *Proceedings of the 3rd international topical meeting on reactor thermal hydraulics*, Newport, Rhode Island, USA, October 1985.
- [70] B. R. Seghal, W. A. Stewart and W.T. Sha, Experiments on natural circulation during PWR severe accidents and their analysis, *International ENS/ANS Meeting on Reactor Safety*, Avignon, France, 1988.
- [71] C. F. Boyd and K. Hardesty, CFD predictions of severe accident steam generator flows in a 1/7th scale pressurized water reactor, *Proceedings of the 10th International Conference on Nuclear Engineering (ICONE10)*, Arlington, Virginia, USA, April 14-18, 2002.
- [72] C. F. Boyd, D. M. Helton and K. Hardesty, CFD analysis of full-scale steam generator inlet plenum mixing during a PWR severe accident, NUREG-1788, 2004.
- [73] H. Mutelle and U. Bieder, Study of severe accident natural gas circulation with the CFD code TRIO-U, *Technical meeting on use of CFD codes for safety analysis of reactor systems, including containment*, Pisa, Italy, November 11-14, 2002.

-
- [74] D.L. Knudson and C. A. Dobbe, Assessment of the potential for high-pressure melt ejection resulting from a Surry station blackout transient, NUREG/CR-5949, 1993.
- [75] <http://www.nea.fr/html/jointproj/rosa.html>
- [76] T. Takeda *et al.*, Analysis of the OECD/NEA ROSA project experiment simulating a PWR small break LOCA with high-power natural circulation, *Annals of nuclear energy* **36** (3), 386-392, 2009.
- [77] Güntay S. *et al.*, ARTIST: introduction and first results, *Nuclear engineering and design* **231** (1), 109-120, 2004.

5.2. *Phenomena liable to result in early containment failure*

5.2.1. *Direct containment heating*

5.2.1.1. Introduction

The phenomenon of direct containment heating (DCH⁴) is diagrammatically represented in Figure 5.12. In the event of a PWR core melt accident, a corium melt composed of uranium and zirconium oxides as well as non-oxidised metals (zirconium and steel) and various fission products may form in the lower head. If the lower head ruptures in this situation, the corium is ejected, along with steam and, in some cases, hydrogen from the RCS and liquid water still present in the reactor vessel head when it fails. Depending on the internal pressure of the reactor vessel when it ruptures, this causes more or less finely-grained corium fragmentation and more or less widespread dispersion of the fragments outside the reactor pit. Corium dispersion leads to very efficient heat exchange between the corium and the gases present, as well as oxidation of metallic components of corium, producing hydrogen as a result. The oxidation is mainly due to the steam present in the RCS but also to the steam contained in the containment. The temperatures reached by the gases in the containment and the presence of very hot corium particles then triggers the combustion of the hydrogen created through oxidation of the dispersed corium. This combustion could cause the hydrogen already present in the containment to ignite at the time the reactor vessel ruptures if the concentration is high enough. These phenomena cause the containment atmosphere to heat up and its pressure to rapidly build up (in a few seconds), resulting in the containment being damaged or its integrity failing. In addition, the loads directly applied to the reactor vessel (thrust due to the gases and liquids leaving the reactor vessel, and pressure in the reactor pit) may result in a more or less significant movement of the reactor vessel itself, possibly causing a shock to the structures, the RCS and the SCS and the possible bypass of the containment if breaks are induced in the exterior of the containment, in a system connected to the RCS and not isolated from it.

The risk of the containment rupturing as a result of the gases inside the containment being directly heated is assessed from a technical point of view, assuming that there is no water in the reactor pit when the reactor vessel ruptures. Tests have shown that the risk of combustion is greater when there is no water in the reactor pit. If there is a large quantity of water in the reactor pit, the main phenomenon that can threaten containment integrity is the steam explosion that could occur when the reactor vessel ruptures as a result of the very hot corium coming into contact with the water in the reactor pit; the subject of steam explosions is discussed in Section 5.2.3. In the case of the reactors in operation in France, if there is no water in the reactor pit when the reactor vessel ruptures, this is because the Containment Spray System (CSS) was not operating before the reactor vessel ruptured. For the PWRs, the objective of "practical elimination" of the steam explosion risk in the reactor pit requires the reactor pit to be kept dry before the reactor vessel ruptures.

4. The acronym DCH (Direct Containment Heating) is generally used.

5.2.1.2. Physical phenomena

Although the phenomena involved in DCH are well understood at the qualitative level, many uncertainties remain regarding the corresponding detailed physical phenomena and their importance in the pressure build-up within the containment [1, 7]. The extent and consequences of DCH greatly depend upon reactor geometry and an experimental approach has been preferred for some time, coupled with the development of simplified models for interpreting the test results and extrapolating them to the case of a power reactor. The particularly violent nature of the phenomenon and the highly specific conditions under which nuclear reactor core melt accidents occur demand the use of simplified geometries and materials and modest instrumentation in the tests, however. Most of the information obtained in experiments is global (corium dispersion rate and pressure peak), includes significant uncertainties (corium oxidation rate and hydrogen combustion) and is often result of analyses performed after the tests are conducted (dispersion and grain size distribution, for example). With the recent development of simulation tools and computational capabilities, certain phenomena can now be assessed in greater detail. All of these phenomena, including dispersion, metal oxidation, hydrogen combustion and the presence of water, have not yet been combined in CFD modelling, however, and it seems difficult to envisage doing so in the short term.

Figure 5.12 shows a diagram of the phenomena and the associated risks. When the reactor vessel ruptures, it contains, apart from the structural elements still in place,

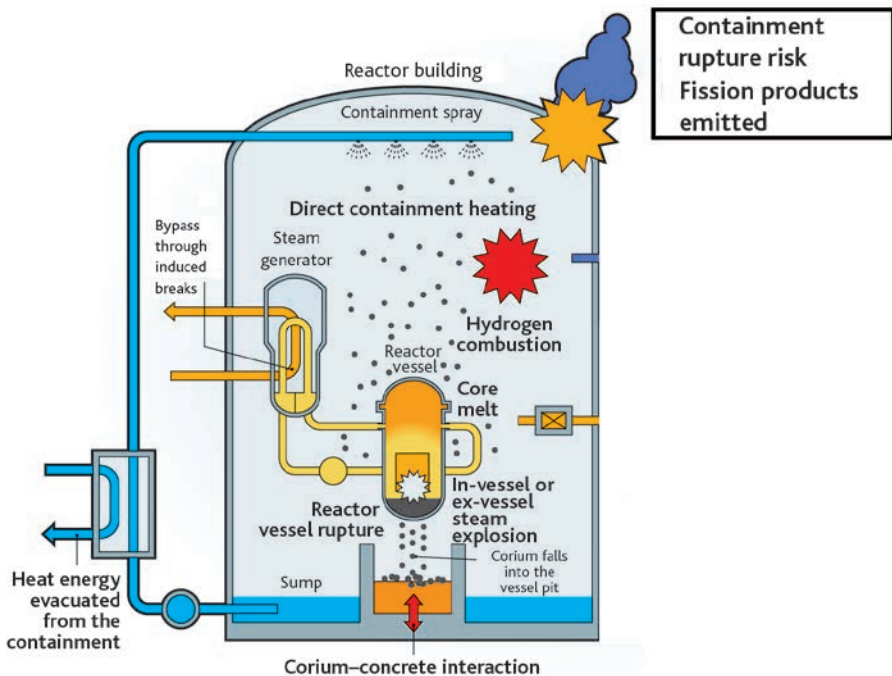


Figure 5.12. Schematic diagram of the physical phenomena occurring during direct heating of the gases in the containment.

a mixture of steam and hydrogen, some corium in the lower head and possibly some water, all of which is subjected to a pressure ranging from the operating pressure of the RCS (approximately 160 bar) to a pressure close to that of the containment (a few bar) if the RCS is completely depressurised. The corium and the steam, and possibly some hydrogen, are ejected under pressure into the reactor pit in different phases (single-phase liquid corium jet, followed by a two-phase corium and gas jet and a gaseous jet). The characteristics of their ejection, of course, depend on the size, shape and location of the break in the reactor vessel wall. The characteristics of the break are currently difficult to predict and so are uncertain (Section 5.1.3).

When the corium is ejected under pressure, it is fragmented into liquid droplets that rapidly oxidise, producing hydrogen. A flow of steam, hydrogen and corium then forms in the reactor pit. This highly complex flow is greatly influenced by the geometry of the reactor pit. It is also central to the following phenomena: the projection of corium onto the reactor pit walls, the formation of a liquid film along these walls and the entrainment and fragmentation of the film by the gases. All these phenomena increase the pressure of the gases in the reactor pit relative to that of the containment. As a result, part of the corium is entrained by the steam into the areas adjoining the reactor pit and towards the containment dome, while another part remains trapped in the pit. During this phase, the gases and the corium droplets interact both thermally and chemically. The gases' temperature and pressure in the reactor pit therefore increase considerably. Hydrogen combustion is not possible in the reactor pit, however, because its atmosphere contains little oxygen (it was driven out by the gases leaving the reactor vessel). When hot gases and corium particles enter the containment, they contribute to the superheating and rapid pressurisation of its atmosphere. The greater the mass of corium dispersed and the finer its fragmentation, the greater the containment pressure build-up. The distribution of corium in the different areas of the containment and the duration of the flow also play an important role in defining the pressure build-up. Furthermore, when the very hot gases and corium particles enter the containment they provoke hydrogen combustion. This combustion is highly complex because it combines turbulent diffusion flames (in the containment area into which the jet leaving the reactor pit spreads) with premixed flames (in the containment areas outside the jet). In most situations, hydrogen combustion does most to heat up and pressurise the containment gases.

It should be noted that the above description of DCH and its current modelling has been simplified compared with reality for various reasons including the following:

- the presence of water, both in the reactor vessel and in the reactor pit, affects the phenomenon in various ways by creating the opposite effects. The water present in the reactor vessel, which is strongly depressurised when it ruptures, very rapidly vaporises (referred to as “flash vaporisation”). This causes the reactor vessel to depressurise more slowly, on the one hand (increasing the corium dispersion time), and causes a greater thrust upon the reactor vessel, on the other hand. This water does not entirely vaporise, however, and the water present in the reactor pit also disperses and so, firstly, acts as a heat sink and, secondly, disrupts or even inhibits combustion. As a result, it is difficult to know whether the presence of water has a generally beneficial effect or not;

- as a result of the pressure in the reactor pit, the water can move and so modify the geometric configuration and close flow routes or open others.

Technically, therefore, the problem is very difficult to model precisely.

5.2.1.3. Experimental programmes

The existing knowledge of phenomena involved in DCH has mainly been gained through test programmes conducted on mock-ups, which provide small-scale reproductions of the main geometrical characteristics of reactors. The different geometries studied are presented in the following paragraphs, after which the results of the tests are discussed, based on the temperature and materials used to simulate the corium and the presence of water in the reactor pit.

In the late 1980s and early 1990s, many tests were conducted on more or less detailed mock-ups of American reactors at scales varying from 1/40 to 1/25 [1-4]. The most widely studied and documented geometry is that of the ZION reactor. The link between the reactor pit and the containment dome (through which the gases and corium pass *via* the annular passage around the reactor vessel) was not represented in the purpose-built mock-up of the Zion reactor in the Sandia National Laboratory's Surtsey facility in the United States (Figure 5.13). An instrumentation tunnel represented the connections between the reactor pit and the intermediate compartments of the containment. In addition, the system simulating the reactor vessel was positioned outside the containment. The integral tests were conducted at high pressures (around 60 bar).

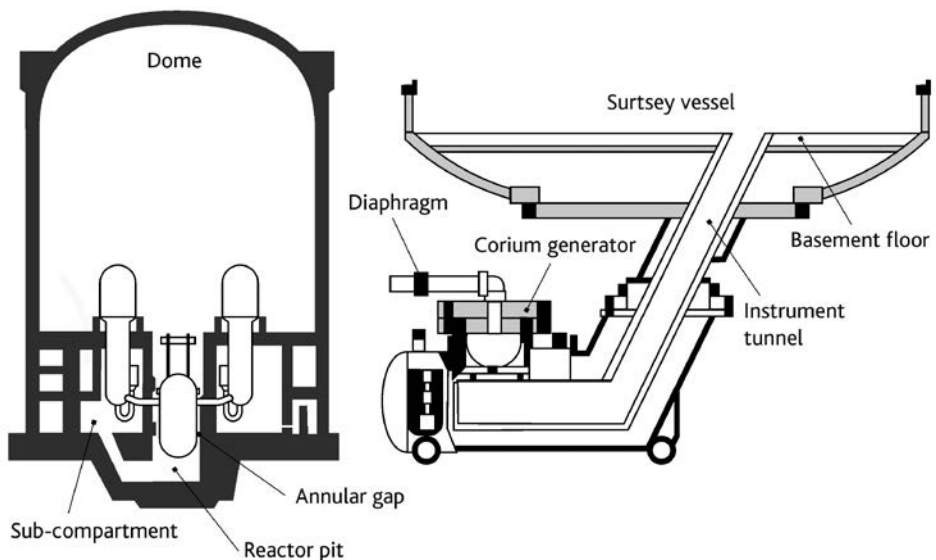


Figure 5.13. Diagram of the Zion reactor (left) and its representation in the experiments conducted in the Sandia National Laboratory's Surtsey facility (right) [1].

The second geometry studied was that of the Surry reactor. Some of the corresponding tests took into consideration the annular passage around the reactor vessel, directly linking the reactor pit with the containment dome, and the presence of thermal insulation around the reactor vessel. A limited number of experiments have been conducted with this geometry. Lastly, a third geometry, that of the Calvert Cliffs reactor, was studied; in this geometry, there is a larger annular passage around the reactor vessel, whose configuration is more like that of the French reactors.

In 1997, KAERI (South Korea) conducted a test campaign for IRSN (IPSN at that time). These tests were the first to study the DCH phenomenon, albeit solely in cold tests, in a geometry similar to that of a French 900 MWe reactor at a 1/20 scale.

More recently, tests were conducted in the DISCO facilities of Forschungszentrum Karlsruhe (FzK), now called Karlsruhe Institut für Technologie (KIT), in Germany [5, 7]. The initial test facilities, referred to as DISCO-C, were used to conduct cold tests, whereas another, referred to as DISCO-H, was used to conduct integral tests simulating all of the thermal and chemical phenomena. The DISCO facilities, which were initially constructed for studies on the PWR reactor (1:18 scale), were then modified so that the geometry of the 1300 MWe P'4 reactors could be studied (in collaboration with IPSN, Figure 5.14), for that of the KONVOI reactors (German reactors whose geometry is similar to that of the PWRs) and for that of the VVER-1000 reactors (a single test in DISCO-H). The PWR and KONVOI geometries are unusual as their reactor pit is very small, encouraging corium dispersion outside the reactor pit, particularly as there is no access corridor; in the case of the 900 MWe and 1300 MWe French reactors (Figure 5.14), the reactor pit is much deeper and there are three possible exit routes from the reactor pit: to the upper part of the containment (dome), to the compartments at the bottom of the containment and to the reactor pit access corridor. The DISCO tests were limited to reactor vessel internal pressures below 25 bar.

► Low-temperature simulant tests (dynamic aspects)

These tests aim to establish correlations relating to the entrainment of the simulant to the compartments adjacent to the reactor pit and to the containment based on experimental parameters, which generally consist of the size of the break in the lower head, the internal pressure of the reactor vessel when it ruptures, and the physical properties of the corium simulant and of the carrier gas leaving the reactor vessel. Various simulants have been used for the tests of this type: water (Figure 5.14), oils, Wood metal (a eutectic alloy composed of bismuth, lead, tin and cadmium) and gallium. The latter two simulants offer the advantage of possessing properties (density, viscosity and surface tension) that are similar to those of corium, whereas water is a poor simulant (its physical properties are very different from those of corium, and its phase changes — evaporation or freezing — are unrepresentative of it).

The KAERI tests, whose geometry is representative of that of the 900 MWe French reactors, have shown that when the internal pressure of the reactor vessel is high enough, up to 80% of the simulant can be entrained into the annular space around the reactor vessel and into the passage towards the containment dome, and then released

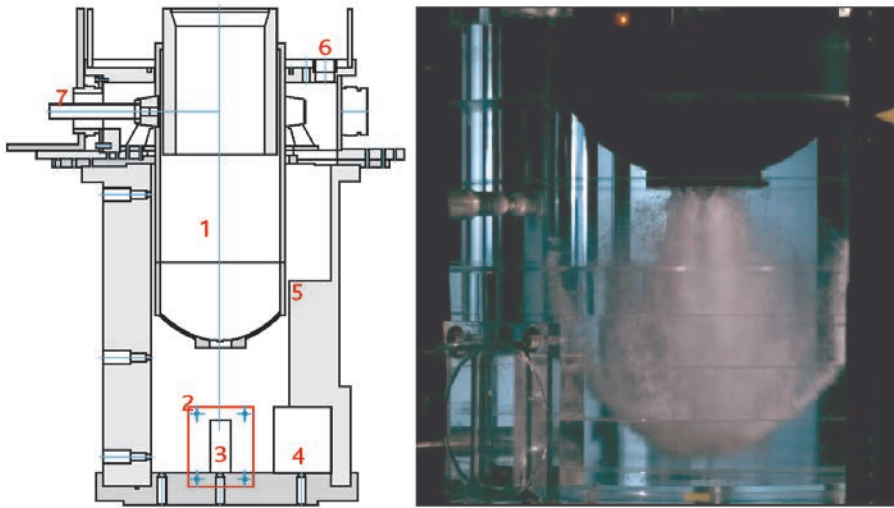


Figure 5.14. Representation of the reactor pit geometry of a P'4 reactor for the DISCO-C tests: 1-reactor vessel, 2-reactor pit, 3-reactor pit access corridor, 4-niche, 5-annular passage, 6-exit to the containment dome, 7-exit to the intermediate compartments of the containment. Right: photograph of a high-pressure water ejection.

into the containment. In this geometry, the passage to the intermediate compartments of the containment is in fact very small and most of the fuel is ejected into the containment. In the case of the 1300 MWe reactors, a smaller fraction of the fuel is dispersed into the annulus (60%), as a substantial proportion of the fuel (~30%) is trapped in the reactor pit access corridor. Of the 60%, approximately 20% is directly entrained towards the containment dome and the rest is entrained into the intermediate compartments of the containment.

The geometry of the EPR reactor pit is very different. Due to the very small volume of the reactor pit, almost all of the corium may be drawn into the containment even if the internal pressure of the reactor vessel is very low (a few bar). The geometry of the EPR reactor pit has changed since the DISCO tests were conducted on EPRs and no longer includes a direct passage between the reactor pit and the containment; most of the ejected corium would then be entrained towards the intermediate compartments of the containment housing the equipment (SGs and pressuriser). The effect of various lower head rupture modes (break in the centre of the lower head, lateral break or partial de-capping of the lower head) upon simulant ejection dynamics has also been studied in tests on EPR geometries [6]; these tests have shown that greater masses are dispersed in the case of central breaks.

► High-temperature integral tests

In addition to the dynamic aspects, these tests provide an insight into heat exchange phenomena and chemical interactions. Table 5.3 lists all integral tests conducted until 2010. The most frequently-used simulant in tests of this type consists of an iron and alumina

mixture (Al_2O_3) resulting from a thermitic reaction⁵, with small quantities of chrome and zirconium sometimes added. Some tests have also been conducted using a composition more similar to that of an actual corium (containing a $\text{UO}_2 + \text{ZrO}_2$ mixture). The main differences between thermite ($\text{Fe-Al}_2\text{O}_3$) and corium are their density (approximately 4000 kg/m^3 , compared with 8000 kg/m^3) and their oxidisable metal composition (Fe, compared with Zr + Fe + Cr). Consequently, the results of the tests conducted using thermite cannot be directly extrapolated to the case of a DCH incident. Many tests have been conducted in the United States, mainly by the Sandia laboratories (SNL) and Argonne laboratories (ANL), for three types of geometry (principally that of the Zion reactor, the Surry reactor and the Calvert Cliffs reactor) and different experimental conditions [1]. These tests were conducted using high reactor vessel pressures between 60 and 120 bar: as a result, dispersion of the simulant and the pressure build-up within the containment were both high.

In the case of Zion reactor geometry, the different tests (conducted using the Surtsey mock-up with no direct connection between the reactor pit and the containment dome⁶) showed that the intermediate compartments of the containment retained 90% of the simulant and that there was a limited containment pressure build-up of approximately 2.5 bar (Figure 5.15). On the basis of these results, the US NRC has estimated that, in the case of this reactor, the risk of the containment rupturing as a result of DCH was zero [8].

Table 5.3. Main experimental programmes studying DCH.

Series	Number of tests	Scale	Geometry	ΔP (bar)	Material	$D_{\text{break}}^{(4)}$ (m)	Direct connection with dome	Water
DCH/WC ⁽¹⁾	7	1/10	Zion	26–67	Fe- Al_2O_3	0.4–1	No	Pit
TDS/LFP ⁽¹⁾	13	1/10	Surry	25–40	Fe- Al_2O_3 -Cr	0.4–0.9	No	No
IET-Zion ⁽¹⁾	9	1/10	Zion	60–70	Fe- Al_2O_3 -Cr	0.4	No	Pit
IET-Surry ⁽¹⁾	3	1/6	Surry	120	Fe- Al_2O_3 -Cr	0.7–1	Depending on the test ⁽⁵⁾	Pit
ANL-IET ⁽²⁾	6	1/40	Zion	57–67	Fe- Al_2O_3 -Cr	0.4	No	Pit
U ⁽²⁾	3	1/40	Zion	30–60	$\text{UO}_2 + \text{ZrO}_2$ + Z ₂ -stainless steel	0.4	No	No
CE-CES ⁽¹⁾	7	1/10	Calvert Cliffs	40–80	Fe- Al_2O_3	0.4–0.5	Yes	Reactor vessel
DISCO-H ⁽³⁾	6	1/18	EPR	8–22	Fe- Al_2O_3	0.5–1	Depending on the test	No
DISCO-FH ⁽³⁾	5	1/16	P'4	15–25	Fe- Al_2O_3	0.5–1	Yes	No
DISCO-KH ⁽³⁾	2	1/18	Konvoi	20–25	Fe- Al_2O_3	1	No	No

⁽¹⁾Sandia NL, ⁽²⁾Argonne NL, ⁽³⁾FzK, ⁽⁴⁾reactor vessel break diameter relative to the scale of the reactor vessels concerned, ⁽⁵⁾study of the effect of the thermal insulation, depending on whether it remains in place or not.

- When an iron oxide and aluminium are brought into contact, a highly exothermic chemical reaction occurs in which the aluminium reduces the iron oxide to produce what is called "thermite", an iron and alumina mixture (Al_2O_3); the reaction raises the temperature of the mixture, resulting in it melting.
- In reality, there is a connection between the reactor pit and the dome in the reactor, but this has been ignored.

The various subsequent tests, including those conducted in the DISCO facility, suggest that when no combustion occurs (due to the inert atmosphere in the containment), the compartmentalisation of the containment plays an important role in DCH and only the simulant fraction dispersed into the containment dome effectively heats its atmosphere. This is because the thermal equilibrium is reached more rapidly in a small volume, as the ratio between the volume of corium and the volume of gas is greater and so the gases are heated more rapidly.

The chemical phenomena of oxidation and combustion play a key role in DCH. The first tests to study the effect of these phenomena are the IET tests conducted for the Zion and Surry reactors' geometries (in most cases, with no direct connection between the reactor pit and the containment dome). In these tests, there was initially a moderate hydrogen concentration of approximately 2–3% in the containment. The metals were always very intensely oxidised. Hydrogen combustion rate was around 70%, resulting in the pressure doubling or tripling within the containment (Figure 5.15, left).

The DISCO-H tests confirmed these experimental findings [7]. They also showed that the oxidation not only occurs with the steam initially present in the reactor vessel, but also with the steam present in the containment (this could not be observed in the IET tests conducted with no direct connection between the reactor pit and the containment dome). Hydrogen combustion rate is very high in these tests — around 80% for initial hydrogen levels of 4.5–6%. Above all, they showed that there is a linear relationship between the pressure build-up in the containment and the estimated quantity of hydrogen contributing to combustion (Figure 5.15, right). If there is considerable hydrogen combustion, therefore, the heat transfers between the corium and the gas play a smaller

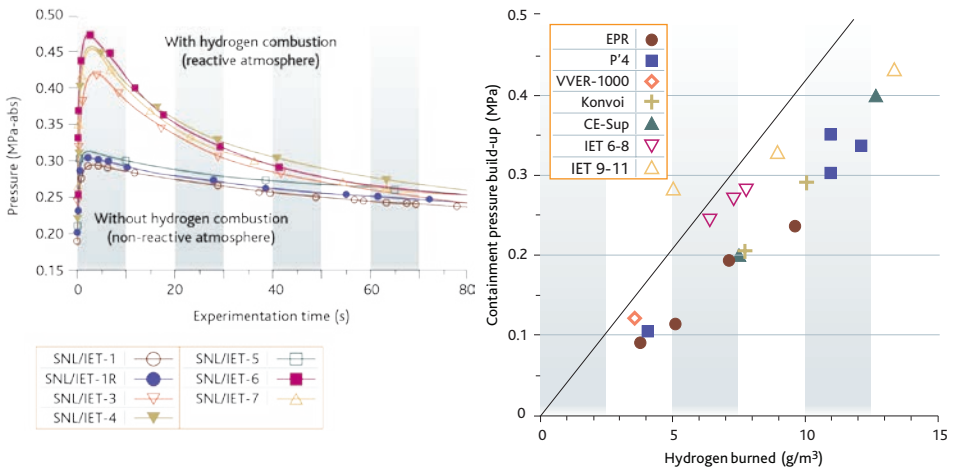


Figure 5.15. Influence of combustion upon the pressure build-up in the containment. Left: comparison of the pressure build-up observed for an atmosphere with and without hydrogen combustion in the IET-Zion tests (Sandia NL) [1]. Right: relationship between the pressure build-up and the estimated quantity of burnt hydrogen (per unit of volume) for a selection of DISCO (FzK), CE and IET tests (Sandia, IET6-8: Zion geometry, IET9-11: Surry geometry) [7]. The line represents the theoretical envelope values of the pressure build-up linked with hydrogen combustion.

role in DCH. This can be explained by the fact that the gas heating up due to combustion limits the thermal transfers between the corium droplets and the gas.

In addition, the DISCO tests conducted using the geometries of the PWR and 1300 MWe reactors show that the effect of compartmentalising the containment is less marked if combustion occurs. The combustion itself is less sensitive to compartmentalisation with high hydrogen concentrations (5–6%). When the initial hydrogen concentration is low (less than 3%), however, combustion has difficulty in propagating to the regions that the corium has not entered.

► Tests with real materials

Following the IET tests using thermite, three similar tests were conducted using a mixture of UO_2 , Zr, ZrO_2 , Fe and Cr in the COREXIT facility (1/40 scale mock-up of the Zion reactor) in order to demonstrate the effect of using real materials in place of thermite [2]. Very little data is therefore available on tests using real materials, and only very partial conclusions can be drawn from these tests.

Two tests were conducted using an almost inert containment atmosphere, eliminating all hydrogen combustion as a result; corium oxidation was possible, however, as the reactor vessel had a high steam content. For these two tests without combustion, which were conducted using a material whose specific energy is lower than that of thermite (approximately 1.2 MJ/kg, in the case of actual corium, instead of 2.7 MJ/kg for thermite), the pressure build-up in the containment dome was lower than in the tests conducted under similar conditions using thermite. The production of hydrogen due to oxidation of the materials by steam was much greater for corium, with corium oxidation of around 70%, compared with only 30–40% for thermite. This strong oxidation is mainly due to oxidation of the metals of which the corium is composed. Uranium dioxide (UO_2) can also be “superoxidised” by steam if enough is present; this “superoxidation” is probably limited, however, and produces little hydrogen.

In these two tests, it is also probable that corium oxidation was limited by the quantity of steam contained in the reactor vessel, which was insufficient to oxidise all of the oxidisable component materials of the corium. These tests therefore show that very high corium oxidation can occur for coriums whose compositions are representative of those that would form in a PWR core melt accident. For power reactors, a conservative approach to processing DCH consists in supposing that all the metals in the corium are completely oxidised when they are dispersed and ignoring uranium dioxide oxidation.

► Effects of the presence of water

The effect of water being present when the reactor vessel ruptures, either in the reactor vessel or in the reactor pit, has also been studied in the United States. The small number of tests conducted, coupled with the lack of even simplified models, only allows qualitative interpretations to be made, however. In the CE-CES tests (Calvert Cliffs reactor geometry, [4]), the corium simulant was initially in the bottom of the reactor pit, and water or steam that had previously been pressurised to between 40

and 80 bar was ejected from the reactor vessel through a break 4 cm in diameter (corresponding to a 40 cm diameter when scaled up to the real size of the reactor vessel). When the water was initially saturated (and so flash-vaporised on leaving the reactor vessel), this was not seen to have a significant influence upon the pressure build-up in the containment; the pressure build-up due to the water vaporising was therefore offset by a reduction in the effects of combustion and oxidation (approximately 30%). When the water temperature was close to the ambient temperature (meaning that the water did not vaporise on depressurisation), a significant drop (of around 30%) in the pressure loads was seen. In the CE-CES tests in which water was present in the reactor vessel, approximately 60% of the simulant was entrained towards the containment dome through the annular space.

Several tests were conducted by adding a small quantity of water in the reactor pit (the WC and IET tests). Some IET-Zion tests were also conducted using various quantities of water in the reactor pit. In these tests, the pressure build-ups were similar to those observed in tests with no water in the reactor pit; the presence of water therefore does not seem to have any overall effect upon the pressure build-up. The temperature measurements established that 50% less hydrogen was burned up than when there was no water in the reactor pit; in this case, therefore, the pressure build-up is largely due to water vaporisation. As a result, the presence of water has a very considerable effect upon the phenomena occurring in DCH and so could affect the pressure build-up under conditions different from those of the test. The current studies are based on the experimental results, however, and, as no adequate modelling is available, ignore the effect of the presence of water.

The presence of water in the reactor vessel or reactor pit seems fairly beneficial to DCH by limiting hydrogen combustion, although this must be confirmed by more detailed studies. When water is present, however, a steam explosion resulting from the interaction between the fragmented corium and the water may occur. Considering the measures taken to limit the possibility of high-pressure corium ejection in the event of a power reactor core melt accident (consisting of intentionally depressurising the RCS, see Section 4.3.3.3) and, therefore, the possibility of DCH occurring, conducting steam explosion studies is considered a priority in terms of risk mitigation.

The Sandia laboratories in the United States have conducted experiments in which molten corium was ejected at high pressure in a 1:10 scale mock-up of a flooded reactor pit (SPIT/HIPS experiments) [15]. In every case, a steam explosion destroyed the reactor pit in the tests. Details of the research results regarding the steam explosion are provided in Section 5.2.3.

5.2.1.4. Modelling

The complexity of DCH prevents it from being modelled in detail by coupling all of the important phenomena (corium ejection and fragmentation, heat transfers, oxidation of the component materials of the corium, hydrogen combustion and the presence of water).

Until the middle of the 2000s, the only existing models were constructed from simplified models mainly based on experimental correlations that were themselves implemented in “integral” computer codes used to calculate more or less complete accident sequences (MELCOR, MAAP, CONTAIN, ASTEC, etc.; see Chapter 8). These simplified models are mainly parametric, and their purpose is not to study and precisely understand the phenomena occurring in a DCH incident. They reflect the state of knowledge of these phenomena and can be coupled to provide a complete, albeit approximate, means of studying the progression of an accident.

For some years, FzK then IRSN have been conducting studies using multiphase, multidimensional simulation codes (the AFDM and MC3D codes, respectively). Unlike the parametric models discussed above, these computer codes represent certain important aspects of DCH more precisely, notably corium geometry and behaviour at different scales, but they do not represent the coupling of all phenomena. Furthermore, they process the complex chemistry occurring during DCH in a very simplified form. The AFDM and MC3D computer codes firstly aim to provide the parametric models with more appropriate correlations.

The modellers are now mainly focusing their attention on questions regarding corium dispersion. The experiments conducted show that both the oxidation of corium component materials and the hydrogen combustion are very closely linked with corium dispersion, and the simplified approaches producing envelope estimates of their effects upon the oxidation and combustion pressure do not excessively overestimate the pressures reached.

5.2.1.4.1. Parametric models

The DCH module of the US CONTAIN computer code [9] is the most advanced 0-D code available, and offers many computational options. Thus it also highlights the difficulties involved in modelling corium dispersion in DCH, as more than a dozen models or correlations may be used to describe how the corium debris is transported and the flows take place between the compartments of a containment, as well as describing how the structures trap debris.

The DCH module of the CONTAIN code contains relatively mechanistic models for describing how the corium is fragmented and the corium debris is entrained. It assesses the convection and radiant heat transfers between the debris and the atmosphere by means of conventional heat exchange laws. The code processes the chemical reactions involved in corium oxidation as well as in the combustion of hydrogen (both that produced through DCH and that already existing in the containment). Hydrogen combustion is evaluated by means of a simplified approach. Although the DCH module of the CONTAIN code provides a solid basis for qualification [10], its use is limited to US Zion or Surry reactors (GRS found it difficult to use when interpreting the results of the DISCO tests, which consisted of PWR and P'4 geometries) [11, 12]; this may be due to software complexity (notably its large choice of options) and, therefore, the need for its users to be highly experienced.

The other integral codes used to analyse core melt accidents adopt simpler approaches. The DCH module of the MAAP code, for example, uses correlations (based on the

geometry) to evaluate the total fraction of the dispersed corium [12]. The corium droplets are assumed to be in dynamic and thermal equilibrium with the gases. The distribution of droplets in the different outlets of the reactor pit then depends on the gas flow rates that the code computes for each outlet. Although this type of modelling can hardly be used to process precisely the geometry (notably that of the outlets) and the flows in the outlets (which depend on their geometry), it nevertheless offers the advantage of being simple.

The ASTEC computer code evaluates the pressure loads due to DCH by means of the RUPUICUV, CORIUM and CPA modules (see Chapter 8). The reactor pit phenomena are addressed by means of the RUPUICUV module. The CPA thermal-hydraulics module, which is used to compute the gas flows within the containment, cannot directly handle the special DCH phenomena associated with the presence of corium particles (heat transfers from the corium particles to containment gases, and corium oxidation), and an intermediate module — the CORIUM module — serves as an interface and processes corium energy contributions for use by the CPA module itself. The total dispersed fraction of the corium is determined using correlations. IRSN plans to revise the DCH modelling while still maintaining a simplified approach. Notably, it will introduce new correlations deduced from the results of the DISCO tests and the modelling conducted using the MC3D computer code.

5.2.1.4.2. Simulation software

IRSN and KIT have chosen to use multiphase thermal-hydraulics simulation codes to improve the state of knowledge of flows during DCH and simplify the development of simple models [13].

KIT uses the AFDM computer code, which was initially developed for conducting safety studies on fast neutron reactors (FNRs). This is a forerunner of the SIMMER III computer code, to which physical models relating to DCH have been added in order to simulate the chemical reactions between the metals and the steam or oxygen, for example, or else hydrogen combustion in the containment (parametric simplified model). The code processes gas flow configurations and thermal transfers between the gases and the corium in a comparatively comprehensive way, including the formation of corium films and crusts on the reactor pit cavity walls. Its use is limited to axisymmetrical 2D geometries, however. Promising results have been obtained for interpreting the DISCO tests conducted using the geometries of the EPR and Konvoi reactors; in particular, it has enabled IRSN to perform comparative analyses with the MC3D computer code.

The MC3D code is developed by IRSN and CEA; it is mainly used to evaluate the pressure loads caused by a steam explosion (Section 5.2.3). It can, however, also process many multiphase phenomena including — partially — DCH. This code is distinctive in that it describes the corium in detail: the “droplet field” (dispersed corium) is handled separately from the “jet field” (continuous corium) (see Figure 5.33 in Section 5.2.3, which illustrates this point). A detailed model of corium fragmentation and droplet coalescence allows users to move from one field to another. It includes a corium oxidation model. The MC3D code does not handle combustion, however. As combustion is the main contributor to the pressure build-up in the containment, the studies conducted

using the MC3D code only address corium dispersion and aim to develop simplified dispersion models for the ASTEC computer code and the probabilistic safety assessments (PSAs). The MC3D code can also be used to perform 3D computations that handle the French reactors' special geometries more precisely. As an example, Figure 5.16 shows a reactor geometry processed using the MC3D computer code (simplified P'4) as well as the computed results for corium dispersion in the annulus, as a function of the internal pressure of the reactor vessel.

As well as providing a direct comparison of the computational results at several experimental points, this type of code can be used to study, by means of many computations and fairly coarse meshes, the sensitivity of corium dispersion to parameters such as the internal pressure of the reactor vessel, the gas temperature and the break size. A correlation for processing corium dispersion has therefore been developed on the basis of the DISCO test results. This correlation predicts, for example, that when water is used as the simulant, the threshold pressure (minimum) resulting in dispersion is around 5 bar (see also Figure 5.16). In the case of P'4 reactors, the studies show that, for a reactor vessel break approximately one metre in diameter, the corium dispersion threshold pressure (minimum) is around 20 bar and the pressure above which maximum corium dispersion occurs is around 40 bar. Figure 5.17 shows these results, based on the internal pressure of the reactor vessel for three break diameters (the size of the break is not known precisely; it can vary from a few centimetres to a metre, as described in Section 5.1.3).

It has also been observed, again for the P'4 reactors, that the cross-section of the reactor pit access corridor only affects the maximum quantity of corium dispersed in the containment; the other characteristics such as the dispersion threshold pressure are barely affected. This has been confirmed by additional DISCO experiments.

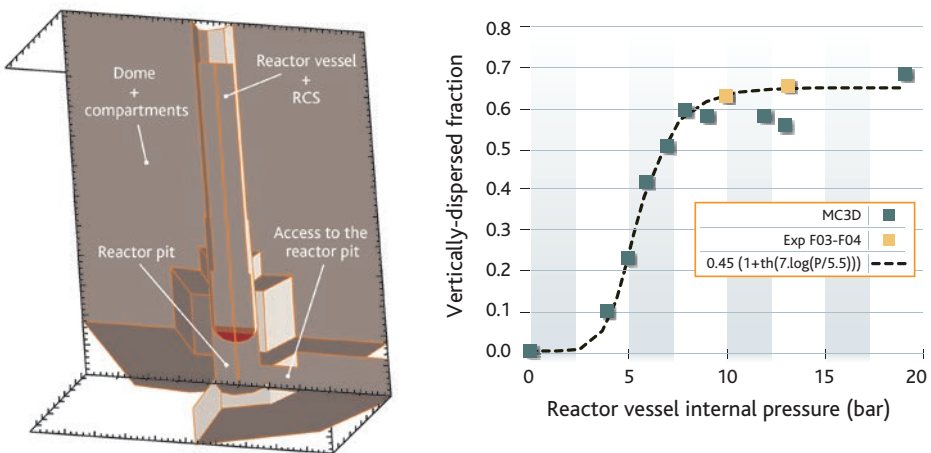


Figure 5.16. Left: 3D geometry used when interpreting the DISCO tests conducted using the geometry of the P'4 reactors (simplified geometry) processed by the MC3D code. Right: MC3D code evaluation of the fuel fraction dispersed towards the top of the reactor pit compared with the results of the tests conducted using water as the simulant and a reactor vessel break diameter of 60 mm.

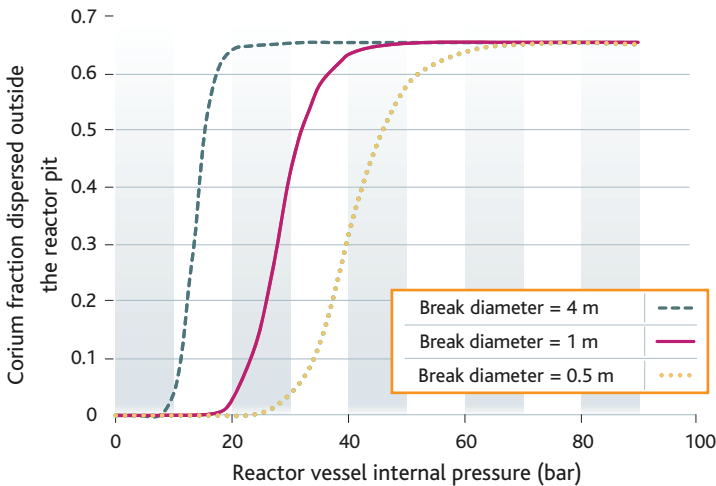


Figure 5.17. IRSN evaluation of corium dispersion outside the reactor pit depending on the internal pressure of the reactor vessel for different break diameters, in the case of P'4 reactors. The 4 m diameter corresponds to the lower head being torn off.

The great weakness in the existing models concerns hydrogen combustion. The combustion computer codes cannot compute corium dispersion and oxidation; conversely, the MC3D and AFDM codes do not include an adequate combustion model. It appears necessary to model combustion if these computer codes' predictive abilities are to be improved. Work on this point began in 2009 in the European [SARNET](#) system, under the supervision of KIT, with the aim of determining the most appropriate models and the way of introducing them into the multiphase simulation codes.

5.2.1.5. Summary and outlook

It is not easy to study the DCH risk. The risk is different for each type of reactor and, for a given geometry, depends on factors including the following:

- the internal pressure of the RCS at the moment the reactor vessel ruptures;
- the size of the break in the reactor vessel;
- the quantity of unrecombined hydrogen still present in the containment and in the RCS when the reactor vessel ruptures;
- the quantity of unoxidised metal in the corium.

The surest way of avoiding or limiting the effect of DCH upon the containment is to intentionally depressurise the RCS. This is incorporated into the design of PWR and AP1000 reactors. Depressurising the RCS is generally considered to be a key action in PWR safety during operation, notably in the Severe Accident Management Guidelines. Figure 5.17 shows the benefits of depressurising the RCS for the P'4 reactors and undoubtedly more generally, taking into account the uncertainties listed above, for all of the reactors in operation in France. DCH at a reactor vessel internal pressure of less

than 10 bar seems impossible for these reactors. Depending on the hydrogen concentration present in the containment, the corium melt outside the reactor vessel may result in hydrogen combustion without DCH in such a situation. The pressure loads on the containment would then only be due to hydrogen combustion.

The experimental data also show that the consequences of DCH are essentially related to reactor pit geometry and to the routes between it and the other areas of the containment. In particular, it is accepted that the consequences of DCH are reduced in reactors with no direct route for the corium and gases between the reactor pit and the containment dome; this solution has notably been chosen for the PWR reactors.

The combustion of the hydrogen created through oxidation of the corium dispersed by steam and of any initially present in the reactor vessel as well as in the containment atmosphere appears to be the main phenomenon responsible for building up the pressure in the containment. A detailed knowledge of the constituent metals of the corium as well as of the hydrogen quantities present in the containment and in the reactor vessel is needed to be able to evaluate precisely this pressure build-up. In situations in which there is considerable corium dispersion (dispersion of 30–50 tonnes of liquid corium; depending on the envisaged core melt accident scenarios, 100 tonnes or corium or even more may be dispersed), the studies conducted by IRSN show that containment mechanical strength limits may be reached during the resulting hydrogen combustion.

DCH is difficult to model. This is because the complexity and diversity of the phenomena involved in DCH, coupled with their dependence upon reactor building geometry, do not lend themselves to simple modelling. Parametric studies have been developed and used to conduct studies to estimate the pressure build-up in the containment during DCH, but their usefulness is highly doubtful outside their precise fields of validation (notably concerning the geometry of the reactor pit and the adjoining compartments). Multi-phase simulation codes have been used to obtain important results, notably concerning corium dispersion depending on the internal pressure of the reactor vessel. These are also difficult to use, however, and they cannot precisely determine all consequences of DCH in 2015, notably because of the difficulties of modelling corium oxidation and particularly, hydrogen combustion. In addition, the meshes used to process the complex real geometries are quite crude, and some geometric details cannot be modelled without simplification, resulting in inaccuracies in the flow computation.

The impact of water present in the reactor vessel or in the reactor pit during DCH has not really been characterised either. A better knowledge of this effect is necessary, but this can only be achieved by developing models coupled in a simulation code such as MC3D.

It appears necessary to use more precise simulation codes to compensate for the lack of experimental results (notably using real materials) and the limitations of the correlations developed on the basis of the existing results as well as to allow the results to be extrapolated to the case of a power reactor; this is why IRSN began development to improve DCH modelling for the French nuclear reactors in the middle of the 2000s.

5.2.2. *Hydrogen risks and means of mitigating their consequences*

5.2.2.1. Introduction

In the context of core melt accident studies on pressurised water reactors (PWRs), “hydrogen risk” is defined as the possibility of containment integrity being lost in a reactor or its safety systems as a result of hydrogen combustion. The hydrogen is principally produced through oxidation of the metals present in the reactor core (mainly the zirconium contained in the cladding of the fuel elements) during the core degradation phase (Section 5.1.1), and oxidation of the metals present in the corium pool or in the basemat during the molten corium-concrete interaction phase (Section 5.3). The hydrogen produced in this way is released into the containment. The hydrogen distribution in the containment is more or less homogeneous depending on the degree to which the atmosphere is mixed (this is mainly linked with the convection loops resulting from steam condensation within the containment). If it is heterogeneous, there may be local hydrogen concentrations that exceed the flammability limit of the gaseous mixture; if it ignites, this may result in pressure loads that can threaten containment or safety component integrity. The distribution and concentration of hydrogen within the containment may also be modified by the use of safety systems, such as the Containment Spray System (CSS), which homogenise the containment atmosphere and lead to an increase in hydrogen concentration due to steam condensation on water droplets. Moreover, systems such as recombiners and igniters already installed inside the reactor containments may affect hydrogen distribution by avoiding hydrogen building up in part or all of the structure (the PWRs in operation in France are only equipped with recombiners).

5.2.2.2. Physical phenomena

When a PWR core melt accident occurs, the hydrogen released from the RCS enters the containment atmosphere, which initially mainly consists of air and steam. In this atmosphere, convection movements are caused by the presence of steam and its condensation on cold surfaces. The hydrogen then plays a role in increasing the natural convection movements due to its low density and in reducing steam condensation on the walls by hindering steam diffusion. Convection within the containment may therefore be altered, and it is important to know whether the entire contained volume is set into movement as a result. If it is, the hydrogen and the air mix rapidly enough for it to be assumed that, outside the regions in which the gases are released and near to the walls, the atmosphere is homogeneous. Otherwise, only part of the contained volume — probably the upper part of the containment — is mixed, and the homogeneity of that part of the containment atmosphere is initially concerned; if its volume is small, that part can contain a gas mixture that is relatively rich in hydrogen. The hydrogen will then migrate more slowly (over the course of several hours, given the containment geometry and compartmentalisation) to the “dead” regions, which are probably in its lower part. In these regions, the hydrogen will be incorporated into the gas mixture, but the hydrogen level of the mixture will never exceed that found in the homogeneous region.

The flammability of the gas mixture in the containment depends on the temperature, pressure and composition of the mixture, as well as its ignition mode. In practice, however, the position of the point representing the composition of the mixture (hydrogen, air and steam) in the Shapiro diagram (see Figure 5.18) can be used to determine whether the mixture is flammable. In this diagram, the ignition and detonation regions are bounded by curves: the flammability limit curve bounds the flammability region, and the detonation limit curve bounds the detonation region. The detonation region, which is smaller, is within the flammability region. The flammability and detonation limits depend on the temperature and pressure; furthermore, the detonation limit is not an intrinsic characteristic of the gas mixture; it is only valid for the geometry in which it is obtained.

In a mixture flammable, combustion may be triggered by an energy source of a few millijoules. Consequently, in the presence of electrical power sources or hot points, it seems probable that ignition would occur rapidly once the gas mixture enters the flammability domain. In contrast, more energy (at least 100 kilojoules) is required to trigger a stable detonation. This explains why direct detonation can be ruled out for practical purposes; the only mechanism considered likely to provoke detonation is flame acceleration and the deflagration-to-detonation transition. In fact, due to hydrodynamic instabilities and turbulence (primarily caused by obstacles in the path of the flame), an initially laminar deflagration (with a flame velocity of around 1 m/s) may accelerate. Rapid combustion conditions may also develop, involving rapid deflagration (a few hundred m/s), deflagration-to-detonation transition (DDT) and detonation (over 1000 m/s). These explosive phenomena pose the biggest threat to the mechanical integrity of the containment walls, as they can produce very large, localised dynamic loads. The higher the combustion speed, the higher the pressure peak, albeit with a shorter peak application time.

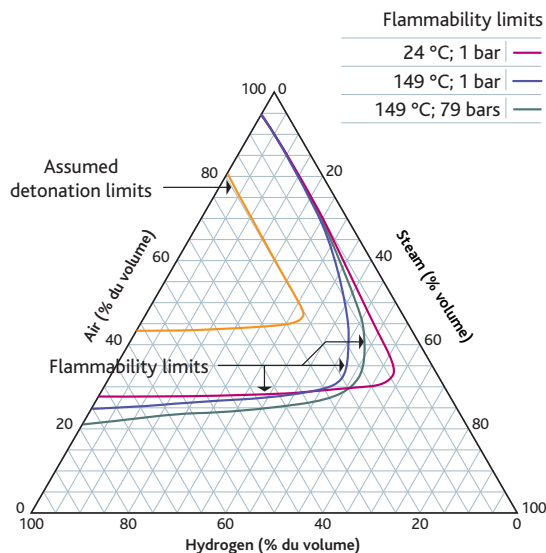


Figure 5.18. Shapiro diagram for the hydrogen, air and steam mixtures.

Due to the large volume and geometric complexity (mainly due to its compartmentalisation) of the containment, it is currently not possible to perform predictive computations concerning flame acceleration. Based on their understanding of the mechanisms involved, researchers have nevertheless developed prerequisite criteria, i.e. conditions required for the various combustion modes. Two types of criteria have been defined in this way:

- the criterion “ σ ” concerns the flame acceleration; the value σ is the expansion factor of the mixture, the relationship between the cold gas and burnt gas densities at a constant pressure, and so is an intrinsic property of the mixture in question; the critical value σ^* above which flame acceleration is possible depends on the initial temperature of the gases and the stability of the flame and has been determined using the results of many experiments at different scales and in different geometries;
- similarly, the necessary conditions have been established for assessing the possibility of a deflagration-to-detonation transition (DDT); these are based on comparing a length typical of the geometry of the studied chamber with the size of the detonation cells (marked λ) characterising the sensitivity of the mixture.

These criteria were initially established for homogeneous gas mixtures and then extended to cover mixtures in which there are hydrogen concentration variations, on the basis of ENACCEF programme results (Section 5.2.2.3.2). These criteria are used to determine the situations presenting a rupture risk to the containment for which it appears necessary to compute the loads resulting from possible combustion, by studying the hydrogen distribution in the containment (taking into account its geometry). It should be noted that before these criteria can be applied, the codes used to compute the hydrogen distribution in the containment must be validated based on situations representative of core melt accident conditions; this has been the aim of experimental programmes on hydrogen distribution in recent years.

5.2.2.3. Experimental programmes

5.2.2.3.1. Hydrogen distribution

Hydrogen distribution in the containment is controlled by various coupled complex physical phenomena, such as:

- the flows in the release region and the transporting of gases in the containment, notably hydrogen and steam;
- natural convection induced by temperature differences between the atmosphere and the walls and by density differences between the various gases present;
- steam condensation on the containment walls and internal structures;
- heat and mass stratification of the gases;
- diffusion in flows and turbulence;
- the effect of spray droplets on flows or of steam condensation on spray droplets.

Many analytical experiments have studied these phenomena separately. Regarding condensation, for example, the Dehbi experiments [31] on natural convection, together with those of Tagami, Uchida and Huhtiniemi [32] on forced convection, have enabled global models for steam condensation to be developed. The resulting correlations are more or less dependent on the test conditions and geometry, however. As the various phenomena governing hydrogen distribution are strongly coupled, large-scale global experiments have been conducted in addition to the analytical tests. A state-of-the-art report sponsored by EOCED on containment thermal-hydraulics and hydrogen distribution was completed in 1999 by a group of international experts (including IRSN experts) [16]. It provides a description of all of the experiments (HEDL, HDR, BMC and NUPEC) conducted since the beginning of the 1980s. In most cases, they consist of large-scale global experiments using limited instrumentation and an imprecise knowledge of the boundary conditions, meaning that they can only be used to validate 0D computer codes and are unsuitable for validating multidimensional codes.

To overcome the lack of data, well-equipped new facilities were constructed at the beginning of the 2000s to validate the multidimensional, multi-compartment computational tools. These include the PANDA, THAI, TOSQAN and MISTRA facilities (Figures 5.18, 5.19, 5.20 and 5.21).

► PANDA facility programme

The PANDA facility at the Paul Scherrer Institute in Switzerland was initially designed for studying containment thermal-hydraulics in boiling-water reactors (BWRs). It consists of four interconnected compartments with a total volume of 460 m³ [28].

As part of the OECD SETH (SESAR Thermal-Hydraulics) project between 2004 and 2006, tests were conducted (mostly without condensation) on a test facility mainly

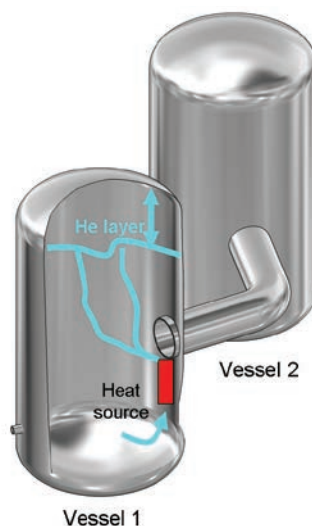


Figure 5.19. Diagram of the PANDA facility.

consisting of two compartments with a total volume of 180 m^3 , using instrumentation specially designed to accurately measure the flows in order to validate the multidimensional codes. The test grid for this project concerned flows resulting from a lateral or central injection of steam or helium, gas jet interaction with the containment wall within the injection region, and the impact upon gas distribution of an opening between the two compartments in the upper part of the containment and those in its lower part. The PANDA facility offers the possibility of studying complex flows; the lack of control over the temperature of the facility walls prevents the condensation phenomenon from being precisely characterised, however.

More recently, a new experimental programme, OECD/SETHII [35], was conducted in the PANDA and MISTRA facilities to obtain additional data on transient flows under conditions that could result in the homogenisation of an initially-stratified environment. Various configurations covering the effect of hydrogen recombiner use and the spraying or injection of steam at different flow rates upon the elimination of previous hydrogen stratification were studied as a result.

► THAI programme

Becker Technology's THAI facility in Germany is dedicated to analysing phenomena associated with the "hydrogen risk", iodine chemistry, and the transport and deposition of aerosols in PWR containments.

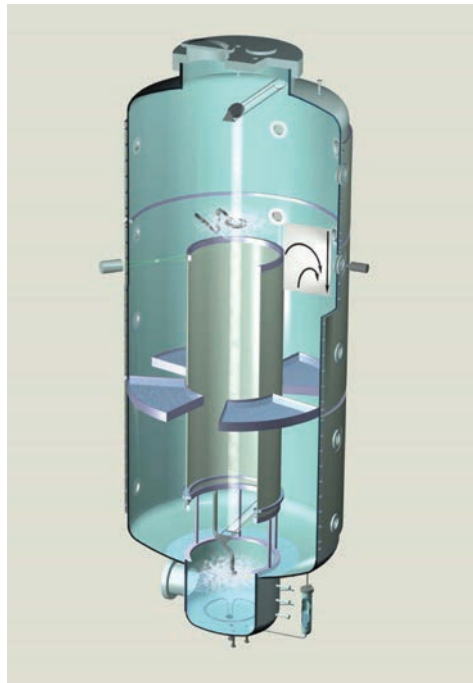


Figure 5.20. Diagram of the THAI facility [36].

The 60 m³ containment has a multi-compartmented internal structure with thermally-insulated external walls. With regard to the hydrogen risk, the THAI facility is designed for the study of hydrogen distribution and combustion, and the characterisation of catalytic recombiner operation. Between 1999 and 2002, the THAI facility was used to conduct thermal-hydraulics tests, one of which served as the basis of the OECD *International Standard Problem* (ISP) no. 47, which was completed in 2007 [18]. In this test, stratification of the gas mixture used (air, helium and steam) was created by injecting the helium and steam into the upper part of the containment (vertical injection); a lateral, low-flow-rate steam injection into its lower part could not cause movement throughout the compartmentalised containment atmosphere and so could not homogenise the gas mixture. This unexpected finding has shown the failings of the existing computer codes, which computed containment atmosphere homogenisation, and revealed the need to model flows in the injection regions in greater detail.

As a result, the study of phenomena governing the creation or destabilisation of stratification was continued as part of the OECD/THAI study [36] in order to improve the modelling of hydrogen distribution in a containment in the event of a core melt accident. As we will see later, the purpose of this project was also to study hydrogen combustion, recombiner behaviour and iodine chemistry. The tests conducted in this project also confirmed that the helium spread in the same way as hydrogen in the containment, meaning that it can be used in tests to study hydrogen distribution.

► TOSQAN programme

The TOSQAN facility, which IRSN has set up and operates at its Saclay site, consists of a cylindrical steel vessel with an internal volume of 7 m³ (excluding the sump, the lower part of the containment containing water). The wall temperature of this containment is adjusted, allowing the cold area in which condensation occurs to be delimited. Instrumentation for the gas volume includes equipment for measuring its pressure, temperature, concentration of gas species (by mass spectrometry and spontaneous Raman scattering) and velocity (by laser velocimetry). The water droplets dispersed by the spray system are measured in terms of their size (using imaging), velocity (using laser velocimetry) and temperature (using refractometry). The test programme studies the phenomena of steam condensation, containment spray, condensation and evaporation at the interface between the sump and the containment atmosphere as well as the spraydown of aerosols by aspersion [26].

The condensation tests, one of which served as the basis of ISP47, have been completed; they studied the stabilised conditions (constant steam injection condensation flow rates) with and without helium. In the test on which ISP47 was based, the helium added to the steam injection began to spread homogeneously in the upper part of the facility (above the injection point). This is where the main convection loop is situated. Instability then develops as a result of the fluid heated by the walls in the containment lower areas, curtailing the slow helium enrichment phase there and causing movement throughout the atmosphere, homogenising the mixture as a result. Under steady-state conditions, the atmosphere is homogeneous.

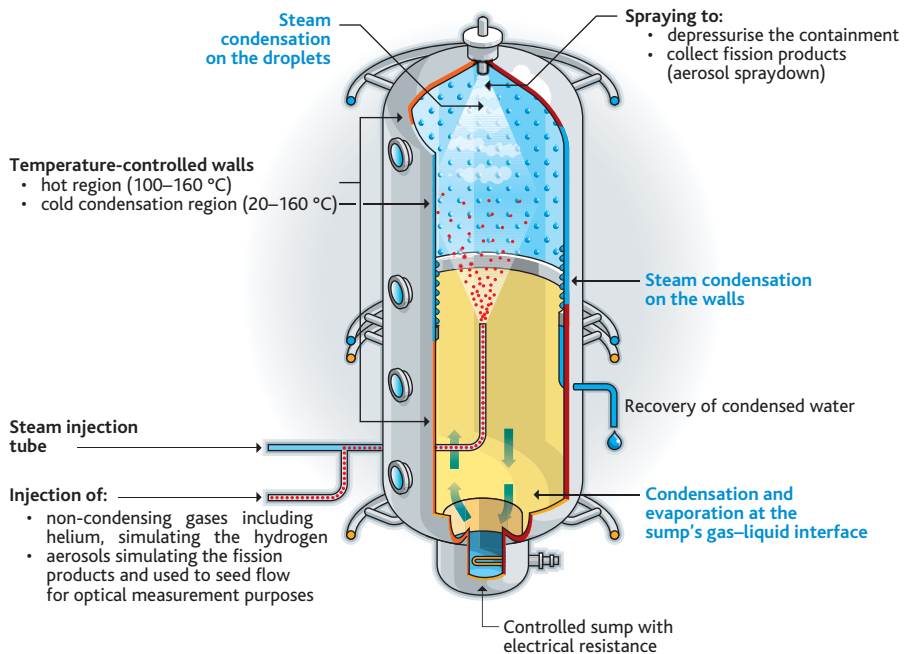


Figure 5.21. Diagram of the TOSQAN facility.

Spraying tests with centred and off-centre spray nozzles have been conducted. In addition, an international comparative study has been organised on the basis of the tests conducted in the European [SARNET](#) network. Test campaigns have been also conducted to study the interactions between the containment atmosphere and the sump as well as aerosol spraydown, and their results have been analysed.

► MISTRA programme

The main objective of the CEA MISTRA programme is to study condensation on the walls and on water droplets (from spraying) in a containment that is larger than that of TOSQAN and may contain compartments [27]. To be exact, the MISTRA facility consists of a 100 m³ stainless-steel containment (diameter 4.25 m; height 7 m) that is thermally-insulated and has three temperature-controlled internal condensing surfaces. The instrumentation used includes equipment for measuring pressure, temperature, gas concentration and flow velocities (using laser Doppler anemometry). It can be used to qualify multi-compartment and multidimensional computer codes and their coupling.

The condensation tests conducted in the MISTRA facility, one of which served as the basis of ISP47, were carried out under stabilised conditions to reach a balance between the steam injection and condensation rates when steam is injected into the uncompartimentalised or compartmentalised containment from centred and off-centre nozzles. In the test used for ISP47, in which helium was added to the steam injection flux, the helium distribution results were similar to those obtained in the TOSQAN test used for



Figure 5.22. Picture of the MISTRA facility (building 452) [reference document PAR-20050629-003, credit: A. Gonin/CEA].

the same ISP. A homogeneous atmosphere was firstly created in the uniform part of the containment under the effect of convection currents; below the helium injection level, the helium concentration slowly increased until the containment atmosphere was completely homogenised in approximately three hours. The overall movement observed in the TOSQAN test described above did not occur because the lower part of the containment was colder than its other parts (in a stable configuration). The TOSQAN and MISTRA test programmes on spraying showed that it was effective in homogenising an initially-stratified gaseous atmosphere. The MISTRA containment is also used in the OECD/SETHII project to study the effect of low-velocity steam injection upon an initially-stratified atmosphere.

IRSN and CEA conducted a study of the effect of scale between the TOSQAN and MISTRA facilities in order to assess the possibility of using the existing computer codes for a PWR building. This study was based on tests for which the initial conditions and the limit conditions were similar, resulting in homogeneous mixtures. This work on

the heterogeneous gas mixtures is being continued in the European ERCOSAM project (2011–2015). In this project, the study involves tests defined using the results of severe accident scenario computations and conducted in the TOSQAN, MISTRA and PANDA facilities in Switzerland (see above) and SPOT and HYMIX facilities in Russia on volumes ranging between 7 and 1920 m³; it will be used to assess the ability of the models developed and validated on the basis of small-scale tests to predict hydrogen distribution within a power reactor containment [33].

5.2.2.3.2. Hydrogen combustion

As for hydrogen distribution in the containment, many experimental programmes have been conducted on flame propagation in a premixed atmosphere containing hydrogen. These tests have two objectives: 1) to characterise the transition between slow and fast conditions and between deflagration and detonation; and 2) to produce a database for validating computer codes. There are two types of tests:

- analytical tests to determine the laminar flames' characteristics and to construct a database for qualifying the different flame conditions;
- dedicated tests for studying turbulent flames with the aim of validating computer codes and establishing criteria for characterising the possible flame conditions.

As was the case for hydrogen distribution in the containment, a state-of-the-art report on flame acceleration and the deflagration-to-detonation transition was produced in 2000 by a group of international experts (including IRSN experts) within the framework of OECD [21]. This report provides a description of the major experiments conducted in the facilities of BMC, NUPEC, VIEW, HTCF, FLAME, RUT, etc. on flame acceleration and the deflagration-to-detonation transition. Criteria for the transition between the different combustion conditions were developed on the basis of the results obtained from the tests conducted in these facilities; these criteria were then refined as part of the European HYCOM programme and the ENACCEF programme (both these programmes are presented later in this document). It also reports on the state of the art in combustion models.

► RUT experimental programme

The RUT facility, which is operated by the Kurchatov Institute in Russia, has studied the turbulent combustion of hydrogen in a large-scale facility. IRSN and FzK (Germany) have helped to define and finance a set of tests in this facility. The facility, with a total volume of 480 m³ and total length of 62 m, consists of three parts: one channel that is completely rectilinear, a second —shorter— channel that is curved at one end and a "canyon" or cavity in the intermediate area. All three regions have a rectangular cross-section and may possibly be blocked by obstacles.

These geometric characteristics can be used to study both the mono-directional acceleration of a flame produced as a result of hydrogen combustion in the channels and more complex 3D effects or interactions in the "canyon". It is the only facility of its size used to study turbulent hydrogen combustion and thus the only one subjected to



Figure 5.23. Diagram of the RUT facility.

pressure loads that can be transposed to reactor scenarios. The gas mixtures used in the tests, which contained hydrogen, air and possibly steam, are supposed to be representative of the mixtures present in a containment when a core melt accident occurs. The instrumentation is highly suitable for validating CFD computer codes [22].

The various test campaigns have investigated the following combustion conditions:

- slow deflagration, in which flame velocities are below the speed of sound in the case of cool gases and the pressure levels are below the adiabatic isochoric complete combustion (AICC) pressure;
- fast deflagration, in which flame velocities are around the speed of sound in the case of burnt gases and the pressure levels are above the AICC pressure;
- “critical” conditions, in which a deflagration-to-detonation transition (DDT) occurs but the resulting detonation does not spread or is not directly transmitted to the entire mixture;
- stable detonation, in which the detonation forms after a DDT in one region of the facility and in which the velocities and pressure peaks are close to the Chapman-Jouguet values (CJ) and propagate to the rest of the fuel mixture.

The objectives of the different programmes conducted in the RUT facility have included the establishment and validation of the criteria σ and λ (defined in Section 5.2.2.2).

► HYCOM European programme

The European HYCOM programme has been designed to build upon the first tests conducted in the Kurchatov Institute RUT facility in the context of a collaboration between FzK, the US NRC, IRSN and the Kurchatov Institute; its objective is to study flame acceleration in hydrogen-air mixtures and especially to validate the σ criterion [25]. The effect of burnt gas expansion (the “piston” effect) and the impact of compartmentalisation were studied using the RUT facility; the impact of venting was studied using the DRIVER and TORPEDO facilities operated by FzK, consisting of cylindrical tubes that are 174 mm in diameter and 12.2 m long and 520 mm in diameter and 12.4 m long, respectively.

This programme, in which IRSN and EDF participated, also added to the available data on flame acceleration and validated the criteria for special situations in which there are gas mixture richness and containment geometry differences.

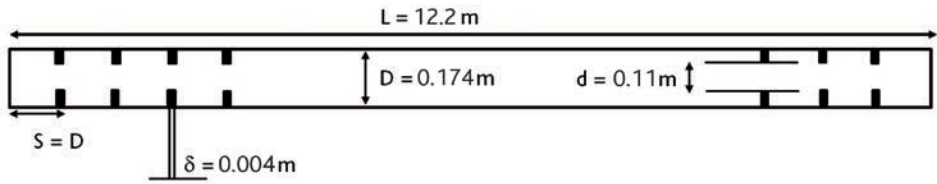


Figure 5.24. Diagram of the DRIVER facility.

► ENACCEF programme

The ENACCEF (flame acceleration containment) programme on flame acceleration was conducted for IRSN by CNRS and, during its initial years, EDF. Its primary goal was to validate the criterion σ using tests conducted on a vertical structure representing an SG bunker opening up into the dome [17]. The ENACCEF facility contains an acceleration tube forming the lower part of the containment and an adjustable dome forming the upper part of the containment. The acceleration tube, which was 168.3 mm in diameter and 3.2 m high, can be fitted with obstacles of various shapes, resulting in different blockage rates and notably an obstacle simulating an 11.12-litre SG. The adjustable dome volume may be 780.9 litres or 957.8 litres.

The instrumentation used includes photomultiplier and pressure sensors for measuring the progression of the flame front and the pressure generated as a result of hydrogen combustion. In addition, gas sampling points are positioned along the facility's acceleration tube to measure the composition of the gas mixture within the facility. Lastly, laser Doppler velocimetry (LDV) and particle image velocimetry (PIV) are used to determine the velocity field of the gas flow before the combustion flame reaches it. The ENACCEF facility is therefore well equipped with instrumentation and particularly well suited to validating CFD computer codes. It can also be used to study the flames' upward and

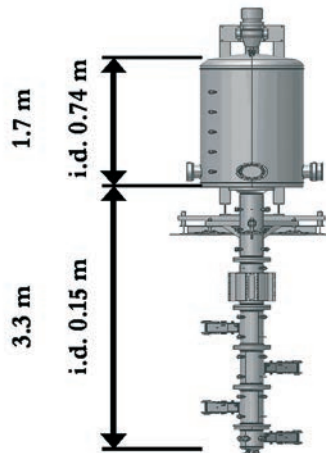


Figure 5.25. Diagram of the ENACCEF facility [17].

downward propagation, taking into account the ignition points at the bottom and top of the facility. The effects of dilution by steam simulant gases and of the volume and heterogeneity of the mixture have been studied in addition to those of the ignition position; this has confirmed and improved the criterion σ developed in the RUT and HYCOM programmes as well as obtaining data for the validation of CFD computer codes. The ENACCEF facility has also studied the effect upon flame propagation of the presence of water droplets due to spraying. These results showed that under certain conditions, the flames progressed more rapidly when the spray system was activated. This statement had been confirmed by the experiments results performed in framework of the OECD/THAI II project (2011–2014).

Some tests were also conducted in the ENACCEF facility and serve(d) as the basis for the international comparative exercises organised within the European SARNET network and the OECD *International Standard Problem* no. 49 [34].

5.2.2.3.3. Means of reducing the hydrogen risk

Catalytic hydrogen recombiners (see Figure 5.26) have been set up in the French PWRs' containments to reduce their hydrogen content in the event of a core melt accident. They are usually constructed from a catalytic material (platinum or palladium on an alumina mounting) and housed in a metallic casing whose purpose is to enable the gases to circulate inside the catalyser (consisting of a bed of beads or a row of vertical plates). On contact with the catalytic recombiner plates, the hydrogen and oxygen present in the containment atmosphere react to produce steam.

Many test programmes, most of which were conducted by the recombiners' manufacturers (SIEMENS, AECL, etc.) [20], have studied the behaviour of the recombiners in the event of a core melt accident in order to evaluate their recombinatory capacity.

The H2PAR programme, conducted by IRSN at its Cadarache facilities with financial support from EDF, was mainly intended to investigate the behaviour of the catalytic hydrogen recombiners [19] in an atmosphere representative of that found in the

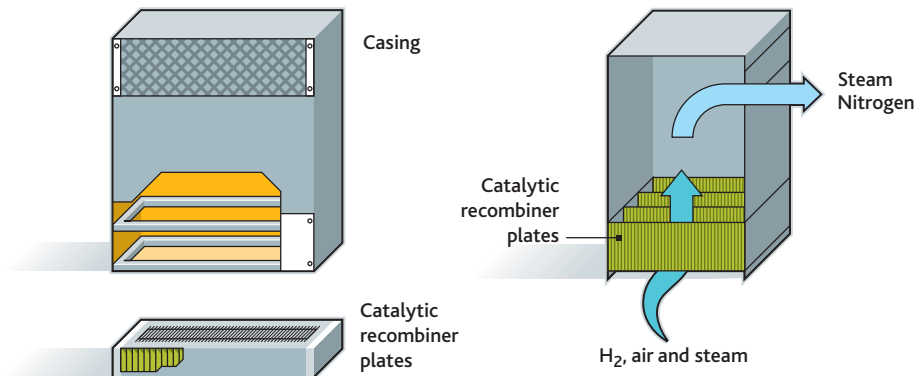


Figure 5.26. Block diagram of a passive catalytic hydrogen recombiner.



Figure 5.27. Picture of the REKO 4 facility (credit: Jülich Institute).

containment in the event of severe accident within chemical compounds in aerosol form (creating a risk of catalyser poisoning). It also studied the risk of the mixture present in the containment igniting as a result of the recombiner (which heats up in the recombination reactions) and determined the limits above which such ignition would occur for a given recombination model. In addition, it analysed recombination sensitivity to different geometric parameters (number of catalytic recombiner plates and height of the passage between the plates (called the "stack"), physical parameters (molar fraction of hydrogen) and chemical parameters (replacing several catalytic plates by chemically neutral plates) [29]. These tests notably demonstrated the aerosols' limited impact upon recombination efficiency.

The aims of the KALIH2 test programme, conducted by CEA with financial support from EDF, were complementary to those of the H2PAR programme and concerned the behaviour of the recombiners in special situations (when not poisoned by the fission products). It evaluated the effects of the following upon recombiner

performance: humidity, exposure to smoke from cable fires, and the presence of carbon monoxide [23, 24]. Unlike H2PAR, KALIH2 studied the impact of spray system use and overpressure upon recombiner efficiency. The tests revealed that spray system use has little effect recombiner efficiency but overpressure has a major effect upon it.

More recently, the OECD/THAI project confirmed and supplemented the H2PAR and KALIH2 programmes' results concerning the limits of ignition by the hydrogen recombiners and their performance under conditions in which there is little oxygen.

The effect of the hot plumes emitted from the recombiners upon hydrogen distribution in the containment, which the H2PAR and KALIH2 programmes did not address, was also studied in the OECD/SETHII programme tests as well as in additional tests as part of the European ERCOSAM project, in which recombiner models were used in the PANDA, MISTRA and KMS facilities. It is also being studied in the European SARNET project by conducting tests with recombiners in the REKO 4 facility operated by the Jülich Institute.

5.2.2.4. Modelling and simulation codes

The computer codes used to predict hydrogen distribution in the containment are based on a multi-compartmental approach. These include the CONTAIN, MAAP, GOTHIC, MELCOR and COCOSYS codes, the ASTEC code CPA module and the TONUS code multi-compartment computation module. These codes have demonstrated their ability to compute hydrogen distribution in small- and large-scale experiments, with or without the use of a spray system. The models used by these codes are too simple to precisely describe the complex gas flows likely to be produced locally at the power reactor scale, notably in the volumes in which concentration differences can appear (stratification, jets, etc.).

The codes that use a multidimensional approach, such as the TONUS code multidimensional module or the GASFLOW code developed by KIT, can model complex flows much more precisely and so can be used to complete the studies conducted using the codes listed above in the case of complex flows. They may be of limited use in some cases, however, due to the geometric complexity of the internal structures of the containment as well as to the costs involved, which may be considerable.

The comparative computational exercises (ECORA and ISP47) based on the experimental results of the four programmes named above have led to the following conclusions.

The ECORA exercise, which involved a gas injection transient with no steam condensation, used CFD tools and showed that the main limitation in the use of this type of computer code lay in the computation of large-scale slow transients. The existing means of computation are not powerful enough to allow computation convergence or mesh sensitivity over time to be studied. The models used have accurately predicted steam transport between the compartments of the PANDA facility, however, which was one of the key points of this exercise.

In the ISP47 exercise, multi-compartment and multidimensional computer codes were used. Furthermore, as several research bodies have used the same tool, it has been possible to assess the user effect more accurately. The following points were emphasised in the final conclusions of the exercise:

- the CFD tools have not shown any significant advantages over the multi-compartment tools, possibly due to the relatively simple flow structures in the case of the TOSQAN and MISTRA tests;
- the results obtained using multi-compartment tools varied greatly depending on the user. They have therefore highlighted the need to draw up and implement best practices (this recommendation is also true of the CFD codes that use the correlations);
- the “blind” exercises, which are important in assessing the codes’ predictive aspect, produced a wide range of results;
- supplementary studies are needed in order to model the condensation of steam on the walls, notably concerning the effect of the presence of helium;
- the processing of the effects of scale in computer codes has not been fully resolved: this is the objective of the European ERCOSAM project.

Additionally, the pressure loads resulting from hydrogen combustion and applied to the containment can be computed using codes adopting multi-compartment or multi-dimensional approaches. The multi-compartment codes are generally used to compute slow flames whose pressure loads can be considered as being static. Multidimensional CFD codes must usually be used to compute the dynamic pressure loads, however. For example, the HYCOM project has produced very complete results with regard to hydrogen combustion in reactor containments and the modelling of this phenomenon. In particular, this project has revealed the following:

- global values such as the maximum pressure are relatively well-computed by the CFD and multi-compartment codes. CFD codes give better results for fast flames, however, whereas multi-compartment codes are better suited to slow flames;
- differences exist between the results obtained using the various codes for “dynamic” values, such as the flame velocity or pressure build-up;
- the computer codes do not accurately compute some experimentally-observed phenomena such as smothering;
- modelling the energy dissipation of the flame during its progression is an important point and must be improved.

Above all, however, the HYCOM project has highlighted the difficulties of modelling hydrogen combustion when the mixtures are not homogeneous, particularly when this is accompanied by a change in the combustion conditions. These situations — which are nevertheless similar to actual conditions — are not modelled satisfactorily and require additional experimental data, notably concerning the turbulence level, to allow the computer codes to be validated. This was also the finding of the comparative exercises

applying the codes to the OECD *International Standard Problem* (ISP49) and in the [SARNET](#) project.

5.2.2.5. Summary and outlook

Research and development on the hydrogen risk have produced a number of results reinforcing the decision to install passive hydrogen recombiners in all French nuclear power plants. Studies of core melt accident scenarios in the case of the existing reactors and the EPR have shown that despite the installation of recombiners, it is difficult to prevent, at all times and locations, the formation of a combustible mixture potentially resulting in local flame acceleration.

Furthermore, the events that occurred at the [Fukushima Daiichi](#) nuclear power plant in Japan have shown that the R&D studies must be continued in order to advance the state of knowledge of hydrogen risk phenomena.

Additional research is being conducted to improve the tools needed to evaluate the hydrogen risk. This concerns the following:

- in the case of hydrogen distribution, studies of transient flows with stratification. This aspect was studied in the SETHII project and is now being studied in the test programmes of the European ERCOSAM project, notably in the TOSQAN, PANDA and MISTRA facilities;
- in the case of combustion, studies of the effect of the presence of water droplets upon hydrogen flame acceleration. This subject is covered in the ENACCEF programme and is part of the current OECD/THAI II project;
- in the case of recombiners, studies of how the recombiners' location affects the recombination rate as well as flame ignition by the recombiners. Both these subjects are covered in the European [SARNET](#) network and are being studied in a programme based on the tests conducted in the REKO3 and REKO4 facilities. The effects of the recombiners' location upon the surrounding atmosphere are also discussed in the OECD/SETHII project;
- in the case of hydrogen distribution, the development of models representing steam condensation in the presence of incondensable gases and stratification, as well as “destratification” mechanisms. Furthermore, the comparative exercise organised by [IRSN](#) regarding spraying have shown the limits of the computer codes in describing the effect of spraying upon atmospheric mixture kinetics;
- in the case of hydrogen combustion, additional work to improve and validate the models is needed in order to better simulate flame propagation in a heterogeneous environment, notably when there are differences in the hydrogen concentrations enabling the flame propagation condition to change.

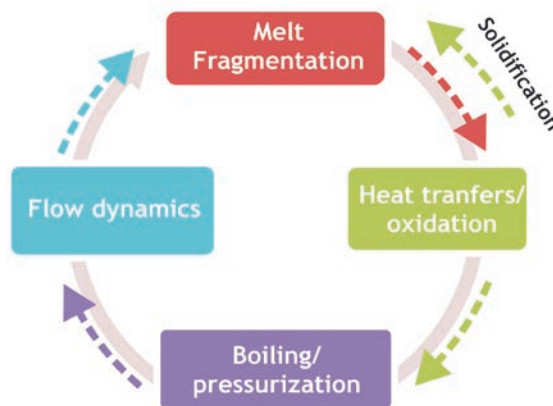
In conclusion, the R&D conducted to date has significantly increased our knowledge of the phenomena governing the distribution of gas mixtures and their combustion in the containment when a core melt accident occurs. In particular, by enabling us

to establish criteria that have been validated using experimental data, it has enabled us to more accurately determine which situations involve hydrogen combustion risks. Although the computer codes have now achieved a significant level of maturity, their predictive capabilities must be further improved by defining best practice guidelines to mitigate the “user” effect, by improving the models (notably regarding combustion), or else by improving the numerical performance of the CFD multidimensional tools and increasing the computing power of the computers permitting their widespread use.

5.2.3. Steam explosions

5.2.3.1. Introduction

The phenomenon of steam explosions is relatively well understood since the 1970s. When two fluids come into contact, with one (the molten fuel, or corium, resulting from core meltdown) being at a temperature higher than the boiling point of the other (the coolant), an explosive interaction may be caused. This phenomenon is the result of the chained interaction of several mechanisms shown below:



Corium fragmentation into ultra-fine fragments below a hundred microns in diameter causes the transfer of energy from the corium fragments into the coolant. The associated phase change (or simply density changes) may induce a pressure build-up faster than the pressure release. The pressure build-up causes relative motion in the fluids (the water moves faster than the fuel because their densities are different). This leads to substantial overpressure, followed by a more or less slow expansion that may damage surrounding structures (overpressures of up to 1000 bar have been measured in the KROTOS tests conducted in the Joint Research Centre (JRC) at Ispra in Italy, using alumina as a simulant of corium. Two additional phenomena have significant impacts. The heat transfer induces a cooling of the melt and thus its solidification, which, to a degree to be specified, will prevent the fragmentation. Experiments have also shown that oxidation may be very intense. Through the associated energy and through the

production of hydrogen, a non-condensable gas, oxidation has strong impacts which may either limit or enhance the explosion strength.

The prerequisite condition for triggering a steam explosion is the contact between the two fluids, but the situations generating most energy are those in which the two fluids are mixed before they are finely fragmented (hence the terms “pre-mix” or “pre-mixing”). In the case of PWR or BWR core melt accidents, such mixtures may form after core meltdown and while the corium is flowing in the lower head if any water remains (“in-vessel” explosion), and then possibly in the flooded reactor pit when the vessel is penetrated (“ex-vessel” explosion).

This condition is not sufficient in itself, however: an explosion does not necessarily occur when the fluids are in contact or mixed. The corium then remains at the coarse fragmentation stage (with fragments millimetres or centimetres in diameter) and its energy is transferred to the coolant relatively slowly (approximately a second for one droplet), resulting in the pressure slowly building up (this is what occurred in the Three Mile Island-2 accident, described in Section 7.1). In order for an explosion to occur, there must be an “internal” triggering event (producing what is referred to as a spontaneous explosion) or an “external” event (shock wave), causing fine fragmentation somewhere in the pre-mix and then propagating throughout the rest of the pre-mix. Such spontaneous or artificially-triggered explosions have been experimentally produced with the molten materials of which a PWR corium is composed (a mainly U–O–Zr–Fe mixture).

In its most extreme form, a steam explosion is similar to a detonation due to a chemical reaction, with a shock wave propagating at the speed of sound and heat transfers between the fragmented corium and the water playing an equivalent role to the release of energy in chemical reactions. The analogy is somewhat limited, however, and quite unrealistic approximations are needed in order to construct analytical models (based on detonation models), which have very little potential for practical application. This is why complex multiphase and multidimensional models are needed in order to compute steam explosions. The most frequently-used computer code in France is the MC3D code developed by IRSN in collaboration with CEA (Section 5.2.3.3.3).

The OECD SERENA (Steam Explosion REsolution for Nuclear Applications) programme brought together the leading steam explosion specialists. In its initial phase between 2001 and 2005, they evaluated the current state of knowledge of the phenomenon and assessed the computational capabilities of the main dedicated software solutions [44]. The second phase of the programme, which took place between 2008 and 2012, consisted of an experimental programme devoted to studying steam explosions with various corium compositions likely to be found in a power reactor core melt accident, with the aim of improving the existing models (Section 5.2.3.3.2).

5.2.3.2. Physical phenomena

While the corium melt is in the water present in the lower head or, after the vessel ruptures, in the reactor pit, the explosive interaction appears as a two-stage dispersion and fragmentation phenomenon shown diagrammatically in Figure 5.28. The first

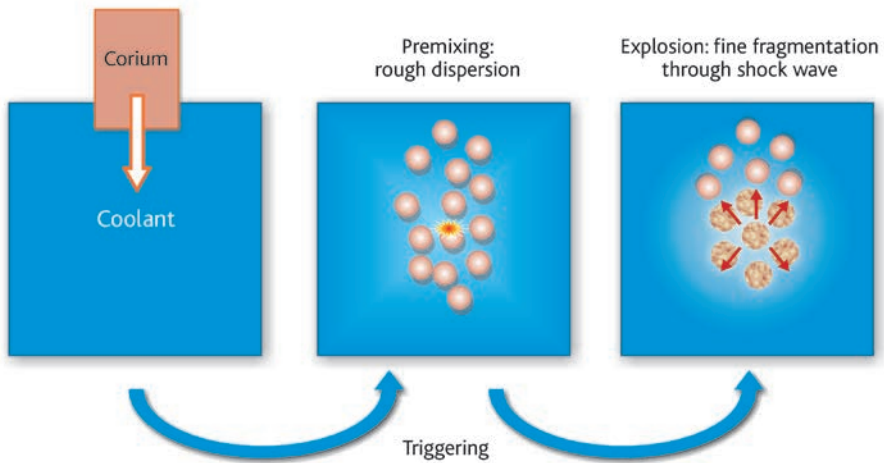


Figure 5.28. Schematic diagram of the phases in a steam explosion.

stage — the pre-mixing phase — may, depending on how it occurs, result in the explosion itself (the second stage) due to the fundamental, self-sustaining mechanisms described in the introduction: fine corium fragmentation, energy transfer between the fragmented corium and the water, and the associated pressure build-up and differentiated motion in the fluids. As the pre-mixing and explosion phases' timescales are very different (seconds compared with milliseconds), the explosion takes place within a virtually static pre-mix that determines the initial conditions of the explosion.

As a result, the explosion greatly depends on the pre-mix characteristics at that time; these consist of the composition and distribution of the various phases present (corium, water and steam) and the corium interface, including its temperature and its possible state of solidification. It is thus essential to accurately describe this first phase in order to obtain the initial conditions of the explosion. Accurate prediction of the explosion phase is therefore achievable only if pre-mixing is accurately described. This first phase was neglected for some time but has been the subject of most R&D efforts for the last ten years.

The explosion therefore begins with a “trigger” phase and is followed by a phase referred to as the “escalation” phase, during which the intensity of the explosion increases until a stationary state is reached. There is no phenomenological difference between these two steps of the explosion and they are modelled in the same way in the current computer tools. On the following pages, we will use the more general term “explosion phase” to describe them both. The pre-mixing, the triggering of the explosion and the explosion itself are described in detail in the following sections.

5.2.3.2.1. Pre-mixing

The importance of pre-mixing has been clearly demonstrated, particularly in the KROTOS experiments, in which the very different pre-mixes observed with the alumina and the corium (Figure 5.29) resulted in very different explosion intensities (alumina

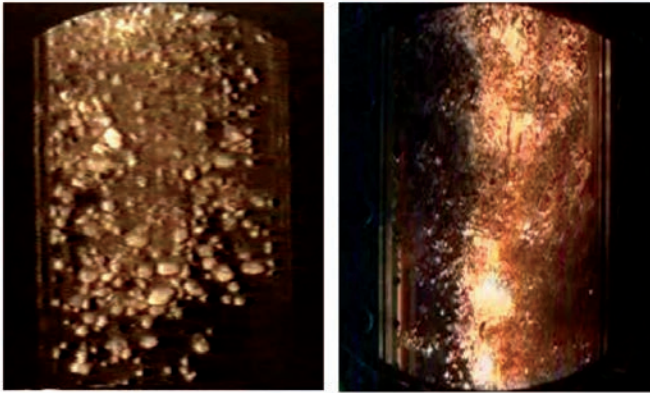


Figure 5.29. View of an alumina and water pre-mix (left: KROTOS-57 experiment) and a corium and water pre-mix (right: KROTOS-58 experiment). 10 x 20 cm window [37].

releases ten times more energy than corium) [37]. In all the tests, mostly qualitative information was obtained on the pre-mixing of materials with high melting points ($> 2000\text{ }^{\circ}\text{C}$). This information is not sufficient to explain the observed differences in behaviour. The second phase of the OECD/SERENA programme sought more detailed information on the pre-mixing, notably concerning the fragmentation and boiling processes (Section 5.2.3.3.2).

With regard to modelling, pre-mixing is evaluated using multidimensional, multiphase thermal-hydraulic computer codes (Section 5.2.3.3.3), as the many dynamic, thermal and chemical interactions prevent pre-mixing from being modelled simply.

The three essential points upon which R&D concentrates, namely corium fragmentation, determining of the void fraction (the fraction of the volume occupied by the steam) and fuel solidification, are presented below. For the sake of completeness, the effects of oxidation of the corium materials — which could greatly modify each of these points — should also be studied.

► Corium fragmentation

During the pre-mixing phase, fragmentation occurs in two stages: primary fragmentation, from the continuous phase (typically a corium jet), produces a first generation of droplets that may then undergo secondary fragmentation. In reality, jet fragmentation is a highly complex phenomenon and involves several instability and then fragmentation processes, as Figure 5.30 shows.

Secondary fragmentation continues until the droplets formed cannot become any smaller (the droplets consist of fragments wrenched from larger droplets by the gas flow; this fragmentation is only possible if the droplet is unstable under hydrodynamic flow conditions).



Figure 5.30. Illustration of fragmentation process complexity in the case of a liquid jet in a coaxial air flux [63].

Considerable research has been conducted on the primary fragmentation of corium jets (in particular, see the results of the doctoral theses presented in references [42, 43]). The models developed in these theses are mainly devoted to direct fine fragmentation (atomisation)⁷ of the corium jet. It was, however, seen that the corium jet can be fragmented by other mechanisms involving “large-scale” hydrodynamic instabilities causing larger fragments to be formed and greater spatial dispersion of the corium fragments (Figure 5.31). These mechanisms are believed to cause the behaviour observed during tests with alumina in the KROTOS facility [37], where the fragments filled the entire cross-section of the experimental tube (see Figure 5.29).

Secondary fragmentation was the subject of substantial work until the 1980s. This work revealed trends and fundamental characteristic numbers (Weber number: $We = \frac{\rho_{amb} V^2 D}{\sigma}$; characteristic fragmentation time: $\frac{D}{V} \sqrt{\frac{\rho_{comb}}{\rho_{amb}}}$). The knowledge acquired as a result only provides a qualitative description of the pre-mixing, however.

Apart from the fact that the theoretical knowledge must be improved, the modelling of fragmentation in the computer codes faces two difficulties. The first concerns the local aspect of the phenomena, resulting in the need for fine spatial resolution, whereas the second lies in the models’ extreme sensitivity to the local flow conditions, which are quite unstable and can trigger the explosion themselves. Parametric modelling of flow dynamics is therefore often preferred to more-detailed modelling; this approach, which is based on simplified models of the gravitational fall of corium fragments, is of limited use, however, as these simplified models have not been sufficiently validated to compute corium–water pre-mixes when a core melt accident occurs in a power reactor.

7. This must not be confused with the “fine fragmentation” process during the explosion, in which the fragments are much smaller.

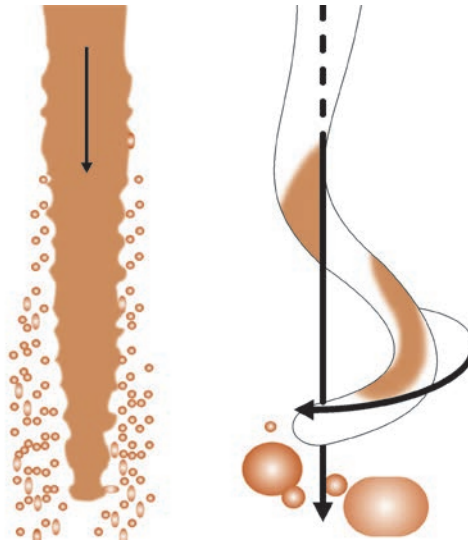


Figure 5.31. Schematic diagram of the primary fragmentation of a corium jet upon contact with water: liquid jet fragmentation due to atomisation (left) and fragmentation due to large-scale hydrodynamic instabilities (right); these instabilities result in corium jet deformation (torsion around the flow's vertical axis) and, therefore, greater spatial dispersion of the fragments.

► Void production

The volumetric fraction of the gases in the corium–water mixture is called the “void fraction”. There are still many uncertainties regarding the effect of the void fraction upon steam explosion, however. The greater the void fraction is, the more the average compressibility of the mixture increases and the more explosion becomes difficult. Predicting the void fraction in the pre-mix (the initial state of the explosion) is a complex task, mainly because of the corium’s very high temperatures (it should be remembered that at 3000 K, the steam is already greatly dissociated). The steam production processes of film boiling are poorly understood. Similarly, the steam condensation processes are very difficult to model. The flow configurations used in modelling are based on studies of isothermal two-phase flows in piping. Their suitability for describing pre-mixing is therefore uncertain. The presence of non-condensing gases produced through oxidation of corium metallic phases modifies the boiling and condensation processes, making the void fraction even more complex to model.

This results in a certain degree of disparity between the existing models, and this disparity is largely the cause of the uneven computational results obtained during phase 1 of the SERENA programme. Due to the lack of detailed experimental results, particularly concerning the local void fractions and the corium’s configuration, the validity of the various models cannot be established with sufficient certainty. Correctly evaluating the void fractions and their distribution was thus a major objective of phase 2 of the SERENA programme, as described in Section 5.2.3.3.2.

► Corium solidification

An additional phenomenon must be taken into account when the models are applied to power reactors. This concerns corium solidification during the pre-mixing phase, which inhibits the fine fragmentation process and, therefore, the explosion. This phenomenon is particularly difficult to study because of the complex mixtures of component materials in corium and the complex pre-mixing conditions (gas and corium flows, corium fragmentation, high temperatures, etc.). As a result, considerable uncertainties remain regarding the solidification processes themselves. The codes computing these processes (including MC3D) assume that solidification occurs under thermodynamically balanced conditions, and that there is a solid surface crust and a well-defined solidification front.

5.2.3.2.2. Triggering of the explosion

The steam explosion triggering phase is undoubtedly the most difficult phase to process when evaluating the steam explosion risk. There are no reliable models for predicting when and where an explosion will be triggered. The physical parameters that determine the triggering of the explosion are not precisely known. The existing knowledge is mainly based on experimental results. In the case of corium, it has been experimentally observed that spontaneous explosions occur when the corium makes contact with the test system lower head containing the corium-water mixture. However, nothing says that an explosion could not occur before or after this contact.

From a theoretical point of view, it is known that a hot corium droplet may explode under the influence of a low-pressure disturbance of a few bar (Figure 5.32). The phenomenon includes isotropic fragmentation, unlike the fragmentation linked with dynamic effects (the fragments are found in the flow's wake). Despite many research studies, this "thermal fragmentation" phenomenon is still poorly understood. However, a doctoral thesis study conducted from 2005 to 2008 at IRSN [45] added to our understanding of this phenomenon and validated the most widely-posed hypothesis whereby the phenomenon is due to the steam film surrounding the corium droplet becoming destabilised. This destabilisation causes localised contact between the corium and the coolant, thereby creating local build-ups in pressure that, in their turn, destabilise the corium droplet. The corium's "thermal fragmentation" phenomenon only appears possible under fairly specific conditions of ambient pressure (approximately 2–15 bar) and water under-cooling (above 70 °C according to the experimental results obtained by the Sandia National Laboratories [64], and above 40 °C according to the model in this doctoral thesis). It is thought to contribute to the triggering and escalation of the explosion, but its actual importance has not yet been determined. A spontaneous explosion was therefore observed at a pressure of 50 bar in a programme at the British Winfrith nuclear centre under apparently unfavourable conditions for thermal fragmentation [38].

An explosion may also be triggered by the corium enveloping some coolant when it lands on the floor (the bottom of the testing cross-section), which would explain the spontaneous explosions occurring when the corium comes into contact with the floor. Furthermore, the small scales of the tests do not encourage spontaneous explosions.

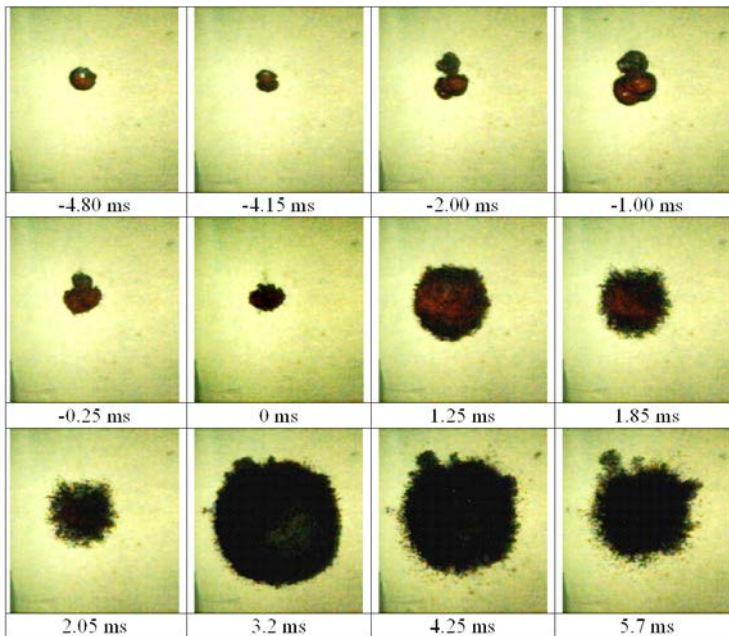


Figure 5.32. View of a WO_3 -CaO droplet ($1500\text{ }^\circ\text{C}$) exploding in water at $25\text{ }^\circ\text{C}$ due to thermal fragmentation [65].

Spontaneous explosions therefore occur more frequently in the experiments conducted with wide testing cross-sections (the FITS [32-34] or TROI [62] programmes) than in geometries with narrow cross-sections (KROTOS [37]).

In the probabilistic safety assessments, a triggering probability is sometimes used. No probabilistic quantification is currently based on precise physical arguments, however. Uncertainties regarding the triggering of the explosion therefore lead us to consider that steam explosion risk cannot be eliminated and to study the consequences of such an explosion. It should be noted, however, that the triggering caused by a pressure disturbance does not necessarily result in an interaction likely to endanger the structures if the temperature and pressure conditions are not combined. In the computations as well as in some experiments, therefore, certain situations that notably have a high void fraction or high solidification do not result in an explosion that threatens the structures (or any explosion whatsoever).

5.2.3.2.3. Explosion

The explosion is caused by very intense heat transfers between the corium and the coolant and the resulting coolant vaporisation⁸. In the case of the violent explosions such as those obtained in the KROTOS facility's mono-dimensional geometry using

8. It may seem surprising to speak of vaporisation when the pressure exceeds the critical pressure. In this case, we are misusing the term to describe the fact that, even under supercritical conditions, the hot fluids are still less dense than the cold fluids, a phenomenon similar to evaporation.

alumina (with pressure peaks of 500–1000 bar), the explosion may be approximately described as follows:

- propagation of a detonation-type shock wave with intense isochoric thermal transfers;
- expansion of the mixing region behind the passing shock wave.

Because of the obvious instrumentation limitations, experimental studies on the detailed mechanisms of the explosion are extremely complicated. As a result, very little data — which have often been obtained under questionably representative conditions — are available. The analytical models, concerning complex phenomena that are frequently unbalanced, reach their limits comparatively rapidly. It is, however, interesting to note that with the increase in computing power, it is becoming feasible to study these highly localised phenomena using numerical simulation tools (such as the MC3D code itself, described later in this document).

Paradoxically, however, the explosion is comparatively “simpler” to model than the pre-mixing phase, subject to the use of suitable approximations for the corium’s fine fragmentation as well as heat and mass transfers between the corium and the coolant, as these processes produce the pressure peak. For one thing, these two processes are clearly predominant mechanisms; for another, many aspects can be simplified or even ignored because of the timescale of the explosion (a few milliseconds). The studies therefore concentrate on understanding the two predominant phenomena, consisting of the fine fragmentation of the corium and the boiling of the coolant, both of which are briefly described below.

► Fine fragmentation

The fragmentation mechanisms are astonishingly complex (see, for example, reference [66]). The fine fragmentation of a corium droplet in water when subjected to a shock wave is illustrated in Figure 5.33, from reference [46]. Traditionally, the fragmentation phenomena are characterised by means of the Weber number ($We = (\rho V^2 D / \sigma)$, which expresses the ratio between the destabilising dynamic forces (ρV^2) and the stabilising force due to surface tension (σ/D .) When the Weber number is not too large, the droplet surface layers are firstly detached due to water friction. The fragmentation occurs later behind the film drained by the friction. With high Weber numbers, instability occurs earlier and directly results in droplet fragmentation.

When the corium is finely fragmented, the size of the droplets is reduced by one or two orders of size in approximately one millisecond. Opinions differ regarding the way in which the phenomenon develops. The studies conducted by IRSN using the MC3D computer code suggest that the corium’s fine fragmentation is the result of Kelvin-Helmholtz shearing instabilities (because the flow speeds of the corium and coolant droplets are different). These studies have led to the development of a model describing the changes in the fragments’ size; this model is integrated into the MC3D code.

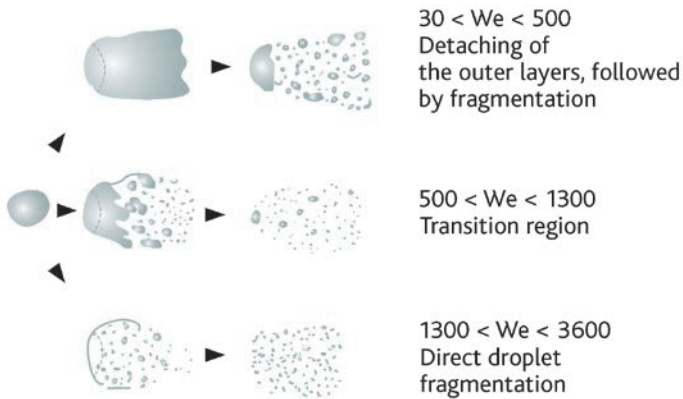


Figure 5.33. Fine fragmentation mechanisms observed by Bürger *et al.* [46] depending on the Weber number ($\rho V^2 D / \sigma$).

Corium solidification tends of course to modify or even inhibit the phenomenon, potentially explaining the (relative) weakness of the explosions observed with corium oxide ($UO_2 + ZrO_2$). It is difficult to model the solidification phenomenon during the pre-mixing phase, however. This is because its effect upon fine fragmentation is difficult to quantify. In some models, the crust has an effect similar to an elastic shell. The models remain highly parametric, however, due to the many approximations and uncertainties concerning, for example, the mechanical properties of the solid corium layers.

► Pressurisation mechanisms

The initial steam explosion models [47] assumed that there was an instantaneous balance between the resulting corium fragments and the coolant; in these models, the coolant temperature increase due to direct contact with the hot corium fragments directly results in the pressure build-up, either through boiling or simply through thermal expansion. This approach has been refined by Theofanous [48] with the so-called "micro-interaction" approach, which considers that only a fraction of the water is heated. The term "micro-interaction" comes from the hypothesis that the interaction between the fragment and the water is highly local and that only a part of the water is involved (except in transmitting the pressure build-up). Experimental observations show that in reality, at least up to the critical pressure, the hot corium fragments are surrounded by a thin film of steam, affecting the heat transfers between the corium fragments and the coolant as well as coolant vaporisation. The model representing the interaction between the corium fragments and the water integrated into the MC3D code assumes that the pressure build-up is the result of the direct vaporisation accompanying the heat transfers through the steam film between the hot corium fragments and the coolant (the so-called "imbalance" model); this model, which is more mechanistic *a priori*, assumes that the mass

transfers associated with the heat transfers between corium fragments (whose average size is 100 μm in the KROTOS experiments) and the coolant are known. It is important to remember that these transfers occur during a pressure transient of a few hundred bar lasting a few milliseconds, which are difficult conditions to achieve in experiments.

5.2.3.3. Experimental programmes, modelling and computer code

5.2.3.3.1. Mechanical efficiency concept

Before we present the main experimental programmes, it is important to discuss the mechanical efficiency concept, as it is often used to characterise the intensity of an explosion in the experiments (as well as in the initial thermodynamic models). This concept is intended to represent the efficiency of the transfer of the heat energy contained in the fuel, the source of the explosion's energy (excluding chemical phenomena), into mechanical energy. In reality, this concept is rather vague, as the mechanical energy concerned can be defined in several ways. In the initial estimates, the energy in question was that linked with the system's overall pressure build-up — in other words, the gaseous atmosphere in the test section (the compression is assumed to be adiabatic). In reality, this definition created considerable difficulties and expression used for the energy was revised several times. It was then judged preferable to use the kinetic energy of the mixture. To avoid confusion, we will talk of kinetic efficiency in the rest of this document. This kinetic energy is also impossible to measure accurately, and it is generally obtained by evaluating load impulsion (the pressure build-up integral, $I = S \int \Delta P dt$, where S is the bottom surface area of the test cross-section to which the pressure load ΔP is applied). Although the mixture is assumed to be non-deformable (like a slug) and expelled by the explosion, the approximate value of its kinetic energy is provided by the expression $I^2/2M$, where M is the mass of the mixture. This approximation leads to a minimisation of the actual energy but provides acceptable orders of magnitude.

The efficiency concept must therefore be used with caution, and any comparisons between different experiments must be purely qualitative.

5.2.3.3.2. Experimental programmes

Table 5.4 shows the main programmes that have studied the pre-mixing phase or the steam explosion using corium or simulant jets and whose results have been used as the basis for developing and qualifying computational models. The FITS programme, which was the "pioneer" in the domain, was conducted by the Sandia laboratories in the United States and included many experiments in the different configurations and on different materials described in references [38-41]. Notably, spontaneous violent explosions were obtained using a corium consisting of a $\text{UO}_2 + \text{ZrO}_2$ -steel mixture (little information is provided on the corresponding tests, unfortunately) [49]. The programme ended with the loop being unexpectedly destroyed in the RC2 test. These experiments are not used to qualify the codes, however, as little is known of the experimental conditions under which the fluids come into contact, and so the conditions are often poorly known and difficult to reproduce in the computations.

Table 5.4. Experimental programmes studying steam explosions resulting from an interaction between a corium jet or a simulant jet and the coolant (water).

Programme	Laboratory	Type of test	Materials	Conditions and key facts
FITS [5.2_38] at [5.2_41]	Sandia (USA)	Explosion	Al ₂ O ₃ -Fe thermite or corium A few kg	<ul style="list-style-type: none"> - First major programme - Many tests - Series of extended conditions materials (MDC) tests with corium: spontaneous explosions (approx. 2% efficiency) - Series of extended efficiency (RC) with thermite: RC2 experiment with the highest observed efficiency (8–15%, gas compression work)
CCM [5.2_53]	ANL (USA)	Pre-mixing	UO ₂ + ZrO ₂ - steel mixtures at 2800 °C A few kg	<ul style="list-style-type: none"> - Well-controlled conditions - 6 tests under different conditions (including geometry, jet diameters and water temperature) - No spontaneous explosions
FARO [5.2_54] [5.2_55]	CCR Ispra (European Commission)	Pre-mixing Explosion	UO ₂ + ZrO ₂ at 2800 °C 100–200 kg	<ul style="list-style-type: none"> - Very large programme - Reference for pre-mixing phase model qualification - Large masses - No spontaneous explosions - Explosion test with trigger (low efficiency)
KROTOS [5.2_37]	CCR Ispra (European Commission)	Explosion	Sn at 1000 °C Al ₂ O ₃ at 2300– 2800 °C UO ₂ + ZrO ₂ at 2800 °C 1 litre	<ul style="list-style-type: none"> - Reference programme for explosion code validation - One-dimensional (narrow test cross-section) - Influence of the composition (alumina or corium UO₂ + ZrO₂) - No spontaneous explosions with corium
ZrEX-ZrSS	Sandia (USA)	Explosion	Zr + ZrO ₂ mixtures Zr-steel A few kg	<ul style="list-style-type: none"> - Triggered explosions - Very great impact of Zr rate upon efficiency
TROI [5.2_56]	KAERI (South Korea)	Explosion + Pre-mixing	UO ₂ + ZrO ₂ corium Around 10 kg	<ul style="list-style-type: none"> - Poorly defined conditions - Spontaneous explosions - Low efficiency - Only 2 kg in the mixture at the time of explosion - Influence of corium composition

The reference results regarding the pre-mixing phase are based on the FARO experiments (conducted by the European Commission Joint Research Centre (JRC) at Ispra in Italy) [54], which used 100–200 kg of corium oxide (UO₂ + ZrO₂). The KROTOS

programme (which was also conducted at the JRC in Ispra) [37] was similar to the FARO programme in studying the explosion, albeit at a smaller scale (fuel volume was approximately one litre); this programme demonstrated a lower tendency towards explosion as well as lower pressure loads for a corium oxide ($\text{UO}_2 + \text{ZrO}_2$) in comparison with alumina (Al_2O_3). This result was the subject of considerable speculation regarding the “material effect”. The difference in density between the corium oxide and the alumina may explain this result; the lower density of the alumina has two effects: firstly, jet fragmentation into larger particles, resulting in less vaporisation and solidification, and secondly, an increase in the volume of fuel in the mixture because the speed of deposition on the bottom of the test cross-section is lower. The kinetic efficiencies (Section 5.2.3.3.1) of the strongest explosions were evaluated at approximately 2%, which is similar to those of the explosions in the FITS programme.

We should also mention the programmes whose results are little used, either because of a specific complication in the results or because of limitations in the dissemination of the results. The former category notably includes the ZREX tests by the Argonne National Laboratory in the United States [50], which revealed that explosion intensity was very greatly increased due to oxidation of the zirconium contained in the $\text{Zr} + \text{ZrO}_2$ and Zr-steel mixtures.

The TROI programme, which was conducted by the Korea Atomic Energy Research Institute (KAERI) in South Korea, confirmed that spontaneous explosions were possible with corium [56].

To support modelling, experimental programmes investigating separate effects (thermal transfers, fragmentation, etc.) have been conducted, generally in a national context. Notably, the TREPAM tests (CEA/IRSN) have made it possible to specify the heat transfers associated with the corium fragments under fairly representative conditions (pressures of up to 240 bar, speed differences between fragments and water of up to 46 m/s and temperatures of approximately 2200 °C). In the case of fine fragmentation, the DROPS programmes (conducted at the Institut für Kernenergetik und Energiesysteme (IKE) in Stuttgart, Germany, and then at CEA) [60] and MISTEE (conducted at the Royal Institute of Technology (KTH) in Stockholm, Sweden) [61] were devoted to studying the fragmentation of the corium droplets in the water by using simulants (generally liquid metals) at relatively low temperatures.

In order to validate the codes, various programmes also tried to represent the corium jets by jets of solid beads, thereby eliminating the fragmentation-related difficulties in order to concentrate on the heat transfer and friction aspects. In particular, the QUEOS programme conducted by Forschungszentrum Karlsruhe in Germany [51] studied the pre-mixing phase of solid sphere packets for temperatures of up to 2200 °C.

At the end of the programmes described above, many uncertainties remained at the beginning of the '00s regarding the steam explosions potentially resulting from interactions between a hot corium and the coolant. This conclusion explained the launch of the international SERENA programme described below, in line with the conclusions of OECD's “Technical opinion paper on fuel coolant interaction” and with the summary

report published by OECD in 2001 concerning the [nuclear safety](#) research conducted in the OECD countries, which show the usefulness of continuing R&D on the corium–water interaction [52].

The OECD international SERENA programme took place between 2001 and 2005, to provide a state of the art on steam explosions resulting from the interaction between hot corium and the coolant in a core melt accident and evaluating the existing codes' ability to describe this interaction. It showed that there were many differences of opinion between the experts, mainly due to the few experimental results available, highlighting the need for a new experimental programme.

This programme was implemented as part of a second phase of the programme, called SERENA-II, which took place between 2008 and 2012; its main objective was to study the effect of the corium's composition upon the explosion in integral tests and obtaining results to improve the state of understanding of certain points and qualify the computer tools.

The studies conducted in the first phase of SERENA made it possible to confirm that there was little risk of the containment rupturing as the result of a steam explosion in the reactor vessel ("Alpha" mode) and that the studies conducted in the second phase of the programme should give priority to studying the steam explosions that might occur in the reactor pit after the reactor vessel fails. From the point of view of the phenomena involved, there are no fundamental differences between in-vessel and ex-vessel interactions (in the reactor pit). The difference lies in the conditions under which the fluids come into contact. In particular, the mode of corium transfer into the water differs: in the ex-vessel case, it depends on the conditions under which the reactor vessel is ruptured and generally occurs in the form of a wide, non-central jet that may possibly be ejected under pressure. The nature of the corium may also differ, notably with a high probability of separation of its metallic (oxidisable) and oxidised phases (in the corium in the lower head). Containment internal pressure is of course generally lower than in the reactor vessel, and the water is assumed to be colder. The studies conducted in this context have also led to the deduction that the main uncertainties regarding steam explosions were due to a lack of detailed results on the pre-mix region and on the behavioural differences between the corium and the simulants such as alumina (the material effect) when they interact with the coolant. A small number of the experiments showed that the interaction between the corium and the water generated less energy than that between the alumina and the water. This finding has to be confirmed and explained.

CEA (supported by [IRSN](#) and EDF) and KAERI, an institute in South Korea (supported by KINS, the Korea Institute of Nuclear Safety) proposed the second phase of the SERENA programme with the aim of obtaining further information on pre-mix flow configuration, as well as on the effects of the materials and geometry. Fourteen organisations participated in this phase: CEA, IRSN and EDF in France, the KAERI and KINS institutes in South Korea, IKE-Stuttgart (Institut für Kernenergetik und Energiesysteme) and GRS (Gesellschaft für Anlagen und Reaktorsicherheit) in Germany, JNES (Japan Nuclear Energy Safety) in Japan, AECL (Atomic Energy of Canada Limited)

negative outcome is the fact that the explosion strengths (peak pressures, impulses) were higher than in previous experiments (with the same melt composition). This is attributed to larger melt masses in the test sections at the moment of triggering the explosion. The analyses of the TROI results indicated also an important “venting effect”, i.e. decrease of the pressure waves while travelling from the interaction zone to the walls. The pressure inside the interaction zone can be far higher than the resulting pressure at the wall. Due to this effect, in the hypothetical case of a central vessel break, the loads on the containment structures might be admissible or at least might not lead to immediate failure of the containment integrity (at least for the studied PWR geometry). Another positive outcome, from the point of view of the research efforts, was also the observation that the difference in explosion strengths owing to the exact composition of UO_2/ZrO_2 compositions was of second order.

5.2.3.3.3. Software

The MC3D computer code is developed and used in France to perform numerical simulations, notably of the pre-mixing and explosion phases [58, 59]. Its development by CEA to simulate steam explosions has mainly been financed by IRSN and partly by EDF. EDF ceased to support this code’s development in 2002 and then resumed its support in 2009 when it decided to participate in phase 2 of the SERENA programme. Since 2003, IRSN has been managing and developing the code in collaboration with CEA. Since 2006, the Slovenian JSI institute and the University of Stuttgart Institute of Research (IKE) in Germany have also helped to develop or qualify the code. The MC3D code is now considered as being one of the most advanced steam explosion simulation tools (mainly with JEMI/IDEMO [Germany, GRS/IKE], PM-ALPHA/ESPROSE [United States, UCSB] and JAS-MINE [Japan]) [59]. MC3D offers many functionalities described later in this document. It is distributed to various international bodies for studying the fuel-coolant interaction (as well as Direct Containment Heating (DCH)) in nuclear reactors.

A steam explosion computer code must process the many interactions between the different phases of the corium and coolant. This involves highly complex modelling with detailed numerical schemes, particularly in order to ensure its robustness. Furthermore, some codes such as MC3D are designed with the dual aims of obtaining results that can be used to assess safety in nuclear installations and improving our understanding of the phenomena involved. This dual purpose (studies and research) involves constraints that are often difficult to reconcile (robustness vs. accuracy).

In the MC3D code PREMIX application, the corium can be modelled in three different ways depending on whether it is in the form of a jet or in the form of droplets:

- the corium jet is modelled by a continuous field by means of a method of monitoring the volume (VOF-PLIC, see Figure 5.35); this numerical methodology is difficult to manage but its handling is a characteristic of the MC3D code, providing a wider scope of investigation than that of the other computer codes;
- the corium droplets are modelled by a field of drops by means of a Eulerian approach; the drops are created through fragmentation of the continuous field.

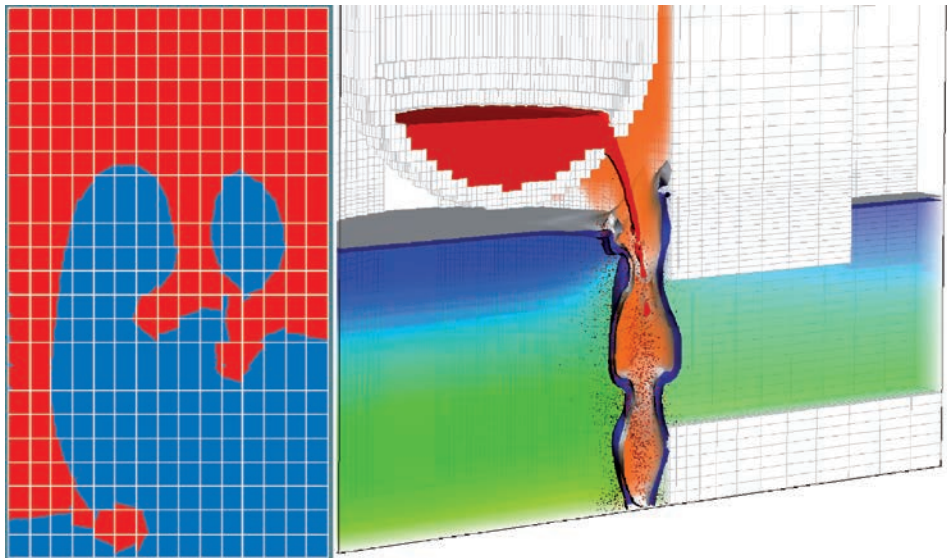


Figure 5.35. Illustrations of the MC3D code VOF-PLIC volume monitoring method for a continuous corium jet (continuous field in red (right) or brown (left); the droplet field is represented by dots). Left to right: Rayleigh-Taylor instabilities, high-pressure corium ejection from a reactor vessel (passage to a two-phase flow at the breach), 3D computation of an ex-vessel interaction, displaying fuel ex-vessel ejection [58] and interaction with the water (displayed in blue) in the reactor pit.

The MC3D code is also special in that it can take into consideration many non-condensing gases and corium oxidation by means of a parametric model. It should be remembered that the oxidation occurring during the explosion may result in a considerable increase in explosion energy. Unfortunately, the oxidation occurring under steam explosion conditions is poorly characterised (or even poorly understood) and the model is currently not sufficiently predictive.

There are fewer functional differences between the codes regarding the explosion phase modelling, and most of them use two fields for the fuel, namely a droplet field and a fragment field recording droplet fragmentation [59].

Some codes, such as PM-ALPHA and IDEMO, use what is known as the “micro-interaction” approach, in which the heating of a fraction of the water results in the pressure build-up. The MC3D and JASMINE codes’ models assume that, as in the pre-mixing phase, the pressure build-up is due to film vaporisation around the fragments generated by the explosion. IRSN and IKE (using the IDEMO model) are jointly analysing the difference between the two approaches in order to better understand the implications of the various approximations and assumptions.

Although these tools’ predictive capabilities are still somewhat limited at this time (they include major uncertainties), they have significantly enhanced overall understanding of the phenomena and the multiple interactions. The MC3D code, despite the constant efforts made to improve the user interface, is still difficult to use because of its complexity, which is itself due to the complexity of the phenomena involved.

During the SERENA-2 programme, a remarkable evolution of the capabilities of the MC3D code but also of the JEMI/IDEMO codes was obtained. This concerned mainly the physical mechanisms of melt fragmentation and solidification. More recently, JASMINE (JNES) and TEXAS (UW) also received substantial improvements related to solidification and the melt drop description. One important outcome of the analyses conducted during SERENA-2 is the recognition that, in the reactor applications undertaken, mainly due to the large scale, a large fraction of drops are solidified and a large void develops around the melt jet. Both effects, together with the venting effect discussed before, lead to a strong reduction in the potential loads resulting from FCI on the reactor pit walls. It was also demonstrated that 3D calculations are practically feasible. This is important as it is believed that 2D approximations with a central jet are not fully representative. The real impact of asymmetry of both the flow and the reactor geometry is unclear but it can be investigated only with 3D models.

Following the SERENA-2 conclusions and the Fukushima nuclear accident, a five-year programme was launched in 2014. Called ICE, the programme involves the major actors involved in nuclear safety research in France, namely IRSN, CEA, EDF and AREVA. The University of Lorraine is also participating and the programme is partly funded by the French government. The project combines integral experiments in the KROTOS facility, measurements of corium melt properties, dedicated analytical experiments on fragmentation and oxidation and model development for the MC3D code. A significant step forward in knowledge and understanding is expected from the development and use of methods for directly modelling complicated phenomena such as fragmentation, film boiling or oxidation ("quasi" direct simulation). Such methods are expected to give insights that cannot be obtained from experiments due to the very specific conditions (high temperature, high pressures). Some of these developments are done directly in the MC3D code, through specialised new applications.

5.2.3.4. Summary and outlook

The results of the research on steam explosions may appear modest in light of the problems left to solve. This is due to the complexity of the phenomena involved in the interactions between the hot corium and the coolant, on the one hand, and to the difficulty of obtaining experimental data on these interactions for simulants whose composition is typical of a corium formed when a power reactor core melt accident occurs.

The complexity and costliness of the interaction tests using coriums containing uranium have led to the experiments being jointly conducted at the international level, notably resulting in the OECD SERENA programme. This programme aims to provide the missing experimental data for coriums representative of those found in a power reactor accident.

The computer codes include increasingly accurate modelling of the pre-mixing phase and the explosion phase. In this domain too, the work must be shared; this is done by means of partnerships or exchanges, notably in the context of the European SARNET network of excellence (Section 1.3.2). The most difficult key points to describe are jet fragmentation during the pre-mixing phase, corium solidification and its impact upon

the explosion. A better description of the pressure build-up process during the explosion is also required. These key points form the core of the French ICE project, started in 2014, for five years, which is expected to yield a further step in understanding, modelling and simulation capabilities.

From the power reactor safety point of view, it is generally agreed that there is little risk of a containment rupturing as a direct result of a steam explosion in the reactor vessel (at least in the case of reactors with a large containment, such as the French PWRs). As the flooding of the reactor pit is one of the measures taken or envisaged to limit the consequences of a core melt accident in the operational reactors (with the aim of cooling the corium in the reactor pit and slowing the interaction between the corium and pit concrete, as described in Section 5.3), however, the risk of the containment rupturing as a result of a steam explosion in the reactor pit must be evaluated. Questions also remain concerning the strength of the containment concrete structures, due to the pressure loads caused by a steam explosion.

It should be noted that, in the case of an EPR, the risk of a steam explosion in the reactor pit must be “practically eliminated” by setting up measures guaranteeing that the pit does not contain any water at the time of the corium melt.

Reference documents

- [1] *Nuclear Engineering and Design*. Special issue on DCH, Vol. 164, 1996.
- [2] J.L. Binder, L.M. McUmbler, B.W. Spencer, Direct Containment Heating Integral Effects Tests at 1/40 Scale in Zion Nuclear Power Plant Geometry, NUREG/CR-6168, ANL-94/18, 1994.
- [3] T.K. Blanchat, M.D. Allen, M.M. Pilch, R.T. Nichols, Experiments to Investigate Direct Containment Heating Phenomena with Scaled Models of the Surry Nuclear Power Plant, NUREG/CR-6152, SAND93-2519, 1994.
- [4] T.K. Blanchat, M.M. Pilch, M.D. Allen, Experiments to Investigate Direct Containment Heating Phenomena with Scaled Models of the Calvert Cliffs Nuclear Power Plant, NUREG/CR-6469, SAND96-2289, 1997.
- [5] L. Meyer, G. Albrecht, M. Kirstahler, M. Schwall, E. Wachter, G. Wörner, Melt Dispersion and Direct Containment Heating (DCH) Experiments in the DISCO-H Test Facility, FZKA 6988, 2004.
- [6] L. Meyer, M. Gargallo, M. Kirstahler, M. Schwall, E. Wachter, G. Wörner, Low Pressure Corium Dispersion Experiments in the DISCO Test Facility with Cold Simulant Fluids, FZKA 6591, 2002.
- [7] L. Meyer, G. Albrecht, C. Caroli, I. Ivanov, Direct containment heating integral effects tests in geometries of European nuclear power plants, *Nuclear Engineering and Design* **239** (10), 2070-2084, 2009.
- [8] M.M. Pilch, M.D. Allen, Closure of the direct containment heating issue for Zion, *Nuclear Engineering and Design* **164**, 37-60, 1996.

- [9] K.K. Murata, D.C. Williams, J. Tills, R.O. Griffith, R.G. Gido, L.G. Tagios, F.J. Davis, G.M. Martinez, K.E. Washington, Code Manual for CONTAIN 2.0: A Computer Code for Nuclear Reactor Containment Analysis, NUREG/CR-6533, SAND97-1735, 1997.
- [10] D.C. Williams, R.O. Griffith, Assessment of cavity dispersal correlations for possible implementation in the CONTAIN code, SAND94-0015, 1996.
- [11] R. Meignen, S. Mikasser, C. Spengler, A. Bretault, Synthesis of analytical activities on Direct Containment Heating, ERMSAR-2007, Fzk GmbH, Germany, 12-14 June 2007, session-3, 2007.
- [12] R. Meignen, S. Mikasser, C. Spengler, A. Bretault, D. Plassart, L. Meyer, Direct Containment Heating: Comparison and Analysis of ASTEC, CONTAIN and MAAPE, Calculations of the LACOMERA L-1 Test, SARNET-CONT-P09, 2004.
- [13] R. Meignen, D. Plassart, C. Caroli, L. Meyer, D. Wilhelm, Direct Containment Heating at Low Primary Pressure: Experimental Investigation and Multi-dimensional Modeling, NURETH-11, Avignon, France, 2005.
- [14] S. Mikasser, R. Meignen, Computation and analysis of the Direct Containment Heating dispersion process with the multiphase flow software MC3D, *Proceedings of ICAPP 2007*, Nice, France, May 13-18, 2007.
- [15] W. W. Tarbell, M. Pilch, Pressurized melt ejection into water pools, Sandia National Laboratories, NUREG/CR-3916, 1991.
- [16] D. Karwat *et al.*, State-of-the-Art Report on containment thermal hydraulics and hydrogen distribution, [NEA/CSNI/R\(1999\)16](#).
- [17] H. Cheikhvat, Étude expérimentale de la combustion de l'hydrogène dans une atmosphère inflammable en présence de gouttes d'eau, University of Orléans doctoral thesis, September 2009.
- [18] H. J. Allelein, K. Fischer, J. Vendel, J. Malet, E. Studer, S. Schwarz, M. Houkema, H. Paillère, A. Bentaib, International Standard Problem ISP-47 on containment thermal hydraulics, Final Report, [NEA/CSNI/R\(2007\)10](#).
- [19] (a) D. Leteinturier *et al.*, Essais H2PAR: période mi-98 à fin 2000 synthèse des essais conclusions du programme, IRSN/DPEA/DIR/02/01 - Not publicly available;
(b) E. Studer, M. Durin, M. Petit, P. Rongier, J. Vendel, D. Leteinturier, S. Dorofeev, Eurosafe Forum, <http://www.eurosafe-forum.org/files/b4.pdf>
- [20] J. Loesel-Sitar *et al.*, Environmental Qualification of Hydrogen Recombiners, Test Report, AECL 00-68460-TR-001 - Not publicly available.
- [21] W. Breitung *et al.*, OECD State-of-the-Art Report on Flame Acceleration and Deflagration-to-Detonation Transition In Nuclear Safety, [NEA/CSNI/R\(2000\)7](#).
- [22] S. Dorofeev *et al.*, Large scale experiments for validation of hydrogen combustion models and criteria, article presented to the Jahrestagung Kerntechnik, Stuttgart, May 2002.

- [23] E. Bachellerie *et al.*, Generic approach for designing and implementing a passive autocatalytic recombiner PAR-system in nuclear power plant containments, *Nuclear Engineering and Design* **221** (1-3), 151-165, 2003.
- [24] E. Bachellerie *et al.*, EC PARSOAR project - State-of-the-art report on passive autocatalytic recombiners - Handbook guide for implementing catalytic recombiners, 2002, EUR report, June 2002.
- [25] W. Breitung *et al.*, Integral large scale experiments on hydrogen combustion for severe accident code validation HYCOM, *Nuclear Engineering and Design* **235** (2-4), 253-270, 2005.
- [26] J. Malet *et al.*, OECD International Standard Problem ISP-47 on containment thermal-hydraulics - Conclusions of the TOSQAN part, *Nuclear Engineering and Design* **240** (10), 3209-3220, 2010.
- [27] E. Studer, J.-P. Magnaud, F. Dabbene, I. Tkatchenko, International Standard Problem on containment thermal-hydraulics ISP47, step 1 – Results from the MISTRA exercise, *Nuclear Engineering and Design* **237** (5), 536-551, 2007.
- [28] D. Paladino, J. Dreier, PANDA: a multipurpose integral test facility for LWR safety investigations, *Science and Technology of Nuclear Installations*, vol. 2012, Article ID 239319, 9 pages.
- [29] P. Rongier, T. Bonhomme, C. Perez, 1^{re} Synthèse H2PAR – Résultats expérimentaux: Fiches d'expériences, expériences E1 à E19 et PHEB 02 - IPSN/DPRE/SERE n° 98/014 (I) - Not publicly available.
- [30] P. Rongier, T. Bonhomme, C. Perez, 2^e Synthèse expérimentale H2PAR - Détermination des conditions d'inflammation d'un mélange Air/H2/H2O par les recombineurs Siemens et A.E.C.L – Fiches d'expériences – IPSN/DPRE/SERLAB n° 99/004 (I) – Not publicly available.
- [31] A.A. Dehbi, The effects of noncondensable gases on steam condensation under turbulent natural convection conditions, Ph.D. Thesis, MIT, USA, 1991.
- [32] W. Ambrosini, N. Forgione, A. Manfredini, F. Oriolo, On various forms of the heat and mass transfer analogy: discussion and application to condensation experiments, *Nuclear Engineering and Design* **236**, 1013–102, 2006.
- [33] ERCOSAM: containment thermal-hydraulics of current and future LWRs for severe accident management, SP5-Euratom, collaborative project, small or medium-scale focused research project, FP7-Fission-2009, Grant agreement N°249691, 2010.
- [34] ISP-49 on hydrogen combustion, [NEA/CSNI/R\(2011\)9](#).
- [35] OECD/NEA SETH-2 project PANDA and MISTRA experiments, final summary report, [NEA/CSNI/R\(2012\)5](#).

- [36] OECD/NEA THAI project final report – Hydrogen and fission product issues relevant for containment safety assessment under severe accident conditions, [NEA/CSNI/R\(2010\)3](#).
- [37] I. Huhtiniemi, D. Magallon, H. Hohmann, Insight into steam explosions with corium melts in KROTOS, *Nuclear Engineering and Design* **204**, 391-400, 2001.
- [38] G. Berthoud, L'interaction corium-eau, synthèse et analyse des résultats expérimentaux, STT/LPML/87/28/C, 1987. Not publicly available.
- [39] D. E. Mitchell, M. L. Corradini, W. W. Tarbell, Intermediate Scale Steam Explosion Phenomena: Experiments and Analysis, NUREG/CR-2145, SAND81-0124, 1981.
- [40] D. E. Mitchell, N. A. Evans, Steam Explosion Experiments on Intermediate Scale: FITSB Series, NUREG/CR-3983, SAND83-1057, 1986.
- [41] B. W. Marshall Jr., Recent Fuel-Coolant Interaction Experiments Conducted In The FITS Vessel, SAND87-2467C, 1988.
- [42] R. Meignen, G. Berthoud, Fragmentation of molten fuel jets, *Proceedings of the International Seminar of Vapor Explosions and Explosive Eruptions*, pp. 83–89, 1997.
- [43] J. Namiech, G. Berthoud and N. Coutris, Fragmentation of a molten corium jet falling into water, *Nuclear Engineering and Design* **229** (2-3), 265-287, 2004.
- [44] SERENA – Steam Explosion Resolution for Nuclear applications, final report, December 2006. [NEA/CSNI/R\(2007\)11](#).
- [45] J. Lamome, R. Meignen, On the explosivity of a molten drop submitted to a small pressure perturbation, *Nuclear Engineering and Design* **238** (12), 3445-3456, 2008.
- [46] M. Bürger, S.H. Cho, E.V. Berg, A. Schatz, Modelling of drop fragmentation in thermal detonation waves and experimental verification, *Specialists Meeting on FCI*, Santa Barbara, California, USA, Jan 5-8, 1993.
- [47] S.J. Board, R.W. Hall and R.S. Hall, Detonation of fuel coolant explosions. *Nature* **254** (3), 319–321, 1975.
- [48] W. W. Yuen and T. G. Theofanous, On the existence of multiphase thermal detonations, *International Journal of Multiphase Flow* **25** (6-7), 1505-1519, 1999.
- [49] M. Berman, Light water reactor safety research program, quarterly report, January–March 1981, NUREG CR-2163/lof4, SAND81-1216/lof4, 1981.
- [50] D.H. Cho, D.R. Armstrong and W.H. Gunther, Experiments on Interactions Between Zirconium-Containing Melt and Water, NUREG/CR-5372, 1998.
- [51] L. Meyer, QUEOS, An Experimental Investigation of Pre-mixing Phase with hot spheres, *Proc. OECD/CSNI Specialist Meeting on FCI*, Tokai-Mura, Japan, 19-21 May 1997, pp. 155-166.
- [52] (a) Technical opinion paper on fuel coolant interaction. [NEA/CSNI/R\(99\)24](#).

- (b) Nuclear Safety Research in OECD Countries, Major Facilities and Programmes at Risk. NEA # 03145, ISBN: 92-64-18468-6, 2001.
- [53] S.K. Wang, C.A. Blomquist, B.W. Spencer, L.M. Mc UMBER and J.P. Schneider, Experimental Study of the Fragmentation and Quench Behaviour of Corium Melts in Water, *Proc. 5th Nuclear Thermal Hydraulics*, San Francisco, 1989, pp. 120-135.
- [54] D. Magallon, H. Hohmann and I. Huhtiniemi, Lessons Learnt from FARO/TERMOS Corium Melt Quenching experiments, *Nuclear Engineering and Design* **189**, 223-238, 1999.
- [55] D. Magallon and I. Huhtiniemi, Energetic event in fuel-coolant interaction test FARO L-33, ICONE-9 Conference, Nice, France, 8-12 April 2001.
- [56] J.H. Song, J. H. Kim, S. W. Hong, B. T. Min, H. D. Kim, The effect of corium composition and interaction vessel geometry on the prototypic steam explosion", *Annals of Nuclear Energy* **33** (17-18), 1437-1451, 2006.
- [57] Characterization of Molten-Fuel Coolant Interaction Processes, EUR 19567 EN, 4th EC Framework Program, 1999.
- [58] R. Meignen, Status of the Qualification Program of the Multiphase Flow Code MC3D, *Proceedings of ICAPP '05*, Seoul, KOREA, 15-19 May 2005, paper 5081.
- [59] R. Meignen *et al.*, Comparative Review of FCI Computer Models Used in the OECD-SERENA Program, *Proceedings of ICAPP '05*, Seoul, KOREA, 15-19 May 2005, paper 5087.
- [60] M. Bürger, Comparison and Theoretical Interpretation of Experiments on Hydrodynamic Drop Fragmentation. IKE 2-FB-16, (CEC-RCAMFCI Project, Report INV-MFC(98)-D014), Universität Stuttgart, July 1998 — Not publicly available.
- [61] H.S. Park, R.C. Hansson, B.R. Sehgal, Fine fragmentation of molten droplet in highly subcooled water due to vapor explosion observed by X-ray radiography, *Experimental Thermal and Fluid Science* **29** (3), 351-361, 2005.
- [62] J. H. Song, I. K. Park, Y. S. Shin, J. H. Kim, S. W. Hong, B. T. Min and H. D. Kim, Fuel coolant interaction experiments in TROI using a UO_2 - ZrO_2 mixture, *Nuclear Engineering and Design* **222** (1), 1-15, 2003.
- [63] P. Marmottant, E. Villermaux On spray formation, *Journal of Fluids Mechanics* **498**, 73-111, January 2004.
- [64] L. S. Nelson, P. M. Duda, Steam explosion experiments with single drops of iron oxide melted with a CO_2 laser, NUREG/CR-2295, SAND81-1346, 1981.
- [65] R.C. Hanson, An experimental study on the dynamics of a single droplet vapor explosion, Doctoral thesis, School of Engineering Science, KTH, Sweden, 2010.
- [66] E. Villermaux, Fragmentation, *Annu. Rev. Fluid. Mech.*, 419-446, 2007.

5.3. Phenomena that could lead to delayed containment failure: Molten Core-Concrete Interaction (MCCI)

5.3.1. Introduction

In the event of reactor-vessel failure during a core melt accident, the corium resulting from this core melt and the melting of internal structures will pour onto the reactor pit basemat. Contact between corium and concrete leads to what is called Molten Core-Concrete Interaction. This interaction involves gradual erosion of the concrete basemat (see Figure 5.36) and the walls of the reactor pit, which could lead to basemat penetration, and consequent release of radioactive substances outside the containment building into the ground. Furthermore, contact between the corium and any water present in the reactor pit and adjacent rooms could contribute an increase in the pressure inside the containment building *via* vaporisation of this water, or could even lead to a steam explosion (see Section 5.2.3). Gases resulting from reactions between corium and concrete also contribute to increasing the pressure inside the containment building. Taking uncertainties into account, the penetration time for the concrete basemat will be from one to several days, depending on the quantity of corium, its possible cooling and the type of concrete (siliceous or calcareous). It should be noted finally that the aerosol production that accompanies MCCI also affects how the behaviour of radioactive aerosols inside the containment changes and therefore affects any resulting releases.

5.3.2. Physical phenomena involved

The residual heat released by fission products within the corium spread on the basemat of the reactor building (20 to 30 MW at the start of the accident for a 900 MWe PWR) cannot be removed by conduction *via* the basemat due to its thickness and the very low thermal conductivity of concrete; it is only partially dissipated by radiative heat transfer from the surface of the corium. The corium, whose liquidity depends on its composition (which depends on the development of core damage during the accident), therefore heats up to the melting point of the oxide materials (UO_2 , ZrO_2) and the metals from the vessel (i.e. to a temperature of approximately 2200 °C), leading to the formation of a corium pool with a temperature exceeding the decomposition temperature of concrete. The heat released by the fission products is transferred by convection to the edges of the corium pool and provokes the destruction of the concrete walls of the reactor pit and their loss of integrity by decomposition of concrete (this process is generally called erosion or ablation). Siliceous or silico-calcareous concrete erodes from 1330 °C and calcareous concrete from a temperature several hundred degrees higher than that. After an initial corium heating phase, MCCI therefore leads to a phase of continuous erosion of the concrete walls. During this phase, the residual heat is largely dissipated at the corium-concrete interfaces *via* erosion of the concrete, and to a lesser extent by radiative heat transfer from the surface of the corium pool (see Figure 5.36).

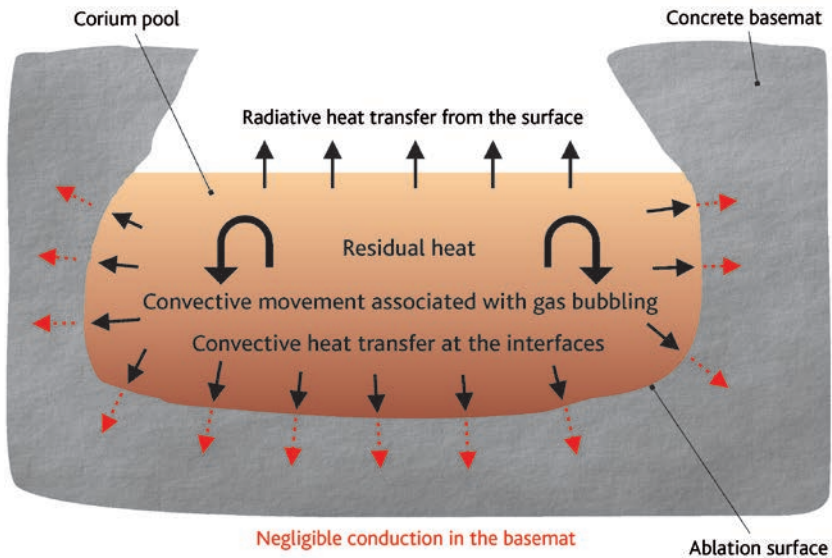


Figure 5.36. Formation of a cavity by erosion of the reactor-pit basemat.

As the concrete is made up mainly of SiO_2 , CaCO_3 and H_2O , its decomposition leads to the release of condensed (SiO_2 and CaO) and gaseous (H_2O and CO_2) phases into the pool. The corium pool therefore contains heavy oxides from the reactor core (UO_2 and ZrO_2), light oxides from the concrete (mainly SiO_2 and CaO) and metals (Fe , Cr , Ni and Zr), all subject to the mixing induced by the concrete decomposition gases. The mixing of metals with oxides in condensed or gaseous form can lead to exothermic oxidation reactions that produce gases such as H_2 , CO and $\text{SiO}(\text{g})$. Finally, contact between hot corium and colder concrete can lead to local formation of a crust by solidification, and fragments of this crust can become suspended in the liquid corium. The corium pool therefore has several constituents and several phases (liquid, solid and gas) whose composition and physical properties constantly change during MCCI, due to decomposition of the concrete and to chemical reactions.

As the rate of erosion of the horizontal and vertical walls is directly correlated to the relationship between the heat flux received by the walls and the energy density required for their erosion, determination of the rate of erosion of these walls requires calculation of the heat flux distribution at the edges of the corium pool. Even if there are multiple immiscible phases, the liquid pool produced by MCCI is uniform due to the mixing induced by the gases; however, steep temperature and concentration gradients may exist at the interfaces (see Figure 5.37). The heat flux at the pool interfaces may therefore be calculated using a convective heat transfer coefficient (h_{conv}), the pool temperature (T_b) and the temperature of the interface (T_i) between the corium pool and an interface layer separating the concrete from the corium (the composition and temperature of this interface layer are intermediate between those of the corium pool and those of the concrete; the layer may be liquid or solid depending on the conditions); the interface temperature

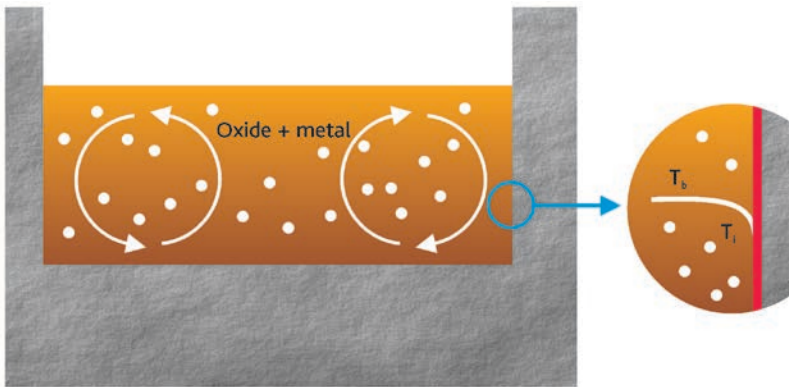


Figure 5.37. Perfectly mixed oxide-metal pool produced by an MCCI. Right: Detail of the pool-concrete interface.

depends on the type of interface between the corium and the concrete (i.e. whether a stable crust forms or not). The configuration of the pool produced by MCCI may be single layer (oxide and metal mixed) or two layer (oxide and metal stratified based on their respective densities), depending on the gas flowrate released by the concrete and the densities of the oxide and metal phases (which are only partially miscible). In the latter case (see Figure 5.38), determination of temperature at the interface, and of heat transfer coefficient is therefore necessary not only for the interfaces between the layers and the concrete, but also for the interface between the "oxide" liquid and the "metal" liquid.

To facilitate reading of the rest of this section, three phases of MCCI are distinguished: short term, medium term and long term. As will be seen below, the behaviour of the pool produced during MCCI depends on:

- its physical transport properties (density, thermal conductivity, specific heat capacity, viscosity and, to a lesser extent, liquid-gas surface tension) and its

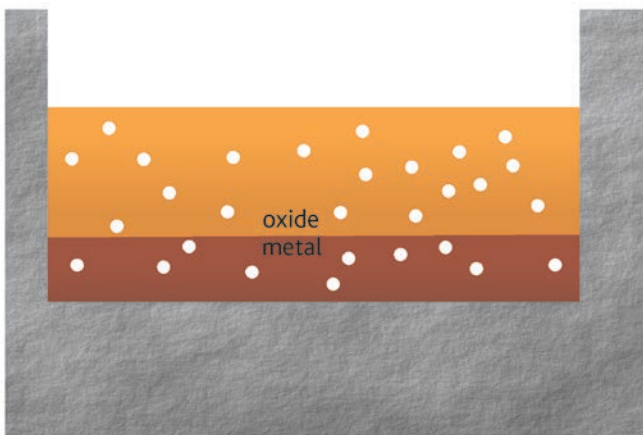


Figure 5.38. MCCI pool in a stratified configuration.

thermochemical properties, which are themselves a function of the composition of the pool, in particular the concentration of compounds from concrete erosion;

- the heat flux at the pool interfaces, which is a function of pool volume, and therefore of the quantity of matter from concrete erosion;
- the superficial gas velocity (volume flowrate of gases per unit surface area) along the interface between pool and concrete, proportional to the heat flux.

It therefore seems appropriate to distinguish various phases of MCCI, depending on the concentration of "concrete oxides" in the pool:

- the short-term phase corresponds to a mass fraction of "concrete oxides" in the pool below 25% (in practice, for a power reactor this corresponds to the initial hours of MCCI), with physical and thermochemical properties little different from those of the materials coming from the core, and vigorous gas bubbling;
- the medium-term phase corresponds to a higher mass fraction of "concrete oxides" in the pool (up to around 50%), i.e. in practice, for a power reactor, to the period between 5 and 15 hours from the start of MCCI, where the physical and thermochemical properties have significantly changed from those of the materials coming from the core but where heat flux at the pool interfaces and gas bubbling remain strong;
- finally, the long-term phase corresponds to a mass fraction of "concrete oxides" in the pool over more than 50%, i.e. in practice, for a power reactor, to the period beyond 15 hours from the start of MCCI, where heat flux at the interfaces and gas bubbling are significantly lower.

5.3.3. *Experimental programmes*

Study of MCCI includes experiments and computer models. The purpose of the experiments is to identify and understand the corresponding phenomena (heat transfers, solidification, mixing etc.); they are supplemented by studies using simulation software that include models that have been qualified on the basis of experimental data.

Tests devoted to the study of molten core-concrete interactions can be classified into two categories:

- analytical tests, which study one or more specific phenomena using simulant materials at a reduced scale; these tests can determine certain physical values concerning the phenomena studied (interface temperatures, heat transfer coefficients etc.);
- integral tests during which concrete erosion rates are measured, and in certain cases, pool temperatures during MCCI for coriums made up of simulant materials (containing alumina or thermite) and for coriums more representative of the composition expected during a core melt accident on a power reactor (generally containing a $\text{UO}_2 + \text{ZrO}_2$ mixture).

5.3.3.1. Analytical tests

► Heat transfer coefficients

Numerous analytical tests were performed between 1980 and 2010, see [1], [2] and [3], aiming to determine the heat transfer coefficients between a liquid pool and a bubbling porous wall. Examination of the results of these various tests, see [5], shows that the physical properties of the liquids used have often been close to those of water and that the data available mainly involves horizontal walls. For water, measurements performed during the various experimental programmes give similar results for the same superficial gas velocity. Data regarding viscous liquids (as for corium “enriched” with concrete erosion compounds) and vertical walls are quite rare, see [4]. However, test results in water show that the heat transfer coefficients between a fluid and a vertical wall are similar to those obtained for a horizontal wall. The CLARA experiments [6], which are described below, were launched in 2007, with a view to filling in gaps in knowledge regarding distribution of heat transfer coefficients along pool interfaces, which influence the distribution of heat fluxes and radial and vertical erosion of concrete during an MCCI.

Results pertaining to heat transfer coefficients between two immiscible liquids with gas bubbling (stratified pool configuration, see Figure 5.38) are less common, see [7] and [8]. In particular, examination of these results shows a significant dispersion of results (by around a factor of 5). Furthermore, the tests are not representative of situations where there is solidification at the interface between the pool and the concrete. However, the ABI tests, see [9], performed until 2008, show that the order of magnitude of the heat transfer coefficient between two stratified oxide and metal layers is comparable to that determined using the correlation deduced from the Werle tests, see [8], and that this heat transfer coefficient is probably large compared with the heat transfer coefficient between a liquid pool and a porous wall mentioned above. These results mean that, in a stratified configuration, heat transfer from the oxide layer into the metal layer could accelerate erosion of the concrete wall in contact with the metal layer (in the lower part, see Figure 5.38). This also highlights the interest of a reliable prediction of pool stratification (mixing and separation phenomena).

► Interface temperatures at the edges of a corium pool

The ARTEMIS programme (see [10]), performed by CEA from 2003 to 2008, is the only one that aimed to determine temperatures at the edges of a corium pool. It studied the coupling between physico-chemistry and thermal-hydraulics through tests conducted with simulant materials (LiCl and BaCl₂ salt mixtures), whose phase diagram has a similar form to that of the compounds present during an MCCI for a power reactor, as shown in Figure 5.39.

Tests performed in one-dimensional configurations (horizontal corium-concrete interface) confirmed that, under test conditions representative of the long-term phase of MCCI for a power reactor in terms of concrete erosion rate and gas bubbling,

the interface temperatures at pool edges were close to the liquidus temperature of the pool and that the pool temperature decreased with liquidus temperature due to enrichment of the pool with compounds from concrete erosion. However, the interface structure seems to be more complex than expected, with the formation near the interface of a solid porous zone out of thermal equilibrium (i.e. with liquid-solid interface temperature and composition that deviate from those imposed by thermal equilibrium between the liquid and solid phases). Examination of the results of ARTEMIS 1D experiments, see [11] and [12], also shows that, under conditions comparable to those of the short-term and medium-term phases of an MCCI for a power reactor, the results are not compatible with an assumption of thermodynamic equilibrium: the temperature of the pool-crust interface deviates from the liquidus temperature, the pool becomes mushy in the event of significant gas bubbling, and crusts form at the corium-concrete interface with a composition less refractory than that deduced from the phase diagrams.

Following an initial stage of the ARTEMIS programme dedicated to tests with purely axial erosion, the second stage (ARTEMIS 2D) was dedicated to the study of configurations with two-dimensional concrete erosion (i.e. in both axial and radial directions) during MCCI tests with differing compositions between pool and concrete and "concrete-concrete" tests with no difference in composition between pool and concrete. The results show significant concrete erosion on the upper part of the concrete side walls for all tests, very little erosion on the lower interface between pool and concrete during concrete-concrete tests and the formation, during MCCI tests, of a very thick

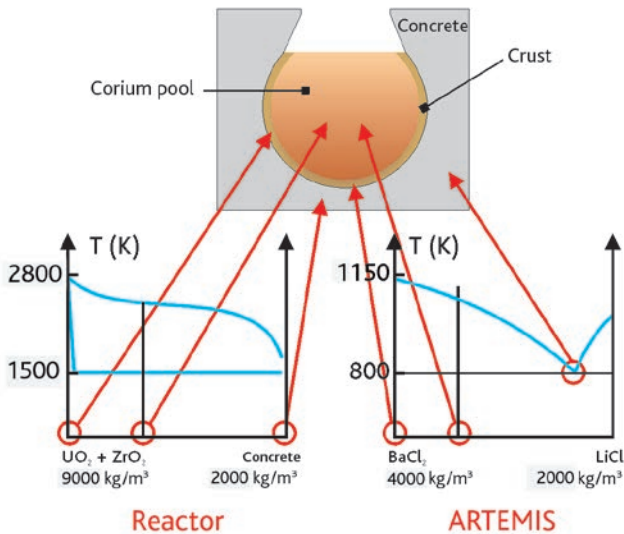


Figure 5.39. Comparison between the phase diagrams of simulant materials from ARTEMIS tests and those of corium materials which would form during a core melt accident on a power reactor (the BaCl_2 salt simulates the refractory behavior of corium and the $\text{LiCl}-\text{BaCl}_2$ eutectic simulates the behavior of concrete), see [10].

mushy crust of corium at the lower interface between the pool and the concrete (covering around a third of the pool); during the tests, this crust remained hot and embedded itself into the concrete. These unexpected results in terms of concrete erosion (in all cases, more concrete erosion was expected in the lower part of the pool) are probably explained by pool bypass by the gases injected into the lower part, due to the formation of stable, leaktight crusts at the lower pool-concrete interface; these crusts meant that gases could not pass during most of the tests. At the scale of a power reactor, it is unlikely that a large non-cracked crust would form at the lower pool-concrete interface. The results of the ARTEMIS 2D tests are therefore not directly applicable to a power reactor; however, they have brought to light the strong dependence of the 2D erosion profile on gas flow conditions in the pool.

► Mixing and separation of immiscible liquids with gas bubbling

The mixing and separation of immiscible liquids with gas bubbling has been studied with the aim of predicting the corium pool configuration during MCCI (i.e. whether the pool is mixed or stratified). The main experimental work on this subject was performed using simulant materials at the Argonne National Laboratory (ANL, [13]) and the University of Wisconsin (see [14]) in the United States, and more recently at CEA Grenoble (BALISE tests), see [15]; all experiments were purely hydrodynamic (with no study of phase change effects). They aimed to determine limit values in terms of superficial gas velocity (or void fraction) leading to a mixed or stratified pool depending on the density difference between the liquids. The results summary given in [15] shows a – sometimes wide – dispersion of results, partially due to differences in the physical properties of the liquids used. Nevertheless, these experiments clearly demonstrate that stratification of a corium pool can only take place for low superficial gas velocities, which are only possible during the long-term phase of MCCI for a power reactor.

► Physical properties of the materials

Analytical tests with prototypic corium compositions, like those which would form during core melt accident on a power reactor, have also been performed to validate and supplement knowledge regarding the thermophysical properties (in particular viscosity, see [21]) and thermochemical properties of corium, which are needed for the computer models of heat transfer and solidification phenomena for the corium pool outside the reactor vessel. These tests meant that improved estimates could be made of the viscosity of a corium formed from a mix of oxides (as a function of silica concentration), and of the solidus and liquidus temperatures of the corium-concrete mixes.

5.3.3.2. Integral tests

Integral tests provide an overview of MCCI, with all phenomena involved operating in a coupled manner. These tests are difficult to perform given the associated technological difficulties (very high temperatures and materials used etc.). All integral MCCI tests performed up to 2012 are summarised in Table 5.5 below.

Table 5.5. Summary of integral MCCI tests.

Programme	Characteristics	Mass of corium	Geometry	Parameters
SURC (1D)	Prototypic corium compositions + fission products	200 kg	0.4-m-diameter cylinder	Concrete composition, power
ACE (1D)	Prototypic corium compositions + fission products	250 to 450 kg	Rectangular box 0.5 m x 0.5 m x 0.4 m	Concrete composition, power
MACE (1D)	Prototypic corium compositions water injection	100 to 1800 kg	Rectangular box (0.5 to 1.2 m) x (0.5 to 1.2 m) x 0.4 m	Concrete composition, power, water flowrate
BETA (2D)	Thermite-alumina + iron oxide-metal stratified pool	450 kg	0.4-m-diameter conical frustum	Concrete composition, power
COMET-L (2D)	Thermite-alumina + iron oxide-metal stratified pool	920 kg	0.6-m-diameter cylinder	Concrete composition, power
OECD-MCCI (2D)	Prototypic corium compositions	350 to 550 kg	Rectangular box 0.5 m x (0.5 m or 0.7 m) x 0.6 m	Concrete composition, power, pool geometry
ARTEMIS 2D	Simulants (salts)	110 kg	0.3-m-diameter, 0.6-m-high cylinder	Power, gas flowrate
VULCANO-ICB (2D)	Prototypic corium compositions	40 kg	0.3-m-diameter, 0.3-m-high half-cylinder	Concrete composition, power

Interpretation of these integral tests is complex due to the limited number of measurements and the lack of precision associated with some of them, the difficulty of estimating heat losses and sometimes the difficulty in quantifying the influence of certain phenomena associated with the test set-up which may affect heat transfers above the pool: effects of the heating method and scale effects which could affect pool formation, ejection of matter (which changes the inventory of corium participating in MCCI), and crust adhesion on the walls. Despite these difficulties, the tests performed have brought to light phenomena which had not been previously identified and which could be significant: the strong influence of the type of concrete on the progress of axial and radial erosion and on the ejection of corium during an MCCI under water during the MACE tests; MCCI under water is presented in more detail in Section 5.4.2.

From a chronological standpoint, 1D tests with oxides (ACE, MACE and SURC) date from twenty years ago or more. Their analysis has provided an improved understanding of MCCI, supported certain assumptions regarding the corium behaviour models (decrease in pool temperature close to the liquidus temperature) and partially validated simulation software.

2D tests performed between 2003 and 2012 with oxides representative of a corium which would form during a core melt accident on a power reactor, have provided information on the 2D heat flux distribution during MCCI (see [16] and [17]). The results of these tests tend to show that, at least at the beginning of MCCI (the first four hours), concrete erosion is preferentially in the radial direction for siliceous concrete and similar in both radial and axial directions for silico-calcareous concrete (see [18]), as shown in Figure 5.40.

Tests using siliceous concrete show a possible scale effect on the anisotropy of erosion during the initial phase of MCCI. Analysis and interpretation of these results helped better understand the effect of the type of concrete on 2D erosion and to produce a model to better appreciate the erosion kinetics for the case of a power reactor.

Very few results exist for tests performed with materials representative of a corium which would form during a core melt accident on a power reactor and with pool heating representative of the residual heat of a corium for oxide-metal stratified configurations. The BETA and COMET tests were performed with simulant materials and their (induction-based) heating method meant that the heat was injected into the metal phase, whereas it would come from the oxide phase for a power reactor. The BETA tests showed preferential concrete erosion in the axial direction; however, this behaviour cannot be extrapolated to a power reactor for the reasons mentioned above and because the mass of metal is overestimated with respect to that of a power reactor, see [19]. Only the VULCANO tests, performed with a more representative heating method and composition of pool oxides and metals (see [20]), could provide answers to the question of possible existence of pool stratified during MCCI, which would lead to a high axial erosion rate, as illustrated by the applications to a power reactor presented in Section 5.3.5.

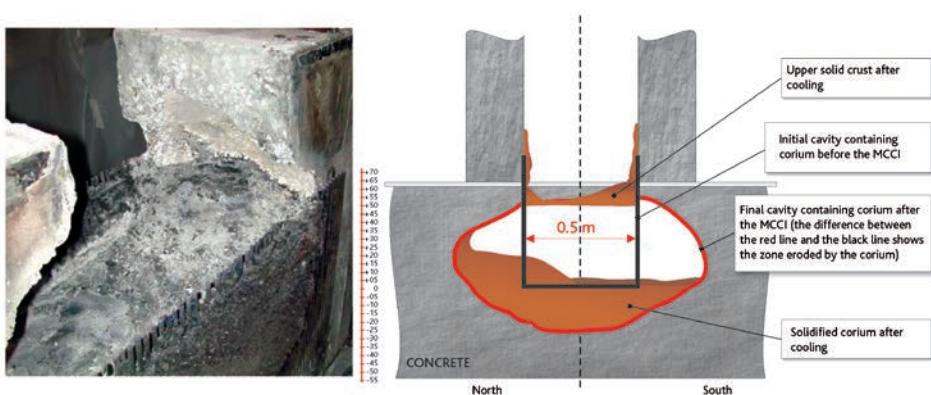


Figure 5.40. Final cavity obtained during the OECD-MCCI CCI-2 experiment, performed with a silico-calcareous concrete; the photo on the left shows the cavity formed in the concrete; this is represented in red on the diagram on the right (cross-section on the vertical axis).

5.3.4. Computer modelling and simulation software

5.3.4.1. Models

► Pool behaviour and pool-concrete interface temperatures

The oldest approach to determining the behaviour of the corium pool and pool-concrete interface temperatures during an MCCI assumed that, if the mean temperature of the corium pool is between the liquidus temperature and the solidus temperature, the pool is in a “mushy” state, intermediate between a solid phase and a liquid phase. The crust that forms at the interfaces has the same composition as the corium pool and the same solid fraction as the corium at the pool-crust interface. The interface between the pool (with or without crust) and the concrete is made up of a thin layer of decomposed concrete, called the “slag layer”. The solid-liquid equilibrium temperature is therefore the solidus temperature and the entire mushy zone is assumed to participate in convective flow near the solid interface. However, use of this assumption does not reproduce the temperature variations measured during certain ACE and OECD-MCCI tests.

In 2000, CEA produced a model called the “phase-segregation model” to describe the behaviour of the corium pool during an MCCI. This model is deduced from the model that couples thermal-hydraulics and physico-chemistry, used to describe the behaviour of the corium in the reactor vessel, see [21]. It is assumed that the pool is liquid and that crusts made up of refractory compounds (UO_2 and ZrO_2) form at the interface between the corium pool and the concrete. These crusts may be unstable. Mechanisms of crust formation at the interfaces and mechanisms that could affect their stability are little understood, in particular those that could explain the instabilities of the crusts formed at the interfaces with the vertical concrete walls, the presence of crusts during initial corium-concrete contact, and then the longer-term disappearance of crusts even at the bottom of the pool, as shown by certain inspections performed after VULCANO tests with an oxide pool. For applications to power reactors, the permanent existence of crusts at the interfaces is considered plausible given the duration of MCCI and the large pool volume. At the pool-crust interfaces, thermodynamic equilibrium is assumed to exist between the two physical phases present (the pool liquid and the crust solid), with the interface temperature being the liquidus temperature of the pool. If a departure from equilibrium occurs, liquid-solid segregation is partial or absent in the pool, which becomes mushy and the pool-crust transition may therefore correspond to a solid fraction threshold above which conduction dominates convection. The pool-crust interface temperature would then be lower than the liquidus temperature of the pool. This type of approach is adopted in the model used in the MEDICIS code developed at IRSN [27], described in detail in Section 5.3.4.2.

The phase segregation model has been partially validated using the results of ARTEMIS 1D tests, with regard to interactions with a horizontal wall and for low erosion and bubbling rates, which correspond to the long-term phase of MCCI for a power reactor. However, this “ideal” model, which assumes thermodynamic equilibrium at the pool-concrete interface, does not satisfactorily explain the results of the ARTEMIS 1D tests, with rapid erosion and significant bubbling, which corresponds to the initial

highly-transitory phase of the interaction; furthermore, this model is not relevant for the long-term phase for a power reactor, despite the good agreement with the ARTEMIS 1D test results corresponding to these conditions, due to the high concentration of silica in the pool in the long-term phase, which reduces the diffusion of chemical species in the pool and delays attainment of equilibrium at the interface, see [22].

► Distribution of heat fluxes at the corium-concrete interface

Numerous correlations of heat transfer between a pool and a bubbling horizontal wall are cited in the literature, see [1] to [4] and [7]. They have been produced on the basis of the experimental data mentioned above, or from more theoretical approaches. They are expressed as correlations which give the Nusselt number Nu as a function of the Reynolds number Re and the Prandtl number Pr under the assumption that heat transfer is associated with a forced convection produced by the concrete decomposition gases, or Nu as a function of the Rayleigh number Ra and Pr under the assumption that heat transfer is associated with natural convection; the Prandtl number Pr only depends on the fluid properties; the Reynolds number Re depends on the transport properties of the pool and the superficial gas velocity; the Rayleigh number Ra depends on the transport properties of the pool and the void fraction, and therefore indirectly on the superficial gas velocity. The ranges of variation of the physical properties of fluids used for the tests with simulant materials (see Section 5.3.3.1) are narrow and do not always cover those of a corium pool representative of an MCCI, see [23]. Although the correlations give identical results for the experimental conditions of tests performed with simulant materials, a wide dispersion of results is observed when these correlations are used with parameters representative of a power reactor. This dispersion probably shows that the dimensionless numbers used in the correlations do not correctly reflect all physical phenomena involved or the respective weightings of the various physical parameters, due to the narrow range of experimental data used to establish these correlations. For this reason, a model based on a more phenomenological approach was proposed in 2005, see [24]; it provides satisfactory results for the conditions of available experimental data (horizontal wall and vertical wall, see [5]) but would need additional validation for viscous liquids. Finally, it is important to note that, rather than the local value of the heat transfer coefficient between pool and the crusts, it is the distribution of the value of the heat transfer coefficient at the surface of the pool that is crucial to determining the distribution of local heat fluxes and erosion rates during the pseudo-steady state which exists during the longest part of MCCI.

For this reason, the CLARA analytical test programme was launched by CEA and IRSN to improve understanding of the distribution of heat transfer coefficients along the pool interfaces and their variations as a function of superficial gas velocity and pool viscosity.

With regard to heat transfers between the oxide and metal layers which form during pool stratification, several models are found in the bibliography, deduced from analytical tests, see [7], [8] and [25]. Due to the lack of experimental results and the dispersion of the available results, these models were reviewed in 2010, see [1] taking into account the most recent results obtained for measurement of the convective heat

transfer coefficient in the context of the ABI experimental programme performed at CEA Grenoble, see [9]. The main conclusion of this work, see [1], is that convective heat transfer between the layers is greater than radial heat transfer, which leads to a rate of axial concrete erosion that is higher than that of radial erosion; however, possible formation a permeable crust at the interface between the two liquids, which would reduce this heat transfer, is difficult to model, precisely because of the probable instability of this crust.

► Mixture and separation of immiscible liquids with gas bubbling

Test results produced with simulant materials are the basis of the development of experimental correlations, see [15], used to estimate the superficial gas velocity thresholds that lead to mixture or stratification of the pool; the values obtained present a non-negligible dispersion (several tens of%). These correlations have not been validated on test results with real materials, and their use for a power reactor would lead to highly varied configurations: a largely mixed configuration or a stratified configuration or a partially stratified configuration over a longer or shorter period of MCCI. In particular, uncertainties concern the dependence of the correlations on the physical properties of the liquids, the respective volumes of the metal and oxide layers and the size of bubbles.

5.3.4.2. Simulation software

Various software packages developed for MCCI studies, see [26], [27] and [30], are based on identical basic assumptions:

- the corium pool is made up of various layers (of oxides or metals) each of uniform temperature and chemical composition;
- the corium pool can be in a mixed (uniform) or stratified configuration;
- the structure of the interface is described by a thermal resistance model that takes into account the possible formation of a solid crust or a zone of concrete decomposition products (a thin layer of decomposed concrete called the “slag layer”). The concrete erosion rate is estimated using Stefan’s law, which determines the quantity of heat coming from the corium pool that is not removed by conduction in the concrete and which serves to erode the concrete.

These software packages are mainly distinguished by their corium behaviour models and by the sub-models (or correlations) that they use (such as correlations to calculate void fraction, heat transfers etc.).

The TOLBIAC-ICB code (see [26]), developed by CEA, is based on the phase segregation model described above, which assumes the pool of liquid corium and the formation of crust of refractory material at the interface: the interface temperature is the liquidus temperature of the pool (over 2200 K for a large part of MCCI). It is calculated from the pool composition using a coupling with the GEMINI2 thermodynamic code.

In contrast, the CORCON code (see [30]), developed by Sandia National Laboratories in the United States, considers that the pool is a mix of liquid and solid debris in suspension and assumes the existence of a mushy zone, if the pool temperature is between the liquidus and solidus temperatures. The thin layer of decomposed concrete ("slag layer") model is used describe the corium-concrete interfaces. In this approach, the pool-crust interface temperature is close to the concrete decomposition temperature.

The MEDICIS code (see [27]), developed by IRSN, uses a more flexible model to describe the behaviour of the pool interfaces: it is assumed that a mushy zone exists at the interface between the liquid pool and the concrete, including a convection zone and a conduction zone. In this approach, the interface temperature used for convective heat transfers from pool to interface is the threshold temperature at the border between the convective part of the pool and the conductive part of the mushy zone ($T_{\text{solidification}}$ on Figure 5.41). As no model can satisfactorily determine this interface temperature in all circumstances, it is arbitrarily set by the user between the liquidus temperature and the solidus temperature, or deduced from a threshold value for the molten fraction of pool corium. The extreme options correspond to the interface model in TOLBIAC (liquidus temperature) and that adopted in CORCON (solidus temperature). MEDICIS validation leads to recommending an interface temperature value a little lower than the liquidus temperature, or a molten fraction threshold of approximately 50%. Phase segregation in the crusts is not taken into account, as the crusts are usually thin at the corium-concrete interface; however, liquidus and solidus temperatures and the relationship between the molten corium fraction, its composition and its temperature are assessed using the GEMINI2 code prior to an MCCI calculation. It is also assumed that a thin layer of decomposed concrete (the "slag layer") exists between the concrete and the pool (with or without crusts).

The main steps of an MCCI calculation are as follows:

- calculate the physical properties of the pool;
- calculate the (possible) solid fraction in the pool;
- determine the interface temperature;
- calculate the heat transfer coefficients;
- estimate the concrete erosion rates;

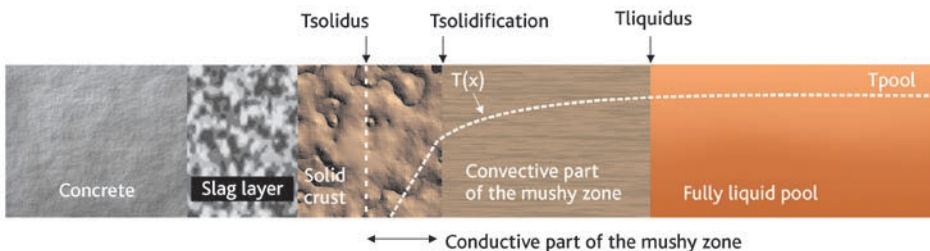


Figure 5.41. Model of the corium-concrete interface used in the MEDICIS code.

- perform a mass balance (taking chemical reactions into account) and an energy balance (including radiative heat transfer from the surface) to obtain the composition and temperature of each pool zone;
- calculate the thicknesses of crusts and erosions;
- update the form of the cavity and the heat transfer surfaces.

Simulation software is validated using the test results presented in the previous section. For integral tests, this validation process is made more complex by the numerous phenomena observed during these tests that are not covered by the computer models (such as corium ejection and deposits of matter on the walls of the test sections) and the specifics of the experimental set-ups, as mentioned previously.

Generally, the validity of simulation software for application to a power reactor is limited by uncertainties on scale effects, as the models implemented in this code have only been validated using test results at a scale 10 to 20 times smaller than that of a power reactor. The obvious solutions for overcoming this difficulty are the performance of larger-scale tests with prototypic materials, or the development of mesh-based simulations able to represent the thermal-hydraulics and heat transfer physics at various scales, in order to confirm extrapolation from the scale of the tests to that of a power reactor. The first solution runs into issues of technical feasibility and cost. The second solution assumes development and validation of turbulence models applicable to a pool with gas bubbling; these models would only be applicable to idealised situations with regard to the structure of the pool interfaces and would require the implementation of simulations that may not be available for many years.

5.3.5. Application to a power reactor

As an example, this section presents application to a 900 MWe PWR performed using the MEDICIS code, see [27] and [28], for the case of a reinforced siliceous-concrete basemat with an axial thickness of 4 m. Conservative bounding assumptions have been used for the initial conditions to obtain bounding results in terms of concrete erosion; in particular, all the reactor core that becomes corium is assumed to be present in the reactor pit at the beginning of MCCI and the effects of any water present and of radial erosion of the basemat are ignored.

The main calculation assumptions adopted are similar to those used for interpreting the MCCI tests of the MCCI programme at the ANL, see [16], leading to 2D isotropic erosion, see [29]. For a uniform pool, a heat transfer model is adopted that is independent of the orientation of the interfaces, and an interface temperature slightly below the liquidus temperature is used. The convective heat transfer coefficient between the oxide and metal layers, which applies to the stratified configuration, has been deduced using Greene's correlation, see [7], which tends to overestimate heat transfer.

Large uncertainties exist regarding pool configuration and how it changes over time. For this reason, three very different scenarios have been considered for the concrete erosion calculation.

(1) A scenario with a uniform pool maintained throughout MCCI (see Figure 5.42), which leads to slow erosion and a basemat penetration time of approximately 5 to 9 days, depending on the thickness of concrete to be eroded (3 m to 4 m).

Axial and radial erosion rates remain low due to the uniform distribution of heat flux at the pool-concrete interfaces, leading to uniform erosion and a very large zone of eroded concrete as shown in Figure 5.42.

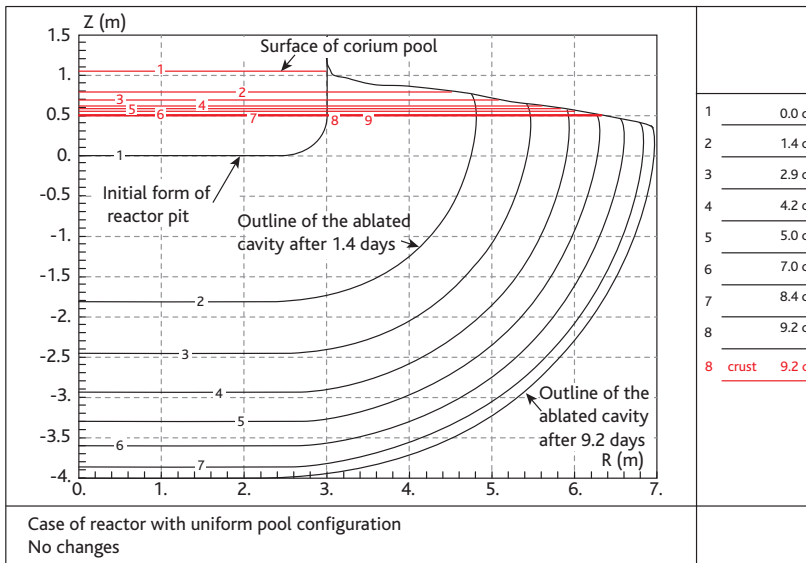


Figure 5.42. Case of a power reactor with a uniform pool configuration changes calculated for the cavity resulting from concrete erosion (axial erosion along the Z-axis and radial erosion along the R-axis) until basemat penetration after 9.2 days. The last curve corresponds to the time that axial basemat penetration occurs.

(2) For illustrative purposes, an unrealistic scenario with a stratified pool where the metal layer is assumed to be below the oxide layer from the start of the interaction, which leads to a very high rate of axial erosion, with a basemat penetration time of between 14 and 24 hours depending on its thickness. The reason for rapid erosion in this case is the high heat transfer coefficient at the metal-oxide interface, which leads to residual heat removal being concentrated at the bottom of the pool, thereby promoting axial erosion (see Figure 5.43).

(3) A more realistic scenario, which involves four phases with changing pool configurations (see Figure 5.44). In this scenario, the pool is assumed to be initially stratified with the oxide layer below the metal layer due to the higher density of the oxides (initial short-term phase), then it mixes and becomes uniform due to significant gas bubbling (second medium-term phase); then, in a third phase (start of the long-term phase), the pool become stratified again but with the metal layer below the oxide layer due to the reduction in oxide density caused by the addition of compounds from concrete erosion;

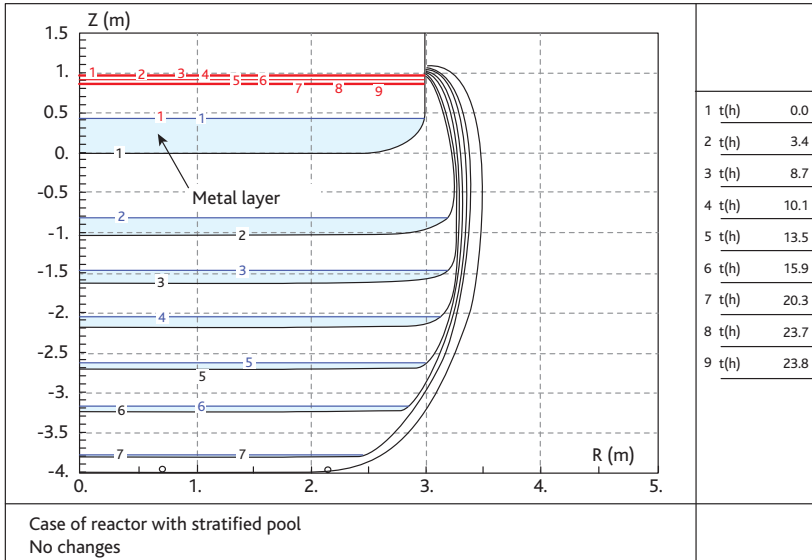


Figure 5.43. Case of a power reactor with a stratified configuration – changes calculated for the cavity resulting from concrete erosion (axial erosion along the Z-axis and radial erosion along the R-axis) in approximately 3-hours steps, with axial penetration after approximately 24 hours. The last curve corresponds to the time that axial basemat penetration occurs.

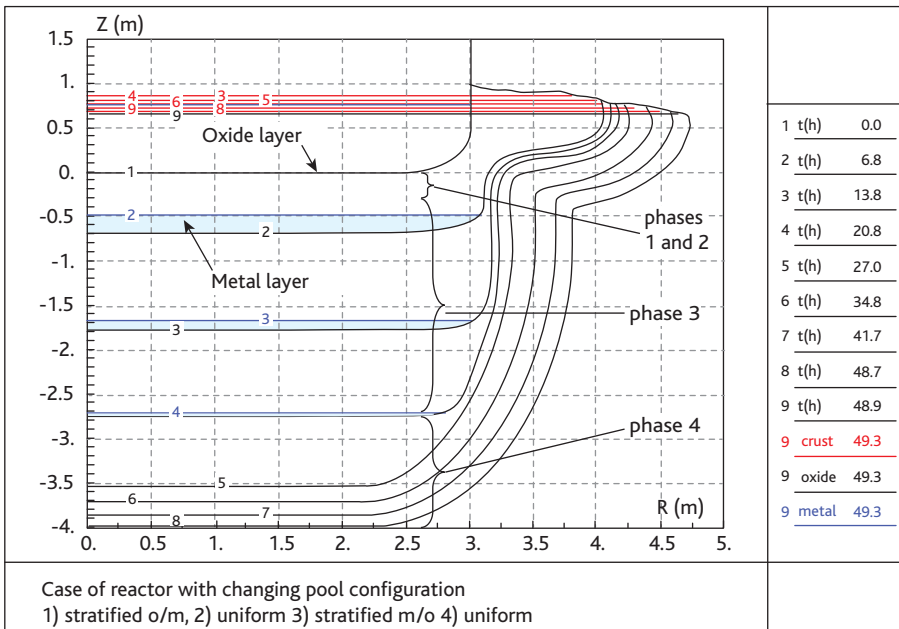


Figure 5.44. Case of a power reactor with changing pool configuration – changes calculated for the cavity resulting from concrete erosion in approximately 6-hours steps, with axial penetration after approximately 49 hours (o/m: the oxide layer is above the metal layer; m/o: the metal layer is above the oxide layer).

finally in a fourth longer-term phase, the pool becomes uniform again as the metal layer disappears due to oxidation. Changes in pool configuration are determined using criteria deduced from the BALISE tests mentioned above in Section 5.3.3.1, see [15]. When configuration changes are taken into account, basemat penetration time is extended by at least 24 hours with respect to a fixed stratified configuration with the metal layer below the oxide layer (compare Figures 5.43 and 5.44).

The results of basemat penetration time calculations are given in Figure 5.45 below. This figure shows that the effect of pool stratification on basemat penetration time would only disappear if the heat transfer coefficient between the oxide and metal layers was very small (by a factor of more than 20) compared with the available experimental data. However, high values of the oxide-metal heat transfer coefficient due to the mixing caused by gas bubbling have been confirmed (at least in terms of order of magnitude) by the experiments in the ABI programme cited in Section 5.3.3.1, see [9].

It should be noted that the calculations given above are based on certain conservative assumptions:

- the assessment criteria for pool configuration assumes that its stratification occurs from the beginning of separation of the oxide and metal phases and that this stratification is maintained even for a thin metal layer; a more realistic criterion for configuration changes, taking into account limitation of stratification in the event of a thin metal layer which is still to be confirmed, would probably lead to axial penetration times of several days;
- the heat transfer coefficient at the pool-concrete interface is assumed to be independent of the orientation of this interface for an oxide pool (and for a metal pool). However, for a siliceous concrete and in an oxide pool configuration, heat transfers could be less at the lower interface than at the lateral interface, as shown by certain results from the MCCI-OECD programme, see [16]; a model taking these results into account leads to a reduction in axial erosion rates;
- corium reflooding in the event of water injection is ignored.

Figure 5.45 shows that penetration of the reactor-pit walls (leading to partial spillage of corium outside the reactor pit into the containment building) takes place before axial penetration in the event of slow to moderate axial erosion, and slows later axial erosion by reducing the corium inventory in the reactor pit.

Finally, it should be noted that axial erosion is slower for a silico-calcareous concrete than for a siliceous concrete:

- gas velocity is greater for a silico-calcareous concrete due to the concrete's greater gas content, which has the effect of reducing the period during which stratification is possible;
- the decomposition enthalpy is higher, which reduces axial and radial erosion rates in a uniform configuration.

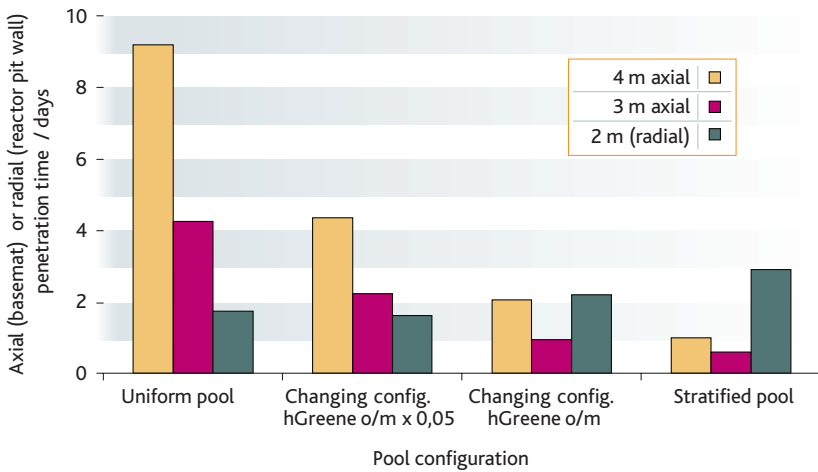


Figure 5.45. Reactor-pit basemat and wall penetration times as a function of pool configuration: uniform pool (see Figure 5.42); stratified pool (see Figure 5.43); changing pool configuration for a calculation performed using a convective heat transfer coefficient between the oxide and metal layers deduced from Greene's correlation ($h_{\text{Greene}} \text{ o/m}$, see Figure 5.44); changing pool configuration for a calculation performed using a heat transfer coefficient reduced by a factor of 20 compared with that given by Greene's correlation ($h_{\text{Greene}} \text{ o/m} \times 0.05$) and convective heat transfers between the oxide and metal layers.

5.3.6. Summary and outlook

The results of experiments and calculations performed for a power reactor using the MEDICIS and TOLBIAC-ICB code bring to light the following main areas of uncertainty, see [31]:

- the nature and properties of the corium pool interfaces: pool solidification temperature, and heat and mass transfers at the corium-concrete interfaces;
- the 2D (radial and axial) distribution of convective heat fluxes in a uniform pool;
- heat and mass transfers between metal and oxide layers in a stratified configuration;
- changes in pool configuration (stratification).

Knowledge of the interface structure has progressed over the last decade but remains inadequate. Indeed, analysis of the ARTEMIS 1D experiments, performed with a uniform pool and a horizontal interface, shows that the phase segregation model at thermal equilibrium (with a pool-crust interface temperature close to the liquidus temperature) applies well to a case of slow concrete erosion and low gas velocities, a situation that could correspond to the long-term phase for a power reactor; however, the high pool viscosity in this phase slows diffusion of chemical species and could lead to a different composition at the interface than that for thermodynamic equilibrium. For faster erosion, a situation that corresponds to the short- and medium-term phases for a power reactor, the phase segregation model is no longer suitable due to being far from thermodynamic equilibrium. Furthermore, analysis of 2D MCCI tests performed with real

materials also shows that the pool is often mushy and the pool-crust interface temperature lower than the liquidus temperature, in particular for siliceous concrete, see [29]; in addition, associated inspections did not bring to light a crust on any corium-concrete interface, including the horizontal interface, contrary to what was observed during tests with simulant materials (ARTEMIS 1D tests).

Major uncertainties also exist regarding the last three points mentioned above, i.e. the distribution of heat fluxes at pool interfaces, heat transfers between the metal and oxide layers in the stratified configuration, and changes in pool configuration. In particular, improved understanding of heat transfers between the metal and oxide layers and of the types of pool configuration and their changes, would strongly reduce uncertainties regarding axial and radial erosion rates for a stratified pool configuration, which remain major, see [33].

In 2015, end of the VULCANO MCCI experiments (with materials representative of a power-reactor corium) and associated work – such as interpretation of the tests and comparison of the results obtained with various code packages – provided further understanding of the physical phenomena that govern the structure of the interfaces, and supplemented knowledge of the 2D distribution of heat fluxes for a uniform pool configuration. Additional MCCI tests for stratified pool configurations are envisaged to contribute to reducing remaining uncertainties by providing results regarding heat transfers between oxide and metal layers and regarding changes to the pool configuration.

The CLARA programme, which ended in 2012 and used simulant materials, aimed for better understanding of 2D erosion for a uniform pool, by detailed study of convective heat transfers between a heated pool and a bubbling porous wall, in a 2D situation with simplified boundary conditions (without erosion) over a large range of pool viscosities.

Qualification using a large-scale test would be necessary, due to probable scale effects on convective heat transfer and on the structure of the corium-concrete interfaces. Such a test, with an initial pool size of around one metre, was planned in Russia in 2011 in the context of the programmes of the International Science and Technology Center (ISTC), but the project was not completed due to administrative difficulties.

Pool stratification criteria should also be better defined and better validated, in particular the superficial gas velocity threshold and maximum thickness of metal below which stable pool stratification appears.

Furthermore, a programme of additional studies aiming to reduce uncertainties on the thermochemical properties of corium was performed in the context of the ISTC programme (the PRECOS project) and mainly involved determination of the phase diagrams for certain mixtures of oxides and metals of compositions selected in a range where thermochemical data is inadequate or uncertain. Analysis of the associated experimental results should provide additional data for the thermochemical databases used by software (such as GEMINI2, see [32]) to calculate thermodynamic values for corium.

Reference documents

- [1] [S.S. Kutateladze](#), Boiling and bubbling heat transfer under free and forced convection of liquid, *Int. J. Heat Mass Transfer* **22**, 1979.
- [2] M.R. Duignan, G.A. Greene, T.F. Irvine Jr, Heat transfer from a horizontal bubbling surface to an overlying water pool, *Chem. Eng. Comm.* **87**, 1990.
- [3] J.M. Bonnet, Thermal-hydraulic phenomena in corium pools for ex-vessel situations: the BALI experiments, *8th Int. Conf. On Nuclear Engineering (ICONE)*, Baltimore, USA, April 2-6, 2000.
- [4] [D.K. Felde](#), H.S. Kim, S.I. Abdel-Khalik, Convective heat transfer correlations for molten core debris pools growing in concrete, *Nuclear Engineering and Design* **58**, 1980.
- [5] [B. Tourniaire](#), O. Varo, Assessment of two-phase flow heat transfer correlations for molten-core concrete interaction study, *Nuclear Technology* **164**, 2008.
- [6] M. Amizic, E. Guyez, J-M. Seiler, Experimental investigation on heat transfer for two-phase flow under gas-driven convection, *Proceedings of ICONE20-PWER2012, 20th Int. Conf. on Nuclear Engineering*, July 30-August, 2012, Anaheim, California, USA.
- [7] [G.A. Greene](#), Heat, mass and momentum transfer in a multi-fluid bubbling pool, *Advances in Heat Transfer* **21**, 1991.
- [8] [H. Werle](#), Enhancement of heat transfer between two horizontal liquid layers by gas injection at the bottom, *Nuclear Technology* **59**, 1982.
- [9] J. Excoffon, Rapport d'essais ABI-Gallium, Rapport CEA/ DEN/DTN/SE2T/ LPTM/ RT/008-312a – 2008 – Reference not publicly available.
- [10] J.M. Veteau, ARTEMIS program: investigations of MCCI by means of simulating materials experiments, *Proceedings of ICAPP '06*, Reno, NV USA, June 4-8, 2006.
- [11] [M. Guillaumé](#), H. Combeau, J.-M. Seiler, An improved interface model for MCCI for LCS or Limestone concrete, *Nuclear Engineering and Design* **239** (6), 1084-1094, 2009.
- [12] [B. Michel](#), M. Cranga, Interpretation and calculations for the first series of tests for the ARTEMIS program (corium-concrete interaction with simulating materials), *Nuclear Engineering and Design* **239** (3), 600-610, 2009.
- [13] [M. Epstein](#), D.J. Petrie, J.H. Linehan, G.A. Lambert, D.H. Cho, Incipient stratification and mixing in aerated liquid-liquid or liquid-solid mixture, *Chem. Eng. Science* **36**, 1981.
- [14] [J.L. Casas](#), M.L. Corradini, Study of void fractions and mixing of immiscible liquids in a pool configuration by an upward gas flow, *Nuclear Technology* **99**, 1992.

- [15] B. Tourniaire, J.M. Bonnet, Study of the mixing of immiscible liquids by sparging gas: results of the BALISE experiments, 10th International Meeting on Nuclear Reactor Thermal-Hydraulics (NURETH10), Seoul, Korea, October 5-9, 2003.
- [16] M.T. Farmer, S. Lomperski, S. Basu, A summary of findings from the melt coolability and concrete interaction (MCCI) program, *Proceedings of ICAPP07*, Nice, France, May 13-18, 2007.
- [17] C. Journeau, J.M. Bonnet, E. Boccaccio, P. Piluso, T. Sevón, P.H. Pankakovski, S. Holmström, J. Virta, Current European Experiments on 2D Molten Core Concrete Interaction: HECLA and VULCANO, *Proc. ICAPP'08*, Anaheim, California, 2008.
- [18] M. Farmer, S. Lomperski, The results of the CCI2 reactor material experiment investigating 2-D core-concrete interaction and debris coolability, *11th International Topical Meeting on Nuclear Reactor Thermal-hydraulics (NURETH-11)*, Avignon, France, 2005.
- [19] H. Alsmeyer, BETA experiment in verification to the WECHSL code: experimental results on the melt concrete interaction, *Nuclear Engineering and Design* **103**, 1987.
- [20] C. Journeau, P. Piluso, J. F. Haquet, E. Boccaccio, S. Saretta, J.M. Bonnet, Oxide-Metal Corium-Concrete Interaction Test in the VULCANO facility, *Proc. ICAPP'07*, Nice, France, 2007.
- [21] J.M. Seiler, K. Froment, Material effects on multiphase phenomena in late phases of severe accidents of nuclear reactor, *Multiphase Science and Technology* **12**, 2000.
- [22] Ch. Journeau, C. Jegou, J. Monerris, P. Piluso, K. Frolov, Phase macrosegregation during the slow solidification of prototypic corium, 10th International Meeting on Nuclear Reactor Thermal-Hydraulics (NURETH10), Seoul, Korea, October 5-9, 2003.
- [23] D.R. Bradley, Modelling of heat transfer between core debris and concrete, *ANS Proceedings of the 1988 ASME Nat. Heat Transfer Conf.*, Houston, USA, June 1988.
- [24] B. Tourniaire, A heat transfer correlation based on a surface renewal model for molten core concrete interaction study, *Nuclear Engineering and Design* **236**, 2006.
- [25] F.G. Blottner, Hydrodynamics and heat transfer characteristics of liquid pools with bubbles agitation, NUREG Report CR-0944, 1979.
- [26] B. Spindler, B. Tourniaire, J.M. Seiler, K. Atkhen, MCCI analysis and applications with the TOLBIAC-ICB code based on phase segregation model, ICAPP'5, Seoul, Korea, May 15-19, 2005.
- [27] M. Cranga, R. Fabianelli, F. Jacq, M. Barrachin, F. Duval, The MEDICIS code, a versatile tool for MCCI modelling, ICAPP'5, Seoul, Korea, May 15-19, 2005.

- [28] M. Cranga, B. Michel, F. Duval, C. Mun, Relative impact of MCCI modeling uncertainties on reactor basemat ablation kinetics, *MCCI-OECD seminar*, Cadarache, St-Paul-lez-Durance, France, October 10-11, 2007.
- [29] M. Cranga, C. Mun, B. Michel, F. Duval, M. Barrachin, Interpretation of real material 2D MCCI experiments in homogeneous oxidic pool with the ASTEC/MEDICIS code, *Proc. ICAPP'08*, Anaheim, California, June 8-12, 2008.
- [30] D.R. Bradley, D.R. Gardner, J.E. Brockmann, R.O. Griffith, CORCON-MOD3: an integrated computer model for analysis of molten core concrete interactions, NUREG Report CR-5843, 1993.
- [31] B. Tourniaire, B. Spindler, V. Coulon, A.C. Augé, M. Cranga, Transfert de chaleur entre le bain de corium et le béton en cours d'interaction corium/béton – Analyse du groupe de travail CLARA, Rapport CEA/DEN/DTN/SE2T/LPTM/05-105 – 2005 – Reference not publicly available.
- [32] B. Cheynet, P.Y. Chevalier, E. Fischer, Thermo suite, *Calphad* **26** (2), 167-174, 2002.
- [33] M. Cranga, L. Ferry, J.F. Haquet, C. Journeau, B. Michel, C. Mun, P. Piluso, G. Ratel, K. Atkhen, MCCI in an oxide-metal pool: lessons learnt from VULCANO, Greene and BALISE experiments, *ERMSAR-10 Conference*, Bologna, Italy, May 11-12, 2010.

5.4. Retention and cooling of corium inside and outside the reactor vessel

5.4.1. In-vessel corium retention

5.4.1.1. Physical phenomena and associated safety issues

In-vessel corium retention assumes that reactor vessel integrity is preserved during an accident that causes reactor core melt.

Corium may be retained in the vessel either as a result of core reflooding leading to interruption of its melting, or flooding of the reactor pit with the aim of removing heat from the corium (debris or pool) while it is in the lower plenum of the vessel and thereby preventing vessel failure.

Research into in-vessel corium retention became one possible research option after the Three Mile Island 2 (TMI-2) accident in 1979 (see Section 7.1). During this accident, part of the core (approximately 20 tonnes of corium) was found at the bottom of the reactor vessel and the vessel did not fail, see [1]. The resistance of the reactor vessel to the thermal stresses caused by the residual heat released by this corium was attributed [2] to the fact that the molten corium flow at the bottom of the vessel was under-water (reactor flooded and pressurised (~ 100 bar)), but this has never been completely confirmed.

However, core reflooding may not be beneficial in all conditions. The following phenomena can occur during reflooding:

- massive steam generation, with hydrogen production and an increase in reactor coolant system pressure;
- steam explosion through corium-water interaction;
- continuation of core melt, despite water inflow;
- faster release of fission products.

Theoretically, reflooding could take place in all possible core configurations (fuel rods intact, rods slightly damaged but with ballooned cladding, rods melted leading to one or more flows of molten material, debris bed, corium pool, etc.). It is therefore necessary to determine the effects of reflooding on the subsequent development of the accident, based on the core configuration at the time when water is injected into the core.

After the TMI-2 accident, studies into the possibility of in-vessel corium retention following reactor pit flooding (cooling from outside the vessel) led to reactor designs 15 years later that incorporated this possibility (examples include the Westinghouse AP600 and AP1000 in the USA [3], the KAERI APR1400 in South Korea and the European ESBWR. However, it remains difficult to demonstrate the effectiveness of external cooling in retaining corium inside the vessel.

5.4.1.2. In-vessel corium retention through RCS flooding

5.4.1.2.1. Physical phenomena and state of current knowledge

► Conditions with fuel rods intact or only slightly damaged

If the core is reflooded when the fuel rods are intact or only slightly damaged (rod temperatures between approximately 1200 °C and 1800 °C), high levels of hydrogen can be generated, as demonstrated by the QUENCH test results by Forschungszentrum Karlsruhe (Fzk) in Germany (programme described in Section 5.1.1.3.1). The speed of the cladding oxidation reaction caused by the steam depends on the cladding temperature and the steam flowrate through the core, which is itself related to the progress of the quench front. Current software is able to satisfactorily estimate the progress of the quench front for a geometry with fuel rods intact. For these conditions, the model has been validated by various experimental results [25] (including the PERICLES tests by the CEA and the RBHT tests at the University of Pennsylvania in the United States). The thermal-hydraulic models are still sufficiently accurate when the fuel rod cladding begins to undergo deformation or the first molten material flows appear, because these deformations are not significant enough to lead to major disruption of the flow patterns. The main uncertainties are due to imprecision regarding rod geometry at the time of reflooding (in particular, the heat exchange surface) and the related laws of heat exchange. For these conditions in which core geometry has not been significantly altered, if the flowrate is high enough, core damage is likely to be halted, provided that reflooding does not cause the mechanical destruction and collapse of a large proportion of the fuel rods due to thermal shock. Any debris bed obtained in this way could no longer be properly cooled. The conditions under which the fuel rods might collapse and the size of the resulting debris are unknown, but interesting data has been deduced from test results from an OECD programme performed in the HALDEN reactor at the Norway Institute for Energy Technology (accumulation of irradiated fuel pellet debris in a rod that swelled during a LOCA). The ISTC-1648 test programme, funded by the International Science and Technology Centre (ISTC) and performed by NIIAR in Russia (Research Institute of Atomic Reactors), which aimed to study the reflooding of a length of irradiated fuel rod (see Section 5.1.1.3.1) also provided some data. The evidence gathered can be summarised briefly as follows, based on three fuel rod temperature ranges:

- below 1200 °C, it is unlikely that the fuel rods will fragment and only small amounts of hydrogen will be released due to cladding oxidation; the core can therefore be cooled if the water flowrate is high enough;
- between 1200 °C and 1600 °C, the fuel rods may become fragmented and collapse, forming a debris bed if the cladding is embrittled by significant oxidation; if the rods do not collapse, hydrogen production remains low and the core can without doubt still be cooled if the steam flowrate is high enough;
- above 1600 °C, oxidation of the zirconium alloy cladding leads to a runaway oxidation reaction, resulting in high hydrogen production and major rod damage, possibly with flows of liquefied materials. The core can no longer be cooled, at least locally in the places with molten material flows had occurred.

► Conditions with debris bed formation

If the fuel rods collapse inside the core, the fuel fragments form a porous medium known as a debris bed. If a debris bed forms, the pressure loss increases significantly and makes it a lot more difficult to access the collapsed areas. If the flooding water cannot reach some parts of the debris bed, these parts can only be cooled if the steam flow produced downstream at the quench front is sufficient, otherwise they heat up to melting temperature, creating a molten pool of core material. A debris bed can also form at the bottom of the reactor vessel when the corium flows through the water. The maximum heat that can be removed from a debris bed by water, before it dries out and melting occurs, is called the "critical heat flux". It is expressed per m^2 of the upper surface of the debris bed. The phenomena that occur when a debris bed is reflooded are satisfactorily understood, because a number of experiments have been performed and various models developed since the 1980s. However, the only data developed are point models or 1D models, validated with 1D experimental results. There is still uncertainty about the extrapolation of reflooding calculation results to multi-dimensional and heterogeneous geometries. In particular, some experimental calculations and observations, which unfortunately are incomplete, suggest that the heat removed from a debris bed for a multi-dimensional configuration may be higher than the heat removed from a debris bed in a one-dimensional configuration (possibly as much as twice as high), and that even after the debris bed has dried out, the steam flowing through the bed may keep some of the debris below melting point. However, much uncertainty remains, because in the TMI-2 accident (discussed in detail in Section 7.1), the heterogeneity of the debris formed (including the presence of liquid "pockets") and the presence of small debris ($< 1 \text{ mm}$) may be the reason why corium melt could not be prevented after reflooding. Reflooding of a heavily damaged core or a debris bed remains poorly modelled by calculation software.

The main multi-dimensional thermal-hydraulic models that exist for a porous medium are included in the ICARE/CATHARE ([IRSN](#)), WABE (IKE/GRS) and MC3D (CEA/IRSN) software packages. The multi-dimensional effects on heat removal through reflooding in particular remain to be confirmed with experimental data from sufficiently large experimental set-ups that can provide reliable local temperature measurements and steam generation during reflooding. This is the aim of the PEARL programme of experiments, initiated by IRSN in 2010, in partnership with EDF, with the participation of the European network [SARNET-2](#).

► Conditions with a liquid corium pool

What happened at the TMI-2 accident? When the corium flowed to the bottom of the reactor vessel, the vessel was full of water. Around ten tonnes of corium in oxide form (approx. 1 m^3) had flowed in compact form to the bottom of the reactor vessel and around ten further tonnes of debris were above the corium in compact form. Analysis of reactor vessel samples showed that the temperature of the internal surface in contact with the compact corium mass at the bottom of the vessel reached approximately $1100 \text{ }^\circ\text{C}$ and the external surface reached approximately $800 \text{ }^\circ\text{C}$. The internal pressure in the reactor vessel was around 100 bar at the time. The vessel then cooled

very slowly. Assuming perfect contact between the compact corium and the reactor vessel, all thermal calculations have shown that the reactor vessel temperature should have continued to rise, eventually causing vessel failure. The explanation put forward as to how the reactor vessel withstood these conditions assumes that a gap formed between the corium and the vessel. According to this assumption, the gap would have formed due to two phenomena:

- traces of water in porosities within the steel boiling and preventing contact between the corium and the steel;
- a process of differential expansion between the solidifying corium and the reactor vessel, which was heating up.

It is thought that the ingress and flow of water in this gap cooled the reactor vessel sufficiently and sustainably enough to prevent failure.

Some experiments have been performed to try to confirm this hypothesis of a gap between the corium and the reactor vessel in the TMI-2 accident. Small-scale tests have been performed on corium flows at the bottom of reactor vessels containing water, to reproduce the TMI-2 corium flow conditions and analyze the results. Such tests have been performed by FAI (FAUSKE & Associates, Illinois, USA) [11], JAERI (Japan) and KAERI (South Korea) [12]. All these tests were carried out with an alumina thermite mixture to simulate the corium. Other tests to determine the maximum power (or critical heat flux) that could be removed by water flowing in a gap between the corium and the reactor vessel have been carried out by IBRAE (Russia) [13], Siemens (Germany) [14] and KAERI [15].

These tests have not been highly conclusive and the main finding is that the gap is likely to have been formed solely by the traces of water boiling. The hypothesis of differential expansion appears less plausible. However, as suggested by a CEA study [4], the possibility of heat removal through water boiling in a gap is also very slim. It remains difficult to explain with certainty why the reactor vessel withstood failure in the TMI-2 accident conditions.

In more general terms, for a power reactor core meltdown accident, this CEA study shows that the heat (or critical heat flux) that can be removed by boiling water in a gap is very approximately proportional to the square root of the pressure. For instance, for a 3 mm gap and pressure of 1 bar, the critical flux is of the order of 0.02 MW/m², which should be compared with the 0.5 MW/m² that needs to be removed if half the mass of the core were at the bottom of the reactor vessel in the form of a corium pool. The conclusion is that too little is known about the real conditions at the bottom of the reactor vessel (Is water present permanently or not? What is the critical flux value? Is there a gap in the event of meltdown? etc.) for the cooling mechanism through gap formation to be considered plausible for most foreseeable core meltdown accident conditions on a PWR at low pressure.

Without more pertinent experimental results, with the reactor coolant system depressurised and with no reactor pit reflooding, it would appear difficult to demonstrate

that reflooding the reactor coolant system would prevent reactor vessel failure once a large pool of molten material has formed within the core.

5.4.1.2.2. Experimental programmes

The main programmes of experiments studying core reflooding for pressurised water reactors are LOFT-FP, PBF-SFD, CORA, QUENCH, ISTC 1648 (QUENCH) and PARAM-ETER. These programmes are briefly described in Section 5.1.1.3.1.

5.4.1.2.3. Review and future outlook

Two reviews [22, 23], dating from 2005 and 2006, summarise current knowledge of the various risks associated with PWR core reflooding. These documents identify the main uncertainties and the R&D programmes that will be required.

The themohydraulics and fuel behaviour during a core meltdown accident require finer modelling in order to better understand accident development in the core of a power reactor. This implies more precise and detailed modelling of transient conditions, in particular the two “key” transitions from a damaged core to a molten pool and then from a molten pool in the core to a molten pool at the bottom of the reactor vessel. The models used in the software for fuel rod deterioration in the core are based on a multi-dimensional description of the material transfers in order to better calculate the transient changes to materials in the reactor vessel, but there are no experimental results from relatively large-scale tests to deal with the scale effects and validate these multi-dimensional models.

The three priorities for further study are as follows:

1. the geometric evolution of a heavily damaged core or a debris bed during reflooding (can a damaged core be cooled or not?); tests will be required to more clearly understand the progress of the quench front in a damaged core, according to its geometry, particularly for conditions involving a debris bed and the specific geometric features of debris from irradiated fuel rods. The size distribution of the debris will be a significant result that could be obtained through additional out-of-pile tests with real rods. This is the aim of the reflooding tests with lengths of fuel rods under the ISTC 1648 (QUENCH) programme;
2. the evolution of a dry debris bed and its transformation into a molten pool (if it cannot be cooled); it would be good to study dissolving and oxidation, two phenomena that have an impact on stratification in the pool;
3. the arrival of corium at the bottom of the reactor vessel, in particular when it is full of water; it would be good to study corium fragmentation, oxidation and cooling when it gets into the water and when it spreads at the bottom of the vessel. These issues were partially examined in the programmes that looked at steam explosion (see Section 5.2.3).

5.4.1.3. In-vessel retention with reactor pit flooding

5.4.1.3.1. General approach: orders of magnitude

Two main parameters affect the integrity or otherwise of the reactor vessel under core melt accident conditions with molten corium flowing to the bottom of the vessel:

- the mechanical strength of the reactor vessel at all points, particularly in areas subjected to the highest thermal load;
- the mechanical strength of the reactor vessel to withstand a steam explosion caused by an in-vessel corium water interaction.

Order of magnitude calculations have shown that, following core degradation, the materials in the core of a PWR 900 would take up a volume of a similar order of magnitude to the hemispherical vessel bottom, if they formed a very compact mass at the bottom of the reactor vessel with no voids (e.g. a corium pool). Assuming that the residual power of these materials is 20 MW and that they emit a uniform heat flux, the heat flux calculated at the edge of the pool is of the order of 0.8 MW/m^2 . This heat flux is extremely high and can only be removed if there is efficient convection at the free surface of the corium pool and the interfaces between the corium pool and the reactor vessel. Even in this case, part of the vessel wall would melt and its residual solid thickness would only be a few centimetres. With a simple calculation, it can also be shown that if this heat flux is not efficiently removed (e.g. if there is no steam flow above the corium pool), the reactor vessel will be perforated after only a few minutes. Ensuring vessel integrity therefore requires a way of removing the heat flux from the corium pool at all points in the reactor vessel. This condition is essential, but it is not the only criterion. The weakened vessel also needs to continue to withstand the pressure. Given that the residual thickness of the steel is reduced, the reactor vessel cannot resist high pressure in the reactor coolant system, requiring the RCS to be depressurised. The mechanical strength of the reactor vessel is therefore assessed at final pressure, after depressurisation, taking into account the thermomechanical loads caused by the corium pool. It also needs to be evaluated for a pressure peak in the reactor coolant system. A pressure peak could, for example, result from a steam explosion following inflow of water from the RCS onto the corium pool at the bottom of the reactor vessel [10].

5.4.1.3.2. Mechanical strength of the vessel depending on corium pool configuration

To assess the mechanical strength of the reactor vessel when in contact with a corium pool in core melt accident conditions, vessel behaviour is studied under the worst-case limit conditions, which are no core reflooding, flow of all corium mass to the vessel bottom and stationary thermal-hydraulic conditions in the molten pool. These are the conditions in which the highest heat flux is received by the reactor vessel.

The heat flux distribution on the vessel wall depends on the configuration of the corium at the vessel bottom (whether or not it is stratified). The core materials can be distributed

according to their respective densities in order to define the various possible corium configurations for a given core inventory (masses of oxides, zirconium and steel in the core). There are however other parameters that affect the corium pool configuration:

- the degree of zirconium oxidation (which can range between 25% and 80% depending on the accident scenarios considered, see Section 5.1.2.1);
- the mass of molten steel (between a few tonnes and several tens of tonnes);
- the possibility of solid layers (debris and solid crusts), in particular at the corium pool interfaces.

One of the most critical configurations for the reactor vessel is when low-density molten metals (mainly containing steel) float on top of a pool of high-density corium “oxides” (approximately 8000 kg/m^3) (Figure 5.46). These are the bounding conditions in terms of thermal loading on the reactor vessel that have been most extensively studied and for which the limit conditions and heat transfer to the pool have been determined. This configuration was also used to support the first external vessel cooling studies, in particular the AP600 concept. This configuration will be referred to as the “reference configuration” hereinafter.

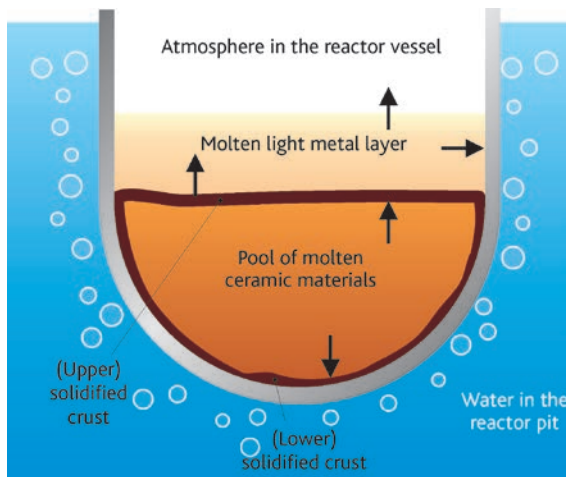


Figure 5.46. Configuration of the corium pool at the bottom of the reactor vessel with external cooling.

5.4.1.3.3. Study of the corium pool stratified configuration

► Heat flux distribution and cooling for the stratified configuration

For any given corium configuration, the heat flux distribution depends on the limit conditions between the melting mass and the solid wall (either the crust or the steel of the vessel) and the coefficients of heat transfer by natural convection. The temperatures at the edge of a corium pool have been determined in various studies, which are summarised in [5]. The main difficulty in determining the temperatures is related to the fact that the melting materials are a mixture of oxides and metals. These mixtures melt over a relatively

wide range of temperatures that depends on the composition of the mixture. Such a mixture may also contain a soft zone, between the molten pool and the solid crust by the vessel wall, which could affect heat transfer. Reference [5] has shown that in steady-state thermal-hydraulic conditions (i.e. when the heat fluxes have been established), no such soft zone can exist, because the pool composition becomes homogeneous and will solidify in the same way as a pure body (with a flat interface between the solid and liquid). In addition, when there is sufficient external cooling, the solid crust has a constant thickness (i.e. the speed of progress of the solidification front is zero). In this case, the temperature at the liquid-solid interface tends towards the liquidus temperature corresponding to the liquid mixture. There is a clear separation between the solid and liquid. Experimental confirmation of this conclusion has been provided by various tests (PHYTHER by the CEA (described in [5], RASPLAV (Kurchatov Institute, Russia) [16], and SIMECO (Royal Institute of Technology, Sweden). The solidification transient was studied by IRSN in 2005 [17].

The assumption of thermochemical equilibrium in determining the interface temperatures also applies to the metallic layer of a stratified corium pool. If the liquidus temperature corresponding to the composition of the metallic layer (chiefly formed of steel and zirconium) is lower than the melting point of steel, the steel may be dissolved by the molten metal. The interface temperature with the solid steel of the reactor vessel establishes itself at this liquidus temperature. To put things simply, depending on the composition of the liquid metal layer, the temperature of the inner surface of the reactor vessel wall may be substantially lower than the melting point of steel. Temperatures at the liquid-solid interface are calculated with thermodynamic software (such as GEMINI) on the basis of the composition of the liquid layer in question. The corollary of this choice is that the pool is completely liquid and the heat transfer laws identified from tests with simulation materials (pure bodies like water) can be transposed to the real materials.

Heat transfer correlations have been deduced from tests with simulation materials (BALI, COPO, ACOPO, RASPLAV-Salt, etc.) for various geometrical configurations [9]. Efforts have also been made to validate CFD software for natural convection. The results are encouraging, but further improvements to the turbulence model are still required in order to improve the precision of the results. The use of such software on the scale of a power reactor vessel gives results with a wide uncertainty interval. Given the current state of knowledge, it is preferable to use a simpler approach based on correlations from the tests.

► Order of magnitude of the heat fluxes and focusing effect

To give an order of magnitude, for the reference configuration shown in Figure 5.46, the residual heat is distributed as follows, assuming that the entire mass of oxides from the core is at the bottom of the reactor vessel:

- half the residual heat released from the pool of oxides is transferred to the bottom of the vessel;
- the other half is transferred from the pool of oxides to the upper layer of liquid metals.

If there is no water inside the reactor vessel, the metal layer transfers most of the heat received from the pool of oxides and the internal heat it releases to the steel vessel wall, which is in contact with the liquid metal layer. The metal layer can generate a heat flux “focusing effect” on the wall surface that is in contact with the liquid metal. At the point of contact with the metal layer, the heat flux is very approximately inversely proportional to the thickness of the metal layer. For a thickness of more than 50 cm (corresponding to approximately 50 tonnes of steel), the heat flux is below 1.5 MW/m^2 . Reactor vessel integrity is only assured if the heat flux transferred to it can be removed by two-phase natural convection from the cooling water outside the vessel. This naturally raises the question of the critical flux on the external vessel wall (upper limit higher than the heat flux that can be removed by external reactor vessel flooding).

► Critical flux for natural external water circulation

The critical heat flux associated with external cooling of the reactor vessel, in particular in the area around the metallic layer, will therefore be the limiting factor for heat removal from the vessel. Significant efforts have been made around the world to determine this critical flux and to increase it. Various tests have been performed (with 2D or 3D geometries and different wall heating modes). The most interesting of these include tests by ULPU (University of California, Santa Barbara) [19], the SULTAN tests (CEA) [18] and tests by KAIST (Korea Advanced Institute of Science and Technology, South Korea).

The first phenomenon that determines the critical flux value if the reactor pit is reflooded is the water circulation by natural convection within the reactor pit. Simply reflooding the reactor pit is not enough to cool the reactor vessel. The water circulation needs to be organised such as to “maximise” liquid flowrate along the vessel walls. This implies the existence of a “rising hot leg” (the reactor vessel) and a cold leg. The geometry of the vessel (radius and spherical or elliptical shape of the vessel bottom) and the presence of insulating materials around the vessel may affect water circulation and pressure loss. For a geometry that maximises water circulation and in the absence of elements to hinder flow, maximum critical heat flux is obtained when the water flow-rate is high enough to limit boiling close to the wall in the heating zone (no mass boiling in this area). However, above the heating zone, boiling should be higher to create a strong enough “chimney effect”, whereby the steam generated drives an increased liquid flow. If water flowrate is not high enough, there is mass boiling around the heating zone and the critical flux is reduced because the heat is removed less effectively. Having said that, the water flowrate cannot exceed the flow created by the chimney effect related to mass boiling above the heating zone. This maximum flowrate corresponds to a maximum critical heat flux of the order of 1.5 MW/m^2 .

Analysis of the test results mentioned above show that the spread of estimated critical flux values is often fairly high. Results from the ULPU tests give values close to 2 MW/m^2 (but with a wide spread of experimental results), whereas results from the SULTAN and KAIST tests show critical flux values on a vertical wall that range from 1.2 to 1.5 MW/m^2 .

Various effects have been studied in an attempt to identify provisions that could increase the critical heat flux, in particular effects linked to the condition of the reactor vessel's outer surface. According to some authors, [6], a spray-on porous metal coating on the outer surface of the reactor vessel could significantly increase the critical flux (by a factor of up to 2). However, this conclusion is not universally shared and experimental verification is still required.

► Limitation linked to vessel mechanical strength

For a heat flux of 1.5 MW/m^2 , the vessel thickness supporting the mechanical load (i.e. the place where the temperature is below $600 \text{ }^\circ\text{C}$) is 1 centimetre. This thickness can withstand pressures up to a few tens of bar. An increase in critical flux would lead to an inversely proportional decrease in the thickness supporting the mechanical load, and a consequent reduction in the yield pressure of the reactor vessel. These considerations strongly temper the potential benefits of any work to demonstrate critical flux values of above 2 or 3 MW/m^2 .

► Limitation linked to the minimum mass of molten steel

One of the key parameters that determines the thickness of the metallic layer above the oxide pool, and hence the highest thermal loads on the reactor vessel, is the mass of molten steel in the corium produced by core melt. For a critical heat flux of 1.3 to 1.5 MW/m^2 , the minimum thickness of molten steel required to prevent the thermal focusing effect is of the order of 50 to 60 cm for a 1000 MWe PWR. Given the characteristics of these reactors, this thickness corresponds to a mass of molten steel of the order of 50 to 60 tonnes. According to studies by Westinghouse for the AP600 and AP1000, this quantity of steel would be found at the bottom of the reactor vessel after the lower in-vessel structures and part of the vessel walls have melted. Findings from the OECD MASCA programme [20] suggest that complex physical phenomena could reduce the mass of metal and lead to a focusing effect. These phenomena are as follows:

- part of the liquid metals (e.g. the lower in-vessel structures) getting trapped in solid oxide debris;
- part of the molten metal flowing to the bottom of the reactor vessel due to physico-chemical effects related to the presence of non-oxidised zirconium (details below);
- for a fixed quantity of metal, this would lead to reduced thickness of the metallic layer on the top of the corium pool (see Figure 5.47).

The physico-chemical effects are linked to the presence of non-oxidised zirconium in a metallic phase. This zirconium can react with the uranium dioxide in the oxide phase and lead to the formation of a uranium metal phase. This phase can mix with the liquid steel and lead to the formation of a liquid metal layer that is denser than the pool of oxides that would now be at the bottom of the vessel. By using thermodynamic software (such as GEMINI2 from Thermodata), the composition of complex

metal-oxide mixtures can be calculated in equilibrium at various temperatures. If the density of the phases resulting from these calculations is determined, the maximum mass of metal that might end up below a pool of oxides can be estimated and, by subtraction, for any given quantity of steel, the mass of metal present in the upper layer. This method was used by CEA and IRSN to calculate the mass of metal necessary to prevent the heat flux transferred from the metal layer to the reactor vessel exceeding the critical flux [7]. Calculations were performed for different reactor types: the French 900 MWe and 1300 MWe PWRs, the AP600 and AP1000 reactors developed by Westinghouse, and the Korean APR1400 reactor. The results showed that one key parameter is the fraction of non-oxidised zirconium present in the molten pool. The higher this fraction, the greater the mass of metallic uranium produced and the greater the mass of metal at the bottom of the reactor vessel. The question of keeping the corium inside the vessel is thus more complex if the mass of metallic zirconium is higher. The results are also sensitive to the databases used for thermodynamic calculations and the critical flux values outside the vessel. In particular, for reactors of greater than 600 MWe, a natural circulation system needs to be set up in order to remove a high heat flux.

It should be noted that the above studies were performed for a stationary corium pool configuration. The formation of metallic layers and the pool of oxides will necessarily involve transients of growth in the metal layer thickness and increase in the heat released by the pool of oxides. These transients were not incorporated in the calculations, but they could cause the critical heat flux to be reached.

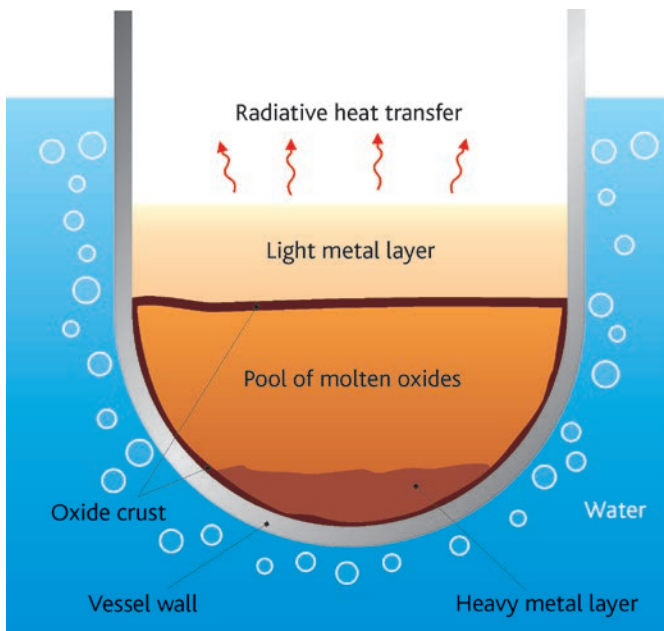


Figure 5.47. Corium recovery from the bottom of the vessel with inversed stratification of metals and oxides.

5.4.1.3.4. Possible progress for in-vessel corium retention with reactor pit flooding

The studies described in the foregoing paragraph do not yet demonstrate that reactor pit flooding would ensure, for any given reactor type, that the corium would be retained inside the reactor vessel for all foreseeable core melt accidents. Further studies are required on the following issues, in particular:

- more realistic corium configurations, in which the metallic layer can be in various positions (above or below the pool of oxides) over time;
- the possibility of simultaneous external (reactor pit) flooding and internal core reflooding;
- conditions that could lead to several successive corium flows within the reactor pit, for which the heat fluxes on the reactor vessel may differ significantly from the very schematic situation usually considered (see Figure 5.46).

An inflow of water onto the corium pool inside the vessel could eliminate the heat flux focusing effect. The ANAIS tests by CEA [8] have shown that, in this case, the metal layer on the surface could solidify, transferring a significant proportion of the residual heat to the water. These same ANAIS tests also showed that, under these conditions, the steam explosion risk would be limited to the area in which the water spray hit the liquid corium. A large explosion following accumulation of water seems unlikely because the surface of the corium pool would quickly be solidified by a significant inflow of water.

In order to better assess the possibility of in-vessel corium retention for reactor pit flooding, it will be necessary to improve the model of corium flow to the bottom of the reactor vessel and development of the corium pool at the vessel bottom.

For 900 MWe and 1300 MWe reactors, there are not currently provisions to ensure in-vessel corium retention for all foreseeable core melt accidents. Reactor vessel failure (Section 5.1.3) and the possibility of cooling the corium outside the vessel (Section 5.4.2) at the time of molten core-concrete interaction (MCCI) have therefore been studied in detail.

For the EPR reactor design, specific provisions have been adopted (the corium spreading and cooling compartment, presented in Section 5.4.3) in order to cool the corium outside the vessel.

5.4.2. *Cooling of corium under water during MCCI*

5.4.2.1. Physical phenomena involved

One possibility for accelerating cooling of a corium pool during MCCI (see Section 5.3), and stopping its development, would be to direct water into the reactor pit onto the corium surface.

Radiative heat transfer between the corium pool and the reactor-pit walls leads to the formation of a crust on the surface of the corium, due to the high solidification temperature of corium (around 2400 K for a corium containing little concrete). This crust would apparently be thicker if the corium were covered by water, but would also act as an insulator between the corium pool and the water, thereby restricting heat transfer between corium and coolant. Order of magnitude calculations show that if heat transfer between pool and water were only by conduction *via* the crust, then the slowing of concrete erosion due to directing water onto the corium would be minimal. For the cooling of corium under water to be truly effective, other heat transfer mechanisms would need to be involved. The purpose of R&D work (experiments and models) performed on the subject is to identify and quantify the effectiveness of these other modes of heat transfer.

5.4.2.2. Experimental programmes

The main experimental programmes that have been performed on this subject are: the Melt Attack and Coolability Experiments (MACE, see [26]) programme performed at the Argonne National Laboratory (ANL, USA) from 1989 to 2010 using real materials, MSET (see [27]) and OECD-MCCI (see [28] and [29]) – with the last programme divided into three sub-programmes, namely SSWICS, MET and CCI –, plus CEA's PERCOLA programme using simulation materials, see [30]. The ANL programmes involve both integral experiments and more analytical tests.

5.4.2.2.1. MACE and CCI tests

These integral tests aimed to study the possibility of cooling the corium during an MCCI by directing water onto the pool surface, using materials representative of corium formed during a core melt accident on a power reactor. Three tests were performed with 1D devices (concrete erosion only in the downwards direction: M1B, M3B and M4) and five tests with 2D devices (concrete erosion downwards and on the sides: M0 in the MACE programme, and CCI-1, CCI-2, CCI-3, and CCI-4 in the OECD-MCCI programme). Test performance was essentially the same for all tests; it initially involved forming a corium pool, with a composition representative of that of a core melt accident on a power reactor at the beginning of MCCI, by using a thermite reaction (a highly exothermic reaction, which for these tests involved a mixture of U_3O_8 , CrO_3 , CaO , SiO_2 , silicon, zirconium and aluminium) that produces a molten mixture mainly made up of UO_2 and ZrO_2 along with a smaller proportion of oxides representative of concrete erosion (mainly SiO_2 , CaO , etc.), alumina and chromium oxide. The corium pool was then maintained in a molten state by direct heating. Concrete erosion was initially obtained *via* a dry MCCI. Water was then directed onto the corium after a time delay or a maximum specified ablation, and MCCI continued under water. The effectiveness of directing water onto the corium can be understood by comparing concrete erosion rates with and without water, and by measuring the heat flux at the surface of the corium pool (associated with the quantity of steam produced). Pool temperature is also an indicator of the effect of water supply. However, it is important not to directly extrapolate test results to the case of a power reactor, to the extent

that tests involve non-representative aspects: in particular, the corium is heated *via* the Joule effect in the liquid corium, whereas for a power reactor, the residual heat would be spread between the liquid (pool) and the solid (crust).

The tests mentioned above brought to light several possibilities for corium cooling by water:

- during numerous tests (M0, M3B and CCI2), part of the corium pool was entrained by the gases produced by concrete decomposition and ejected above the pool's upper crust, forming a bed of centimetre-sized debris. Furthermore, analytical tests have shown that it is possible to cool debris of this size dispersed in water but it has not been shown that cooling of a thick bed of debris emitting significant residual heat would be as effective as cooling of dispersed debris;
- the pool's upper crust could crack and water could penetrate under this crust, due to the effect of temperature differences between the water and the corium and thermomechanical stresses. This water could propagate in the pool and cool it completely (a mechanism called "water ingressión"). However, models that describe this mechanism suggest that the cracks created by temperature differences would be too small for water ingressión alone to effectively cool a corium pool, see [31]. Nevertheless, the presence of cracks plays an important role in the thermomechanical behaviour of the crust (cracks reduce the mechanical resistance of the crusts) and could contribute to corium cooling;
- effective cooling of the corium surface has been measured during direct contact between water and liquid corium. This highly transient phenomenon can occur during sudden mechanical failures of the crust or when water first arrives on the corium pool. However, during the tests performed, it may have been promoted by the geometry of the experimental set-up; it is not possible to directly extrapolate this result to a power reactor.

Under these conditions, it is not possible to conclude on the effectiveness of cooling of a corium pool during an MCCI by directing water onto the surface of the pool for a power reactor, although it would seem that the various phenomena mentioned above would tend to slow concrete erosion. The performance of more representative tests runs up against technological difficulties that limit the scope of the experiments and study of the phenomena:

- given the limited scale of existing test equipment, in most cases a crust forms on the upper part of the pool and bonds to the walls of the test section. As concrete erosion progresses, the liquid corium descends and separates from the crust; this separation limits the effectiveness of corium ejection. In the case of a power reactor, it is more likely that the crust would remain in contact with the liquid corium due to the size of the reactor pit;
- direct corium heating means that it is not possible to heat the solid crusts. The solidification observed during the tests is therefore not representative of that which might occur on a power reactor.

5.4.2.2.2. MSET test

The purpose of the MSET test, performed in 2001, was to study corium ejection through the crust, a phenomenon brought to light during the MACE tests. The MSET test was performed with materials representative of corium formed during a core melt accident on a power reactor, without concrete erosion and with water directed onto the upper part of the pool. Gas release was simulated by using a porous material at the base of the corium pool, through which gas was injected at a controlled rate.

The MSET test led to the formation of bed of debris but no corium ejection was observed for superficial gas velocities below 10 cm/s, which posed the question of the effectiveness of such a phenomenon for a power reactor, where the superficial gas velocity would be less than 5 cm/s during the long-term MCCI. However, analysis of the MSET results brought to light as possible causes of this behaviour:

- bonding of the crust onto the walls of the test section, leading to separation of pool and crust;
- the presence of a significant solid fraction, due to pool temperature (well below the liquidus temperature).

The results of this test do not therefore provide insight into the importance of corium ejection for the cooling of corium during an MCCI on a power reactor.

5.4.2.2.3. SSWICS tests

The purpose of the SSWICS tests (see [31]), performed with materials representative of corium formed during a core melt accident on a power reactor, was to study the mechanism of water ingress after thermomechanical cracking of the corium pool's upper crust. Water penetrates *via* this mechanism into the cracks which form in the upper crust when cold water comes into contact with the hot crust; the cooling of corium under the crust leads to its solidification, which increases crust thickness.

Under the SSWICS programme, separate-effect tests were performed without heating the corium pool, and with simulated release of concrete gases for some tests. The corium pool, which was produced in a test section using a thermite reaction similar to the one described in Section 5.4.2.2.1, sat on an inert support. Water was gradually directed onto the corium pool and the cooling kinetics were deduced from the water vaporisation rate. The effectiveness of water ingress was assessed by comparing the heat flux extracted during the tests with that obtained under conditions where only conduction was involved (thermite cooling without water). The permeability of the crust was measured after the tests, which meant that the removed heat fluxes could be assessed using specific models.

The tests performed (see Figures 5.48 and 5.49) enabled quantification of the influence of concrete type (siliceous or silico-calcareous), corium pool composition (between 4% and 25% concrete by mass), gas injection, and pressure (between 1 and 4 bar). The lumps of corium obtained at the end of the tests were cut into pieces and subjected to mechanical resistance tests.

The main lessons drawn from the SSWICS tests were the following:

- these tests confirmed that cracking of the upper crust and water ingestion into these cracks cools the corium in certain cases (increasing crust thickness). With no gas injection, corium cooling is only effective for low concrete concentrations in the corium (less than 15% by mass); for a power reactor, these conditions would correspond to water arriving soon after the corium had flowed into the reactor pit during a core melt accident. The tests also demonstrated the effects of gas injection into the corium; indeed, the programme's last tests performed with counter-current gas flow in the corium showed more effective corium cooling for lower concrete concentrations. This was the case in the SSWICS-11 test performed with 15% concrete, which led to high heat-flux removal, similar to that obtained without gas injection for a low (4%) concrete concentration (Figure 5.48). Gas

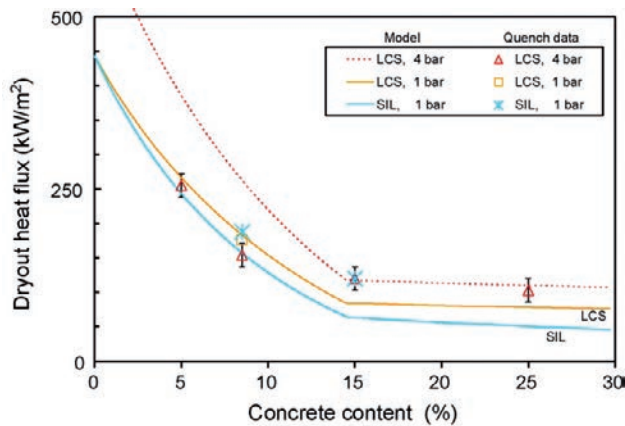


Figure 5.48. Measurement of heat fluxes removed by water ingestion during SSWICS tests, as a function of concrete concentration in the corium (without gas injection into the corium), see [31].



Figure 5.49. Appearance of the resolidified lump of corium at the end of the SSWICS-11 test, performed with gas injection into the corium, see [32]; reproduced by permission of OECD.

flow could lead to the opening of pores in the corium during solidification, which would facilitate its cooling. However, it should be noted that, due to the lack of heating, SSWICS tests did not reproduce effects associated with residual heat in the pool and crust, effects which could be significant for a power reactor;

- measurements of mechanical stresses leading to crust failure (see [33]), in particular, the *in situ* measurements obtained during certain CCI tests show that crust failure occurs for low levels of stress. For a power reactor, it is very unlikely that the crust would remain a single block and bond to the reactor-pit walls.

During MCCI tests performed under more representative conditions with sustained corium heating (in particular during the CCI tests, see [29]), water ingress and corium ejection phenomena occurred simultaneously and were difficult to distinguish, as the corium ejections were close together.

5.4.2.2.4. PERCOLA programme

The PERCOLA experimental programme was performed by CEA between 1999 and 2002. Drawing lessons from the MACE tests and the results of calculations (see [34]) showing that it would be possible to cool a corium pool which would transform into a bed of debris, the purpose of this programme was to study corium ejection above a cracked crust caused by gases coming from concrete erosion. This analytical programme, performed with simulant materials (water, oil) brought to light several ejection regimes and meant that the influence of numerous parameters (see [30]) could be quantified, such as:

- fluid viscosity (a parameter representative of the increasing quantity of concrete in the corium as MCCI progresses);
- superficial gas velocity (a parameter representative of the type of concrete and the decreasing gas flowrate during MCCI);
- hole density in the crust (a parameter little understood for a power reactor);
- hole diameter (a parameter little understood for a power reactor);
- thicknesses of crust and bed of debris (parameters representative of the thickening of the crust and the bed of debris during MCCI after ejection).

The results of the PERCOLA programme have enabled development of an analytical model covering corium ejection during MCCI (this model is described in the next section).

5.4.2.3. Modelling

The main modelling work has covered corium ejection via holes in the upper crust and water ingress into corium.

An analytical model taking into account corium ejection⁹ was developed in the context of the PERCOLA programme in 2004, see [35]. It takes into account the effect of

9. This model provides an estimate of the corium entrainment rate, i.e. the ratio of the volumetric flowrate of the liquid ejected and the volumetric flowrate of gases released during MCCI.

the major physical parameters for MCCI (superficial gas velocity, pool viscosity etc.) and the geometry of the ejection holes which were not covered in the Ricou and Spalding model (see [36]), which was used prior to the PERCOLA programme and describes liquid entrainment by a turbulent gas jet in a specific geometry. Application of the PERCOLA model to power-reactor scenarios tends to show that a bed of debris could quickly form if corium ejection is effective, see [37]. The stability of this bed of debris would then depend on the size of the debris particles formed. The PERCOLA model has been validated using the results of PERCOLA tests, but requires validation on the basis of more representative tests (with concrete erosion and prototypic compositions). To this end, large scale tests have been performed since 2012 at the Argonne National Laboratory (ANL in the USA); these are described in Section 5.4.2.4. Some of the model's input parameters are subject to very large uncertainties, such as the density and size of holes in the crust through which corium can pass. They are the subject of a specific model proposed by Farmer, see [38]. However, there is no experimental data that is sufficiently representative to validate these models for a power reactor.

In order to ensure the validity of the PERCOLA model in the long-term cooling phase for a power reactor, the model should also be supplemented to cover development of the bed of debris, in particular the effect of its thickening on corium ejection¹⁰.

With regard to water ingress, it should be noted that a critical heat flux correlation, deduced from a model of crust cracking during water ingress, has been developed as part of the SSWICS programme, see [31]. This correlation has been adjusted using the results of tests performed without gas injection during corium solidification. On the basis of this correlation, it would appear that water ingress is much less effective for corium cooling than corium ejection.

As the possibility of cooling corium under water is strongly associated with MCCI, the modelling of cooling under water is covered by the same software as used for modelling MCCI. For example, the TOLBIAC-ICB code (see [39]) contains the corium ejection model developed after the PERCOLA test programme. Similarly, most models developed in the context of studies on the possibility of cooling corium by directing water onto it have been implemented in the CORQUENCH code (see [40]) developed by ANL to simulate 1D concrete erosion and the coupling between MCCI and heat transfer phenomena in the presence of water at the surface of the corium pool. Simplified models concerning water ingress into the upper crust and corium ejection, drawn from the first version of the CORQUENCH code, have been integrated into the MEDICIS code developed by IRSN, see [41]. More detailed models have subsequently been developed for the MEDICIS code, based on the PERCOLA model for hydrodynamics, see [35], and the literature available for assessing the geometry (density and diameter) of holes through which corium can be ejected, see [38] and [47]. Applications to a power reactor show that corium ejection is the dominant mechanism for corium cooling, and can significantly slow concrete erosion, especially in the case of a siliceous concrete, without stopping it completely, see [38] and [43].

10. The PERCOLA model assumes that gases and corium escape along vertical channels (or "chimneys") which develop in the bed of debris regardless of its thickness.

5.4.2.4. Summary and outlook

As shown by the overview above, in 2015, it is not possible to draw conclusions on the possibility of stabilising and cooling a corium pool during an MCCI by directing water onto the surface on the basis of the results of the tests performed (1D and 2D integral tests, corium ejection tests, and water ingress tests).

Progress in this area is hindered by the technological difficulties surrounding the performance of sufficiently large-scale tests with real materials (scale effects on the corium pool, crust bonding onto test set-up walls, representativeness of the corium heating mechanism etc.).

Given the results obtained and in the face of the difficulties encountered, other specific provisions aiming to cool corium were proposed and studied over the years 1995 to 2010.

Three very different types of corium cooling device have been considered:

- the first type is a corium spreader, that collects all the corium leaving the vessel and spreads it out on a large-surface “spreading compartment” to reduce the heat to be removed per unit surface area and to cool it using a passive water circulation system, as planned for the EPR, see [42]; this system has been studied in depth and is described in detail in Section 5.4.3;
- the second type of device is a core catcher in the form of a crucible, see [44], made up of a large cavity covered with a thick layer of “sacrificial” refractory materials (materials that are eroded by the corium), which reduces heat flux *via* corium “dilution” (due to the addition of the sacrificial materials) and cools the corium using a passive water circulation system outside the core catcher; an example of such a device is the one implemented in the VVER reactor on the Tianwan Nuclear Power Plant in China;
- a third type of device, based on corium cooling by directing water at the bottom, has been successfully tested on the COMET facility at Forschungszentrum Karlsruhe in Germany, using simulant materials, see [45], and also in Cadarache with materials more representative of corium that could form during a core melt accident on a power reactor, see [46]. In the tested device, corium is collected in a porous concrete core catcher, covered with sacrificial concrete. Once this layer has eroded, the corium is reflooded by a passive system that directs water *via* the porous concrete and fragments the corium; corium spreading is not necessary for cooling and such a device can be installed in the reactor pit, just under the reactor vessel.

Experiments performed on these types of devices, in particular those performed on the core catcher and spreader system described in Section 5.4.3, show that, during a core melt accident on a power reactor, the devices should be able to effectively cool the corium after reactor-vessel failure and prevent the basemat penetration which could result from MCCI. Such devices are implemented in some new generation reactors; in particular, this is the case for EPRs, which are fitted with a core catcher and spreader system.

At least in the short term, it is not planned that such corium-cooling devices be installed on second-generation reactors in the operating fleet, because such installation would involve expensive, complex modifications. Furthermore, the significant worker exposure to ionising radiation that would result from such installation work should be taken into account. For this reason, studies are also being pursued with regard to cooling corium by directing water onto it, especially by using existing spray systems in the containment building. In particular, a new large-scale test programme was launched at ANL in 2011, dedicated to the study of corium cooling during MCCI by directing water from above under representative conditions, especially with regard to changes in residual heat in the pool during its flooding with water; this programme is part of collaboration between EDF, IRSN and the US Nuclear Regulatory Commission (NRC). In the case where corium cooling by existing devices that can direct water from above is found to be inadequate, recourse to other corium cooling devices and, in particular, those studied in the COMET facility could be considered, including for second-generation reactors.

5.4.3. Corium spreading for the EPR

5.4.3.1. Physical phenomena involved

Development of a core catcher with a corium spreader for the EPR required a European R&D programme. The purpose of the spreading is to prevent reactor-building basement penetration by facilitating corium cooling. To achieve this, spreading aims to ensure a sufficiently thin layer of corium, which minimises the surface heat flux due to residual heat to be removed.

Studies on corium spreading have therefore been performed to understand the ability of corium to spread on a substrate of fixed geometry and composition, with the corium flow conditions on the spreading surface determined by the accident sequence. The key parameters for corium spreading are the compositions of corium and substrate, the initial temperature and flowrate of the corium, and the geometry of the spreading compartment. References [60] and [76] give a summary of the work performed on this subject.

5.4.3.2. Description of the EPR core catcher

The concept used is based on spreading the corium over a large surface area, with the corium flooded and cooled by water from the In-containment Refuelling Water Storage Tank (IRWST) located in the containment building (see Figure 5.50 and Section 2.3.2.4 for a description of the EPR's engineered safeguard systems).

To promote corium spreading, the EPR core catcher temporarily retains the corium in the reactor pit before spreading. During this phase, the corium erodes a layer of "sacrificial" concrete, which is approximately 50 cm thick, before flowing into the melt discharge channel that connects the reactor pit to the "spreading compartment". This layer of sacrificial concrete is laid on a protective 10-to-14-cm-thick zirconium layer, which aims to ensure the integrity of reactor-pit concrete structures, even in the event

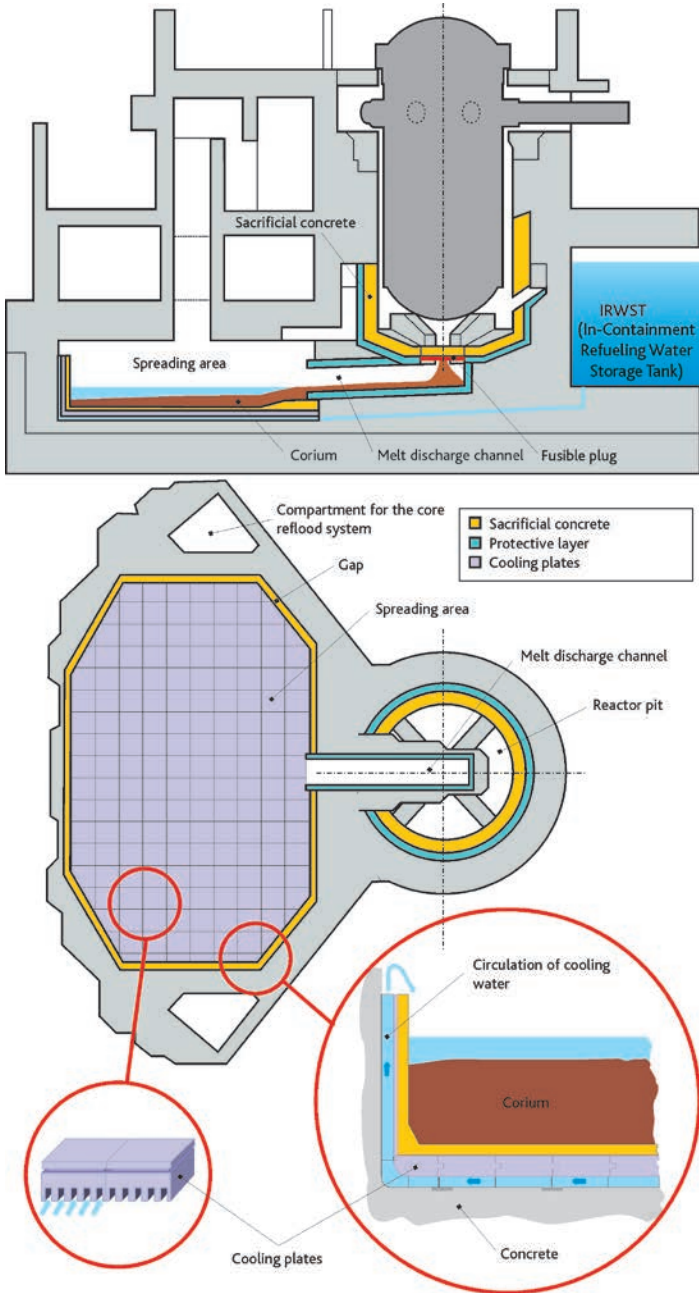


Figure 5.50. The upper part of the figure represents a cross-section view of the main components of the EPR core catcher (from [78]). The lower part of the figure represents the cooling system for the EPR core catcher with details: lower right, a vertical cross-section of the walls of the spreading compartment showing how the cooling water circulates under these walls; lower left, a vertical cross-section of the horizontal cooling channels located under the spreading compartment. The central part shows a top view of reactor pit, melt discharge channel and spreading compartment.

of non-uniform erosion of the sacrificial concrete by the corium (see Figure 5.50). During this temporary retention, the physico-chemical properties of the corium are modified (becoming more fluid, uniform in composition and of low viscosity) to facilitate its flow in the melt discharge channel and the spreading phase itself. If there are several successive corium flows following reactor-vessel failure, this temporary retention also means that the corium from the various flows can be gathered to obtain a uniform corium and a single flow towards the spreading compartment. In the zirconium layer under the sacrificial concrete at the bottom of the reactor pit, there is a wire-mesh insert which acts as a melt plug. This “gate” gives access to the melt discharge channel; it is a by-design weak point, as it is the only place where the sacrificial concrete is not reinforced by a protective layer, and it therefore fails relatively quickly on contact with the corium (after erosion of the sacrificial concrete), providing a sufficiently wide flow cross-section for rapid flow of all the corium into the spreading compartment.

The spreading compartment has a surface area of approximately 170 m². The floor and sidewalls of this compartment are assembled from a large number of individual elements made of cast iron. This structure is largely insensitive to thermal expansion and steep temperature gradients. The floor elements have rectangular, horizontal cooling channels. The inside of the spreading compartment is covered with a layer of sacrificial concrete. The arrival of corium triggers the opening of valves that initiate gravity-driven flow of water from the IRWST into the spreading compartment. The water first fills the horizontal cooling channels below the spreading compartment, and then fills the space behind the side-wall cooling structure before reflooding the corium from above. The system is shown in Figure 5.50.

5.4.3.3. Physics of corium spreading

Corium spreading is governed by competition between hydrodynamic driving forces (hydrostatic pressure and, to some extent, inertia), which promote progress and thinning of the flow, and gradual corium solidification, which leads to increasing apparent viscosity and the appearance of crusts in contact with the substrate and surface.

The hydrodynamics of lava spread has been studied by several authors in the field of volcanology, see [48], [49] and [50]. Numerical models and semi-analytical solutions have been developed for the flow of a fluid whose properties remain constant during the flow. Spreading on a horizontal surface is a free-surface flow, whose driving force is a function of the downslope. Corium flow during a core melt accident depends on gravity, inertia (at high flowrates) and viscous friction forces (at lower flowrates).

Corium rheology, see [73] and [74], changes strongly during its cooling, in particular below the liquidus temperature when crystalline phases appear. It depends on both the viscosity of the liquid phase (a mixture in which the silicate ions from the sacrificial concrete increases the viscosity by forming networks), which has been described by Urbain in [51] for example, and on the effect of crystals which solidify during the flow (the type of complex fluid formed, called semi-solid, is described by Flemmings in [52] and an empirical viscosity formula has been proposed for corium, see [73] and [77]).

Corium cooling is due to radiative heat transfer from the surface of the flow and by convection in contact with the substrate. Crusts may form at these two interfaces and contribute to slowing the flow. Nevertheless, there is significant thermal contact resistance, of around $5 \cdot 10^{-3} \text{ m}^2 \cdot \text{K/W}$, at the corium-substrate interface, which contributes to reducing corium cooling in contact with the substrate, see [53]. The effect of residual heat is small, given the short duration of spreading (no more than a few minutes).

In reference [54], Griffiths and Fink have published a detailed study of the various models of the spreading of solidifying lavas as a function of dominant forces (gravity and inertia, gravity and viscosity, gravity and complex rheology, gravity and crust strength etc.). These models mean that the speed of corium spreading can be assessed as a function of its flowrate in the melt discharge channel and its viscosity. They are used to assess the validity of corium spreading calculations performed for simplified boundary conditions, that do not take corium cooling into account.

5.4.3.4. Experimental programmes, modelling and simulation software

5.4.3.4.1. Experimental programmes

The first test programmes regarding spreading corium from a core melt accident on a power reactor were performed at Brookhaven in the USA, see [55]. Their purpose was to study corium spreading on the bottom of a reactor pit on a Mark I BWR. In Europe, experimental and numerical studies of spreading have been performed with a view to development of a core catcher for the EPR. Most of this work has been performed in the context of European projects: COMAS, large-scale corium cooling tests performed by AREVA, see [57]; Corium Spreading and Coolability (CSC), qualification tests for the concept of a core catcher with corium spreading and of the COMET concept of reflooding from below, see [56]; and Ex-vessel CORE melt STABILISATION Research (ECOSTAR), tests pertaining to the study of the physico-chemical phenomena that occur during spreading and the effectiveness of reflooding spread corium by directing water onto the top or bottom, see [58].

Experimental programmes include analytical experiments that aim to study the effect of various physical phenomena involved in corium spreading and cooling (for example, the CORINE programme using simulant materials performed at CEA Grenoble and jointly funded by IRSN, see [59] and [60]), semi-analytical experiments with simulant materials and tests with prototypic materials¹¹. Tables 5.6 and 5.7 present the characteristics of main test programmes, whether with simulant materials or with prototypic corium compositions. As an example, Figure 5.51 illustrates a corium spreading test.

These experimental programmes (in particular, the CORINE, VULCANO and KATS programmes) cover the greater part of the range of possible variations of the parameters accessible to experimentation with regard to the geometry, properties of materials and boundary conditions.

11. (Non-radioactive) corium of identical chemical composition to that expected during a core melt accident, but of different isotopic composition (for example using depleted or natural uranium instead of enriched uranium).

Table 5.6. Experimental spreading programmes performed with simulant materials.

Programme	Laboratory	Materials	Scale (volume poured)	Geometry	Parameters or effects studied
CORINE [59, 60]	CEA (France)	Low-temperature simulant materials (water, glycerol, low-melting point metal alloys)	~ 50 litres	19° angular sector	<ul style="list-style-type: none"> Flowrate (from 0.5 to 3 L/s) Effect of material (viscosity, single substances or non-eutectic mixtures). Cooling from above or below. Effect of a gas flow coming from the substrate.
Greene [55]	BNL (USA)	Lead	~ 1 litre	Square cross-section	<ul style="list-style-type: none"> Spread mass. Heating. Effect of water depth.
S3E [61]	KTH (Sweden)	Low- and intermediate-temperature (1200 °C) simulant materials	5 to 20 litres	Rectangular channels	<ul style="list-style-type: none"> Flowrate. Heating. Effect of material. Effect of (concrete) substrate. Effect of water, with or without boiling.
SPREAD [62]	Hitachi Energy Research Laboratory (Japan)	Steel	1 to 15 litres	Rectangular channel Half-disk	<ul style="list-style-type: none"> Spread mass. Heating. Flowrate. Effect of inlet geometry. Effect of substrate. Effect of water depth.
KATS [63-65]	FzK (Germany)	Aluminium thermite ($Al_2O_3 + Fe$) around 2000 °C	Up to 850 litres	Rectangular channel 90° angular sector	<ul style="list-style-type: none"> Spread mass. Flowrate. Effect of substrate. Effect of adding "sacrificial materials" Type of phase(s) spread (oxide or metal). Reflooding.

Table 5.7. Experimental programmes performed with prototypic materials.

Programme	Laboratory	Materials	Scale (volume poured)	Geometry	Parameters or effects studied
COMAS [57]	Siempelkamp (Germany)	Corium-concrete-iron mixtures Liquidus temperature around 1900 °C	20 to 300 litres	Rectangular channels 45° angular sector	<ul style="list-style-type: none"> High flowrates (> 150 kg/s). Effect of silica. Effects of substrate (ceramic, metal or concrete).

Programme	Laboratory	Materials	Scale (volume poured)	Geometry	Parameters or effects studied
FARO [66]	CCR Ispra (European Commission)	UO ₂ + ZrO ₂ Liquidus temperature around 2700 °C	~ 20 litres	19° angular sector	<ul style="list-style-type: none"> • Presence or otherwise of a thin layer of water. • Effect of a metal substrate.
VULCANO [67]	CEA (France)	UO ₂ + ZrO ₂ + concrete erosion products Liquidus temperature of 1900 to 2700 °C	3 to 10 litres	19° angular sector	<ul style="list-style-type: none"> • Flowrate. • Corium composition. • Effects of the substrate.

The spreading experiments performed show that, for corium flows during solidification, the liquid and solid phases remain mixed (there is no macrosegregation, unlike that which occurs during slower transitions). The solid fraction varies continually during flow. Furthermore, for a corium where the difference between solidus and liquidus temperatures is large, a "skin" forms in a mushy (liquid-solid) state rather than as a solid crust, at least initially. Conversely, in the case of a more refractory corium where the solidus and liquidus temperatures are close, a solid crust forms on the upper flow surface, which cracks and lets molten corium pass. In this case, the phenomena observed depend strongly on the scale of the flow, which means that the available experimental data remains inadequate on this specific point of the effect of the crust on flow dynamics, as it only involves small-scale tests with masses at least 1000 times smaller than those which would be involved in the case of a power reactor. Erosion of the concrete substrate during spreading remains minor; an effect on the spreading speed has been brought to light but is of little importance.

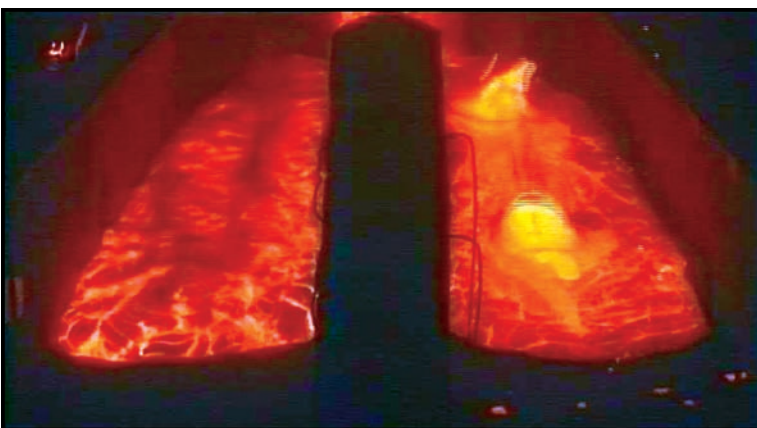


Figure 5.51. Spreading of corium representative of that produced during a core melt accident on a power reactor onto ceramic (left) and concrete (right) substrates, from the VULCANO VE-U7 spreading test performed by CEA with a mixture of UO₂, ZrO₂ and concrete erosion products, see [58]; credit: CEA.

Knowledge of dry corium spreading for the case of a large difference between solidus and liquidus temperatures (i.e. for corium rich in non-refractory materials from sacrificial concrete) is sufficient to validate calculation software and extrapolations to the case of a power reactor.

With regard to corium spreading under water, CORINE tests, performed with simulant materials and a water depth of around 10 cm, show that there could be an accumulation of corium whose thickness could reach that of the depth of water downstream of the corium flow, but that this would have little effect on the spreading. However, extrapolation of these results concerning spreading under water, which depend on scale (in particular the flow height), to the case of a power reactor is not possible with existing knowledge.

5.4.3.4.2. Models and simulation software

Several simulation software packages have been developed in Europe to model corium spread. Table 5.8 presents their main characteristics. This software has been the subject of significant validation work using the results of flow tests performed using simulant or prototypic materials. For example, comparison exercises for the calculation results produced using different software systems on the basis of the VULCANO VE-U7 test (with prototypic corium compositions, see [72]) and calculations performed on the basis of the ECOKATS-1 test (with simulant materials, see [64]) have shown that the software produces a good estimate of the spreading surfaces observed during tests; the uncertainty is around 20%.

The Stockholm Royal Institute of Technology (KTH) has developed a simplified analytical model for corium spreading, which has been satisfactorily validated (the mean precision is around $\pm 50\%$ on the spreading surface calculations), see [61] and [76].

To supplement the modelling of corium spreading, an R&D programme was performed by CEA at the end of the 1990s, dedicated to the study of corium rheology during its solidification, taking into account the variation of corium viscosity as a function of the corium spreading speeds along the vertical axis, see [73]. This means that viscosity models applicable to liquids with or without silica can be applied to corium, and therefore the viscosity of semi-solid corium as a function of the solid volume fraction can be predicted with adequate accuracy (i.e. within a factor of 3), see [73], [74] and [75]. These calculation results for the viscosity of corium are used in the spreading calculations.

All this work has led to a level of corium-spreading modelling that is sufficient to predict the spreading kinetics under the conditions of a core melt accident on a power reactor. In particular, the software developed is used to check, with reasonable uncertainty, the correct spreading of corium as a function of the boundary conditions of various accident scenarios, especially as a function of corium temperature and changes in corium flowrate.

Table 5.8. The main simulation software for corium spreading.

Code	Origin	Geometry	Characteristics	Validation
MELTSPREAD [68]	ANL for EPRI (USA)	1D	<ul style="list-style-type: none"> Covers substrate erosion and corium oxidation. 	<ul style="list-style-type: none"> Mainly based on the results of Greene's tests.
THEMA [60]	CEA (France)	2D temperature and horizontal speed averaged over the vertical axis	<ul style="list-style-type: none"> Covers corium solidification (in mass and in crusts) and substrate erosion. 3D resolution of heat equations in the substrate. 	<ul style="list-style-type: none"> Analytical tests. Tests with simulant materials and prototypic corium compositions.
LAVA [69]	GRS (Germany)	2D temperature and horizontal speed averaged over the vertical axis	<ul style="list-style-type: none"> Detailed analysis of corium cooling and rheology. 	<i>Idem</i>
CROCO [70]	IRSN (France)	2D horizontal and vertical	<ul style="list-style-type: none"> Detailed modelling of convection in the flow. Calculation of the free surface using Lagrangian modelling and resolution of conservation equations on a Eulerian mesh. 	<i>Idem</i>
CORFLOW [71]	FzK (Germany)	3D	<ul style="list-style-type: none"> Detailed modelling of convection in the flow. Free surface represented by a "corium height" function deduced from the equations for conservation of mass and momentum. 	<i>Idem</i>

5.4.3.5. Summary and outlook

R&D programmes performed to study corium spreading have established that dry spreading of the corium formed during a core melt accident on a power reactor enables its later cooling (the corium layer produced is sufficiently thin). It has been found, in particular during VULCANO tests, that even when the temperature of a corium-concrete mixture is 100 to 200 °C below the liquidus temperature, this mixture spreads adequately, as long as the flowrate is sufficiently high.

The presence of a thin water layer (simulating the water which would condense in the reactor building during an accident) or that of a concrete substrate (releasing steam and CO₂ during its interaction with the corium) have little effect on spreading. However, the influence of a deeper layer of water on corium spreading cannot be determined on the basis of existing knowledge. In this case, corium flow depends on the mechanical behaviour of the crusts formed on the surface and at the front of the flow (in particular

their cracking), and on fragmentation of the corium; study of the behaviour of crust and corium would require additional tests to provide a validated model.

Due to uncertainties concerning the ability of a layer of corium to spread under water, design provisions were taken for the EPR, aiming to ensure collection of corium from the reactor vessel in the reactor pit, followed by its dry spreading (no water in the spreading compartment before the corium arrives) then its cooling by water circulating in cooling channels located under the spreading compartment and finally its cooling by reflooding from above.

Reference Documents

- [1] *Nuclear Technology*, Special edition devoted to TMI-2, 87, 1989.
- [2] Three Mile Island reactor pressure vessel investigation project, *Proc. of an Open Forum Sponsored by OECD NEA and US NRC*, 1993.
- [3] [NUREG/CR-6849](#), Analysis of in-vessel retention and ex-vessel fuel coolant interaction for AP1000, 2004.
- [4] J.M. Seiler, Analytical model for CHF in narrow gaps on plates and in hemispherical geometries, *Nuclear Engineering and Design* **236** (19-21), 2211-2219, 2006.
- [5] J.M. Seiler, K. Froment, Material effects on multiphase phenomena in late phase of severe accidents of nuclear reactor, *Multiphase Science and Technology* **12**, 2000.
- [6] F.M. Cheung, Limiting factors for external vessel cooling, *10th Int. Topical Meeting on Nuclear Reactor Thermalhydraulics* (NURETH 10), 2003.
- [7] J.M. Seiler, B. Tourniaire, F. Defoort, K. Froment, Consequences of physico-chemistry effects on in-vessel retention issue, *11th Topical Meeting on Nuclear Reactor Thermalhydraulics* (NURETH 11), 2005.
- [8] M. Amblard, K. Froment, J.M. Seiler, B. Tourniaire, ANAIS experiment: consequence of water injection on a molten metal layer in the lower head, *10th Int. Topical Meeting on Nuclear Reactor Thermalhydraulics* (NURETH 10), 2003.
- [9] J.M. Bonnet, J.M. Seiler, In-vessel corium pool thermalhydraulics for the bounding case, *Salt Expert Group Meeting RASPLAV Seminar*, 2000.
- [10] T. Laporte, Synthèse des études réalisées au DMT sur les conséquences d'une explosion de vapeur en cuve ou hors cuve en cas d'accident grave de REP, CEA/DEN/DMT/LM2S/RT/00-039, 2000.
- [11] E.H. Henry, R.J. Hammersley, An experimental investigation of possible In-Vessel cooling mechanisms, FAI note I:\HPA\97-1, 1997.
- [12] K.H. Kang, R.J. Park, S.D. Kim, H.D. Kim, Simulant melt experiments on the coolability through external vessel cooling strategy, *ICAPP'05 conference*, Seoul, Korea, May 15-19, 2005.

- [13] V. Asmolov, L. Kobzar, V. Nickulshin, V. Strizhov, Experimental study of heat transfer in the slotted channel at CTF facility, *OECD/CSNI Workshop on In-Vessel Core Debris Retention and Coolability*, Garching, Germany, March 3-6, 1998.
- [14] W. Köhler, H. Schmidt, O. Herbst, W. Krätzer, Thermohydraulische Untersuchungen zur Debris/Wand-Wechselwirkung (DEBRIS), Abschlussbericht Project N° 150 1017, November, 1998.
- [15] J.H. Jeong, R.J. Park, K.H. Kang, S.B. Kim, H.D. Kim, Experimental study on CHF in a Hemispherical Narrow Gap, *OECD/CSNI Workshop on In-Vessel Core Debris Retention and Coolability Garching*, Germany, March 3-6, 1998.
- [16] S.S. Abalin, I.P. Gnidoi, A.I. Surenkov, V.F. Strizhov, Data base for 3rd and 4th series of RASPLAV salt tests, OECD RASPLAV Report, 1998.
- [17] P. Roux, F. Fichot, S. De Pierrepont, D. Gobin, B. Goyeau, M. Quintard, 2005 Modelling of binary mixture phase change: assessment on RASPLAV Salt Experiments, *NURETH 11*, Avignon, 2-6 October, 2005.
- [18] S. Rougé, SULTAN test facility; Large scale vessel coolability in natural convection at low pressure, *NURETH 7*, Saratoga Springs September 10-15, 1995.
- [19] T.N. Dinh, T.G. Salmassi, T.G. Theofanous, The limits of coolability in AP 1000 related ULPU-2400 confi V facility, *Proceedings of the 10th Intern Topical Meeting on Nuclear Reactor Thermalhydraulics*, October 5-9, 2003, Séoul, Korea.
- [20] J.M. Seiler, A. Fouquet, K.F. Froment, F. Defoort, Theoretical analysis for corium pool with miscibility gap, *Nuclear Technology* **141** (3), 233-243, 2003.
- [21] J.L. Rempe, K.H. Suh, F.B. Cheung, Insights from investigations of In-Vessel retention for high powered reactors, *NURETH 11*, Avignon, octobre 2-6, 2005.
- [22] J.M. Seiler, G. Ducros, Reflooding of a PWR core assessment of knowledge and R&D needs. Potential contribution by Phébus, DEN/DTN/SE2T/LPTM/05-117, 2005.
- [23] M. Zabiego, F. Fichot, Experimental needs for reflooding models validation, NT SEMCA 2006/257, IRSN/DPAM, 2006.
- [24] K. Atkhen, G. Berthoud, Experimental and numerical investigations based on debris bed coolability in a multidimensional and homogeneous configuration with volumetric heat source, *Nuclear Technology* **142**, June 2003.
- [25] N. Chikhi, F. Fichot, Reflooding model for quasi-intact rod configuration quench front tracking and heat transfer closure laws, *Nuclear Engineering and Design* **240** (10), 3387-3396, 2010.
- [26] M.T. Farmer, B.W. Spencer, J.L. Binder, D.J. Hill, Status and Future Direction of the Melt Attack and Coolability Experiments (MACE) Program at the Argonne National Laboratory, *Proc. of 9th Int. Conf. on Nuclear Engineering, ICONE-9697*, April 2001.

- [27] M.T. Farmer, D.J. Kilsdonk, R.W. Aeschliman, MSET-1 test data report, MACE-TRD18, 2002 – Reference not publicly available.
- [28] M.T. Farmer, S. Lomperski, S. Basu, Results of reactor material experiments investigating 2D core-concrete interaction and debris coolability, *Proc. of 4th Int. Conf. on Advances in Nuclear Power Plants*, 2004.
- [29] M.T. Farmer, S. Lomperski, S. Basu, A summary of findings from the melt coolability and concrete interaction (MCCI) program, *Proceedings of ICAPP07*, Nice, France, May 13-18, 2007.
- [30] B. Tourniaire, J.M. Seiler, J.M. Bonnet, M. Amblard, Experimental study and modelling of liquid ejection through orifices by sparging gas, *Nuclear Engineering and Design* **236** (19-21), 2281-2295, 2006.
- [31] S. Lomperski, M.T. Farmer, Experimental evaluation of the water ingression mechanism for corium cooling, *Nuclear Engineering and Design* **237** (9), 905-917, 2007.
- [32] S. Lomperski, M.T. Farmer, D. Kilsdonk, R. Aeschlimann, Small-Scale Water Ingression and Crust Strength Tests (SSWICS) SSWICS-11 Test Data Report: Thermal Hydraulic Results, OECD/MCCI-2009-TR01, Rev. 2, September, 2009.
- [33] S. Lomperski, M.T. Farmer, Measurement of the mechanical strength of corium crusts, *Proc. of 8th Int. Conf. on Advances in Nuclear Power Plants*, Seoul, Korea, June 8-12th, 2008.
- [34] J.M. Bonnet, J.M. Seiler, Coolability of corium spread onto concrete under water, the PERCOLA model, *Proc. of the 2nd OECD (NEA) CSNI specialist meeting on Core Debris-Concrete Interaction*, 1992.
- [35] B. Tourniaire, J.M. Seiler, Modeling of viscous and inviscid fluid ejection through orifices by sparging gas, *Proc. of 4th Int. Conf. on Advances in Nuclear Power Plants*, 2004.
- [36] F.P. Ricou, D.B. Spalding, Measurements of entrainment by axisymmetrical turbulent jets, *Journal of Fluids Mechanics*, 1961.
- [37] B. Tourniaire, Application of the PERCOLA ejection model to reactor scenario of molten core concrete interaction under water, *Proc. of 5th Int. Conf. on Advances in Nuclear Power Plants*, 2005.
- [38] M.T. Farmer, Phenomenological Modeling of the Melt Eruption Cooling Mechanism during Molten Corium Concrete Interaction, *ICAPP'06*, Reno, Nevada, USA, June 2006.
- [39] B. Spindler, B. Tourniaire, J.M. Seiler, K. Atkhen, MCCI analysis and applications with the TOLBIAC-ICB code based on phase segregation model, *Proc. of 5th Int. Conf. on Advances in Nuclear Power Plants*, 2005.

- [40] M.T. Farmer, B.W. Spencer, Status of the CORQUENCH model for calculation of ex-vessel corium coolability by an overlying water layer, *OECD Workshop on Ex-vessel Debris Coolability*, 1999.
- [41] M. Cranga, R. Fabianelli, F. Jacq, M. Barrachin, F. Duval, The MEDICIS code, a versatile tool for MCCI modelling, *Proc. of 5th Int. Conf. on Advances in Nuclear Power Plants*, Seoul, Korea, May 15-19, 2005.
- [42] M. Fischer, The severe accident mitigation concept and the design measures for core melt retention of the European pressurized water reactor (EPR), *Nuclear Engineering and Design* **230** (1-3), 169-180, 2004.
- [43] M. Cranga, B. Michel, F. Duval, C. Mun, Relative impact of MCCI modeling uncertainties on reactor basemat ablation kinetics, *MCCI-OECD seminar*, Cadarache, St-Paul-lez-Durance, France, October 10-11, 2007.
- [44] J.M. Seiler, B.R. Sehgal, H. Alsmeyer, O. Kymäläinen, B. Turland, J.L. Grange, M. Fischer, G. Azarian, M. Bürger, C.J. Cirauqui, European Group for Analysis of Corium recovery Concepts (EUROCORE), *FISA Conference*, 2003.
- [45] H. Alsmeyer, C. Adelhelm, H. Benz, T. Cron, G. Dillmann, W. Tromm, S. Schmidt-Stiefel, H. Schneider, G. Schumacher, T. Wenz, F. Ferderer, Corium cooling by bottom flooding: Results of the COMET investigations, *Proc. OECD Workshop on Ex-Vessel Debris Coolability*, Karlsruhe, Germany, Nov. 1999, FZKA 6475, pp. 345-355, 356-364 (2000).
- [46] C. Journeau, H. Alsmeyer, Validation of the COMET Bottom-Flooding Core-Catcher with Prototypic Corium, *Proc. of 6th Int. Conf. on Advances in Nuclear Power Plants*, Reno, NV USA, June 4-8th 2006.
- [47] K.R. Robb, M.L. Corradini, Towards understanding melt eruption phenomena during molten corium concrete interactions, *Proc. Of ICONE 18 Conf. Xi'an, China*, May 2010.
- [48] M. Dragoni, M. Bonafede, E. Boschi, Downslope flow models of a Bingham liquid: Implications for lava flows, *J. Volcanol. Geotherm. Res.* **30**, 305-325, 1986.
- [49] H.E. Huppert, The propagation of two-dimensional and axisymmetric viscous gravity currents over a rigid horizontal surface, *J. Fluid Mech.* **121**, 43-58, 1982.
- [50] N. Didden, T. Maxworthy, The viscous spreading of plane and axisymmetric gravity currents, *J. Fluid Mech.* **121**, 27-42, 1982.
- [51] G. Urbain, Viscosity estimation of slags, *Steel Res.* **58**, 111-116, 1987.
- [52] M.C. Flemmings, Behavior of metal alloys in the semisolid state, *Metall. Tran.* **22B**, 269-293, 1991.
- [53] G. Berthoud, *Freezing of Pure Melt Flowing into Tubes*, In: Ehrhard, P., Riley, D.S., Steen, P.H., Édition, *Interactive Dynamics of Convection and Solidification*, Kluwer Acad. Publ., Dordrecht, NL, pp. 249-26, 2001.

- [54] R.W. Griffiths, J.H. Fink, Effects of Surface Cooling in the Spreading of lava flows and domes, *J. Fluid Mech.* **252**, 667-702, 1993.
- [55] G.A. Greene, C. Finrock, J. Klages, C.E. Schwarz, S. B. Burton, Experimental Studies on Melt Spreading, Bubbling Heat Transfer and Coolant Layer Boiling, *Proc. 16th Water Reactor Safety Meeting*, NUREG/CP-0097, pp. 341-358, 1988.
- [56] G. Cognet, A. Alsmeyer, W. Tromm, D. Magallon, R. Wittmaack, B.R. Sehgal, W. Widmann, L. De Cecco, R. Ocelli, G. Azarian, D. Pineau, B. Spindler, G. Fieg, H. Werle, C. Journeau, M. Cranga, G. Laffont, Corium spreading and coolability: CSC Project, *Nuclear Engineering and Design* **209**, 127-138, 2001.
- [57] W. Steinwurz, A. Alemberti, W. Häfner, Z. Alkan, M. Fischer, Investigations on the phenomenology of ex-vessel core melt behaviour, *Nuclear Engineering and Design* **209** (1-3), 139-146, 2001.
- [58] H. Alsmeyer, G. Alberecht, L. Meyer, W. Häfner, C. Journeau, M. Fischer, S. Hellmann, M. Eddi, H.-J. Allelein, M. Bürger, B.R. Sehgal, M.K. Koch, Z. Alkan, J.B. Petrov, M. Gaune-Escart, E. Altstadt, G. Bandini, Ex-vessel core melt stabilization research (ECOSTAR), *Nuclear Engineering and Design* **235** (2-4), 271-284, 2005.
- [59] J.M. Veteau, R. Wittmaack, CORINE experiments and theoretical modelling. In: G. Van Goetem, W. Balz, E. Della Loggia (Eds) *FISA 95 EU Research on severe accidents*, Official Publ. Europ. Communities, Luxembourg, 1996, p. 271-285.
- [60] B. Spindler, J.M. Veteau, Simulation of spreading with solidification: assessment synthesis of THEMA code, Rapport CEA-R6053, 2004.
- [61] T.N. Dinh, M.J. Konovalikhin, B.R. Sehgal, Core Melt Spreading on a reactor Containment Floor, *Progr. Nucl. Energ.* **36** (4), 405-468, 2000.
- [62] H. Suzuki, T. Matsumoto, I. Sakaki, T. Mitadera, M. Matsumoto, T. Zama, Fundamental experiment and analysis for melt spreading on concrete floor, *Proc. 2nd ASME/JSME, Nucl. Eng. Conf.* **1**, 403-407, 1993.
- [63] G. Engel, G. Fieg, H. Massier, U. Stiegmaier, W. Schütz, KATS experiments to simulate corium spreading in the EPR code catcher concept, *OECD Workshop Ex-Vessel Debris Coolability*, Karlsruhe, Allemagne, 15-18/11/1998, 1999.
- [64] C. Spengler, H.-J. Allelein, J.-J. Foit, H. Alsmeyer, B. Spindler, J.M. Veteau, J. Artnik, M. Fischer, Blind benchmark calculations for melt spreading in the ECOSTAR project, *Proc. ICAPP '04 (Int. Conf. Advances in nuclear Power Plants)*, Pittsburg, PA, Communication n° 4105, 2004.
- [65] H. Alsmeyer, T. Cron, G. Messemer, W. Häfner, ECOKATS-2: A Large Scale Experiment on Melt Spreading and Subsequent Cooling by Top Flooding, *Proc. ICAPP '04 (Int. Conf. Advances in nuclear Power Plants)*, Pittsburg, PA, Communication n° 4134.
- [66] W. Tromm, J.J. Foit, D. Magallon, Dry and wet spreading experiments with prototypic materials at the FARO facility and theoretical analysis, *Wiss. Ber. FZKA*, 6475, 2000, pp. 178-188.

- [67] C. Journeau, E. Boccaccio, C. Brayer, G. Cognet, J.-F. Haquet, C. Jégou, P. Piluso, J. Monerris, Ex-vessel corium spreading: results from the VULCANO spreading tests, *Nuclear Engineering and Design* **223** (1), 75-102, 2003.
- [68] M.T. Farmer, J.J. Sienicki, C.C. Chu, B.W. Spencer, The MELTSPREAD-1 computer code for the analysis of transient spreading and cooling of high temperature melts, Rapport EPRI TR-103413, 1993.
- [69] H.-J. Allelein, A. Breest, C. Spengler, Simulation of core melt spreading with LAVA: Theoretical background and Status of Validation, *Wiss. Ber. FZKA*, 6475, 189-200, 2000.
- [70] B. Piar, B.D. Michel, F. Babik, J.-C. Latché, G. Guillard, J.-M. Ruggieri, CROCO: A Computer Code for Corium Spreading, *Proc. Ninth International Topical Meeting on Nuclear Thermal Hydraulics (NURETH-9)*, San Francisco, Ca., USA, 1999.
- [71] R. Wittmaack, CORFLOW: A code for the numerical simulation of free-surface flow, *Nucl. Technol.* **116**, 158-180, 1997.
- [72] C. Journeau, J.-F. Haquet, B. Spindler, C. Spengler, J. Foit, The Vulcano VE-U7 corium spreading benchmark, *Progr. Nucl. Energ.* **48**, 215-234, 2006.
- [73] M. Ramacciotti, C. Journeau, F. Sudreau, G. Cognet, Viscosity models for corium melts, *Nuclear Engineering and Design* **204** (1-3), 377-389, 2001.
- [74] J.M. Seiler, J. Ganzhorn, Viscosities of corium-concrete mixtures, *Nuclear Engineering and Design* **178** (3), 259-268, 1997.
- [75] M. Perez, J.C. Barbé, Z. Neda, Y. Bréchet, L. Salvo, Computer simulation of the microstructure and rheology of semi-solid alloys under shear, *Acta Mat.* **48** (14), 3773-3782, 2000.
- [76] C. Journeau, L'étalement du corium: hydrodynamique, rhéologie et solidification d'un bain d'oxydes à haute température, Doctoral thesis, University of Orléans, 2006.
- [77] C. Journeau, G. Jeulain, L. Benyahia, J.-F. Tassin, P. Abélard, Rheology of mixtures in the solidification range, *Rhéologie* **9**, 28-39, 2006.
- [78] M. Fischer, A. Henning, EPRTM engineered features for core melt mitigation in severe accidents, *Proc. ICAPP'09*, Tokyo, Japon, 2009.

5.5. Release of fission products during a core melt accident

This section deals with releases of fission products (FPs) from degraded fuel or corium during an in-vessel or ex-vessel core melt accident. In the latter case, the accident is considered to lead to vessel failure and relocation of corium into the containment. It also discusses the transfer of FPs from the reactor to the containment *via* the gas mixture produced during the progression of the accident in the core (mixture of steam and hydrogen; this hydrogen is produced primarily by oxidation of the zirconium [Zr] in the cladding) in the event of an RCS break. Lastly, it describes the behaviour of FPs in the containment.

Figure 5.52 summarises the sequence of the processes involved in the release and transfer of FPs to the environment during a core melt accident. The main parameters governing these processes are also listed in Figure 5.52. Their effects on the release of FPs from the reactor core, their transport in the RCS and their behaviour in the containment are discussed in greater detail in the following sections.

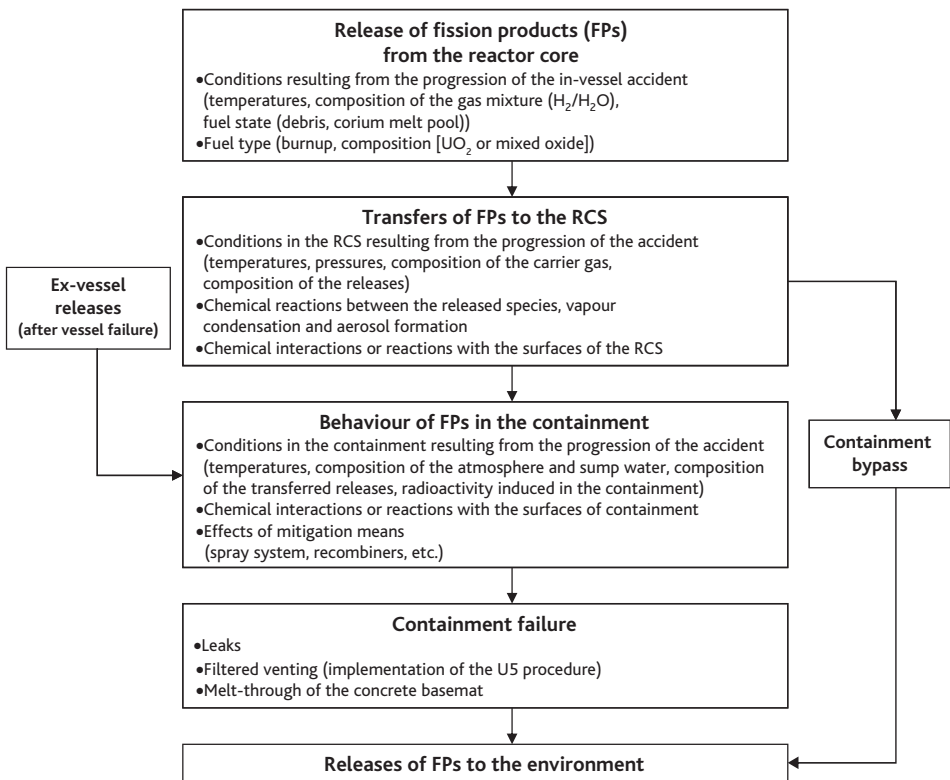


Figure 5.52. Summary description of the processes involved in the release and transfer of FPs to the environment during a core melt accident.

OECD/CSNI reports published in 1994 [1] and 2000 [2] provide an overview of the matter. More recent state-of-the-art reports are available on iodine chemistry [3] and nuclear aerosols [4].

5.5.1. Inventory and relative importances of FPs

Fission products are produced during fission reactions caused by the effect of neutrons on fuel. Each FP has a specific yield that depends on the type of fission (thermal neutrons for ^{235}U or ^{239}Pu , fast neutrons for ^{238}U , etc.). It should be noted that, fission yields of some FPs, such as ruthenium (Ru), can differ greatly from one isotope to another depending on whether fission concerns ^{235}U or ^{239}Pu . For example, the fission yield (in percent) of ^{103}Ru is 5.8% from ^{239}Pu and 3.0% from ^{235}U . However, the yield of ^{106}Ru is 5.0% from ^{239}Pu but only 0.38% from ^{235}U .

The inventory of FPs in terms of mass or number of atoms increases virtually in a near-linear fashion depending on the burnup rate (around 75 kg/(GWd/t)) to around 2 tonnes of FPs in the core of a 900 MWe PWR at balance. Table 5.9 lists this inventory for each fission product and each heavy nucleus together with the change in total core activity from the time of reactor shutdown to one month later.

Under nominal burnup conditions of a PWR, the FPs in the fuel matrix are at various chemical states [5]:

- in the form of *dissolved oxides* for nearly half and in particular strontium (Sr), yttrium (Y), zirconium (Zr), lanthanum (La), cerium (Ce) and neodymium (Nd);
- in the form of *oxide precipitates* primarily for barium (Ba) and niobium (Nb);
- in the form of *metal precipitates* for molybdenum (Mo), technetium (Tc), ruthenium (Ru), rhodium (Rh) and palladium (Pd);
- mainly in the form of *dissolved atoms* for the volatile FPs: bromine (Br), rubidium (Rb), tellurium (Te), iodine (I) and caesium (Cs). However, the chemical state of these FPs is not fully known. Above a certain temperature, they can migrate radially into the fuel pellets and condense in the colder sections, where they form more complex compounds with fuel elements or other FPs. For example, caesium can form compounds such as caesium molybdates and uranates;
- in the form of *dissolved atoms* or *intergranular or intragranular gas bubbles*: xenon (Xe) and krypton (Kr) in the case of the fission gases. It should be noted that gases that accumulate at the grain boundaries are more easily released during accident situations.

Radioactive FPs, especially those with short half-lives, have a smaller mass but generate most of the radioactivity and residual heat. Their relative importance can be assessed using two main criteria:

- their dosimetric impact if released to the environment: this impact varies depending on the half-life and type of radiation emitted. For example, Figure 5.53 shows the relative importance of FPs and actinides on the dose to the lungs. Figure 5.54

Table 5.9. Change in the activities of the FPs and actinides in a 900 MWe PWR (1) after reactor shut-down (RT = reactor trip).

Fission products	Total mass at RT, in kg (2)	Activities as a fraction of the total activity			
		at RT	at 1 hour	at 1 day	at 1 month
As	7.39E-03	0.20%	0.01%	0.00%	0.00%
Se	3.14E+00	0.58%	0.02%	0.00%	0.00%
Br	1.16E+00	1.17%	0.20%	0.00%	0.00%
Kr	2.21 E+01	2.32%	1.46%	0.03%	0.06%
Rb	2.03E+01	3.22%	0.84%	0.01%	0.00%
Sr	5.51 E+01	4.50%	3.85%	2.57%	6.10%
Y	2.89E+01	5.84%	5.11%	3.40%	8.16%
Zr	2.10E+02	4.73%	3.83%	4.63%	10.30%
Nb	3.24E+00	7.09%	5.68%	5.93%	13.18%
Mo	1.84E+02	4.28%	2.28%	2.90%	0.01%
Tc	4.52E+01	4.82%	2.50%	2.77%	0.01%
Ru	1.37E+02	1.85%	3.11%	3.67%	10.27%
Rh	2.36E+01	2.30%	3.42%	4.96%	10.26%
Pd	5.93E+01	0.19%	0.33%	0.18%	0.00%
Ag	3.97E+00	0.14%	0.11%	0.12%	0.05%
Cd	4.00E+00	0.03%	0.02%	0.01%	0.00%
In	8.20E-02	0.13%	0.03%	0.01%	0.00%
Sn	2.65E+00	0.66%	0.15%	0.02%	0.01%
Sb	8.98E-01	1.76%	0.68%	0.17%	0.06%
Te	2.62E+01	3.85%	4.16%	2.88%	0.69%
I	1.27E+01	5.70%	8.94%	6.39%	0.65%
Xe	3.07E+02	4.33%	3.60%	5.12%	0.41%
Cs	1.61 E+02	3.82%	1.27%	0.46%	1.61%
Ba	8.21 E+01	4.67%	3.75%	3.46%	3.45%
La	6.99E+01	4.71%	5.22%	3.57%	3.25%
Ce	1.63E+02	3.61%	5.04%	7.41%	16.01%
Pr	6.21 E+01	3.10%	4.63%	5.49%	11.76%
Nd	2.07E+02	0.68%	1.07%	1.25%	0.82%
Pm	1.24E+01	0.65%	1.22%	1.65%	1.48%
Sm	3.57E+01	0.21%	0.46%	0.54%	0.00%
Eu	8.90E+00	0.08%	0.19%	0.29%	0.36%
Actinides					
U	6.99E+04	9.37%	3.91%	0.00%	0.00%
Np	3.15E+01	9.37%	22.76%	29.86%	0.02%
Pu	5.89E+02	0.05%	0.11%	0.19%	0.80%
Am	6.18E+00	0.00%	0.00%	0.00%	0.00%
Cm	2.09E+00	0.01%	0.03%	0.06%	0.21%

(1) 900 MWe PWR with UO_2 fuel enriched to 3.70% of ^{235}U , 72.5 tons of initial uranium, with the fuel loaded into four regions of the core (burnup rate of the assemblies: 10.5 GWd/tU for the first region [one burnup cycle], 21 GWd/tU for the second region [two cycles], 31.5 GWd/tU for the third region [three cycles] and 42 GWd/tU for the last region [four cycles]).

(2) Total mass of the stable isotopes and the radioactive isotopes.

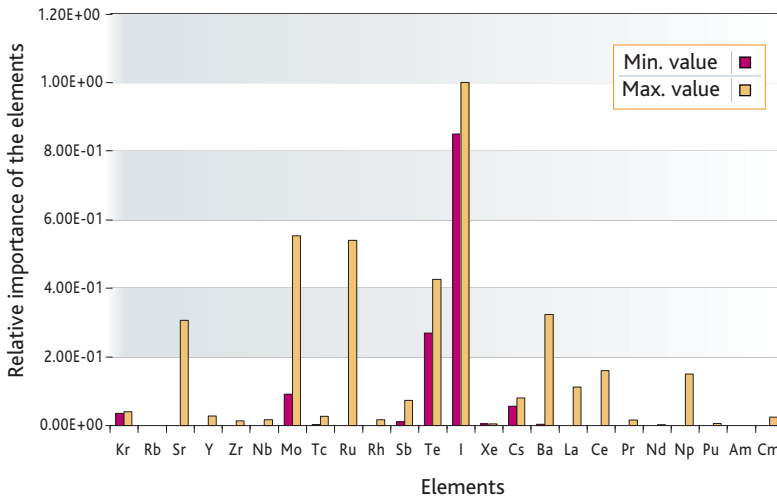


Figure 5.53. Relative importance of the elements released during a PWR core melt accident (100% core melt) on the dose to the lungs.

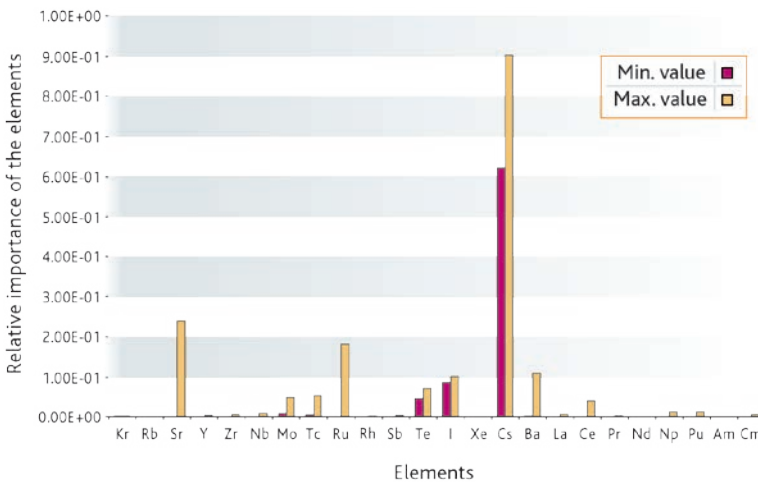


Figure 5.54. Relative importance of the elements released during a PWR core melt accident (100% core melt) on latent cancers (long-term exposure).

shows the same information, but for the long-term consequences (latent cancer). The relative importance indicated for each element are derived from studies conducted by the US NRC [6]. The minimum and maximum values shown on the graphs are derived from studies conducted by IRSN on the variability and uncertainty of the release rates;

- their contribution to the residual heat generated in fuel or corium, which is illustrated by Figure 5.55. Residual heat influences accident progression, such as the moment of vessel failure or the moment of corium melt-through of the containment basemat.

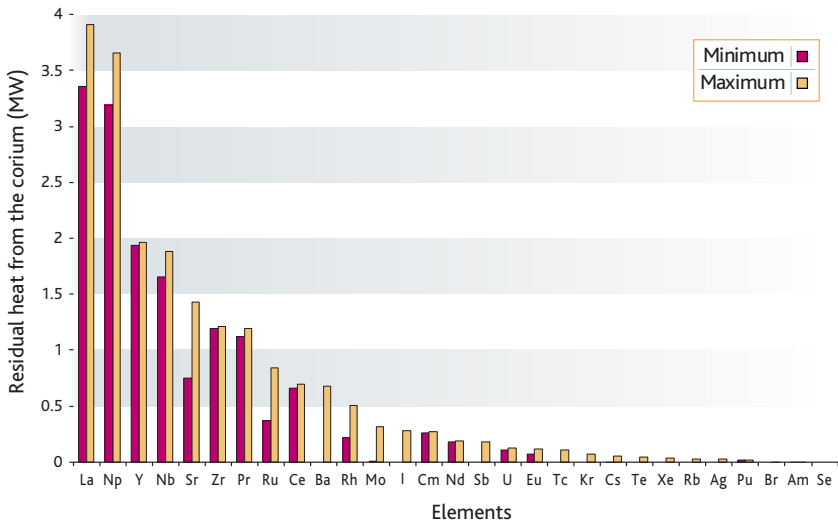


Figure 5.55. Minimum and maximum residual heat associated with the elements in corium at the time of vessel failure during a large-break LOCA in the RCS.

Stable FPs, which have a higher mass, can influence core degradation because the formation of eutectic mixtures of uranium dioxide-fission product (UO_2 -FP) seems to lower the fuel-melting temperature [7]. The concentration of FPs in the fuel is not negligible at high burnup (they may account for more than 10% of the total number of atoms beyond 50 GWd/t). Furthermore, under oxidising conditions, the hyperstoichiometry of the fuel (oxygen content greater than the stoichiometric content UO_2) lowers its melting temperature [8].

5.5.2. Release of FPs into the reactor vessel

The chemical state of the FPs initially present in the fuel matrix in the form of dissolved atoms or oxides, oxide precipitates and metal precipitates is not permanent. Some FPs may shift from one chemical state to another depending on the temperature of the fuel, the oxygen content in the fuel (which increases with the burnup rate) and the burnup rate (increase in the concentration of FPs in the fuel matrix). This is especially true for molybdenum, which precipitates in fuel mainly in metal form but can also be in oxidised form (especially on the surface of MOX fuel pellets), and for niobium and strontium, whose oxides may be partly dissolved and precipitated in the fuel.

5.5.2.1. Physical phenomena involved in the release of FPs

► Fission gases

During fuel irradiation, fission gases form as atoms in the grains of UO_2 . These atoms of gas either diffuse toward the grain boundaries or precipitate into nanometre-sized intragranular bubbles, slowing down their rate of migration towards the grain boundaries. The bubbles may then redissolve under the influence of fission spikes (defects

created along the path of the fission fragments just after their formation), which speed up the rate at which gas is supplied to the grain boundaries. Once on the grain surface, (mainly by atomic diffusion, but also by bubble migration), the fission gases accumulate to a point where they coalesce to form larger bubbles and fill the boundaries. These bubbles are then capable of moving into the free volume of the rod [9].

At the onset of the accident, the gases consist of:

- gas atoms dissolved in the fuel matrix;
- intragranular gas bubbles with little mobility;
- gases accumulated in the grain boundaries (intergranular bubbles).

Their release is governed by a number of mechanisms. The first release phase (often referred to as “burst release”) corresponds to the *release of gases accumulated in the intergranular spaces*. The fraction already released into the rod plenum during normal irradiation must also be taken into account, ranging from a few percent to 10%, depending on the burnup, the irradiation power and the fuel type. Such releases occur at the beginning of the temperature rise at around 1000 °C, though this is sometimes lower for high burnup fuels.

The second phase involves the *release of the intragranular gases via a thermally activated diffusion process* that begins with dissolved atoms. The *gases trapped in the intragranular bubbles* (which are of nanometre size) are the last to be released, which generally occurs when the fuel melts.

It is therefore important to correctly quantify the respective fractions of these three phases when modelling gas releases, which depend on their radial position in the pellet and on the fuel type (high burnup fuels [the granular structure on the periphery of the pellets is degraded, resulting in more pores where the gases can accumulate] and heterogeneous MOX fuels have a higher intragranular fraction).

During a core melt accident, all the fission gases are released from the fuel when it melts.

► Non-gaseous FPs

It is generally accepted that the release of non-gaseous FPs follows a two-phase process: (1) the FPs in solution in the matrix (or the precipitates when the solubility limit has been reached) diffuse as far as the grain boundaries, and then (2) a mechanism of mass vaporisation transfers the FPs from the grain surface outside of the fuel matrix. This mechanism also involves a number of chemical aspects. The potential formation of species (such as molybdates, uranates, zirconates) can determine transfers of FPs (caesium, barium and strontium) in the fuel. Likewise, oxidation or reduction of FP precipitates by water vapour or hydrogen has a significant impact on transfers of these species in the fuel. It should be noted that the basic thermodynamic data on the formation and destruction of these species currently are subject to high uncertainties that affect the

calculation of FP chemistry – and thus FP transport – in the fuel and, consequently, affect the calculation of FP releases from fuel. The predictive capability of the release models is discussed in Section 5.5.2.3.

Outside the fuel matrix, chemical interactions with the cladding or elements of the core structures can then reduce the volatility of some elements through the formation of more refractory species.

Lastly, once released from the core, a significant fraction of the FPs condenses in the colder sections of the upper core structures before even reaching the hot legs of the RCS or the containment. This is especially true for low-volatile FPs.

Qualitatively speaking, the main physical parameters influencing the release of FPs are as follows:

- the fuel *temperature* is the main parameter, at least until loss of integrity of the fuel assemblies in the core leads to loss of core geometry;
- the *oxidising-reducing conditions* have a significant impact on fuel. The release kinetics of volatile FPs are particularly accelerated under oxidising conditions. Furthermore, the overall release of certain FPs is very sensitive to the oxidising-reducing conditions. For example, the release of molybdenum increases in steam, whereas that of ruthenium can be very high in air. Conversely, the release of barium (as for strontium, rhodium, lanthanum, cerium, europium [Eu] and neptunium [Np]) increases under reducing conditions;
- *interactions with the cladding and/or elements of the core structures* can play a major role. For example, the presence of tin in the cladding delays the emission of the volatile elements tellurium and antimony (Sb). Barium significantly contributes to the decay heat (*via* its daughter product ^{140}La) and is also partially trapped in both the cladding (probably due to the formation of zirconates) and in the steels of the structures.
- the *burnup* accentuates releases, in terms of both the kinetics of volatile FPs, and the magnitude of release of low-volatile species such as niobium (Nb), ruthenium, cerium and neptunium (Np);
- The *fuel type* also has a significant impact: MOX releases tend to be higher than those of UO_2 . This phenomenon is probably related to its heterogeneous microstructure, with the presence of plutonium (Pu)-rich agglomerates where the local burnup can be very high;
- Last of all, the *physical state of the fuel* (fragmented, solid, liquid) during its in-vessel degradation has a significant influence. The transition from a “degraded rod” geometry to a “debris bed” geometry also involves an increase in releases *via* the increase in the surface-to-volume ratio. Conversely, the transition from a debris bed to a molten pool slows down the release of FPs as a solid crust forms on the surface of the molten corium pool.

► Degrees of volatility of the various FPs

The current state of knowledge, obtained in particular thanks to the analytical experiments of the VERCORS programme and the integral tests of the **Phebus** programme (Section 7.3), make it possible to schematically classify FPs and fission gases into four categories of decreasing volatility (Figure 5.56):

- *fission gases and volatile FPs* (Kr, Xe, I, Cs, Br, Rb, as well as Te, Sb and silver [Ag]): almost all of these products are released even before reaching molten pool conditions. The release kinetics of these elements are accelerated under oxidising conditions and are slightly retarded for Te and Sb than for the other volatile FPs due to interactions with tin in the cladding;
- *semi-volatile FPs* (Mo, Ba, Y, Rh, Pd, Tc): their release rates can be very high and are sometimes equivalent to those of volatile FPs yet are highly sensitive to the oxidising-reducing conditions and result in significant retention in the upper vessel internals;
- *low-volatile FPs* (Sr, Nb, Ru, La, Ce, Eu, Np): they are characterised by low but significant levels of release, ranging from a few percent to 10% during the fuel-rod degradation phase (prior to loss of fuel rod geometry). Nevertheless, some of these releases can reach much higher levels for fuels with very high burnups under specific conditions (this is especially the case of Ru in air). Retention of these FPs is nevertheless expected to be significant in the upper vessel internals;
- *non-volatile FPs* (Zr, Nd): to date, no significant release of these two elements has been demonstrated experimentally. These are the two most refractory FPs.

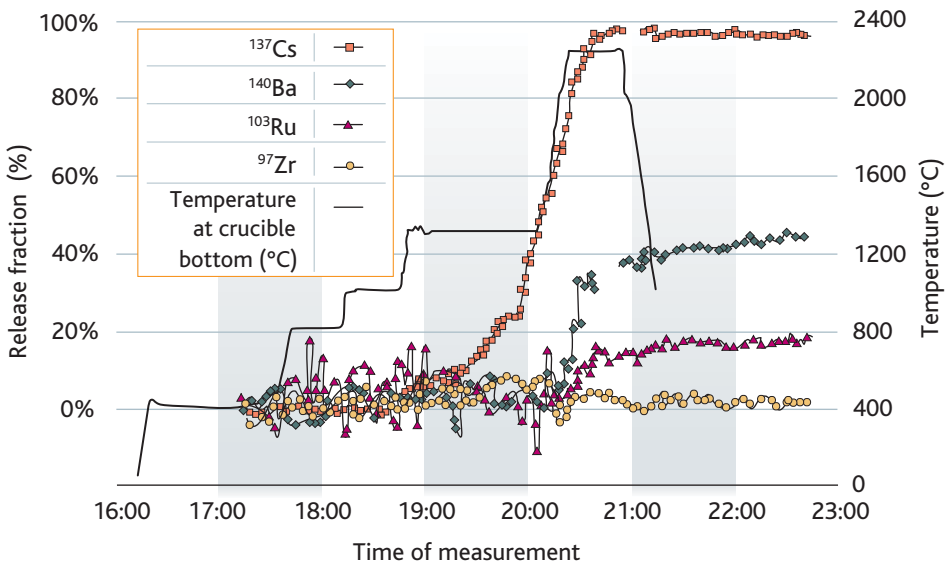


Figure 5.56. Illustration of the four volatility categories for FPs according to the results of a VERCORS test [10].

► Actinides

Most of the quantitative data on releases of actinides during a core melt accident come from the VERCORS programme [10]. The behaviour of uranium and neptunium is similar to that of low-volatile FPs whereas the behaviour of plutonium is rather more similar to that of non-volatile FPs.

5.5.2.2. Experimental programmes

Experimental programmes on FP releases have mainly relied on analytical experiments performed on sections of irradiated fuel. They were eventually supplemented by integral tests performed on reduced-scale fuel assemblies particularly to study the effects of changes in core geometry (particularly debris bed and molten pool formation) during core degradation on the release of FPs.

► Analytical experiments

Five major analytical programmes have been conducted since the late 1970s: SASCHA in Germany [11], HI/VI in the United States [12], CRL in Canada [13], VEGA in Japan [14] and HEVA/VERCORS [15] in France. The HEVA/VERCORS programme is described in greater detail on account of its significant contributions to the development and validation of the FP release models developed by IRSN (Section 5.5.2.3):

- the first analytical experiment of its kind, the SASCHA programme was performed by FZK on *unirradiated* UO_2 fuel under various atmospheres, including argon, air and steam. The UO_2 pellets were specially manufactured *with additives that simulate FPs*. Although the SASCHA programme was not really representative of the real location of the FPs in fuel during irradiation, it did provide a series of preliminary estimates for iodine and caesium releases up to 2000 °C;
- ORNL conducted the HI/VI programme between 1981 and 1993 (13 tests in total). The experimental configuration, at least for the VI tests, was similar to that of the VERCORS programme, i.e., a test loop equipped with thermal-gradient tubes (TGT) to collect condensable gases (these samples were used to determine the condensation concentrations and temperatures), a series of filters to trap aerosols and a condenser and cartridges to trap fission gases. The fuel samples were cladded sections of irradiated UO_2 measuring around 15 cm in length and sealed at the ends. A hole was drilled in the cladding at midplane height. This programme provided *highly representative results on the release of FPs, but only in relation to long-lived FPs* (mainly ^{85}Kr , ^{106}Ru , ^{125}Sb , ^{134}Cs , ^{137}Cs , ^{144}Ce and ^{154}Eu) as the samples were not re-irradiated prior to the tests;
- AECL's CRL programme was a highly analytical programme conducted to study CANDU fuels. It consisted of many tests on fragments of irradiated fuel (from 100 mg to 1 g) and on short sections of cladded fuel. The resistive furnace used during the tests limited temperatures to a maximum of 2100 °C. Some samples were pre-irradiated to measure the release of short-lived FPs. One of the

important results of this programme was the first quantification of the *very high release of ruthenium in air*;

- performed by JAERI (Japan), the VEGA programme was very similar to the VERCORS programme in terms of its experimental configuration and conditions, especially the VERCORS HT series (see next paragraph). A total of 10 tests were carried out: eight on UO_2 fuel and two on MOX fuel. Some of the tests were carried out in a *steam atmosphere up to fuel melting temperatures*. Some of the samples were re-irradiated prior to the tests but under less than optimal conditions. The irradiation time, which was shorter than the in-reactor irradiation time, and the long decay time did not result in a sufficient quantity of short-lived FPs. A unique feature of these tests was the inclusion of *tests at a pressure of 10 bar*, which notably demonstrated a reduction in caesium releases;
- the HEVA/VERCORS programme, performed by the CEA and financed by IRSN (IPSN at the time) and EDF, aimed at quantifying releases of FPs and actinides (kinetics and total release rates) from irradiated nuclear fuel under conditions representative of a core melt accident. These tests were performed in a high-activity cell on different types of fuel sample irradiated in a PWR (around 20 g of fuel) under a range of experimental conditions. Most of the samples were re-irradiated for a few days at low power in an experimental reactor in order to build up an inventory of short-lived FPs. These samples were then heated in an induction furnace under a variable atmosphere of steam and hydrogen simulating core melt accident conditions (Figure 5.57). FP releases from the fuel samples were measured by gamma spectrometry of the decrease of the FPs in the fuel samples during the test. Twenty-five tests were carried out between 1983 and 2002 in three phases: (1) eight HEVA tests (release of volatile and semi-volatile FPs up to 2100 °C); (2) six VERCORS tests (release of volatile and semi-volatile FPs and some low-volatile FPs up to 2300 °C, the limit for the onset of fuel collapse in the sample), (3) eleven HT/RT tests (release of all types of FP until the melting point was reached). These tests resulted in the compilation of an extensive database on the release of FPs: the parameters that varied during these tests were the maximum temperature reached (below or above fuel melting temperature), the oxidising-reducing conditions, the burnup, the fuel type (usually UO_2 , although MOX was used in two tests) and the initial fuel geometry (intact fuel or fuel debris to simulate the formation of a debris bed during a core melt accident).

There still are, however, uncertainties about the release of FPs. This is particularly the case for very-high-burnup UO_2 fuels (70 GWd/t and beyond), MOX fuels, and accidents with in-vessel ingress of air or in-vessel fuel reflooding.

The VERDON programme, conducted at the CEA facility of the same name as part of the International Source Term Programme (ISTP) [16], aims to address these issues, apart from aspects related to reflooding. Tests on FP releases from samples of high burnup fuels, MOX fuel samples and fuel samples in an air atmosphere have been conducted since 2011 at a facility similar to that where the VERCORS HT tests were carried out.

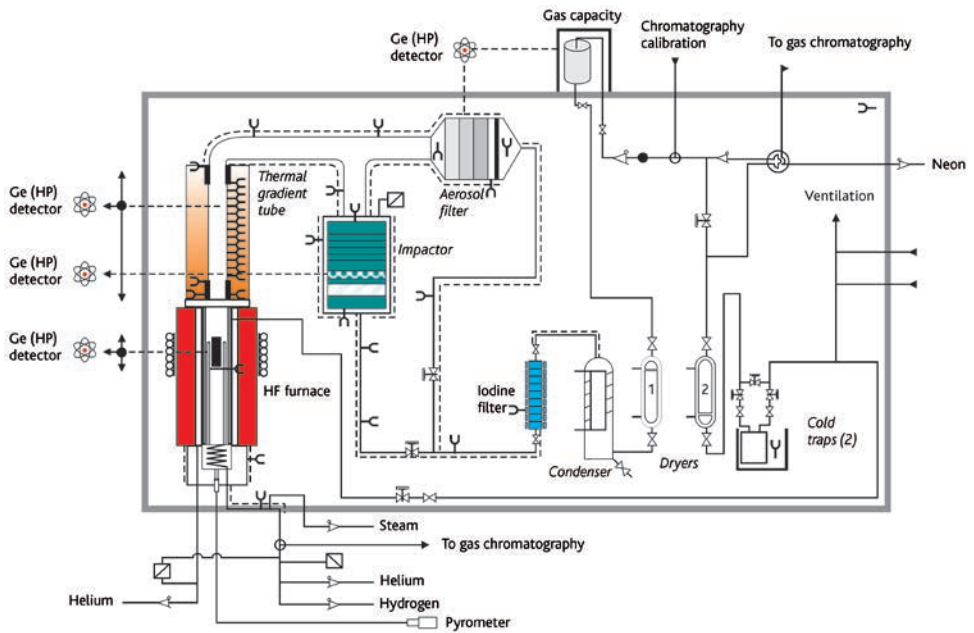


Figure 5.57. The VERCORS HT loop [15].

► Integral tests

Among the experimental programmes devoted to fission product releases, the **Phébus FP** programme is one of the most representative of core melt accident conditions, particularly with regard to releases from fuel, transport in the RCS and the behaviour of FPs in the containment [16]. Four bundles of 20 fuel rods (three of which were re-irradiated in order to obtain inventories representative of the short-lived FPs) with burnup of between 20 and 40 GWd/tU were brought to fuel melting conditions. In three tests, the bundles were brought to molten pool conditions. A specific test was conducted to study degradation of a debris bed up to molten pool conditions. The programme and the lessons learnt are described in Section 7.3.

In terms of in-vessel FP releases, the **Phébus FP** programme made a huge contribution in addition to the analytical tests by providing better understanding of two aspects: (1) releases of FPs depending on the progression of the accident in the vessel and (2) the effect, on such releases, of the chemical interactions with the cladding material or structural steels in the core. For example, lower FP releases were observed with molten corium melt pools than with releases from solid fuels. In-core fuel collapse during degradation (collapse of the fuel rods with the formation of debris and the relocation of corium to the cool areas at the bottoms of the bundles) results in spikes in FP releases. The case of barium is a good example in terms of the effects of the chemical interactions, with these releases being much lower than those recorded

in the analytical tests. This difference in behaviour is ascribed to interactions with the fuel rod cladding and possibly iron from the molten structural steels of the core, which reduced the volatility of the barium.

For the other fission products, the total releases were highly consistent with those obtained from the analytical tests.

5.5.2.3. Physical models and simulation codes

Two approaches are used in computer codes to model FP releases: (1) a simplified approach that allows models to be easily integrated into integral codes (see Chapter 8), and (2) a mechanistic approach that describes, at best, all the physical phenomena that come into play. Both approaches can be illustrated by two tools used at IRSN: (1) the Franco-German ASTEC code, which uses semi-empirical release models, and (2) the MFPR mechanistic code developed jointly by IRSN and the Russian institute IBRAE.

► Simplified approach used in the ASTEC code

The ASTEC code [17] models releases of FPs according to three categories:

- so-called *volatile* FP releases (Xe, Kr, I, Br, Cs, Rb, Sb, Te) are governed by their *diffusion* in fuel grains. Their diffusion coefficient is a function of the temperature and oxygen content of fuel. This coefficient is the same for all FPs, excepting Sb and Te, for which a release delay is applied to take into account their retention in the cladding provided the latter has not oxidised completely;
- so-called *semi-volatile* FP releases are governed by *mass transfers* induced by their vaporisation at grain boundaries. Their vapour pressures are determined using thermodynamic correlations made with the GEMINI2 (Sr, Ru, Ba and La) or FACT (Mo, Ce and Eu) solvers, which calculate the equilibrium state of the chemical system involved by minimising its free enthalpy (Gibbs free energy). The same mass-transfer mechanism is applied to all FPs released from a molten corium pool;
- so-called *non-volatile* FP releases are governed by the *vaporisation of UO_2* when it becomes hyperstoichiometric (UO_{2+x} with an oxygen content higher than that of stoichiometric UO_2) and oxidises until UO_3 forms. This category also covers the actinides U, Np, Pu, Am and Cm.

► Mechanistic approach of the MFPR code

MFPR [18] is an 0-D mechanistic code designed to simulate FP releases from solid UO_2 fuel. FPs are assumed to be present in fuel in atomic or oxide form. Two types of modelling are performed: one for fission gases, the second for other FPs.

Modelling of FPs includes all the physical phenomena described in Section 5.5.2.1: intragranular diffusion of atoms and bubbles to the grain boundaries with modelling of the bubble formation (nucleation, growth) and destruction (return to solution form)

mechanisms. Releases from the grain boundaries occur after coalescence and interconnection of the gas bubbles.

In 2015, modelling of other FPs involved 13 elements: Cs, I, Te, Mo, Ru, Sb, Ba, Sr, Zr, La, Ce, Nd and Eu. They are assumed to diffuse to the surface of the grain boundaries, with some oxidation occurring during their transfer to the fuel matrix. They then form three distinct phases: a metallic phase, a ternary phase (known as the grey phase and composed of FP oxides) and a specific phase for CsI (caesium iodide). Releases from fuel are governed by the thermodynamic equilibrium of these three phases, with the gas contained in spaces between the grains (grain boundaries).

Much progress has been made in the validation of the simplified and mechanistic release models. The experimental observations are well reproduced by the calculated releases of the volatile FPs. However, the ASTEC results slightly underestimate the releases at intermediate temperature (between 1000 and 1500 °C) because the model does not take into account the intergranular inventory. The greatest uncertainties relate to the results for the semi-volatile and low-volatile FPs and are due in particular to the difficulty in properly addressing the chemical reactions with the structural elements of the core (control rods, reactor core internals, etc.).

5.5.2.4. Releases of structural materials

The radioactivity of structural materials, due mainly to their activation, is relatively low. Nonetheless, it is important to evaluate releases of these materials for two reasons: (1) they may chemically react with FPs, such as iodine with the silver in silver-indium-cadmium (SIC) control rods or tellurium with the tin in cladding, and (2) they significantly contribute to the quantity of aerosols released into the containment. Structural materials agglomerate with FP-laden aerosols, increasing the average size of the particles and contributing to increasing their gravitational settling.

Releases of components from SIC control rods (rods in French 900 MWe reactors and in many other PWRs of Western design) depend primarily on their degradation mechanisms described in Section 5.1.1.2. When the cladding and guide tubes of SIC rods fail, the liquid SIC alloy inside comes into contact with the surrounding fluid and vaporises. The release rates then depend on the vapour pressures of these three metals. This is well known and correctly modelled. What remains uncertain is the degradation phenomena of the control rods and guide tubes. Depending on the level of degradation of these components, the liquid alloy may remain at high temperature for a variable period of time before flowing to the colder sections in the lower end of the core and solidifying. This has an effect on the quantities that are vaporised.

The boron carbide in other types of control rod (those used in French 1300 MWe reactors along with SIC rods, also in BWRs, and in VVERs (PWRs of Russian design)) begin to oxidise when it comes into contact with the surrounding fluid, i.e., after cladding and guide-tube failure. The resulting oxidation products are boric oxide and carbon monoxide or carbon dioxide (depending on the oxidising potential of the fluid). The boric oxide is converted into boric acid as it is transferred from the RCS to the containment.

Theoretically, the carbon monoxide could turn into methane in the RCS if reducing conditions prevail there. In practice, the formation of methane in the RCS remains negligible at low pressure and is very low at high pressure because the reactions that allow it to form are too slow to achieve a significant yield.

In the case of Zircaloy fuel-rod cladding, significant amounts of tin are released (tin is a minor component of Zircaloy). It is the form SnO_2 (tin dioxide) that is volatile and released. The degradation mechanisms of the cladding govern the releases of tin. Satisfactory models are obtained by taking into consideration that the release kinetics of tin follow those of the oxidation of Zircaloy cladding.

5.5.2.5. Summary and Outlook

The experimental database of analytical tests performed on sections of irradiated fuel is relatively broad in the case of UO_2 fuels with average burnups. It is supplemented by integral **Phebus FP** type tests. These experiments have helped improve understanding of the effects of the different parameters influencing releases, such as temperature, oxidising-reducing conditions, interactions with structural materials (especially cladding), burnup and the type (UO_2 or MOX) and state of the fuel (solid or liquefied).

These results have made it possible to develop and validate two types of model. Mechanistic models are used to describe most of the interactions in the fuel and above all to interpret the tests. Simplified models describing the main phenomena can be derived from these mechanistic models and used in integral codes such as ASTEC (see Chapter 8).

The hypotheses formulated to interpret the tests are based mainly on the physico-chemical changes in the fuel and make it possible to correctly reproduce the influence of the various parameters on releases (temperatures, burnup, composition of the atmosphere surrounding the fuel). Apart from predicting the behaviour of fission gases, the MFPR code is used to determine variations in the composition of the different phases containing FPs inside the fuel as well as the chemical species of the elements involved. However, these hypotheses still lack sufficient validation. Such validation should be made possible by the fuel sample microanalysis performed in one part of the ISTP (the aim is to determine FP distributions and, if possible, the chemical species of FPs in matrices of fuel-samples obtained from fuel degradation tests conducted as part of the VERCOR and VERDON programmes).

The experimental database has been extended to cover MOX fuel (two tests) and high-burnup UO_2 fuel (one test) in the VERDON programme, which is part of the ISTP and which ended in 2014.

Releases during reflooding of solid high-burnup fuels were experimentally studied in the QUENCH-ISTC programme. This programme did not provide any significant lessons about releases.

The case of accidents with air ingress into the vessel, such as when the reactor is shut down, is also explored. The available data, primarily Canadian, show that in such

accidents ruthenium behaves like a volatile FP and may be almost completely released from fuel [19]. Models have been developed and in 2012 a specific test in the VERDON programme was conducted to study releases in air from MOX fuel, another one in 2015 will study releases in air from high burn up UO_2 fuel.

5.5.3. Fission product transport in the reactor coolant system and secondary loops (fission gases excluded)

FPs and structural materials are released primarily as gases or vapours. These vapours cool in the vessel upper head and then in the RCS. A number of phenomena occur during this cooling:

- the vapours condense on nuclei and form fine particles in a phenomenon commonly known as homogeneous nucleation;
- the vapours condense on pre-existing particles in a phenomenon commonly known as heterogeneous nucleation;
- the vapours condense on the walls, forming deposits.

The temperatures at which these phenomena occur depend on the chemical form of the FPs and structural materials. Fission product chemistry is discussed in Section 5.5.6. After the vapours condense, the FPs and structural materials are entrained into the RCS primarily in aerosol form. Notable exception are iodine and ruthenium, which can in some circumstances remain in gas form. The main processes involved in such transfers are shown in Figure 5.58.

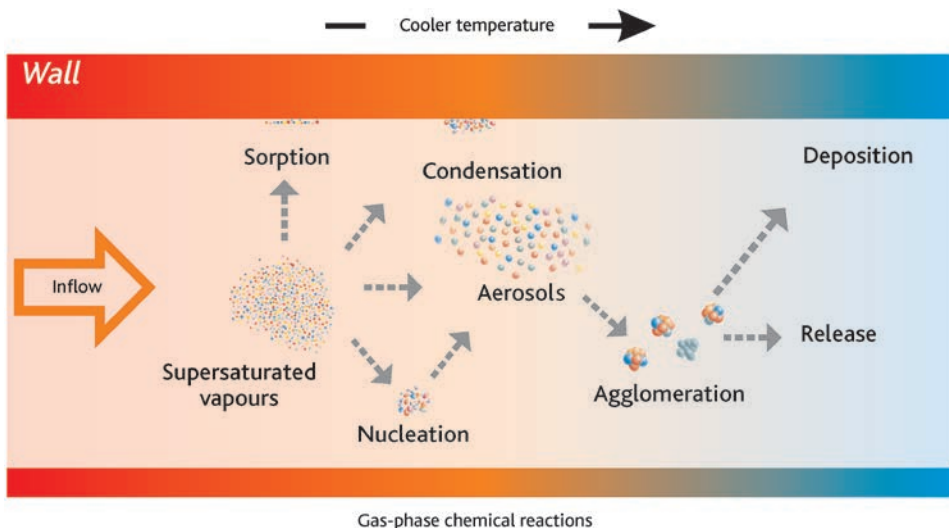


Figure 5.58. Process determining FP transfers to the RCS in aerosol form.

5.5.3.1. Physical phenomena involved in aerosol transfers

► Nucleation phenomena

The formation of particles through homogeneous nucleation can be described at the scale of the atoms and molecules produced or at a more macroscopic scale by directly taking into account particle formation. This macroscopic description is easier to model and yields results similar to those of the atomic-scale description. As a result, it is generally used in computer codes to analyse homogeneous nucleation.

In heterogeneous nucleation, vapours condense on existing aerosol particles consisting of less-volatile elements that have condensed at higher temperatures. The existing models, which analyse the diffusion of molecules in a carrier fluid, are considered to be satisfactory.

► Coagulation (or agglomeration) phenomena

The motion of aerosols formed through nucleation is relative to the fluid carrying them and due especially to Brownian diffusion, turbulence and gravitational settling (sedimentation). This motion leads aerosol particles to collide with each other and stick together (agglomeration). The aerosols grow as they are carried and typically reach a size of a few micrometres in the RCS.

These phenomena are well understood and the available models yield computational results that are satisfactory for the experimental conditions. It should be noted however that some parameters of the models, such as the form factor of the particles (which indicates their deviation from sphericity) are poorly known. However, this lack of understanding does not give rise to any significant uncertainties.

► Deposition by vapour condensation

Part of the FPs and structural materials released as vapours from the reactor core will condense and deposit on the cool walls. This deposition phenomenon is generally modelled using an analogy of mass transfers and heat transfers whereby the values of the dimensionless numbers governing these transfers (Sherwood and Nusselt numbers) are considered to be the same. This assumes that the properties of the vapour species involved, especially their saturation pressure, are known. The associated chemical aspects are discussed in Section 5.5.6.

Prior to the [Phebus FP](#) integral tests, there was a high degree of confidence in the deposition-by-condensation models. But these tests have shown that deposition by condensation was underestimated by a factor of as much as two. A number of assumptions have been explored by CFD calculations. These calculations have made it possible to conclude that this underestimation was caused by effects related to the fact that the flow of fluid in the system was neither thermally nor hydraulically stable [20]. In such situations, the heat-exchange and mass-transfer coefficients are increased, leading to a corresponding increase in the deposits.

► Deposition by gravitational settling (sedimentation)

Aerosols move under the action of gravity and settle on horizontal surfaces. This deposition phenomenon is only significant when the carrier fluid velocity is low and thus the system transit time is long.

This phenomenon is well understood and the available models yield computational results that are satisfactory under the experimental conditions.

► Deposition by Brownian or turbulent diffusion

Brownian motion of particles, particularly those with a diameter of less than $0.1\ \mu\text{m}$, can cause particles to collide with and deposit on walls. This phenomenon is significant only in laminar flows. At high flow rates, aerosols deposit on walls by means of turbulent diffusion. These phenomena are well understood and the available models give computational results that are satisfactory under the experimental conditions.

► Deposition by impaction

This phenomenon occurs especially where there are changes in system geometry: elbows, changes in cross-section, obstacles, etc. The inertia of the particles moves them away from the lines of flow and can cause them to collide with the walls. Aerosol size is an important factor. Deposition by impaction occurs primarily with large aerosols.

In the RCS, most deposition by impaction occurs in elbows and where there are changes in cross-section (e.g., steam generator tube inlets). This deposition is modelled using physical correlations that generally yield satisfactory results. The case of deposition on the secondary side following an SGTR is discussed below.

► Deposition by thermophoresis

When aerosols are carried by a hot fluid into a system where the walls are cooler than the hot fluid, the temperature gradient between the centre of the hot flow and the cooler flow along the walls results in more collisions between the molecules of the carrier fluid and the aerosols at the centre of the flow than in the vicinity of the walls. This causes the aerosols to move towards the walls, favouring deposition there. Many theoretical and experimental studies have made it possible to establish widely accepted formulae for deposition rates by thermophoresis [21]. Examples of past experimental studies include the TUBA thermophoresis tests carried out by IPSN [22].

The models have been satisfactorily validated by the calculation of the TUBA thermophoresis experiments. Nonetheless, the **Phebus FP** integral tests revealed significant differences between the calculation results and the experimental results for deposition by thermophoresis in steam generators. The calculations overestimate this deposition by a factor of around two. This is true for all the codes used to calculate core melt accidents. A number of areas have been investigated to explain these differences, including

the influence of the differences between the **Phebus** tests and those used to validate the models (e.g., the temperature differences between the fluid and the wall or the differences in aerosol concentrations). CFD calculations following the trajectories of aerosols have also been conducted [24], but a convincing explanation has yet to be found. In the case of core melt accidents following a large RCS break, the differences between the calculation results and the experimental results have little impact on the releases calculated in the containment because the retention in the RCS is low. However, retention in pipes has a strong impact on the possible releases in the case of accidents with containment bypass (e.g., V-LOCA; see Section 4.2.1.3).

► Deposition by diffusiophoresis

Condensation occurs when the walls of the RCS are cooler than the saturation temperature of the steam. This condensation causes a flow of gas that carries particles towards the walls [23]. The models available for calculating deposition by diffusiophoresis are based in particular on the results of the TUBA-diffusiophoresis tests performed by IPSN [25]. They yield satisfactory results for calculating deposition in the RCS.

► Mechanical resuspension

A number of phenomena, such as the production of steam during core reflooding, may lead to significant flows in the pipework. Deposited particles may then be mechanically entrained. This entrainment may be high in the case of a highly turbulent flow and dry deposits. Resuspension phenomena are quite complex. To simplify, resuspension occurs when the aerodynamic forces exerted on aerosols deposited on walls are stronger than the forces causing them to adhere to walls. A number of models have been developed, including one that considers a single layer or several layers of aerosol deposits. The validation of these models is based primarily on the results of the STORM tests [26] conducted at the Joint Research Centre in Ispra, Italy.

A state of the art study on aerosol resuspension, conducted as part of the European **SARNET** network, found that the validation of the models was insufficient, particularly regarding the evaluation of releases from accidents with containment bypass (V-LOCA or SGTR) for which aerosol retention in pipes is an important factor in reducing releases.

► Revolatilisation

This phenomenon is the opposite of deposition by vapour condensation. When the thermodynamic conditions in the RCS (temperature of the fluid carrying the aerosols, oxidising-reducing conditions and vapour concentration in the fluid) change, deposited vapours can revolatilise. Due to the importance of the associated chemical aspects, revolatilisation is discussed in Section 5.5.6.

It should be noted that this phenomenon was clearly demonstrated during the **Phebus FP** integral tests and in the VERCORS tests.

► Deposits in the secondary loop (steam generators and tubes)

During an SGTR (initial or induced rupture), the secondary side of the affected steam generator may be dry or flooded. This can have a significant effect on aerosol deposits in the secondary loop and thus on releases. Considering that very few experiments have been conducted under representative conditions, lower-bound deposition assumptions are currently being used to evaluate aerosol retention in the secondary side of damaged steam generators (these assumptions thus increase the calculated releases). A more realistic assessment of aerosol retention in the secondary side of damaged steam generators was therefore deemed necessary. As a result, the ARTIST experimental program [27] was conducted at the Paul Scherrer Institute (PSI) in Switzerland as part of an international consortium project. The programme led to the development of a new model of aerosol retention usable for cases where the secondary side of a steam generator is flooded.

5.5.3.2. Experimental programmes, physical models and simulation codes

The aerosol physics phenomena have been the subject of many experimental and theoretical studies often conducted outside the field of nuclear engineering, which have led to the creation of basic models. These models show a good consensus and have been implemented in computer codes used to analyse core melt accidents, such as the SOPHAEROS module of IRSN's ASTEC integral code.

SARNET identified two additional priority areas regarding transfers of aerosols in the RCS and the secondary loop:

- mechanical resuspension: efforts were made to better assess the validity of the models using existing data [28] (the STORM programme conducted by the JRC/IE [Joint Research Centre/Institute for Energy]) in the late 1990s;
- deposition in the secondary sides of damaged steam generators: as mentioned above, this topic was explored in the ARTIST programme conducted by PSI, a partner of IRSN [29]. The design of the experimental steam generator was representative of the design of Framatome steam generators, but with a reduced height of 3.8 metres. The steam generator internals and upper structures (separators and dryers) were of the same scale as that of a real steam generator used in the Beznau nuclear power plant in Switzerland. The experiments studied the aerosol retention in broken tubes near and beyond the break, in the separators and dryers, under dry secondary side conditions. Retention in a flooded steam generator was also investigated. The retention factors deduced from these experiments (dry or flooded secondary side) are used to assess the validity of the models of retention in the secondary side of a damaged steam generator.

5.5.3.3. Summary and Outlook

The phenomena associated with the transport of aerosols in the RCS are now generally well understood and satisfactory models, often based on data from fields other than nuclear engineering, have been developed to describe them. The main deposition

phenomena, such as thermophoresis and diffusiophoresis, have been the subject of specific experimental programmes conducted to validate the corresponding models.

The models describing the phenomena of mechanical resuspension of deposited particles due to high flow rates are less well validated. An effort is being made to improve these models.

Because aerosol retention in the secondary sides of steam generators remains poorly quantified, lower-bound retention coefficients are used in safety studies. This matter is the subject of supplementary studies based on the findings of the international ARTIST programme.

5.5.4. Ex-vessel fission product releases

Ex-vessel releases of FPs and aerosols can be caused by several phenomena that can occur inside the containment:

- releases of aerosols from boiling sump water;
- releases during MCCI;
- resuspension of aerosols deposited on containment walls.

The specific aspects of iodine and ruthenium, both of which have a complex chemistry, are discussed in section 5.5.6.

5.5.4.1. Physical phenomena

► Releases from boiling sump water

Aerosols released into the containment during a core melt accident end up primarily in the sump water after settling. Resuspension of these aerosols may occur if the sump water begins to boil. The results of past REST tests [30] carried out by FzK (Germany) have been used to develop semi-empirical models for both soluble and insoluble aerosols.

► Releases during MCCI

Such releases primarily relate to semi-volatile FPs and low-volatile FPs, as volatile FPs are released beforehand during in-vessel degradation and core melt. The release rates depend on the composition of corium and particularly its metallic zirconium content, which determines the oxygen potential of the corium and influences the chemical form of the FPs and thus their volatility. The concrete composition (siliceous concrete or silico-calcareous concrete) also plays a role, particularly because of differences in the production of gases during erosion of the concrete.

Releases during MCCI can be estimated from the FPs vapour pressures calculated using a thermodynamic code such as GEMINI for different corium compositions and concrete types. The highest values are obtained for zirconium-rich corium and siliceous

concrete. The only elements with significant releases (greater than 1%) are barium and strontium.

As the release rates are low, it has not been considered necessary to conduct R&D programmes to refine the results.

► Resuspension of aerosols deposited on the containment walls

Some events, such hydrogen combustion or corium-water interaction may result in high gas velocities near the containment walls and allow resuspension of deposited aerosols. Such resuspension is not addressed by existing models, but experiments are planned to assess if it can have a significant radiological impact on the environment.

5.5.4.2. Experimental programmes, physical models and simulation codes

The effect of possible releases from a boiling sump and during MCCI on releases during core melt seems to be relatively low. Specific models for assessing these releases exist, but they are not implemented in the ASTEC integral code presented in Chapter 8.

5.5.4.3. Summary and Outlook

Ex-vessel releases of FPs can occur if sump water boils (aerosol releases) or during MCCI. Studies conducted on these two issues have revealed only low release rates, which are lower than those in-vessel.

Nor has the possible resuspension of aerosols deposited on containment walls during violent events (such as hydrogen combustion) been investigated in detail. The reason is that such resuspension is not expected to significantly contribute to releases to the environment.

5.5.5. *Behaviour of aerosols in the containment*

Aerosols released into the containment are subjected to the phenomena of agglomeration, deposition and, in some cases, resuspension. The basic physical phenomena are the same as those governing the transport of aerosols in the RCS. They depend on thermal-hydraulic conditions in the containment (humidity rate, condensation or non-condensation of steam). The main deposition phenomena are gravitational settling and diffusiophoresis. Some safety systems, such as sprays, can also have a major influence on aerosol concentrations in the containment.

5.5.5.1. Physical phenomena

► Hygroscopicity and agglomeration phenomena

Aerosol agglomeration phenomena are the same as those at play in the RCS. They cause the particles to increase in size, accelerating their deposition by gravitational settling.

Hygroscopicity can play a major role. Some compounds, such as caesium hydroxide, are able to absorb water molecules and form droplets. This, too, causes aerosol particles to increase in size and accelerate their gravitational settling.

Models for calculating the size of the droplets formed at equilibrium as a function of temperature and relative humidity are available.

A difficulty in using such models lies in the limited knowledge of the chemical species formed by FPs. Prior to the [Phebus FP](#) tests, it was generally accepted that caesium was released into the containment in highly hygroscopic hydroxide form. The first two Phebus FP tests showed that this was not the case. Thermodynamic calculations taking account of the molybdenum releases show that the most likely chemical form of caesium is caesium molybdate. This is consistent with the caesium volatility measured during the tests. However, this finding cannot be directly extrapolated to all possible accident situations because the formation of caesium molybdate depends on the oxidising-reducing conditions in the RCS. Furthermore, the same tests show that the aerosols were agglomerates composed of released structural materials and FPs, the majority of which are poorly soluble. These agglomerates are much less hygroscopic than caesium hydroxide.

Aerosol hygroscopicity and assessments of aerosol settling rates in the containment must therefore be considered with caution. Nonetheless, these uncertainties probably have very little effect on the estimation of releases outside the containment.

► Washout of deposits by water vapour condensation

Aerosols deposited on the containment walls can be washed away by water condensed from vapour and be drawn down into the sumps. A simplistic approach to studying this phenomenon in the computer codes considers that insoluble aerosols are not washed out but that soluble aerosols are. However, the difficulty is the same as that described above regarding aerosol hygroscopicity, i.e., uncertainties exist as to the type of chemical species making up the aerosols and thus their solubility. As most of the chemical species of barium and caesium are soluble, both elements are considered to be soluble.

► Spray removal of aerosols in the containment

The main purpose of the containment spray system in France's PWRs is to prevent excessive pressure from building up in the containment. It also significantly lowers the concentration of suspended aerosols in a matter of hours. In the past, airborne concentrations were assessed using simple time-constant models. More recent studies allow current computer codes to obtain a better physical description of the phenomena involved.

Spray removal of aerosols in the containment depends on the characteristics of the droplets, particularly their masses, velocities and temperatures as they fall. Changes in these characteristics depend on evaporation and condensation phenomena as well as coalescence of the droplets.

The trapping of aerosols by droplets involves the following mechanisms:

- inertial impaction and interception, mechanisms that primarily apply to large aerosols;
- Brownian diffusion, a mechanism that is particularly effective in the case of small particles near droplets;
- phoretic capture, which is associated with movements of particles in a temperature field. This mechanism is particularly effective in the upper part of the containment before the droplets reach thermal equilibrium with the atmosphere.

5.5.5.2. Experimental programmes, physical models and simulation codes

The basic mechanisms involved in aerosol deposition in the containment (deposition by diffusio-phoresis and thermophoresis on the containment walls, deposition by gravitational settling) are well known. Models have been developed to describe these basic mechanisms, often using data from outside the field of nuclear engineering. Where necessary, these basic models were validated by specific experiments such as the PITEAS experiments, which were conducted at Cadarache by IPSN to study of the behaviour of aerosols in the containment [31].

More recently, R&D work conducted in the 2000s have made it possible to explore more deeply issues relating to spray removal of aerosols in order to quantify the kinetics and efficiency of removal of aerosols and gaseous iodine in the containments of France's PWRs. This work includes:

- the CARAIDAS [32] tests conducted by IRSN in a cylindrical enclosure measuring 5 metres high and 0.6 m in diameter. The tests made it possible to determine the individual efficiencies of various mechanisms for collecting aerosols and gaseous iodine species by drops under steady-state conditions, under various conditions representative of a core melt accident (temperature, pressure, humidity, pH of the drops, iodine concentration);
- in terms of modelling, the development of a detailed description of the physical change in the drops during their fall as well as the various aerosol capture mechanisms. This description was implemented in the ASTEC integral code. Its thermal-hydraulic aspects were validated using the results of the CSE [33] tests conducted in the USA and its aerosol aspects were validated using the results of the CARAIDAS tests.

5.5.5.3. Summary and Outlook

The various phenomena governing the behaviour of aerosols in the containment are generally well understood and physical models have been developed to describe them, often using data from outside the field of nuclear engineering. The main deposition phenomena, such as diffusio-phoresis and gravitational settling, have been the subject of specific experimental programmes conducted to validate the corresponding models.

5.5.6. Fission product chemistry

During a core melt accident, FPs are released from fuel as vapours. The chemical form in which they are released depends on the equilibrium with their condensed phase in the fuel. This equilibrium varies during the course of an accident, mainly due to variations in temperature and oxidising-reducing conditions. Once released, FPs soon find themselves in a different environment during their transport in the RCS, with variations in temperature and in the composition of the carrier fluid and changes in their chemical speciation in the RCS. Most of the chemical reactions take place in the gas phase, but the vapours may also interact with pipe walls. The structural materials released to outside the core also play a role (SiC and/or boron carbide control rod materials, tin in the Zircaloy cladding, etc.).

Most of the FPs are released into the containment either in condensed form (aerosols) or rapidly condense there. The behaviour of aerosols in the containment atmosphere is determined primarily by the deposition processes described in Section 5.5.5.1. The chemistry of the FPs has little effect on these processes. A large fraction of the aerosols is washed down into the sump water, where they dissolve depending on their respective solubility.

Iodine [3] and ruthenium are two FPs that exhibit specific behaviour and can be present in significant quantities as gases in the containment. These two highly radiotoxic elements (Section 5.5.1) have a complex chemistry in both their gas and liquid phases and can react with painted surfaces and metal surfaces in the containment. Their interactions with the water and air radiolysis products, formed under the radiation emitted by the FPs in the atmosphere and sumps of the containment, also play an important role.

5.5.6.1. Physical phenomena

► Chemistry of gaseous FPs in the RCS

The chemical speciation of FPs in the RCS during a core melt accident can be estimated by assuming, as a first approximation, that the chemical reactions have reached thermodynamic equilibrium, with understanding of the concentrations of the various chemical elements and of the thermodynamic properties of the various chemical species likely to be formed. However, given the complexity of the chemical systems involved, particularly due to the large number of elements involved in the chemical reactions (FPs, elements released by degradation of the control rods and core structures, hydrogen and oxygen in the carrier gas molecules), the existing thermodynamic databases are not comprehensive enough. Furthermore, some of these databases contain significant uncertainties. It is for these reasons that the chemical species of FPs in the RCS cannot be determined with certainty by thermodynamic calculations.

Furthermore, the thermodynamic equilibrium is not always reached. This is particularly true when chemical reactions occur at a rate too slow for equilibrium concentrations of the species formed to be obtained. While thermodynamic equilibrium is most probably reached at high temperature in the vessel near the core (chemical reactions occur very quickly at high temperature), this is most likely not to be the case in the cold legs,

where the temperatures are lower, and for some species in the parts of the RCS where the temperature of the carrier fluid drops quickly (the steam generators in particular). Thus, in the parts where the temperature drops quickly, the reaction rates become sufficiently slow to have an effect on the final speciation of the FPs. As a result, the species found are not always those that would have been formed at thermodynamic equilibrium.

Studies conducted to determine the species formed initially looked at the volatile elements (particularly iodine) and the simple reaction system limited to the elements Cs, I, O, H [34], while taking into consideration the influence of boric acid. These studies led to the conclusion that, in the absence of boron, iodine is transported as caesium iodide (CsI) with the remaining caesium in hydroxide form (CsOH). The presence of boron may lead to the formation of caesium borate, which is less volatile than CsOH, and where part of the iodine converts to hydroiodic acid (HI), which is more volatile than CsI [36]. These studies are based on the results of experiments conducted with simulated FPs, such as the British FALCON programme [35].

The results of these preliminary studies led developers of computer codes such as MELCOR (an American code; see Chapter 8) to set the chemical forms of the transported elements without taking the chemical reactions into account. The computer codes, such as SOPHAEROS (a module of the ASTEC integral code; see Chapter 8), for which modelling of the transport of FPs in the RCS was developed more recently, calculate the chemical speciation of FPs. These are not thermodynamic calculations of the complete reaction systems. Rather, they are simplified calculations limited to reaction systems most important for the chemical speciation of FPs and which were carried out using a thermodynamic database that was as comprehensive and validated as possible.

The chemical forms selected based on the aforementioned preliminary studies were challenged primarily by the results of the *Phebus FP* programme (Section 7.3). One strong point of this programme is that the source of the FPs and structural materials is the most realistically achievable both in terms of its composition and the release kinetics. This is because the source comes from an irradiated fuel rod cluster undergoing degradation.

In the *Phebus FP* tests, the chemical forms are not determined directly, owing to the detection limits of the various techniques for low amounts of radioactive materials. However, indirect indications are provided by the volatility of the elements (their condensation temperatures) and their solubility in water or acid.

Regarding caesium, the results of the *Phebus FP* programme (Section 7.3) showed that in the presence of a carrier gas rich in water vapour, caesium was primarily in the condensed phase at 700 °C. This is incompatible with caesium hydroxide, which is in the vapour phase at this same temperature. These tests also showed that with a steam-rich carrier gas, two things occur: (1) molybdenum releases are higher than initially expected and (2) molybdenum is present in the RCS at a much higher concentration than caesium, thus promoting the formation of caesium molybdate, a less-volatile species than caesium hydroxide. The concentration of this species is correctly calculated by the ASTEC code, which uses thermodynamic data for the species involving molybdenum. After

reviewing the results of the [Phebus FP](#) tests, the developers of the MELCOR (US NRC) code modified it to take into account the formation of caesium molybdate.

In the case of iodine, calculations made with the ASTEC code predict the formation of caesium or rubidium iodide (equivalent properties). The [Phebus](#) tests, particularly FPT2, showed that this is not always the case. Depending on the oxidising-reducing conditions and the concentration of elements from the control rods in the RCS (Ag, In and Cd or B), caesium iodide and at least one more-volatile species may be present or absent. This chemical speciation is not currently predicted by the models. The aim of the CHIP experimental programme, conducted at Cadarache by [IRSN](#) and devoted to iodine chemistry in the RCS in event of a core melt accident, is to provide indications on the chemical reactions involved and the species formed. This programme is discussed more in detail in Section [5.5.6.2](#).

► Interactions of FPs with the walls of the RCS

Fission product vapours can react with the walls of the RCS. Elements such as tellurium can also be chemisorbed, increasing deposition. However, this does not seem to occur if sufficient amounts of tin (a component of Zircaloy) are transported with tellurium to form tin telluride. If degradation of Zircaloy cladding leads to a significant release of tin, higher amounts of tellurium may be transported by the aerosols in the containment.

The FP vapours condense on the metal walls and react with them. This is particularly the case with caesium in the hot leg of the RCS. This interaction has been demonstrated by many experimental programmes, including the DEVAP programme [\[37\]](#) conducted for [IRSN](#) at CEA's centre in Grenoble, and the [Phebus FP](#) programme. Deposit revaporisation tests conducted on hot-leg samples from the FPT1 test of the Phebus FP programme showed that interactions between caesium and steel may lead to the formation of several different volatile species [\[38\]](#). Revolatilisation of deposited FPs may occur after their main release from the core during a core melt accident. This can lead to long-term releases, particularly in the case of delayed containment failure (failure occurring at least 24 hours after the onset of the accident *via* mode δ or mode ϵ , for example; see Section [4.3.3.3](#)). Such releases are determined by the volatility of the species in the deposits.

► Iodine chemistry in the RCS

In the RCS, iodine is likely to combine with many other elements (FPs or structural materials), particularly caesium, rubidium, silver, indium and cadmium. Iodine may also be present in the RCS as atoms (I), molecules (I₂) or hydroiodic acid (HI). These species have the particularity of being in the gas phase in the conditions that prevail in the RCS during a core melt accident.

Following the studies conducted after the TMI-2 accident, it was generally accepted in the 1980s and 1990s that iodine was transported primarily as caesium iodide (CsI). In 1995, the US NRC conducted a new set of studies aimed at better estimating releases

to the containment during a core melt accident. These studies were summarised in benchmark report NUREG-1465 [40], which indicated that a significant fraction (5%) of volatile iodine (I and HI) may be released into the containment. This percentage was not determined based on experimental results but rather on calculations, for several accident sequences, of the thermodynamics of the Cs, I, O, H simple system supplemented by assessments of the speeds of the chemical reactions for the iodine speciation. As mentioned above, when the reaction rates are sufficiently low, iodine does not have time to fully react with the caesium in the RCS. As a result, non-negligible fractions of volatile iodine (I and HI) remain.

The results of the **Phebus FP** tests show that the behaviour of iodine in the RCS is in reality more complex. Iodine is not always present primarily in the form of caesium iodide, but rather forms species with other elements released during degradation of fuel and structural materials. In particular, thermodynamic assessments have shown that the silver and cadmium in SIC control rods can affect the iodine chemistry in the RCS depending on the oxidising-reducing conditions and temperature levels. Thermodynamic data of the species that may be present in the RCS were compiled and verified. This considerable task has made it possible to implement extensive databases in computer codes such as ASTEC. Despite this work, however, the thermodynamic calculations still do not make it possible to reproduce the iodine behaviour observed during the tests of the Phebus FP tests.

Another notable result of the **Phebus FP** tests is that the presence of gaseous iodine in the containment at the onset of fuel degradation cannot be explained by chemical reactions in the containment. This presence is attributed to an influx of gaseous iodine from the RCS. The fractions of gaseous iodine transported in the RCS at a given moment in relation to the total iodine (gaseous iodine and iodine aerosols) reached 30% during the FPT-0 test and 4% during the FPT1 test [39, 41]. It should be noted that:

- during these tests, the maximum fractions of gaseous iodine were measured when the hydrogen content in the RCS was at its highest (approx. 50%);
- these are estimates for a cold-leg break; the results of the FPT1 test seem to show that the fraction of gaseous iodine is higher for a hot-leg break;
- the difference in iodine concentrations between the two tests (30 times less iodine during test FPT0, which was conducted with only very slightly irradiated fuel) suggests that the reaction rates for the formation of iodine compounds have an influence on the fraction of gaseous iodine;
- the relationship between the fraction of gaseous iodine and the hydrogen concentration is less clear for the FPT2 test;
- the FPT0 test is a special case in that the test fuel was very slightly irradiated and, as a result, the iodine concentrations were not representative of an actual accident sequence.

Phebus tests FPT0, FPT1 and FPT2 were conducted using a SIC control rod like those used in French 900 MWe PWRs (also in most PWRs of Western design) for example. On

the other hand, **Phébus** test FPT3 was conducted using a boron carbide (B_4C) control rod, like the ones used in 1300 MWe and 1450 MWe PWRs. The iodine fraction in the gaseous phase measured in the containment during this test was significantly higher (more than 80% [43]) than during the other tests in the programme. This result can be explained by a number of assumptions, including the absence of silver, indium and cadmium (which reduces the number of elements with which iodine can chemically combine) and the presence of high concentrations of boric acid from oxidation of the control rod (boric acid can combine with caesium, preventing the formation of caesium iodide). The combination reactions of iodine with other elements may be lower and more iodine may remain in gaseous form. The CHIP experimental programme conducted at Cadarache by **IRSN** aims to test these assumptions.

Nevertheless, caution should be exercised in extrapolating these experimental results to real accident sequences in a power reactor. Although studies conducted around the year 2000 on possible releases during core melt accidents took into account the results of the FPT0 and FPT1 tests (by taking a 5% fraction of gaseous iodine in the fluid leaking from an RCS break), supplementary studies are necessary to take into account the implications of the results of the FPT3 test for power reactors.

► Iodine chemistry in the containment sump

Iodine released in aerosol form in the containment behaves like the other aerosols (Section 5.5.5) that are primarily entrained into the sump water. With the notable exception of silver iodide (AgI), most of the metal iodides (CsI , RbI , CdI_2 , InI) are soluble. The soluble iodides dissolve in water, forming I^- and IO_3^- ions.

The large amount of FPs in the containment sump create significant dose rates in the sump water, leading to the formation of water radiolysis products including reactive molecules and radicals such as $\cdot OH$, $\cdot O_2^-$, H_2O_2 , etc. Many chemical reactions take place, the net result of which is radiolytic oxidation of the iodide ions (I^-) into volatile molecular iodine (I_2). The formation of I_2 depends on many parameters, the most important being water pH. If the pH is kept basic, the I_2 production rate is very low.

The sump water also contains organic compounds primarily from submerged paintwork. The iodine reactions with the organic radicals formed through decomposition of these organic compounds due to the dose rates produce volatile organic iodides such as methyl iodide (CH_3I) or low-volatile organic iodides such as compounds of higher molecular weight.

These reactions in the liquid phase (see Figure 5.59) have been studied in depth both experimentally and theoretically, and the associated phenomena are reasonably well understood [45, 46]. However, there remain uncertainties about the effect of some impurities, such as the NO_3^-/NO_2^- ions produced by radiolysis of the gases in the containment atmosphere (a product of radiolysis is nitric acid [HNO_3], which is drawn into the sump by the condensing water vapour), the Fe^{2+}/Fe^{3+} ions from the steel surfaces in contact with the liquid phase in the sump (these ions are formed by corrosion reactions), or the Cl^- ions that may come from cable pyrolysis during an accident involving fire in

the containment. The effect of these impurities is still being investigated by experimental programmes conducted in Canada and Switzerland, primarily as part of the OECD's international *Behaviour of Iodine Project* (BIP).

During the first *Phebus FP* tests, it was noticed that the silver released from the SIC control rods reacted with the iodine in the sump to form insoluble silver iodide. If there is sufficiently more silver than iodine (since this is a reaction between silver particles and iodine solubilised in the form of iodide (I^-) or iodine (I_2), the number of active sites on the surface of the silver particles must be high enough to react with most of the iodine) the concentration of iodide ions (I^-) drops sharply in the sump, leading to very little production by radiolysis of gaseous iodine (I_2). These phenomena have been quantified and models have been developed from the results of dedicated experiments, particularly the *Phebus RTF* tests conducted by AECL to study the reactions of iodine with silver in the sump [47] and the tests conducted by PSI, under the *Phebus FP* programme, to study the stability of silver iodide (AgI) [48].

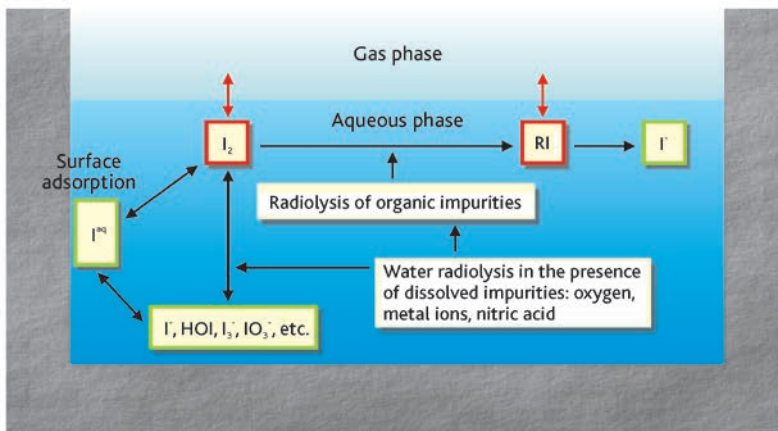


Figure 5.59. Main reactions involving iodine in the liquid phase in the containment sump (taken from [3], reproduced by courtesy of the OECD).

► Iodine chemistry in the containment atmosphere

Gaseous iodine in the containment atmosphere has two origins:

- gaseous iodine exiting the break in the RCS;
- gaseous iodine produced by radiolytic reactions in the sump water.

Transfers of gaseous iodine from the sump obey classic laws of mass transfer. Mass-transfer models exist that can be applied to a sump with and without evaporation of water vapour to the containment atmosphere.

Iodine in the gas phase of the containment reacts with the surfaces in the containment, mainly those made of metal or covered by paint, in physical and chemical adsorption and desorption reactions. These reactions are a function of the temperature and dose rate.

Existing data on iodine adsorption and desorption are derived from laboratory-scale experiments or more integral tests such as those conducted in the RTF [49] in Canada and the CAIMAN facility [50] in France. The experimental parameters investigated were primarily the type of paint, its ageing, temperature and dose rate. The derived correlations correspond to first-order kinetics.

In safety terms, the iodine-paint interactions are highly significant because they lead to the formation of gaseous organic iodides that are not retained by the filters, especially when the containment filtered venting system is opened (U5 procedure in France, see Section 4.3.3.3). Organic iodide production rates were established from the results of a large number of small-scale tests that involved taking painted surfaces on which iodine had been deposited and irradiating them in an atmosphere representative of the containment atmosphere. These tests show that radiation has a greater effect than temperature and their results have been used to develop semi-empirical models. However, given the dispersion of the results and the difficulty in distinguishing the influence of the various parameters, the models are only capable of reproducing the experimental results to within about one order of magnitude.

When exposed to radiation, molecular iodine (I_2) is oxidised by the radiolysis products of the gases in the containment atmosphere (ozone and nitrogen oxides) to form iodine oxides and nitroxides. These compounds are less volatile than molecular iodine particularly because they react with the water vapour to form compounds that are entrained down to the sump. Several reactions occur simultaneously (Figure 5.60):

- the oxidising species (ozone and nitrogen oxides) are formed and destroyed by irradiation;
- the oxidising species interact with the metal surfaces and painted surfaces;
- the oxidising species react with the iodine;
- the iodine reacts with the metal surfaces and painted surfaces.

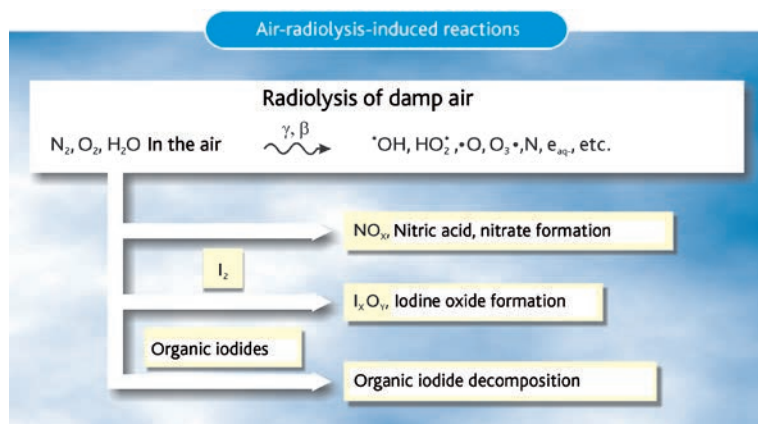


Figure 5.60. Main reactions involving iodine and radiolysis products in the containment atmosphere sump (taken from [3], reproduced by courtesy of the OECD).

The tests conducted during the preliminary studies on the effect of air radiolysis products, particularly ozone, found high iodine concentrations. The models derived from these tests could not be easily extrapolated to the conditions of a core melt accident in a power reactor. More recent tests (PARIS project [51]) have made it possible to gain a better understanding of the phenomena and identify the most influential parameters.

Organic iodine (CH_3I) is also destroyed by reactions with air radiolysis products. The tests carried out show that the destruction rate of organic iodine is proportional to the dose and that temperature has little effect on the rate of the destruction reaction.

An important mechanism that lowers the concentration of gaseous iodine in the containment is its capture by the spray droplets [32]. This mechanism involves the following process:

- transfer of the iodine from the gas phase to the droplets;
- transfers at the gas-droplet interface and within the droplets;
- in-sump liquid-phase chemical reactions.

Capture of gaseous molecular iodine depends on the pH of the droplets. It is more efficient when the pH is basic, which is the case when the containment spray system (CSS) is used in direct mode. Unlike molecular iodine (I_2), organic iodine (CH_3I) is not efficiently scavenged by the droplets.

The RECI tests [52] conducted by IRSN in the early 2000s studied the possible interactions of iodine in the recombiners. The following phenomena are involved in these interactions:

- heating of the metal halide aerosols (CsI , AgI , CdI_2 , etc.) as they pass between the plates of the recombiners;
- vaporisation and dissociation of the iodides, leading to the formation of dissociated gaseous iodine in the hottest sections;
- quenching at the outlets of the recombiners, with the formation of gaseous molecular iodine and fine aerosols by nucleation.

The small-scale RECI tests have more recently been supplemented by larger-scale tests using real recombiners and conducted as part of OECD/NEA THAI project [53]. The production of gaseous iodine by iodide dissociation in the recombiners has been quantified and its impact on iodine releases during a core melt accident has been assessed. Although this impact is not zero, it is lower than that of other phenomena, such as gaseous iodine injected into the containment from the RCS.

► Ruthenium chemistry

As mentioned in Section 5.5.2, large amounts of ruthenium may be released from fuel during an accident with fuel degradation in the presence of air. Such an accident may be a core melt accident caused by vessel melt-through, a spent fuel handling accident, or a spent fuel pool uncover accident [54]. If released to the environment, the dosimetric impact of ruthenium may be high and similar to that of iodine in the short term and caesium in the medium term [6]. Furthermore, ruthenium has a very complex chemistry.

Ruthenium is in metal form in the fuel. However, in the presence of air, it is released primarily as ruthenium(IV) oxide (RuO_2). When it reaches the colder sections of the RCS, RuO_2 can either condense on the walls or oxidise to form gaseous ruthenium tetroxide (RuO_4). This gaseous RuO_4 can then react with the walls and deposit on them in the form of RuO_2 . Due to its kinetics, this last reaction may not be complete in the colder sections of the RCS, allowing ruthenium to persist in the form of gaseous RuO_4 . The behaviour of ruthenium in the RCS was investigated during the RUSSET tests [55-57] conducted by AEKI (Hungary) and tests conducted by VTT [58] in Finland. Conducted under various oxidising-reducing conditions, these ruthenium vaporisation tests revealed, despite significant deposits on the walls of the loops, the existence of gaseous ruthenium in the coolest sections of the loops. During the RUSSET tests, partial pressures of gaseous ruthenium corresponding to the equilibrium between the gaseous RuO_4 and the deposited dioxide were measured at temperatures of around 600-700 °C.

As mentioned above, the gaseous RuO_4 can react with the walls of the pipes and remain trapped there. These effects were studied experimentally by VTT [58] in Finland. The ruthenium deposition (in the form of RuO_2 , as the RuO_4 had been reduced during the reactions with walls) was measured on aluminium oxide and steel pipes. This deposition was light on the aluminium oxide pipes but heavy on the steel pipes except in the presence of water vapour. No explanation was given for this result. The conclusion drawn from these tests is that a significant fraction of ruthenium can be released in gaseous form in the containment.

The behaviour of gaseous ruthenium in the containment was the subject of experiments conducted at IRSN [59-63] as part of the "containment ruthenium" section of the ISTP. These experiments investigated three areas: (1) adsorption and desorption phenomena of gaseous ruthenium on steel walls and painted surfaces; (2) radiation effects that lead to the formation of air radiolysis products such as ozone; and (3) reactions of ruthenium deposited on the containment walls or dissolved in the sump water with these products, which can lead to revolatilisation of gaseous ruthenium.

The results of these tests suggest that, if gaseous RuO_4 is present in the containment, a significant portion of this gaseous ruthenium can remain suspended in the containment atmosphere despite being deposited on its walls. These results also suggest that the ruthenium deposited on the walls or dissolved in the sump water can be revolatilised by radiation. Having been established, the kinetics of these reactions are used to build viable models for determining the quantities of gaseous ruthenium present in the containment of a power reactor during a core melt accident.

5.5.6.2. Experimental programmes, physical models and simulation codes

► Fission product chemistry in the RCS

Regarding the behaviour of FPs in the RCS, the calculation and experimental results are compared primarily for deposition of FPs on the walls of the RCS and for quantities of FPs released to the containment. Work in interpreting these results, especially for

the **Phebus FP** and VERCORS HT tests with the ASTEC code, made it possible to supplement the thermodynamic databases used for relative calculations of the chemistry of the FPs in the RCS. The results obtained using the supplemented thermodynamic databases, now integrated into the ASTEC software, are satisfactory, except for simulating the behaviour of the iodine measured during the Phebus FP tests.

In particular, the ASTEC calculations do not correctly predict the fractions of gaseous iodine present in the RCS. As a result, the CHIP experimental programme was launched in 2005 to obtain additional data on the iodine chemistry in the RCS, both in terms of its thermodynamics and its chemical kinetics. This programme consists of two types of tests conducted at Cadarache by IRSN:

- analytical tests that study chemical systems consisting of, in addition to hydrogen and oxygen (elements that make up the carrier gas), iodine and only one other element in order to obtain data on the kinetics and thermodynamics of the chemical reactions involving iodine;
- larger-scale studies for studying more complex chemical systems having a higher number of elements (representative of the FPs, control-rod components and core structures) in order to obtain data on the amounts of volatile iodine in the RCS as a function of the elements present and the boundary conditions (oxidising-reducing conditions, element concentrations, temperatures, carrier gas flow rates).

These tests are supplemented by literature reviews to establish kinetic and thermodynamic databases for developing kinetic models. When this data are missing or too uncertain, they are obtained using methods of theoretical chemistry (*ab initio* calculations). The models are then validated by comparison with results of the CHIP tests and progressively integrated in the ASTEC code.

The behaviour of ruthenium is studied in the experimental programmes led by AEKI and VTT described in the previous section (5.5.6.1). The results obtained confirm that a significant portion of ruthenium is transported as metastable gaseous RuO_4 to the free volume of the containment even if the gaseous ruthenium deposits onto the steel pipes.

► Fission product chemistry in the containment

Research on this topic primarily covers iodine and ruthenium chemistry in both experimental and modelling terms.

Iodine chemistry in the containment during a core melt accident has been the subject of many research programmes in several countries since the 1980s. There are detailed reviews that present the main advances made in this area (see [3] in particular).

Until the mid-1990s, before the first results of the **Phebus FP** tests had been analysed, the research programmes conducted on iodine chemistry in the containment during a core melt accident primarily focussed on studying volatilisation of molecular iodine from the sump and its adsorption on the metal and painted surfaces in the containment.

This was because it was assumed that iodine was released in the containment exclusively in the form of CsI aerosols, that these aerosols were drawn down to the sump and that they led to the formation of iodides (I^-) through solubilisation of the CsI.

The research programmes conducted at the time made it possible to satisfactorily understand and model the kinetics of the chemical reactions involving, with or without radiation, the inorganic iodine species in the sump (primarily iodides [I^-], iodates [IO_3^-] and molecular iodine [I_2]) [45, 46]. The main parameters that influence the kinetics of the reactions and the volatilisation of molecular iodine from the sump are the pH, the dose rate, the temperature and the oxidising-reducing conditions in the liquid phase. The effect of each of these parameters on iodine volatility has been studied in detail (up to an in-sump temperature of 80-90 °C). It turns out that pH is the parameter that has the greatest influence: a basic pH (in the sump or spray droplets) sharply reduces volatility of iodine in the containment.

Based on the results of these programmes, the conclusion was made that the effect of high temperatures (beyond 90 °C) and of the presence of impurities in the sump on iodine volatility had to be quantified. The aim of the EPICUR programme (conducted by IRSN as part of the ISTP and described in detail below), and the OECD BIP (conducted by CNL, formerly AECL) is to obtain sufficient data to be able to model these effects. It should be noted that PSI has conducted a programme complementary to the OECD BIP to study the effect of the presence of impurities in the sump on iodine volatility.

Research programmes have also made it possible to obtain a database for assessing the adsorption rates of molecular iodine on the metal walls and painted walls of the containment in order to obtain preliminary results for assessing the production of organic iodides from painted surfaces (see, for example, [49, 50], which present the results obtained during the RTF integral tests conducted by AECL and the CAIMAN tests conducted by the CEA for IRSN).

However, the results obtained from the **Phebus FP** tests showed that iodine volatility in the containment could be affected by other processes, particularly:

- releases of gaseous iodine from the RCS. This gaseous iodine, which is not produced by the chemical reactions occurring in the sump, can react directly with the painted walls of the containment and ultimately lead to releases of organic iodides. Furthermore, gaseous iodine can also react with gas radiolysis products in the containment atmosphere. Until the mid-1990s, all these chemical reactions in the containment atmosphere had been studied very little;
- releases of silver through degradation of the SIC control rods. The silver that ends up in the sump forms silver iodide, which sharply reduces the volatilisation of gaseous iodine from the sump. Like the reactions in the containment atmosphere, the influence of silver on the iodine chemistry in the sump had not been studied as part of specific research programmes.

Since then, research programmes studying the influence of silver on iodine volatility in the containment have been conducted by AECL, as part of the international **Phebus FP**

programme, and by PSI [48, 49]. These programmes have made it possible to model the reactions involving silver. This model is integrated in most integral codes for core melt accidents, particularly ASTEC. These models allow a satisfactory understanding of the influence of silver on iodine volatility.

A research programme studying the reactions between gas radiolysis products in the containment atmosphere and gaseous iodine was recently conducted by AREVA-NP in collaboration with IRSN [51]. The results of these tests have increased understanding and modelling of chemical reactions that affect iodine volatility. However, they do not make it possible to precisely quantify this effect. It should be noted that iodine volatility is reduced by the reactions between air radiolysis products and gaseous iodine in the containment atmosphere. The reason is that the products thus formed react with the water vapour and form compounds that are entrained down to the sump.

In 2005, IRSN launched the EPICUR programme as part of the ISTP. The programme aims to study more particularly the processes whose effects on iodine volatility in the containment were insufficiently quantified:

- the formation of organic iodides in the containment atmosphere from painted surfaces;
- in-sump iodine radiolysis, particularly at high temperatures (beyond 90 °C);
- iodine radiolysis in the containment atmosphere.

The EPICUR facility (see diagram in Figure 5.61) consists of a vessel that can hold a liquid phase in its bottom section. This vessel can be exposed to irradiation by ^{60}Co source. Small painted specimens can be placed in either the liquid phase or the gas

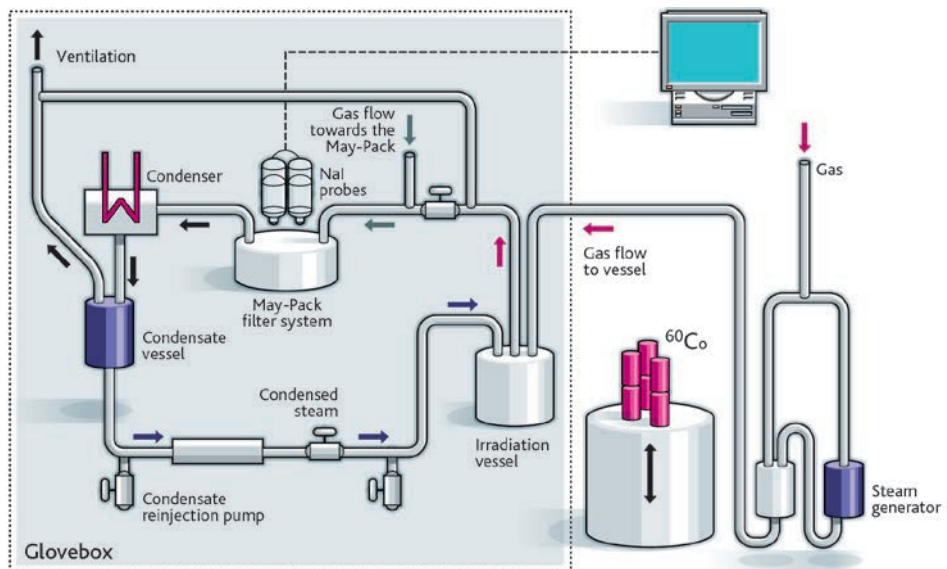


Figure 5.61. Schematic view of the EPICUR facility.

phase of the vessel. The liquid phase can hold iodide ions or molecular iodine solubilised according to its pH. Likewise, iodine can be deposited on the painted specimens before they were placed in the vessel.

Volatile iodine (molecular and organic) produced by radiation from either the liquid phase or the painted specimens, as well as the iodine oxide aerosols produced by radiation in the vessel atmosphere, are continuously entrained by a gas flow and collected in selective filters that separate the iodine, molecular iodine and organic iodine aerosols. The use of iodine containing iodine-131 (^{131}I) makes it possible during a test to perform gamma spectrometry measurements at each filtration stage and determine the kinetics of the processes of volatile iodine production.

The ASTEC code is used at IRSN to interpret these tests. The first part of the programme, which looked at iodine radiolysis in the liquid phase, was fully implemented and made it possible to improve the in-ump iodine radiolysis models. The results obtained also showed that releases of organic iodine from the liquid phase are low but that releases of organic iodine from the painted specimens placed in the vessel atmosphere are high. It remains to be examined whether this mechanism of organic iodine production on the painted surfaces in the containment atmosphere can have an effect on the possible releases during a core melt accident.

It should be noted that, in addition to the tests of the influence of the presence of in-ump impurities on iodine volatility, some of the OECD BIP tests, complementary to the EPICUR tests, investigate the formation of organic iodides from painted surfaces in the containment for the purposes of validating the reaction models involving organic iodides and developed using the results of the EPICUR programme.

At the same time, work on interpreting the Phebus FP tests is continuing, with the participation of a number of partners from outside the programme. The results of the Phebus FPT3 test are drawing special attention. Analyses of these results show that the concentration of gaseous iodine in the containment, very high at the start of the test, decreased quickly and that much iodine is trapped on the painted surfaces of the containment.

In 2010, IRSN published a summary detailing the model of the iodine chemistry in the containment during a core melt accident implemented in the ASTEC code and its use for interpreting the Phebus FPT2 test [65].

An experimental programme on the behaviour of ruthenium in the containment was conducted at IRSN between 2004 and 2008 [59, 63]. This programme investigated a number of areas, including:

- adsorption of gaseous ruthenium by the metal surfaces and the painted surfaces in containment and its desorption from these surfaces;
- revolatilisation of the ruthenium deposited on the surfaces of the containment under the action of ozone and radiation;
- revolatilisation of the ruthenium from the liquid phase of the sump under the action of ozone and radiation.

The results of this programme made it possible to develop models of ruthenium chemistry in the containment during a core melt accident.

5.5.6.3. Summary and Outlook

► Fission product chemistry in the RCS

The **Phebus FP** integral tests have prompted a review of a number of assumptions on the chemistry of FPs – particularly caesium and iodine – in the RCS. Recent studies of degradation in air of fuel have also shown that a review of ruthenium chemistry was necessary.

Contrary to assumptions prior to the **Phebus** tests, caesium is not necessarily in the form of CsOH but can be in the form of caesium molybdate, which is less volatile. The models now take this into account. Phenomena of revolatilisation from deposition in the RCS have also been observed and may lead to delayed releases, after the main release phases associated with fuel degradation, in the containment.

Iodine chemistry is more complex. Iodine is not always in the form of caesium iodide in the RCS. The **Phebus FP** tests show that, apart from the gaseous forms, at least two other species could be present depending on the conditions prevailing in the RCS (other elements present, oxidising-reducing conditions, temperature in the RCS). Part of the iodine is also in gaseous form in the RCS until its release in the containment. Exploitation of the results of the **Phebus FP** tests as well as of the results of the specific studies using the entire set of available experimental data resulted in using a gaseous iodine quantity of 5% in relation to the total iodine released in the containment for studies on releases during core melt accidents. However, the percentage observed during the last test in the **Phebus FP** programme (**Phebus FPT3**) exceeded 80%. This percentage was probably due to highly different chemical conditions in the RCS during the test resulting from the absence of species from degradation of a SIC control rod and the presence of species from degradation of a boron carbide control rod (for this test, the SIC control rod had been replaced by a boron carbide rod). That said, there are two reasons why caution should be exercised in relation to the consequences of this result in terms of the possible releases during a core melt accident:

- the control rods in 1300 MWe and 1450 MWe power reactors are not made solely of boron carbide but are composed in part of a silver-indium-cadmium alloy;
- during the **Phebus FPT3** test, the concentration of gaseous iodine in the containment decreased rapidly and much of this iodine was trapped on the painted surfaces.

As regards more specifically iodine chemistry in the RCS, critical reviews of the thermodynamic data for the various possible chemical species have been conducted and have enabled chemical speciation calculations to be made. However, these calculations do not make it possible to fully reproduce the iodine behaviour observed in the RCS during the **Phebus FP** tests, particularly the existence of several non-gaseous species of metal iodide. A possible hypothesis is that the thermodynamic calculations are

insufficient for modelling iodine chemistry in the RCS, particularly in the sections where the temperature falls sharply (at the core outlet and the inlets of the steam generators), and that they must be supplemented by calculations of the kinetics of the chemical reactions. Indeed, if they are sufficiently slow, the kinetics of some reactions can lead to incomplete reactions of iodine with metallic elements (such as caesium, silver or cadmium) and gaseous iodine. The CHIP experimental programme is continuing to identify the important chemical reactions of iodine with silver, indium and cadmium and determine the kinetic data needed to conduct chemical kinetics calculations.

Experiments conducted in Hungary and Finland have shown that, during a core melt accident with vessel melt-through and air ingress, the ruthenium released from the fuel can be transported as metastable gaseous RuO_4 to the free volume of the containment although a significant amount of the ruthenium remains on the pipes. Additional data on the behaviour of ruthenium in the RCS were collected during a test conducted at the CEA's VERDON facility as part of the ISTP (Section 5.5.2.2) to study in-air degradation of the irradiated fuel, FP releases and associated transfers to the RCS and are collected as part of the OECD STEM project.

Lastly, the experimental data on revolatilisation of FPs deposited in the RCS are insufficient for quantifying the possible effect of this process on releases during a core melt accident. Additional experiments aimed at allowing this quantification are being conducted as part of the OECD STEM project conducted by IRSN and which began in 2011.

► Fission product chemistry in the containment

During a core melt accident, the two FPs whose chemistry in the containment can strongly influence radioactive releases and their consequences are iodine and ruthenium¹². This is due to the fact that both FPs can exist in gaseous form under the conditions prevailing in the containment. These gaseous species may be released to the environment by either direct or indirect leaks from the containment or during implementation of the containment filtered venting procedure.

Iodine

Many experimental and theoretical studies have been conducted on iodine chemistry in the containment during a core melt accident. These studies have looked at iodine chemistry in the sump and the containment atmosphere, its interactions with the surfaces of the containment and the influence of radiation on these various processes [3]. The available models describing this chemistry are either mechanistic, spanning several hundred reactions, or simplified to cover a smaller range of reactions. The latter type of model is generally used in the integral codes such as ASTEC [65].

12. Other FPs, such as caesium, may significantly contribute to the radiological consequences of a core melt accident with containment failure. However, their chemistry in the containment has not a strong influence on their behaviour during releases.

Despite these research efforts, substantial uncertainties remain about the estimation of radioactive iodine releases during a core melt accident. This was brought to the fore during the OECD International Standard Problem (ISP) exercises, which compare the results of calculations and experiments. ISP 41 dealt with iodine chemistry in the containment for an RTF experiment conducted by AECL. ISP 46 dealt with iodine chemistry in the RCS and the containment for the *Phebus* FPT1 experiment. This is particularly true for the formation of organic iodides in the containment atmosphere. The EPICUR, OECD STEM, and OECD BIP experimental programmes aim to provide new data on this matter as well as certain aspects related to liquid-phase and gas-phase iodine radiolysis.

The effect of spraying, which enables partial capture of iodine in droplets, has been quantified and validated models are available.

Analytical experiments have revealed that the interactions between iodine aerosols and the plates of hydrogen recombiners could lead to the formation of gaseous iodine in the containment. A larger-scale experiment was conducted as part of the OECD/NEA THAI project led by Becker Technology in Germany [53]. The transposition of these results to the recombiners in the containment shows that the production of gaseous iodine by the recombiners in the containment is not zero but lower than that due to other sources such as gaseous iodine from the RCS.

Another source of gaseous iodine in the containment is related to radiation-induced decomposition of the metal halides (e.g., caesium iodide) and iodine oxides deposited on the walls of the containment. This is one of the themes of the experimental studies of the OECD STEM project conducted by IRSN which began in 2011.

Ruthenium

Regarding ruthenium chemistry in the containment during a core melt accident, the experiments conducted show that part of the ruthenium can be in gaseous form in the containment. Experiments have made it possible to study adsorption of gaseous ruthenium on the surfaces of the containment and its desorption from the surfaces as well as revolatilisation of ruthenium deposited or trapped in the liquid phase of the sump under the action of radiation [59, 63]. The kinetics of the various processes have been established so that it is possible to assess gaseous ruthenium concentrations in the containment during a core melt accident. Ruthenium transport in the RCS is being studied as part of the OECD STEM project.

5.5.7. Conclusion

Releases and transfers of FPs in the RCS during a core melt accident has been the subject of many research programmes. Releases of FPs from fuel inside the reactor core are in overall terms well understood. Nevertheless, improvements in physical modelling are expected between now and late 2015 on the basis of the results of a few additional tests (VERDON programme conducted by the CEA as part of the ISTEP). The current state of knowledge of releases from corium outside the vessel seems satisfactory.

Transfers and behaviour of FPs in the RCS and the containment are governed by physical processes that depend primarily on aerosol physics and chemical processes. Aerosol physics is well established and the corresponding models seem satisfactory. Nevertheless, it would be desirable to have additional data in order to better analyse some complex situations, such as aerosols in the secondary sides of steam generators during an accident with steam generator tube rupture. The situation is different for the chemical processes. Although the analysis of the results of the programmes conducted between 1990 and 2010, particularly those of the [Phebus FP](#) programme, have made it possible to improve understanding and modelling of the most important processes, additional programmes remain necessary to reduce the uncertainties, particularly regarding iodine chemistry. Improvements in modelling are expected to be made by late 2015 on the basis of the experimental results of the ISTP programmes (CHIP, EPICUR) and OCDE BIP-2, THAI-2 and STEM. The research conducted on this topic brings aspects of chemical kinetics into play in complex reaction systems.

The models developed are implemented in computer codes, such as ASTEC. These codes play a role in the capitalisation of knowledge and are used to conduct safety studies for power reactors.

Reference documents

- [1] A.L. Wright, Primary System Fission Product Release and Transport, A state-of-the-art report to the Committee on the Safety of Nuclear Installations, NUREG/CR-6193, [NEA/CSNI/R\(94\)2](#), ORNL/TM-12681 (1994).
- [2] Insights into the Control of the Release of Iodine, Caesium, Strontium and other Fission Products in the Containment by Severe Accident Management, Report [NEA/CSNI/R\(2000\)9](#), 2000.
- [3] B. Clément (coordinator) *et al.*, State of the Art Report on Iodine Chemistry, Report [NEA/CSNI/R\(2007\)1](#), 2007.
- [4] H. J. Allelein (coordinator) *et al.*, State of the Art Report on Nuclear Aerosols, Report [NEA/CSNI/R\(2009\)5](#), 2009.
- [5] [H. Kleykamp](#), The chemical state of the fission products in oxide fuels, *Journal of Nuclear Materials*, **131**, 221-246, 1985.
- [6] D.J. Alpert, D.I. Chanin, and L.T. Ritchie, Relative Importance of Individual Elements to Reactor Accident Consequences Assuming Equal Release Fractions, NUREG/CR-4467, SAND85-2575, Sandia National Laboratories, Albuquerque, NM, March 1988.
- [7] [Y. Pontillon](#) *et al.*, Lessons learnt from VERCORS tests. Study of the active role played by UO₂-ZrO₂-FP interactions on irradiated fuel collapse temperature, *Journal of Nuclear Materials* **344**, 265-273, 2005.
- [8] [M. Barrachin](#), P.Y. Chevalier, B. Cheynet, E. Fischer, New modelling of the U-Zr-O phase diagram in the hyper-stoichiometric region and consequences for the fuel

- rod liquefaction in oxidising conditions, *Journal of Nuclear Materials* **375**, 397-409, 2008.
- [9] S. Valin, Étude des mécanismes microstructuraux liés au relâchement des gaz de fission du dioxyde d'uranium irradié, Thèse à l'Institut National Polytechnique de Grenoble, 1999.
- [10] Y. Pontillon *et al.*, Behaviour of fission products under severe accident conditions: The VERCORS experimental programme - part 1: General description of the programme - part 2: Release and transport of fission gases and volatile fission products - part 3: Release of low-volatile fission products and actinides, *Nuclear Engineering and Design* **240** (7), 1843-1852, 2010.
- [11] H. Albrecht *et al.*, Release of Fission and Activation Products during Light Water Reactor Core Meltdown, *Nuclear Technology* **46**, 559-565, 1979.
- [12] R.A. Lorenz, M.F. Osborne, A summary of ORNL Fission Product release tests with recommended release rates and diffusion coefficients, ORNL/TM-12801 – NUREG/CR-6261, 1995.
- [13] D.S. Cox *et al.*, Fission Product releases from UO₂ in air and inert conditions at 1700-2350 K: analysis of the MCE-1 experiment, ANS-ITM on the safety of thermal reactors, Portland, USA, 1991.
- [14] T. Kudo *et al.*, VEGA; an experimental study of radionuclides release from fuel under severe accident conditions, ANS Water reactor fuel performance meeting, Kyoto, October 2005.
- [15] G. Ducros *et al.*, Fission Product release under severe accidental conditions; general presentation of the program and synthesis of VERCORS 1 to 6 results, *Nuclear Engineering and Design* **208** (2), 191-203, 2001.
- [16] B. Clément and R. Zeyen, The Phebus Fission Product and Source Term International Programme, *Int. Conf. Nuclear Energy for New Europe*, Bled, Slovenia, 2005.
- [17] W. Plumecocq *et al.*, Fission product release modelling in the ASTEC integral code: the status of the ELSA module, *8th Int. Conf. On CANDU fuel*, Honey Harbour, Ontario, 2003.
- [18] G. Nicaise *et al.*, Analysis of accidental sequence tests and interpretation of fission product release: interdependence of Cs, Mo and Ba release, *8th Int. Conf. On CANDU fuel*, Honey Harbour, Ontario, 2003.
- [19] R.D. Barrand, R.S. Dickson, Z. Liu, D.D. Semeniuk, Release of fission products from CANDU fuel in air, steam and argon atmosphere at 1500-1900 °C: the HCE3 experiment, Canadian Nuclear Society, *6th Int. Conf. CANDU fuel*, Niagara Falls, 26-30 Sept., 1999.
- [20] M. P. Kissane, I. Drosik, Interpretation of fission-product transport behaviour in the PHEBUS FPT-0 and FPT-1 tests, *Nuclear Engineering and Design* **236** (11), 1210-1223, 2006.

- [21] L. Talbot *et al.*, Thermophoresis of particles in a heated boundary layer, *Journal of Fluid Mechanics*, **101**, 737-758, 1980.
- [22] A. Zoulalian, T. Albiol, Analysis of fluid-wall interactions in an open material system where the residence time distribution of a fluid is known. Application of aerosol deposition by diffusiophoresis, *Canadian Journal of Chemical Engineering* **73** (6), 800-897, 1995.
- [23] M. Missirlian, Modélisation des dépôts d'aérosols par diffusiophorèse dans un écoulement. Application aux réacteurs à eau sous pression en situation accidentelle, thèse de l'université de Provence/ Aix-Marseille I, 1999.
- [24] C. Housiadas, K. Müller, J. Carlsson, Y. Drossinos, Two-dimensional effects in thermophoretic particle deposition: the PHEBUS FP steam generator, *Journal of Aerosol Science* **32** (Suppl.1), 1029-1040, 2001.
- [25] A. Zoulalian, T. Albiol, Evaluation of aerosol deposition by thermo- and diffusiophoresis during flow in a circular duct – application to the experimental programme 'Tuba diffusiophoresis', *Canadian Journal of Chemical Engineering* **76** (4), 799-805, 1998.
- [26] A. De los Reyes *et al.*, International Standard Problem 40 – Aerosol Deposition and Resuspension, Final Comparison, Report [NEA/CSNI/R\(99\)4](#), 1999.
- [27] S. Güntay, D. Suckow, A. Dehbi, R. Kapulla, ARTIST: introduction and first results, *Nuclear Engineering and Design* **231** (11), 109-120, 2004.
- [28] A. Bujan, L. Ammirabile, A. Bieliauskas, B. Toth, ASTEC V1.3 code SOPHAEROS module validation using the STORM experiments, *Progress in Nuclear Energy* **52** (8), 777-788, 2010.
- [29] T. Lind, A. Dehbi, S. Güntay, Aerosol retention in the flooded steam generator bundle during SGTR, *Nuclear Engineering and Design* **241**, 357-365, 2011.
- [30] W. Shoek, M. Wagner-Amb, Resuspension of fission product aerosols from the boiling sump, *Proceedings of the International Centre for Heat and Mass Transfer*, pp. 539-546, 1990.
- [31] V. Saldo, E. Verloo, A. Zoulalian, Study on aerosol deposition in the PITEAS vessel by settling, thermophoresis and diffusiophoresis phenomena, *J. Aerosol Science* **29** (Suppl.2), S1173-S1174, 1998.
- [32] V. Fournier-Bidoz, V. Layly, D. Roblot, J. Vendel, Efficiency of the PWR spray system – information derived from the CARAIDAS tests, Rapport scientifique et technique IRSN, 2000.
- [33] R.K. Hilliard, A.K. Postma, Large-scale fission product containment tests, *Nuclear technology* **53** (2), 163-175, 1981.
- [34] E.C. Beahm, C.F. Weber, T.S. Kress, Iodine chemical forms in LWR Severe Accidents, NUREG/CR-5942 (ORNL/TM-11861), April 1992.

- [35] A.M. Beard, L. Codron, A. Mason, Boric acid experiments: vaporisation, deposition on Inconel and interaction with caesium hydroxide, EUR 15766/1 EN, Commission of the European Communities.
- [36] E. Hontanon, M. Lazaridis, Y. Drossinos, The effect of chemical interactions on the transport of caesium in the presence of boron, *J. Aerosol Sci.* **27** (1), 19-38, 1996.
- [37] G. Le Marois, M. Megnin, Assessment of fission product deposits in the reactor coolant system: the DEVAP program, *Nuclear Safety* **35** (2), 213-222, 1994.
- [38] A.B. Anderson, A. Auvinen, P.D.W. Bottomley, C.J. Bryan, N.E. Freemantle, J.P. Hieraute, J.K. Jokiniemi, A.F. Kingsbury, A.T. Tuson, Revaporisation tests on samples from Phebus FP: final report, European Commission 4th framework programme, Report ST: RVP(00)-P029, 2000.
- [39] B. Clément, N. Hanniet-Girault, G. Repetto, D. Jacquemain, A.V. Jones, P. von der Hardt: LWR Severe Accident Simulation: Synthesis of the results and interpretation of the Phebus FP experiment FPT0, *Nuclear Engineering and Design* **226** (1), 5-82, 2003.
- [40] L. Suffer, S.B. Burson, C.M. Ferrell, Accident Source Terms for Light-Water Nuclear Power Plants, NUREG-1465, 1995.
- [41] N. Hanniet, D. Jacquemain, An overview of the iodine behaviour in the first two PHEBUS tests FPT0 and FPT1, *Proceedings of OECD Workshop on Iodine Aspects in Severe Accident Management*, Vantaa (Finland), NEA/CSNI/R(99)7.
- [42] N. Hanniet, S. Dickinson, F. Funke, A. Auvinen, L. Herranz, E. Kraussmann, Iodine behaviour under LWR accident conditions: lessons learnt from analyses of the first two Phebus FP tests, *Nuclear Engineering and Design* **236** (12), 1293-1308, 2006.
- [43] Ph. March *et al.*, First Results of the Phebus FPT3 test, *Proceedings of ICONE 14, 14th International Conference on Nuclear Engineering*, Miami, Florida, USA, July 17-20, 2006.
- [44] B. Xerri, S. Canneaux, F. Louis, J. Trincal, F. Cousin, M. Badawi, L. Cantrel, Ab initio calculations and iodine kinetic modeling in the reactor coolant system of a pressurized water reactor in case of severe nuclear accident, *Computational and Theoretical Chemistry* **990**, 194-208, 2012.
- [45] J.C. Wren, J.M. Ball, G.A. Glowa, The Chemistry of Iodine in Containment, *Nuclear Technology* **129**, 297, 2000.
- [46] E. Kraussmann, A state-of-the art report on iodine chemistry and related mitigation mechanisms in the containment, Report EUR 19752 EN, 2001.
- [47] J.M. Ball, G.A. Glowa, J.C. Wren, Summary of the Phebus Radioiodine Test Facility, *Proceeding of the 4th Technical Seminar of the Phebus FP Programme*, Marseille, France, March 2000.

- [48] S. Güntay, R.C. Cripps, B. Jäckel, H. Bruchertseifer, On the radiolytic decomposition of colloidal silver iodide in aqueous solution, *Nuclear Technology* **150**, 303-314, 2005.
- [49] G.J. Evans, W.C.H. Kupferschmidt, R. Portman, A.S. Palson, G.G. Sanipelli, Radiochemical analysis of iodine behaviour in the Radioiodine Test Facility, *Journal of Radioanalytical and Nuclear Chemistry* **180** (2), 225-235, 1994.
- [50] L. Cantrel, Radiochemistry of iodine: Outcomes of the CAIMAN programme, *Nuclear Technology* **156**, (1), 11-28, 2006.
- [51] L. Bosland, F. Funke, N. Girault, G. Langrock, PARIS project: Radiolytic oxidation of molecular iodine in containment during a nuclear reactor severe accident -- Part 1. Formation and destruction of air radiolysis products - Experimental results and modelling, *Nuclear Engineering and design* **238** (12), 3542-3550, 2008.
- [52] F. Deschamps, J.C. Sabroux, Étude de la production d'iode gazeux par un aérosol d'iodure de césium soumis à des températures élevées dans l'air humide, ASFERA, *Actes du 18^e congrès français sur les aérosols*, Paris, 11-12 décembre, 2002.
- [53] CSNI report, OECD/NEA THAI Project Hydrogen and Fission Product Issues Relevant for Containment Safety Assessment under Severe Accident Conditions, Final Report, JT03285992, [NEA/CSNI/R\(2010\)3](#), 2010.
- [54] D.A. Powers, L.N. Kmetyk, R.C. Schmidt, A review of the technical issues of air ingress during severe accidents, US NRC NUREG/CR-6218, 1994.
- [55] L. Matus, O. Prokopiev, B. Alföldy, A. Pintér, Z. Hózer, Oxidation and release of ruthenium in high temperature air, IRSN-AEKI Phebus FP Programme Agreement, Report on in-kind contribution of AEKI part 1, November 2002.
- [56] L. Matus *et al.*, Oxidation and release of ruthenium from short fuel rods in high temperature air, IRSN-AEKI Phebus FP Programme Agreement, Report on in-kind contribution of AEKI part 2 and part 3, December 2004.
- [57] I. Nagy *et al.*, Oxidation and release of ruthenium from short fuel rods above 1500 °C, EUR 21752 EN, April 2005.
- [58] U. Backman, M. Lipponen, A. Auvinen, J. Jokiniemi, R. Zilliacus, Ruthenium behaviour in severe nuclear accident conditions – final report, VTT report PR03/P27/04, June 2004.
- [59] C. Mun, L. Cantrel, C. Madic, A literature review on ruthenium behaviour in nuclear power plant severe accidents, *Nuclear Technology* **156** (3), 332-346, 2006.
- [60] C. Mun, J.-J. Ehrhardt, J. Lambert, C. Madic, XPS investigation of ruthenium deposited onto representative inner surfaces of nuclear reactor containment buildings, *Applied Surface Science* **253** (18), 7613-7621, 2007.
- [61] C. Mun, L. Cantrel, C. Madic, Study of RuO₄ decomposition in dry and moist air, *Radiochimica Acta* **95** (11), 643-656, 2007.

-
- [62] C. Mun, L. Cantrel, C. Madic, Oxidation of ruthenium oxide deposits by ozone, *Radiochimica Acta* **96** (6), 375-384, 2008.
- [63] C. Mun, L. Cantrel, C. Madic, Radiolytic oxidation of ruthenium oxide deposits, *Nuclear Technology* **164** (2), 245-254, 2008.
- [64] L. Cantrel, E. Krausmann, Reaction kinetics of a fission product mixture in a steam-hydrogen carrier gas in the Phebus primary circuit, *Nuclear Technology* **144** (1), 1-15, 2003.
- [65] L. Bosland, L. Cantrel, N. Girault, B. Clément, Modelling of iodine radiochemistry in the ASTEC severe accident code: description and application to FPT2 Phebus test, *Nuclear Technology* **171** (1), 88-107, 2010.

Chapter 6

Behaviour of Containment Buildings

6.1. Introduction

The characteristics of the containment buildings of French PWRs are described in Section 2.3.2.3. Essentially, the containment building, sometimes called the third containment barrier for French reactors, must provide confinement of radioactive substances in the event of failure of the fuel rod cladding (first barrier) and reactor coolant system (second barrier). The best possible leak tightness for the containment building must therefore be sought from design and throughout the service life of the facility.

The containment building is the final barrier implemented to protect the public from radioactive substances released during an accident inside the containment. It includes:

- the reactor building itself (described in Section 2.3.2.3);
- penetrations into this building, which constitute containment discontinuities (i.e. the equipment hatch, personnel airlock, fluid penetrations, electrical penetrations and fuel assembly transfer tube);
- certain pipes, which constitute containment extensions, especially parts of the secondary systems inside the reactor building (in particular the main feedwater pipes and main steam pipes, and the secondary shell and tube bundles of the steam generators, where the tube bundles are also part of the second barrier).

Penetrations are designed to maintain adequate leak tightness under design-basis accident conditions. To achieve this, penetrations that carry fluids are fitted with check valves and isolation valves, most of which are automatically closed by the protection system.

Furthermore, certain systems are considered extensions of the third barrier outside the containment building itself. These are sections of pipes and associated equipment that simultaneously meet the following criteria:

- they are outside the reactor building;
- they may carry either reactor coolant, following an accident that could lead to deterioration of fuel rod cladding (failure of the first barrier), or the containment atmosphere, to the outside of the containment following an accident that could lead to both deterioration of the first barrier and a release of activity from the reactor coolant into the containment (failure of the second barrier).

For example, for reactors in the current French fleet (excluding the EPR), systems could remain open to the outside of the containment or be brought into service by automatic opening of the containment isolation valves during an accident, for recirculation of water from the safety injection system (SIS) and the containment spray system (CSS), or *via* application of operating documents or guides (in particular, the Severe Accident Operating Guide).

On systems that constitute extensions of the third containment barrier, a failure (such as a line break) could lead to transfer of radioactive substances into buildings around the reactor building or into the environment (i.e. to bypass of the third containment barrier).

In situations where the first and second barriers have deteriorated, the integrity and leak tightness of the third containment barrier are essential for preventing the spread of radioactive substances into the environment. This is particularly true during loss of coolant accidents (LOCA), during which radioactive substances are released into the reactor coolant system (RCS) and the containment building. Their spread into the external environment therefore depends on the containment leakage rate and on any containment bypass, which could lead to direct releases of radioactivity into the environment. The quantity of radioactivity that escapes therefore depends on multiple phenomena: overpressure in the containment caused by the accident itself, the reactor building leakage rate at this pressure, and the quantity of radioactive substances present in the containment as gases or aerosols.

In the event of a core melt accident on reactors in the current fleet, the increase in pressure inside the containment would exert large loads onto it (which could be greater than those under the operating conditions used for design of the facility), eventually leading to deterioration of its walls. Increases in temperature and pressure inside the containment could lead to loads such that the maximum leakage rate of the containment adopted in design would be exceeded. This increase in the leakage rate could result from deterioration of the containment walls (in particular, permeability or cracking of the concrete walls could increase under the effect of the thermal and mechanical loads applied throughout facility operations and during the accident) or from changes in leakage around discontinuities in the containment building (penetrations, airlocks etc.).

In this chapter, Section 6.2 describes the behaviour of containment buildings under design-basis conditions for reactors in the current French fleet and the EPR. In particular,

it covers leakage *via* the containment walls and the various penetrations for design-basis operating conditions.

Section 6.3 describes the behaviour of containment buildings under core melt accident conditions for reactors in the current fleet (900 MWe and 1300 MWe reactors).

Section 6.4 describes situations where there could be bypass of the third containment barrier (or its extension) on the current fleet, corresponding to reactor coolant, or the containment atmosphere following an accident, coming into direct contact with the exterior of the containment building (i.e. with peripheral buildings or the environment), due to deterioration of equipment (such as leakage or failure of pipes or equipment on systems that constitute an extension of the third barrier).

Leakage *via* the secondary shell of the steam generators or the external pressure boundary of the water or steam systems located inside the reactor building is not covered.

6.2. Behaviour of containment buildings under design-basis conditions

The reactor building of a facility in the current French fleet comprises:

- either a containment building with a single concrete wall covered with an internal metal sealing liner (900 MWe units);
- or a containment building with double concrete walls (1300 and 1450 MWe units): an inner prestressed concrete wall with no metal sealing liner and an outer reinforced concrete wall. The space between the two walls is maintained below atmospheric pressure by a ventilation system that collects and filters leakage from the inner wall and penetrations prior to its release into the environment (using HEPA filters and iodine traps).

The characteristics of these buildings are specified in Section 2.3.2.3.

It should be noted that the EPR containment building has a double-wall system with dynamic confinement as for the 1300 and 1450 MWe units. In addition, the inside face of the inner wall is covered with a metal sealing liner.

In studying containment leakage, a distinction should be made between:

- leaks *via* peripheral buildings or *via* the annulus between the double walls (on 1300 MWe, 1450 MWe and EPR units), for which radioactive substances could either be deposited inside the facility, or be filtered by the filtration devices fitted to the ventilation systems of peripheral buildings or the annulus; these leaks are called “collected” leakage;
- leaks that are directly released into the environment (on 900 MWe, 1300 MWe and 1450 MWe units); these leaks are called “uncollected” leakage.

For the EPR, design provisions have been made aiming to “practically eliminate” the possibility of direct leakage into the environment.

6.2.1. Single wall containment buildings (900 MWe reactors)

Figure 6.1 below shows the various leakage paths from the containment:

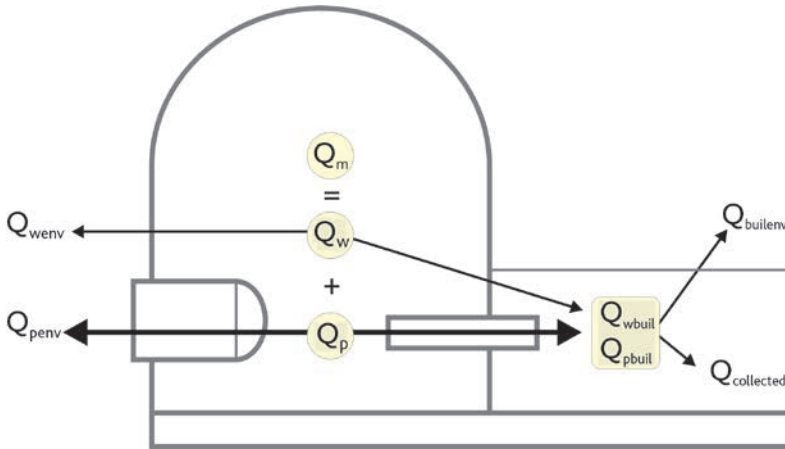


Figure 6.1. The various leakage paths for single containment.

Overall containment leakage (Q_m) includes leakage *via* penetrations (Q_p) and leakage *via* the containment wall (Q_w), which is covered by the metal sealing liner over its whole inner surface (including the basemat), i.e.: $Q_m = Q_p + Q_w$.

Leakage *via* the containment wall or *via* penetrations can be broken down into two main types:

- leakage collected in buildings with a filtration system (with flowrate Q_c). However, part of the leakage *via* these buildings (noted $Q_{builenv}$) could be released into the environment without being filtered, so $Q_c = Q_{wbuil} + Q_{pbuil} - Q_{builenv}$ (where Q_{pbuil} and Q_{wbuil} are the leaks *via* penetrations and the wall that are collected in buildings with filtration systems).
- uncollected leakage (Q_{nc}), which escapes outside the containment without filtration ($Q_{nc} = Q_{wenv} + Q_{penv} + Q_{builenv}$) and has a predominant impact in terms of radiological consequences (Q_{penv} and Q_{wenv} are direct leaks *via* penetrations and the wall).

The construction licences for the 900 MWe PWRs state that the containment building must be designed to withstand, without loss of integrity, the loads resulting from an accident consisting of a sudden double-ended guillotine break (i.e. the loss of coolant accident studied in the context of design-basis accidents). Under the conditions of this accident, the containment’s maximum leakage rate (*via* the wall and penetrations) must not exceed 0.3% per day of the mass of gas inside the containment.

Given that the metal sealing liner provides good leak tightness, only the containment discontinuities (i.e. the various penetrations) are susceptible to causing a significant increase in containment leakage during an accident.

There are several types of containment penetration:

- penetrations comprising one or more pipes crossing the containment wall;
- penetrations for electrical wiring;
- penetrations for ventilation ducts;
- “reserved” penetrations for possible future pipes or wiring not planned in the initial design;
- containment building basemat penetrations;
- the special penetration for the fuel assembly transfer tube;
- the penetration specially designed for moving large equipment items into or out of the containment building, known as the equipment hatch: IRSN and the operator have paid special attention to equipment hatch leak tightness under accident conditions (see Section 6.3);
- the penetration designed for the personnel airlock.

Containment building penetrations are designed to ensure containment leak tightness under the maximum temperature and pressure conditions inside the containment during normal operation and during reference operating conditions (transients, incidents and accidents).

For example, penetrations for pipes include:

- a double seal barrier system comprising the pipe and the cylindrical carbon steel sleeve containing¹ it, along with the isolation valves and non-return valves fitted on the pipe inside and outside the containment building;
- a system for periodically measuring their leakage rate (including the isolation valves);
- provisions for periodic testing of automatic isolation valve operation.

These systems are designed to remain leaktight under all the operating conditions mentioned above, and to withstand the loads associated with a line break and the design-basis earthquake. In all cases, containment isolation must be ensured without manual intervention.

1. The carbon steel sleeve is welded to the metal sealing liner inside the containment; it is embedded and anchored into the concrete wall. Penetration leak tightness is provided by:

- the weld between sleeve and sealing liner;
- the sleeve for all its surface inside the containment building;
- the connector between the sleeve and its pipe.

6.2.2. Double-wall containment buildings (1300 and 1450 MWe reactors)

For reactors in the 1300 and 1450 MWe series, containment is provided by a double-wall structure, with:

- dynamic confinement, provided by the annulus ventilation system (AVS), which creates negative pressure in the annulus and recovers and filters leakage from the inner concrete wall; after filtration, leaks are discharged *via* the nuclear auxiliary building stack;
- static confinement, based on the leak tightness of the inner prestressed concrete wall and the penetrations fitted with seals or with isolation valves on pipes.

Figure 6.2 and the definitions below present the distribution of the various leakage categories for double-wall containments.

The overall containment leakage (Q_m) comprises leaks recovered by the AVS (Q_t) and leaks not recovered by this system (Q_{nt}), i.e.: $Q_m = Q_t + Q_{nt}$.

Leaks not recovered by the AVS (Q_{nt}) comprise:

- leakage *via* penetrations that discharge directly into the external environment (such as the equipment hatch): Q_{1env} ;
- leakage *via* the basemat: $Q_{basemat}$;
- leaks that arrive in buildings fitted with filtration systems, $Q_{building}$, part of which may be released into the environment (Q_{2env}).

Leakage not recovered by the AVS can therefore be expressed as follows:

$$Q_{nt} = Q_{1env} + Q_{basemat} + Q_{building} \quad \text{where } Q_{building} = Q_{2env} + Q_{collected}$$

Non-collected leaks are (Q_{nc}) those released into the environment ($Q_{nc} = Q_{nt} - Q_{basemat} - Q_{collected} = Q_{1env} + Q_{2env}$); they have a predominant impact in terms of radiological consequences. Containment penetrations that do not discharge into the AVS are therefore sensitive elements.

The licence applications for 1300 MWe and 1450 MWe units specify that:

- the internal leakage rate (Q_m) must not exceed 1.5% per day of the mass of gas inside the containment under temperature and pressure conditions consistent with an accident involving a sudden double-ended guillotine break – i.e. the loss of coolant accident (LOCA) studied as part of the design-basis accidents;
- the outer containment leakage rate must not exceed 1% per day of the total mass of gas contained in the volume delimited by the internal face of the outer containment for a negative pressure of 3 mbar in the annulus.

The AVS flowrate is set to ensure that there is a negative pressure of approximately 15 mbar in the annulus under the LOCA conditions cited above. This flowrate means that

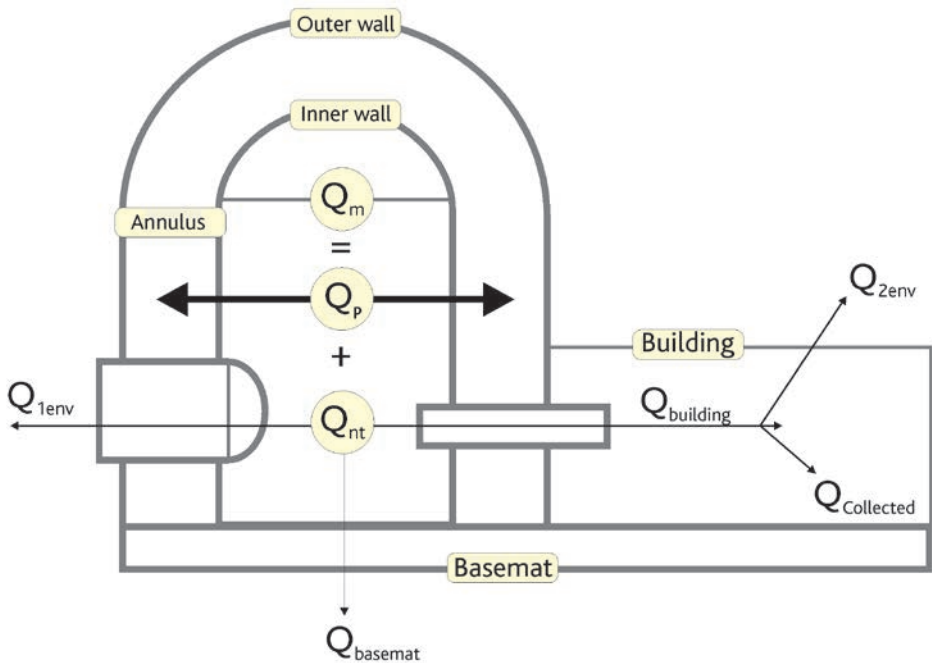


Figure 6.2. Distribution of the various leakage categories for double-wall containments.

negative pressure can be maintained in the annulus under these conditions and prevents any leakage from the annulus to the outside other than *via* the AVS, for the maximum inner containment leakage rate specified in the license application (see above) and for a windspeed of approximately 120 km/h (under these conditions, the negative pressure counteracts the wind suction effect).

Under accident conditions, changes in overall containment leaks and their distribution depend on changes in leaks from the inner containment due to increases in concrete permeability and cracking, on leaks *via* containment penetrations and also on leaks from the outer containment depending on the collection efficiency of the AVS.

6.2.3. Double-wall containment on the EPR

As stated above, for the EPR, design provisions have been made aiming to “practically eliminate” the possibility of direct leakage into the environment.

There must therefore be no direct leakage path from the containment building to the external environment. Pipes that could convey radioactive substances to the outside of the reactor building must lead into peripheral buildings with suitable confinement capacities. Certain buildings around the reactor building, in particular the nuclear auxiliary building, the safeguard auxiliary building and the fuel building, contribute to the containment function (*via* maintenance of dynamic confinement in these buildings by ventilation and filtration systems for aerosols and iodine).

The containment design takes into account core melt accidents with low-pressure failure of the reactor vessel. In the event of an accident of this type, containment integrity must be maintained for 12 hours even with no cooling of the containment building.

The following criteria have been adopted:

- the leakage rate of the inner containment must not exceed 0.3% per day of the gas contained in the inner containment under the accident conditions considered in the design basis (LOCA and core melt accidents);
- the outer containment leakage rate must not exceed 1.5% per day of the total mass of gas contained in the volume delimited by the internal face of the outer containment for a negative pressure of 6.2 mbar in the annulus (which can compensate for the suction effects of an 80 km/h wind).

For accidents considered for the design of the containment including core melt accidents, the AVS must ensure negative pressure in the annulus, and collect and filter leakage from the inner containment which is subject to overpressure due to the accident.

6.2.4. Monitoring the integrity and leak tightness of containment buildings

After the first two “barriers”, confinement of radioactive substances is ensured by the integrity and leak tightness of the containment building and its penetrations under the various temperature and pressure conditions considered.

The containment is subjected to:

- mechanical resistance pressure tests;
- two types of leak tightness tests:
 - overall tests by pressurising the containment;
 - partial tests by local pressurisation of penetrations and isolation systems.

6.2.4.1. Mechanical resistance test

► Initial pressure test

Prior to reactor commissioning, the reactor building is subjected to a mechanical resistance test performed by gradually pressurising the containment up to the test pressure at ambient temperature. Measurements provided by mechanical monitoring devices are recorded during containment pressurisation and depressurisation.

For 900 MWe reactors with a metal sealing liner, the test pressure used is 1.15 times the design pressure of the containment, to take into account the thermal thrust of the metal sealing liner in the event of LOCA.

For the EPR inner containment, which also has a metal liner, this thrust leads to using an initial test pressure of 1.10 times the design pressure.

The test pressure is the design pressure for reactors without a metal sealing liner (1300 MWe and 1450 MWe reactors of the P4, P'4 and N4 series).

► Periodic tests

After the initial pressure test, the containment is subject to mechanical tests at the design pressure during the pre-service inspection and during each of the ten-yearly outage programmes. Measurements provided by mechanical monitoring devices are recorded during containment pressurisation and depressurisation.

Monitoring measurements performed regularly during operation are used to track delayed deformation of the unpressurised structure (concrete shrinkage and creep).

6.2.4.2. Leak tightness tests

► Overall containment leak tightness tests ("type A" tests)

The purpose of overall leak tightness tests is to measure the overall leakage rate for containment buildings with a metal liner (900 MWe reactors and the EPR) and the leakage rate of the inner containment and its components for double-wall reactors without a metal liner (1300 MWe and 1450 MWe reactors). They are performed at the end of construction, i.e. as pre-operational tests prior to first core loading, then every ten years.

Overall leak tightness tests are performed at the design pressure of the containment.

Leakage flowrates are determined by measuring the dry air pressure in the containment (corrected for the partial pressure of water vapour obtained by hygrometer measurements), by measuring the temperature at various places inside the containment and by applying the ideal gas law: variation of the quantity PV/T over time indicates the loss of mass over time and therefore the leakage rate, which is defined as the ratio of the mass of air escaping from the containment in 24 hours to the total mass of air under pressure in the containment.

The leakage rate (including uncertainties) is compared with the criterion, which is 0.162% per day for reactors with a metal liner (900 MWe reactors and the EPR) and 1.125% per day for the inner containment of reactors with double-wall containment with no metal liner (1300 MWe and 1450 MWe reactors).

► Overall leak tightness tests on the outer containments of 1300 MWe and 1450 MWe reactors, and the EPR.

An overall leak tightness test on the outer containment and its penetrations is performed during tests of the AVS, prior to "type A" overall tests.

Essentially, this test is performed by using the AVS to put the annulus under negative pressure (compared with atmospheric pressure) and then measuring the flowrate discharged by this system, which is equal to the flowrate entering the annulus.

For 1300 MWe and 1450 MWe reactors, the acceptability criteria for this test is that the measured flowrate be less than 1% per day of the mass of air in the space delimited by the inner wall of the outer containment for a negative pressure of 3 mbar in the annulus.

► Partial leak tightness tests for penetrations into the reactor building

Partial leak tightness tests are performed for penetrations into the reactor building (into the containment wall for 900 MWe reactors and into the inner wall for 1300 MWe and 1450 MWe reactors and the EPR) to detect and measure local leaks that may affect certain penetrations and associated isolation valves. These tests are subdivided into “type B” and “type C” tests.

The “type B” tests cover:

- “electrical” penetrations (including those for the airlocks);
- sealing systems on personnel airlock doors, including penetrations for door controls;
- the equipment hatch sealing system;
- penetrations fitted with removable blind flanges with seals (in particular, the penetration used for fuel transfer).

The “type C” tests cover isolation valves on pipes that penetrate the containment, other than those subject to “type B” tests and other than those of the secondary systems, which are considered to be closed systems within the containment, maintained above the pressure of the containment atmosphere.

► Leak tightness tests for sections of systems outside the containment that may carry contaminated fluids out of the containment during accidents involving failure of the first two barriers (extensions of the third barrier, see Section 6.1).

For reactors in the current French fleet, this concerns the safety injection system (SIS), the containment spray system (CSS) and the containment atmosphere monitoring system (ETY).

Leak tightness tests on the sections of the SIS, CSS and ETY systems outside the containment are performed at the same frequency as overall leak tightness tests.

6.3. Mechanical behaviour of containments in the event of a core melt accident

6.3.1. Introduction

During a severe accident, the containment building of the concerned reactor may be subject to several types of load that exceed the temperature and pressure conditions adopted for its design. These loads would be induced by the physical phenomena described in Section 5.1 to 5.3, which occur during different phases of core degradation, in particular possible combustion of hydrogen produced during degradation of fuel rod cladding or during reflooding of the degraded core, a vapour explosion inside or outside the reactor vessel, and the slow pressure increase in the containment during the interaction between the corium and the basemat concrete.

Extensive research has been performed and is underway to understand the behaviour of containment buildings on French reactors under the effect of such loads, outside the design basis of the containments. The approach differs depending on the type of containment building, but the objective is the same, as it ultimately involves determining the leakage flowrate from the containment to the environment beyond the temperature and pressure conditions adopted for its design.

The problem is complex and solving it requires sophisticated mechanical studies, in particular involving theoretical assessments of containment stresses and strains, supplemented by experimental studies to confirm the theoretical assessments. R&D work is also needed, in particular regarding the cracking of concrete subject to loads corresponding to a core melt accident. On this subject, EDF has undertaken significant experimental and theoretical work (see the MAEVA Model described in Section 6.3.3.2 and Reference [1] respectively), which mainly applies to the double-wall containments of 1300 MWe reactors.

IRSN has also performed studies to support the Level 2 Probabilistic Safety Assessments (PSA2) for the 900 MWe and 1300 MWe reactors.

As an example, a relatively detailed overview of these studies and the results obtained is given in Section 6.3.2 for the containments of 900 MWe reactors. IRSN has also developed studies for the containments of 1300 MWe reactors. The approach used for the simulations concerning this type of containment is described in Section 6.3.3.

6.3.2. Mechanical behaviour of the containments of 900 MWe PWR power plants

The studies undertaken were based on simulations using nonlinear finite element methods. Models representing the containment at different scales were constructed so that the behaviour of the containment at different levels of detail could be understood (this is called a multi-scale approach), making a distinction between the containment wall, the equipment hatch area and its cover. This approach meant that the various

thermo-mechanical phenomena could be reproduced realistically, while maintaining reasonable times and simulation costs.

A sequence of mechanical simulations were performed using meshes suitable for the level of detail desired for the modelling: complete overall model of the containment building, quarter containment model, local model of the equipment hatch penetration, see References [3] and [4]. However, it was first necessary to specify bounding profiles for the loads to which the containment building would be subjected during a core melt accident.

6.3.2.1. Selection of the core melt accident scenarios used in the studies (increases in temperature and pressure in the containment)

The purpose of the mechanical studies performed by IRSN as part of the level 2 PSA for 900 MWe PWR power plants was to assess the response of the containment building to pseudo-static loads, corresponding to a pressure peak or to a slow rise in pressure, see Reference [1].

Linear calculations, performed for several core melt accident scenarios, were used to determine the scenario leading to the most severe degradations of the containment building. This is the “AF scenario”, which has three phases (see Figure 6.3):

- a thermal pre-loading phase corresponding to core degradation; times P1 and P2 on Figure 6.3 correspond to the beginning and end of this phase respectively;
- the temperature and pressure peak corresponding to adiabatic isochoric combustion of the hydrogen produced by oxidation of core materials; time P3 on Figure 6.3 corresponds to the peak;
- a phase of slowly rising temperature and pressure, corresponding to the molten-core concrete interaction (MCCI) with the corium coming into contact with water from the containment sump; a large quantity of hot gases is produced during this interaction, which causes rising temperature and pressure in the containment; times P4 and P5 on Figure 6.3 correspond to the beginning and end of this phase respectively; P5 has been set to a pressure assumed to be above the maximum resistance pressure of the containment.

A prior parametric study performed for various values of the temperature and pressure peak at time P3 produced a pressure peak value of approximately 11.4 bar abs. (i.e. about 2.3 times the design pressure of the containment). This pressure corresponds to that produced by the adiabatic isochoric combustion of 125% of the maximum quantity of hydrogen produced by core oxidation. Selection of the extreme temperature and pressure values of the AF scenario provides a margin for the mechanical loads on the containment for the core melt accident scenarios covered in the IRSN level 2 PSA. Furthermore, with the aim of quantifying the thermal effects of the accident on the mechanical behaviour of the containment, the AF scenario includes two different temperature rise kinetics (see Figure 6.3): one at time P3, corresponding to a rapid rise in containment temperature, and the other between times P4 and P5 (MCCI phase), corresponding to a

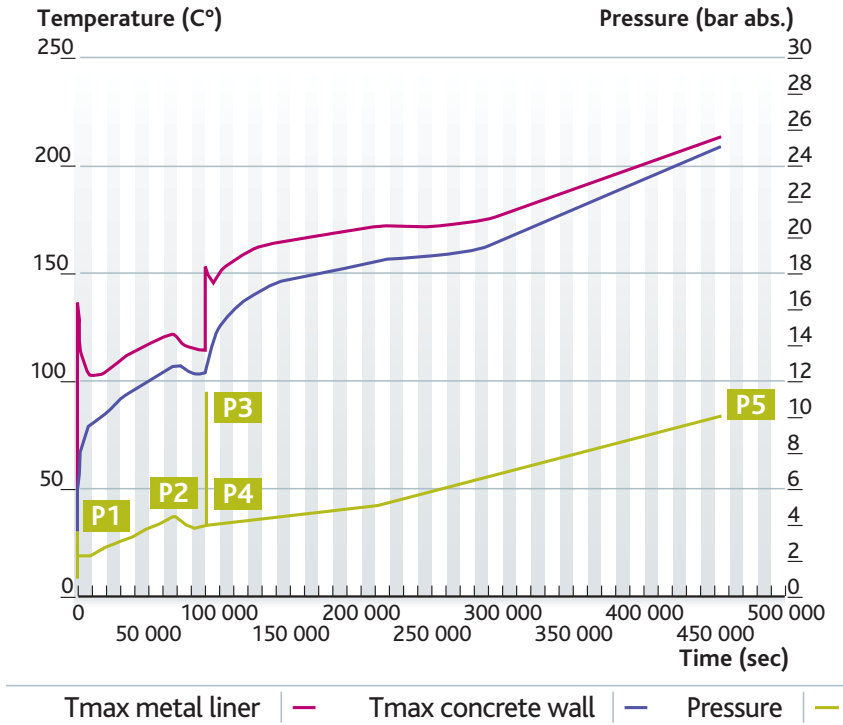


Figure 6.3. Changes in containment temperature and pressure for the AF scenario.

slow temperature rise. This gives the possibility of extrapolating the results of the study performed to other core melt accident scenarios, with different containment temperature change profiles.

6.3.2.2. Complete overall model of the containment building (simulation of the initial state of the containment)

Simulation of the behaviour of the containment building during an “AF” core melt accident scenario requires the most realistic possible knowledge of the state of the structure prior to the accident under the effects of shrinkage and creep phenomena. The age of the containment was taken to be 30 years. A simulation of prestress and creep to determine the state of the structure at 30 years was performed for a containment representative of a 900 MWe PWR power station. This simulation, whose geometrical modelling and mechanical loads are described below, served as a basis for all the simulations performed with the various models described in Sections 6.3.2.3 to 6.3.2.5.

The position and tensioning of prestressing tendons was not sufficiently symmetrical to avoid performing the simulation over the whole containment (360°).

The mesh used reproduced the various containment components: wall concrete, passive reinforcements, metal liner, protective concrete on the basemat, and a simplified model of the equipment hatch penetration with sleeve, flanges and cover. All prestressing tendons, their geometry and their deviations were modelled with precision, in particular around the equipment hatch and the two personnel airlocks. The model also reproduced the effects of the ground and backfill. The images in Figure 6.4 (first left) and Figure 6.5 present the meshes used.

The concrete containment was subject to its own weight and to the prestress of the tendons, simulated taking into account the various phases of tensioning, the various causes of loss of tension (friction, retreat of anchoring heads etc.) and the geometrical specifics of all tendons.

Concrete shrinkage and creep were estimated, during tendon tensioning and over a period of 30 years, using the formulae in French Regulations (BPEL 1999). They were introduced at each step in the simulation in the form of a standard "initial strains"

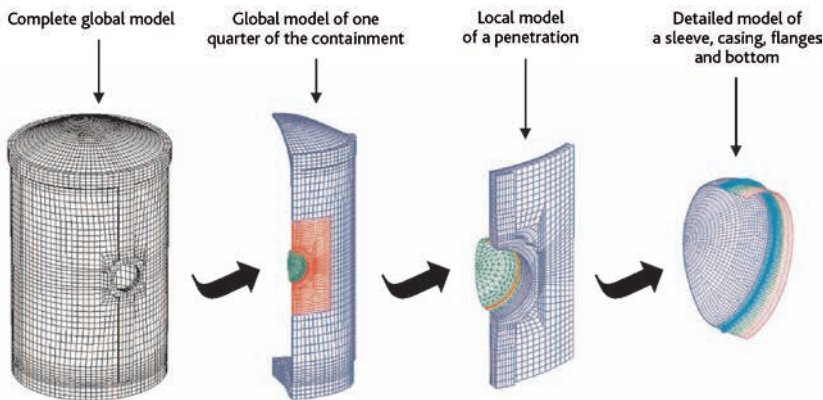


Figure 6.4. Nested models used: complete overall model, overall quarter containment model, local model of a penetration, detailed model of sleeve/penetration/flanges/cover.

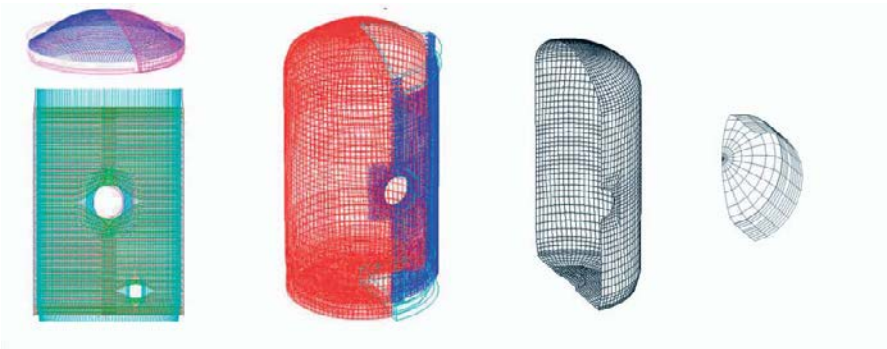


Figure 6.5. Mesh representing the prestressing tendons, passive reinforcements, metal liner, and equipment hatch used for the complete overall model.

loading, based on the drying characteristics of the concrete, the age of the loading and the stress field.

The delayed behaviour of the containment simulated using finite element methods was compared with the results of monitoring measurements performed by EDF at 20 years, which meant that the parameters in the BPEL formulae could be adjusted with respect to the results of these measurements.

6.3.2.3. Quarter containment model

The thermo-mechanical simulation of containment behaviour under the conditions of the "AF" core melt accident scenario was performed using a mesh representing a quarter of this containment to reduce simulation times.

The simulation of prestress and creep performed using the complete model of the containment was used for the quarter containment model, prior to applying the temperature and pressure loads due to the core melt accident.

As for the complete model, the quarter containment model represented the containment concrete, prestressing tendons, passive reinforcements, metal liner, protective concrete laid on the basemat, internal structures, and the equipment hatch penetration with its sleeve, flanges and cover. Figure 6.4 shows the mesh used for this simulation.

The finite element model for the concrete used linear eight-node solid elements with a nonlinear behaviour law that took into account uniform volume cracking of the concrete (using the Ottosen Fictitious Crack Model for the rheology). The finite element model for prestressing tendons and passive reinforcements used two-node bar elements with an isotropic strain-hardening nonlinear behaviour law. The finite element model for the metal liner used shells with an isotropic strain-hardening nonlinear behaviour law. The ground was simulated using a single element extending beyond the horizontal surface of the basemat, which allowed for basemat uplift depending on the loads due to the core melt accident, see Reference [4].

6.3.2.3.1. Analysis of the results of simulations performed using the "quarter containment" model

Analysis of the results of the simulations for the core melt accident studied leads to the following observations:

- the simulations confirm the locations of the most sensitive areas on the containment building, in particular the equipment hatch and the gusset area (see Figure 6.6) which presented through-wall cracks in relation with the tendon gallery;
- comparison of the results of simulations for the AF scenario and those obtained for the scenario without pressure peak P3 shows that this peak has little effect on the later behaviour of the containment building (containment displacements are pseudo-reversible in the main body during the pressure peak);



Figure 6.6. Containment strain amplified 100 times and concrete cracks, in the equipment hatch axis and the main body, at the pressure peak of the AF scenario (time P3).

- overall stability of the structure is provided by the integrity of the prestressing tendons;
- the maximum equivalent plastic strain of the metal liner just after the pressure peak (time P4 on Figure 6.3) is greater than during the pressure peak itself (time P3 on Figure 6.3);
- the mechanical behaviour of the containment can be extrapolated to other scenarios because the results of the simulations show that the mechanical phenomena depend mainly on the pressure;
- possible tears in the metal liner and cracks in the prestressed concrete wall constitute leakage paths;
- the strains calculated for the metal liner remain well below the breaking strain of steel; according to the modelling results, there should not be any tearing of the liner and containment building leak tightness should be maintained.

Analysis and interpretation of the results of the studies described above required recourse to experimental results, in order to define acceptability criteria for the results of the nonlinear simulations performed, so that the risk of containment failure (i.e. of the metal liner or prestressed concrete wall) could be estimated on the basis of the strains observed. To achieve this, the results of the simulations were compared with certain experimental results obtained on scale models, in particular the prestressed concrete containment vessel (PCCV) model used by the American-Japanese programme (NUPEC – NRC – Sandia) described in the following section. A group of

experts was involved in this comparison between simulations and experiments with the aim of specifying these criteria.

6.3.2.3.2. Analysis of the test results on the scale model

Recourse to test results representative of the problem studied is an important aspect for validation of the simulations performed using the CAST3M code for mechanical simulations. The difficulty is in finding tests that are representative of the load conditions under consideration, see Reference [5].

The PCCV model is a 1/4-scale representation of a prestressed concrete containment building with a metal liner. Sandia National Laboratories performed pressure tests on the model with dry air at ambient temperature. These were followed by a destructive test on the containment (to understand its ultimate behaviour).

The tests performed on the PCCV model demonstrated the existence of tears in the metal liner leading to significant leaks for a pressure of around 10.7 bar abs. (which is 2.5 times the design pressure of the model, see Reference [6]).

Analysis of the results of tests performed using this model and of computer modelling of these tests was performed as part of International Standard Problem 48 (ISP48) organised by the OECD, in which IRSN participated. Simulations were run on CAST3M using the same approach as in the simulations for the level 2 PSA project, see Reference [6].

The simulations performed by IRSN and the various teams involved in this comparison did not predict the tears observed at a pressure of 10.7 bar abs., even when taking the various geometrical discontinuities into account, see Reference [7].

For this containment pressure, the circumferential strain measured on the metal liner in the main body was 0.17% and the calculated equivalent plastic strain was around 0.3 to 0.5%. The same order of magnitude for the strain was obtained by the simulations. However, this value is lower than the breaking strain (of the order of 10%) obtained during liner characterisation tests performed after the tests on the scale model.

In order to reproduce the tears in the metal liner, which are a local phenomenon, the computer models used must be at the scale of this phenomenon taking into account the discontinuities constituted by the various welds and liner embedments and by any cracks created in the concrete, by using codes that can simulate strain localisation and tearing of the metal liner.

This difficulty in interpreting the results of the tests performed on the PCCV model led IRSN to call on the group of experts mentioned above. The purpose of this group was to advise IRSN on the best way to use the test results in their application to simulations of containment buildings performed as part of the IRSN level 2 PSA project. At the end of its consultations, the group proposed the following application criterion: the maximum plastic strain in the main body of the metal liner obtained by nonlinear simulations of the main body must be less than $0.30\% \pm 0.15\%$. Beyond this value, tearing of the metal liner is highly likely due to strain localisation. This localisation

effect concentrates the strain at a point in the structure where the strain will exceed the tearing criterion for the material.

A strain value of 0.3% for the metal liner corresponds to a containment pressure of around 10.5 bar abs. for the AF scenario, which would suggest that the pressure that would lead to containment failure is approximately 10 bar abs. (i.e. twice the design pressure of the containment building).

It should be noted that the breaking strength of the penetrations has not been considered in this study.

6.3.2.4. Local model of the equipment hatch penetration

Modelling of a quarter containment, with its prestressing tendons and passive reinforcements, using nonlinear mechanical behaviour laws, requires considerable simulation time, despite relatively coarse spatial discretisation of the geometry. A more specific model was therefore used to study the behaviour of the sensitive areas, such as the equipment hatch, in particular with regard to the risk of separation of the flanges that make up the hatch closure system (such a separation would lead to direct leakage into the environment). This modelled the precise geometry of the flanges and the bolts that keep them together. This local model included the same components as the overall model (the concrete, metal liner, passive reinforcements and prestressing tendons making up part of the 10.60-m-wide and 23.40-m-high cylindrical containment, with the equipment hatch sleeve, flanges and bolts, gussets and anchoring collars in the concrete etc.). The same thermo-mechanical loads and the same material behaviour laws were applied to this local model, along with the prestressing, creep and shrinkage of the concrete used in the overall model.

Several simulations were performed for the penetration, on the basis of the same quarter containment simulation, by modifying certain parameters such as the mechanical characteristics of the bolts, passive reinforcements, mesh, boundary conditions and bolt tightening. These sensitivity studies provide insight into the uncertainties due to the model, the simulations and the materials, which are around 15%.

The flanges were modelled using shell elements, as were the liner, the gussets, the collars and the sleeve/penetration/flanges/cover assembly. Rebars and tendons, and the 44 bolts used to close the equipment hatch were modelled using two-node bar elements (see Figure 6.7). Three types of bolt were considered: the bolts originally used for the containments of 900 MWe PWR power plants (33 mm diameter; yield strength 238 MPa) and two other types of bolt that are considered stronger (33 mm diameter; yield strength 729 MPa, and 24 mm diameter; yield strength 852 MPa).

Over the scope of the local model, the displacement fields obtained using the quarter containment simulation were used as boundary conditions for the local model for each time step. The validity of this method was checked, in particular by comparison of the results obtained with local models of different scales.

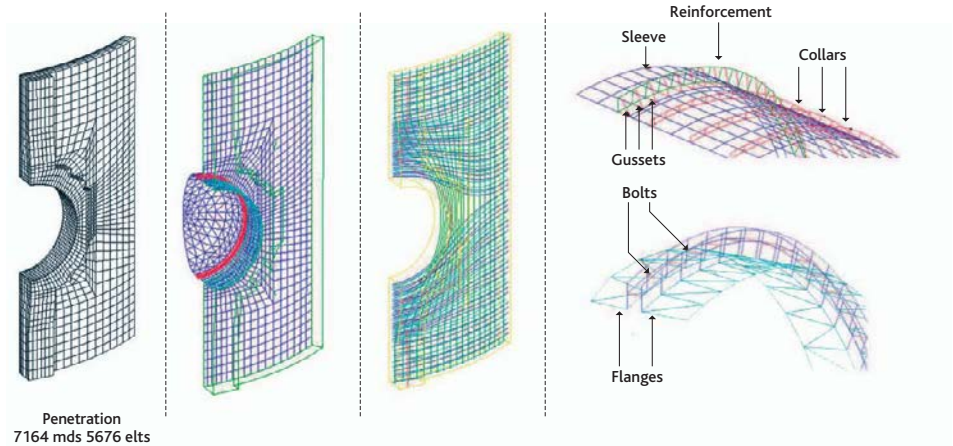


Figure 6.7. Concrete penetration (a), liner/sleeve/flanges/cover (b), tendons (c), sleeve detail (d), details of flanges and bolts (e).

In the absence of experimental data regarding the mechanical behaviour of seals subject to ageing, the studies performed do not take into account the presence of the seal between the two flanges, and only provide the separation between flanges as the result. The main results obtained were as follows:

- the choice of bolts (characterised by their diameter and the yield strength of the steel) is the critical parameter of the mechanical study, with major repercussions on the amplitude of flange separation;
- the temperature and pressure peak (time P3) has relatively little effect on the value of separation as a function of pressure. Flange spacing is therefore mainly conditioned by buckling and ovalisation of the containment around the equipment hatch sleeve, which are not very temperature sensitive;
- regardless of scenario, flange reclosure is only partial after the pressure drops. This is due to plastification of the bolts and irreversible deformations of the concrete containment around the equipment hatch penetration;
- flange separation is approximately constant around the circumference of the sleeve, with an opening length of around 4 m (for the half-circumference). The leakage cross-section is more or less proportional to maximum flange separation.

6.3.2.5. Detailed model

Modelling the flange connection is one of the most complicated aspects of the thermo-mechanical study, and the most sensitive in terms of flange separation. In the local model, use of shell elements leads to overestimating flange separation. This was the motive for producing a detailed model with the following main characteristics:

- solid elements were used to model the metal sleeve, flanges, bolts and hemispherical hatch cover, in order to overcome the difficulties associated with specifying the boundary conditions when using shell or bar elements;

- the mesh was much finer meaning that the real geometry could be more faithfully reproduced (changes in thickness, weld grooves etc.);
- the gussets, collars, concrete and passive reinforcements were not represented in the model. It was assumed that the concrete imposes its displacements and deformations onto the metal parts which are less rigid.

The behaviour laws used were identical to those used for the penetration simulation. Due to symmetry, the mesh used represented a half-circumference (see Figures 6.8 and 6.9).

The detailed model was implemented in a similar way to the local model. The displacement boundary conditions applied were those resulting from the local model simulation. They were applied to the scope of the detailed model. The detailed model with its solid elements and more precise representation of the flanges, spacers and clamps provides better understanding of the behaviour of the closure system. In particular, it brought to light the predominant effect of shear loads on the bolts up to their failure, for moderate pressures in the containment building, with a significant risk of loss of hatch cover leak tightness.

This model therefore demonstrated:

- the complexity of the flange strain mechanisms, excluding any possibility of extrapolation from simplified models, and the strong coupling between flange buckling and ovalisation phenomena;
- the weak effect of axisymmetric loads, from the concrete *via* the sleeve, on flange separation and bolt shear (loads due to pressure in the containment building, and sleeve pinching under the effect of the prestressed compression imposed in the concrete by tendon tensioning) and the importance of non-axisymmetric strain imposed on the sleeve by the containment building, responsible for flange buckling and ovalisation;

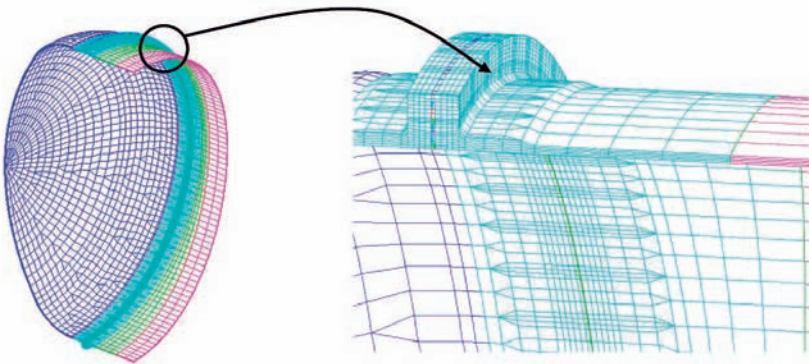


Figure 6.8. Mesh for the whole sleeve and the flange on the hatch cover side (with spacers and bolts).

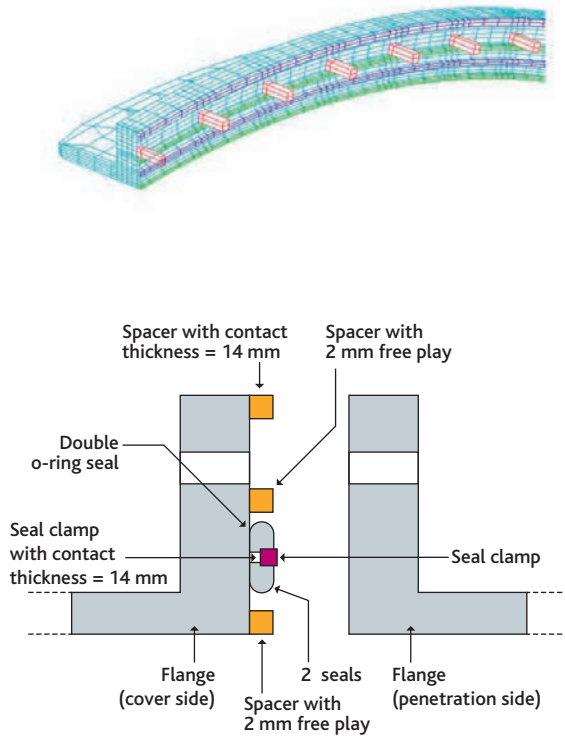


Figure 6.9. Mesh for a flange (with spacers, clamp and bolts) and cross-sectional diagram of the flanges.

- the importance of the choice of bolts (in particular, their diameter and yield strength of the steel), which are subject to shear loads;
- the influence of the free play between bolts and flanges.

With regard to this last point in particular, if the free play between flanges and bolts was not taken into account, the results showed that the bolts plastic yielded at low pressures (between 3.2 and 5.5 bar abs. depending on the bolts selected) if the two flanges were free to slide with respect to each other. These low values, due to bolt shear, were strongly sensitive to the free play between bolts and flanges.

During hydrogen combustion, the margin with respect to shear provided by around 3 mm of free play, which is acceptable with regard to the risk of the bolts yielding, led to irreversible separation of the flanges from pressures of between 6.2 and 8.5 bar abs. depending on the bolts selected. It would appear that reducing the diameter of the bolts is detrimental to their tensile strength, while increasing their yield strength improves their mechanical shear strength.

6.3.3. Mechanical behaviour of the containments of 1300 MWe PWR power plants

6.3.3.1. Approach used in the mechanical studies

The objective for this type of containment is similar to that of the mechanical studies performed for the containment of a 900 MWe PWR. It involves determining the leak tightness limit of the containment building under the thermal and mechanical loads to which this containment is subject during a core melt accident. However, a different approach is used for two key reasons:

- the internal face of the inner containment does not have a metal liner. The purpose of mechanical studies is therefore to determine the ability of the prestressed concrete of the inner containment to maintain confinement under various accident loads;
- leakage from the inner containment appears in the annulus. This space is normally under negative pressure and the gases and aerosols extracted by the annulus ventilation system (AVS) are filtered before discharge. Mechanical studies, as described above, must therefore be supplemented by an examination of possible failures of this system and of the outer containment during a core melt accident, taking severe weather conditions into account (in particular strong winds).

IRSN has performed studies regarding these containments in support of its Level 2 Probabilistic Safety Analysis (PSA2) for 1300 MWe PWR power plants. These studies also support assessment of the studies submitted by EDF as part of the third ten-yearly outage programme for 1300 MWe PWR power plants, in particular studies concerning the management of core melt accidents, bearing in mind that EDF is developing its own studies on this subject. One of the specific difficulties that appeared in the level 2 PSA quantifications and during technical discussions with the operator, is the assessment of leakage *via* the prestressed concrete wall of the inner containment when under pressure, an assessment which affects the quantity of releases of radioactive substances into the annulus and the ability of the AVS to maintain this space below atmospheric pressure. Difficult questions need to be answered to obtain this quantification, in particular:

- understanding of concrete cracking (crack spacing, opening, length, etc.) on the basis of the mechanical stress states in the containment walls. The formulae in French Regulations that apply to concrete shrinkage and creep provide values that are very different from those measured. On this subject, EDF has launched a national study project (the CEOS project) in which IRSN is participating. Results of research actions performed under this project and their analysis are expected this year;
- quantification of leakage *via* a network of intercommunicating cracks which are not necessarily themselves through-wall cracks. IRSN has studied this question as part of the ECOBA project regarding the containment properties of reinforced concrete structures, funded by the French National Research Agency (ANR). Results of research actions performed under this project and their analysis are expected this year.

Given the difficulties stated above and awaiting the results of the aforementioned projects, a semi-empirical approach is used in IRSN studies. The steps of this approach can be summarised as follows:

- the degree of cracking of the inner containment wall is simulated using CAST3M code, using a finite element model of this wall based on the prestress in the tendons, and concrete shrinkage and creep;
- the results of these simulations are adjusted using experimental results obtained during containment pressure tests at design pressure (in particular, concrete cracking measurements are performed following these tests);
- the adjusted model is then validated by comparing the results with those of experiments performed on scale models under conditions similar to those of a core melt accident (see the description of MAEVA tests in Section 6.3.3.2);
- the validated simulation model, performed using CAST3M code, is then applied to the inner containment of a 1300 MWe PWR assumed to be subject to the temperature and pressure loads of a core melt accident deemed adequately bounding.

Completion of these various steps should allow estimates of releases into the annulus to be made this year.

It should be noted that experience feedback on pressure tests performed at design pressure and the results of the initial simulations regarding the mechanical behaviour of 1300 MWe PWR containments show that the concrete of the inner containment does not remain in compression everywhere but has areas in traction that could crack. Furthermore, given the delayed deformations of prestressed concrete, the prestress reduces over time, which increases the extent of the areas that may be found in traction. The areas involved (along with those where concreting faults were observed during the pressure tests) have been covered with a coating to restore leak tightness, in compliance with the leakage rate requirements.

In parallel, IRSN performed a study of the various possible failures of the AVS under core melt accident conditions, in the context of studies to support its level 2 PSA. The purpose was to determine the operating limits of the ventilation system (i.e. its ability to maintain the annulus below atmospheric pressure), its filtration systems, and iodine traps which are very sensitive to the humidity.

6.3.3.2. Experiments performed to support mechanical studies for 1300 MWe PWRs: MAEVA tests

In 1994, EDF decided to produce a scale model of a containment building, in order to study the mechanical resistance of the containment buildings of French reactors. The scale model represents the main wall of the inner containment at a scale of 1/3 for diameter and 1/1 for wall thickness. The annulus is also represented but the concrete outer containment is replaced by a metal wall on the model (see Figure 6.10). EDF's objective was to perform an experimental study of the thermo-mechanical behaviour of the prestressed concrete inner containment for design-basis and beyond-design-basis conditions.

More precisely, the main objectives of the tests were as follows:

- study of heat transfer in a prestressed concrete wall in the presence of a mixture of air and steam;
- study of the behaviour of a prestressed concrete wall under beyond-design-basis conditions, by subjecting the model to scenarios of rising temperature and pressure;
- assessment of air and steam leakage rates under accident conditions by comparison with those measured with dry air during pressure tests;
- study of the behaviour of composite-material coatings for the pressure test sequences and the various accident scenarios, and validation of their implementation conditions at industrial scale.

The results should enable assessment of the ability of the inner containment to provide the confinement function under design-basis and beyond-design-basis accident conditions, and specification of the margins on the leakage rates with respect to pressure test conditions.

The MAEVA scale model consisted of a cylindrical prestressed concrete wall, 16 m in diameter, 1.2 m thick and 5 m tall (see Figure 6.10). It was built on the Civaux site, using high-performance concrete with the same characteristics as the concrete used for the containment on Unit 2 of the Civaux power plant. The upper slab was supported by four prestressed concrete pillars located in the four quadrants of this slab. The inner wall was

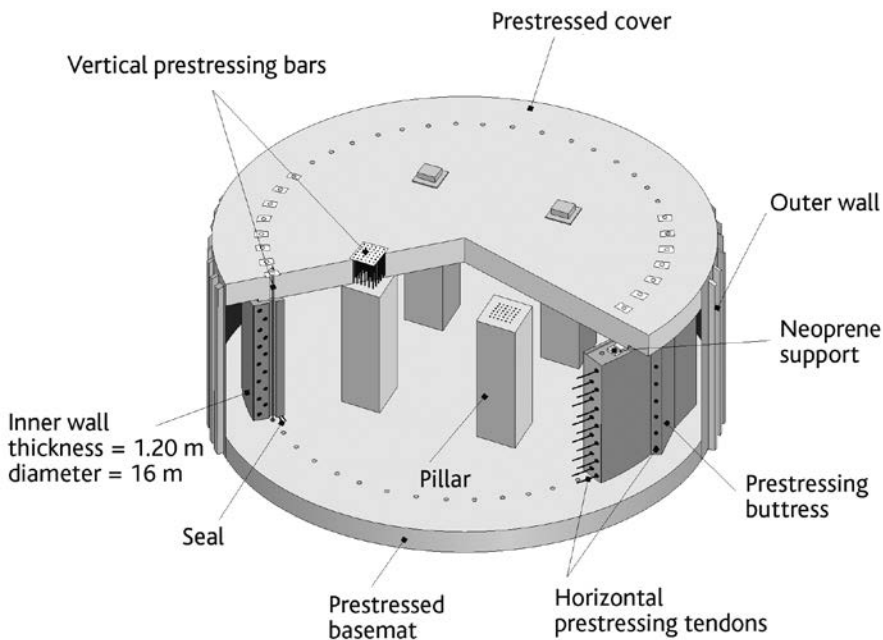


Figure 6.10. Schematic diagram of the MAEVA scale model.

divided into quadrants, two of which were covered with a composite-material sealing layer similar to that used for repairs on units in operation.

As for units in operation, the prestress was calculated to obtain, at a pressure of 6.5 bar abs., a mean residual compression of 1 MPa.

Several tests were performed on this scale model, with air and with a mixture of air and steam, up to the design pressure of the scale model (5.5 bar rel.). To represent core melt accidents, a test with air was performed at a pressure of 9.75 bar rel. (see Figure 6.11).

During each test, the purpose of the measurements performed was to determine leakage rates into the annulus, divided into four sealed quadrants (each quadrant was called a chamber), with dry air and with a mixture of air and steam, along with temperatures in the containment and the concrete wall, pressure in the containment and displacements of the inner wall of the scale model. In addition, a survey of cracks, visual monitoring of the composite-material coatings and bond tests for these coatings were performed. These last tests quantified the adhesion of the coatings on the concrete wall after the test sequences.

Analysis of the results also determined the adjustment coefficient to be used between the leakage rate for dry air and the leakage rate for a mixture of air and steam. This coefficient was then used to determine the leakage rate of real containments under accident conditions based on leakage rates measured during tests. In addition, changes in cracking and measured leakage rates were determined for several accident scenarios. In particular, these results on changes in cracking and measured leakage rates have been used to validate the method for quantifying leaks described in Section 6.3.3.1 (the CEOS project launched by EDF and the ECOBA project funded by ANR, which have just been completed at the time of writing).

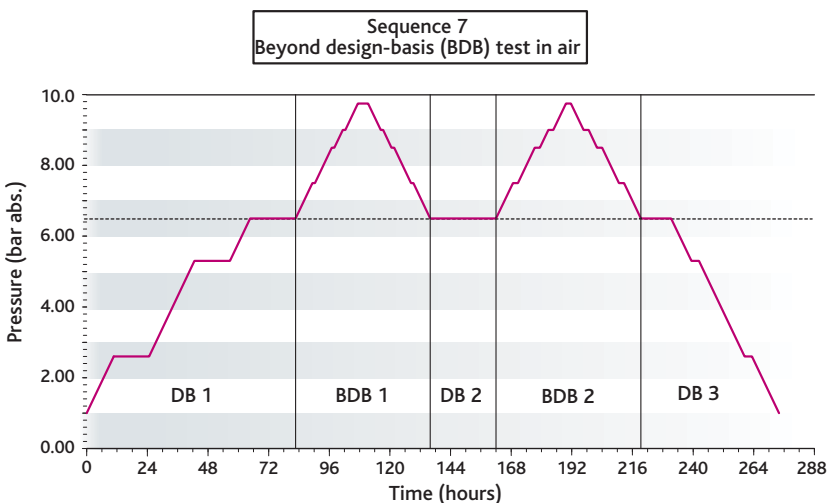


Figure 6.11. Pressure changes during the test performed on the MAEVA model, for core melt accidents.

6.3.4. Summary and outlook concerning studies performed by IRSN regarding the mechanical behaviour of containment buildings under core melt accident conditions

6.3.4.1. Summary and outlook for the containments of 900 MWe PWR power plants

The nonlinear simulations performed by IRSN determined the mechanical behaviour of the containment buildings of 900 MWe power plants under core melt accident conditions, and specifically, the behaviour of the sensitive areas of these structures. Leak tightness of these containments is provided by a metal layer on the internal face of the containment. Taking experience feedback into account, the test results were used to specify a criterion for loss of leak tightness of the metal layer, suitable for finite element simulations.

The value adopted for the pressure leading to loss of leak tightness of such a containment is about 10 bar abs. (twice the design pressure). However, it should be noted that the simulations were performed for an ideal liner, without taking into account any defects that might exist in the welds or any degradation by corrosion, as these phenomena are very difficult to simulate on a computer. For this reason, a safety coefficient should be assigned to the pressure given above, depending on the extent of knowledge of the aforementioned phenomena, in order to determine the failure pressure for such a containment.

The results could be extrapolated to core melt accident scenarios other than the AF scenario. This extrapolation is possible because the mechanical phenomena depend mainly on the pressure.

With regard to the leak tightness of the equipment hatch, the local and detailed models brought to light two modes of loss of confinement, corresponding to tensile failure and shear failure of the bolts. These two failure modes show threshold effects that depend on the choice of bolts and the specific conditions of each facility (initial free play between bolt shank and flange bore, the surface state of the flanges, friction etc.). In all cases, regardless of the failure mode, these studies confirmed the vulnerability of the flange closure system adopted at design, under core melt accident conditions. In order for the containment to resist an accident pressure of at least 8 bar abs., EDF has decided to change the bolts (changing both grade and diameter) on the equipment hatch.

Other than the equipment hatch, the behaviour of the other sensitive areas of the containment, such as the various penetrations, must also be considered for core melt accident conditions, as the containment failure pressure also depends on this behaviour. EDF is working on this subject as part of safety reviews to check the behaviour of equipment under severe accident conditions.

6.3.4.2. Summary and outlook for the containments of 1300 MWe PWR power plants

In the context of performing a level 2 PSA for 1300 MWe PWR power plants, IRSN produced an approach to the study of the behaviour of double-wall containments. This will be used from 2014 during discussions concerning the safety review associated with the third ten-yearly outage programme for 1300 MWe PWR power plants.

However, this approach, which is based on the results of containment pressure tests and tests performed using the MAEVA scale model, is subject to significant uncertainties as concrete cracking is difficult to characterise and the quantification of leakage via cracks is therefore imprecise.

Improvement of knowledge in these two areas is the subject of two projects whose results and their analysis are expected in 2015:

- the 4-year CEOS project, led by the institute for applied research and experimentation in civil engineering (IREX). IRSN was a participant in this project, whose objectives were to study the cracking of concrete walls or shells under various loads (static monotonic loading, early behaviour in the ten days after pouring, effect of constrained deformations, and cracks due to an earthquake);
- the ECOBA project, funded by the French National Research Agency (under the ANR Blanc programme) for a period of three years. The objective of this project was to develop a reliable tool for assessing leakage through a reinforced or pre-stressed concrete wall under severe pressure load conditions possibly combined with a thermal load.

These two projects had complementary objectives, and include a computer modelling and an experimental aspect. Studies using the developed modelling are expected this year.

6.4. Containment bypass

6.4.1. Introduction

The term “containment bypass” covers situations which, following equipment failure, lead to reactor coolant being put into direct contact with the outside of the containment building (i.e. into peripheral buildings or directly into the environment).

Containment bypass could occur during normal reactor operation, during a design-basis accident (in particular, a steam generator tube rupture accident), or during a core melt accident.

Core melt accidents with containment bypass are among the situations that should be “practically eliminated” because they could lead to large early release of radioactive materials. Generally, these situations have not been covered in design for the reactors in the current French fleet, because they result from multiple failures or have a very low probability of occurring.

In contrast, these containment bypass situations have been covered in EPR design *via* suitable design and operating provisions. The purpose of these provisions is to prevent failures on the secondary systems in the event of steam generator tube rupture (SGTR), and failures on systems connected to RCS that leave the containment building. They also aim to ensure reliable confinement in these situations (such that the objectives set for the EPR in terms of limiting releases are met in all cases). The following provisions are among those that contribute to practical elimination of accident sequences with containment bypass for the EPR:

- design provisions on the low head safety injection system (LHSI/RHR, connected to the RCS in particular in certain LOCA situations or during reactor shutdown), whose injection lines outside the containment building are fitted with motor-driven isolation valves that can prevent flow of any fluid from the RCS (in the event of failure of the isolation devices – three non-return check valves – located upstream inside the containment building). The valves are therefore designed to maintain their integrity and provide their isolation function for RCS temperatures and pressures and for two-phase water-steam mixtures;
- design provisions on the medium head safety injection system (MHSI, connected to the RCS in particular in certain LOCA situations) similar to those implemented for the LHSI/RHR;
- design provisions made to detect and isolate breaks in the thermal barriers of the reactor coolant pumps (RCP);
- design and operating provisions implemented for SGTR situations with a view to reducing releases outside the containment building:
 - the MHSI has been designed with a sufficiently low discharge pressure as to avoid loading the relief and blowdown valves of the relevant steam generator secondary system with a two-phase water-steam flow that could damage them;
 - in the event of high water level on the secondary side, the chemical and volume control system (CVCS) is automatically shut down for the same reasons;
- for reactor shutdown states, design and operating provisions for containment isolation systems which must be implemented to ensure that the containment building will be closed before any significant release of radioactive substances into it; this requirement affects the equipment hatch in particular.

Practical elimination of containment bypass situations during a core melt accident is based on systematic consideration of all conceivable bypass sequences, with a deterministic analysis of the corresponding lines of defence, supplemented by probabilistic safety analyses, taking into account uncertainties due to limited knowledge of certain physical phenomena. As specified in the technical directives for the design and construction of the next generation of PWR power plants, practical elimination of an accident sequence cannot be based uniquely on compliance with a generic probabilistic cut-off point. This applies to containment bypass sequences, especially as probabilistic assessments of such sequences, which are associated with large early releases into the

environment, generally depend mainly on estimating the frequency of failure modes for equipment that may contribute to confinement. These failure modes include those already encountered on operating reactors (non-return check valve leakage, isolation valve failure, pipe break on a system connected to the RCS outside the containment building, failure of an RCP thermal barrier, SGTR etc.), and others that have not been encountered in operating experience. For this reason, uncertainties regarding the reliability data for various systems and equipment items whose failure could lead to containment bypass must be assessed and taken into account during use of the results of probabilistic safety analyses.

6.4.2. Possibilities for containment bypass

During normal reactor operation, failure of isolation between the RCS and one of the systems connected to it (in particular, the SIS, RHR, CVCS and CCWS for reactors in the current French fleet) could lead to a line break outside the containment building on the system involved. These systems are not designed to withstand loads resulting from the arrival of reactor coolant (a water-steam mixture at high temperature and pressure) following isolation failure (i.e. failure of a check valve or isolation valve for the SIS, RHR and CVCS, failure of an RCP thermal barrier for the CCWS). Along with the possibility of a pipe break outside the containment building, the heat exchangers used for cooling the RHR, CVCS and CCWS are mechanical weak points. Leakage possibilities are therefore considered.

During design-basis accidents such as SGTR or LOCA, containment bypass may occur in the following cases:

- the combination of a main steam line break (MSLB) and an SGTR;
- a valve on the main steam relief train (MSRT) or a steam generator relief valve jamming in the open position following an SGTR;
- rupture on a system in a peripheral building that constitutes an "extension of the third containment barrier" (see Section 6.1), including the safety injection system (SIS) and the containment spray system (CSS), following LOCA.

Finally, the following types of containment bypass could occur during a core melt accident:

- a single or multiple SGTR caused by an increase in pressure in the RCS when water drains back onto the molten core;
- a line break on the SIS due to a leak affecting the isolation valves fitted to the safety injection lines;
- a line break on a system that is part of the extensions to the third containment barrier (line break on a system connected to the RCS or failure of an RCP thermal barrier).

The following sections give examples of several types of containment bypass.

6.4.3. Types of containment bypass that could occur during reactor operation

6.4.3.1. Rupture on the safety injection system (SIS) following a leak affecting the isolation valves fitted to the safety injection lines in the RCS

In the event of a sealing fault on the isolation devices (check valves) located between the "low head" part of the SIS and the RCS, rupture could occur on the low head part of the SIS (LHSI), due to pressurisation of this part if the leak exceeds the capacity of the SIS safety valves. Such rupture would lead to water from the RCS draining outside the containment building. Depending on valve failure mode, the calculated flowrate from the RCS would be between 25 m³/h and 1000 m³/h.

Estimated frequencies for these "type V" accident sequences, depend on the number of isolation devices and the probabilities of failure, including common cause failure, assigned to these devices. As these probabilities of common cause failure for the various check valves providing RCS isolation are low, the probability of a core melt accident with containment bypass is estimated at approximately 10⁻⁸ per reactor-year for 900 MWe reactors, given that there are three check valves, two of which are diversified. However, this value is subject to large uncertainties.

6.4.3.2. Break on the component cooling water system (CCWS) outside the containment building following failure of a reactor coolant pump thermal barrier

The RCP thermal barriers are cooled by coils which are part of the CCWS. Failure of such a coil could lead to rupture on sections of the CCWS not designed for RCS pressure. This would lead to an RCS break that cannot be isolated. As described below, the break could occur inside or outside the containment building, leading to containment bypass in the latter case.

For 900 MWe units, each RCP is cooled by a part of the CCWS that penetrates the containment building. Inside the containment, isolation of each cooling line (one line per RCP) is reliant on the closure of a non-return check valve located on the CCWS upstream of the RCP and on closure of a pneumatic valve located on the CCWS downstream of the RCP. Valve closure is automatic in the event of excessive flowrate in the CCWS at the outlet of the RCP thermal barrier (excessive flowrate may occur following coil rupture leading to reactor coolant leaking into the CCWS). The section between the non-return check valve and the isolation valve is able to mechanically withstand the temperatures and pressures associated with leakage of reactor coolant into the CCWS, as shown by mechanical calculations performed by IRSN to this end. However, in the event of failure of the non-return check valve or the isolation valve, which are not designed to ensure isolation of the CCWS during a reactor coolant leak (in particular for the corresponding temperatures and pressures and two-phase water-steam mixtures), a break in the CCWS could occur inside or outside the containment

building on sections of the system other than the section between the non-return check valve and the isolation valve.

The estimated frequency of a core melt accident with containment bypass during such a break in the CCWS depends on the ability of the CCWS isolation valve to close. Given the large uncertainties concerning this ability and as part of the safety review associated with the third ten-yearly outage programme for 900 MWe units, ASN requested implementation of a design modification to ensure the availability of the CCWS in the event of thermal barrier coil rupture.

For 1450 MWe reactors, following their first ten-yearly outage programmes, ASN requested that the operator present a detailed analysis of accident scenarios of this type in 2014.

For 1300 MWe reactors, the subject is under examination as part of the safety review associated with the third ten-yearly outage programmes.

For the EPR, the estimated frequency of core melt is very low given that CCWS isolation is qualified to be operable in the event of a guillotine break in the coil and is provided by two diversified valves. Furthermore, by design, only partial loss of CCWS would occur in the event of failure of this isolation.

6.4.4. *Types of containment bypass that could occur during a design-basis accident*

This section describes containment bypass associated with steam generator tube rupture (SGTR).

SGTR leads to reactor trip and automatic startup of the safety injection system (SIS) and the emergency feedwater system (EFWS). The main actions to be performed by the operator are as follows:

- identify the affected steam generator and isolate it on the secondary side. This isolation must be performed quickly to avoid the steam generator filling with water and consequent loading of the associated blowdown and relief valves;
- cool the reactor *via* the healthy steam generators and reduce RCS pressure to stop the primary-secondary leak as quickly as possible and create the conditions for startup of the RHR system. Using specific criteria, operators must shut down the SIS to limit filling of the steam generator with water and allow depressurisation of the RCS.

The path to cold shutdown is pursued by starting up the RHR system.

Following an SGTR, containment bypass may result from a leak of reactor coolant *via* the secondary system blowdown or relief valves occurring after filling of the secondary side of the affected steam generator by reactor coolant. Such a situation could occur if there were a delay in the operator isolating the affected steam generator or shutting down the safety injection system and if the secondary system blowdown or relief valves

should fail to close after operating with water, followed by failure of the RHR system during its startup or operation, which would lead to complete drainage of the refuelling water storage tank (RWST) to the outside of the containment building, thereby making it impossible to provide water injection into the RCS.

In order to reduce the risk of a combination of an SGTR and failure of a secondary-side relief-valve, modifications have been made to reactors in the current French fleet to limit filling of the secondary side of the affected steam generator with water from the RCS, in order to prevent steam generator overflow. Note that the situation is more favourable on 1300 MWe and 1450 MWe units and the EPR, as the SIS discharge pressure (MHSI on the EPR, see Section 6.4.1) is lower than on 900 MWe units. Results of the PSAs show that the probability of a core melt accident with containment bypass associated with an SGTR is very low (less than 10^{-8} per reactor-year for 900 MWe reactors).

6.4.5. Types of containment bypass that could occur during a core melt accident

6.4.5.1. Induced breaks on steam generator tubes

One of the main risks associated with high-pressure core melt accidents is containment bypass following steam generator tube rupture (SGTR).

Existing studies concerning high-pressure core melt accidents, in particular those performed at IRSN, show that RCS failure would initially occur on steam generator tubes (i.e. before hot leg or reactor vessel failure) when these are depressurised (see Section 5.1.4). Furthermore, operating experience feedback has shown that certain steam generator tubes are weakened by reactor operation (weakening by corrosion and fatigue mechanisms). Despite provisions made to monitor the state of the tubes and isolate weakened or corroded tubes (see Section 2.4.2.3), the existence of weakened tubes which constitute one of the mechanical weak points of the RCS pressure boundary cannot be ruled out.

Provisions have been made that aim to prevent high-pressure core melt accidents, given the possible consequences of this type of accident on the third and final containment barrier, in particular in the event of direct containment heating (DCH, see Section 5.2.1). These provisions include deliberate depressurisation of the RCS by opening the pressuriser steam bleed valves. This depressurisation of the RCS is included in the accident operation procedures and is performed immediately by the operators as soon as the Severe Accident Operating Guide is in use (see Section 4.3.3.4).

It should be noted that, in the context of the safety review associated with the third ten-yearly outage programme for 900 MWe reactors, it has been decided to modify the opening control for pressuriser steam bleed valves to make their operation more reliable and thereby make it possible to depressurise the RCS during a core melt accident.

For the EPR, design provisions have been made aiming to "practically eliminate" high-pressure core melt accidents. These are described in Section 4.3.4.2.

Please refer to Section 5.1.4 for more details regarding high-pressure core melt accidents and "induced breaks".

6.4.5.2. Failure of a system that constitutes an extension of the third containment barrier

Systems called "extensions of the third containment barrier" (E3B) are systems required for the management of a given accident situation, whose startup requires the opening of containment isolation valves. A failure (such as a leak or line break) on these systems may lead to transfer of radioactive substances into the buildings around the reactor building or into the environment.

For 900 MWe units, systems that constitute an extension of the third containment barrier during a core melt accident include, in particular:

- the section of the containment building venting and filtration system between the containment isolation valve and the outlet of the sand filter. This system and its uses are described in Section 4.3.3.3;
- the sections of the SIS and CSS systems outside the containment, which carry contaminated water from the sumps located at the bottom of the reactor building when these systems are used in recirculation mode (see Section 2.4.2).

The decision to start up an E3B system can be made by applying the Severe Accident Operating Guide. The decision could also have been made earlier in the course of an accident, in application of the Assistance Guide for Emergency Response Teams.

The definition of an extension of the third containment barrier, the list of E3B systems and the requirements to be applied to these systems are subject to detailed examination by IRSN and EDF, in particular during safety reviews.

In this respect, it should be specified that the concept of an E3B system appeared after the design phase for the facilities. For this reason, the process of applying the requirements associated with the third containment barrier to its extensions has been performed in a checking framework rather than a design framework for reactors in the current French fleet. Initially, this process aimed to check the ability of E3B systems, as designed, to:

- mechanically withstand the loads induced by their role which involves checking via mechanical studies performed on all series;
- ensure confinement of radioactive substances under all conditions to which they might be subject, in particular under accident conditions that require their use.

This IRSN examination of the requirements that apply to E3B systems as part of the safety reviews associated with the third ten-yearly outage programmes for 900 MWe reactors and the second such programmes for 1300 MWe reactors has led to requests to check the mechanical resistance of certain systems which could carry a water-steam mixture under accident conditions (in particular for the NSS/RCS) and the irradiation

resistance of certain equipment items (in particular the seals required for leak tightness of E3B systems).

This examination also led to implementation of modifications to equipment and procedures, with the aim of both ensuring better detection of possible failures on E3B systems and of mitigating consequences in the event of failure of these systems.

With regard to monitoring the leak tightness of E3B systems (in particular the SIS and CSS), additional activity measurements (on the plant radiation monitoring system) and measurements of the water level in the sumps of the nuclear auxiliary building, fuel building and auxiliary safeguard building have been implemented on the facilities.

With regard to means for mitigating any consequences in the event of failure on the systems, EDF's current strategy consists of reinjecting the contaminated effluents recovered outside the containment back into the containment, whether for design-basis accidents or core melt accidents. Analysis of the modifications associated with this strategy, which have already been implemented for the 900 MWe series as part of the third ten-yearly outage programmes, is currently underway at IRSN for the 1300 MWe series as part of the safety review associated with the third ten-yearly outage programmes for these reactors.

6.5. Conclusion

As shown by the Three Mile Island accident in the United States (see Section 7.1), the containment building provides effective confinement during a core melt accident when its integrity and leak tightness can be ensured. Studying possible failure modes of the containment building and assessing means to confront them contributes to reducing the possibility of radioactive releases into the environment for all conceivable accident situations, including core melt accidents.

As we have seen in this section, studies regarding containment consist of systematic examination of possible failure modes under all conceivable operating conditions: leak tightness failure on the reactor building itself, leak tightness failure on containment penetrations, failure on systems connected to the RCS which under certain operating conditions constitute "extensions of the containment building".

In particular, the purpose of these studies is to improve the design and operating provisions implemented on containments in the current French fleet, to prevent the risk of large releases into the environment in the event of a core melt accident as far as possible. For reactors in the current fleet, studies have also enabled improvements to equipment hatch leak tightness by modifying the associated fastenings.

For the design of the EPR, a stricter objective was adopted: to "practically eliminate" core melt accidents that could lead to large early releases.

Reference Documents

- [1] B. Masson, Tenue du confinement, évaluation des transferts à travers la paroi de l'enceinte, réunion sur la recherche et développement concernant les accidents graves, SFEN, Cadarache, France, 2009 (in French).
- [2] E. Raimond, B. Laurent, R. Meignen, G. Nahas, B. Cirée, Advanced Modelling and Response Surface Method for Physical Models of Level 2 PSA Event Tree. *CSNI-WG-RISK-Workshop level 2PSA and Severe Accident Management*, Cologne, Germany, 2004.
- [3] B. Cirée, G. Nahas, Mechanical analysis of the equipment hatch behaviour for the French PWR 900 MWe under severe accident, *H01/3 – Proc. SMiRT*, Toronto, CANADA, 2007.
- [4] G. Nahas, B. Cirée, Mechanical analysis of the containment building behaviour for the French PWR 900 MWe under severe accident, *H05/5 – Proc. SMiRT*, Toronto, CANADA, 2007.
- [5] [M. F. Hessheimer](#), R. A. Dameron, Containment Integrity Research at Sandia National Laboratories, NUREG/CR-6906 SAND2006-2274P, 2006.
- [6] OECD International Standard Problem No. 48, Containment capacity, Phase 2 Report Results of Pressure Loading Analysis, Organization for Economic Cooperation and Development, Nuclear Energy Agency, Committee on the Safety of Nuclear Installations, [NEA/CSNI/R\(2004\)11](#), 2004.
- [7] OECD International Standard Problem No. 48, Containment capacity, Synthesis Report, Organization for Economic Cooperation and Development, Nuclear Energy Agency, Committee on the Safety of Nuclear Installations, [NEA/CSNI/R\(2005\)5](#)/ Vol. [1](#), [2](#) and [3](#), 2005.

Chapter 7

Lessons Learned from the Three Mile Island and Chernobyl Accidents and from the Phebus FP Research Programme

7.1. Lessons learned from the Three Mile Island accident

7.1.1. Introduction

On 28 March 1979, a core-melt accident occurred on the second unit of the Three Mile Island nuclear power plant (TMI-2, an 800 MWe reactor designed by Babcock and Wilcox) near Harrisburg in Pennsylvania, USA¹ (see Figure 7.1). This accident, which had been considered utterly improbable, caused considerable repercussions around the world. For those in the nuclear industry, it led to a sudden awareness that the risks associated with nuclear power plants needed be reconsidered in depth [1-7].

1. The TMI-2 reactor is similar in its major design principles to the pressurised water reactors (PWRs) operating in France (see Figure 7.1). However, it differs from French PWRs on two main points for facility operation and safety: it only had two core cooling loops, while French PWRs have three or four loops (see Section 2.3.2.2) and the steam generators were countercurrent heat exchangers with straight tubes, whereas French PWRs have U-tubes. In the event of its water supply being interrupted, a straight-tube steam generator dries out in two minutes, whereas a U-tube steam generator takes about 10 minutes to dry out.

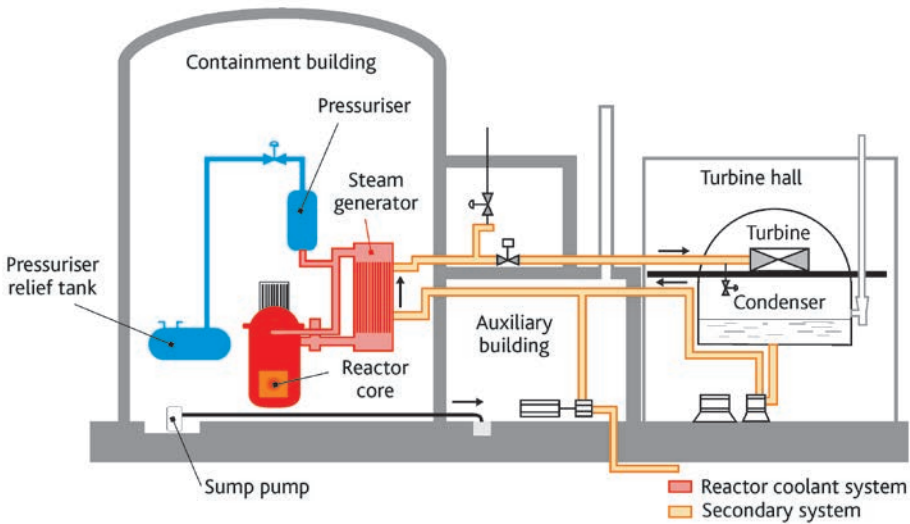


Figure 7.1. Diagram of the Three Mile Island power plant

Previously, it had never really been considered that the core of a reactor could melt. The speed with which this melting occurred was also a surprise. After the accident, when observation of the degraded core became possible, it was discovered that nearly half the core had melted and that approximately 20 tonnes of molten materials produced by this degradation had reached the vessel lower head. This raises the question of what would have happened if the operators had not finally closed the breach in the reactor coolant system (RCS) and reflooded the core with water during the accident, or if a larger quantity of molten materials had ultimately accumulated at the bottom of the vessel. The vessel could then have failed, allowing molten materials to flow into the containment building, which would have led to interactions between these materials and the containment concrete, with the eventual risk of a large release of radioactive substances into the environment *via* containment pressurisation or basemat piercing².

All these uncertainties and questions raised by the Three Mile Island accident have led to large-scale analysis work in the nuclear industry, a large number of international discussions, and a general review of risks and safety approaches for nuclear reactors [3-7].

A summary of the accident sequence and a physical analysis, in which experts from many countries have participated, is given in the following sections. The analysis is based on interpretation of the data recorded by the power plant's instrumentation during the accident, on knowledge of the final state of core degradation observed after the reactor vessel head was opened (in late 1984, over five years after the accident), on extraction

2. In 2011, the accident on the Fukushima Daiichi nuclear power plant in Japan demonstrated that external hazards (earthquake followed by a tsunami significantly greater than the design-basis tsunami for the facilities) can lead to a core-melt accident. Unfortunately, this accident led to fuel melt and probably to reactor vessel and containment failure on three of the power plant's reactors, along with large releases of radioactive substances into the environment [12].

and examination of the core debris in hot laboratories, and on simulation of aspects of the accident scenario. Collaboration between specialists from various countries has enabled the accident sequence to be largely reconstructed, in particular the thermal-hydraulics in the core and associated systems during the accident, and the stages of core degradation [6, 8 and 9].

The consequences and lessons learned from the accident are presented at the end of Section 7.1. These lessons marked a major turning point in the development of the safety approach for nuclear reactors worldwide.

7.1.2. Accident and core-degradation sequence

The accident's initiating event was a relatively banal operating incident: failure of the main feedwater supply to the steam generators while the reactor was operating at nominal power. This failure was probably caused by an error made during maintenance work on the reactor's auxiliary systems. Due to the low thermal inertia of this steam-generator design, the sudden loss of heat removal *via* the steam generators led to an increase in cold leg temperature and pressure in the reactor coolant system within a few seconds.

As planned for this situation, the RCS relief valve, located at the top of the pressuriser, opened to reduce the pressure in this system by discharging its coolant into the pressuriser relief tank located in the containment building. The incident also very quickly led to reactor trip. Up to this point, control systems functioned as expected.

Two failures then occurred which determined the development of the situation. The first failure was that the pressuriser relief valve did not automatically close when the RCS pressure had fallen sufficiently. Reactor coolant therefore continued to discharge into the relief tank and then into the containment building *via* the tank's overflow once it was full; this corresponds to a loss of coolant accident (LOCA). The second failure was that the emergency feedwater system for the steam generators did not take over from the main feedwater system because its valves, which should have been open, were closed (they had been closed during a regulatory test performed several days previously). The secondary side of the steam generators then dried out in a few minutes, leading to loss of cooling of the RCS by the steam generators.

The first failure had serious consequences because the operators in the control room did not realise that the pressuriser valve had remained open. For over two hours, approximately 60 tonnes per hour of reactor coolant poured into the containment building (for an initial reactor coolant inventory of 200 tonnes). The jammed valve was not quickly diagnosed, as the operators in the control room had no indication of the real position of the valve, only a light that indicated that the close command had been sent. They therefore had no way of knowing if closure had been successfully performed.

The second failure may not have had a major impact on the accident sequence. However, for nearly 25 minutes, operator attention was focussed on re-establishing stable cooling conditions on the secondary side, which probably partly explains why the initial critical phases on the RCS side were not correctly analysed.

The accident sequence can be described in several phases from the initiating event, as suggested in earlier publications [6, 8, and 9].

► Phase 1 of the accident: LOCA (estimated duration 100 minutes)

RCS pressure continued to decrease because the pressuriser relief valve remained open. When it reached approximately 110 bar, two minutes after the start of the accident, the high-pressure safety injection system (SIS) started up automatically and cold water was therefore injected into the RCS. Operators then monitored pressure regulation in the RCS by following the pressuriser water-level measurement. In normal operation, with the relief valve tightly closed, the upper part of the pressuriser is filled with a small volume of steam that determines RCS pressure. An instruction tells operators to check that this volume of steam (and therefore the water level in the pressuriser) varies little, which is a sign of RCS pressure stability. However, as the relief valve was open, a two-phase water-steam mixture was escaping from the breach. The apparent water level in the pressuriser, measured using the static pressure difference between the top and bottom of the pressuriser (weight of the water column), therefore seemed to rise quickly, given the large proportion of water in the mixture leaving by the relief valve. Believing the relief valve tightly closed, the operators attributed the rising water level in the pressuriser to the water supplied by the safety injection system and assumed that this rising water level would be accompanied by rising pressure in the RCS. Five minutes after the start of the accident, they took the decision to manually stop the high-pressure safety injection, which would have major consequences. From then on, there was an open breach in the second barrier and emergency cooling was not operating.

From this point, the water that continued to leave *via* the pressuriser relief valve was no longer replaced in the RCS; make-up *via* the chemical and volume control system (CCVS) was not adequate. Approximately 16 minutes after the start of the accident, the volume of reactor coolant lost *via* the breach and the loss of pressure were such that steam started to form in the RCS.

The RCS was now carrying a mixture of steam and water, with an increasing steam fraction over time. Its operation was maintained under these conditions for over an hour, despite a certain number of indications (increase in core neutron flux, reactor coolant pump vibrations, increasing water level in the pressuriser relief tank, and increasing temperature and pressure in the containment building) and alarms that should have alerted the operators to the state of the RCS. Residual heat from the core was being removed both by the steam generators – the operators having succeeded in restoring emergency feedwater supply, which had occupied all their attention – and by the water and steam discharging into the containment building *via* the pressuriser discharge valves (but the operators were unaware of this).

The two reactor coolant pumps were shut down at 73 minutes and 100 minutes from the start of the accident respectively. Given the parameters measured in the containment (in particular temperature and pressure), the operators suspected an RCS leak on the steam generators. They were now counting on core cooling by natural convection.

► Phase 2 of the accident: core heating with the RCS and high-pressure SIS shut down (from 100 minutes to 174 minutes)

Shutting down the reactor coolant pumps led to separation of the water and steam phases in the RCS and creation of a volume of steam in the upper part of the reactor vessel. As later estimated, the water level was now around the top of the core.

The reactor was now only cooled by water from the chemical and volume control system. This make-up was not adequate to compensate for the loss of water from the pressuriser relief valve. Loss of water led to a decrease in the water level in the reactor vessel. It was later estimated that the decreasing water level reached the top of the fuel rods in the core 112 minutes after the start of the accident. This point therefore marks the start of uncovering of the fuel rods, which then heated up as they were inadequately cooled.

Between 130 and 140 minutes after the start of the accident, the upper part of the fuel rods was sufficiently hot (a temperature of approximately 800 °C) to cause ballooning and failure of their zirconium alloy cladding, leading to release of gaseous fission products into the containment building *via* the RCS breach (the “high dose rate” alarm in the containment triggered at 134 minutes). At this point, the operators could no longer be in doubt that the situation was serious.

Leakage *via* the pressuriser relief valve was finally diagnosed 142 minutes after the start of the accident. The operators closed an upstream isolation valve, which eliminated the RCS breach and restored the second barrier. However, later assessments show that at this point, half of the height of the fuel rods was uncovered and it was too late to prevent their degradation.

Until 174 minutes from the start of the accident, no means other than the CCVS would be used to cool the core (as the RCS and SIS were shut down). Under the effect of the exothermic oxidation reaction between zirconium alloy and steam (see Sections 4.3.1.2 and 5.1.1.2), the core continued to heat up, which caused increased steam production and increased pressure in the RCS, which was now sealed following closure of the pressuriser relief line. The water level in the core continued to decrease until only one metre of the 3.6 metre height of the fuel rods was covered.

With the gradual drop in water level, heating of the uncovered part of the cladding led firstly to cladding rupture, then to its significant oxidation, and finally to the initial flows of melted metal materials by the formation of eutectic mixtures. Fe-Zr, Ni-Zr, and Ag-Zr eutectics can form at temperatures of several hundred degrees below the melting point of zirconium alloy (see Section 4.3.1.2 and Figure 4.3). The initial liquid formed was most probably the Ni-Zr eutectic between the cladding zirconium alloy and the Inconel of the spacer grids in the central part of the core. Then around 1400 °C, at the same time as exothermic oxidation, melting of the control rod cladding led to a flow of a silver-indium mixture. The stainless steel of the control rod cladding could also have been attacked at around 1300 °C by interaction with the nickel-zirconium eutectic.

When the molten materials reached the water-steam interface, they solidified in contact with water, which led to the formation of a crust around the core axis, called the lower crust in the following text (see Figure 7.2). This crust remained in place until the end of the accident, and samples could be taken and analysed after the reactor vessel head was removed. These analyses showed that it was made up of metal alloys of Zr, Ag, In, Fe and Ni, which coated columns of fuel pellets.

The lower crust's bowl shape can be explained by the changing conditions for core cooling: the central blockage of flow by the forming crust redirected steam towards the perimeter, causing a gradual increase in cooling at the perimeter such that the molten metal alloys resolidified in these areas at levels much higher than the water level in the core.

In the upper parts of the core, continued highly exothermic oxidation of zirconium alloy by the steam led to local attainment of the melting point of zirconium alloy (which ranges from 1800 °C to 1950 °C depending on its oxygen content). Flowing zirconium alloy melted the fuel pellet uranium oxide to form a bimetallic compound (mainly U, Zr, and O). Similarly, zirconium alloy oxidation led to degradation of the fuel rods, leading to solid fuel-pellet fragments falling in the core. This degradation process is assumed to have progressed towards the core perimeter until 174 minutes after the start of the accident.

The lower crust now constituted a crucible that collected metal and oxide compounds. This was probably a mixture of solid debris and molten materials, with a mean temperature of between 2300 °C and 2500 °C at this time.

While the lower crust itself was cooled convectively by steam and also by radiative heat transfer to the water surface, the materials collected in the crucible were poorly cooled and gradually heated up until the centre melted. Figure 7.3 shows a schematic diagram of the state of the core at 174 minutes:

- in the lower part of the core, the fuel rods are intact over a height of approximately one metre;
- a leaktight bowl-shaped crust, made up of resolidified materials, has formed above these intact fuel rods;
- the crucible thus formed contains a mixture of solid debris, along with a pool of molten materials in its central part;
- in the upper part of the core, the fuel rod cladding is highly oxidised, but the majority of fuel rods are still in place.

► Phase 3 of the accident: partial reflooding of the core - formation of a debris bed (between 174 and 180 minutes)

At 174 minutes from the start of the accident, the operators restarted the reactor coolant pump on one of the cooling loops to try and restore reactor coolant circulation. This brought 28 m³ of water into the reactor vessel in 6 minutes. This was the largest supply of coolant since the reactor coolant pumps had been stopped 100 minutes after the start of the accident.

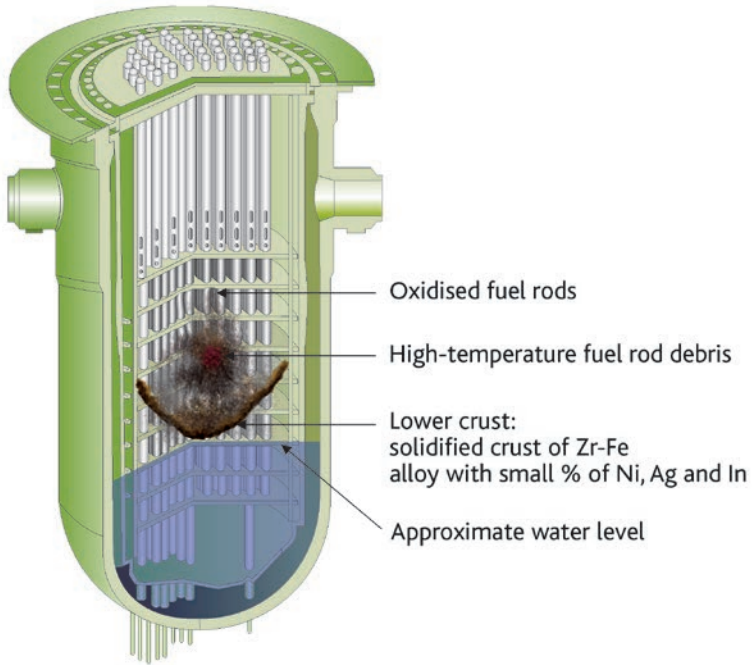


Figure 7.2. Assumed state of the core after lower crust formation.

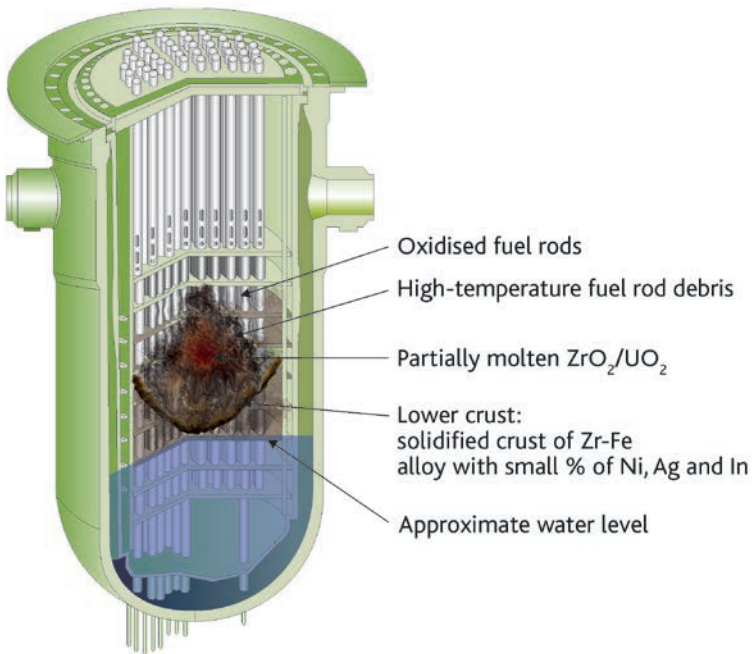


Figure 7.3. Assumed state of the core 174 minutes after the start of the accident.

It caused a rapid increase in RCS pressure, associated with the vaporisation of water in contact with the overheated core components, rapid oxidation of the remaining unoxidised zirconium alloy in the upper half of the core, and probably deterioration of heat exchange in the steam generators due to the hydrogen produced by zirconium alloy oxidation.

This water supply to the core probably stopped development of the corium pool above the crust. However, the thermomechanical stresses caused by partial quenching of the damaged oxidised fuel rods in the upper part of the core led to fragmentation of the oxidised cladding and fuel pellets, which then formed a debris bed in the upper part of the core (see Figure 7.4). Later observations and analyses have shown that the bed was made up of several tonnes of compact debris.

Six minutes after restarting, the reactor coolant pump was stopped by the operators because RCS pressure was rising sharply.

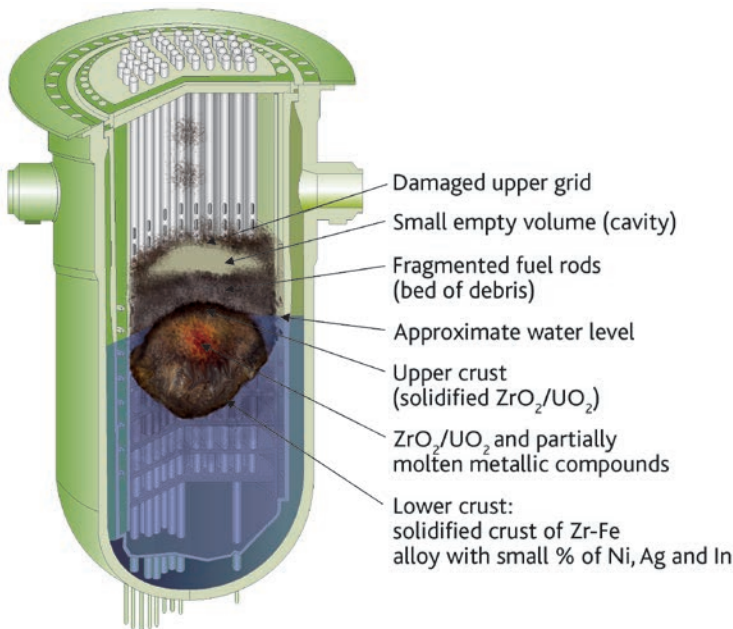


Figure 7.4. Assumed state of the core during Phase 3 of the accident.

► Phase 4 of the accident: heating of the debris bed – development of the corium pool (between 180 and 200 minutes)

The sharp rise in RCS pressure associated with supply of water to the core led operators to reopen the isolation valve of the pressuriser relief line. This opening caused radioactivity alarms to trigger, including some outside the reactor building. At this point, the first two barriers were “breached” and isolation of the third and final containment barrier (the containment building) had not yet been performed.

In the absence of containment isolation, the triggering of alarms outside the reactor building was due to automatic transfer of contaminated liquid from the containment sumps into storage tanks located in the non-leaktight auxiliary building. These tanks themselves overflowed and contaminated liquid poured into the auxiliary building, leading to releases outside the facility.

An emergency situation was declared 200 minutes after the start of the accident and this led to isolation of the containment building, interrupting transfer of radioactivity to the auxiliary building.

According to the later reconstruction of the accident, the quantity of water in the reactor vessel decreased during Phase 4, due to water boiling off under the effect of the residual heat. At 200 minutes from the start of the accident, the water level in the core was only about 2 m.

Between 180 and 200 minutes, the cooling water flowrate was low. The centre of the debris bed was not cooled due to its mass, its low permeability, the residual heat released inside it and the presence of the lower crust that hindered coolant flow. The debris bed therefore heated up around the corium pool and the pool grew towards the top of the core through gradual melting of debris.

► Phase 5 of the accident: total reflooding of the core - continued development of the corium pool (between 200 and 224 minutes)

At 200 minutes after the start of the accident, the operators started up the high-pressure safety injection system and ran it for 17 minutes. Later analysis of the data gathered on RCS temperatures and pressures shows that the reactor vessel was full of water 7 minutes after this system restarted.

It is estimated that during vessel filling, water managed to penetrate the upper debris bed, cool it and rewet it. However, the corium pool continued to heat up. The restarting of the high-pressure safety injection system, between 200 and 217 minutes after the start of the accident, occurred when the corium pool was already too large to be effectively cooled. It is estimated that at 224 minutes, almost all the compacted debris in the crucible formed by the lower crust had melted (see Figure 7.5).

► Phase 6 of the accident: movement of core materials towards the reactor vessel's lower plenum (between 224 and 226 minutes)

At 224 minutes from the start of the accident, while the operators were occupied with cooling the core which they did not suspect to be badly damaged, a certain number of measurements suggested that fuel movements were occurring in the core. It was only much later, after examination of the vessel's lower plenum, that the events that occurred at this time could be reconstructed. The crust finally failed on one side and 20 tonnes of molten materials flowed to the bottom of the core, destroying the internal structures located in the core perimeter as they passed (see Figure 7.6).

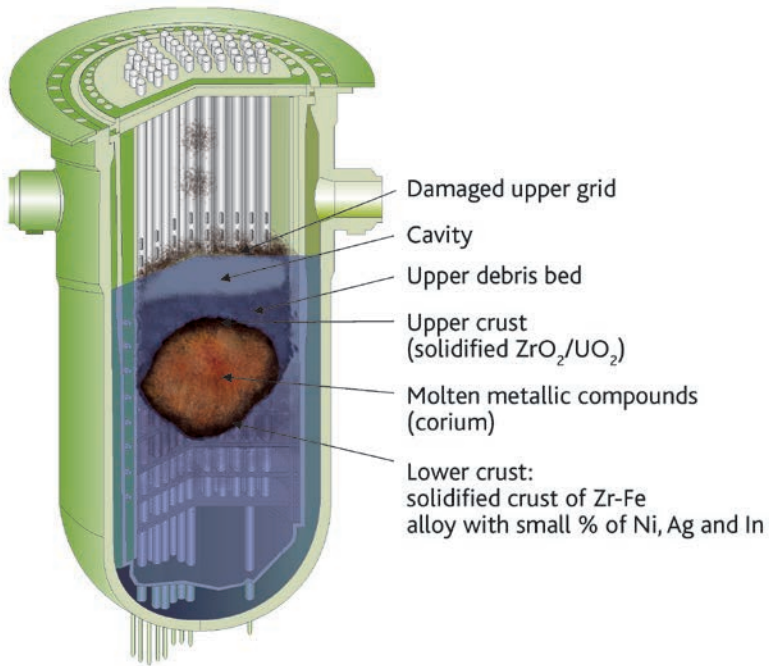


Figure 7.5. Assumed state of the core at the end of Phase 5 of the accident.

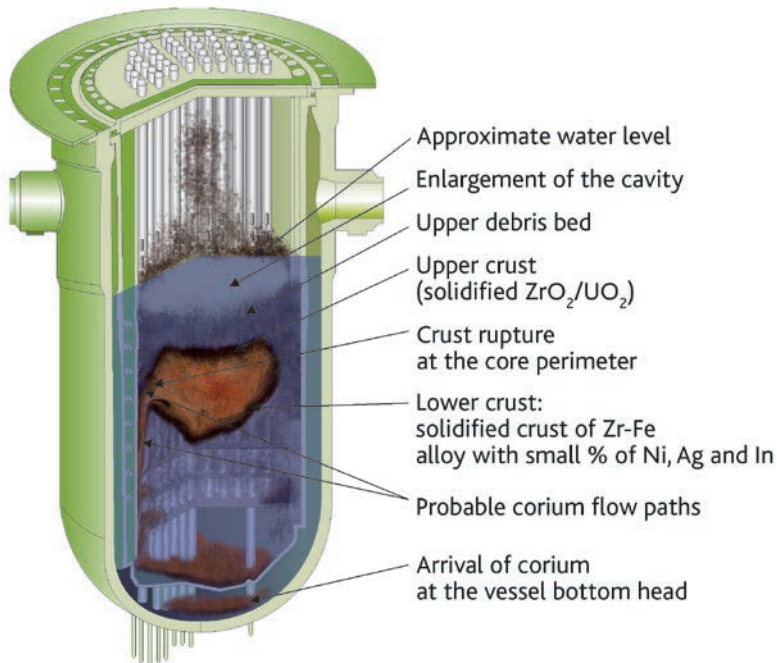


Figure 7.6. Assumed state of the core after the flow of molten materials (Phase 6 of the accident).

The mechanism of crust rupture is not known with certainty. Some writers have emphasised compression of the corium pool under the weight of the upper debris bed, while others emphasise the mechanical loads on the crust due to the partial depressurisation of the RCS which occurred between 220 and 224 minutes, after high-pressure safety injection was stopped.

The flow of molten materials to the vessel lower head while the vessel was practically full of water could theoretically have led to a violent vapour explosion (see Section 5.2.3). It is important to note that nothing in the recorded data, or in the state of the core observed after the accident, suggests that such a sudden mechanical phenomenon occurred during the flow of 20 tonnes of molten materials into the lower plenum. One possible explanation is that the relatively long duration of the flow of molten materials (of the order of a minute) did not promote their mixture with the coolant.

The water present in the reactor vessel was finally able to solidify and cool the molten materials after several hours. The vessel lower head did not fail despite the flow of molten materials. One possible explanation, which has already been mentioned in Section 5.1.3.1, is the existence of a gap between the molten corium and the vessel wall, which would have allowed circulation of water or steam and reduced heat exchange between the molten materials and the vessel lower head.

► End of the accident: restoration of stable cooling (to 16 hours after the start of the accident)

During Phases 3 and 5 of the accident, operators had attempted to restart RCS cooling. These attempts were hindered by the large quantity of non-condensable hydrogen in the RCS, produced by oxidation of the zirconium alloy cladding and other core materials. Nevertheless, these actions did cool the degraded core as the hydrogen was vented by opening the pressuriser relief line. In doing this, hydrogen and radioactive products entered the containment building.

Hydrogen thus accumulated in the containment building. Hydrogen combustion occurred 9 hours 30 minutes after the start of the accident. It has been shown that, at this time, the molar concentration of hydrogen in the containment was slightly below 8%, along with a small quantity of water vapour (around 3.5%). This combustion led to a pressure peak of 2 bar in the containment (which was designed to withstand 5 bar). The containment suffered no damage, but when entered several months later, fire and pressure damage was observed on some parts of the internal structures.

At 11 hours 8 minutes after the start of the accident, the isolation valve on the pressuriser relief line was definitively closed, bringing to an end transfer of contamination into the containment building.

At 13 hours 23 minutes after the start of the accident, the safety injection system was restarted to fill the RCS.

At 15 hours after the accident, the quantity of water in the RCS was sufficient for reactor coolant pumping to recommence. The reactor coolant pumps were restarted from 15 hours 49 minutes after the accident. Normal, stable cooling was thus obtained approximately 16 hours after the start of the accident. One day after the start of the accident, the reactor coolant pumps were again stopped, as the natural convection flowrate between the reactor vessel and the steam generators had become adequate to remove the residual heat from the core.

The final state of the core is shown in Figure 7.7.

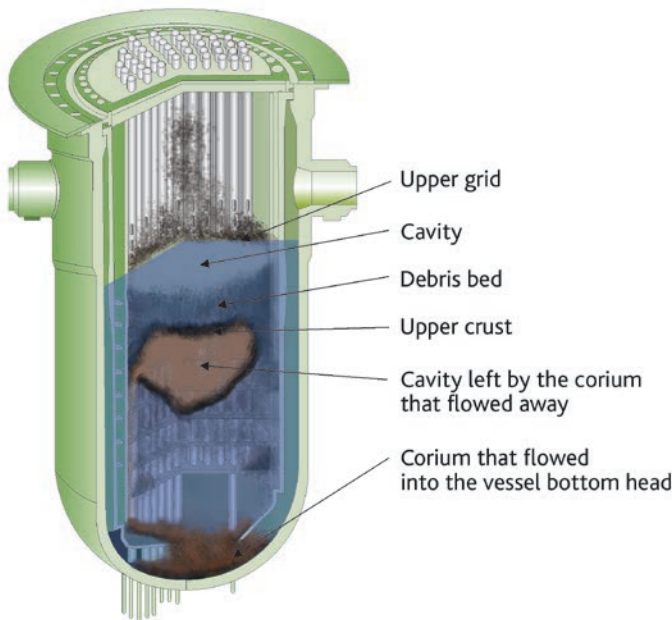


Figure 7.7. Final state of the core.

7.1.3. *Environmental and public health consequences of the accident*

As stated above, there was considerable internal damage to the power plant: nearly half the fuel melted, nearly half the gaseous and volatile fission products (krypton, xenon, iodine and caesium) passed into the reactor coolant, whose radioactivity concentration reached 2.96×10^{16} Bq/m³. Over 2000 m³ of this radioactive water poured into the containment via the RCS breach.

Despite partial melting of the reactor core and the significant release of radioactive products into the containment building, the immediate radiological consequences on the environment were negligible [1 and 2]. The containment building performed its function. The small releases into the environment that did occur prior to containment isolation

were caused by contaminated liquid from the containment sumps being pumped into a non-leaktight auxiliary building.

In the design of the Three Mile Island facility, start-up of the safety injection system did not automatically provoke isolation of the containment building, i.e. closure of isolation valves on all pipes entering or leaving the reactor building that are not indispensable for reactor core safety. For several hours, the sump pumps therefore transferred water that was increasingly loaded with radioactive products into an auxiliary building. Due to the lack of leak tightness on certain systems, hot contaminated water escaped into this building and evaporated, releasing the iodine and xenon that it contained. These gases and vapours were taken up by the building's general ventilation system and discharged outside *via* iodine filters whose efficiency was found to be inadequate (it was later observed that the filters had not been subject to suitable inspections to check their efficiency). It was only when these transfers of radioactive products triggered alarms that the order to isolate the containment building was given manually.

On the basis of radioactivity measurements performed on the accident site, it has been estimated that only 0.01% of the fission product inventory was transferred from the core to the environment, even though the auxiliary building in question was not designed to constitute a leaktight containment building. With regard to iodine, whose ^{131}I isotope produces the most significant short-term environmental consequences (see Section 5.5), it has been determined that the total release of this radionuclide into the environment did not exceed 10^{-5} % of the inventory present in the reactor core. In the 16 hours following the accident, 37×10^{10} Bq of ^{131}I were released, and in the thirty days that followed approximately 259×10^{10} Bq were released. Releases of other radioactive products were estimated at approximately 18.5×10^9 Bq of ^{137}Cs and 3.7×10^9 Bq of ^{90}Sr .

Many studies have shown that the accident had no health consequences for the general public and had no significant impact on the environment [1 and 2]. However, the Three Mile Island accident traumatised the public. For a whole week, the authorities in charge of public safety were unsure of the degree of severity of the accident and whether partial or total evacuation of nearby inhabitants was required. In particular, they were afraid that the hydrogen bubble formed in the upper part of the reactor vessel could explode (falsely, because this explosion is not possible without oxygen), leading to catastrophic failure of the containment and large releases of radioactive products into the environment.

The contradictory information drip fed by the authorities during the accident did nothing to reassure the public, and over 200,000 people fled the region during the crisis.

7.1.4. *Lessons learned from the accident with regard to the physics of core melt accidents*

The Three Mile Island accident led to the development of numerous R&D programmes with regard to the physics of core melt accidents, with the aim of better understanding the phenomena which occur during this type of accident (see Chapter 5).

Numerous experimental results have since been obtained internationally with regard to the phenomena associated with a core melt accident on a water-cooled reactor. Knowledge and understanding of the complex phenomena involved in such an accident have greatly increased, and the ability to predict changes in reactor state under severe accident conditions using simulation software (see Chapter 8) has greatly improved.

The multiple analyses and studies of the Three Mile Island accident mean that it is possible to assess the ability of software to simulate core melt accidents, from the initiator event to possible releases outside the containment building. Since the accident, numerous comparisons of simulation software have been performed at the international level to understand the remaining uncertainties in simulating the accident [8-10].

The first two phases of the accident, corresponding to LOCA and the beginning of core heating (see Section 7.1.2), are now correctly modelled by existing software with regard to changes in RCS thermal-hydraulic parameters and the core degradation sequence (hydrogen production, formation of the lower crust, and melting and flow of materials into the crucible formed by the lower crust).

On the other hand, the core reflooding phase (Phase 3) and the later core degradation phases (beyond Phase 3) are not yet correctly modelled. The main weakness of current simulation software concerns reflooding of the degraded core. The phenomena which require more precise modelling to simulate reflooding are the circulation of fluids (water and steam) in the degraded core, heat transfers and zirconium alloy oxidation. These phenomena affect hydrogen production and the flow of molten materials (see Section 5.4.1 for further details). As part of the European Severe Accident Research Network (SARNET), IRSN is leading a research programme, PEARL, on the reflooding of a degraded core, with a view to reducing the associated uncertainties by 2015.

7.1.5. Lessons learned from the accident for the safety of French nuclear power plants

7.1.5.1. Introduction

The Three Mile Island accident caused considerable shock and many lessons have been learned in the area of **nuclear safety**, particularly in France.

While core melt accidents on water-cooled reactors had already been the subject of in-depth scientific analysis in the USA from the 1970s (see the WASH 1400 report [11]), it was not until the Three Mile Island accident that the designers and operators of nuclear facilities became aware that core melt accidents were really possible. However, it should be noted that, since publication of the WASH 1400 report, French and other safety bodies have sought to draw practical conclusions from this report in terms of improving the safety of nuclear facilities and drawing up emergency plans for accident scenarios.

While the Three Mile Island accident did not call into question the overall design of nuclear facilities³, it clearly showed that accidents more severe than those considered up to that point in the design of nuclear facilities (i.e. LOCA resulting from a double-ended guillotine break on the RCS) were possible and that they could result from a series of technical failures and human errors.

The Three Mile Island accident raised a series of questions, such as:

- during an accident, how can inappropriate operator actions, which could aggravate the consequences and lead to core melt, be avoided?
- how best to use the containment building, the final barrier against the dissemination of radioactive substances?
- among real incidents, how can those that could be precursors to core melt accidents be identified, and necessary preventive measures be taken in time?
- how to prepare to confront a core melt accident (a question that applies to both operators of nuclear facilities and public authorities)?

7.1.5.2. Analysis of the causes of the accident

The error committed by the operators in picturing the events – they did not understand the origin of the difficulties encountered and persisted in an incorrect picture of the sequence of events – highlights the importance of human factors in the safety of nuclear facilities. The operators did follow the applicable instructions, but on the basis of incorrect or incomplete information:

- with regard to the position of the pressuriser relief valve, the operators saw the indication “valve closed”, but this information was incorrect because it was associated with the command to close the valve and not its actual position; this was a crucial aspect of the accident;
- although the operators focussed their attention on the water level in the pressuriser, following the applicable instructions, they had neither the training nor the procedures to deal with a breach located in the upper part of the pressuriser;
- faced with the rapid rise of the pressuriser water-level indicator, and believing the relief valve to be closed, the operators manually stopped the safety injection. The mental picture that the operators had of the situation was false and they lacked direct data on the state of the reactor core.

3. Application of the defence-in-depth concept requires implementation of provisions with regard to a certain number of accidents, which has led to the idea of strong containment in particular. This containment provided significant protection for the general public and staff on the Three Mile Island power plant.

The combination of the following failures and technical inadequacies played a significant role in the accident sequence:

- inadequate indicators in the control room (for example, the position of the pressuriser relief valve, and the water level in the pressuriser relief tank, which would have indicated that the tank was filling up during the accident);
- the lack of prioritisation on alarm signals in the control room; several alarms triggered at the same time, which contributed to disorientating the operators and meant that they could not correctly analyse the situation;
- incorrect positioning of the valves on the emergency feedwater system for the steam generators;
- by design, the start-up of the safety injection system did not automatically lead to isolation of the containment building;
- non-leaktight systems and poor iodine trap efficiency in the auxiliary building, into which contaminated liquids from the containment sumps were pumped.

7.1.5.3. Safety lessons

The partial core melt accident on the Three Mile Island reactor confirmed that combinations of failures could lead to a severe accident.

Independently of research performed on core melt accidents, safety reviews have covered three major subjects: human factors in facility operation, experience feedback from operation of nuclear power plants, and management of emergency situations.

► Human factors in facility operation

Prior to the Three Mile Island accident, safety analyses mainly assessed the reliability of safety-related reactor components. The Three Mile Island accident highlighted the fact that people are also an essential aspect of safety, which was already known but little considered.

While operator actions are usually positive from a safety perspective, in certain cases, human actions can contribute to the initiation or development of incidents. It is now important to study operating and working conditions in detail to identify, in particular, the safety problems that could result from organisational difficulties, or from inadequate or unsuitable resources and data.

The explicit acknowledgement of human factors in safety has led to improvements in two technical areas that aim to improve the organisational structure, and specify the allocation of responsibilities and what is expected of each person involved:

- Improving the conditions for operation
Conditions for operation have been improved by better selection, initial training and ongoing training of operators, and now involve the systematic use of simulators in training. In this regard, the standardisation of the French nuclear fleet

means that simulators are available that are directly representative of the various types of facility. Training covers normal operation, incidents and accidents.

During the accident, the procedures available in the Three Mile Island plant were clearly inadequate. In most countries, particularly in France, procedures and instructions have been reviewed and rewritten. The revision included both the form and content of the documents.

A new approach to accident operation of facilities was thereby implemented (see Section 2.5.2) in order to:

- ensure the “human redundancy” of operators, in particular during an accident, by a safety engineer whose role is to provide independent verification of the relevance of the operating strategy implemented, by monitoring a certain number of safety parameters (using a “safety parameter display console”);
- cover the simultaneous occurrence of several apparently independent events as well as possible. In France, an approach has been developed and implemented to give operators the means to bring the facility back into a safe state, independently of the path that led to the situation in question; this is called the “state-oriented approach” (see Section 2.5.2).

In the state-oriented approach, the procedures to be followed are no longer based on the operator’s understanding of the sequence of events to which the reactor has been subject (the event-oriented approach) but rather on its actual state at a given moment (characterised by physical data: core sub-criticality, residual heat in the core, water inventory in the RCS, water inventory in the steam generators, leak tightness of the containment building, etc.).

The event-oriented approach is not able to cover all possible combinations of equipment failures and human errors, which may be simultaneous or separated in time. Furthermore, it makes diagnostics difficult in the event that the facility changes in ways that were not foreseen.

In the state-oriented approach, each abnormal state is associated with actions to be performed to bring the facility back to a satisfactory condition. The operating team may perform the corresponding actions without necessarily having understood the sequence of prior events. A key element in the state-oriented procedures has been the addition of a “water level in the reactor vessel” indicator, which means that the operator can know if the core is correctly covered by water (which was not the case during the Three Mile Island accident).

Furthermore, since 1981, beyond design-basis procedures that aim to prevent core melt (H1 to H4 Procedures, described in Section 2.5.2) and ultimate procedures that aim to prevent core melt and mitigate the radiological consequences (U Procedures, described in Section 2.5.2) have been adopted as a principle in France. In the event of core melt, these latter procedures aim to limit releases of radioactive products outside the containment building and therefore into the environment.

All procedures have been tested on a simulator.

- Control room improvements

The observations made following the Three Mile Island accident, with regard to inadequacies in terms of indicators and prioritisation of alarms in the control room, led to modifications in unit control rooms, including those currently in operation. Better presentation of information was sought, by replacing the majority of “command-sent” indicators by valve-position indicators. Certain measurement ranges have been widened. New indicators have been added to supply more complete information on the state of the core (which was lacking during the Three Mile Island accident), such as the indicator of boiling margin (the difference between the actual temperature of the reactor coolant and the boiling point at the RCS pressure) and measurement of the water level in the reactor vessel. In addition, alarms have been prioritised and key data duplicated on a safety parameter display console. This console guides the safety engineer during implementation of accident procedures.

► The importance of precursor events

Another important lesson from the Three Mile Island accident concerns taking into account experience feedback from the operation of nuclear power plants.

A precursor incident very similar to the Three Mile Island accident (pressuriser relief valve jammed open) took place in 1977 on an American reactor of the same type (on the Davis–Besse nuclear power plant), but with no damage to the reactor. The operators committed the same analysis error as at Three Mile Island (shutting down the cooling). The lessons from this incident had not been converted into instructions for operators when the Three Mile Island accident occurred. This example illustrates that the systematic study of significant incidents, and any changes to operator procedures and instructions that could be recommended following such studies to prevent such incidents recurring, could in fact prevent more serious accidents.

Since the Three Mile Island accident and the analyses that followed, detection of precursor events that could lead to an accident has become a major concern for operators and [nuclear safety](#) bodies. The organisation of operational monitoring and experience feedback has therefore been developed with this new objective.

Following the Three Mile Island accident, a systematic analysis of the possible causes of a breach in the second barrier (the RCS) has been performed, in particular leading to development of more reliable valves for opening and closing the pressuriser relief line.

► Managing emergency situations

The Three Mile Island accident demonstrated that the operators, power station managers and authorities responsible for public safety were not sufficiently prepared to manage a core melt accident. Power station managers, and local and federal authorities, did not know how things could develop and whether it was necessary to evacuate. For over a week, the authorities believed in the possibility of a hydrogen explosion which

could damage the reactor vessel and the containment building, causing a large release of radioactive products into the environment. This possibility should have been quickly discounted because the low oxygen concentrations in the core meant that such an explosion was impossible. In uncertainty, people left their homes in a large area around the plant, although the authorities never ordered an evacuation.

From then on, it has been seen as essential that the necessary resources be developed to manage such situations in a less improvised manner in the event that a new situation of this type should occur:

- improved confidence in the behaviour of the containment building, even under conditions very different than those foreseen in design;
- tools available to predict possible changes in the situation, the corresponding releases and their transfer into the environment under accident conditions.

The Three Mile Island accident was partly associated with a false understanding of the situation by operators. It is very difficult for a given team to call into question its initial interpretation of events. It therefore became clear that implementation of crisis teams, distinct from the operating teams and able to take a step back from the situation, could provide alternative insights. Similarly, it was seen necessary to clarify the roles of the various people, and manage the distribution of information in an accident situation. Emergency plans were developed on these bases. The necessity of regular training (crisis drills) was also brought to light.

Since the early 1980s, specific emergency plans have been implemented for nuclear facilities in France. On-site emergency plans have been developed by operators of nuclear facilities with the goal of managing any possible accidents as well as possible, mitigating the consequences, providing help for anyone injured on site and informing the authorities and the press. The authorities have drawn up off-site emergency plans that meet the general objective of public safety in the event of an accident occurring on the facilities.

7.1.6. Conclusion

The Three Mile Island accident has provided many lessons: the importance of defence-in-depth and human factors, along with thorough operating procedures and alarm prioritisation, and the essential role of the containment building, the final barrier between radioactive substances and the environment. All reactors worldwide have benefited from the lessons learned from the Three Mile Island accident. Taking these lessons into account has meant that the calculated probability of core melt on second-generation PWRs has been reduced by a factor of 10. Furthermore, in France, the drawing up of ultimate procedures means that the consequences of such an accident can be mitigated.

For safety experts, the Three Mile Island accident remains a major source of lessons that help understanding of the complex phenomena that occur during a core melt accident. The repercussions of this accident still influence certain research programmes and efforts are continued, in particular to better understand and correctly model the development of such an accident.

Third-generation reactors and the EPR in particular, take lessons from the Three Mile Island accident into account from the beginning. Core melt accidents have therefore been considered in the EPR design. In particular, a core catcher located at the bottom of the containment can collect and cool molten core materials in the event of failure of the vessel lower head (see Section 5.4.3).

7.2. Lessons learned from the Chernobyl disaster

7.2.1. Introduction

On April 26 1986, seven years after the Three Mile Island accident (see Section 7.1), the reactor exploded on the fourth unit of the [Chernobyl](#) nuclear power plant in Ukraine, which was then a Soviet Socialist Republic. This accident is the worst that has ever occurred on a civilian nuclear facility. Prior to the [Fukushima](#) accident in 2011, it was the only example of an accident on a power reactor with core destruction and uncontained radioactive releases⁴. This disaster caused considerable consternation worldwide, in particular in what were then Soviet Socialist Republics and in Western Europe.

There were 31 fatalities among the staff present on-site during the reactor explosion and among those who intervened on the site during the days immediately following (notably fire-fighters). Furthermore, several hundred people received high doses of radiation, in particular among the “liquidators⁵”. This accident also drew public attention onto the issues of large-scale radioactive contamination. Fallout from the radioactive cloud, which followed highly varied trajectories during the ten days that followed the destruction of the reactor core, affected a large part of what was then the Soviet Union and practically all of Europe.

Since this accident, the authorities in many countries have more actively considered the short-term and long-term management of a post-accident situation. Following the disaster, resources were deployed on an impressive scale in an attempt to mitigate the effects on people and the environment. This involved fire-fighting in a highly radioactive environment, evacuation of a vast number of people, treatment of those who received the highest doses of radiation, protection against the dissemination of radioactivity, decontamination of large areas, monitoring programmes for the food chain, and medical monitoring of the affected population. Greater attention has since been

4. The Fukushima Daiichi accident led to fuel melt and probably to reactor-vessel and containment failure on three of the power plant’s reactors, along with large releases of radioactive substances into the environment. In contrast to the reactivity accident at Chernobyl, the cores of the damaged reactors on the Fukushima Daiichi plant did not explode. Initial estimates of the releases performed following this accident show that they were smaller than the releases from the Chernobyl accident (same level for noble gases, approximately 10 times lower for ¹³¹I and three times lower for ¹³⁷Cs) [12].
5. “Liquidators” is the name given to the civilian and military workers who were sent onto the accident site in the days that followed the explosion, and until the early 1990s, in particular to construct a rudimentary protective barrier around the damaged reactor, with a view to preventing new releases of radioactive substances (a concrete “sarcophagus” was thereby built around the damaged reactor in the six months following its explosion), and to clear the most contaminated soils over a radius of 30 km around the plant. It is estimated that approximately 600,000 people were involved.

paid to the long-term social and economic disruption caused by an accident affecting a nuclear facility.

Finally, with regard to the important topic of public information and communication, the difficulties encountered during the [Chernobyl](#) disaster have led to discussions on the need for better “transparency”. The Three Mile Island accident had already highlighted the need for progress in this area.

7.2.2. Accident sequence, releases and consequences

7.2.2.1. The RBMK reactor

In 1986, the [Chernobyl](#) nuclear power plant had four operating RBMK reactors (in Russian, *Reactor Bolshoy Moshchnosty Kanalny*, which can be translated “high-power pressure-tube reactor”). Two other RBMK reactors were under construction on the site.

The design of an RBMK reactor (see [Figure 7.8](#)) is very different from that of the pressurised water reactors (PWR) that EDF operates for power generation in France. The [Chernobyl-4](#) 1000 MWe (3600 MWth) RBMK reactor was a thermal neutron reactor, moderated by a graphite stack (whereas water fulfils the role of moderator in a PWR⁶). Each RBMK on the Chernobyl site contained approximately 190 tonnes of uranium oxide (slightly enriched in uranium-235, to around 2%) with zirconium-niobium alloy cladding. The core was cooled by ordinary “boiling” water, circulating from bottom to top in zirconium-niobium pressure tubes (sometimes called “channels”). The neutron moderator was graphite. The water circulating in the pressure tubes was a neutron absorber.

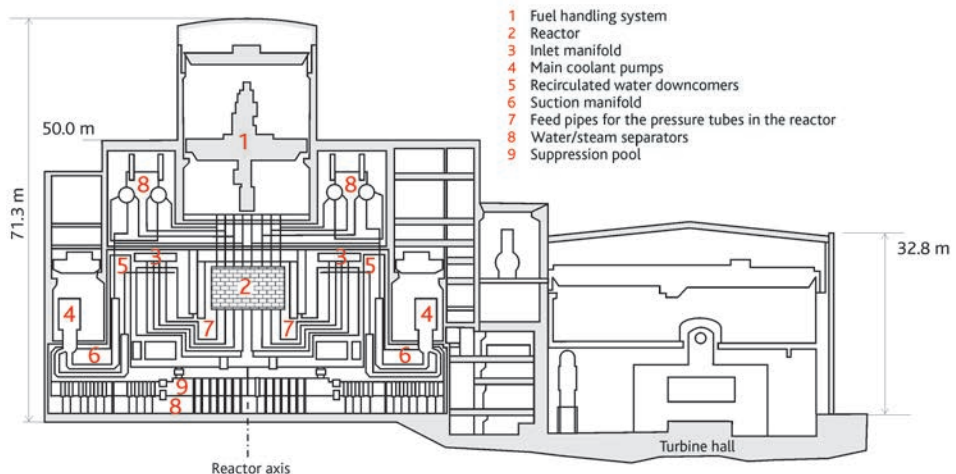


Figure 7.8. Schematic diagram of the Chernobyl-4 reactor.

6. The moderator slows down neutrons, so that they produce fission reactions in the fuel more efficiently (see Section 2.1 for further details).

The reactor core was installed in a cylindrical vessel (14 m in diameter, 7 m high). This vessel was filled with a graphite stack, traversed by 1681 pressure tubes containing fuel assemblies and control rods. Cooling water was circulated in these pressure tubes. The water was heated in contact with the fuel and turned into steam, which was sent directly to the turbines *via* two independent cooling loops with no secondary system. The part containing the reactor core was closed off by a 2000-tonne upper concrete slab.

The power level in the core and its distribution were controlled by 211 absorber rod assemblies, which occupied pressure tubes distributed across the whole reactor core just as the fuel assemblies occupied the other pressure tubes. Motorised mechanisms were used to extract or insert these assemblies. The maximum speed of assembly movement was 0.4 m/s, i.e. very slow, taking 18 to 20 seconds for complete insertion (in French PWRs, control rod drop time is around 2 to 3 seconds). These absorber rod assemblies were made of boron carbide with graphite at the bottom, which had the following disadvantage: when the assemblies were in the upper position, their insertion initially replaced water, which is a neutron absorber, with graphite, which is less of an absorber, thereby increasing core reactivity rather than reducing it.

According to the designers, the advantages of the RBMK reactor were the lack of a pressure vessel, as each pressure tube constituted a small reactor coolant system, the lack of steam generators, the ability to continuously renew the fuel (which provided fuel-cycle flexibility), the ability to adjust the flowrate of each channel, and the ability to manage them individually both thermally and with regard to fuel cladding integrity.

The disadvantages of such a reactor were the complexity of the coolant distribution system and, more importantly, the difficulty and complexity of managing power level and distribution, which was the main cause of the accident. RBMK reactors were therefore characterised by:

- possible instability due to radial and azimuthal power fluctuations, more marked for larger cores, due to core poisoning by the xenon (^{135}Xe)⁷ produced following a power step;
- the possibility of exceeding prompt criticality, leading to runaway reactor power due to a positive void coefficient (see Section 2.1): as water is a neutron absorber, a reduction in water flowrate or increase in steam production in the core leads to a reduction in neutron absorption and an increase in the number of fissions.

During a power increase, the variation in core reactivity is the result of the combination of positive effects (such as the void coefficient) and negative effects (such as

7. In a thermal reactor, one of the products of fission reactions is iodine-135 which decays to xenon-135 in a few hours. This is then transmuted by absorbing neutrons from the fission reactions. Under normal operation, power is relatively stable, and formation and transmutation of xenon-135 are in equilibrium. In the event of a sudden reduction in power, and therefore in the number of fissions, there are insufficient neutrons to transmute the xenon-135 and so it accumulates, as it continues to be produced from the iodine-135 produced by fissions prior to the power reduction. If an attempt is now made to increase reactor power by extracting control rods, the power increase does not occur because xenon-135 is a neutron absorber. It takes around 10 hours to return to a normal neutron balance.

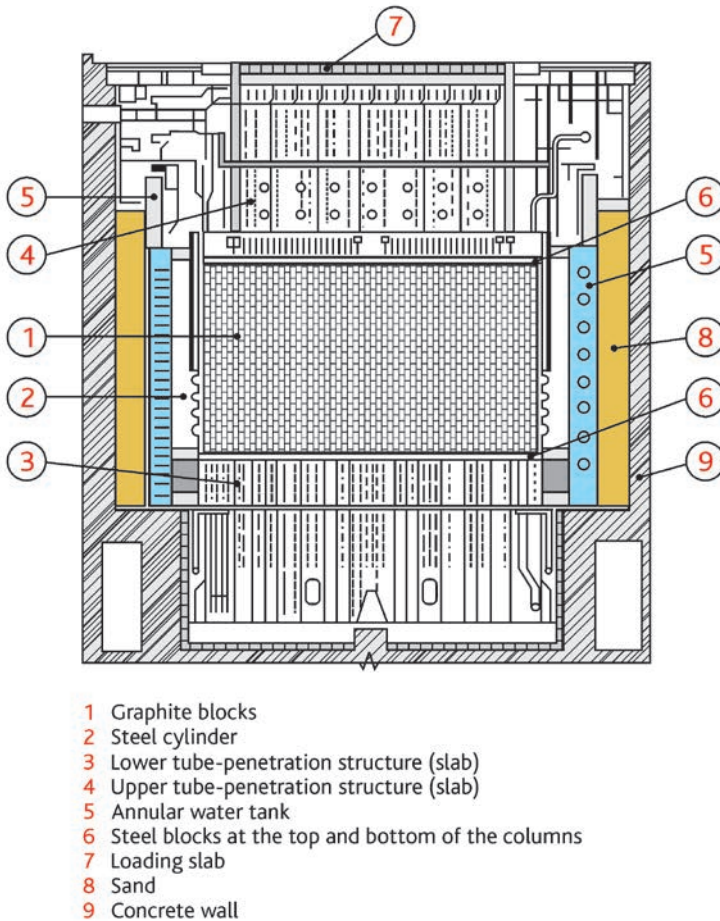


Figure 7.9. Schematic diagram of the Chernobyl-4 reactor core

dilation of structures that support the core, and the Doppler Effect⁸ associated with the higher fuel temperature). In RBMK reactors, negative effects dominate at nominal power due to the temperatures in the core. On the other hand, at low thermal power (below 700 MWth), the effect of the positive void coefficient dominates, and the power coefficient can become positive (during a voluntary increase in the neutron flux produced, for example, by reducing the penetration of the absorber rods in the core, accentuated by the water vaporisation that accompanies this variation). The increase in reactivity is normally compensated by the control rods. However, if this is not the case, it can lead to exceeding prompt criticality and runaway reactor power (see Section 2.1). Also note

8. The Doppler effect corresponds to a broadening of ^{238}U neutron absorption resonances in the neutron energy spectrum. This broadening increases with fuel temperature and leads to a reduction in fission reactions and core reactivity as it heats up (see Section 2.1).

the disadvantage mentioned above, regarding the transitory increase in reactivity when control rods are inserted into the core.

Another problem with the RBMK design was the lack of a large containment building that could withstand significant overpressure around the reactor core. There were just several containment compartments designed to provide confinement of radioactive substances in the event of an accident involving failure of a single pressure tube (the case of an accident involving failure of multiple pressure tubes had not been taken into account in the containment design).

7.2.2.2. Accident sequence

The [Chernobyl](#) disaster is very well documented; in particular, readers may refer to the reference documents for further details [4, 13-17].

The accident occurred during a test to check the possibility of powering the main reactor coolant pumps from one of the turbo-generators for a few seconds while it was slowing down under its inertia in the event of loss of offsite power, thereby providing additional time for emergency takeover by the diesel generators. This test was performed neither under the planned conditions nor in compliance with reactor operating procedures. In particular, several safety systems were disabled. Furthermore, as described below, although the test was planned at medium power of around 700 MWth, it was performed at lower power and with a delay compared to the planned schedule.

The sequence of events that led to the disaster can be summarised as follows:

- reactor power reduction was started on April 25 at 1:00 am; power was gradually reduced from an initial 3200 MWth to approximately 1600 MWth by around 1:00 pm;
- at the request of the Grid Control Centre in Kiev, the reactor was maintained at half power for around 10 hours to supply the grid. This unplanned period at half power led to reactor poisoning by xenon. The control rods were therefore gradually removed from the core to maintain the power level;
- power reduction was resumed around 11:00 pm;
- at 0:28 am on April 26, the power level was down to 850 MWth; the operators then switched over to the medium-power control system. This switchover, which was poorly controlled, led to an excessive power drop to 30 MWth and further increased core poisoning by xenon. The operators sought to perform the test at all costs and withdrew a large number of control rods from the core;
- the operators started up the two recirculation pumps at 1:03 am and 1:07 am respectively; the increase in fluid flowrate in the core led to a reduction in steam formation and a consequent reduction in reactivity. The operators decided to withdraw more control rods;
- at 1:15 am, the operators disabled the reactor trip signals so that they could perform the test;

- between 1:15 am and 1:22 am, cold water was injected into the core, which further decreased the reactivity. The automatic control rods reached their high position at 1:19 am. The operators then decided to further withdraw manual control rods, dangerously reducing the shutdown margin in the core;
- at 1:22 am, the computer indicated that the shutdown margin was equivalent to only 6 to 8 control rods, whereas the instructions prescribed immediate reactor shutdown if the shutdown margin was less than the equivalent of 15 bars. Despite all this, the operators decided to perform the test;
- four seconds after 1:23 am, the test was started; the slowing of the generator leading to slowing of the reactor coolant pumps, caused a decrease in water flow-rate and increased vaporisation in the core, which led to a reactivity insertion and an increase in power, which further accelerated vaporisation. The situation became divergent;
- forty seconds after 1:23 am, the head operator hit manual reactor trip; however, given the design of the control rods (with graphite tips), their entry into the core caused a reactivity insertion, which was probably the final trigger of the reactivity accident;
- forty-four seconds after 1:23 am, the reactivity insertion caused a sudden power surge followed by an explosion. According to some witnesses, a second explosion occurred two seconds later.

An attempt to reconstruct the behaviour of the reactor core during the accident has been made on the basis of later examinations of samples of fuel-bearing materials taken from the damaged facility and the environment. The power excursion probably caused fuel fragmentation, in particular in the lower part of the core. Water in the core would have interacted with very hot dispersed fuel particles, leading to massive vaporisation, an increase in pressure and probably a steam explosion (see Section 5.2.3). This explosion would have led to failure of the pressure tubes, followed by lifting of the reactor's upper slab. The energy released by the explosion has been estimated as equivalent to 30 to 40 tonnes of TNT. The explosion destroyed the reactor building and led to direct releases of radioactive substances into the environment.

Later examinations suggest that:

- high temperatures, of at least 2600 °C, were attained in the reactor core;
- molten core materials flowed towards the lower parts of the reactor and formed several pockets of accumulated "lavas", resulting from interactions between the molten corium and the structural materials (steel, concrete etc.) encountered; this took place over a period of approximately six days following the explosion;
- a large pocket of molten materials, resulting from drainage of local lava pockets, then formed within a crucible-shaped crust located above the concrete structures under the core; this stable, thermally-insulating crust held out for four days following the previous phase;

- this crust gave way about ten days after the explosion, forming three flows. The lava flows then cooled and solidified, resulting in a major reduction in the emission of radioactive substances.

Due to the lack of confinement, a large fraction of the radioactive products contained in the fuel were released into the atmosphere over several days (see Section 7.2.2.3). Large releases were produced over a ten day period from April 26 to May 5, 1986, despite the efforts of the plant operator and the authorities to manage the accident (between April 27 and May 2, approximately 1800 helicopter runs were made to cover the reactor by pouring about 5000 tonnes of materials such as sand, boron, clay, lead and dolomite).

Within the facility, incandescent debris were projected by the explosion and caused various fires, in particular on the roof of the turbine hall. It took fire-fighters about three hours to extinguish them and fire-fighters were exposed to high doses of radiation during their interventions. At about 5 am, a graphite fire was declared. Numerous fire-fighters were exposed to additional radiation attempting to extinguish this fire. The core's enormous mass of graphite burned for ten days after the accident and, after the initial explosion, was probably the main cause of the dispersal of radioactive substances to high altitudes. Radioactive releases continued for about twenty days, but were much smaller after the tenth day when the graphite fire was finally extinguished. A photograph of Unit 4 of the power plant taken just after the accident is given below in Figure 7.10; it shows the immediate damage to the facility.

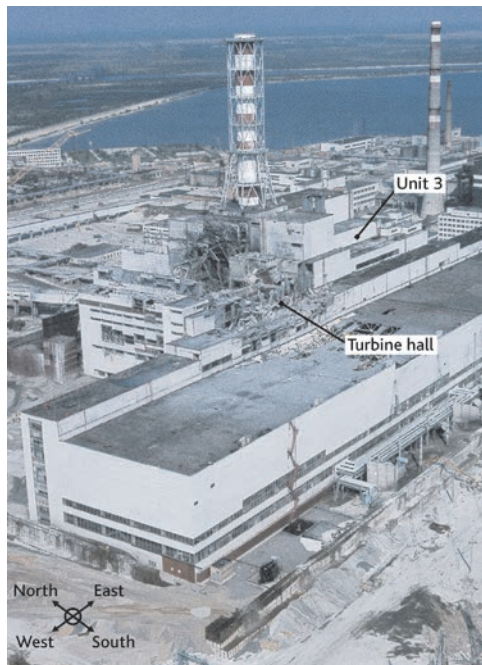


Figure 7.10. Photograph of the power plant after the accident (Source: DR).

7.2.2.3. Releases and consequences

A third of the releases of radioactive substances occurred at the time of the explosion, which put the reactor core into direct contact with the environment. This large initial release can be largely attributed to mechanical fragmentation of the fuel during the explosion. It mainly contained volatile compounds (noble gases, and iodine and caesium isotopes). The other two-thirds of releases were produced over the following ten days, when molten fuel remained in the reactor and the graphite was on fire. These releases were at their most intense between the seventh and tenth day when core temperatures were at their highest. The sharp reduction in releases observed after ten days may possibly be attributed both to rapid cooling of the fuel, as the molten materials and core debris crossed the lower biological shield and reacted with other colder materials in the reactor, and to extinction of the graphite fire.

Estimates of total releases produced using all available sources [16] (environmental measurements and analyses of what remained in the facility) show that, as percentages of the initial core inventory, 100% of noble gas radioisotopes were released, 50 to 60% of the radioiodine, 20 to 40% of the radioactive caesium, and around 3 to 6% of other radioisotopes (including actinides and fuel fragments that fell near the reactor). This corresponds to release of approximately 2×10^{18} Bq of ^{131}I (an isotope with a half-life of about 8 days that plays an essential role in short-term effects) and approximately 10^{17} Bq of ^{137}Cs (an isotope with a half-life of about 30 years that plays an essential role in medium to long-term effects).

Due to the explosion and the intense heat produced by the fuel itself and by combustion of hydrogen (produced by zirconium oxidation) and graphite, the radioactive substances released rose to a relatively high altitude (between 1000 and 1500 m), which contributed to reducing local contamination but led to contamination over long distances [17]. The winds at this altitude carried radioactive substances firstly towards Scandinavia (contamination was first detected in Sweden, prior to any official announcement regarding the accident), then towards Central and Western Europe. Given the duration of the releases and the changes in weather conditions, all of Europe (excluding Spain and Portugal) was ultimately affected by part of the releases. As there were numerous, often very localised, precipitation events during contamination transfers, significant fallout occurred locally, leading to non-uniform contamination of soil and vegetation. Most typical are the “leopard skin” contamination patterns observed in the south of Belarus in particular. Similar phenomena, but at a lower level of contamination, have been observed in Italy, Switzerland and France (in the Vosges, Corsica and the Mercantour Massif). Reference Document [17] gives a detailed description of the dispersion of radioactive pollutants released during the accident at the European and French scales, and estimate mappings of ^{131}I and ^{137}Cs deposits in France (for 2007).

From a health perspective, 28 people (notably fire-fighters) died quickly due to the very high radiation doses they received (three other people had been killed during the explosion). Many health problems have been observed among the 600,000 “liquidators” (soldiers and civilians who built the rudimentary concrete sarcophagus to contain the damaged reactor and who cleared the most contaminated soils over a radius of 30 km

around the plant). However, the lack of systematic medical monitoring of the liquidators means that the health consequences of the accident on these people cannot be established with certainty. Discussion of these highly complex and controversial aspects is outside the scope of this work.

In the most contaminated areas of Belarus, Ukraine and Russia, an undeniable health effect of the radiation is the very marked increase in thyroid cancer among children under 15 at the time of the accident. The incidence rate is between 10 and 100 times the "natural" rate [17]. Thyroid equivalent doses are mainly due to iodine-131. These doses were received in the three months following the accident. Consumption of contaminated produce and, to a lesser extent, inhalation of radioactive substances during the radioactive releases, were the cause of these thyroid doses.

The inhabitants of the most exposed zone (116,000 people), located in a radius of 30 km around the damaged reactor, were evacuated in the days following the accident. This zone is called the "exclusion zone". Deposits of caesium-137 (the main contributor to long-term doses) generally exceeded 500,000 Bq/m² in this zone, and reached several million Bq/m² in the most affected areas. Distribution of the deposits is not uniform around the site; it depends on the various wind directions during the releases.

At greater distances (of the order of several hundred kilometres) caesium-137 deposits are non-continuous; there are patches of contamination wherever the releases encountered precipitation. Three countries were affected over vast expanses by caesium-137 deposits exceeding 37,000 Bq/m² (the threshold adopted after the accident to define contaminated areas): approximately 41,840 km² in Ukraine, 46,450 km² in Belarus and 56,930 km² in Russia. In these areas, deposits are variable and can reach several hundred thousand Bq/m², and in places even exceed a million Bq/m².

In addition to the people evacuated in the days that followed the accident, 250,000 people were evacuated from the most contaminated areas between 1986 and 1995. This large number of people evacuated is explained by the decision of the Soviet authorities to evacuate people from areas where ¹³⁷Cs soil contamination exceeded the threshold of 555 kBq/m² [18]. Relocation proved to be a deeply traumatic experience for those affected.

The consequences of the accident in France are incomparable with those observed in the most affected countries around the [Chernobyl](#) site. However, France was affected by arrivals of contaminated air from the beginning of May via the south-east and north-east, which mainly affected the eastern half of the country and had little effect in the western part. Forest soils were the most contaminated, especially in mountain areas, and contamination patches of several thousand Bq/m² were measured, mainly in Alpes-Maritimes, Corsica and the Vosges. However, recent studies confirm that the doses received by the French public and the associated health risks may be considered as low [17]. In particular, the mean thyroid doses received by children in France are approximately 100 times lower than those received by children in Belarus, where a significant number of thyroid cancers were observed. No epidemiological study has brought to light an excess of thyroid cancers at the dose levels received in France. Nevertheless, the possibility of such an excess cannot be excluded, in particular among children.

7.2.3. *Lessons learned in France regarding safety*

The **Chernobyl** disaster was very different from the Three Mile Island accident. Chernobyl was a reactivity accident, mainly associated with the specific characteristics of RBMK reactors (in particular, that their operation could lead to a positive void coefficient, which is not the case for PWRs, see Section 2.1). Nevertheless, in terms of safety, the Chernobyl disaster led to the following actions for French nuclear power plants:

- research and emphasis on possibilities for reactivity accidents other than those covered in existing safety reports;
- research and emphasis on physical and organisational possibilities for operation with safety systems disabled;
- enhancement of the safety culture among nuclear facility licensees, in particular with the aim of preventing the disabling of safety systems and deviations from operating technical specifications;
- research and emphasis on situations where there has been non-compliance with the operating technical specifications;
- improvement of systems for measuring radioactive releases into the environment;
- development of dialogue to specify measures that the public authorities could implement to mitigate the consequences of radioactive releases in the medium and long term after the emergency phase;
- movement towards greater information transparency: in particular by the production and use of the International Nuclear and Radiological Event Scale (INES) for accident and incident severity, and by increased involvement of civil society (via local information commissions and their national association) in the institutional framework responsible for **nuclear safety**, which includes public authorities (French Nuclear Safety Authority [ASN]), institutional consultancy (IRSN) and licensees.

In particular, the **Chernobyl** disaster, a criticality accident not covered by the designers and unknown to plant operators in what was then the Soviet Union, led to a review of the way in which reactivity accidents are considered and covered in France. The possibility of sequences not covered in existing safety reports was explored, bringing to light potentially hazardous scenarios, especially during a reactor outage. These scenarios include accidental injection of “clear” water (i.e. water with a low boron concentration, boron being a neutron absorber) into the core. Additional provisions have since been taken to eliminate, as far as possible, this type of “non-uniform dilution” accident.

Although very different from the Three Mile Island accident, the **Chernobyl** disaster led to an acceleration of research work regarding reactor core melt accidents, including research and studies on the possibilities of early containment failure. The three phenomena that could lead to sudden loss of containment in the short term – steam explosion, direct containment heating and hydrogen explosion –, have been, and continue to be, the subject of major research programmes (see Section 5.2).

The **Chernobyl** disaster also raised awareness of the possible long-term effects of a nuclear accident. For the EPR, this led to specification of general safety objectives regarding core melt accidents (see Section 4.3.4.1 for further details).

- core melt accidents that could lead to large early releases must be “practically eliminated”; this includes high-pressure (> 20 bar) core melt accidents;
- low-pressure core melt accidents must be managed such that the associated maximum conceivable releases would only require very limited public protection measures in terms of scope and duration.

7.2.4. Lessons learned in France regarding “nuclear crisis” management

The **Chernobyl** accident made the issue of assessing and managing large-scale contamination by massive ejection of radionuclides from a nuclear facility into an urgent practical question. In France, lessons learned from analysis of the consequences of the accident, and changes to techniques for assessing environmental contamination, have identified areas for improvement in the management of a nuclear crisis. The lessons concern two key questions: “How can the consequences of accidental environmental contamination on people and the environment be assessed with adequate precision and speed?” and “What provisions can best mitigate the impact of such contamination on public health?”.

After the **Chernobyl** disaster, the French authorities decided to enhance their means to assess the radiological consequences on people and the environment by:

- expanding and improving systems for the early detection and characterisation of airborne contamination;
- developing software to model radionuclide transfers into the environment (fallout and contamination of the food chain);
- developing methods to assess and monitor dosimetry consequences for the public (external irradiation from the ambient environment and internal contamination *via* inhalation and ingestion) and implementing protective actions to mitigate such internal exposure.

These developments are described in detail in Reference [17].

Ten years after the accident, in the context of provisions that aim to enhance public protection, the French government decided to distribute stable iodine tablets to people living near a nuclear facility that could release radioactive iodine, so that they would be immediately available to be taken, if needed, on instruction from the prefecture. This would prevent thyroid cancer (taking stable iodine protects the thyroid by saturating the gland – thus preventing it from absorbing radioactive iodine). It was also found necessary to improve the effectiveness of the on-site emergency plans implemented by licensees and the off-site emergency plans implemented by the authorities. More frequent drills, including drills involving the public, have been performed to validate and improve the corresponding provisions.

7.2.5. Conclusion

The **Chernobyl** disaster led the affected countries to review the safety of RBMK reactors, and more generally, the safety of all nuclear power plants in Eastern Europe. International cooperation programmes for technical and financial assistance have been developed to this end. Under international pressure, the **Chernobyl** power plant was definitively shut down at the end of the year 2000. Other reactors of the same type were also shut down when former Soviet countries joined the EU.

Lessons have also been learned from the **Chernobyl** disaster for French and other Western European reactors. New research has been launched with regard to reactivity accidents. Measures have been taken to enhance the safety culture among licensees (in particular, with the aim of preventing the disabling of safety systems and deviations from operating technical specifications). However, this disaster has specifically demonstrated that the contamination resulting from a severe accident can be very widespread, cover a whole continent, and have large-scale, long-term socio-economic consequences. In France, lessons learned from the disaster mainly concern the development of resources to manage a nuclear crisis in both the short-term (emergency phase) and the medium to long term (post-accident phase). Environmental monitoring networks (for air, soils and animal and vegetal produce) have also been considerably enhanced. Research has been developed regarding possible measures for mitigating the consequences of a nuclear crisis (such as radiological protection and public health monitoring, radiological monitoring and rehabilitation for affected areas, redeployment of industrial and agricultural activities from those areas, economic support for the affected sectors, and relationships with other countries affected by the accident).

The consequences and health effects of the disaster are still only partially known. In particular, large-scale epidemiological research is being undertaken for the “liquidators” and the populations affected by the evacuations.

7.3. The Phebus FP programme

7.3.1. Background

Since the Three Mile Island (TMI-2) accident on March 28, 1979, which led to approximately half the reactor core melting, albeit with minimal releases of fission products into the environment, a series of experimental safety-research programmes has been performed by various entities worldwide. Numerous computer models have also been developed to simulate a core melt accident sequence, assess the consequences, and determine the effectiveness of various provisions that could be implemented to mitigate the effects. Launched by IPSN (the forerunner of **IRSN**) in 1988, the **Phebus FP** (FP for fission products) programme of experiments was one of the main research programmes focussed on core melt accidents for water-cooled reactors. This programme was launched in partnership with the European Commission and EDF, and performed in close collaboration with CEA, which operates the Phebus reactor. Collaboration quickly expanded to include the USA, Canada, Japan, South Korea and Switzerland. The

collaborative nature of the programme enabled regular international discussions with regard to understanding and interpreting results, and the ability of simulation software to reproduce these results. This was a key factor in the programme's success.

A number of the results obtained under this programme were unexpected. Such results, which are important for safety analyses, regard fuel rod degradation and cladding oxidation, the effect of control rod materials on fuel degradation and fission-product chemistry, and the behaviour of iodine in the reactor coolant system (RCS) and the containment. Analysis of the results as a whole, and their use in studies on the radioactive releases into the environment that could result from a core melt accident, has revealed a certain number of lessons [21, 24, 37 and 58]. Software to simulate the various physical phenomena involved during such an accident has been significantly improved via the development of new models. Specific small-scale tests have been performed to understand the unexpected phenomena observed and to validate new models. A list of the main remaining uncertainties was drawn up at the end of the *Phebus FP* programme. The European EURSAFE Project [50], part of the Fifth Framework Programme for Research and Technological Development (FP5), whose objective was to develop a realistic assessment of possible releases into the environment for better management of the associated risks, has specified research priorities with a view to reducing these uncertainties. Part of this research is the subject of the International Source Term Programme (ISTP) [27, 30], jointly launched by IRSN, CEA and EDF in 2005, which involves a series of analytical tests, in particular regarding iodine chemistry, fuel degradation in the presence of boron carbide (a neutron absorber), oxidation of cladding in air, and the release kinetics of fission products from the fuel. This programme is due to be completed in 2014.

7.3.2. Description of the *Phebus FP* test setup and test matrix

Five integral in-pile tests were performed during the *Phebus FP* programme. By providing experimental conditions representative of a PWR under core-melt accident conditions [25 and 57], the setup can be used to study fuel degradation including formation of a molten pool, hydrogen production, the release and transport of fission products in the RCS, aerosol physics, and iodine chemistry in the RCS and containment.

The various physical phenomena studied occur in 1) the reactor core, which is represented by 20 fuel rods, analogous to those in a PWR, along with a 1-metre-long absorber rod, 2) the RCS, whose steam generator is represented by an inverted U-tube, 3) the containment, represented by a 10 m³ vessel with a water-filled part for the sump, a gas-filled part and painted surfaces. These three areas are reproduced at 1:5000 scale compared to a 900 MWe PWR (see Figure 7.11).

The test matrix for the series of tests performed is described in Table 7.1. The experimental conditions were identical for the first two tests (FPT0 and FPT1), except with regard to the fuel: new fuel was used during test FPT0, while fuel with burnup of 23 GWd/tU was used for test FPT1 (burnup equivalent to two fuel cycles in a PWR). The main characteristics of these two tests were a relatively high steam flowrate at the test device inlet to maintain a fairly oxidising atmosphere during the entire phase of

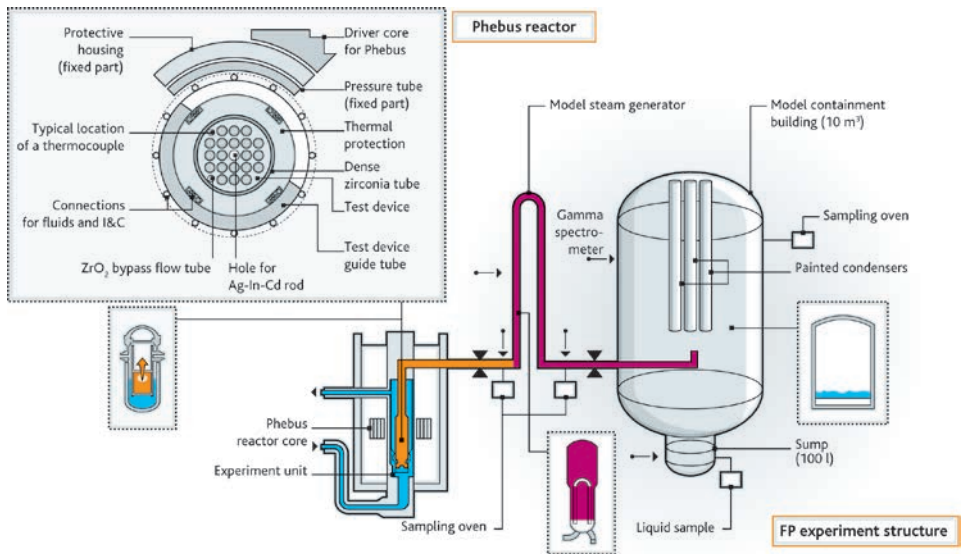


Figure 7.11. Schematic diagram of the Phebus FP test setup. Top-left box: test device (assembly of 20 fuel rods).

zirconium alloy cladding oxidation by steam, the use of a silver-indium-cadmium control rod (neutron absorber), an RCS adjusted to 700 °C on the hot leg and 150 °C on the cold leg, painted surfaces in the containment building to study iodine interactions with paints (painted condensers), and an acidic aqueous solution in the containment sump. During the FPT2 test, the injected steam flowrate was much lower, leading to a less oxidising (hydrogen-rich) atmosphere during fuel rod cladding oxidation, and with the aqueous solution in the containment maintained alkaline at a temperature above that of the gas phase to cause evaporation from the sump, unlike in the previous tests. The experimental conditions for the FPT3 test were identical to those of the FPT2 test, except with regard to the type of control rod, where a boron carbide rod was used, and the pH of the sump (which was acidic rather than alkaline). Finally, the main objective of the FPT4 test was to study the release kinetics of low-volatile fission products and actinides from a debris bed made up of fragments of fuel pellets and oxidised cladding, typical of what was found after the TMI-2 accident.

Each test was performed in two phases. During the first phase, which lasted several hours, the fuel temperature was gradually increased up to its melting point and fuel assembly failure. This led to the release of fission products and structural materials into the containment vessel via the RCS. Then, over a four-day period, the behaviour of these fission products and structural materials in the containment was studied, whether they were in the form of aerosol particles (agglomeration, transport and deposition phenomena, etc.) or gases, in particular with regard to iodine. The radioactivity of the released fission products produced a significant dose rate in the containment and the effect of radiation on fission-product chemistry was also studied.

Table 7.1. Objectives and experimental conditions for the Phebus FP tests

Test	Main objective	Experimental conditions			
		Fuel assembly ⁽¹⁾	Reactor coolant system	Containment vessel	Date
FPT0	Formation and development of a corium pool and release of fission products into a steam-rich mixture	New fuel 1 Ag-In-Cd rod "re-irradiation" for 9 days	No steam condensation in the steam generator	Painted surfaces Sump at pH 5	December 2, 1993
FPT1	As for FPT0 but with irradiated fuel	Fuel with burnup of 23 GWd/tU 1 Ag-In-Cd rod "re-irradiation" for 9 days	As for FPT0	As for FPT0	July 26, 1996
FPT2	As for FPT1 but with release of fission products into a hydrogen-rich mixture	Fuel with burnup of 32 GWd/tU "re-irradiation" for 9 days	As for FPT1 but with boric acid injection	As for FPT1 but with sump at pH 9 with evaporation	October 12, 2000
FPT3	As for FPT2	As for FPT1 but with B ₄ C rod Fuel with burnup of 24 GWd/tU "re-irradiation" for 9 days	As for FPT0	As for FPT2 but with sump at pH 5 with evaporation, hydrogen recombiner coupons	November 18, 2004
FPT4	Release of low-volatile fission products and actinides from a bed of UO ₂ + ZrO ₂ debris	Fuel with burnup of 38 GWd/tU no "re-irradiation"	Addition of integral filters upstream of the test device Chemical analyses of the samples taken		July 22, 1999

(1) The fuel was "re-irradiated" in the Phebus reactor in order to reproduce the inventory of short half-life fission products, in particular ¹³¹I, which had decayed from the fuel since its unloading from the reactor where it had been irradiated.

7.3.3. Main lessons regarding fuel rod degradation

7.3.3.1. Oxidation of fuel rod cladding

In the event of a core melt accident on a water-cooled reactor, fuel degradation begins by oxidation of the cladding with rapid temperature rise (see Section 5.1.1.2). During the first **Phebus FP** test, FPT0, the observed temperature rise was faster than predicted by prior simulations, with significant hydrogen production, beyond the design of the measurement devices (see Figure 7.12), and with fuel-rod temperatures rising to very high levels, above 2400 °C. The initial simulations performed after the

test, using the same models as for the pre-test simulations but with the real boundary conditions from the tests, did not reproduce the observed data. Due to the sudden increase in cladding temperature, there was competition between its oxidation, which progressed from the external surface forming an oxide layer, and the dissolution of UO_2 fuel in contact with the remaining molten metal cladding. These phenomena were interrupted when the outer zirconium oxide layer (ZrO_2) became too weak to retain the liquid metal within (this is called “cladding dislocation”). The computer models used to simulate these phenomena include correlations that specify a cladding dislocation criterion based on its temperature and the thickness of the ZrO_2 layer. These correlations have been modified to provide correct simulation of cladding oxidation and the associated hydrogen production (see Figure 7.12) for the FPT0, FPT1 and FPT2 tests [54], and the FPT3 test [56].

Furthermore, hydrogen production kinetics were strongly influenced by the steam flowrate injected into the assembly. At low flowrates, the steam was almost entirely consumed by cladding oxidation in the lower part of the fuel rods, and the fluid was steam depleted in the upper part, leading to a significant period of “steam starvation” (i.e. the phase in which steam has been almost entirely consumed by oxidation) during the main cladding oxidation phases for the FPT2 and FPT3 tests. Hydrogen production calculated using these correlations is seen to be a slight overestimate [56], which is probably associated with the coupling between oxidation phenomena, fuel dissolution and cladding failure.

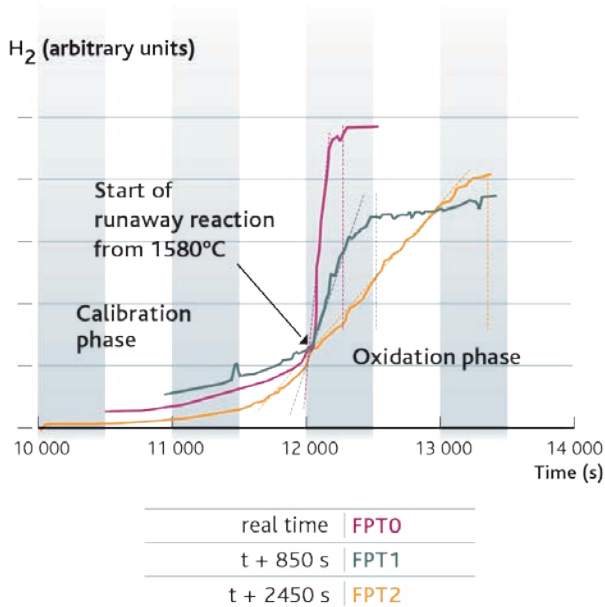


Figure 7.12. Hydrogen production kinetics measured during the FPT0, FPT1 and FPT2 tests (solid lines) and calculated using correlations revised following the Phebus FP tests (dotted lines). In order to aid comparison, the curves for the FPT1 and FPT2 tests have been drawn with a time shift compared to the real start time of the test.

7.3.3.2. Fuel degradation

The **Phebus FP** experiments produced greater fuel degradation than had been previously obtained in integral experiments of the same kind. In particular, it was observed that fuel melt, and structural failure of the rod assembly into a pool of molten materials, could occur at a temperature of 2350 °C (± 200 °C), which is much lower than the melting point of pure UO_2 (2830 °C) [54]. The very severe degradation observed during the Phebus FP tests seems to be associated with significant interactions between the fuel and the structural materials (mainly steel structures and zirconium alloy cladding), probably intensified by fuel swelling, due to the presence of large quantities of gaseous and volatile fission products. Fuel oxidation by steam leads to a change in its stoichiometry (an increase in the quantity of oxygen with respect to uranium during the tests), reducing its melting point, which seems to have played an especially significant role [20]. Although detailed modelling of these phenomena still needs to be improved and developed, current simulation software correctly reproduces the final state of assembly degradation (see Figure 7.13) as long as a suitable reduction is applied to the fuel rod relocation temperature⁹ [55].

The sensitivity of degradation models to significant parameters (cladding dislocation criteria and fuel relocation temperature) has been assessed for simulations of the TMI-2

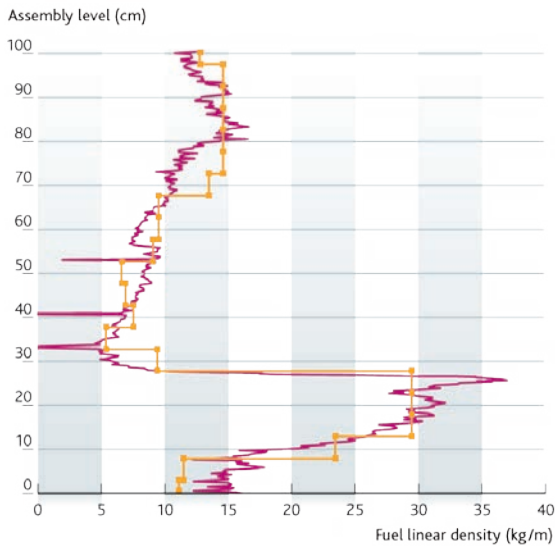


Figure 7.13. Examples of axial fuel distributions as measured (in purple) and as calculated using the ICARE2 code (in orange) [55] at the end of the FPT2 test, which highlights an accumulation of materials on the lower part of the degraded assembly (area where a corium pool formed) and a lack of materials above (area where a cavity formed).

9. “Fuel relocation temperature” is the name given to the temperature at which the simulation software assumes fuel assembly failure and large-scale downward movement of the fuel, whether due to melt phenomena or solid-phase flows.

accident using the American MELCOR code [43]. During this study, it was shown that the calculated behaviour of the core is strongly dependent on the degradation models used and the values of their parameters. A fuel relocation temperature of 2230 °C for structural failure, deduced from the results of the *Phebus FP* tests, has now been adopted for the MELCOR code and gives quite good results. The same conclusions and experience feedback have been drawn from studies performed using the ICARE/CATHARE and ASTEC code developed by IRSN (described in Sections 5.1.1.3.2 and 8.3).

Degradation of the debris bed in the FPT4 device, including transition from a debris bed to a pool of molten materials, has been reproduced (see Figure 7.14), assuming fuel swelling [31] that causes a reduction in porosity inside the debris bed and the consequent redirection of steam towards the bed perimeter (and a reduction in convective heat exchange).

Following the FPT4 test, analysis of the results of destructive tests on the fuel show that it appears to have been oxidised during the transient, solid-state interactions led to partial early melting (at 2530 °C, which is low in the absence of unoxidised metals), and part of the corium was formed by separate melting of the two components (UO_2 and ZrO_2). While no direct measurement of post-test fuel porosity is available, these observations are consistent with the assumption of fuel swelling. Finally, analysis of the composition of the molten phases shows that temperatures exceeding 2700 °C were attained.

The FPT3 test [53] was performed under conditions very similar to those of the FPT2 test, except for the presence of a boron carbide (B_4C) control rod instead of a silver-indium-cadmium alloy (Ag-In-Cd) absorber. Although the power transient was stopped at a lower level than in the FPT2 test, with less extensive assembly degradation, earlier degradation

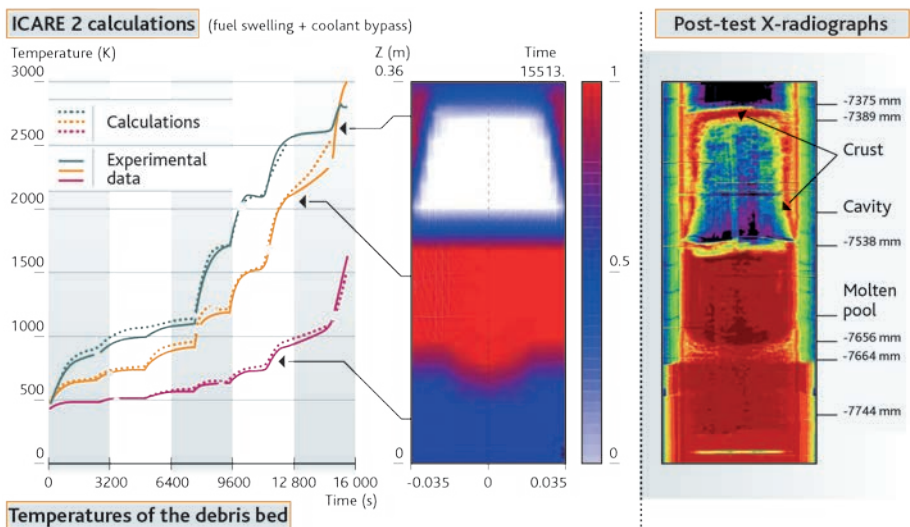


Figure 7.14. Changes in (calculated and measured) temperatures in the FPT4-test debris bed and the final state of fuel degradation indicated by the ICARE2 code (calculated specific gravity) and by post-test X-radiograph (measured specific gravity).

occurred, in particular during the cladding oxidation phase. Furthermore, simulation software is currently unable to correctly reproduce all the results of the FPT3 test, in particular the duration of the hydrogen-rich (steam-starved) phase (see Figure 7.15). Some hypotheses have been formulated regarding the possible role of B_4C to explain early cladding degradation [28 and 56] and have been explored using separate-effects experiments (the BECARRE programme, completed in 2010 as part of the ISTP [27]). These experiments demonstrated that a molten B_4C -steel mixture could be projected onto the fuel rods next to the boron carbide control rod and accelerate cladding degradation.

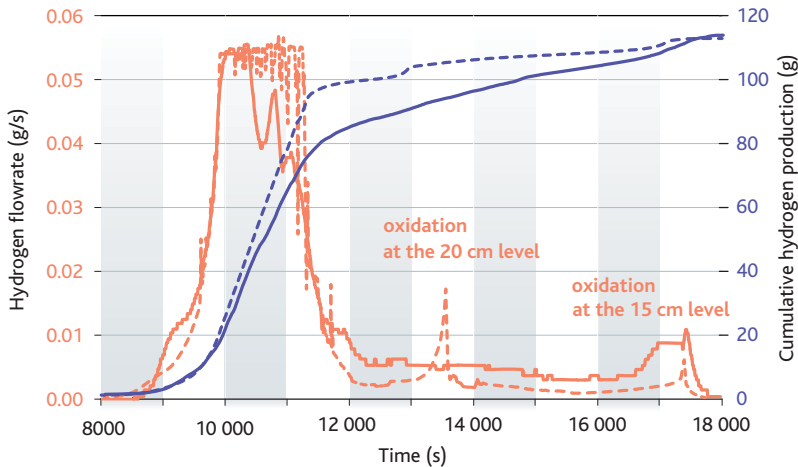


Figure 7.15. Hydrogen release flowrate and cumulative hydrogen production during the FPT3 test. Comparison between (ICARE2) calculation (---) and experiment (—).

7.3.4. Releases from the core

7.3.4.1. Fission product releases

Generally, very similar percentages of fission product inventories were released from the fuel during the three tests FPT0, FPT1 and FPT2. However, due to the lower flowrate of steam injected into the test device during test FPT2, a non-negligible fraction of the volatile fission products (Mo, Cs, I and Te) released was deposited in the upper part of the fuel assembly and in the non-thermally-regulated area located just above it. This was also observed during test FPT3.

Fission product releases depend on the characteristics of the UO_2 fuel (temperatures, degree of oxidation, and burnup) and its interactions with the other components that make up the core as degradation of the materials progresses. These dependencies were clearly revealed during the *Phébus FP* tests. Volatile fission product releases are generally well predicted by all simulation software (see the results for caesium in Figure 7.16), although some software, in particular codes based on a CORSOR-type approach¹⁰, overestimates

10. CORSOR-type models use “releases as a function of temperature” correlations derived from small-scale experiments.

fission product release kinetics at the beginning of the power transient, specifically during the runaway cladding oxidation reaction [26 and 29]. Semi-empirical software adequately simulates volatile fission product releases both for analytical tests and for Phebus-type integral tests despite the fact that it does not simulate all phenomena in detail, but rather uses simplified models to take into account the most influential phenomena, such as the significant increase in diffusion inside the uranium oxide matrix during its oxidation. This is true of the ASTEC code for example.

It should be noted that in the specific case of the FPT0 test, characterised by fuel with very low burnup, the early release of volatile fission products can only be explained by partial dissolution of the fuel from the cladding oxidation phase [35].

Semi-empirical simulation software has been less successful in predicting the release kinetics of semi- and low-volatile fission products, which are strongly dependent on chemical interactions (see the results for barium in Figure 7.16). However, better understanding of the phenomena that govern these releases has been obtained *via* use of mechanistic models [35], such as those included in the Modelling Fission Product Release (MFPR) code (see Section 5.5.2.3 for more details). This knowledge has been gradually integrated into the software by using simplified models. Barium releases during the Phebus FP tests performed using a fuel-rod assembly are much lower than those measured during analytical tests. The difference has been attributed to interactions between the fuel and the cladding materials (such as the zirconium and iron in the control rod cladding), leading to a marked reduction in barium volatility [34]. This hypothesis is confirmed by the results of the FPT4 test (using a debris bed made up of fuel and cladding fragments with no control rod material), during which barium releases were much higher during the initial test phases, while the materials were still solid, than during the higher-temperature phases when melting started along with interactions between the fuel debris and fragments of oxidised cladding [22].

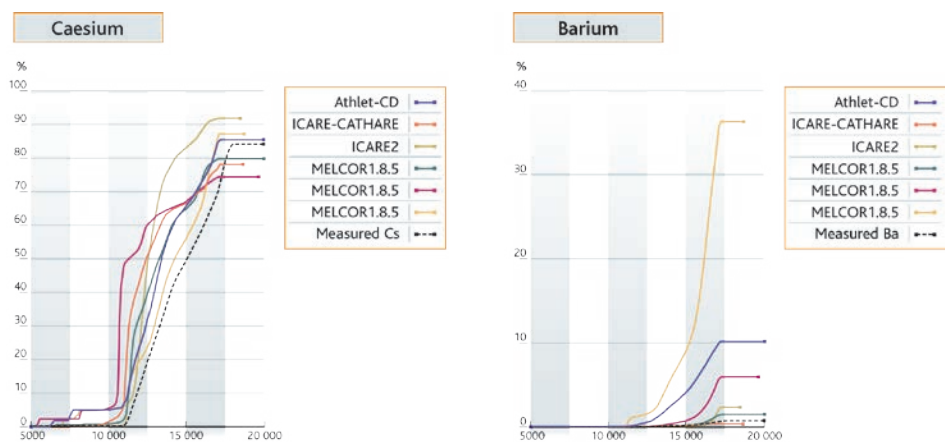


Figure 7.16. Caesium (left) and barium (right) release kinetics during the FPT1 test, as simulated by various computer models (results from International Standard Problem 46 (ISP-46) [26]). Comparison with experimental measurements (black dotted line).

The results of the **Phebus FP** tests therefore clearly demonstrate a link between fission product release kinetics and fuel degradation phenomena.

7.3.4.2. Aerosol emissions from structural materials

Aerosol emissions from structural materials and control rods are significant for two reasons:

- the mass of structural materials in the core is much greater than the mass of fission products. These materials make up a large share of the mass of aerosols circulating in the RCS and released into the containment. This share represented the majority during the first two tests (over 50% of the total mass of aerosols), but was lower during the FPT2 and FPT3 tests (approximately 35% of the total mass of aerosols in the containment vessel). The total mass of aerosols present in the containment over time and the deposition kinetics of these aerosols therefore depend on the emission of structural materials;
- certain elements involved interact with the fission products (e.g., silver reacts with iodine), which can modify the behaviour and volatility of the fission products.

Emission of materials from silver-indium-cadmium control rods was poorly simulated by most of the software [26], in particular with regard to silver (see Figure 7.17). The major phenomena governing the emission of these elements are now relatively well understood and models have been developed and integrated into some simulation software, such as ICARE, ASTEC and MELCOR. However, the impact of control rod degradation on the emission of some of its constituent elements still needs to be better taken into account. Emission of the tin originally contained in the zirconium alloy cladding (see Figure 7.17) has also been reconsidered. On the basis of experimental results from the **Phebus FP** programme, a new model was produced that predicts gradual release of this element as the cladding oxidises during a core melt accident on a water-cooled reactor.

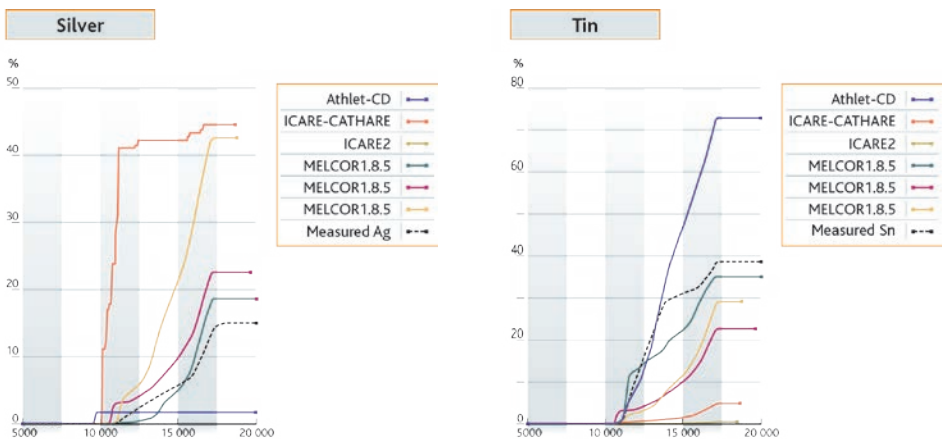


Figure 7.17. Silver (left) and tin (right) release kinetics during the FPT1 test, as simulated by various computer models (results from ISP-46 [26]). Comparison with experimental measurements (black dotted line).

Finally, models for uranium emission, one of the major constituents of the aerosols emitted and released into the containment, have also been reviewed on the basis of the results of the **Phebus** FPT4 test. A wide range of predictions for uranium emission from various computer models was clearly observed during simulations prior to the test, demonstrating the need to improve models. According to simulations performed after the test using the thermal conditions from the experiment, uranium emission from the lower part of the debris bed should have reached 60 g (for a total uranium mass of approximately 4.5 kg in the debris bed) [52]. However, a large unmeasured fraction of this uranium was deposited in the upper part of the bed, such that the calculated fraction of uranium released from the fuel is compatible with the value from the experiment, estimated at approximately 11 g following chemical analysis of the integral filters located downstream of the test device [22].

7.3.5. Transport of fission products and aerosols in the RCS

During the **Phebus** FP tests, two main retention zones for aerosols and fission products were identified in the part of the test setup that represented the RCS. These zones, where wall and fluid temperatures dropped rapidly, were the vertical part of the hot leg immediately above the fuel assembly (cooling from around 1750 °C to 700 °C) and the steam generator rising leg (cooling from 700 °C to 150 °C).

During the first two **Phebus** FP tests, FPT0 and FPT1, most elements, with the exception of iodine, cadmium and some of the caesium, were transported as aerosols into the RCS hot leg, where the temperature was maintained at 700 °C. During these tests, iodine and cadmium were deposited in large quantities at the steam generator inlet via condensation of their vapours. In contrast, due to its lower volatility, caesium was deposited in equal quantities in each of the two zones with steep thermal gradients mentioned above. Finally, other elements, such as molybdenum and silver, which are even less volatile, were mainly deposited in the RCS vertical line located above the fuel assembly.

During the FPT2 test, several notable differences were observed with respect to the previous tests. In particular, besides the three elements cited above (I, Cs and Cd), indium and tellurium were also partially transported in vapour form at 700 °C. For each of these elements, the fraction transported in vapour form was relatively constant throughout the test and represented over half its total mass. An identical deposition rate in the steam generator hot leg was measured for these elements and for molybdenum.

Partial, temporary revaporisation phenomena for deposits on the RCS hot leg were clearly demonstrated during the FPT1 and FPT2 tests. Such phenomena were mainly observed for caesium after its releases from the fuel had ceased, and are explained by a reduction in the partial pressure of various caesium species in the fluid.

Tellurium seemed to have a very particular behaviour during the FPT2 test, with a large fraction deposited in the RCS upstream of the steam generator, possibly by chemisorption. In the long term, these deposits could lead to releases of iodine (daughter isotopes of tellurium).

Finally, various chemical forms of iodine, transported into the RCS hot leg in vapour form during the FPT2 test, have been brought to light *via* analysis of the condensates deposited on the walls of the sampling lines, in an area where the temperature dropped from 700 °C to 150 °C. Several chemical species were found: caesium iodide was only detected after the main cladding oxidation phase (mass-spectrometry detection of Cs and I in equal proportions) and other unidentified more volatile species, whose condensation temperatures were approximately 200 °C and within a range of 330 °C to 430 °C respectively (see Figure 7.18). The specific case of the presence of gaseous iodine in the RCS is covered in Section 7.3.7.

Analysis of aerosol and fission-product transport in the RCS during the FPT0 and FPT1 tests, performed using the ASTEC code [46], shows that calculations generally adequately predict the behaviour of vapours and aerosols, along with the overall quantities deposited in the RCS. However, fission-product retention is underestimated in the vertical line above the fuel assembly and overestimated in the steam generator. Underestimation of deposits in the vertical line may be explained by the fact that the fluid flow

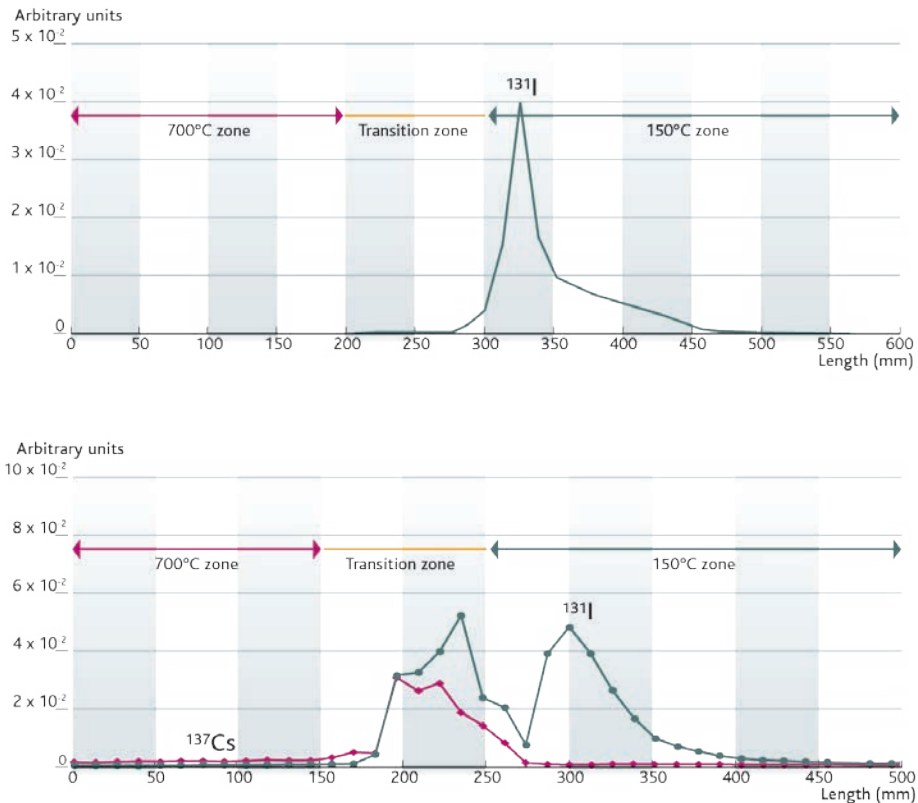


Figure 7.18. Caesium (in pink) and iodine (in green) vapour condensation profiles on the lines with a temperature gradient from 700 °C to 150 °C for the initial cladding oxidation phase (top) and for the fuel heating phase (bottom) during the FPT2 test.

in this area is not hydraulically or thermally established, given the steep temperature gradients and sudden changes in geometry (transition from flow in a fuel assembly to flow in a cylindrical pipe). Non-established flow conditions promote mass transfer to the walls. Furthermore, most simulation software overestimates retention in the steam generator rising line by a factor of 2. No significant improvement has been obtained even though a number of hypotheses have been put forward to explain this discrepancy [46] and two-dimensional simulations have been performed to follow particle paths [44].

With regard to fission-product speciation, it should be noted that, during the **Phebus FP** tests, caesium is mainly transported in condensed form from the RCS hot leg onwards. This clearly shows that the hydroxide (CsOH) is not the predominant chemical form, whereas this was generally assumed to be the case prior to the Phebus FP programme. According to thermodynamic equilibrium calculations, formation of caesium molybdate (Cs_2MoO_4) in the RCS would be promoted under the experimental conditions of the first two Phebus FP tests. This species is predicted by the ASTEC/SOPHAEROS simulation software (see Section 5.5.6) and has been introduced into other code packages such as MELCOR [40]. With regard to the FPT2 test, analysis of data from the tubes with thermal gradients and the sampling lines (see Figure 7.18) highlights the difficulties of simulating iodine species, in particular with the prediction of the presence of caesium iodide in all test phases, which is not always in agreement with experimental results [42].

7.3.6. Thermal-hydraulics and aerosol behaviour on the containment vessel

Thermal-hydraulics in the **Phebus** vessel that represents the containment building were mainly governed by the steam injection and condensation flowrates. Simplified simulations, performed using a coarse mesh to represent this containment (one or more compartments), reproduce the results of thermal-hydraulics measurements (temperatures, pressures, humidities, etc.) and the distribution of aerosols at the end of the test [26] fairly successfully. In line with the results of experimental measurements, they predict that the majority of the aerosols would settle on the elliptical lower head of the containment vessel, the remainder being deposited on the surfaces where water vapour condensed. In the simulations, for the first two tests, a small fraction would deposit on the side walls of the containment vessel (walls which were heated to prevent condensation of water vapour). The kinetics and distribution of aerosol deposits measured during the FPT2 test differ somewhat from the results of the previous tests, in particular with slower deposition kinetics (for all phenomena), a smaller fraction deposited on the surfaces where water vapour condenses, and a larger fraction deposited on the vessel side walls. These differences can be explained by the lower steam injection flowrate and consequent lesser condensation in the vessel during this test, and by smaller, less dense particles on average (less structural materials): the lower condensation rate reduced deposits on condensing surfaces and the smaller aerosol particles deposited onto the side walls more easily by Brownian diffusion.

The mass of aerosols retained on the elliptical lower head of the containment vessel and the condensing surfaces at the end of the **Phebus FP** tests is generally well simulated

by “point” code using standard models for aerosol deposition by sedimentation and dif-fusiophoresis [26 and 47], although for some models, the respective fractions of aerosols deposited *via* these two mechanisms were not accurate. A new model for particle deposition by diffusion onto the vessel side walls, based on a description of turbulence damping in the boundary layer near the walls, correctly predicted the mass of aerosols deposited on these surfaces [49]. Depending on the test, the calculated mass varied from 2 to 4% of the quantity of aerosols in the vessel. It was higher for the FPT2 test, in agreement with the experimental results. In summary, throughout the Phebus FP tests, “point” code adequately predicted the thermal-hydraulics in the containment vessel [48] and the aerosol physics.

7.3.7. Iodine chemistry in the containment vessel

One of the most unexpected results of the Phebus FP tests – a result which is safety related – was experimental evidence of the existence of a small volatile iodine fraction at low temperature in the containment vessel at a very early stage (as soon as fission products started to be released from the fuel) during the FPT0, FPT1 and FPT2 tests [45]. The gaseous iodine measured in the containment vessel during this phase was interpreted as coming from the RCS, contrary to the thermo-chemical models which predicted that all the iodine would be in condensed form (Csl) at its outlet. Kinetic limitations on the gas-phase chemical reactions involving iodine (incomplete reactions) are the most plausible explanation because none of the simulations that assume chemical equilibrium of the gaseous mix in the RCS correctly reproduce the experimental results [23 and 41]. These limitations could be produced by the specific thermal conditions in the RCS during the Phebus FP tests, with steep thermal gradients at the test device outlet and steam generator inlet. These limitations are accentuated for lower concentrations of fission products, which would explain the higher fraction of volatile iodine measured during the FPT0 test performed with very low burnup fuel and levels of fission products 50 times lower than in the FPT1 and FPT2 tests using higher burnup fuel.

The fraction of volatile iodine was found to be even greater during the FPT3 test. The reasons for this are still to be elucidated, but could be associated with the fact that the FPT3 test was performed using a boron carbide control rod instead of the Ag-In-Cd alloy rod used during previous tests. The “CHemistry of Iodine in the Primary circuit” (CHIP) experiment programme is underway as part of the ISTP [30] in order to better understand and quantify the phenomena involved.

The key role of the silver present in the control rod has been clearly shown by the Phebus FP tests, in particular the first two, which were characterised by large fractions of silver released. During the first two Phebus FP tests, iodine was detected and measured in the sump of the vessel representing the containment building, mainly in an insoluble form that was identified as silver iodide. The kinetics of the reaction between iodine and silver can be quite rapid under certain conditions, which leads to a suppression of the expected volatilisation of the iodine in the sump, following either radiolytic oxidation of the I^- ions dissolved in the water, or the formation of organic iodides from the submerged painted surfaces (see Section 5.5.6 for further details). A set of analytical and semi-integral test programmes have quantified the kinetics

of the various silver-iodine reactions, meaning that the phenomena involved can be modelled [19 and 38].

The importance of the non-submerged painted surfaces of the containment vessel in the formation of organic iodides was clearly shown by the first two Phebus FP tests. In fact, this formation dominates that of organic iodides from submerged painted surfaces when the soluble iodine fraction in the sump is low (i.e. when releases of silver fractions significantly dominate releases of iodine fractions) [32]. For this reason, at least during the first two tests in the Phebus FP programme, organic iodides were the most common volatile iodine species measured in the containment atmosphere after approximately one day.

Generally, the Phebus FP tests demonstrated that the long-term concentration of volatile iodine in the vessel that represents the containment building (beyond 24 hours) mainly depends on the physicochemical phenomena affecting the gas phase, and therefore the concentration of volatile iodine arriving from the RCS or formed in the containment vessel. After one day, the concentration of iodine in the containment atmosphere remained constant, which shows that equilibrium was attained both for the reactions that create and destroy volatile iodine and for adsorption and desorption processes (see Figure 7.19). Furthermore, gas-phase radiolytic reactions, such as reactions involving air radiolysis products that break up molecular iodine and organic iodine, are key to long-term iodine speciation and therefore for assessing releases into the environment in the

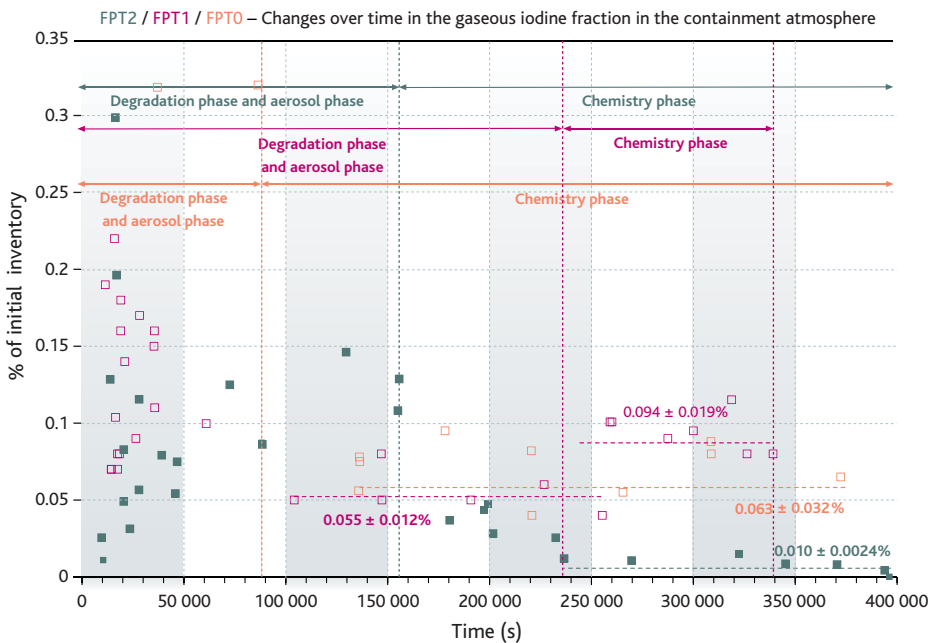


Figure 7.19. Changes over time in the concentration of volatile iodine in the vessel representing the containment building during FPT0, FPT1 and FPT2 tests (percentage of the total inventory in the fuel). Equilibrium values are given for the aerosol phase and chemistry phase for FPT1 and for the chemical phase for FPT0 and FPT2.

event containment failure on a PWR (venting *via* filters or basemat piercing). Radiolytic oxidation of volatile iodine species by ozone, nitrogen oxides and various radicals formed by air radiolysis, leads to the formation of iodine oxides in condensed form [33 and 39]. The concentration of volatile iodine in the containment after one to two days therefore depends on what happens to the products of radiolytic iodine oxidation, in particular their affinities for the surfaces inside the containment (paints, steel, etc.).

The analyses of all results concerning the behaviour of iodine during the FPT0 and FPT1 tests, performed in the context of the international Interpretation Circle¹¹ for iodine chemistry in the containment, are summarised in [41]. These analyses have contributed to improving understanding of iodine behaviour, in particular bringing to light:

- the probable occurrence of kinetic limitations during gas-phase chemical reactions in the RCS, which could account for the formation of volatile iodine at low temperature;
- the key role of silver from the control rods in liquid-phase iodine chemistry in the containment, the irreversible formation of insoluble silver iodide preventing the re-volatilisation of molecular iodine by radiolytic oxidation of iodide ions and the formation of organic iodine in the liquid phase;
- the importance of the unsubmerged painted surfaces of the containment in the production of organic iodides when iodine is not very soluble in the liquid phase (e.g., when significant quantities of silver are released into the containment), leading to the production of mainly organic forms of volatile iodine;
- the equilibrium attained in the containment between the creation and destruction of volatile iodine, which leads to pseudo steady-state concentrations of iodine in the gas phase;
- the importance of gas-phase reactions between iodine and air radiolysis products in long-term iodine speciation (iodine oxides and nitroxides) and consequently in the assessment of possible releases into the environment in the event of core melt.

Lessons learned from the analysis of results concerning the behaviour of iodine during **Phebus FP** tests have been used to improve and develop models, which have then been integrated into most simulation software that covers iodine chemistry in the containment buildings of power reactors, such as:

- liquid-phase reactions between iodine and silver (taking into account the Ag metal/I₂(g), Ag metal/I⁻ and Ag oxide/I⁻ reactions, and oxidation of silver by water radiolysis products);
- radiolytic oxidation of molecular iodine and organic iodine *via* air radiolysis products and the formation of iodine oxides;
- formation of various organic iodides *via* the adsorption of molecular iodine onto unsubmerged painted surfaces.

11. The international partners of the Phebus FP programme share their interpretations of these test results. This is performed in the context of Interpretation Circles, one of which is devoted to iodine chemistry.

7.3.8. Use of Phebus FP test results in safety analyses

Knowledge acquired thanks to the **Phebus FP** programme has been put to use in accident simulation software such as ASTEC, MELCOR and MAAP. These computer codes, described in Chapter 8, are used to perform safety analysis; in some cases, the results of the Phebus FP programme can be used directly. One example is the use made by **IRSN** and the US Nuclear Regulatory Commission (NRC) with regard to the assessment of possible releases into the environment following a severe accident. In particular, at IRSN, this involved quantification of delayed and filtered releases and level-2 probabilistic safety analyses (PSA-2) [27]. The most recent results have been integrated into these analyses.

At US-NRC, a critical analysis, supported by the results of the **Phebus FP** tests, has been performed regarding the recommendations and assumptions gathered in Report NUREG-1465 [59], which covers releases in accident situations, on the basis of the opinions of an Expert Group [36], some members of which were from **IRSN**.

The results of the **Phebus FP** programme were also used to specify the research priorities for core melt accidents under the European EURSAFE project [50]. The lessons which continue to be learned from the Phebus FP tests are used by Severe Accident Research NETwork of Excellence (**SARNET**) [51]; in particular, research priorities are periodically reviewed [60]. The ISTP [27], which aims to reduce the uncertainties brought to light during the Phebus FP programmes, is part of this collaborative effort.

Reference Documents

- [1] <http://www.threemileisland.org/>, in particular the following report:
J. Kemeny, President's Commission Report: The need for change, the legacy of TMI, Washington DC, US Government Printing Office, 1979.
- [2] <http://www.nrc.gov/reading-rm/doc-collections/fact-sheets/3mile-isle.html>
- [3] J. Bourgeois, P. Tanguy, F. Cogné et J. Petit, *La Sûreté Nucléaire en France et dans le monde*, Polytechnica, 1996.
- [4] J. Libmann, *Éléments de sûreté nucléaire*, Collection IPSN, EDP Sciences, 2000.
- [5] J. Walker, J. Samuel, *Three Mile Island: a nuclear crisis in historical perspective*, Berkeley: University of California Press, 2004.
- [6] J. Duco, Accidents nucléaires: *Three Mile Island, techniques de l'ingénieur*, BN3883, <http://www.techniques-ingenieur.fr/book/bn3883/accidents-nucleaires.html>, 2004.
- [7] G. Cenerino, F. Pichereau, E. Raimond, M. Dubreuil, L. Esteller, C. Pignolet, F. Bigot, P. Quentin, R. Gonzalez, B. Clement, K. Herviou, L'accident de Three Mile Island et ses enseignements pour la sûreté des centrales nucléaires en France, <http://www.irsn.fr>, 2009.

- [8] Progress Made in the last fifteen years through analyses of the TMI-2 accident performed in Member Countries, OECD/CSNI/GAMA Report, [NEA/CSNI/R\(2005\)1](#), 2005.
- [9] Ability of current advanced codes to predict core degradation, melt progression and reflooding. Benchmark exercise on an alternative TMI-2 accident scenario, OECD/CSNI/NEA Report, [NEA/CSNI/R\(2009\)3](#), 2009.
- [10] G. Bandini, M. Buck, W. Hering, L. Godin-Jacqmin, G. Ratel, P. Matejovic, M. Barnak, G. Paitz, A. Stefanova, N. Trégourès, G. Guillard, V. Koundy, Progress on ASTEC Validation on Circuit Thermal-Hydraulics and Core Degradation, *Progress in Nuclear Energy* 52 (1), 148-157, 2010.
- [11] N. Rasmussen *et al.*, Reactor Safety Study, WASH-1400, Washington D.C., US NRC, 1975.
- [12] Fukushima, un an après – Premières analyses de l'accident et de ses conséquences, rapport IRSN, IRSN/DG/2012-001, available on the IRSN Internet site, www.irsn.fr, 2012.
- [13] Chernobyl: Assessment of Radiological and Health Impacts: 2002 Update of Chernobyl: Ten Years On <http://www.oecd-nea.org/rp/chernobyl/>
- [14] The Chernobyl accident, IAEA, INSAG-7, 1992.
- [15] J. Duco, Accidents nucléaires, Tchernobyl (URSS), Techniques de l'Ingénieur, BN3884. <http://www.techniques-ingenieur.fr/book/bn3884/accidents-nucleaires.html>, 2003.
- [16] International Atomic Energy Agency (IAEA), Environmental consequences of the Chernobyl accident and their remediation: 20 years of experience, Report of the UN Chernobyl Forum Expert Group «Environment», 2005.
- [17] P. Renaud, D. Champion, J. Brenot, *Les retombées radioactives de l'accident de Tchernobyl sur le territoire français*, Collection sciences et techniques de l'IRSN, Éditions TEC&DOC, Lavoisier, 2007.
- [18] D. Robeau, *Catastrophes et accidents nucléaires dans l'ex-Union Soviétique*, Collection IPSN, Editions EDP Sciences, 2001.
- [19] J. Ball, W.C.H. Kupferschmidt and J.C. Wren, Results from the phase 2 of the Radioiodine Test Facility experimental programme, Chemistry of Iodine in Reactor Safety, Workshop proceedings Würenlingen, Switzerland, 10-12 June, [NEA/CSNI/R\(96\)6](#), 1996.
- [20] M. Barrachin, P.Y. Chevalier, B. Cheynet, E. Fischer, New modeling of the U-O-Zr phase diagram in the hyper-stoichiometric region and consequences for the fuel rod liquefaction in oxidizing conditions, *Journal of Nuclear Materials* 375, 397-409, 2008.

- [21] J. Birchley, T. Haste, H. Bruchertseifer, R. Cripps, S. Güntay and B. Jäckel, Phebus-FP: Results and significance for plant safety in Switzerland, *Nuclear Engineering and Design* **235**, 1607-1633, 2005.
- [22] P.D.W. Bottomley, P. Carbol, J-P. Glatz, D. Knoche, D. Papaioannou, D. Solatie, S. Van Winckel, A-C. Gregoire, G. Grégoire and D. Jacquemain, Fission product and actinide release from the debris bed test Phebus FPT4: Synthesis of the Post test Analyses and of the Revaporisation testing of the plenum samples performed at ITU, *International Congress on Advanced Power Plants (ICAPP-05)*, 15-19 May, Seoul, Korea, 2005.
- [23] L. Cantrel and E. Krausmann, Reaction kinetics of a fission product mixture in a steam-hydrogen carrier gas in the Phebus primary circuit, *Nuclear Technology* **144**, 2003.
- [24] B. Clément, Summary of the Phebus FP Interpretation status, *Proc. 5th Technical seminar on the Phebus-FP programme*, Aix-en-Provence, France, 24-26 June, 2003.
- [25] B. Clément, N. Hanniet-Girault, G. Repetto, D. Jacquemain, A.V. Jones, M.P. Kissane and P. Von der Hardt, LWR severe accident simulation: synthesis of the results and interpretation of the first Phebus FP experiment FPT-0, *Nuclear Engineering and Design* **226**, 5-82, 2003.
- [26] B. Clément and T. Haste, ISP-46 – Phebus FPT-1, *NEA/CSNI/R(2004)18*, 2004.
- [27] B. Clément, Towards reducing the uncertainties on Source Term Evaluations: an IRSN/CEA/EDF R&D programme, *Proc. Eurosafe Forum*, Berlin, Germany, November 8-9, 2004.
- [28] B. Clément, O. De Luze and G. Repetto, Preliminary results and interpretation of Phebus FPT-3 test, MELCOR Cooperative Assessment meeting, 20-21 September, Albuquerque (NM) USA, 2005.
- [29] B. Clément *et al.*, Thematic network for a Phebus FPT-1 international standard problem (THENPHEBISP), *Nuclear Engineering and Design* **235**, 347-357, 2005.
- [30] B. Clément, R. Zeyen, The Phebus Fission Product and Source Term International Programmes, *International Conference Nuclear Energy for New Europe*, Bled, Slovenia, 5-8 September, 2005.
- [31] J.C. Crestia, G. Repetto and S. Ederli, Phebus FPT-4 First post-test calculations on the debris bed using the ICARE V3 code, *Proc. 4th technical seminar on the Phebus FP programme*, Marseille, France, March 2000.
- [32] S. Dickinson, H. E. Sims, E. Belval-Haltier, D. Jacquemain, C. Poletiko, S. Hellmann, T. Karjunen and R. Ziliacus, Organic Iodine Chemistry, *Nuclear Engineering and Design* **209**, 193-200, 2001.
- [33] S. Dickinson, The radiolysis of gaseous iodine species in air, Data Analysis and Modelling of Iodine Chemistry and Mitigation Mechanism, EC Report, SAM-ICHEMM-D010, 2002.

- [34] R. Dubourg and P. Taylor, A qualitative comparison of barium behaviour in the Phebus FPT-0 test and analytical tests, *Journal of Nuclear Materials* **294**, 32-38, 2001.
- [35] R. Dubourg, H. Faure-Geors, G. Nicaise and M. Barrachin, Fission product release in the first two Phebus tests FPT-0 and FPT-1, *Nuclear Engineering and Design* **235**, 2183-2208, 2005.
- [36] Energy Research, Inc., Accident Source Terms for Light-Water Nuclear Power Plants: High Burnup and Mixed Oxide Fuels, ERI/NRC 02-202, October 2002.
- [37] J.M. Evrard, C. Marchand, E. Raimond and M. Durin, Use of Phebus FP Experimental Results for Source Term Assessment and Level 2 PSA, *Proc. 5th Technical seminar on the Phebus FP programme*, Aix-en-Provence, France, 24-26 June, 2003.
- [38] F. Funke, G.-U. Greger, A. Bleier, S. Hellmann and W. Morell, The reaction between iodine and silver under severe PWR accident conditions, Chemistry of Iodine in Reactor Safety, Workshop proceedings Würenlingen, Switzerland, June 10-12, [NEA/CSNI/R\(96\)6](#), 1996.
- [39] F. Funke, P. Zeh and S. Hellmann, Radiolytic oxidation of molecular iodine in the containment atmosphere, Iodine Aspects of Severe Accident Management, *Workshop proceedings* Vantaa, Finland 18-20 May 1999, [NEA/CSNI/R\(99\)7](#), December 1999.
- [40] R.O. Gauntt, Overview of MELCOR Development, Assessment and Applications Activities, *MELCOR Cooperative Assessment meeting*, September 20-21, Albuquerque (NM) USA, 2005.
- [41] N. Girault, S. Dickinson, F. Funke, A. Auvinen, L. Herranz and E. Krausmann, Iodine behaviour under LWR accidental conditions: lessons learnt from analyses of the first two Phebus FP tests, *Nuclear Engineering and Design* **236**, 1293-1308, 2006.
- [42] Girault N., Fiche C., Bujan A., Dienstbier J., Towards a Better Understanding of Iodine Chemistry in RCS of Nuclear Reactors, *2nd European Meeting on Severe Accident Research, ERMSAR 2007*, June 12-14, 2007.
- [43] T. Haste, E. Cazzoli, J. Vitásková, J. Birchley, TMI-2 Analysis with MELCOR 1.8.5 and SCDAPSIM, *MELCOR Cooperative Assessment meeting*, September 20-21, Albuquerque (NM) USA, 2005.
- [44] C. Housiadas, K. Müller, J. Carlsson and Y. Drossinos, Two-dimensional effects in thermophoretic particle deposition: the Phebus-FP steam generator, *Journal of Aerosol Science* **32** (suppl. 1) S1029-S1030, 2001.
- [45] D. Jacquemain, N. Hanniet, C. Poletiko, S. Dickinson, C. Wren, D. Powers, E. Krausmann, F. Funke, R. Cripps and B. Herrero, An Overview of the Iodine Behaviour in

the Two First Phebus Tests FPT0 and FPT1, *OECD Workshop on Iodine Aspects of Severe Accident Management*, Vantaa, Finland, May 18-20, 1999.

- [46] M.P. Kissane and I. Drosik, Interpretation of Fission-product transport behaviour in the Phebus FPT0 and FPT1 tests, *Nuclear Engineering and Design* **236**, 1210-1223, 2006.
- [47] I. Kljenak and B. Mavko, Simulation of containment phenomena during the Phebus FPT-1 test with the CONTAIN code, *Proc. Nuclear Energy for New Europe 2002*, Kranjska Gora, Slovenia, September 9-12, 2002.
- [48] V.D. Layly, P. Spitz, S. Tirini, A. Mailliat, Analysis of the Phebus FPT0 containment thermal hydraulics with the Jericho and TRIO-VF codes, *Nuclear Engineering and Design* **166**, 413-426, 1996.
- [49] V.D. Layly, Aerosol behaviour in a closed vessel: analysis of the Phebus FPT0 test aerosol phase in the containment, Phebus report, Phebus IP 98/391, 1998.
- [50] D. Magallon *et al.*, European expert network for the reduction of uncertainties in severe accidents safety issues (EURSAFE), *Nuclear Engineering and Design* **235**, 309-346, 2005.
- [51] J.C. Micaelli *et al.*, SARNET: A European Cooperative Effort on LWR Severe Accident Research, *European Nuclear Conference 2005*, Versailles (France), 12-15 December, 2005.
- [52] H. Manenc, P.K. Mason and M.P. Kissane, The modelling of fuel volatilisation in accident conditions, *Journal of Nuclear Materials* **294**, 64-68, 2001.
- [53] Ph. March *et al.*, First results of the Phebus FPT-3 test, *Proc. of the 14th International Conference on Nuclear Engineering*, July 17-20, 2006, Miami, Florida, USA, 2006.
- [54] G. Repetto, B. Clément and S. Ederli, Analysis of the FPT0, FPT1 and FPT2 experiments of the Phebus FP program investigating in vessel phenomena during a LWR accident, *10th International Topical Meeting on Nuclear Reactor Thermal Hydraulics (NURETH-10)*, Seoul, Korea, October 5-9, 2003.
- [55] G. Repetto and S. Ederli, Analysis of the FPT0 and FPT2 Phebus FP experiments using porous medium geometry with the ICARE2 code", *11th International Topical Meeting on Nuclear Reactor Thermal Hydraulics (NURETH-11)*, Avignon, France, October 2005.
- [56] G. Repetto, O. De Luze, J. Birchley, T. Drath, T. Hollands, M. Koch, C. Bals, K. Trambauer, H. Austregesilo, Preliminary analyses of the Phebus FPT3 experiment using Severe Accident Codes (ATHLET-CD, ICARE/CATHARE, MELCOR), *2nd European Meeting on Severe Accident Research, ERMSAR 2007*, June 12-14, 2007.

-
- [57] [M. Schwarz](#), G. Hache and P. Von der Hardt, Phebus FP: a severe accident research programme for current and advanced light water reactors, *Nuclear Engineering and Design* **187**, 47-69, 1999.
- [58] [M. Schwarz](#), B. Clément and A.V. Jones, Applicability of Phebus FP results to severe accident safety evaluations and management measures, *Nuclear Engineering and Design* **209**, 173-181, 2001.
- [59] [L. Soffer](#), S.B. Burson, C.M. Ferrell, R.Y. Lee and J.N. Ridgely, Accident Source Terms for Light-Water Nuclear Power Plants, NUREG 1465, 1995.
- [60] [Schwinges et al.](#), Ranking of severe accident research priorities, *Progress in Nuclear Energy* **52**, 11-18, 2010.

Chapter 8

Numerical Simulation of Core Melt Accidents

8.1. *Integral and mechanistic computer codes*

The development of computer codes for the numerical simulation of core melt accidents began in the United States in the 1970s to back up probabilistic studies, such as those referred to in the American WASH 1400 report [1]. The TMI-2 accident in the United States in 1979 spurred efforts to improve simulation of this type of accident and develop level 2 probabilistic safety assessments (PSAs) in the country. Another major report following the WASH 1400 report included a probabilistic study of five US reactors [2]. It was in the late 1980s that the Europeans and Japanese decided to develop their own core melt accident simulation codes and probabilistic safety assessments. Over this period, these codes came into gradual use for elaborating and assessing methods for preventing core melt accidents – or mitigating their impact – as well as for training reactor operators.

Two types of code were developed:

- integral codes (or software systems) designed to simulate the entire core melt accident, from the initiating event up to and including any radioactive release outside the containment;
- detailed or mechanistic codes, used to simulate in greater detail the phenomena involved in a particular accident phase, for example core damage, fission product release or hydrogen combustion inside the containment.

8.1.1. Integral codes

Following the TMI-2 accident, the United States simultaneously started to develop two integral codes in the 1980s, one called MAAP for the nuclear industry and another, MELCOR, intended for the regulatory authorities. At the end of the 1980s, Japan and France began to develop analogue codes, namely THALES [2], developed by JAERI [3] and ESCADRE by IRSN [4]. IRSN then decided to work with GRS on the joint development of ASTEC, an integral code to replace ESCADRE. An ambitious project was started up at NUPEC in Japan using the SAMPSON system of detailed codes [5] but around 2001, related developments came to a virtual standstill owing to a decline in R&D work on core melt accidents in Japan. The Japanese Atomic Energy Agency (JAEA, successor to JAERI) has recently restarted development work on the THALES code. In the early 2000s, Russia began to develop a code system called SOCRAT [6].

There are five integral codes in the world, namely MAAP, MELCOR, ASTEC, SAMPSON and SOCRAT (this excludes certain special codes used to simulate core melt accidents in Canadian-designed CANDU heavy-water reactors, such as ISAAC, a code developed by KAERI in South Korea). Of these five codes, only three are in widespread use:

- ASTEC, jointly developed by IRSN and its German counterpart, GRS;
- MAAP4, developed by the American company Fauske & Associates, Inc. (FAI);
- MELCOR, developed by Sandia National Laboratories (SNL) in the United States for the US Nuclear Regulatory Commission (US NRC).

Integral codes must meet the following requirements:

- provide exhaustive coverage of all the physical phenomena involved in a core melt accident;
- simulate the behaviour of the main reactor safety systems;
- fully incorporate couplings between phenomena, such as the decrease in residual heat according to fission product release from the fuel, metal oxidation according to the quantity of oxygen or steam available, or corium cooling in the reactor pit during corium-concrete interaction as a result of radiation and convection in the containment;
- modular design to allow comparisons with experimental results in particular;
- high-speed performance to calculate a large number of level 2 PSA scenarios in a reasonable time. To achieve this, computing time must be less than real accident time.

Integral codes are used in reactor safety studies, particularly to estimate foreseeable radioactive releases, and in level 2 PSAs. They are also used in studies on the management of a possible core melt accident with a view to defining or improving severe accident operating guidelines. Another example of use is to verify the design of pressuriser steam bleed valves or recombiners in the containment building.

The main physical fields covered are:

- RCS and secondary coolant system thermal-hydraulics from the start of the accident;
- core melting, with the release of fission products from the fuel rods and of aerosols from the structural elements inside the reactor pressure vessel, such as control rods, grids, etc.;
- relocation of corium to the lower head of the reactor vessel, that may result in vessel failure and flow of corium in the reactor pit;
- interaction between the molten core and the concrete of the reactor pit basemat (MCCI);
- transport and deposition of fission products and aerosols in the RCS and secondary coolant system;
- thermal-hydraulics and hydrogen combustion in the containment;
- transport and deposition of fission products and aerosols in the containment;
- fission product chemistry (particularly iodine and ruthenium) in the containment, and the possibility of fission product release to the environment.

Integral codes do not generally cover steam explosion or containment mechanical strength, which are covered by more specific codes.

Core melt accidents include transient phenomena in solid, liquid or gaseous media involving mass, momentum and energy exchanges. Integral codes must couple all these phenomena, which come into play on different spatial and temporal scales. Some phenomena, such as direct containment heating for example, last mere seconds, while others, such as the pressure increase due to gas release during MCCI, chemical reactions between cladding and fuel, or steam flows along the entire height of the core, can last several hours. Of course, these codes also involve various scientific disciplines, including thermal science, thermal-hydraulics, structural mechanics and chemistry.

For each component concerned, equations for conservation of mass and internal energy are solved in volumes, called control volumes, that define a spatial mesh. The RCS and secondary coolant system and the containment may be represented by any number of volumes, usually between 10 and 50 for the containment¹. The reactor core is represented by a 2D axisymmetric mesh, generally composed of four to seven radial rings and 10 to 30 axial volumes.

The corium during MCCI is discretised in one, two or three volumes representing averaged layers (metal on the one hand, heavy and light oxides resulting from concrete decomposition on the other).

1. Except for MAAP4, where the maximum number is 14 for the RCS and two for the secondary coolant system.

Computing time is significantly affected by the degree of refinement selected for discretisation into control volumes. Computing times of one or two hours per day of accident can be achieved using the minimum numbers of volumes mentioned above, but doing so may make results less reliable. Thermal-hydraulic models play a key role in integral codes as they are intricately linked to other models. Each control volume generally contains two temperature zones, a fluid zone (single-phase liquid or two-phase boiling) and a gaseous zone that may include a water mist. These volumes can be surrounded by solid, heat-conducting structures. They are connected by junctions. The velocities of fluids flowing through these junctions are calculated by solving the fluid momentum equations: the average velocity of the fluid is calculated in the transient state using the generalised Bernoulli equation, making allowance for head loss. The difference in velocity between liquid and gas is then calculated from this average velocity using an “inter-phase slip” correlation. For the RCS and secondary coolant system, the ASTEC code uses more complex modelling of 1D “pipe” volumes containing a two-phase mixture. The thermal-hydraulic models of the RCS and secondary coolant system and the containment are closely coupled by the modelling of heat exchanges between the systems and containment or by the discharge of water or steam from the systems to the containment in the event of a pipe break. This allows simple modelling of some automatic reactor functions, such as the start-up of certain systems (safety injection, containment spray) at high containment pressure thresholds.

Integral codes are large, ranging from 400,000 to 500,000 instructions and 1000 to 1500 subroutines for ASTEC and MELCOR, and around 350,000 instructions and 700 subroutines for MAAP. They are made up of modules corresponding more or less to the main areas of the reactor. These modules are connected by a computer program that manages changes in the time steps of the numerical solution scheme, data exchange and conservation of mass and energy. The programming language is Fortran 95 or later.

An essential feature of these codes is that they allow the user to formulate hypotheses for the accident under study as flexibly and as simply as possible, often using a specific command language or a human-machine interface. This makes it possible to simulate the safety systems involved during the accident as well as the accident management procedures implemented by the operators:

- for the RCS and secondary coolant system: intentional depressurisation, pouring water onto the damaged core in the reactor vessel, etc.;
- for the containment: spraying, recombiners, ventilation, filters, etc.

Other requirements for these integral codes concern the numerical robustness and availability of user-friendly tools allowing users to prepare calculations and make use of their results, or stop calculations at any point during the accident, save the results, then continue calculations until the end of the accident, adjusting assumptions as necessary (for example, restarting the safety systems).

Thanks to improved computer performance and expanding knowledge, detailed models can now be incorporated in the integral codes mentioned above. Until the late

1990s, models had to be as simple and fast as possible and highly flexible for the purposes of sensitivity studies. Despite the growing sophistication of models, however, integral codes continue to complement mechanistic codes, which are used to simulate a particular phenomenon. This is the case of Computational Fluid Dynamics (or CFD) codes, which are used to assess the hydrogen risk in the containment or to model steam explosions (Sections 5.2.2 and 5.2.3).

8.1.2. *Mechanistic codes*

The principal mechanistic codes used around the world are, with the developing organisations in parentheses:

- for core damage: ATHLET-CD (GRS in Germany), ICARE/CATHARE (IRSN), RELAP/SCDAPSIM (ISS in the USA), SCDAP/RELAP5 (INL in the USA);
- for the containment: COCOSYS (GRS), TONUS (IRSN), FUMO (University of Pisa in Italy), GOTHIC (AECL in Canada), CONTAIN (developed by ANL in the USA but now replaced by the integral code MELCOR);
- for steam explosion: IKEDEMO (University of Stuttgart in Germany), MC3D (IRSN);
- for large structural mechanics: finite-element codes such as ABAQUS (United States) and CAST3M (CEA);
- for thermal-hydraulics: CFD codes designed to solve Navier-Stokes equations in 3D geometry such as CFX (off-the-shelf software), GASFLOW (KIT, ex-FzK in Germany), TONUS (IRSN).

These codes are generally used to simulate part of an accident scenario or a particular area of a nuclear power plant, such as the RCS and secondary coolant system or the containment. Their main goal is to reduce uncertainties and provide a more detailed understanding of physical phenomena. For this reason, they include detailed, “realistic” state-of-the-art models known as best-estimate models. Mechanistic codes and integral codes adopt different approaches. The first usually calculate numerical solutions for differential equations, while integral codes sometimes use correlations, which implies that they can only be used within the scope of the correlations in question.

Mechanistic codes often serve as references to determine the validity of integral code results.

Computing time is generally long; with very high spatial and temporal discretisation, it can take several weeks to perform calculations for one day of accident.

8.2. General approach to code development and validation

8.2.1. Code development

Code development is generally carried out in the following steps, possibly with iterations between them:

- step 1: defining code objectives, including scope and required performance in terms of computing time, etc.;
- step 2: preparing general specifications such as structure, programming languages, degree of detail in models, numerical solution schemes, etc.;
- step 3: preparing detailed specifications for certain models as required and, where necessary, building prototype;
- step 4: developing physical models, generally based on experimental data;
- step 5: developing the code by implementing the physical models and adjusting them to the appropriate numerical scheme;
- step 6: checking the code by comparing the results it produces for simple problems with analytical solutions, and verifying conservation of mass and energy, consistency of results obtained with various computers systems, correct coupling between phenomena, etc.

8.2.2. Code validation

The purpose of the validation process is to ensure that the code gives a true representation of physical phenomena and that it can reliably simulate a core melt accident in a reactor, from beginning to end.

“Validation Strategy of Severe Accident codes” [7] or VASA, a project carried out between 1999 and 2003 as part of the fourth European R&D framework programme (FP4) and coordinated by GRS with active support from IRSN, studied various approaches to code validation. One of its main conclusions was to recommend a dual approach that not only takes into consideration physical phenomena as such, but also their impact on reactor safety.

The two approaches complement each other as the second determines the degree of accuracy required for simulating phenomena. It should be noted that for the second approach, all the reactor safety systems must be modelled in the code.

Validation is generally carried out in three steps:

- validating a physical model implemented in the code, based on the results of separate-effect tests, often carried out on a small scale, then validating the code based on the results of coupled-effect tests covering a set of several physical

phenomena. The latter tests are often carried out using simulant materials and can also represent the behaviour of a real reactor component;

- validating the code using integral tests. These are often carried out on a relatively large scale (for example on rod clusters of actual height) and using real materials, which makes it possible to check that the various models are suitably coupled and that no important phenomena have been neglected;
- extrapolating the code to accident situations liable to affect power reactors, in particular through scale-effect studies, sensitivity studies on various model parameters (physical and numerical) and comparisons with other codes, and applying it to emergency transients actually encountered in reactors, such as the TMI-2 and Fukushima Daiichi accidents in the United States and Japan respectively.

When these steps are considered sufficiently complete (they need to be repeated regularly as knowledge advances), default values and variation ranges for various model parameters can be recommended to users. The conclusions of this validation process can then point to ways of improving the code models.

The study of core melt accidents involves a number of specific features compared with other scientific disciplines, including extreme conditions, such as high temperatures and pressures and the extremely complex phenomena to be considered. For this reason, numerous specific international experimental programmes had to be carried out for many years. Validation matrices have been developed for all codes based on various available tests. Table 8.1 gives an example of a matrix globally common to integral codes (it does not include the TMI-2 accident). The tests adopted in the International Standard Problem (ISP) [8] exercises organised by the OECD Committee on the Safety of Nuclear Installations (CSNI) are widely used. These exercises involve comparing codes through well-instrumented quality tests.

Table 8.1. Main experimental programmes used in integral code validation.

Field or physical phenomenon concerned (relevant section of book)	Programme name	Organisation (country)
Core melt accident as a whole (Sections 5.1, 5.5 and 7.3)	LOFT-LP-FP2	INEL (USA)
	Phebus FP	IRSN (France)
RCS thermal-hydraulics (Section 5.1.4)	BETHSY [9]	CEA (France)
Core damage (Section 5.1.1)	CORA	KIT (Germany)
	QUENCH	KIT (Germany)
	PARAMETER	LUCH (Russia)
Fission product release (Section 5.5.1)	ORNL HI-VI	ORNL (Canada)
	VERCORS	CEA (France)

Field or physical phenomenon concerned (relevant section of book)	Programme name	Organisation (country)
Fission product transport in the RCS and containment (Section 5.5.2)	FALCON [10]	AEAT (UK)
	VERCORS HT	CEA (France)
	LACE [11]	INEL (USA)
	KAEVER [12]	Battelle (Germany)
Vessel failure (Section 5.1.3)	LHF-OLHF	SNL (USA)
	FOREVER	KTH (Sweden)
Heat transfers in a corium pool (Sections 5.4.1 and 5.4.2)	COPO	VTT (Finland)
	ULPU [13]	UCLA (USA)
	BALI	CEA (France)
Fragmentation of corium in water (Section 5.2.3)	FARO and KROTOS	JRC Ispra
Direct containment heating (Section 5.2.1)	SURTSEY IET	SNL (USA)
	DISCO (C, H)	KIT (Germany)
MCCI (Section 5.3)	BETA	KIT (Germany)
	CCI	ANL (USA)
	ACE and MACE	ANL (USA)
Iodine chemistry in the containment (Section 5.5.5)	ACE/RTF and Phebus/RTF	AECL (Canada)
	CAIMAN	CEA (France)
	EPICUR	IRSN (France)
Thermal-hydraulics in the containment (Section 5.2.2)	NUPEC [14]	NUPEC (Japan)
	VANAM [14]	Battelle (Germany)
	TOSQAN [15]	IRSN (France)
	MISTRA [15]	CEA (France)
Hydrogen combustion in the containment (Section 5.2.2)	HDR	Battelle (Germany)
	RUT	RRC-KI (Russia)

8.3. ASTEC

The Accident Source Term Evaluation Code, or ASTEC, has been jointly developed since 1995 by IRSN and its German counterpart, GRS [16]. It played a key role in the research carried out by the Severe Accident Research Network of Excellence, or SARNET, under the European Commission framework programmes, FP6 and FP7 from 2004 to 2013. Within this context, it gradually incorporated models of all knowledge generated by the network, and is used by the partners to conduct a considerable amount of work on validation and comparison with other codes on reactor applications [17]. ASTEC has now become the European reference code.

8.3.1. Capabilities

An initial series of versions, V0, was developed until 2003, followed by the V1 series until 2009. The first version of the V2 series was commissioned mid-2009. The major change compared with the V1 series concerns core damage: the models in the V2 series, developed using IRSN's mechanistic code ICARE2 [20], are capable of simulating in 2D the flow of corium inside the core, and its progression towards the lower head through the barrel and lower core plates, as observed during the TMI-2 accident (whereas ASTEC V1 modelled flows in one dimension along the rods). Another major improvement concerns iodine and ruthenium modelling in the RCS and secondary coolant system and in the containment.

The V2 versions can be applied to various types of Generation II reactor, French PWRs (900, 1300 and 1450 MWe series), German 1300 MWe Konvoi reactors, Westinghouse 1000 MWe PWRs and Russian-designed 440 and 1000 MWe VVERs. They can also be used for new Generation III reactor designs such as the EPR with its core catcher, or reactors, such as the AP1000, designed to retain the corium inside the reactor vessel and cooling the vessel by flooding the reactor pit (as seen in Generation II VVER 440 reactors on which this cooling system was installed [18]). Research at GRS has shown that the ASTEC V2 code could also be used on boiling water reactors (BWRs), except during the core damage phase, for which models are currently being adapted. The same is true for CANDU and high-temperature reactors (HTRs), as demonstrated by the work of BARC in India and PBMR in South Africa respectively.

Another application of ASTEC is in simulating accidents in fuel storage pools, such as the one that occurred at the Paks NPP in Hungary [19].

IRSN makes intensive use of ASTEC in its Level 2 PSAs and in studies on foreseeable radioactive release in the event of a core melt accident at French 900 MWe and 1300 MWe PWRs. Similar work is in progress for the EPR.

Figure 8.1 shows the different ASTEC modules and how they are coupled. The fact that ASTEC is highly modular simplifies validation, which can be carried out on tests using only one module or suite of modules.

Version V2.0 of ASTEC was distributed to nearly 40 organisations in twenty countries, mostly in the European Union, but also in Russia, China, India, South Korea and South Africa.

All the phases of an accident can be simulated during reactor power operation or with the reactor shut down, except for the detailed effects of air entering the reactor vessel, which will be covered in the next major upgrade, V2.1. All accident scenarios can be simulated – loss-of-coolant accident, steam generator tube rupture, total loss of emergency power supply, and total loss of steam generator feedwater supply – as well as most emergency operation procedures, such as depressurisation of the RCS and secondary coolant system, water injection onto a slightly damaged core, containment spraying, containment venting and filtering radioactive release. Certain devices inside

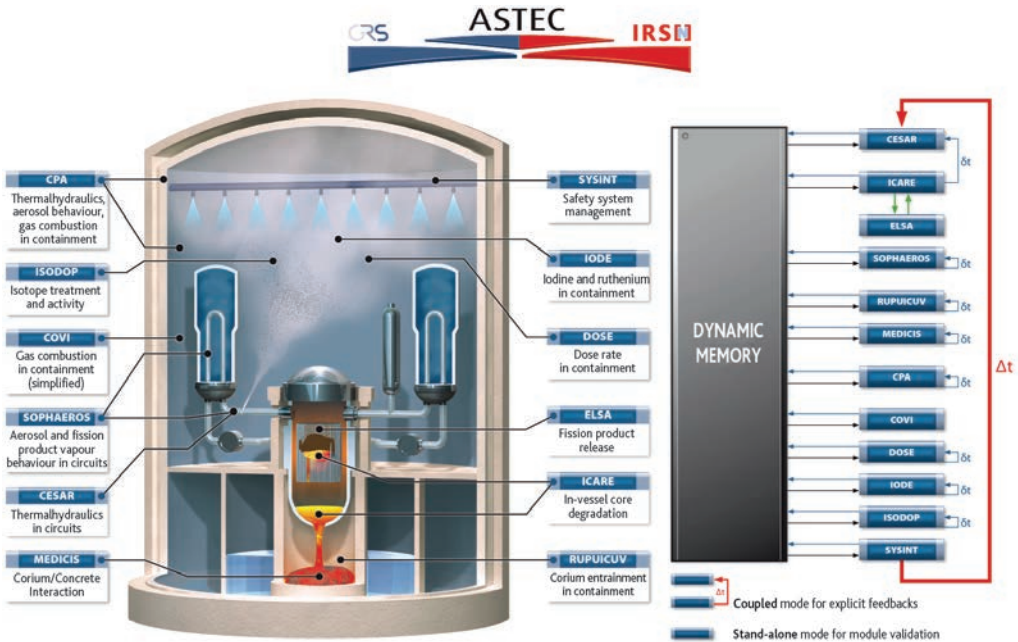


Figure 8.1. ASTEC V2 structure

the containment, such as catalytic hydrogen recombiners, can also be represented, as can suppression pools with gas bubbling in VVER 440 reactors or HTRs.

A numerical approach with five differential equations and an algebraic inter-phase slip algorithm is used to model RCS and secondary coolant system two-phase thermal-hydraulics. A zero-dimensional “zone-based” approach is used to describe corium behaviour in the reactor pit during MCCI. This may involve changes among layers as a result of stratification and layer inversion (see Section 5.3 for further details on MCCI). This approach is also used for modelling thermal-hydraulics in the containment.

All the basic data required for calculations are gathered in a single base called the Material Data Bank, which includes not only the physical properties of materials and mixtures (conductivity, viscosity, etc.) but also chemical reactions and fission product isotopes (radioactive decay). The corium thermophysical properties come from the European reference base, NUCLEA [21].

The computing time for a severe accident scenario is generally close to real time on a PC in a Windows or Linux environment. Less refined spatial meshing can reduce computing time to a few hours per day of accident.

Users have access to SUNSET, a tool designed for automatically launching a series of sensitivity studies for uncertainty analysis.

8.3.2. Validation status mid-2015

During the 1990s, an intensive effort was undertaken to validate codes such as ESCADRE, RALOC and FIPLOC, from which ASTEC was developed. This work laid solid foundations for validation. The basic validation matrix is composed of some thirty experiments, mainly those shown in Table 8.1. As these concern crucial phenomena involved in core melt accidents, the matrix is applied to each major upgrade to specify model uncertainties. For each module, validation is complemented by campaigns which, although less frequent, cover all available experiments (some forty experiments on fission product release for example). It is also performed by IRSN’s partners in SARNET on reference experiments used for international computer code intercomparison exercises (ISP). Examples include BETHSY 9.1b (ISP27) for RCS and secondary coolant system thermal-hydraulics, KAEVER (ISP44) for aerosol behaviour in the containment, and Phebus FPT1 (ISP46) for the accident as a whole.

More than 170 experiments were used to compare all successive versions. The results of the comparison are generally satisfactory and show that ASTEC reflects the state of the art in terms of understanding and modelling, especially concerning fission product behaviour, which takes into account all the knowledge gained from the Phebus FP experimental programme and international analytical tests carried out over many years. To illustrate this, Figure 8.2 gives the validation results vs. the BETHSY 9.1b thermal-hydraulic test performed at CEA on a two-inch break in the cold leg of the RCS, while

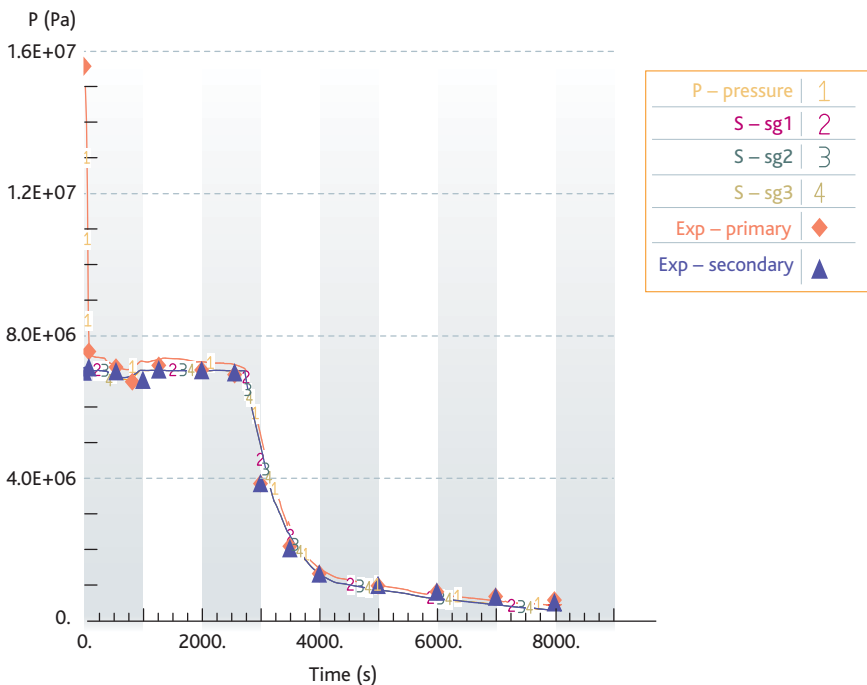


Figure 8.2. Validation of ASTEC on the BETHSY 9.1b test: calculated pressure changes in the RCS and secondary coolant system - Comparison with experimental values.

Figure 8.3 shows the results obtained for the CAIMAN 97/02 test, also performed at CEA, to simulate the production of gas-phase molecular and organic iodine in the containment during a severe accident.

Improvements to ASTEC models currently focus on reflooding of damaged cores, which is a crucial aspect of core melt accident management. As for all other codes, there is considerable room for improvement in ASTEC on this issue. This was highlighted by the interpretation of QUENCH and CORA experiments, especially the failure to reproduce the hydrogen production peaks observed during these reflooding tests.

In addition to comparison with experimental results, it is also necessary to demonstrate that the code is capable of calculating all severe accidents liable to affect power reactors. ASTEC is therefore used in the IRSN level 2 PSA PWR 1300 studies concerning the main scenarios (RCS or secondary coolant system break, loss of emergency power supply, etc.), with variants for examining the impact of whether or not reactor safety systems are used. Nearly a hundred sequence calculations were performed to ensure that results are mutually consistent and that the trends obtained are physically credible.

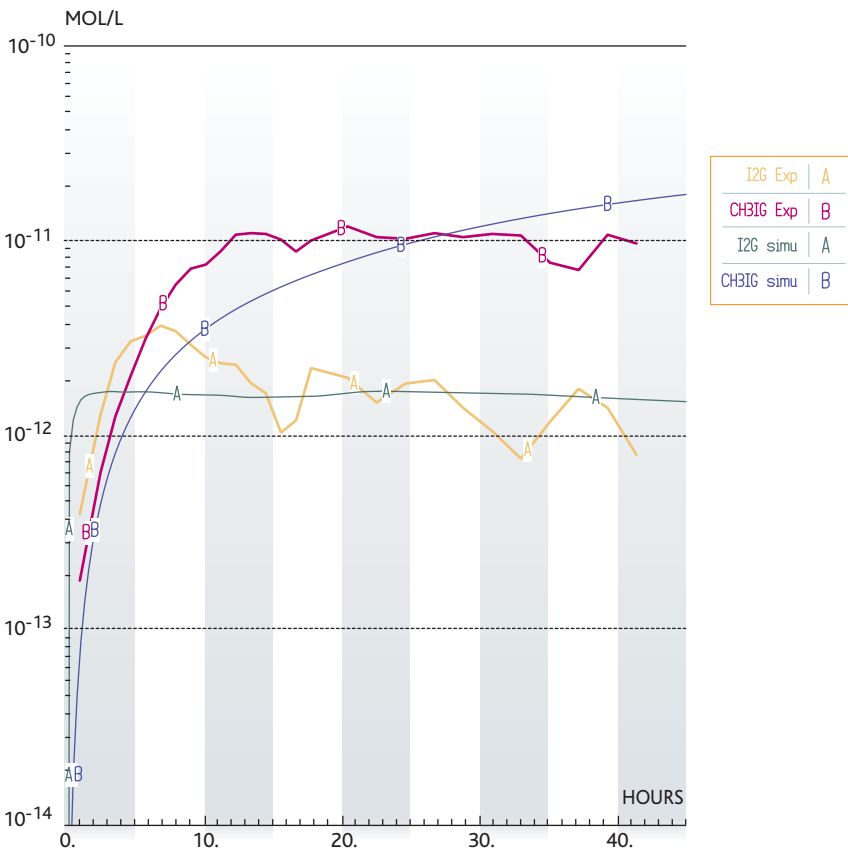


Figure 8.3. Validation of ASTEC on the CAIMAN 97/02 test: changes in gas-phase iodine concentrations in the form of molecular iodine (I_2) and organic iodine (CH_3I).

Comparisons were also made with other codes on certain accident scenarios. This is the case of comparisons made within [SARNET](#) with the MELCOR and MAAP4 integral codes and with mechanistic codes such as ICARE/CATHARE and CONTAIN, for various types of reactor, including PWR 900, PWR 1300, Konvoi 1300, VVER 440 and VVER 1000. Results were generally considered close, although deviations were observed during some phases in the scenarios. The models responsible for these deviations were identified during these comparisons, which helped to quantify uncertainties in the assessment of certain physical phenomena.

8.3.3. *ASTEC upgrade prospects*

Several new models are being implemented in V2.1, the next major upgrade of ASTEC, which is scheduled for release in 2015. These are the results of interpretations of experimental programmes aimed at reducing uncertainties and include:

- for iodine and ruthenium transport chemistry in the RCS: [IRSN](#)'s CHIP tests (Section 5.5.6.2) carried out under the International Source Term Programme (ISTP) to qualify a new chemical kinetics model;
- for iodine and ruthenium chemistry in the containment: [IRSN](#)'s EPICUR tests (Section 5.5.6.2), also carried out as part of ISTP;
- for the spatial distribution of heat flux in the corium pool during MCCI: CEA's VULCANO and CLARA tests and CCI project tests on real materials;
- for the effects of high fuel burnup and MOX fuel on core damage and fission product release: CEA's VERCORS and VERDON tests;
- for damaged core reflooding: [IRSN](#)'s PRELUDE PEARL tests on debris bed cooling (and the related work done by [SARNET](#) partners).

At the same time work was carried out on adapting core damage models to BWRs, in collaboration with GRS and the University of Stuttgart, and to PHWR (Pressurized Heavy Water Reactors [incl. CANDU]), in collaboration with the BARC.

In the future activities of [SARNET](#), ASTEC should continue to be used to build up knowledge on severe accidents. Initiatives are underway to reduce computing speeds, in particular through parallel computing.

Since 2009, work has been carried out on adapting ASTEC to accidents in Gen IV sodium-cooled, fast-neutron reactors and at nuclear fusion facilities such as ITER.

8.4. *MAAP*

Development work on the Modular Accident Analysis Program (MAAP) began in the United States in the early 1980s for the purpose of PSA-related physical studies under the Industry Degraded Core Rulemaking (IDCOR) programme, which brought together some sixty American companies. When IDCOR came to an end, MAAP was acquired by

the Electric Power Research Institute (EPRI), an American organisation, but development work is still carried out by Fauske & Associates, Inc (FAI).

Many nuclear operators have purchased a licence to use MAAP for the purpose of safety studies. They have formed a users' group (MAAP Users' Group or MUG) comprising more than 55 organisations.

EDF uses MAAP for studying PWR core melt accidents including level 2 PSAs, hydrogen recombiner design, reassessment of foreseeable release in the event of a core melt accident, studies to help prepare severe accident operating guidelines (GIAG), direct containment heating (DCH) studies and studying the slow rise in containment pressure.

Since it acquired the code in 1991, EDF has built up specific skills in developing and validating MAAP, in particular by comparing it with results obtained from other codes designed for power reactor applications.

Pursuing the same development approach, it began producing its own versions of MAAP as of 1996, integrating special features. EDF currently uses version 4.07a of the code, which is designed to model EPR accident sequences in addition to those concerning 900 et 1300 MWe PWRs.

8.4.1. Capabilities

The MAAP code is used to simulate accident situations in PWRs, including VVER and EPR designs, BWRs or PHWR reactors, with specific versions for each type of reactor. It focuses in particular on core melt sequences whatever the conditions (whether the reactor is operating or shut down).

Functional modelling is included for examining the impact of operator action on the progression of accident sequences.

Computing time is short - about two hours on a PC in a Linux environment to simulate 24 hours real time for an accident sequence with core damage.

Fission product transport (release in the event of core damage, migration in the RCS and containment, chemistry) can be modelled to determine environmental release and surface and volume contamination in rooms.

For each control volume, MAAP solves conservation of mass and energy equations. Conservation of momentum equations are not differential equations and amount to Bernoulli equations.

The RCS, excluding the pressuriser, is represented by 14 volumes at the most, and the containment by no more than 30. The core is modelled axisymmetrically with a maximum of 175 mesh cells.

Figure 8.4 illustrates the main physical phenomena modelled by MAAP for the RCS and containment.

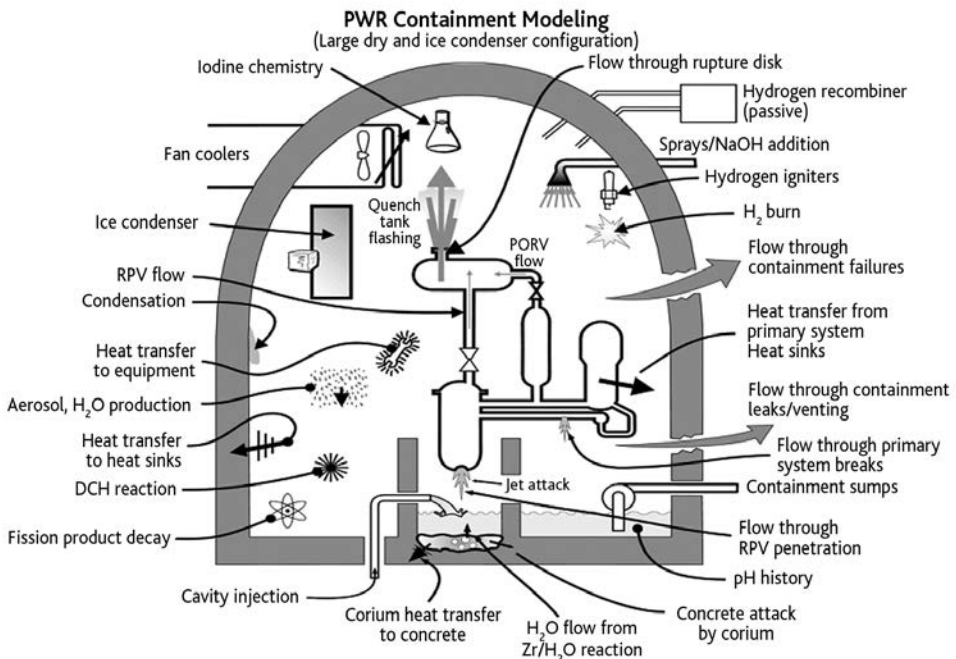


Figure 8.4. MAAP models for physical phenomena in a PWR containment.

The MAAP4.07c version includes specially adapted models for EPR applications [22]. These include:

- modelling the heavy reflector at the edge of the core: the code models the formation of a crust between the molten corium and the heavy reflector and the formation of a layer of molten steel between the crust and solid area of the heavy reflector, the perforation of the heavy reflector, followed by the ablation of the reflector outer wall as the corium flows into the annulus between the reflector and the reactor vessel (Figure 8.5);
- modelling the radiative heat transfer from the corium pool in the reactor pit to the vessel structures and reactor pit walls before the core catcher lower plug melts;
- taking into account the different types of concrete and wall configurations used in partitioning the containment and spreading compartment for the purpose of MCCI calculation.

A new version of the MAAP4 code developed by EDF R&D based on the standard EPRI version was used by EDF in 2012. It incorporates the latest progress in international projects, such as SARNET and ISTP, especially reductions in uncertainties relating to core damage and release assessment. Improvements to the models concern, for example, air-induced oxidation of fuel rod cladding, B₄C oxidation, non-volatile and semi-volatile fission product release from fuel, containment iodine chemistry, MCCI processing and coupling the MAAP code with the NUCLEA base by tabulation for improved assessment of the thermophysical properties of corium.

8.4.3. MAAP upgrade prospects

At the beginning of 2015 EDF switched to MAAP 5.0, a major upgrade to the code. Version 5.0 incorporates most of the physical models developed by EDF for its own versions of MAAP 4, including damage to Ag-In-Cd or B_4C control rods, zirconium oxidation at high temperatures and fission product release from the fuel matrix. It also includes many of the improvements made to physical models by FAI, some of which are listed below:

- RCS thermal-hydraulics: more detailed processing with the RCS broken down into 49 mesh units, single-phase or water-steam two-phase fluid processing, possibility of simulating safety injection in the cold leg only, improved modelling of natural circulation in the reactor vessel (especially between the annulus, core and upper plenum), improved modelling of the formation of water plugs and their impact on natural circulation, taking account of any reversal of flow in steam generator tubes;
- accumulator modelling: accumulators modelled as part of the RCS, accumulator wall modelled as a heat sink, nitrogen injection into the RCS from the accumulators;
- core modelling: addition of 1D neutronic and point kinetic models;
- modelling of corium retention in the reactor vessel: refinement of the reactor vessel axial mesh to 100 meshes, modelling of the variation in the critical dryout heat flux along the outer surface of the reactor vessel (according to the angle of inclination) when the vessel is assumed to be flooded, calculation of heat transfer by nucleate boiling between the outer surface of the reactor vessel and the liquid water in the reactor pit, modelling of insulation and of a gap between the reactor vessel and the insulation;
- new models of phenomena involved in containment heat transfers: natural and forced convection in containment compartments induced by a loss-of-coolant accident, wall condensation allowing for paint, gas entrainment of condensed water droplets on the wall, steam jet condensation in the flooded compartment, hydrogen combustion.

These improvements have been financed by some fifteen MAAP4 licence holders. After improving physical modelling, FAI focused on the numerical stability of MAAP5 in 2011-2012. Since the beginning of 2015, MAAP5 provides an alternative to MAAP4 for EDF research on core melt accidents.

8.5. MELCOR

MELCOR is an integral code developed by SNL since 1982 for the US NRC. It is used as a tool for the comprehensive study of core melt accidents that might occur in light-water reactors (PWR designs including VVERs and BWRs) [23]. Applications also exist for RBMK reactors, as well as for PHWR reactors, albeit only on an exploratory basis. Foreign partners in the US NRC Cooperative Severe Accident Research Program (CSARP) contribute to the code validation process.

The US NRC uses the code in reassessing radioactive releases from MOX or high-burnup fuels for example, appraising new reactor designs (such as the Westinghouse AP1000, ESBWR and US.EPR), realistically estimating the impact of core melt accidents for various types of reactor in operation in the United States, based on state-of-the-art knowledge, methods and software and taking into account the related uncertainties, and for studying accidents in spent fuel pools. On an international level, applications are particularly concerned with optimising accident management guidelines.

MELCOR replaced all the codes developed by the US NRC in the United States in the 1980s and, as can be seen in Figure 8.6, covers almost all the physical phenomena involved in an accident.

A widely used version in 2015 is still MELCOR 1.8.6, which was delivered in 2005. The main improvements made to models at that time concern:

- formation and evolution of a corium pool in the reactor vessel;
- silver release and B₄C oxidation in control rods;
- fission product release from MOX and high-burnup fuels;
- introduction of a point kinetics model to calculate changes in reactivity.

A particular feature of MELCOR compared with the ASTEC and MAAP codes is that it implements the same thermal-hydraulic models for all areas of the reactor, whether in the RCS and secondary coolant system or the containment. A numerical approach with five differential equations and an algebraic inter-phase slip algorithm is used. The time semi-implicit method used to solve the balance equations limits the computing time step to ensure the stability of the numerical scheme.

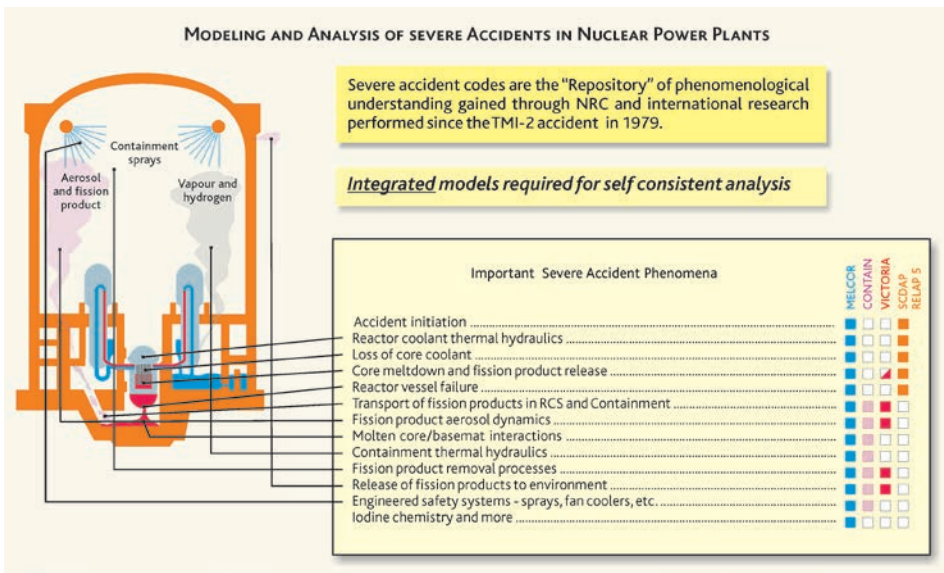


Figure 8.6. Physical phenomena modelled by the MELCOR code.

Users have access to a tool designed for automatically launching a series of sensitivity studies for uncertainty analysis.

Figure 8.7 illustrates an *a posteriori* calculation result of the Phebus FPT1 test performed by IRSN. The test focused on the start of PWR control rod damage (cladding oxidation, UO_2 dissolution, corium flows, etc.). The figure compares calculations with the hydrogen mass release measured during the test.

Validation work on iodine chemistry models, based on Phebus FP results in particular, has highlighted the need for significant improvements to some models, especially those affecting the calculated gas-phase iodine concentration in the containment.

A new series of versions, MELCOR 2, is currently under development. Version 1.8.6 is only concerned by corrective maintenance. Version 2.1 was released in September 2009. The programming of the code was upgraded (e.g. programming language switched to Fortran 95) and the data sets restructured. Significant improvements were made in terms of quality assurance, including the introduction of systematic non-regression tests, user support with an online help tool, and more user-friendly pre- and post-processing tools.

Modelling work in the last years concerned:

- Generation III reactors - PWRs (US EPR, AP1000, etc.) or BWRs (ABWR, etc.). Modelling of some physical phenomena was improved based on new knowledge concerning, for example, gas-phase iodine behaviour in the containment;
- behaviour of spent fuel pools;
- behaviour of UO_2 fuel at high burnups and of MOX fuel;
- Generation IV reactors, with a generalisation of fluids processed (sodium, molten salts, etc.). Modelling efforts have focused chiefly on pebble-bed or prismatic high-temperature reactors and, more specifically, on developing models of heat transfer inside the pebbles or with helium, graphite oxidation, fission product release from fuel and dust generation and transport.

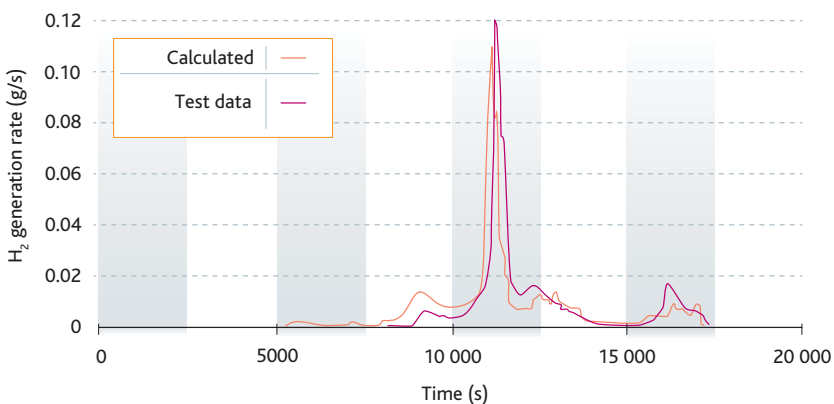


Figure 8.7. Comparison of measurements and MELCOR 1.8.6 calculations of hydrogen release rate during the Phebus FPT1 test.

References

- [1] N. Rasmussen, Rapport WASH 1400, The reactor safety study, 1975.
- [2] NUREG, 1150, Severe Accident Risks: An assessment for five US Nuclear Power Plants, 1991.
- [3] M. Kajimoto *et al.*, Development of THALES2, a Computer Code for Coupled Thermal-Hydraulics and Fission Product Transport Analysis for Severe Accidents at LWRs and its Application to Analysis of Fission Product Revaporization Phenomena, *Proceedings of the ANS International Topical meeting on safety of thermal Nuclear reactors*, Portland (USA), July 1991.
- [4] B. Linet, A. Maillat, ESCADRE code development and validation - An overview, *Proceedings of the International Topical meeting Severe Accident Risk and management (SARM'97)*, Piestany (Slovakia), June 1997.
- [5] M. Naitoh, S. Hosoda, C.M. Allison, Assessment of water injection as severe accident management using SAMPSON code, *Conference ICONE-13*, Beijing, China, 16-20 May 2005.
- [6] L.A. Bolshov, V.F. Strizhov, SOCRAT - The System of Codes for Realistic Analysis of Severe Accidents, *Conférence ICAPP '06*, Reno (United States), June 2006.
- [7] H.-J. Allelein *et al.*, Validation strategies for severe accident codes (VASA), EU Cosponsored research on Containment Integrity, EUR 19952 EN, Brussels, p. 295-324, 2000.
- [8] CSNI: International Standard Problems (ISP), brief descriptions (1975-1999), [NEA/CSNI/R\(2000\)5](#), 2000.
- [9] CSNI integral test facility validation matrix for the assessment of thermal-hydraulic codes for LWR LOCA and transients, [NEA/CSNI/R\(96\)-17](#), 1996.
- [10] A.M. Beard, P.J. Bennett, B.R. Bowsher, J. Brunning, The Falcon Programme: Characterisation of Multicomponent Aerosols in Severe Nuclear Reactors Accidents, *Journal of Aerosol Science* **23**, S831, 1992.
- [11] F. Rahn, R. Sher, R.C. Vogel, *Summary of the LWR aerosol containment experiments (LACE) programme*, IAEA Symposium Severe Accidents in Nuclear Power Plants, Sorrento, 21-25 March 1988, ISBN 92-0-020188-1.
- [12] M. Firnhaber, K. Fischer, S. Schwarz, G. Weber, ISP-44 KAEVER tests – Experiments on the behaviour of core-melt aerosols in a LWR containment, [NEA/CSNI/R\(2003\)5](#), 2003.
- [13] Theofanous and Syri, The coolability limits of a reactor pressure vessel lower head, *Nuclear Engineering and Design* **169** (1-3), 59-76, 1997.
- [14] SOAR on Containment Thermal hydraulics and Hydrogen distribution, [NEA/CSNI/R\(99\)-16](#), 1999.

- [15] H.J. Allelein *et al.*, International standard problem ISP-47 on containment thermal-hydraulics, Final report, [NEA/CSNI/R\(2007\)10](#), 2007.
- [16] P. Chatelard, N. Reinke, S. Arndt, S. Belon, L. Cantrel, L. Carenini, K. Chevalier-Jabet, F. Cousin, J. Eckel, F. Jacq, C. Marchetto, C. Mun, L. Piar. ASTEC V2 severe accident integral code main features, current V2.0 modelling status, perspectives. *Nuclear Engineering and Design* 272 (2014),119-135.
- [17] T. Albiol, J.P. Van Dorselaere, N. Reinke, SARNET: a success story. Survey of major achievements on severe accidents and of knowledge capitalization within the ASTEC code, *Conférence EUROSAFE*, Paris, November 2008.
- [18] D. Tarabelli, G. Ratel, P. Pélisson, G. Guillard, M. Barnak, P. Matejovic, ASTEC application to in-vessel corium retention, *Nuclear Engineering and Design* 239, 1345-1353, 2009.
- [19] J. Elter, P. Matejovic, Proposal of in-vessel corium retention concept for PAKS NPP, *OECD MASCA2 Seminar*, Cadarache (France), 11-12 October, 2007.
- [20] P. Chatelard, J. Fleurot, O. Marchand, P. Draï, Assessment of ICARE/CATHARE V1 severe accident code, *Conférence ICONE-14*, Miami, Florida (USA), 17-20 July 2006.
- [21] B. Cheynet, P. Chaud, P.Y. Chevalier, E. Fischer, P. Mason, M. Mignanelli, NUCLEA: Thermodynamic Properties and Phase Equilibria in the Nuclear Systems of Interest, *Journal de Physique IV* 113, 61-64, 2004.
- [22] E. Williams, R. Martin, P. Gandrille, R. Meireles, R. Prior, C. Henry, Q. Zhou, Recent revisions to MAAP4 for US EPR Severe Accident Applications, *Conference ICAPP 08*, Anaheim (California, USA), June 2008.
- [23] R.O. Gauntt *et al.*, MELCOR Computer Code Manuals, Version 1.8.6, Rapport SAND 2005-5713, 2005.

Chapter 9

Conclusion

Given the technical and organisational measures in place for operating nuclear power plants, a core melt accident or severe accident can only occur in a power reactor following a series of malfunctions (multiple failures, involving human errors and/or equipment failures), as evidenced by the core melt accidents that have occurred since nuclear power plants first came into use. Such an accumulation of malfunctions can be caused by a single hazard for which inadequate provision was made. This was the case, for example, of the [Fukushima Daiichi](#) accident in Japan in March 2011, which was the result of a major external hazard (see below).

In 1979, the accident on reactor 2 of the Three Mile Island (TMI) plant in the United States demonstrated that a series of failures could lead to a core melt accident, even though containment integrity was maintained virtually throughout the accident, which considerably limited radioactive release and avoided any serious environmental impact.

In 1986, the reactivity accident on unit 4 of the [Chernobyl](#) nuclear power plant in Ukraine was the result of reactor design defects and a string of wrong decisions and operator errors that led to the destruction of the reactor core, massive radioactive release to the environment and to large-scale contamination. The accident was classed as an INES level 7 event.

Lastly, in March 2011, the magnitude 9 earthquake in Japan and the ensuing tsunami severely affected the country and had serious consequences for the population and infrastructure. In particular, it devastated a large part of the [Fukushima Daiichi](#) nuclear power plant. These natural events caused an accumulation of malfunctions (in particular the loss of all electrical power supplies, including the emergency power supply for four of the plant's reactors, and of the heat sink), which in turn led to core melt in three nuclear reactors and loss of cooling of several spent fuel pools [1]. Explosions also occurred in

four of the reactor buildings due to the production of hydrogen induced by fuel damage. Very large quantities of radioactive substances were released to the environment. The accident was classed as an INES level 7 event like the [Chernobyl](#) accident.

In 2015, it is not possible to produce detailed descriptions of the accident sequences in the [Fukushima Daiichi](#) reactors for want of sufficiently precise data. Operating experience feedback from the TMI-2 accident, where actual damage to the reactor core could not be confirmed until 1986 when the vessel of the stricken reactor was opened, suggests that it will take several years to reconstruct a detailed account of the Fukushima Daiichi accident based on observations of the final state of damage to the reactor cores and containments. Estimations of the release and environmental dispersal of radioactive substances are provisional and subject to uncertainties.

Following the TMI-2 accident in the United States in 1979, research in the field of core melt accidents in nuclear power reactors benefited from increased material and human resources. Significant progress has been made in understanding the physical phenomena involved in this type of accident and simulation tools have been developed. This publication testifies to this research investment and the considerably improved knowledge of the complex phenomena involved.

Knowledge in the field has now reached a state of the art in severe accident physics that can be shared by various stakeholders in the nuclear sector (industry, research institutes and regulatory authorities) around the world.

Although significant progress has been made, uncertainties still remain. Consequently, it is not possible to determine whether or not radioactive substances resulting from fuel damage will remain within the containment in all foreseeable accident scenarios. In addition, there is still room for progress in defining measures to guarantee the integrity of the reactor vessel and its containment in the event of a core melt accident and thus keep radioactive release to the environment as low as reasonably achievable.

Contextual changes relating to the safety of nuclear facilities in France, such as:

- the coexistence of Generation II and III reactors in the near future;
- the possible lifetime extension of Generation II reactors beyond 40 years;
- the intention of the authorities to see more effective action taken to mitigate the impact of core melt accidents following that at [Fukushima Daiichi](#);

have led the licensees, along with [IRSN](#) and CEA, to submit new research programmes to the authorities aimed at developing knowledge and computing tools in the field of severe accidents. Essentially, these programmes seek to improve the assessment of existing measures concerning Generation II reactors or even propose new ones with a view to:

- arrest as far as possible the progression of the accident in the reactor vessel, in particular by using reactor coolant water to reflood the partially damaged core (when a debris bed or pool of molten materials is involved) in the reactor vessel in all foreseeable core damage configurations;

- arrest as far as possible the progression of the accident in the containment, in particular by pouring water into the reactor pit above or below the pool of molten materials to cool these materials during MCC1; the aim here is to determine how effective cooling is as a means of preventing the ablation of concrete by the corium - and thus avoid basemat penetration – in all foreseeable configurations involving a pool of molten material and for all types of concrete;
- reduce foreseeable iodine and ruthenium releases in the environment in all accident scenarios, including oxidising conditions in the RCS which promote the transfer of gaseous species of these fission products to the containment;
- reduce further the risk of steam explosion in the event of ex-vessel progression, taking into account interactions between molten corium, debris and water in the reactor pit;
- reduce further the flame acceleration risk in the containment in the event of hydrogen combustion.

The acquired knowledge will be used in physical models developed for integral codes, such as ASTEC, and for probability safety analysis to better assess accident risks and their consequences. The results of research on core melt accidents have already had a positive impact on the design of Generation III reactors, like the EPR, with the implementation of equipment and measures aimed at mitigating the consequences of these accidents through the confinement of radioactive substances; the corium catcher is an example of this. Further studies should help to show how effective the systems and measures implemented for this type of reactor are.

It will be important to continue efforts to preserve and develop high-level expertise, drawing on the results of the severe accident research programmes described above. Such efforts should be aimed at:

- improving safety levels for Generation II reactors currently in service by developing increasingly reliable measures to prevent core melt accidents and mitigate their impact on these reactors (not only PWRs but also other reactor systems operated outside France);
- helping to strengthen measures for Europe-wide management of a major nuclear emergency, as the impact of a core melt accident would reach well beyond the borders of any one country;
- for countries like France, which design and export nuclear reactors, sharing their national approach to safety – especially regarding core melt accidents – with countries seeking to develop their nuclear sector.

It will be many years before we have learned all there is to know about reactor safety in light of the [Fukushima Daiichi](#) accident, which demonstrated how overlooking natural phenomena at the facility design stage could lead to a severe nuclear accident. Nevertheless, under initiatives such as European stress tests or complementary safety assessments in France, licensees put forward proposals in 2011 for providing nuclear facilities with greater protection against extreme hazards that were previously considered highly

unlikely. These proposals were examined by IRSN [2]. Ongoing investigations into the need for more effective accident risk reduction measures might also lead to calls for new severe accident research programmes. The accident at the Fukushima Daiichi nuclear power plant shows that stakeholders in the nuclear sector must continue to unite their efforts to prevent and mitigate the impact of severe accidents for even safer nuclear facilities.

References

- [1] Fukushima, un an après, Premières analyses de l'accident et de ses conséquences, Report IRSN/DG/2012-001, www.irsn.fr, 2012.
- [2] Évaluations complémentaires de sûreté post-Fukushima: comportement des installations nucléaires françaises en cas de situations extrêmes et pertinence des propositions d'améliorations, IRSN report No. 679, www.irsn.fr, 2011.

Nuclear Power Reactor Core Melt Accidents

Current State of Knowledge

Didier Jacquemain, Coordinator

For over thirty years, IPSN and subsequently IRSN has played a major international role in the field of nuclear power reactor core melt accidents through the undertaking of important experimental programmes (the most significant being the Phébus-FP programme), the development of validated simulation tools (the ASTEC code that is today the leading European tool for modelling severe accidents), and the coordination of the SARNET (Severe Accident Research NETWORK) international network of excellence. These accidents are described as «severe accidents» because they can lead to radioactive releases outside the plant concerned, with serious consequences for the general public and for the environment.

This book compiles the sum of the knowledge acquired on this subject and summarises the lessons that have been learnt from severe accidents around the world for the prevention and reduction of the consequences of such accidents, without addressing those from the Fukushima accident, where knowledge of events is still evolving.

The knowledge accumulated by the Institute on these subjects enabled it to play an active role in informing public authorities, the media and the public when this accident occurred, and continues to do so to this day.

The Institute for Radiological Protection and Nuclear Safety (IRSN) is a public body undertaking research and consultancy activities in the field of nuclear safety and radiation protection. It provides the public authorities with technical support. It also carries out various public service missions entrusted to it under national regulations. In particular, these include radiological monitoring of French territory and of workers, management of emergency situations, and provision of information to the public. IRSN expertise is available to partners and customers both in France and abroad.

ISBN : 978-2-7598-1835-8

Head Office

31, avenue de la Division Leclerc

92260 Fontenay-aux-Roses

RCS Nanterre B 440 546 018

Telephone +33 1 58 35 88 88

Postal address

B.P. 17 - 92262 Fontenay-aux-Roses Cedex – France

Website: www.irsn.fr

